frontiers | Research Topics

# Women in microorganisms in vertebrate digestive systems 2023

**Edited by**
Karolina Skonieczna-Żydecka, Ekaterina Avershina and Rebeca Martín

**Published in**
Frontiers in Microbiology

ISSN 1664-8714
ISBN 978-2-8325-5931-4
DOI 10.3389/978-2-8325-5931-4

## About Frontiers

Frontiers is more than just an open access publisher of scholarly articles: it is a pioneering approach to the world of academia, radically improving the way scholarly research is managed. The grand vision of Frontiers is a world where all people have an equal opportunity to seek, share and generate knowledge. Frontiers provides immediate and permanent online open access to all its publications, but this alone is not enough to realize our grand goals.

## Frontiers journal series

The Frontiers journal series is a multi-tier and interdisciplinary set of open-access, online journals, promising a paradigm shift from the current review, selection and dissemination processes in academic publishing. All Frontiers journals are driven by researchers for researchers; therefore, they constitute a service to the scholarly community. At the same time, the *Frontiers journal series* operates on a revolutionary invention, the tiered publishing system, initially addressing specific communities of scholars, and gradually climbing up to broader public understanding, thus serving the interests of the lay society, too.

## Dedication to quality

Each Frontiers article is a landmark of the highest quality, thanks to genuinely collaborative interactions between authors and review editors, who include some of the world's best academicians. Research must be certified by peers before entering a stream of knowledge that may eventually reach the public - and shape society; therefore, Frontiers only applies the most rigorous and unbiased reviews. Frontiers revolutionizes research publishing by freely delivering the most outstanding research, evaluated with no bias from both the academic and social point of view. By applying the most advanced information technologies, Frontiers is catapulting scholarly publishing into a new generation.

## What are Frontiers Research Topics?

Frontiers Research Topics are very popular trademarks of the *Frontiers journals series*: they are collections of at least ten articles, all centered on a particular subject. With their unique mix of varied contributions from Original Research to Review Articles, Frontiers Research Topics unify the most influential researchers, the latest key findings and historical advances in a hot research area.

Find out more on how to host your own Frontiers Research Topic or contribute to one as an author by contacting the Frontiers editorial office: frontiersin.org/about/contact

# Women in microorganisms in vertebrate digestive systems: 2023

**Topic editors**

Karolina Skonieczna-Żydecka — Pomeranian Medical University, Poland

Ekaterina Avershina — Oslo University Hospital, Norway

Rebeca Martín — INRAE Centre Jouy-en-Josas, France

**Citation**

Skonieczna-Żydecka, K., Avershina, E., Martín, R., eds. (2025). *Women in microorganisms in vertebrate digestive systems: 2023*. Lausanne: Frontiers Media SA. doi: 10.3389/978-2-8325-5931-4

# Table of contents

frontiers | Frontiers in Microbiology

TYPE Original Research
PUBLISHED 19 June 2023
DOI 10.3389/fmicb.2023.1209158



OPEN ACCESS

EDITED BY
Karolina Skonieczna-Żydecka,
Pomeranian Medical University, Poland

REVIEWED BY
Nadia Andrea Andreani,
Max Planck Institute for Evolutionary Biology, Germany
Tasha M. Santiago-Rodriguez,
Diversigen, United States

*CORRESPONDENCE
Claudia Melis
✉ cme@dmmh.no

RECEIVED 20 April 2023
ACCEPTED 24 May 2023
PUBLISHED 19 June 2023

CITATION
Melis C, Billing AM, Wold P-A and Ludington WB (2023) Gut microbiome dysbiosis is associated with host genetics in the Norwegian Lundehund.
*Front. Microbiol.* 14:1209158.
doi: 10.3389/fmicb.2023.1209158



# Gut microbiome dysbiosis is associated with host genetics in the Norwegian Lundehund

Claudia Melis[1]*, Anna Maria Billing[1], Per-Arvid Wold[1] and William Basil Ludington[2,3]

[1]Department of Nature, Environment and Health, Queen Maud University College, Trondheim, Norway, [2]Department of Embryology, Carnegie Institution for Science, Baltimore, MD, United States, [3]Department of Biology, Johns Hopkins University, Baltimore, MD, United States

A group of diseases have been shown to correlate with a phenomenon called microbiome dysbiosis, where the bacterial species composition of the gut becomes abnormal. The gut microbiome of an animal is influenced by many factors including diet, exposures to bacteria during post-gestational growth, lifestyle, and disease status. Studies also show that host genetics can affect microbiome composition. We sought to test whether host genetic background is associated with gut microbiome composition in the Norwegian Lundehund dog, a highly inbred breed with an effective population size of 13 individuals. The Lundehund has a high rate of a protein-losing enteropathy in the small intestine that is often reported as Lundehund syndrome, which negatively affects longevity and life-quality. An outcrossing project with the Buhund, Norrbottenspets, and Icelandic sheepdog was recently established to reintroduce genetic diversity to the Lundehund and improve its health. To assess whether there was an association between host genetic diversity and the microbiome composition, we sampled the fecal microbiomes of 75 dogs of the parental (Lundehund), F1 (Lundehund x Buhund), and F2 (F1 x Lundehund) generations. We found significant variation in microbiome composition from the parental Lundehund generation compared to the outcross progeny. The variation observed in purebred Lundehunds corresponded to dysbiosis as seen by a highly variable microbiome composition with an elevated Firmicutes to Bacteroidetes ratio and an increase in the prevalence of *Streptococcus bovis/Streptococcus equinus* complex, a known pathobiont that can cause several diseases. We tracked several other environmental factors including diet, the presence of a cat in the household, living in a farm and the use of probiotics, but we did not find evidence of an effect of these on microbiome composition and alpha diversity. In conclusion, we found an association between host genetics and gut microbiome composition, which in turn may be associated with the high incidence of Lundehund syndrome in the purebred parental dogs.

KEYWORDS

**dysbiosis, domestic dogs, genetic diversity, gut microbiome, outcrossing, *Streptococcus equinus-infantarius-lutetiensis***

## 1. Introduction

The gut microbiome of an animal is influenced by many factors including diet (De Filippo et al., 2010), exposures to bacteria during post-gestational growth (Torrazza and Neu, 2011; Dowling and Levi, 2014), lifestyle (Clemente et al., 2015; Tun et al., 2017), disease status (Deng and Swanson, 2015), and host genetics (Hughes et al., 2020). Studies suggest a genetic effect on

the microbiome composition (Blekhman et al., 2015; Weissbrod et al., 2018; Hughes et al., 2020; Bubier et al., 2021), and differences in gut microbiome composition among dog breeds (Hooda et al., 2012; You and Kim, 2021), although the mechanisms through which specific genes modulate microbiome composition is still unclear. Bubier et al. (2021) describes three mechanisms through which genes could control diseases and link to the microbiome: (1) they might cause the disease phenotype, and microbiome is altered as consequence of disease; (2) they might affect gene expression in the host and indirectly alter the microbiome, which causes the disease; (3) they might affect the microbiome directly and cause the disease through the microbiome. Unraveling these mechanisms requires that we have good models where we can consider host genetics, microbiome, disease phenotype and their relationships simultaneously (Bubier et al., 2021).

Several diseases occurring in humans and dogs, such as Inflammatory Bowel Disease (IBD, including Crohn's disease and ulcerative colitis), are characterized by an imbalance in the gut microbiota, called "dysbiosis," where an overgrowth of harmful bacteria, a loss of beneficial bacteria or lowered alpha diversity can occur simultaneously (DeGruttola et al., 2016). It is, however, still unclear whether the dysbiosis is a risk factor or a consequence of the disease (DeGruttola et al., 2016). In both dogs and humans, an association between IBD and dysbiosis has been reported, as seen by an increase of Bacteroidetes (Suchodolski et al., 2012). Additionally, Firmicutes have been found to be decreased in dogs with IBD (Minamoto et al., 2015). However, the dysbiosis in dogs and humans differs in some key bacterial groups (Vázquez-Baeza et al., 2016), possibly due to profound morphological and physiological differences and a relatively recent human adaptation to a more carnivorous diet (Price et al., 2012). For example, *Fusobacterium* appears to be associated with IBD and colorectal cancer in humans, but no association has been established in dogs (Vázquez-Baeza et al., 2016). In humans and mice, obesity has been found to be associated with decreased microbial diversity and an increased Firmicutes/Bacteroidetes (F/B) ratio, whereas in dogs this relationship was not confirmed (Chun et al., 2020; You and Kim, 2021).

The Norwegian Lundehund is a small spitz dog breed that was used to fetch nesting Atlantic puffins *Fratercula arctica* on steep cliffs in the coast of northern Norway (Melis et al., 2013). Towards the end of the 19th century, using nets to hunt puffin became more common than using dogs. Thus, the breed lost its economic importance and was confined to the small fisherman's village of Måstad on the island of Værøy in the Lofoten archipelago. Two bottlenecks, the first caused by an outbreak of canine distemper in the 1940s, and the second caused by the abandonment of the village of Måstad in the 1960s, left only five highly related individuals. Currently, the breed counts more than 1,500 individuals, which all descend from these five dogs. For this reason, the Lundehund has an extremely low level of heterozygosity, which is around 5% as estimated by high-density SNP arrays (Melis et al., 2022), and an effective population size of only 13 individuals (Melis et al., 2013; Kropatsch et al., 2015). The low genetic diversity is associated with low fertility and with high rates of a protein-losing enteropathy localized to the small intestine, often reported as the Lundehund syndrome, but also as intestinal lymphangiectasia and IBD (Berghoff et al., 2007). Chronic atrophic gastritis and gastric neoplasms are also common in dogs with Lundehund syndrome (Kolbjornsen et al., 1994a,b; Qvigstad et al., 2008). Lundehund syndrome is usually treated by administration of immunosuppressant and anti-inflammatory drugs such as prednisone, prednisolone, or azathioprine and with antibiotics to reduce bacterial overgrowth (Berghoff et al., 2007). However, the extremely low genetic diversity also makes the Lundehund a possible genetic model of gut and autoimmune disease. A mortality study estimated that about 40% of deaths before 11 years of age occurs as a consequence of Lundehund syndrome or other gastrointestinal diseases (Norwegian Lundehund Club, 2014). Although a study found an association between Lundehund syndrome and a missense mutation in the gene LEPREL1 (Metzger et al., 2016), the inheritance mechanism of the Lundehund syndrome is not clear, and it is likely that several genes are involved in the development of this illness (Metzger et al., 2016). Very few individuals in the population do not carry the LEPREL1 mutation, making it impossible to use this information to select breeding individuals, without further reducing the already depauperate gene pool.

Because of the extremely low genetic diversity, the associated disease, and low fecundity, the Norwegian Lundehund Club started an outcrossing project in 2014 with three Nordic dog breeds, the Buhund, the Norrbottenspets, and the Icelandic sheepdog. We focus this study on the Buhund outcross, which started earlier and has, so far, produced the most individuals. The outcrossing project started by mating two unrelated females of Buhund with male Lundehunds, in order to avoid problems with gestation and delivery, due to the difference in relative size, the Buhund being about 30% larger than the Lundehund. The first-generation crossings (F1) were then backcrossed to pure Lundehunds, resulting in the second-generation crossings (F2). All dogs included in the project were screened for hip dysplasia and hereditary ocular pathologies before including them in breeding. We previously analyzed the genetic diversity of the parental, F1, and F2 animals from the Lundehund x Buhund outcross and found a restoration of genetic diversity through outcrossing, with F1 animals having highest diversity (Melis et al., 2022). The mean heterozygosity (estimated from 8,184 linkage-disequilibrium-pruned loci) of Lundehund, F1 and F2 dogs was 0.043, 0.272 and 0.153, respectively (Melis et al., 2022). None of the F1 and F2 progeny has, so far, developed Lundehund syndrome.

To ask whether there might be a microbiome basis for Lundehund syndrome, we sampled stool from parental, F1 and F2 dogs. We analyzed the 16S rRNA gene diversity of the fecal microbiome of purebred Lundehund (P), F1 and F2 individuals (Table 1; Figure 1) with the following aims:

1. Characterize the fecal microbiome composition of Lundehund (P) and first (F1) and second (F2) generation of outcrossings with Buhund.
2. Test whether a range of factors including diet type, presence of a cat in the household, administration of probiotics, and living on a farm correlate with microbiome diversity.
3. Test whether microbiome composition clusters according to cohort (P, F1, F2).
4. Explore whether the ratio between Firmicutes and Bacteroidetes (F/B, an index of dysbiosis) differs between dogs who had Lundehund syndrome and those who did not.

TABLE 1 Phenotypical traits and environmental characteristics of the dogs included in this study.

| | Lundehund (P) | | F1 | | F2 | |
|---|---|---|---|---|---|---|
| | *n* | % | *n* | % | *n* | % |
| Gender | | | | | | |
| Females | 28 | 56 | 6 | 75 | 10 | 45 |
| Males | 22 | 44 | 2 | 25 | 12 | 55 |
| Age (years) | | | | | | |
| Mean | 5.7 | – | 5.6 | – | 3 | – |
| SD | 2.7 | – | 1.06 | – | 1.34 | – |
| Weight (kgs) | | | | | | |
| Mean | 7.7 | – | 9.62 | – | 9.41 | – |
| SD | 1.3 | – | 2.13 | – | 2.17 | – |
| Lundehund syndrome history | | | | | | |
| Yes | 11 | 22 | 0 | 0 | 0 | 0 |
| No | 39 | 78 | 8 | 100 | 22 | 100 |
| Probiotics in the last six months | | | | | | |
| Yes | 20 | 40 | 1 | 13 | 1 | 5 |
| No | 30 | 60 | 7 | 88 | 21 | 95 |
| Prevalent diet type | | | | | | |
| Home made | 26 | 52 | 2 | 25 | 4 | 18 |
| Industrial dry | 16 | 32 | 4 | 50 | 13 | 59 |
| Raw | 8 | 16 | 2 | 25 | 5 | 23 |
| Presence of a cat in the household | | | | | | |
| Yes | 9 | 18 | 3 | 38 | 9 | 41 |
| No | 41 | 82 | 5 | 63 | 13 | 59 |
| Antibiotics in the last six months | | | | | | |
| Yes | 5 | 10 | 0 | 0 | 0 | 0 |
| No | 45 | 90 | 8 | 100 | 22 | 100 |
| Home environment | | | | | | |
| Farm | 3 | 6 | 3 | 38 | 7 | 32 |

Lundehund (P), first-generation crosses Lundehund × Buhund (F1) and first-generation backcrosses F1 × Lundehund (F2).

# 2. Materials and methods

## 2.1. Stool samples collection and analysis

In April to August 2021, we collected stool samples from Lundehund (P, $n = 50$), Lundehund x Buhund crosses (F1, $n = 8$), and F1 × Lundehund crosses (F2, $n = 22$). The lower number of individuals in the F1 cohort is due to the challenge in finding owners of Buhund females that were willing to let their dog being paired with a Lundehund. Owners were instructed in how to collect and handle fresh naturally deposited samples, avoiding contamination. The stool samples were stored at room temperature in Stool Nucleic Acid Collection and Preservation Tubes (Norgen BioTek Corp, Cat. 45,660). In September 2021, the samples were analyzed with the ZymoBIOMICS® Targeted Sequencing Service (Zymo Research, Irvine, CA). The ZymoBIOMICS®-96 MagBead DNA Kit (Zymo Research, Irvine, CA) was used to extract DNA using an automated platform. Bacterial 16S ribosomal RNA gene targeted sequencing was performed using the Quick-16S™ NGS Library Prep Kit (Zymo Research, Irvine, CA). The bacterial 16S rRNA primers amplified the V3-V4 region of the 16S rRNA gene. The final PCR products were quantified with qPCR fluorescence readings and pooled together based on equal molarity. The final pooled library was cleaned with the Select-a-Size DNA Clean & Concentrator™ (Zymo Research, Irvine, CA), then quantified with TapeStation® (Agilent Technologies, Santa Clara, CA) and Qubit® (Thermo Fisher Scientific, Waltham, MA). The ZymoBIOMICS® Microbial Community DNA Standard (Zymo Research, Irvine, CA) was used as a positive control for each targeted library preparation. Negative controls (i.e., blank extraction control, blank library preparation control) were included to assess the level of bioburden carried by the wet-lab process. The final library was sequenced on an Illumina® MiSeq™ with a v3 reagent kit (600 cycles). The sequencing was performed with a 10% PhiX spike-in. Unique amplicon sequences variants (ASVs) were inferred from raw reads using the DADA2 pipeline (Callahan et al., 2016). Potential sequencing errors and chimeric sequences were also removed with the DADA2 pipeline. ASVs that were present in only one sample, i.e., singletons, were examined for each cohort and removed from the dataset for clustering analysis. Taxonomy assignment was performed using Uclust from Qiime v.1.9.1 (Caporaso et al., 2010) with the Zymo Research Database. Any taxa that were not represented at over 1% relative abundance in at least one sample were removed. Five purebred Lundehund dogs older than 9 years and two F2 dogs that were under medication at sampling were also removed from further analyses, in order to obtain a sample more homogenous in age and without the influence of antibiotics. Normalization of the data was performed by calculating the relative abundance for each sample by library scaling.

## 2.2. Microbiome statistical analyses

The microbiome analyses were done with a dataset including 306 bacterial species and 73 individual samples in R version 4.1.3 (R Core team, 2021) with RStudio version 2022.07.2 (RStudio Team, 2022) and with the R packages *Phyloseq* (McMurdie and Holmes, 2013) and *Microbiome* (Lahti and Shetty, 2017). We explored the microbiome composition by plotting the relative abundance of bacterial phyla and of the genera present at >1% relative abundance of which there were 15. These plots were produced with the function *comp_barplot* from the package *microViz* version 0.10.8 (Barnett et al., 2021). The R package *plyr* (Wickham, 2011) was used to calculate richness and diversity of bacteria according to the different categories reported in Table 1. We tested for a statistical difference in relative abundance of all phyla and the subset of 15 most abundant genera with the function *xdc.sevsample* in the Human Microbiome Project (*HMP*) R package version 2.0.1 (La Rosa et al., 2012). This function performs a multivariate test for differences in composition between groups assuming Dirichlet-multinomial distribution by testing for a difference in the mean distribution of each taxon across groups and also account for the overdispersion in the count data (Wilks, 1938). Differences in relative abundances of specific phyla between groups were compared by the R package *Maaslin2* (Mallick et al., 2021) with Benjamini-Hochberg correction to control for false discovery

10.3389/fmicb.2023.1209158

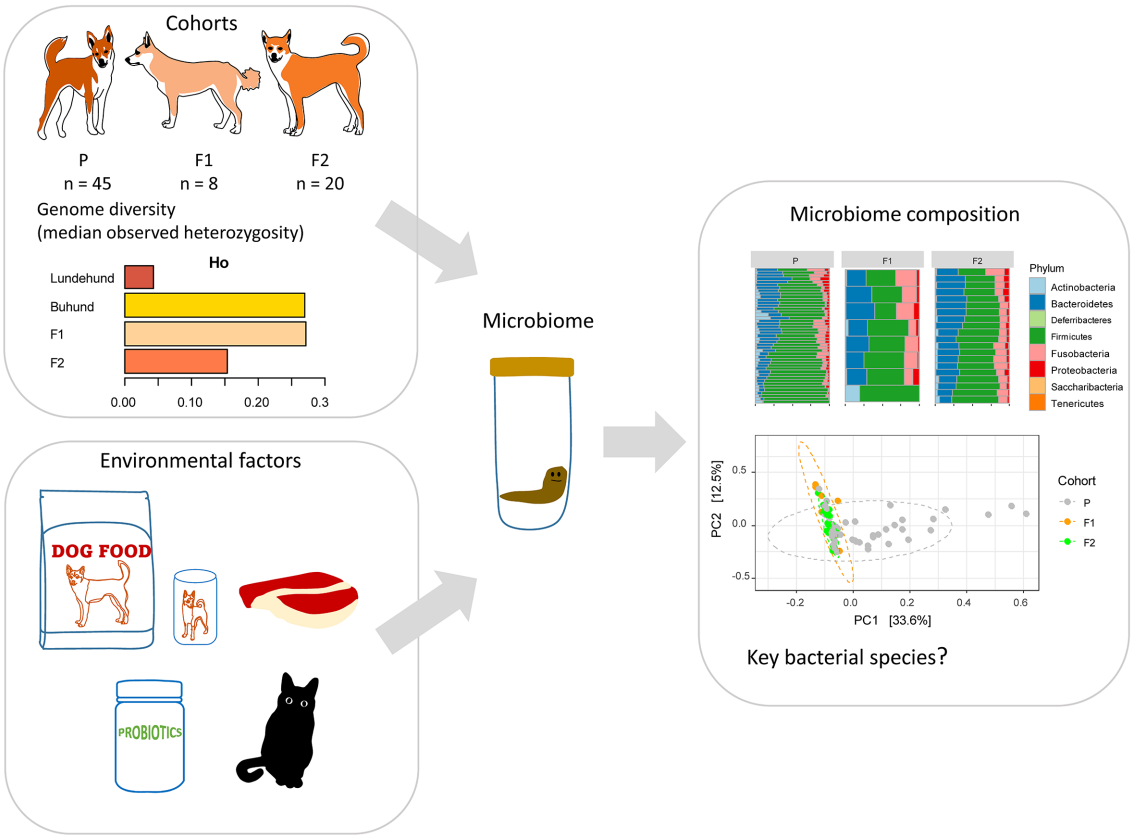


FIGURE 1
Study design to test whether outcrossing Norwegian Lundehund with Buhund is associated with fecal microbiome composition. The dataset included stool samples from 73 dog individuals: 45 Lundehunds (P), eight first-generation crosses Lundehund × Buhund (F1) and 20 first-generation backcrosses F1×Lundehund (F2).

rate. For this analysis, due to the low number of F1 individuals, the F1 and the F2 generations were pooled together and compared to the purebred Lundehund generation (P).

Alpha diversity, as calculated by the Shannon index, was compared across groups according to Table 1. As a measure of beta diversity, a principal component analysis at species level was performed with the R package *Phyloseq* (McMurdie and Holmes, 2013) and the command *ordinate* and "RDA" method (the distance method on the Bray Curtis distance). Comparisons between Shannon indices and F/B ratios were performed by Wilcoxon tests with Bonferroni correction. We also tested whether the samples clustered to a higher degree than expected by sampling variability using permutational multivariate analysis of variance (PERMANOVA). For the permutational analysis the distance method was set to "Euclidean."

## 2.3. Environmental variables

A questionnaire was also sent to the dog owners, together with the stool sampling tubes, to obtain information about environmental factors such as the typical diet, Lundehund syndrome history, antibiotics and probiotics administration (in the previous 6 months), presence of a cat in the household and whether the dog lived on a farm or in a more urban environment (Table 1). Many of the purebred Lundehunds (40%) used a combination of two to three different types of probiotics, whereas probiotics administration was less common among F1 and F2 dogs.

# 3. Results

## 3.1. Microbiome compositional variation is correlated with dog genotype

To assess whether Lundehund syndrome is associated with gut dysbiosis, we collected stool samples and metadata (Table 1) from 73 dogs, comprising 45 purebred Lundehunds, 8 Lundehund × Buhund F1 animals, and 20 F1 x Lundehund crosses, which are the F2 generation. To examine the microbiome of the Norwegian Lundehund and F1 and F2 outcrossing generation, we assessed the bacterial taxonomic composition of the stool by 16S rRNA gene amplicon library sequencing. After assigning taxonomy to the bacteria in each sample based on ASV and filtering the data to remove singletons and rare taxa, the final microbiome data set included 306 bacteria species and 73 individual samples. Five ASVs, with taxonomic assignments to *Collinsella intestinalis-stercoris*, *Blautia hansenii-producta*, *Lachnoclostridium* sp32341-sp32430, Clostridiales (no species), and *Fusobacterium mortiferum*, were present in all samples. A loss of alpha diversity has also been shown by various studies to correlate with microbiome-associated disease. We detected no significant differences

in alpha diversity, as calculated by Shannon index (Appendix S1), as a function of dog generation, Lundehund syndrome history, diet type, administration of antibiotics, administration of probiotics, presence of a cat in the household, or living on a farm versus in a suburban environment (Wilcoxon rank sum test, all $p > 0.05$), although we note that the potential influence of these factors on microbiome composition cannot be ruled out due to the relatively small sample size.

To further assess the microbiome compositional variation between dogs (beta diversity), we performed a principal component analysis at the species level (Figure 2). By defining the centroid of variation for each of the dog generations, we found that purebred Lundehunds were clearly differentiated from F1 and F2 dogs based on principal component #1 (PC1), which explains 33% of the variation in the data (Figure 2A). Whereas there was wide variation in PC1 for purebred Lundehunds, the F1 and F2 generations were much more similar to one another (Figure 2A). The distance-based test of homogeneity of multivariate dispersions showed that the samples clustered beyond the expectation from sampling the total variability ($F = 7.3$, df = 2, $p = 0.002$, Figure 2B). We also performed a principal component analysis with a dataset including only purebred Lundehunds and plotted the ordination by Lundehund syndrome history (Appendix S2). The ellipses overlapped almost totally, showing that there is no difference in beta diversity between purebred Lundehunds which had a Lundehund syndrome history and those which did not.

Overall, our results indicate that microbiome composition is associated with the genetic background of the dogs. The majority of the variation occurred in purebred Lundehunds, suggesting that these dogs lack some control mechanism regulating their microbiome composition. We found no evidence that other known factors associated with microbiome disease contribute to the microbiome composition in Lundehunds.

## 3.2. Lundehunds have a microbiome compositional signature at the phylum and the genus levels

The most abundant bacterial phyla across all samples were Firmicutes (57%), Bacteroidetes (23%), and Fusobacteria (10%), followed by Proteobacteria (4%), and Actinobacteria (4%; Figure 3A). To assess which were the compositional differences based on the genetic background of the dogs, we examined the composition of

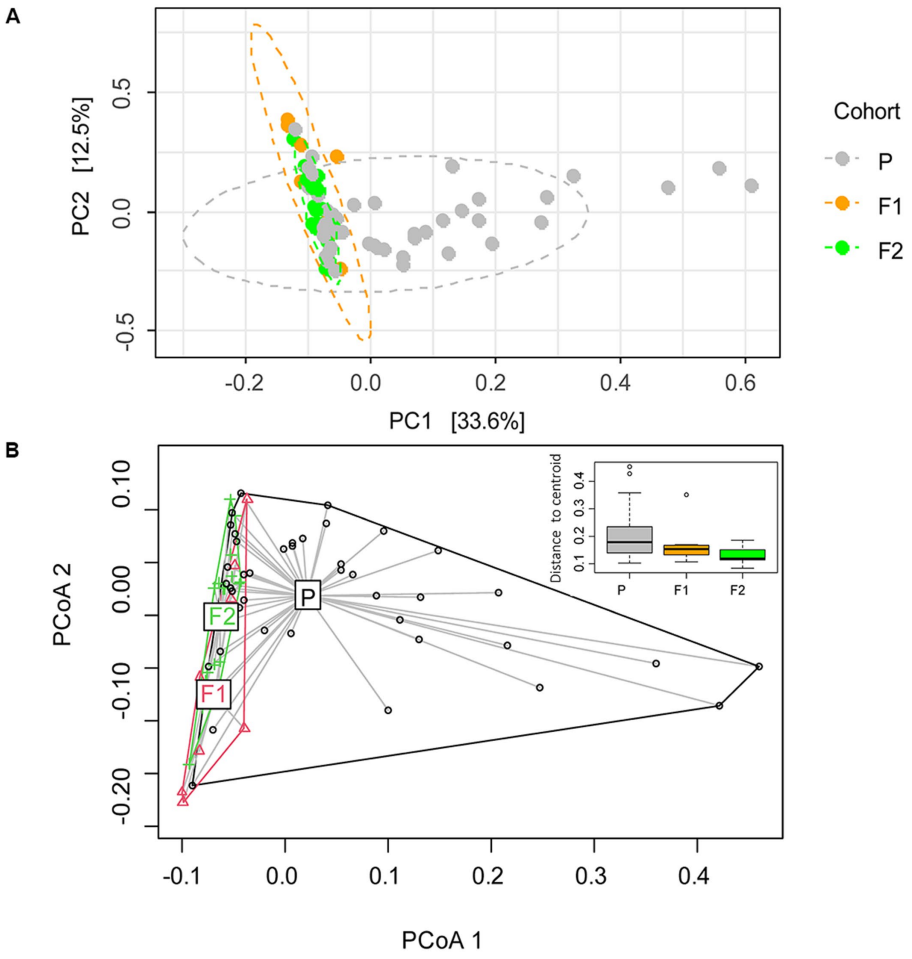


FIGURE 2
**(A)** Ordination analysis performed with *Phyloseq* on gut microbiome of 73 dog individuals, including 45 Lundehunds (P), eight first-generation crosses Lundehund × Buhund (F1) and 20 first-generation backcrosses F1×Lundehund (F2). **(B)** Ordination centroids and dispersion measured by Aitchison distance on gut microbiome composition of the same dataset.

10.3389/fmicb.2023.1209158

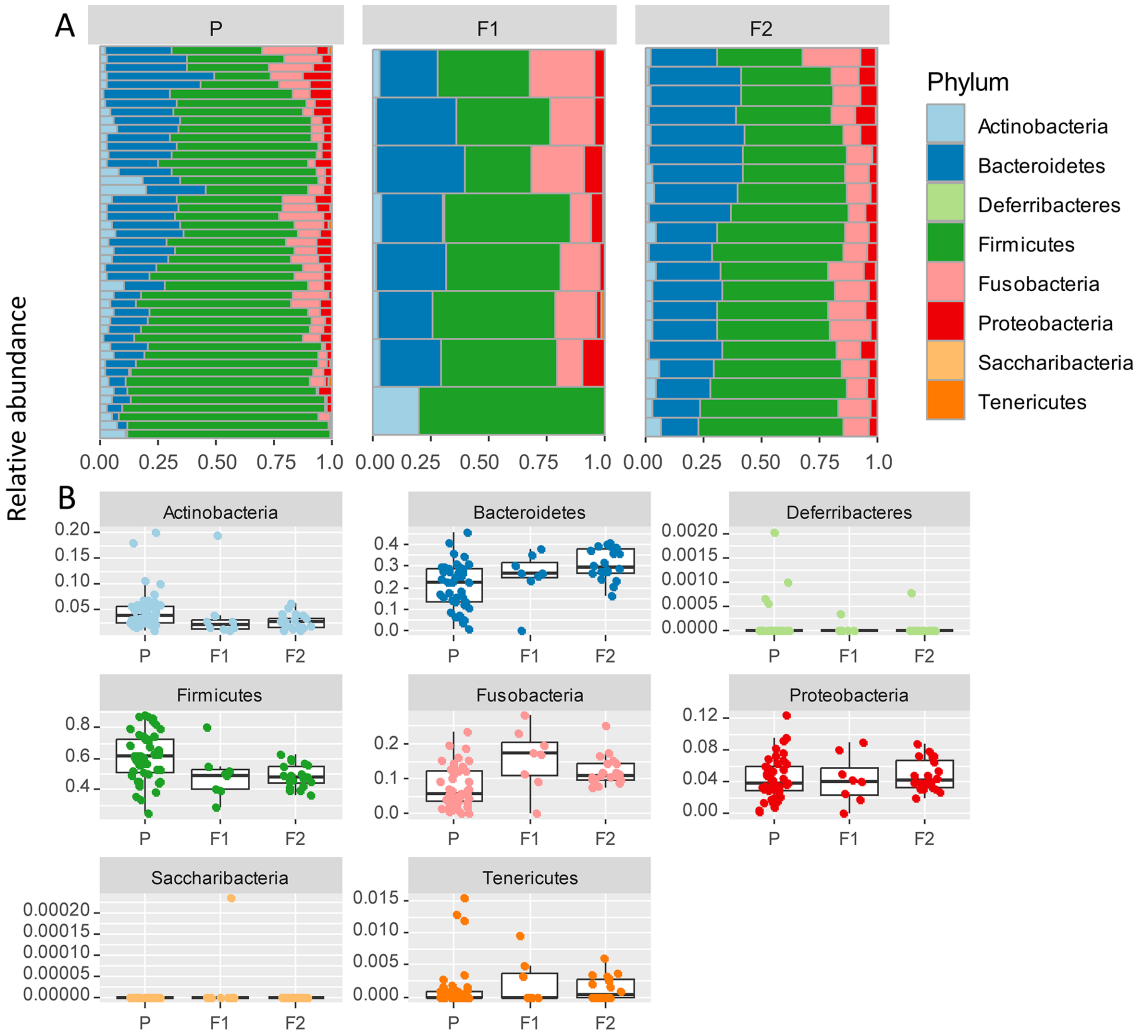


FIGURE 3
**(A)** Relative abundance of bacterial phyla identified in stool samples from 73 dog individuals, including 45 Lundehunds (P), eight first-generation crosses Lundehund × Buhund (F1) and 20 first-generation backcrosses F1×Lundehund (F2). **(B)** Box and whiskers plots of the relative abundance of bacterial phyla identified in stool samples from 73 dog individuals. Whiskers represent 1.5 times the interquartile range past the low and high quartiles. Points outside whiskers range are outliers.

bacteria at the phylum level. We expected that any taxa that are associated with the Lundehund genetic background should be highest in Lundehund, lowest in the F1 generation, and intermediate between Lundehunds and F1 in the F2 backcrosses. Phylum-level differences in relative abundances were evident based on purebred versus outcrossed status of the dogs (Figure 3A).

We plotted the relative abundance of each phylum for each generation of dogs (Figure 3B). The relative abundance at the phylum level was significantly different between the three generations ($X_{\text{several sample test}} = 53.65$, $p = 6 \times 10^{-6}$). Overall, the F1 and F2 progeny were more similar to each other in their microbiome composition than to the purebred dogs. Due to the low number of F1 dogs, we combined the F1s and F2s and compared the phylum-level microbiome abundances for these with the purebred Lundehunds. The abundances of Actinobacteria and Firmicutes were higher in purebred Lundehunds than in the F1 and F2 progeny (both $p = 0.007$). The relative abundance of Fusobacteria showed the opposite pattern, with a lower abundance in purebreds than in the F1 and an intermediate abundance in the F2 progeny ($p = 0.04$). The F1 and F2 dogs also had lower variance in composition at the phylum level (Figure 3B), consistent with the variation observed by principal component analysis (Figure 2A).

To further delineate bacterial taxa associated with the different dog genetic backgrounds, we performed the same analyses as in Figure 3 at the genus level on a subset including the genera present at >1% relative abundance across all samples, amounting to 15 highest abundance genera (Figure 4A). These analyses also revealed some differences between cohorts. To examine more in detail the genus-level variation in relative abundance in the purebred Lundehunds versus F1 and F2 progeny, we plotted the relative abundance of the 15 most abundant genera for each generation of dogs (Figure 4B). The relative abundances of genera were overall significantly different between the three cohorts ($X_{\text{several sample test}} = 110.39$, $p = 4 \times 10^{-11}$). We next made pairwise statistical tests comparing the relative abundance of each genus between purebred and outcrossed dogs (F1 and F2). We detected significant differences for 7 genera by doing pairwise tests, indicating these specific genera are associated with the

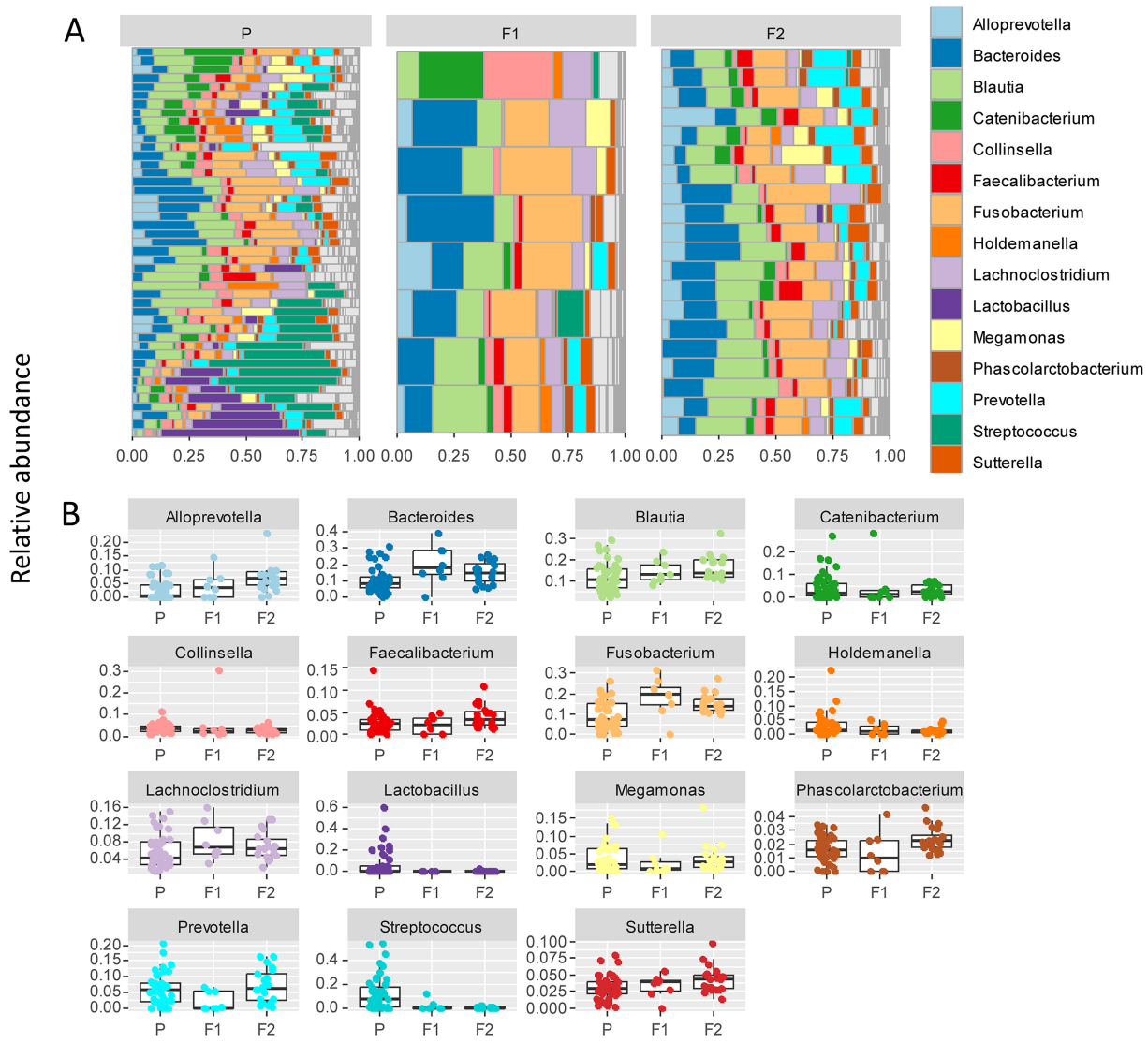


FIGURE 4
**(A)** Relative abundance of the 10 most abundant bacterial genera identified in stool samples from 73 dog individuals, including 45 Lundehunds (P), eight first-generation crosses Lundehund × Buhund (F1) and 20 first-generation backcrosses F1×Lundehund (F2). **(B)** Box and whiskers plots of the relative abundance of the 10 most abundant bacterial genera identified in stool samples from 73 dog individuals. Whiskers represent 1.5 times the interquartile range past the low and high quartiles. Points outside whiskers range are outliers.

genetic background of the dogs. *Streptococcus* ($p = 3 \times 10^{-7}$), *Lactobacillus* ($p = 0.0005$), and *Holdemanella* ($p = 0.01$) were at higher abundance in the purebred Lundehunds whereas *Alloprevotella* ($p = 0.003$), *Blautia* ($p = 0.005$), *Lachnoclostridium* ($p = 0.02$) and *Fusobacterium* ($p = 0.02$) were at higher abundance in the outcrossed dogs. Overall, we detected significant associations between specific bacterial taxa and the Lundehund genetic background, indicating a host genetic basis for the gut microbiome compositional differences.

Since changes in the ratio of Firmicutes to Bacteroidetes have been associated with microbiome dysbiosis in numerous studies of microbiome-associated diseases (e.g., Suchodolski et al., 2012; Minamoto et al., 2015; Vázquez-Baeza et al., 2016; Chun et al., 2020; You and Kim, 2021), we computed the Firmicutes to Bacteroidetes ratio for each dog and compared between the generations. We found that purebred Lundehunds have a higher Firmicutes to Bacteroidetes ratio than F1 and F2 progeny (Wilcoxon test, $W = 943$, $p = 0.0003$). We note that no Lundehund syndrome has been detected to date in any of the F1 or F2 progeny.

## 3.3. The Lundehund microbiome is not indicative of Lundehund syndrome

To examine whether Lundehund syndrome is also associated with microbiome composition, we plotted the relative abundance of each phylum as a function of Lundehund syndrome status (Figure 5) within the purebred Lundehunds. The relative abundance of phyla did not differ significantly between purebred Lundehund who had a diagnosis of Lundehund syndrome at some point in their life versus those who did not ($X_{\text{several sample test}} = 7.56$, $p = 0.48$).

To further examine whether there is a Lundehund syndrome microbiome composition, we calculated the Firmicutes to

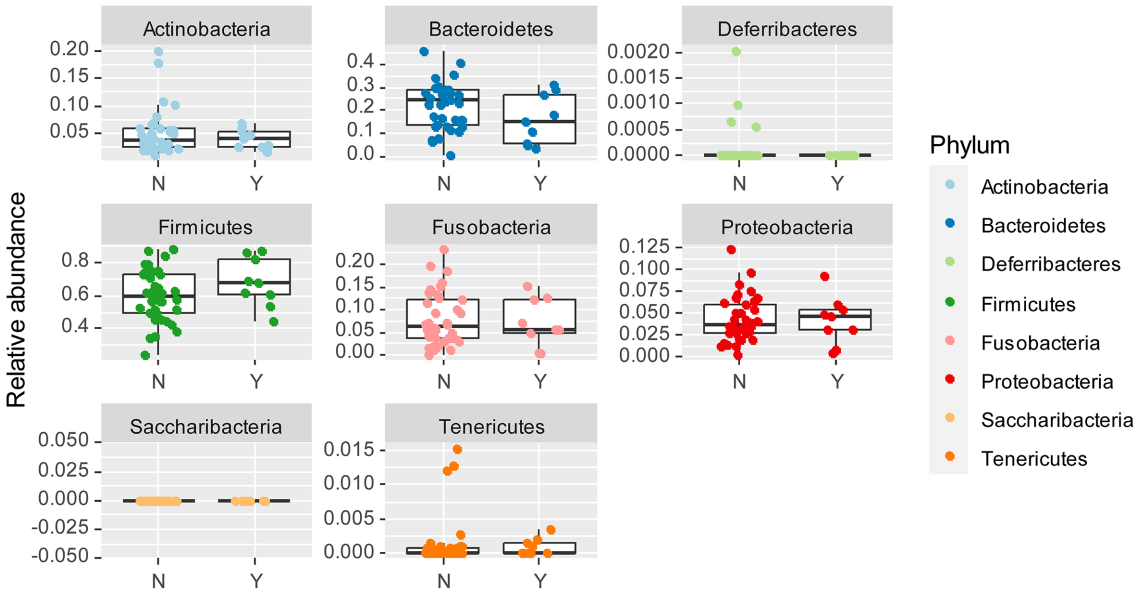


FIGURE 5
Box and whiskers plots of the relative abundance of bacterial phyla identified in stool samples from dogs which Y=had Lundehund syndrome (LS), and N=which did not have LS. Whiskers represent 1.5 times the interquartile range past the low and high quartiles. Points outside whiskers range are outliers. The data set includes 45 purebred Lundehunds (P).

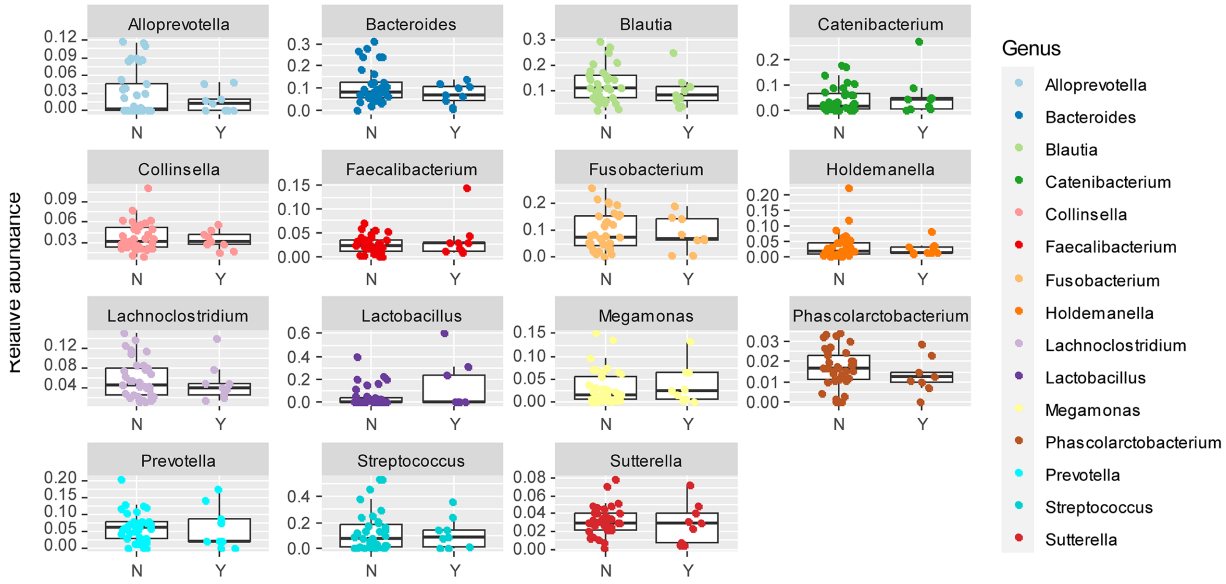


FIGURE 6
Box and whiskers plots of the relative abundance of the 15 most abundant bacterial genera identified in stool samples from Lundehunds which Y=had Lundehund syndrome (LS), and N=which did not have LS. Whiskers represent 1.5 times the interquartile range past the low and high quartiles. Points outside whiskers range are outliers. The data set includes 45 purebred Lundehunds.

Bacteroidetes ratio for purebred Lundehunds with and without a history of Lundehund syndrome. The median ratio of Firmicutes to Bacteroidetes was 4.41 ($n=9$) in dogs who had Lundehund syndrome versus 2.25 ($n=36$) in dogs who did not. While there is a trend of a higher ratio in dogs with a history of Lundehund syndrome, these medians were not significantly different between the two groups (Wilcoxon test, $W=215$, $p=0.1$).

To further delineate the microbiome associated with Lundehund syndrome, we plotted the relative abundance of the 15 most abundant genera as a function of Lundehund syndrome status (Figure 6). Purebred Lundehunds who had a diagnosis of Lundehund syndrome at some point in their life did not differ significantly in the relative abundance at genus level compared to healthy dogs ($X_{\text{several sample test}}=-10.11$, $p=1$). Overall, we found no compositional differences that were significantly associated with Lundehund syndrome within the purebred dogs, consistent with the genotype of the dogs driving the compositional differences we observed between generations.

10.3389/fmicb.2023.1209158

### 3.4. *Streptococcus equinus-Infantarius-lutetiensis* is more abundant in purebred Lundehund

In examining the variation in microbiome composition (Figure 2) and the phylum- and genus-level differences in abundances between purebred dogs and the F1 and F2 progeny (Figures 3, 4), we noticed that the F1 and F2 generations appeared similar to one another and had overall more consistent abundances of each bacterial phylum and genus, whereas purebred Lundehunds have much wider variation in microbiome composition.

To assess whether any specific taxa corresponded to the differences in the variation based on principal component analysis, we examined the major contributing taxa to principal component 1, which clearly differentiated the purebred dogs from the F1 and F2 generations (Figure 2). Based on the loadings (Table 2), we found that *S. equinus-infantarius-lutetiensis* was by far the most important species for principal component #1. We next examined the abundance of *S. equinus-infantarius-lutetiensis* in the individual samples and found that this bacterium is much more abundant in purebred Lundehunds and almost absent in F1 and F2 dogs (Figure 7), indicating that, in addition to the dysbiosis signature in the microbiome in the principal component analysis (Figure 2), and the Firmicutes/Bacteroidetes ratio, Lundehunds also have a characteristic species, *S. equinus-infantarius-lutetiensis*, which is associated with the dysbiosis. When examining the relative abundance of *S. equinus-infantarius-lutetiensis* within the pure bred Lundehunds, we did not find any pattern related to Lundehund syndrome (Appendix S3), indicating that the association is not a potential causative agent in accord with Koch's first postulate on infectious disease (Evans, 1978) which says that the microorganism must be found in the diseased animal, and not found in healthy animals. Rather, *S. equinus-infantarius-lutetiensis* is a species associated with dysbiosis in Lundehunds.

TABLE 2 Most important species dominating the first component of the PCA on microbiome composition of 73 dog individuals, including 45 Lundehund (P), eight first-generation crosses Lundehund × Buhund (F1) and 20 first-generation backcrosses F1×Lundehund (F2).

| Sequence | PCA1 | Species |
|---|---|---|
| 102 | 0.9304039 | *Streptococcus equinus-infantarius-lutetiensis* |
| 34 | −0.1612259 | *Bacteroides* sp12209 |
| 274 | −0.1372722 | *Fusobacterium mortiferum* |
| 278 | −0.1278976 | *Fusobacterium* sp37464 |
| 53 | −0.1040231 | *Alloprevotella* sp13496-sp13497 |
| 195 | −0.0764320 | *Clostridiales* sp. |
| 147 | −0.0737325 | *Lachnoclostridium* sp32341-sp32430 |
| 88 | 0.0693046 | *Lactobacillus reuteri-vaginalis* |
| 72 | 0.0663620 | *Lactobacillus* sp. |
| 124 | −0.0635586 | *Blautia hansenii-producta* |

## 4. Discussion

This study examined the microbiome of purebred Lundehund dogs compared with first and second-generation outcrossings with the Buhund. Consistent with previous studies on the dog fecal microbiome, the dominant phyla in all cohorts were Firmicutes, followed by Bacteroidetes and Fusobacteria (e.g., Swanson et al., 2011; You and Kim, 2021).

We sampled privately owned dogs that had a range of diet and probiotic regimes, therefore our dataset included several potentially confounding factors, such as diet, probiotics regime, different living conditions and age classes. Moreover, Lundehund syndrome is an acute life-threatening disease, which requires immediate treatment with anti-inflammatory drugs and antibiotics. For this reason, we could not collect samples from sick dogs before antibiotics administration and we thus compared the fecal microbiome of healthy dogs (which never had a diagnosis for Lundehund syndrome) with that of dogs which had recovered from the illness.

Despite these limitations, we detected a signature of purebred Lundehund status in the microbiome composition when comparing the different generations of dogs. Given the expectation that Lundehund genetic background-associated taxa should

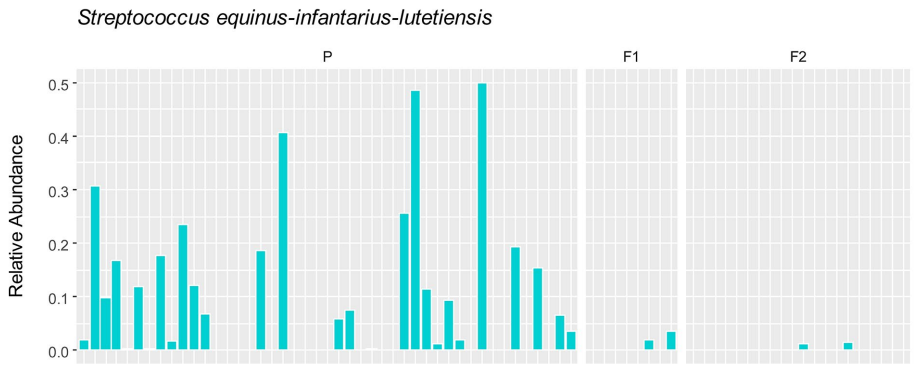


FIGURE 7
Relative abundance of *S. equinus-infantarius-lutetiensis* in gut microbiome of 73 dog individuals, including 45 Lundehunds (P), eight first-generation crosses Lundehund × Buhund (F1) and 20 first-generation backcrosses F1×Lundehund (F2).

be high in purebred dogs, low in F1s, and intermediate in F2, Firmicutes and Actinobacteria appear Lundehund-associated, whereas this was not the case for Fusobacteria and Bacteroidetes. Our results are consistent with several studies which showed that sequences belonging to the phylum Bacteroidetes decreased in dogs with acute diarrhea compared to healthy dogs (Chaban et al., 2012; Guard et al., 2015). Fusobacteria have also been found to be decreased in dogs with clinically active inflammatory bowel disease (IBD; Suchodolski et al., 2012) and are generally associated with a healthy microbiota (Vázquez-Baeza et al., 2016; Pilla and Suchodolski, 2020).

An increased or decreased F/B ratio is considered as a sign of imbalance in the intestine, or dysbiosis. An increased F/B ratio is often observed in humans with obesity (Abenavoli et al., 2019), although there are contradictory results (Chun et al., 2020; Magne et al., 2020; You and Kim, 2021), whereas a decreased F/B ratio is observed in the intestine of humans with IBD (Shen et al., 2018). We observed a significantly increased F/B ratio in purebred Lundehunds. However, contextualizing this result, we might not necessarily expect to be able to compare the relative abundances of functional bacterial groups in humans and dogs, since they have evolved under different pressures, such an omnivorous diet in humans versus a carnivorous diet in dogs (Vázquez-Baeza et al., 2016).

We could not observe any correlation between environmental factors and microbiome alpha diversity as calculated by the Shannon index, but the small size of the dataset and the coexistence of several factors, could make it difficult to disentangle their effects. Despite that, microbiome composition (beta diversity) clustered according to cohort, revealing a signature of the genome in the microbiome. When purebred Lundehunds were compared with F1 and F2 crosses, the variance in microbiomes was larger within the purebred Lundehunds than within F1 and F2 animals. Higher microbiome disparity was evident in purebred Lundehunds when examining the PC1 in the principal component analysis (Figure 2), suggesting the loss of a control mechanism over microbiome composition in Lundehunds.

Interestingly, we found that a single taxon, *S. equinus-infantarius-lutetiensis* was the most important species driving PC1 (explaining 33% of variation in the data). *S. equinus-infantarius-lutetiensis* was much more abundant in the purebred Lundehund, than in the F1 or F2. Several studies suggest an association between gut diseases in humans and bacteria belonging to the *S. bovis* group, which includes *S. equinus-infantarius-lutetiensis*. *S. equinus-infantarius-lutetiensis* was for instance isolated in stool samples of children with diarrhea of unknown origin, suggesting its pathogenic potential (Jin et al., 2013). This bacterium has also been linked to colorectal carcinogenesis in humans, since it could be found at higher rates in the stools of patients with colorectal tumors (Chirouze et al., 2013; Kaindi et al., 2018). In 2005, Vanhoutte et al. (2005) conducted a study on the stability of the gut microbiome after administration of prebiotics, and recommended investigation of *S. equinus-infantarius-lutetiensis* ecology and its role in the gut of healthy dogs, since it was the streptococcal group with the most pronounced population growth observed after administration of the prebiotic, fructan. *S. equinus-infantarius-lutetiensis* was also isolated in a cat with intestinal lymphoma (Piva et al., 2019) and in the equine hindgut, in conjunction with oligofructose-induced laminitis (Milinovich et al., 2008). All of these studies point towards *S. equinus-infantarius-lutetiensis* being a pathobiont, i.e., a commensal bacteria normally present in the gut of healthy humans and other animals, with the potential to either cause serious infections or activate the immune system, causing inflammatory diseases (Chow et al., 2011; Jans and Boleij, 2018). Thus, by being more permissive of this strain, the Lundehund genetic background may increase the risk of *S. equinus-infantarius-lutetiensis* causing pathology.

The fact that the principal component analysis performed on a subset of purebred Lundehunds did not show any difference in fecal microbiome composition between the healthy individuals and that with a history of Lundehund syndrome might indicate that all purebred Lundehunds are genetically predisposed to dysbiosis.

By comparing the microbiome of Lundehunds with that of first and second-generation outcrossings with Buhund, we concluded that Lundehunds have a highly varied microbiome and that Lundehund syndrome is characterized by a dysbiotic state, similar to what is observed in humans and dogs with IBD, which is consistent with the disease etiology. However, the F/B ratio was higher in Lundehunds which have had Lundehund syndrome, whereas a lower F/B ratio is observed in humans and dogs with Crohn's disease (an IBD type) (Minamoto et al., 2015), a difference that might be affected by many factors including both genetic and environmental differences between dogs and humans.

We propose that the loss of microbiome consistency in purebred Lundehunds is due to the loss of genetic loci that are needed for microbiome colonization stability. We further propose that these genetic loci were regained by outcrossing with Buhund in the F1 and F2 dogs, leading to a more stable gut microbiome. Further studies linking microbiome traits with genetic markers at individual level will help elucidate the mechanisms behind gut microbiome specificity in vertebrates.

## Data availability statement

The data presented in this study are available on Dryad, at the URL: https://datadryad.org/stash/dataset/doi:10.5061/dryad.tb2rbp05m.

## Ethics statement

Ethical review and approval were not required for this study because we only collected stool samples and this non-invasive procedure does not require evaluation by an ethics committee in Norway. The owners of the animals were provided with written information about the study and agreed to participate to it by sending stool samples of their dogs.

## Author contributions

CM and WL contributed to conception and design of the study and wrote the first draft of the manuscript. CM and P-AW did the

data collection. CM and AB performed the statistical analyses. All authors contributed to manuscript revision and approved the submitted version.

## Funding

This study was supported by Queen Maud University College, the Norwegian Agriculture Agency (grant Agros 1135359), the Peder Sather Center for Advanced Study, and the Norwegian Lundehund Club. WL was supported by NIH DP5OD017851, NSF IOS 2144342, and the Carnegie Institution for Science endowment.

## Acknowledgments

The authors would like to thank all the owners who participated in the study by providing dog stool samples, members from the Norwegian Lundehund Club who helped with data collection, H. Gautun and I. S. Espelien for reading the draft.

## Conflict of interest

The authors declare that the research was conducted in the absence of any commercial or financial relationships that could be construed as a potential conflict of interest.

## Publisher's note



## Supplementary material

The Supplementary material for this article can be found online at: https://www.frontiersin.org/articles/10.3389/fmicb.2023.1209158/full#supplementary-material

## References

Abenavoli, L., Scarpellini, E., Colica, C., Boccuto, L., Salehi, B., Sharifi-Rad, J., et al. (2019). Gut microbiota and obesity: a role for probiotics. *Nutrients* 11. doi: 10.3390/nu11112690

Barnett, D. J. M., Arts, I. C. W., and Penders, J. (2021). microViz: an R package for microbiome data visualization and statistics. *J. Open Sour. Softw.* 6. doi: 10.21105/joss.03201

Berghoff, N., Ruaux, C. G., Steiner, J. M., and Williams, D. A. (2007). Gastroenteropathy in Norwegian Lundehunds. *Compendium (Yardley, PA)* 29, 468–470. doi: 10.1016/S0925-8574(07)00041-9

Blekhman, R., Goodrich, J. K., Huang, K., Sun, Q., Bukowski, R., Bell, J. T., et al. (2015). Host genetic variation impacts microbiome composition across human body sites. *Genome Biol.* 16:191. doi: 10.1186/s13059-015-0759-1

Bubier, J. A., Chesler, E. J., and Weinstock, G. M. (2021). Host genetic control of gut microbiome composition. *Mamm. Genome* 32, 263–281. doi: 10.1007/s00335-021-09884-2

Callahan, B. J., Rosen, M. J., Han, A. W., Johnson, A. J., Holmes, S. P., and McMurdie, P. J. (2016). DADA2: high resolution sample inference from Illumina amplicon data. *Nat. Methods* 13, 581–583. doi: 10.1038/nmeth.3869

Caporaso, J. G., Kuczynski, J., Stombaugh, J., Bittinger, K., Bushman, F. D., Costello, E. K., et al. (2010). QIIME allows analysis of high-throughput community sequencing data. *Nat. Methods* 7, 335–336. doi: 10.1038/nmeth.f.303

Chaban, B., Links, M. G., and Hill, J. E. (2012). A molecular enrichment strategy based on cpn60 for detection of epsilon-Proteobacteria in the dog fecal microbiome. *Microb. Ecol.* 63, 348–357. doi: 10.1007/s00248-011-9931-7

Chirouze, C., Patry, I., Duval, X., Baty, V., Tattevin, P., Aparicio, T., et al. (2013). *Streptococcus bovis/Streptococcus equinus* complex fecal carriage, colorectal carcinoma, and infective endocarditis: a new appraisal of a complex connection. *Eur. J. Clin. Microbiol. Infect. Dis.* 32, 1171–1176. doi: 10.1007/s10096-013-1863-3

Chow, J., Tang, H., and Mazmanian, S. K. (2011). Pathobionts of the gastrointestinal microbiota and inflammatory disease. *Curr. Opin. Immunol.* 23, 473–480. doi: 10.1016/j.coi.2011.07.010

Chun, J. L., Ji, S. Y., Lee, S. D., Lee, Y. K., Kim, B., and Kim, K. H. (2020). Difference of gut microbiota composition based on the body condition scores in dogs. *J. Anim. Sci. Technol.* 62, 239–246. doi: 10.5187/jast.2020.62.2.239

Clemente, J. C., Pehrsson, E. C., Blaser, M. J., Sandhu, K., Gao, Z., Wang, B., et al. (2015). The microbiome of uncontacted Amerindians. *Advances* 1. doi: 10.1126/sciadv.1500183

De Filippo, C., Cavalieri, D., Di Paola, M., Ramazzotti, M., Poullet, J. B., et al. (2010). Impact of diet in shaping gut microbiota revealed by a comparative study in children from Europe and rural Africa. *Proc. Natl. Acad. Sci. U. S. A.* 107, 14691–14696. doi: 10.1073/pnas.1005963107

DeGruttola, A. K., Low, D., Mizoguchi, A., and Mizoguchi, E. (2016). Current understanding of dysbiosis in disease in human and animal models. *Inflamm. Bowel Dis.* 22, 1137–1150. doi: 10.1097/mib.0000000000000750

Deng, P., and Swanson, K. S. (2015). Gut microbiota of humans, dogs and cats: current knowledge and future opportunities and challenges. *Br. J. Nutr.* 113, S6–S17. doi: 10.1017/s0007114514002943

Dowling, D. J., and Levi, O. (2014). Ontogeny of early life immunity. *Trends Immunol.* 35, 299–310. doi: 10.1016/j.it.2014.04.007

Evans, A. S. (1978). Causation and disease: a chronological journey: the Thomas Parran lecture. *Am. J. Epidemiol.* 108, 249–258. doi: 10.1093/oxfordjournals.aje.a112617

Guard, B. C., Barr, J. W., Reddivari, L., Klemashevich, C., Jayaraman, A., Steiner, J. M., et al. (2015). Characterization of microbial dysbiosis and metabolomic changes in dogs with acute diarrhea. *PLoS One* 10:e0127259. doi: 10.1371/journal.pone.0127259

Hooda, S., Minamoto, Y., Suchodolski, J. S., and Swanson, K. S. (2012). Current state of knowledge: the canine gastrointestinal microbiome. *Anim. Health Res. Rev.* 13, 78–88. doi: 10.1017/S1466252312000059

Hughes, D. A., Bacigalupe, R., Wang, J., Rühlemann, M. C., Tito, R. Y., Falony, G., et al. (2020). Genome-wide associations of human gut microbiome variation and implications for causal inference analyses. *Nat. Microbiol.* 5:1079. doi: 10.1038/s41564-020-0743-8

Jans, C., and Boleij, A. (2018). The road to infection: host-microbe interactions defining the pathogenicity of *Streptococcus bovis/Streptococcus equinus* complex members. *Front. Microbiol.* 9:e00603. doi: 10.3389/fmicb.2018.00603

Jin, D., Chen, C., Li, L. Q., Lu, S., Li, Z. J., Zhou, Z. M., et al. (2013). Dynamics of fecal microbial communities in children with diarrhea of unknown etiology and genomic analysis of associated *Streptococcus lutetiensis*. *BMC Microbiol.* 13. doi: 10.1186/1471-2180-13-141

Kaindi, D. W. M., Kogi-Makau, W., Lule, G. N., Kreikemeyer, B., Renault, P., Bonfoh, B., et al. (2018). Colorectal cancer-associated *Streptococcus infantarius* subsp. infantarius differ from a major dairy lineage providing evidence for pathogenic, pathobiont and food-grade lineages. *Sci. Rep.* 8:9181. doi: 10.1038/s41598-018-27383-4

Kolbjornsen, O., Press, C. M., and Landsverk, T. (1994a). Gastropathies in the Lundehund. 2 A study of mucin profiles. *APMIS* 102, 801–809. doi: 10.1111/j.1699-0463.1994.tb05238.x

Kolbjornsen, O., Press, C. M., and Landsverk, T. (1994b). Gastropathies in the Lundehund. 1 Gastritis and gastric neoplasia associated with intestinal Lymphangiectasia. *APMIS* 102, 647–661. doi: 10.1111/j.1699-0463.1994.tb05216.x

Kropatsch, R., Melis, C., Stronen, A. V., Jensen, H., and Eppelen, J. T. (2015). Molecular genetics of sex identification, breed ancestry and polydactyly in the Norwegian Lundehund breed. *J. Hered.* 106, 403–406. doi: 10.1093/jhered/esv031

La Rosa, P. S., Brooks, J. P., Deych, E., Boone, E. L., Edwards, D. J., Wang, Q., et al. (2012). Hypothesis testing and power calculations for taxonomic-based human microbiome data. *PLoS One* 7:e52078. doi: 10.1371/journal.pone.0052078

Lahti, L., and Shetty, S. 2017. (Bioconductor, 2017–2020). Tools for microbiome analysis in R. Microbiome package version 1.20.0. Available at: https://microbiome.github.io/tutorials/

Magne, F., Gotteland, M., Gauthier, L., Zazueta, A., Pesoa, S., Navarrete, P., et al. (2020). The Firmicutes/Bacteroidetes ratio: a relevant marker of gut dysbiosis in obese patients? *Nutrients* 12. doi: 10.3390/nu12051474

Mallick, H., Rahnavard, A., McIver, L. J., Ma, S., Zhang, Y., Nguyen, L. H., et al. (2021). Multivariable association discovery in population-scale meta-omics studies. *PLoS Comput. Biol.* 17:e1009442. doi: 10.1371/journal.pcbi.1009442

McMurdie, P. J., and Holmes, S. (2013). Phyloseq: an R package for reproducible interactive analysis and graphics of microbiome census data. *PLoS One* 8:e61217. doi: 10.1371/journal.pone.0061217

Melis, C., Borg, Å. A., Espelien, I. S., and Jensen, H. (2013). Low neutral genetic variability in a specialist puffin hunter: the norwegian lundehund. *Anim. Genet.* 44, 348–351. doi: 10.1111/age.12000

Melis, C., Pertoldi, C., Ludington, W. B., Beuchat, C., Qvigstad, G., and Stronen, A. V. (2022). Genetic rescue of the highly inbred norwegian lundehund. *Genes-Basel* 13. doi: 10.3390/genes13010163

Metzger, J., Pfahler, S., and Distl, O. (2016). Variant detection and runs of homozygosity in next generation sequencing data elucidate the genetic background of Lundehund syndrome. *BMC Genomics* 17:535. doi: 10.1186/s12864-016-2844-6

Milinovich, G. J., Burrell, P. C., Pollitt, C. C., Klieve, A. V., Blackall, L. L., Ouwerkerk, D., et al. (2008). Microbial ecology of the equine hindgut during oligofructose-induced laminitis. *ISME J.* 2, 1089–1100. doi: 10.1038/ismej.2008.67

Minamoto, Y., Otoni, C. C., Steelman, S. M., Büyükleblebici, O., Steiner, J. M., Jergens, A. E., et al. (2015). Alteration of the fecal microbiota and serum metabolite profiles in dogs with idiopathic inflammatory bowel disease. *Gut Microbes* 6, 33–47. doi: 10.1080/19490976.2014.997612

Norwegian Lundehund Club. *Rasespesifikk avlsstrategi (RAS) for Norsk Lundehund [breed specific breeding strategy for Norwegian Lundehund, in Norwegian]*. Oslo: Norwegian Lundehund Club. (2014). p 28.

Pilla, R., and Suchodolski, J. S. (2020). The role of the canine gut microbiome and metabolome in health and gastrointestinal disease. *Front. Vet. Sci.* 6:e00498. doi: 10.3389/fvets.2019.00498

Piva, S., Pietra, M., Serraino, A., Merialdi, G., Magarotto, J., and Giacometti, F. (2019). First description of *Streptococcus lutetiensis* from a diseased cat. *Lett. Appl. Microbiol.* 69, 96–99. doi: 10.1111/lam.13168

Price, S. A., Hopkins, S. S. B., Smith, K. K., and Roth, V. L. (2012). Tempo of trophic evolution and its impact on mammalian diversification. *Proc. Natl. Acad. Sci.* 109, 7008–7012. doi: 10.1073/pnas.1117133109

Qvigstad, G., Kolbjornsen, O., Skancke, E., and Waldum, H. L. (2008). Gastric neuroendocrine carcinoma associated with atrophic gastritis in the Norwegian Lundehund. *J. Comp. Pathol.* 139, 194–201. doi: 10.1016/j.jcpa.2008.07.001

R Core team*R: A language and environment for statistical computing*, Vienna, Austria: R Core team (2021).

RStudio Team *RStudio Integrated development environment for R PBC*, Boston, MA: RStudio Team (2022).

Shen, Z. H., Zhu, C. X., Quan, Y. S., Yang, Z. Y., Wu, S., Luo, W. W., et al. (2018). Relationship between intestinal microbiota and ulcerative colitis: mechanisms and clinical application of probiotics and fecal microbiota transplantation. *World J. Gastroentero.* 24, 5–14. doi: 10.3748/wjg.v24.i1.5

Suchodolski, J. S., Markel, M. E., Garcia-Mazcorro, J. F., Unterer, S., Heilmann, R. M., et al. (2012). The fecal microbiome in dogs with acute diarrhea and idiopathic inflammatory bowel disease. *PLoS One* 7:e51907. doi: 10.1371/journal.pone.0051907

Swanson, K. S., Dowd, S. E., Suchodolski, J. S., Middelbos, I. S., Vester, B. M., Barry, K. A., et al. (2011). Phylogenetic and gene-centric metagenomics of the canine intestinal microbiome reveals similarities with humans and mice. *ISME J.* 5, 639–649. doi: 10.1038/ismej.2010.162

Torrazza, R. M., and Neu, J. (2011). The developing intestinal microbiome and its relationship to health and disease in the neonate. *J. Perinatol.* 31, S29–S34. doi: 10.1038/jp.2010.172

Tun, H. M., Konya, T., Takaro, T. K., Brook, J. R., Chari, R., Field, C. J., et al. (2017). Exposure to household furry pets influences the gut microbiota of infant at 3-4 months following various birth scenarios. *Microbiome* 5:40. doi: 10.1186/s40168-017-0254-x

Vanhoutte, T., Huys, G., de Brandt, E., Fahey, G. C., and Swings, J. (2005). Molecular monitoring and characterization of the faecal microbiota of healthy dogs during fructan supplementation. *FEMS Microbiol. Lett.* 249, 65–71. doi: 10.1016/j.femsle.2005.06.003

Vázquez-Baeza, Y., Hyde, E. R., Suchodolski, J. S., and Knight, R. (2016). Dog and human inflammatory bowel disease rely on overlapping yet distinct dysbiosis networks. *Nat. Microbiol.* 1:16177. doi: 10.1038/nmicrobiol.2016.177

Weissbrod, O., Rothschild, D., Barkan, E., and Segal, E. (2018). Host genetics and microbiome associations through the lens of genome wide association studies. *Curr. Opin. Microbiol.* 44, 9–19. doi: 10.1016/j.mib.2018.05.003

Wickham, H. (2011). The Split-apply-combine strategy for data analysis. *J. Stat. Softw.* 40, 1–29. doi: 10.18637/jss.v040.i01

Wilks, S. S. (1938). The large-sample distribution of the likelihood ratio for testing composite hypotheses. *Ann. Math. Stat.* 9, 60–62. doi: 10.1214/aoms/1177732360

You, I., and Kim, M. J. (2021). Comparison of gut microbiota of 96 healthy dogs by individual traits: breed, age, and body condition score. *Animals (Basel)* 11. doi: 10.3390/ani11082432

frontiers | Frontiers in Microbiology

TYPE Original Research
PUBLISHED 22 June 2023
DOI 10.3389/fmicb.2023.1193919



OPEN ACCESS

EDITED BY
Rebeca Martín,
INRAE Centre Jouy-en-Josas, France

REVIEWED BY
Yike Shen,
Columbia University, United States
Feng Gao,
Columbia University, United States

*CORRESPONDENCE
Shoshannah Eggers
✉ shoshannah-eggers@uiowa.edu

†These authors have contributed equally to this work

RECEIVED 26 March 2023
ACCEPTED 23 May 2023
PUBLISHED 22 June 2023

CITATION
Eggers S, Midya V, Bixby M, Gennings C, Torres-Olascoaga LA, Walker RW, Wright RO, Arora M and Téllez-Rojo MM (2023) Prenatal lead exposure is negatively associated with the gut microbiome in childhood.
*Front. Microbiol.* 14:1193919.
doi: 10.3389/fmicb.2023.1193919



# Prenatal lead exposure is negatively associated with the gut microbiome in childhood

Shoshannah Eggers[1,2]*, Vishal Midya[1], Moira Bixby[1], Chris Gennings[1], Libni A. Torres-Olascoaga[3], Ryan W. Walker[1], Robert O. Wright[1†], Manish Arora[1†] and Martha María Téllez-Rojo[3†]

[1]Department of Environmental Medicine and Public Health, Icahn School of Medicine at Mount Sinai, New York, NY, United States, [2]Department of Epidemiology, University of Iowa College of Public Health, Iowa City, IA, United States, [3]Center for Research on Nutrition and Health, National Institute of Public Health, Cuernavaca, Mexico

**Background:** Metal exposures are associated with gut microbiome (GM) composition and function, and exposures early in development may be particularly important. Considering the role of the GM in association with many adverse health outcomes, understanding the relationship between prenatal metal exposures and the GM is critically important. However, there is sparse knowledge of the association between prenatal metal exposure and GM later in childhood.

**Objectives:** This analysis aims to identify associations between prenatal lead (Pb) exposure and GM composition and function in children 9–11 years old.

**Methods:** Data come from the Programming Research in Obesity, Growth, Environment and Social Stressors (PROGRESS) cohort based in Mexico City, Mexico. Prenatal metal concentrations were measured in maternal whole blood drawn during the second and third trimesters of pregnancy. Stool samples collected at 9–11 years old underwent metagenomic sequencing to assess the GM. This analysis uses multiple statistical modeling approaches, including linear regression, permutational analysis of variance, weighted quantile sum regression (WQS), and individual taxa regressions, to estimate the association between maternal blood Pb during pregnancy and multiple aspects of the child GM at 9–11 years old, adjusting for relevant confounders.

**Results:** Of the 123 child participants in this pilot data analysis, 74 were male and 49 were female. Mean prenatal maternal blood Pb was 33.6 (SE=2.1) ug/L and 34.9 (SE=2.1) ug/L at second and third trimesters, respectively. Analysis suggests a consistent negative relationship between prenatal maternal blood Pb and the GM at age 9–11, including measures of alpha and beta diversity, microbiome mixture analysis, and individual taxa. The WQS analysis showed a negative association between prenatal Pb exposure and the gut microbiome, for both second and third trimester exposures (2Tβ=−0.17, 95%CI=[−0.46,0.11]; 3Tβ=−0.17, 95%CI=[−0.44,0.10]). *Ruminococcus gnavus*, *Bifidobacterium longum*, *Alistipes indistinctus*, *Bacteroides caccae*, and *Bifidobacterium bifidum* all had weights above the importance threshold from 80% or more of the WQS repeated holdouts in association with both second and third trimester Pb exposure.

**Discussion:** Pilot data analysis suggests a negative association between prenatal Pb exposure and the gut microbiome later in childhood; however, additional investigation is needed.

KEYWORDS

**human microbiome, weighted quantile sum regression, metal exposure, environmental epidemiology, maternal child health**

# 1. Introduction

Lead (Pb) has been a recognized environmental hazard for centuries (Woolley, 1984), however its etiological pathways to disease are still not entirely understood. One potential mechanistic pathway between Pb exposure and its many downstream adverse health outcomes may be via the human gut microbiome. The collection of trillions of microbes that inhabit the human gut, including bacteria, fungi, viruses, and archaea, as well as their many genetic functions, are known as the gut microbiome (Human Microbiome Project Consortium, 2012). The normal functions of the gut microbiome include nutrient metabolism, support of the mucosal and epithelial barriers within the gut, and interactions with immune, nervous, and cardiovascular systems (Gomaa, 2020; Wilmes et al., 2022). Xenobiotic exposures, including Pb, influence the composition and function of the gut microbiome, affecting its interaction with systemic bodily function, and may lead to altered health status (Claus et al., 2016).

Animal studies have linked Pb exposure to alterations of the gut microbiome including shifts in individual sample diversity (α-diversity), community composition (β-diversity), and individual bacterial taxa and gene abundance (Breton et al., 2013; Wu et al., 2016; Gao et al., 2017; Xia et al., 2018). Moreover, the body of epidemiologic evidence linking Pb exposure to altered gut microbiome composition and function is growing rapidly. Studies have linked human Pb exposure to increased abundance of many specific bacteria, including Proteobacteria (Bisanz et al., 2014; Eggers et al., 2019), a common indicator of gut microbiome dysbiosis, or imbalance (Shin et al., 2015; Litvak et al., 2017). Other analyses have linked Pb exposure to bacteria that are known to affect gut barrier integrity and gut health (Laue et al., 2020; Sitarik et al., 2020; Shen et al., 2022). Alterations in gut and blood–brain barrier integrity resulting from metal-associated shifts in the gut microbiome may allow for increased metal toxicity by allowing for greater absorption into the bloodstream. While this growing field of epidemiologic research has uncovered relationships between Pb exposure and the gut microbiome, so far the analyses have been limited to the use of 16S rRNA amplicon sequencing data, which is less accurate in assigning taxonomy and inferring gene function than metagenomic sequencing. More studies with advanced omics analysis are needed to understand the relationship between Pb exposure and the gut microbiome.

Little is known about the relationship between prenatal exposures and the gut microbiome later in childhood. In fact, there are relatively few studies that investigate the gut microbiome in general between the ages of 5 and 20, especially from populations in low to middle-income countries (Ortega, 2022). Using data and specimens from the Programming Research in Obesity, Growth, Environment and Social Stressors (PROGRESS) cohort, we examine relationships between prenatal Pb exposure and the gut microbiome of 9–11 year old children from Mexico City, Mexico. In this study, we aim to identify critical windows of prenatal Pb exposure that are associated with the gut microbiome later in childhood. Given the existing evidence from epidemiological and animal studies, we hypothesize that elevated prenatal Pb exposure during at least one time point will be associated with altered gut microbiome composition at 9–11 years old.

# 2. Methods

## 2.1. Study design

PROGRESS is an ongoing prospective birth cohort in Mexico City, Mexico. The study enrolled 948 women in early pregnancy who went on to a live birth through the Mexican Social Security System, followed the offspring in infancy every 6 months, and biannually thereafter. The focus of PROGRESS is on neurobehavioral development and child obesity, with emphasis on environmental exposures, like metals, in pregnancy and early life that program later life behavior and growth. Exposures and outcomes were assessed at several time points beginning in the 2nd trimester of pregnancy through a combination of surveys, physical exams, and psychological and behavioral assessments. At each visit, biological specimens (including blood) were collected, processed, aliquoted and stored. Stool samples were collected from a subset of participants ($n = 123$) when the children were between the ages of 9–11. Protocols for the main PROGRESS study, and its ancillary microbiome study were reviewed and approved by the Institutional Review Board at the Icahn School of Medicine at Mount Sinai (STUDY-12-00751A, STUDY-21-00242).

## 2.2. Pb exposure measurement

Prenatal Pb exposure in the PROGRESS cohort has been previously described (Heiss et al., 2020). Briefly, Pb exposure was assessed using maternal whole blood, drawn during the second and third trimesters of pregnancy, at an average of 18.3 and 31.6 weeks gestation, respectively. Pb level was measured using inductively coupled plasma mass spectrometry (ICP-MS) in the trace metals laboratory at the Icahn School of Medicine at Mount Sinai.

## 2.3. Gut microbiome sample collection and processing

Participants were recruited at the PROGRESS clinic visit as part of the 9–11 year visit. Samples were collected in clinic or at home using a sampling kit provided. Once obtained, stool samples were stored in a biosafety bag in the participant's home refrigerator at 4°C. The sample was retrieved by a driver within 24 h, processed following the FAST protocol (Romano et al., 2018), and stored at −70°C within 48 h from sample deposit. Frozen samples were sent to the Microbiome Translational Center at Mount Sinai. Samples were then processed and sequenced in two batches, with $n = 50$ and $n = 73$ samples, respectively. Shotgun metagenomic sequencing was performed using the NEBNext DNA Library Prep kit and sequenced on an Illumina HiSeq. Sequencing reads were quality trimmed with Trimmomatic (Bolger et al., 2014) and human reads removed by mapping to a reference with bowtie2 (Langmead and Salzberg, 2012). The remaining reads were processed using MetaPhlAn2 (Truong et al., 2015) and StrainPhlAn (Truong et al., 2017) to determine microbial taxonomy down to the species/strain level, and HUMAnN2 (Franzosa et al., 2018) to profile microbial gene pathways.

## 2.4. Covariates

Covariates used in this analysis included child sex, child's age at time of stool sample collection, mother's socio-economic status (SES) during pregnancy, mother's age at birth, mother's body mass index (BMI) during pregnancy, and microbiome analysis batch. Mother's height and weight were collected with a professional digital scale and stadiometer at the study visit during the second trimester of pregnancy. Weight and height were used to calculate BMI, which was modeled as a continuous covariate in regression analyses. SES during pregnancy was assessed based on the 1994 Mexican Association of Intelligence Agencies Market and Opinion (AMAI) rule 13*6. Families are classified in six levels based on 13 questions about characteristics of the household (Supplementary Table S1). Most families in the study were low to middle SES, thus the six categories were condensed into three: lower, middle, and higher (Sanders et al., 2022).

Additional covariates were considered for inclusion, such as dietary factors and Pb exposure after birth. While children's dietary patterns are likely to be strongly linked to their gut microbiome composition and function, they are not associated with prenatal Pb exposure, thus they are not confounders of the potential association investigated. Child blood Pb has been measured at several timepoints during childhood. These measurements were not included in the analysis because: (1) in descriptive statistics performed during data processing, the blood Pb concentrations from multiple timepoints before and after birth were not correlated and (2) adjusting for Pb concentration at the intermediate timepoints would give only the direct estimate of association between prenatal Pb concentration and the child gut microbiome, rather than the total estimate of association, which is what we aimed to estimate.

## 2.5. Statistical analysis

All analysis was conducted in R version 4.0.3. Any two tailed value of $p$ less than 0.05 was considered statistically significant, after correction for multiple comparisons if applicable.

### 2.5.1. Data processing

The count data for each Taxa were converted into relative abundance. To consider any possible batch effect while measuring taxa count, (1) only those taxa with at least 5% relative abundance in both batches were further considered in primary statistical analyses. (2) All models were controlled for a batch indicator variable along with other covariates. (3) Further detailed sensitivity analysis was conducted by choosing taxa with at least 25% relative abundance in both batches. The second and third-trimester Pb concentrations were log (base = 2) transformed to meet distributional assumptions with higher confidence.

### 2.5.2. Alpha and beta diversity

We calculated Shannon alpha diversity and Bray–Curtis beta diversity (Shannon, 1948; Bray and Curtis, 1957). To estimate the associations with second and third-trimester lead concentrations, (1) for alpha diversity, we used the Kruskal–Wallis rank sum test (without covariate adjustment) and linear regression (with covariate adjustment), and (2) for beta diversity, we used PERMANOVA with 10,000 permutations and with covariate adjustments (Oksanen et al., 2019).

### 2.5.3. Weighted quantile sum regression

We used the Weighted Quantile Sum ($WQS_{RSRH}$) regression (Carrico et al., 2015) with random subset (Curtin et al., 2019) and repeated holdouts (Tanner et al., 2019), as established for microbiome data (Eggers et al., 2023), to estimate the association between second and third-trimester lead exposures and the effect on the abundance of the overall mixture of microbial taxa. Since the interest lies in the level of the association, and is not a causal analysis, the $WQS_{RSRH}$ model was fitted with all the chosen taxa as exposures and the log transformed Pb concentration as the outcome. This modeling approach is the reverse of how WQS is typically used with chemical concentrations as the exposure, however because this is an association analysis this modeling approach is reasonable. Previously published studies of the human microbiome using WQS have also been conducted using this reverse-modeling approach (Bixby et al., 2022; Eggers et al., 2023). For ease of interpretation, the relative abundance of the taxa was converted into deciles, while a null relative abundance was kept at zero. Moreover, two $WQS_{RSRH}$ models were fitted at each trimester, with the overall mixture effect assumed in the negative or positive directions. The final optimal model (Liao et al., 2018) from each trimester was chosen based on the smallest Akaike information criterion (AIC) (Akaike, 1974) and the Bayesian information criterion (BIC) (Schwarz, 1978). Those microbial taxa were judged important in the final chosen models, which had weight contributions to the overall mixture index above a chance threshold (1/the number of components in the index). Lastly, to account for any between taxa correlations and the relatively smaller sample size, each $WQS_{RSRH}$ model was fitted based on 200 repeated holdouts (with randomly 40% data set aside for validation) and 100 bootstrapped with-replacement sampling at each iteration.

### 2.5.4. Taxa-wide association analysis

To estimate the effect of Pb exposure on individual relative abundance of each chosen taxa, we conducted Taxa-wide association analysis (TWAS) with generalized linear models at both trimesters. Further, the unadjusted raw value of $p$s with respect to regression beta estimates were plotted through Volcano plots. The Bonferroni procedure was adapted for multiple comparison error correction on raw $p$-values. We estimated the effective number of tests for the TWAS using the eigenvalues of the relative abundance of the correlation matrix (Li and Ji, 2005; de Prado-Bert et al., 2021).

### 2.5.5. Gene function analysis

We extracted the microbial gene function pathways of the important taxa from the $WQS_{RSRH}$ analysis at each trimester. We selected the top 20 most frequently occurring pathways in each trimester for ease of interpretation. Through a simple Venn diagram, we further elaborated on the pathways which are common to (a) both trimesters, (b) only present in the second trimester, and lastly, (c) only present in the third trimester.

### 2.5.6. Sensitivity analysis

We also conducted a sensitivity analysis to understand whether the choice of relative abundance in both batches affected the overall mixture effect. To that end, we repeated the entire $WQS_{RSRH}$ analysis with only those taxa having at least 25% relative abundance in both batches.

TABLE 1 Characteristics of the analytical study population by quartile of Pb exposure in the second and third trimester of pregnancy.

| *Exposure* | Total | Quartile 1 | Quartile 2 | Quartile 3 | Quartile 4 |
|---|---|---|---|---|---|
| | *N* =123 | Mean (SE) *n* (%) | Mean (SE) *n* (%) | Mean (SE) *n* (%) | Mean (SE) *n* (%) |
| **Second Trimester Pb (ug/L)** | 33.6 (2.1) | 13.9 (0.5) | 22.2 (0.4) | 32.9 (0.9) | 65.5 (4.3) |
| Child sex | | | | | |
| Male | 74 (60.2) | 10 (58.8) | 19 (59.4) | 19 (65.5) | 26 (57.8) |
| Female | 49 (39.8) | 7 (41.2) | 13 (40.6) | 10 (34.5) | 19 (42.2) |
| Maternal SES | | | | | |
| Lower | 66 (53.6) | 7 (41.2) | 16 (50.0) | 16 (55.2) | 27 (60.0) |
| Medium | 45 (36.6) | 8 (47.0) | 12 (37.5) | 11 (37.9) | 14 (31.1) |
| Higher | 12 (9.8) | 2 (11.8) | 4 (12.5) | 2 (6.9) | 4 (8.9) |
| Maternal age at pregnancy (years) | 28.5 (0.5) | 28.9 (0.5) | 27.2 (0.5) | 29.8 (0.6) | 28.3 (0.5) |
| Maternal BMI during pregnancy (kg/m$^2$) | 27.2 (0.4) | 26.6 (0.4) | 27.8 (0.4) | 27.1 (0.3) | 27.0 (0.5) |
| Child age at gut microbial sample collection (years) | 9.7 (0.7) | 9.7 (0.1) | 9.5 (0.1) | 9.6 (0.1) | 9.8 (0.1) |
| **Third Trimester Pb (ug/L)** | 34.9 (2.1) | 14.6 (0.5) | 23.6 (0.5) | 36.4 (1.1) | 66.4 (4.4) |
| Child sex | | | | | |
| Male | 74 (60.2) | 14 (77.8) | 15 (53.6) | 21 (61.8) | 24 (55.8) |
| Female | 49 (39.8) | 4 (22.2) | 13 (46.4) | 13 (38.2) | 19 (44.2) |
| Maternal SES | | | | | |
| Lower | 66 (53.6) | 8 (44.4) | 15 (53.6) | 24 (70.6) | 19 (44.2) |
| Medium | 45 (36.6) | 7 (38.9) | 11 (39.3) | 10 (29.4) | 17 (39.5) |
| Higher | 12 (9.8) | 3 (16.7) | 2 (7.1) | 0 (0.0) | 7 (16.3) |
| Maternal age at pregnancy (years) | 28.5 (0.5) | 29.6 (0.5) | 28.4 (0.5) | 27.5 (0.5) | 28.7 (0.5) |
| Maternal BMI during pregnancy (kg/m$^2$) | 27.2 (0.4) | 27.5 (0.4) | 26.7 (0.3) | 27.2 (0.5) | 27.4 (0.4) |
| Child age at gut microbial sample collection (years) | 9.7 (0.7) | 9.8 (0.1) | 9.5 (0.1) | 9.86 (0.1) | 9.6 (0.1) |

Further, we chose not to rescale the chosen taxa with at least 5% relative abundance (1) to reflect the original contributions and (2) to make the analysis robust irrespective of the chosen relative abundance cutoff.

#### 2.5.7. Covariate adjustment

Each model was controlled by *a priori* chosen set of covariates. Although we thought Pb exposure during childhood may be a confounder, we tested the correlation between prenatal Pb and childhood Pb at birth, 1 year, 2 years, and 4 years of age, and did not find a correlation, thus we decided to exclude these variables from the models. A few covariates had missing values (less than 5%), which were imputed by the multiple imputation chained equations as implemented in the "MICE" R package (Van Buuren and Groothuis-Oudshoorn, 2011).

## 3. Results

### 3.1. Study population characteristics

Of 123 participants in this study (Table 1), 49 were female, and 74 were male. Mean Pb concentration was 33.6 ug/L and 34.9 ug/L in the second and third trimesters of pregnancy, respectively. Mothers with low SES were more likely to be in the fourth quartile of Pb exposure for both trimesters of pregnancy.

### 3.2. Alpha and beta diversity

In linear regression analysis of alpha (within individual) diversity and prenatal Pb exposure, we found slight negative associations, that were not statistically significant, for both second and third trimester Pb exposures, in unadjusted and adjusted models (Table 2). In PERMANOVA analysis of beta (between individual) diversity (Table 2), second trimester Pb exposure was associated with a non-significant $R^2$ of less than 1% (Adjusted $R^2 = 0.007$, value of $p = 0.515$). However, third trimester Pb exposure was associated with an $R^2$ of 1.1% in the adjusted model, and was directionally trending (Adjusted $R^2 = 0.011$, value of $p = 0.066$).

### 3.3. Microbiome mixture analysis

The primary $WQS_{RSRH}$ analysis was run in the negative direction because we hypothesized the association between prenatal Pb exposure

and the gut microbiome mixture to be negative (Figure 1). Including adjustment for covariates, second trimester Pb exposure was negatively associated with the gut microbiome mixture ($\beta = -0.17$, 95%CI = [−0.46, 0.11]), with 88% of the repeated holdout estimates below zero. Third trimester Pb exposure showed a very similar association with the gut microbiome mixture ($\beta = -0.17$, 95%CI = [−0.44, 0.10]), and had 89% of the repeated holdout estimates below zero. Within the weighted indices, taxa with a weight above 0.027 were considered important in the mixture association. Of the 20 bacterial taxa above the importance threshold for second trimester Pb exposure, 16 were also above the importance threshold in association with third trimester Pb exposure. *Ruminococcus gnavus*, *Bifidobacterium longum*, *Alistipes indistinctus*, *Bacteroides caccae*, and *Bifidobacterium bifidum* all had weights above the importance threshold from 80% or more of the repeated holdouts in association with both second and third trimester Pb exposure.

TABLE 2 Estimates of association between alpha and beta diversity and prenatal Pb exposure.

| | Alpha Diversity (Shannon)* Beta (*p*-value) | Beta Diversity (Bray-Curtis)# $R^2$ (value of *p*) |
|---|---|---|
| Second Trimester Pb | −1.48 (0.38) | 0.73% (0.52) |
| Third Trimester Pb | −1.26 (0.45) | 1.12% (0.06) |

*Linear model adjusted for covariates, #PERMANOVA with adjusted covariates.

In a sensitivity analysis, we ran the same WQS model using only the bacterial taxa that were present in at least 25% (instead of 5%) of participants from both analytical batches, and found associations in the same direction, with slightly larger estimates and confidence intervals that still crossed zero (Supplementary Figure S1). We conducted an additional sensitivity analysis running the $WQS_{RSRH}$ analysis in the positive direction and found null results. When comparing the likelihood estimates between the negative and positive $WQS_{RSRH}$ models, the likelihood was higher for the negative model, confirming our appropriate use of the negative model as the primary analysis.

When examining microbial gene function pathways of the important taxa associated with each of the second and third trimester Pb exposure separately, of the top 20 most abundant gene pathways for each trimester, approximately 1/2 of pathways from each trimester were found to be unique (Figure 2). Overall, common pathways were more likely to do with nucleic acid biosynthesis, and functions essential to all bacteria, while pathways associated with only one trimester Pb exposure or the other, were more likely to be involved in amino acid biosynthesis, and more specialized metabolic functions. A detailed list of the top 20 pathways can be found in Supplementary Table S2.

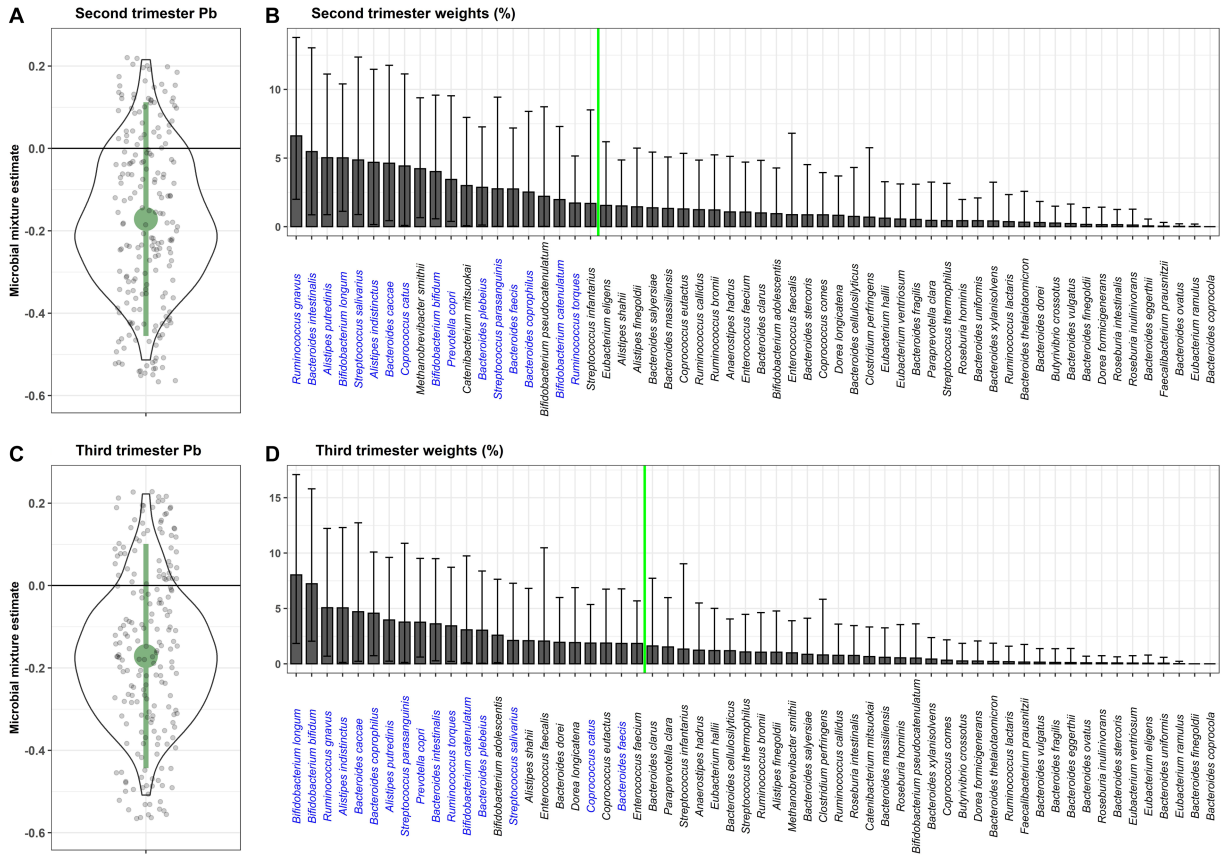


FIGURE 1
$WQS_{RSRH}$ estimates for the association of the gut microbiome mixture with prenatal Pb exposure in the **(A)** second and **(C)** third trimester of pregnancy. Small grey jitter dots represent the $WQS_{RS}$ estimates from each repeated holdout. The violin plot around those points show the density of holdout estimates at each interval. Average percent weight for each taxa within the WQS index are shown for the **(B)** second and **(D)** third trimester Pb exposure. The green line indicates the importance threshold for weights above random chance. Taxa that are labeled in blue are above the threshold for both trimesters of exposure.

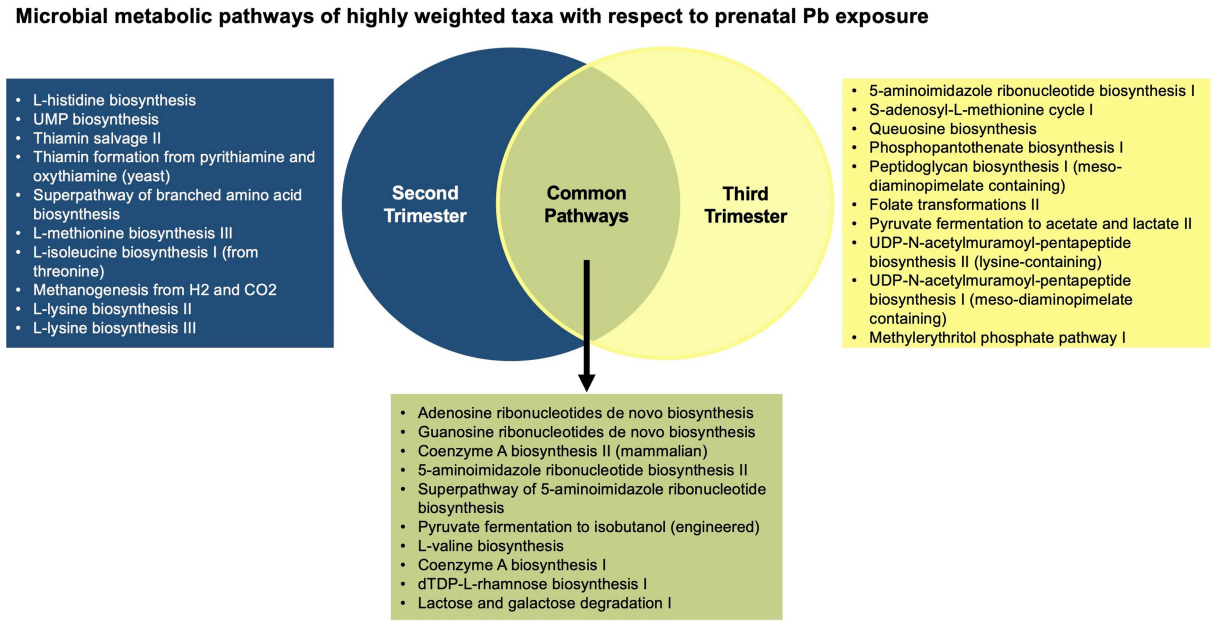


FIGURE 2
Venn diagram of the top 20 most abundant microbial gene functions from the highly weighted taxa in the $WQS_{RSRH}$ analysis.

## 3.4. Individual taxa analysis

In analysis of each individual bacterial taxa with prenatal Pb exposure (Figure 3), we found six taxa (*Alistipes putredinis*, *Ruminococcus ghavus*, *Bacteroides caccae*, *B. intestinalis*, *Coprococcus catus*, and *A. indistinctus*) to be negatively associated, and one (*B. coprocola*) to be positively associated with second trimester exposure. With third trimester exposure, we found three taxa (*Bifidobacterium bifidum*, *B. longum*, and *A. indistinctus*) to be negatively associated, and three taxa (*B. coprocola*, *Eubacterium eligens*, and *B. finegoldii*) to be positively associated with Pb.

# 4. Discussion

In this analysis of pilot microbiome data from the PROGRESS cohort, we examined associations between prenatal Pb exposure and several different components of gut microbiome composition and function. We found consistent negative associations between Pb exposure during the second and third trimester of pregnancy and several assessments of gut microbiome composition and function at 9–11 years old. Associations between prenatal Pb and the gut microbiome later in childhood tended to be strongest for second trimester exposure, providing support for the second trimester of pregnancy in particular as a critical window of exposure.

The focus of this analysis was on the association between prenatal Pb exposure and the gut microbiome later in childhood. There are many other potential exposures that may influence the composition and function of the gut microbiome between the prenatal exposure and the gut microbiome at 9–11 years, including continued exposure to Pb, diet, antibiotic use, animal exposure, child BMI and many others. However, none of these factors were included in this analysis because they are not confounders, as they are either (1) not associated with prenatal Pb exposure, or (2) potentially on the causal pathway between prenatal Pb exposure and the gut microbiome later in life.

The underlying mechanism of association between prenatal Pb exposure and the gut microbiome later in childhood could work in multiple ways. Because the gut microbiome is shaped in part by the host immune system (Petersen et al., 2019; Wong et al., 2022), prenatal Pb exposure may alter the trajectory of immune system development, which can influence gut microbial composition through the life-course. Another possible mechanism is via the maternal gut microbiome. The infant gut microbiome is primarily colonized by bacteria that are transferred from the mother at birth (Ferretti et al., 2018). Pb exposure in adults also influences gut microbiome composition (Eggers et al., 2019), thus Pb induced changes in the maternal gut microbiome during pregnancy may be transferred to children at birth, and carried on into childhood, and even later in life (Gschwendtner et al., 2019). Another potential mechanism may be that maternal Pb exposure is transferred to children through breastmilk, an established Pb exposure pathway (Klein et al., 2017). In that case, postnatal Pb exposure through breastmilk would be along the causal pathway between prenatal Pb exposure and the gut microbiome. Furthermore, all of these mechanisms may be working together. Further mechanistic studies are needed to better understand this complex relationship.

In previously published analyses of prenatal Pb exposure and the gut microbiome in studies with relatively small sample sizes, other researchers have seen similar results. In analysis of a birth cohort based in Detroit, MI ($n = 146$), Sitarik et al., identified associations between prenatal Pb exposure, measured in baby teeth, and decreased abundance of several species of *Bacteroides* within the gut microbiome at 1 month and 6 months of age (Sitarik et al., 2020). They identified *B. caccae* as being negatively associated with second trimester Pb

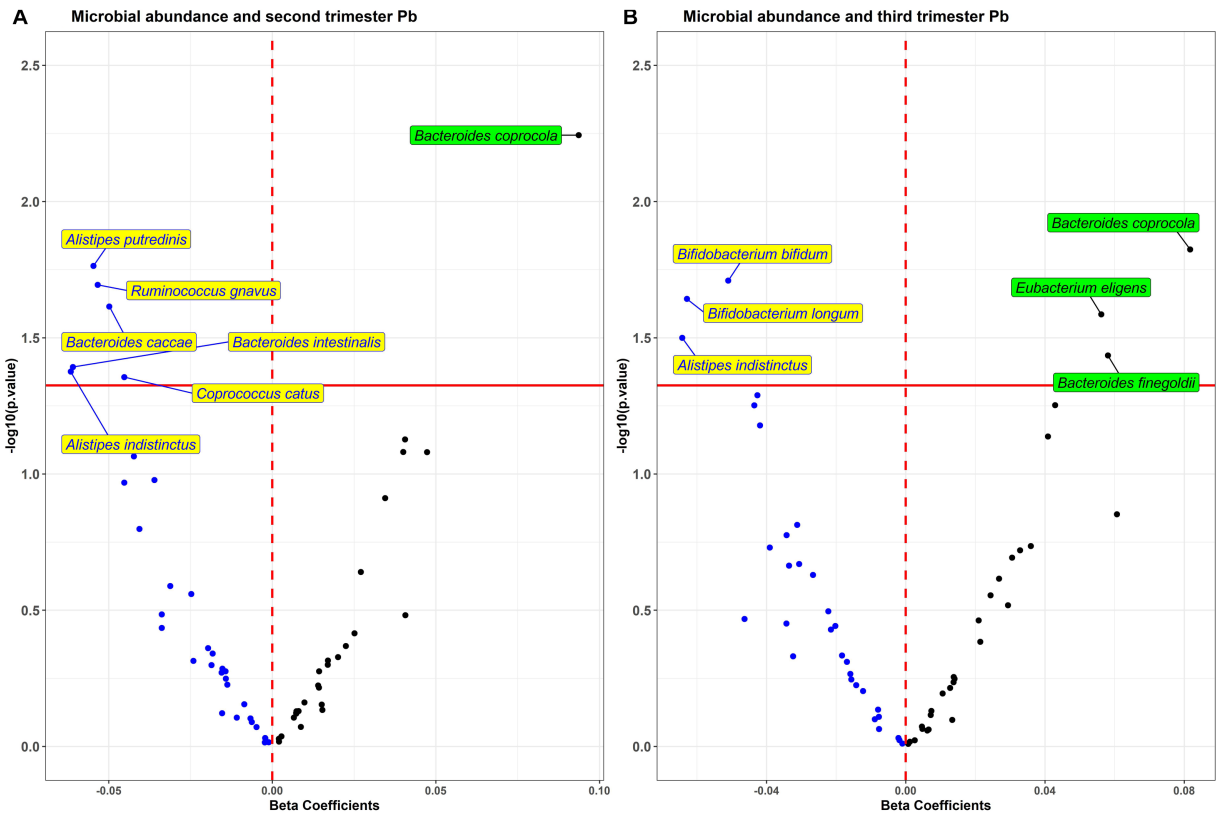


FIGURE 3
Volcano plot of estimates and value of *ps* from the taxa wide association analysis (TWAS) of bacterial abundance in association with **(A)** second and **(B)** third trimester Pb exposure. Blue dots are taxa associated in the negative direction and black dots are associated in the positive direction.

exposure specifically. We also identified a decreased abundance of *B. caccae* in association with Pb exposure in the second trimester using TWAS, and *B. caccae* was also heavily weighted in $WQS_{RSRH}$ for both trimesters of prenatal Pb exposure. *B. caccae* are common fiber degraders in the human gut microbiome, with mixed health effects (Wexler, 2007; Chen et al., 2021; Yang et al., 2022; Zhang et al., 2022). This consistent association of prenatal Pb exposure and decreased *B. caccae* abundance both early and late in childhood, from different populations in different countries, is strong evidence of association in this relatively new field.

In another epidemiologic study using data from a Canadian cohort ($n = 70$), Shen et al., found that prenatal Pb exposure, measured in maternal blood, was associated with increased abundance of *Fusobacteriota* in the gut microbiome at 6–7 years of age (Shen et al., 2022). They did not find a significant association between prenatal Pb and alpha or beta diversity. While the associated gut microbes identified in this analysis and the study by Shen et al., were not the same, it is important to note that links between prenatal Pb and the gut microbiome many years later in childhood were identified, even in these two small data sets. This suggests that there are likely true underlying links between prenatal Pb exposure and the gut microbiome in childhood. Differences in bacterial taxa associated may be due to differences in the study participants, or differences in sample and data processing procedures.

Of all the taxa in this analysis, *Alistipes indistinctus* was the only one identified by both $WQS_{RSRH}$ and TWAS to have a negative association with Pb exposure in the second and third trimesters. *A. indistinctus* is a common member of the human gut microbiome, and relatively newly identified (Nagai et al., 2010). Little is known about the health implications of *A. indistinctus*. However, one study has identified it as protective against liver fibrosis (Shao et al., 2018), and another identified it as a keystone species for restoring a healthy gut microbiome in patients with non-alcoholic fatty liver disease (Wu et al., 2022). Overall, the *Alistipes* genus has been shown to have both beneficial and detrimental health effects in humans (Parker et al., 2020). Continued investigation of the health implications of *A. indistinctus* are necessary to understand the links between prenatal Pb exposure and downstream health status via the microbiome.

In the analysis of microbial gene pathways from the most highly weighted taxa in the $WQS_{RSRH}$ analysis, approximately 1/3 of the gene pathways were shared between the taxa associated with second and third trimester Pb exposure. With a few exceptions, the pathways that were common among these bacteria are used for nucleic acid biosynthesis and other essential functions for bacterial life (Tsuchiya et al., 2018). The pathways that were not shared were more likely to be used in amino acid biosynthesis, fermentation, and other metabolic pathways. Because these more varied pathways provide a wider range of functional capabilities, they are more likely to influence host health, although their direct influence is not yet fully understood.

While this study added to the growing field of evidence around the negative relationship between metal exposure and the human gut microbiome, there are some limitations to consider. The use of metagenomic data to infer functional pathways contains inherent limitations because: (1) the gene sequences can only provide potential functional capabilities, with no information about which genes are actively transcribed and translated and (2) the random sampling approach to shotgun metagenomic sequencing allows for a great deal of missingness along functional pathways within the metagenome, thus prediction of function from a limited number of genes within a functional pathway is imprecise (Wooley and Ye, 2009). However, because the functional pathway analysis is only a minor component of this study, the impact of these inherent limitations on our conclusions are minor. A more substantial limitation of this study is the sample size. Because this was a pilot study, sample size was limited, which limited our power to detect associations. However, because results were primarily in the negative direction across multiple analytical approaches, and over 85% of the beta estimates from the WQS repeated holdouts were negative, we have increased confidence in reporting a negative result. Samples from this pilot study were also analyzed in two batches. Our strategy for reducing batch effects limited the breadth of microbiome data we could include in the analysis; however, similar prevalence thresholds are frequently used as data reduction steps in microbiome data analysis. Another statistical limitation was the use of prenatal Pb exposure as an outcome in the $WQS_{RSRH}$ models rather than a predictor. This model structure was necessary due to WQS format. The implications of this limitation are minimal however, as this analysis was used to determine association, not causation. Lastly, the use of maternal blood Pb during pregnancy to measure prenatal Pb exposure is not ideal, as it is not a direct measure of fetal Pb exposure.

In future analyses based off this work, we hope to examine additional and more nuanced relationships between prenatal environmental metal exposures and the gut microbiome in childhood. We plan to do additional sample collection in this cohort that will expand the sample size for future analyses. Furthermore, we are developing additional methodological approaches to examine relationships between chemical exposures and the gut microbiome, and their combined effect on downstream health.

In conclusion, this pilot study found a consistent negative association between prenatal Pb exposure and the gut microbiome in late childhood. These results support a growing body of evidence that human Pb exposure may alter gut microbial composition and function, leading to downstream health implications. More studies with larger sample sizes are needed to better understand this relationship.

## Data availability statement

Metagenomic data are publicly available at https://www.ncbi.nlm.nih.gov/sra/PRJNA975184. All other data are available upon request to robert.wright@mssm.edu.

## Ethics statement

The studies involving human participants were reviewed and approved by Icahn School of Medicine at Mount Sinai Institutional Review Board. Written informed consent to participate in this study was provided by the participants' legal guardian/next of kin.

## Author contributions

SE, VM, CG, and MA contributed to the conception and design of the study. LT-O, MT-R, and RWr contributed to the data acquisition. VM and MB performed the statistical analysis. SE, VM, CG, and RWa contributed to the data interpretation. SE wrote the first draft of the manuscript. VM wrote sections of the manuscript. All authors contributed to the article and approved the submitted version.

## Funding

This work was supported by the National Institute of Environmental Health Sciences (K99ES032884, P30ES023515 and R01ES013744).

## Acknowledgments

The authors would like to acknowledge the entire PROGRESS study team, as well as the participants. We would also like to thank Jeremiah Faith and the Microbiome Translational Center at the Icahn School of Medicine at Mount Sinai.

## Conflict of interest

MA is an employee and equity holder of Linus Biotechnology Inc., a start-up company of Mount Sinai Health System. The company develops tools for the detection of autism spectrum disorder and related conditions.

The remaining authors declare that the research was conducted in the absence of any commercial or financial relationships that could be construed as a potential conflict of interest.

## Publisher's note



## Supplementary material

The Supplementary material for this article can be found online at: https://www.frontiersin.org/articles/10.3389/fmicb.2023.1193919/full#supplementary-material

# References


Akaike, H. (1974). A new look at the statistical model identification. *IEEE Trans. Autom. Control* 19, 716–723. doi: 10.1109/TAC.1974.1100705

Bisanz, J. E., Enos, M. K., Mwanga, J. R., Changalucha, J., Burton, J. P., Gloor, G. B., et al. (2014). Randomized open-label pilot study of the influence of probiotics and the gut microbiome on toxic metal levels in Tanzanian pregnant women and school children. *MBio* 5, e01580–e01514. doi: 10.1128/mBio.01580-14

Bixby, M., Gennings, C., Malecki, K. M. C., Sethi, A. K., Safdar, N., Peppard, P. E., et al. (2022). Individual nutrition is associated with altered gut microbiome composition for adults with food insecurity. *Nutrients* 14:3407. doi: 10.3390/nu14163407

Bolger, A. M., Lohse, M., and Usadel, B. (2014). Trimmomatic: a flexible trimmer for illumina sequence data. *Bioinforma. Oxf. Engl.* 30, 2114–2120. doi: 10.1093/bioinformatics/btu170

Bray, J. R., and Curtis, J. T. (1957). An ordination of the upland forest communities of southern Wisconsin. *Ecol. Monogr.* 27, 325–349. doi: 10.2307/1942268

Breton, J., Massart, S., Vandamme, P., De Brandt, E., Pot, B., and Foligné, B. (2013). Ecotoxicology inside the gut: impact of heavy metals on the mouse microbiome. *BMC Pharmacol. Toxicol.* 14:62. doi: 10.1186/2050-6511-14-62

Carrico, C., Gennings, C., Wheeler, D. C., and Factor-Litvak, P. (2015). Characterization of weighted quantile sum regression for highly correlated data in a risk analysis setting. *J. Agric. Biol. Environ. Stat.* 20, 100–120. doi: 10.1007/s13253-014-0180-3

Chen, Y., Lin, H., Cole, M., Morris, A., Martinson, J., Mckay, H., et al. (2021). Signature changes in gut microbiome are associated with increased susceptibility to HIV-1 infection in MSM. *Microbiome* 9:237. doi: 10.1186/s40168-021-01168-w

Claus, S. P., Guillou, H., and Ellero-Simatos, S. (2016). The gut microbiota: a major player in the toxicity of environmental pollutants? *NPJ Biofilms Microb.* 2:16003. doi: 10.1038/npjbiofilms.2016.3

Curtin, P., Kellogg, J., Cech, N., and Gennings, C. (2019). A random subset implementation of weighted quantile sum (WQSRS) regression for analysis of high-dimensional mixtures. *Commun. Stat. Simul. Comput.* 50, 1119–1134. doi: 10.1080/03610918.2019.1577971

de Prado-Bert, P., Ruiz-Arenas, C., Vives-Usano, M., Andrusaityte, S., Cadiou, S., Carracedo, Á., et al. (2021). The early-life exposome and epigenetic age acceleration in children. *Environ. Int.* 155:106683. doi: 10.1016/j.envint.2021.106683

Eggers, S., Bixby, M., Renzetti, S., Curtin, P., and Gennings, C. (2023). Human microbiome mixture analysis using weighted quantile sum regression. *Int. J. Environ. Res. Public Health* 20:94. doi: 10.3390/ijerph20010094

Eggers, S., Safdar, N., Sethi, A. K., Suen, G., Peppard, P. E., Kates, A. E., et al. (2019). Urinary lead concentration and composition of the adult gut microbiota in a cross-sectional population-based sample. *Environ. Int.* 133:105122. doi: 10.1016/j.envint.2019.105122

Ferretti, P., Pasolli, E., Tett, A., Asnicar, F., Gorfer, V., Fedi, S., et al. (2018). Mother-to-infant microbial transmission from different body sites shapes the developing infant gut microbiome. *Cell Host Microbe* 24, 133–145.e5. doi: 10.1016/j.chom.2018.06.005

Franzosa, E. A., McIver, L. J., Rahnavard, G., Thompson, L. R., Schirmer, M., Weingart, G., et al. (2018). Species-level functional profiling of metagenomes and metatranscriptomes. *Nat. Methods* 15, 962–968. doi: 10.1038/s41592-018-0176-y

Gao, B., Chi, L., Mahbub, R., Bian, X., Tu, P., Ru, H., et al. (2017). Multi-omics reveals that lead exposure disturbs gut microbiome development, key metabolites, and metabolic pathways. *Chem. Res. Toxicol.* 30, 996–1005. doi: 10.1021/acs.chemrestox.6b00401

Gomaa, E. Z. (2020). Human gut microbiota/microbiome in health and diseases: a review. *Antonie Van Leeuwenhoek* 113, 2019–2040. doi: 10.1007/s10482-020-01474-7

Gschwendtner, S., Kang, H., Thiering, E., Kublik, S., Fösel, B., Schulz, H., et al. (2019). Early life determinants induce sustainable changes in the gut microbiome of 6-year-old children. *Sci. Rep.* 9:12675. doi: 10.1038/s41598-019-49160-7

Heiss, J. A., Téllez-Rojo, M. M., Estrada-Gutiérrez, G., Schnaas, L., Amarasiriwardena, C., Baccarelli, A. A., et al. (2020). Prenatal lead exposure and cord blood DNA methylation in PROGRESS: an epigenome-wide association study. *Environ. Epigenet.* 6:dvaa014. doi: 10.1093/eep/dvaa014

Human Microbiome Project Consortium (2012). Structure, function and diversity of the healthy human microbiome. *Nature* 486, 207–214. doi: 10.1038/nature11234

Klein, L. D., Breakey, A. A., Scelza, B., Valeggia, C., Jasienska, G., and Hinde, K. (2017). Concentrations of trace elements in human milk: comparisons among women in Argentina, Namibia, Poland, and the United States. *PLoS One* 12:e0183367. doi: 10.1371/journal.pone.0183367

Langmead, B., and Salzberg, S. L. (2012). Fast gapped-read alignment with bowtie 2. *Nat. Methods* 9, 357–359. doi: 10.1038/nmeth.1923

Laue, H. E., Moroishi, Y., Jackson, B. P., Palys, T. J., Madan, J. C., and Karagas, M. R. (2020). Nutrient-toxic element mixtures and the early postnatal gut microbiome in a United States longitudinal birth cohort. *Environ. Int.* 138:105613. doi: 10.1016/j.envint.2020.105613

Li, J., and Ji, L. (2005). Adjusting multiple testing in multilocus analyses using the eigenvalues of a correlation matrix. *Heredity* 95, 221–227. doi: 10.1038/sj.hdy.6800717

Liao, J. G., Cavanaugh, J. E., and McMurry, T. L. (2018). Extending AIC to best subset regression. *Comput. Stat.* 33, 787–806. doi: 10.1007/s00180-018-0797-8

Litvak, Y., Byndloss, M. X., Tsolis, R. M., and Bäumler, A. J. (2017). Dysbiotic proteobacteria expansion: a microbial signature of epithelial dysfunction. *Curr. Opin. Microbiol.* 39, 1–6. doi: 10.1016/j.mib.2017.07.003

Nagai, F., Morotomi, M., Watanabe, Y., Sakon, H., and Tanaka, R. (2010). *Alistipes indistinctus* sp. nov. and *Odoribacter laneus* sp. nov., common members of the human intestinal microbiota isolated from faeces. *Int. J. Syst. Evol. Microbiol.* 60, 1296–1302. doi: 10.1099/ijs.0.014571-0

Oksanen, J., Blanchet, F. G., Friendly, M., Kindt, R., Legendre, P., McGlinn, D., et al. (2019). Vegan: Community ecology package. Available at: https://CRAN.R-project.org/package=vegan (Accessed August 12, 2019).

Ortega, R. P. (2022). Microbiome data dominated by wealthy countries. *Science* 375:709. doi: 10.1126/science.ada1336

Parker, B. J., Wearsch, P. A., Veloo, A. C. M., and Rodriguez-Palacios, A. (2020). The genus alistipes: gut bacteria with emerging implications to inflammation, cancer, and mental health. *Front. Immunol.* 11:906. doi: 10.3389/fimmu.2020.00906

Petersen, C., Bell, R., Klag, K. A., Lee, S.-H., Soto, R., Ghazaryan, A., et al. (2019). T cell–mediated regulation of the microbiota protects against obesity. *Science* 365:eaat9351. doi: 10.1126/science.aat9351

Romano, K. A., Dill-McFarland, K. A., Kasahara, K., Kerby, R. L., Vivas, E. I., Amador-Noguez, D., et al. (2018). Fecal aliquot straw technique (FAST) allows for easy and reproducible subsampling: assessing interpersonal variation in trimethylamine-N-oxide (TMAO) accumulation. *Microbiome* 6:91. doi: 10.1186/s40168-018-0458-8

Sanders, A. P., Gennings, C., Tamayo-Ortiz, M., Mistry, S., Pantic, I., Martinez, M., et al. (2022). Prenatal and early childhood critical windows for the association of nephrotoxic metal and metalloid mixtures with kidney function. *Environ. Int.* 166:107361. doi: 10.1016/j.envint.2022.107361

Schwarz, G. (1978). Estimating the dimension of a model. *Ann. Stat.* 6, 461–464. doi: 10.1214/aos/1176344136

Shannon, C. E. (1948). A mathematical theory of communication. *Bell Syst. Tech. J.* 27, 379–423. doi: 10.1002/j.1538-7305.1948.tb01338.x

Shao, L., Ling, Z., Chen, D., Liu, Y., Yang, F., and Li, L. (2018). Disorganized gut microbiome contributed to liver cirrhosis progression: a meta-omics-based study. *Front. Microbiol.* 9:3166. doi: 10.3389/fmicb.2018.03166

Shen, Y., Laue, H. E., Shrubsole, M. J., Wu, H., Bloomquist, T. R., Larouche, A., et al. (2022). Associations of childhood and perinatal blood metals with Children's gut microbiomes in a Canadian gestation cohort. *Environ. Health Perspect.* 130:17007. doi: 10.1289/EHP9674

Shin, N.-R., Whon, T. W., and Bae, J.-W. (2015). Proteobacteria: microbial signature of dysbiosis in gut microbiota. *Trends Biotechnol.* 33, 496–503. doi: 10.1016/j.tibtech.2015.06.011

Sitarik, A. R., Arora, M., Austin, C., Bielak, L. F., Eggers, S., Johnson, C. C., et al. (2020). Fetal and early postnatal lead exposure measured in teeth associates with infant gut microbiota. *Environ. Int.* 144:106062. doi: 10.1016/j.envint.2020.106062

Tanner, E. M., Bornehag, C.-G., and Gennings, C. (2019). Repeated holdout validation for weighted quantile sum regression. *MethodsX* 6, 2855–2860. doi: 10.1016/j.mex.2019.11.008

Truong, D. T., Franzosa, E. A., Tickle, T. L., Scholz, M., Weingart, G., Pasolli, E., et al. (2015). MetaPhlAn2 for enhanced metagenomic taxonomic profiling. *Nat. Methods* 12, 902–903. doi: 10.1038/nmeth.3589

Truong, D. T., Tett, A., Pasolli, E., Huttenhower, C., and Segata, N. (2017). Microbial strain-level population structure and genetic diversity from metagenomes. *Genome Res.* 27, 626–638. doi: 10.1101/gr.216242.116

Tsuchiya, Y., Zhyvoloup, A., Baković, J., Thomas, N., Yu, B. Y. K., Das, S., et al. (2018). Protein CoAlation and antioxidant function of coenzyme a in prokaryotic cells. *Biochem. J.* 475, 1909–1937. doi: 10.1042/BCJ20180043

Van Buuren, S., and Groothuis-Oudshoorn, K. (2011). Mice: multivariate imputation by chained equations in R. *J. Stat. Softw.* 45, 1–67. doi: 10.18637/jss.v045.i03

Wexler, H. M. (2007). Bacteroides: the good, the bad, and the nitty-gritty. *Clin. Microbiol. Rev.* 20, 593–621. doi: 10.1128/CMR.00008-07

Wilmes, P., Martin-Gallausiaux, C., Ostaszewski, M., Aho, V. T. E., Novikova, P. V., Laczny, C. C., et al. (2022). The gut microbiome molecular complex in human health and disease. *Cell Host Microbe* 30, 1201–1206. doi: 10.1016/j.chom.2022.08.016

Wong, C. K., Yusta, B., Koehler, J. A., Baggio, L. L., McLean, B. A., Matthews, D., et al. (2022). Divergent roles for the gut intraepithelial lymphocyte GLP-1R in control of metabolism, microbiota, and T cell-induced inflammation. *Cell Metab.* 34, 1514–1531.e7. doi: 10.1016/j.cmet.2022.08.003

Wooley, J. C., and Ye, Y. (2009). Metagenomics: facts and artifacts, and computational challenges*. *J. Comput. Sci. Technol.* 25, 71–81. doi: 10.1007/s11390-010-9306-4

Woolley, D. E. (1984). A perspective of lead poisoning in antiquity and the present. *Neurotoxicology* 5, 353–361.

Wu, D., Liu, L., Jiao, N., Zhang, Y., Yang, L., Tian, C., et al. (2022). Targeting keystone species helps restore the dysbiosis of butyrate-producing bacteria in nonalcoholic fatty liver disease. *iMeta* 1:e61. doi: 10.1002/imt2.61

Wu, J., Wen, X. W., Faulk, C., Boehnke, K., Zhang, H., Dolinoy, D. C., et al. (2016). Perinatal lead exposure alters gut microbiota composition and results in sex-specific bodyweight increases in adult mice. *Toxicol. Sci. Off. J. Soc. Toxicol.* 151, 324–333. doi: 10.1093/toxsci/kfw046

Xia, J., Lu, L., Jin, C., Wang, S., Zhou, J., Ni, Y., et al. (2018). Effects of short term lead exposure on gut microbiota and hepatic metabolism in adult zebrafish. *Comp. Biochem. Physiol. Toxicol. Pharmacol.* 209, 1–8. doi: 10.1016/j.cbpc.2018.03.007

Yang, X., Xiu, W.-B., Wang, J.-X., Li, L.-P., He, C., and Gao, C.-P. (2022). CO2 is beneficial to gut microbiota homeostasis during colonoscopy: randomized controlled trial. *J. Clin. Med.* 11:5281. doi: 10.3390/jcm11185281

Zhang, Y., Fan, Q., Hou, Y., Zhang, X., Yin, Z., Cai, X., et al. (2022). Bacteroides species differentially modulate depression-like behavior via gut-brain metabolic signaling. *Brain Behav. Immun.* 102, 11–22. doi: 10.1016/j.bbi.2022.02.007

frontiers | Frontiers in Microbiology

TYPE Original Research
PUBLISHED 28 July 2023
DOI 10.3389/fmicb.2023.1205797



OPEN ACCESS

EDITED BY
Rebeca Martín,
INRAE Centre Jouy-en-Josas, France

REVIEWED BY
Anand Kumar,
Los Alamos National Laboratory (DOE), United States
Viera Karaffová,
University of Veterinary Medicine and Pharmacy in Košice, Slovakia

*CORRESPONDENCE
Eliška Valečková
✉ eliska.valeckova@slu.se

RECEIVED 14 April 2023
ACCEPTED 12 July 2023
PUBLISHED 28 July 2023

CITATION
Valečková E, Sun L, Wang H, Dube F, Ivarsson E, Kasmaei KM, Ellström P and Wall H (2023) Intestinal colonization with *Campylobacter jejuni* affects broiler gut microbiota composition but is not inhibited by daily intake of *Lactiplantibacillus plantarum*. *Front. Microbiol.* 14:1205797. doi: 10.3389/fmicb.2023.1205797



# Intestinal colonization with *Campylobacter jejuni* affects broiler gut microbiota composition but is not inhibited by daily intake of *Lactiplantibacillus plantarum*

Eliška Valečková[1]*, Li Sun[1], Helen Wang[2], Faruk Dube[3], Emma Ivarsson[1], Kamyar Mogodiniyai Kasmaei[1], Patrik Ellström[4] and Helena Wall[1]

[1]Department of Animal Nutrition and Management, Swedish University of Agricultural Sciences, Uppsala, Sweden, [2]Department of Medical Biochemistry and Microbiology, Uppsala University, Uppsala, Sweden, [3]Department of Biomedical Science and Veterinary Public Health, Swedish University of Agricultural Sciences, Uppsala, Sweden, [4]Department of Medical Sciences, Zoonosis Science Center, Uppsala University, Uppsala, Sweden

**Introduction:** Lactobacilli may prevent broilers from colonization with *Campylobacter* spp. and other gram-negative zoonotic bacteria through lactic acid production and modulation of the intestinal microbiota. This study evaluated the effects of daily intake of *Lactiplantibacillus plantarum* 256 (LP256) on *Campylobacter jejuni (C. jejuni)* loads in ceca and feces of *C. jejuni* challenged broilers, together with the changes in the gut microbiota.

**Methods:** Two experiments were conducted using the broilers Ross 308 (R-308; Experiment 1) for 42days and Rowan Ranger broilers (RR; Experiment 2) for 63days. The *LP256* strain was administered either via silage inoculated with *LP256* or direct supplementation in the drinking water. Concurrently, haylage as a forage similar to silage but without any inoculum was tested. *C. jejuni* loads in fecal matter and cecal content were determined by plate counts and qPCR, respectively. The cecal microbiota, in response to treatments and the challenge, were assessed by 16S rRNA sequencing.

**Results and Discussion:** Culturing results displayed a significant reduction in *C. jejuni* colonization (2.01 log) in the silage treatment in comparison to the control at 1 dpi (day post-infection) in Experiment 1. However, no treatment effect on *C. jejuni* was observed at the end of the experiment. In Experiment 2, no treatment effects on *C. jejuni* colonization were found to be statistically significant. Colonization load comparison at the peak of infection (3 dpi) to that at the end of the trial (32 dpi) revealed a significant reduction in *C. jejuni* in all groups, regardless of treatment. Colonization dynamics of *C. jejuni* in the cecal samples analyzed by qPCR showed no difference between any of the treatments in Experiment 1 or 2. In both experiments, no treatment effects on the cecal microbiota were observed. However, proportional changes in the bacterial composition were observed after the *C. jejuni* challenge, suggesting that colonization affected the gut microbiota. Overall, the daily intake of *LP256* was not effective in reducing *C. jejuni* colonization in either broiler type at the end of the rearing period and did not cause any significant changes in the birds' cecal microbiota composition.

KEYWORDS

*Lactobacillus plantarum*, *Campylobacter jejuni*, broiler, gut microbiota, qPCR, sequencing

# 1. Introduction

The ceca are believed to have an important role in the gut health and performance of broiler birds. However, its role in the maintenance of gut health and modulation of the gut microbiota is still not fully understood. As the most densely colonized microbial habitat in broilers, its microbial density is estimated to be $10^{11}$–$10^{12}$ bacterial cells per gram (Rinttilä and Apajalahti, 2013). The description and understanding of intestinal microbial communities and their interactions, are essential for the development of feed additives and dietary changes to improve broiler health, performance, and welfare (Sugiharto, 2016). A wide variety of feed supplements, such as prebiotics, probiotics, and organic acids, focus on the stabilization of the gut microbiota to secure intestinal health (Yang et al., 2009).

Probiotics are natural microbes that benefit their host fundamentally through their action in the gastrointestinal tract (Abd El-Hack et al., 2020). Single-strain probiotic species including, among others, species of *Bifidobacterium*, *Bacillus*, *Enterococcus*, *Streptococcus*, and *Lactobacillus* have previously shown positive effects on broiler performance, modulation of the gut microbiome as well as inhibition of pathogens through different principles, i.e., competitive exclusion, production of organic acids, or production of antimicrobial compounds (Neal-McKinney et al., 2012; Prabhurajeshwar and Chandrakanth, 2019; Krysiak et al., 2021). Furthermore, it has been shown that probiotics help to maintain microbial homeostasis thus avoiding colonization by pathogens, and may suppress *Campylobacter* colonization (Di Marcantonio et al., 2022).

Campylobacteriosis is the most commonly reported zoonosis in the European Union (EU), where broiler products are a common source of infection due to insufficient heat treatment or cross-contamination. According to the European Food Safety Authority (EFSA), 58% of human *Campylobacter jejuni* (*C. jejuni*) infections are associated with broiler meat (EFSA, 2020). Poultry feed with low pH and a high number of lactic acid bacteria (LAB) has been shown to reduce the susceptibility to *Campylobacter* colonization in broilers (Heres et al., 2003). This effect might be explained by the principles of pathogen inhibition mentioned above.

Although the prevalence of *Campylobacter* in conventional broiler production in Sweden is currently low, the problem remains in organic production. In 2021, 5% of tested conventional batches were *Campylobacter* positive at slaughter, whereas in organic production, 33% of tested flocks were positive (Swedish Poultry Meat Association, 2021). The higher frequency in the latter is due to the access to outdoor reservoirs of *Campylobacter*, as all organic poultry in the EU must have the opportunity to spend time outdoors (Commission Regulation (EC) 889/2008, 2008). In addition, organic poultry must be provided daily access to forage where silage is provided at some organic broiler farms (Crawley, 2015).

This study aimed to investigate the effects of daily intake of *Lactiplantibacillus plantarum* strain 256 (*L. plantarum* 256; *LP*256) on *C. jejuni* load in broiler's cecum and feces, together with the changes in their gut microbiota. In organic farming, silage can be supplied as forage to the broilers, and therefore we assessed the efficiency of providing *LP*256 both via silage inoculated with the strain and via direct supplementation in the drinking water. Concurrently, impact of haylage as a forage similar to silage but without any inoculum was tested. The effects of the treatments were evaluated on slow-growing (birds used in organic production) and fast-growing (conventional production) broilers in two separate trials under *C. jejuni* challenge.

# 2. Materials and methods

## 2.1. Experimental design and housing

The experimental setting was previously described in detail by Valečková et al. (2020); a brief description follows. Two experiments were conducted concurrently at the Swedish Livestock Research Centre of the Swedish University of Agricultural Sciences, with approval from the Uppsala region's animal ethics committee (approval number 5.8.18-16271/2017). The experiments were conducted using fast-growing broilers Ross 308 (R-308), used in conventional production in Sweden, and the Rowan Ranger broilers (RR), with a slower growth preferred in, e.g., organic broiler production. In Experiment 1, a total of 160 unsexed day-old R-308 broiler chickens were used for the 42-day (6-week) experiment, which is considered a normal period of growth for fast-growing strains in the EU. In Experiment 2 a total of 160 unsexed day-old RR broiler chickens (also referred to as "slow-growing broiler") were used in the 63-d experiment (9 weeks) corresponding to the age at which this broiler type is generally slaughtered in organic production systems in Sweden. In each study, broilers were randomly distributed in groups of eight individuals in 20 raised pens with four dietary treatments and five pen replicates for each treatment, arranged in a randomized block design. In both studies, two random broilers per pen were chosen as focal birds, representatives of the entire pen population. Focals were later on used for the collection of fecal droppings for *C. jejuni* quantification by agar plate culture and at the end of the experiment for cecal content sampling for a quantitative real-time polymerase chain reaction (qPCR) assay to quantify *C. jejuni* loads and for microbiota analysis done by 16S rRNA sequencing.

The experiments were performed in parallel during the winter in an insulated stable equipped with the facilities for automatic control of temperature and light. Each pen had a floor covered by fresh wood shavings and was equipped with a metal feeder and a 3-liter bell drinker.

## 2.2. Experimental diets

Detailed diet specification and forage preservation are stated in Valečková et al. (2020). In brief, fresh feed and water (including

10.3389/fmicb.2023.1205797

treatments) were provided directly after the broilers' arrival and supplied daily. All experimental diets were based on organic compound feed (13 MJ/kg metabolizable energy and 230 g/kg DM crude protein) and the daily requirement of pellets in all treatment groups was estimated (based on production performance objectives) to ensure *ad libitum* provision. Broilers were assigned to four different treatment groups: silage, haylage, *LP*256, or control. Haylage treatment was included in the study as a forage similar to silage but without any inoculum. Silage and haylage experimental diets were composed as total mixed rations (TMR) containing 85% of pellets and 15% of respective forage (on a DM basis). Additionally, the *LP*256 and the control groups received the organic pelleted compound feed (no forage provided). The *LP*256 group had drinking water inoculated with *L. plantarum* 256 ($10^7$ CFU/mL).

Second-cut grass, with a seeding composition of 70% timothy and 30% meadow fescue, was used for the production of forages. Silage was inoculated with *L. plantarum* strain 256 during baling, providing an inoculum concentration of $10^8$ CFU per gram fresh matter. Haylage bales were made without inoculum. After 3 months of storage, bales were separately opened, chopped and thereafter ground to 0.5–1 cm particles. Forage was afterward vacuum-packed (1 kg per bag) and bags were stored at a temperature below 0°C to maintain a similar feed quality throughout the experiments. Enumeration of epiphytic LAB on silage was performed in duplicates monthly (January, February, and March) during the trial period and the pH of silage juice was measured prior to the trials.

## 2.3. Bacterial strains and culturing conditions

Bacterial strains used in this study include *L. plantarum* 256 and *Campylobacter jejuni* #65. The *L. plantarum* strain (also known as *L. plantarum* NC7, Cosby et al., 1989) was previously used in our *in vitro* experiments and proved among other LABs to elicit the best inhibitory effect against *C. jejuni* #65 (unpublished data). The *L. plantarum* strain 256 isolate was stored at – 80°C in Luria Bertani (LB) broth with 20% glycerol. It was propagated in De Man, Rogosa and Sharpe broth for 24 h at 37°C for silage preparation and as a prophylactic probiotic in the study. *C. jejuni* #65 (ST-104, in ST-21 CC; isolated from a broiler chicken in the UK 2006) was cultured in Brucella broth at 42°C under microaerobic (85% N2, 10% CO2, 5% O2) conditions for 24 h. After 24 h incubation, optical density at 405 nm and plate counts were used to determine the infection dose used in the *C. jejuni* challenge.

## 2.4. *Campylobacter jejuni* colonization and quantification

To investigate the effects of the *L. plantarum* treatments on *C. jejuni* colonization of the broilers' ceca, all birds were orally challenged (also referred to as "infected") at 22 d of age in Experiment 1 and 29 d of age (corresponding to the 4 weeks of age at which organic broilers in Sweden must have access to an outdoor environment) in Experiment 2 (Figure 1). On the day of the challenge, 0.5 L of water with $10^6$ CFU/mL of the *C. jejuni* strain #65 was provided in the bell drinker of each pen. The inoculated water was administered for 3 h

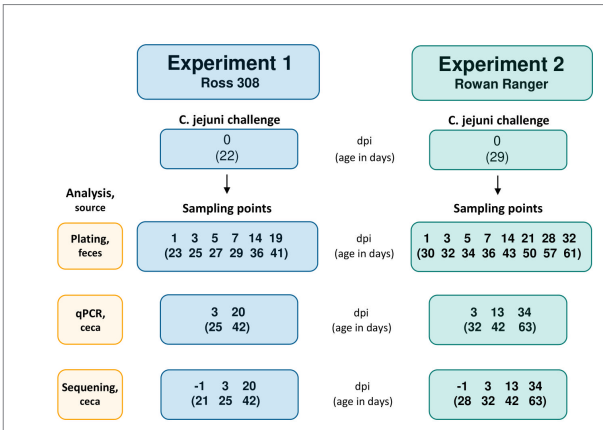


FIGURE 1
Flowchart with the *Campylobacter jejuni* challenge occasion and following sampling points in Experiment 1 (R-308) and Experiment 2 (RR). The challenge occasion and sampling points are presented as days post-infection (dpi), with the corresponding age of the birds (in days) indicated in brackets.

and *C. jejuni* viability in the water was determined by colony counts on blood agar plates at the start and end of the challenge.

The colonization pattern of *C. jejuni* was monitored during 19 days and 32 days for R-308 and RR, respectively, by fecal culture and colony counts on modified Charcole Cefoperazone Deoxycholate (mCCDA) agar plates. For fresh fecal sampling, two focal birds from each pen were placed individually in plastic boxes. Sterile plastic loops were used for the collection of droppings from the box bottom. Fecal samples were collected from all pens 1 day before the challenge with *C. jejuni*, to verify that the broilers were *Campylobacter* negative before the challenge. One hundred mg of fresh fecal droppings from the focal birds in each pen were collected in 1 mL LB medium supplemented with 20% glycerol on 1, 3, 5, 7, 14, and 19 days post-infection (dpi) in Experiment 1 and 1, 3, 5, 7, 14, 21, 28, and 32 dpi in Experiment 2 (Figure 1). Tubes were directly transported on ice to the laboratory for analysis. Samples were vortexed and centrifuged (100 × *g* for 15 s) to pellet crude fecal matter. Next, 100 µL was withdrawn and serially diluted in 10-fold dilution series. Afterward, 100 µL was plated on mCCDA and incubated for 26 h at 42°C under microaerobic conditions (Campygen, Thermo Fisher). After incubation, colonies were counted on the plate corresponding to the dilution that gave approximately 100 CFU per plate. Raw plate counts data are provided in Supplementary Figure 1 (Experiment 1) and Supplementary Figure 2 (Experiment 2).

## 2.5. Cecal samples collection

In both experiments, one random bird per cage was sacrificed 1 day before infection (−1 dpi) and 3 days after infection (3 dpi) by an intravenous injection of sodium pentobarbital through the wing vein; the birds age corresponding to mentioned dpi is stated in Figure 1. The cecal content was sampled with an aseptic procedure into 2.0 mL screw cap microtubes (Sarstedt AG & Co, Germany) and placed in liquid nitrogen (followed by storing at – 80°C until analyzed). At 42 days of age, all focal birds in Experiment 1 (20 dpi), and one random bird in each replicate in Experiment 2 (13 dpi) were sacrificed and sampled. Experiment 2 focal

birds were sacrificed at 63 days of age (34 dpi) followed by cecal sampling as described above. Samples were analyzed by a qPCR assay to assess *C. jejuni* colonization and the microbial composition of cecal content was investigated by 16S rRNA amplicon sequencing.

## 2.6. DNA extraction and qPCR-based *Campylobacter jejuni* quantification

For quantification of *C. jejuni* load in the broiler cecum using qPCR, a standard curve was developed as a reference for the proceeding analysis (Supplementary Table 1). Bacterial colonies of *C. jejuni #65* from a 36-h incubated mCCDA culture were suspended in 300 µL of phosphate-buffered saline (PBS). The suspension was briefly vortexed and divided into 100 µL duplicates, and was diluted in a 10-fold series of PBS for CFU counting on mCCDA plates and incubated under microaerobic conditions for 24 h at 42°C.

Simultaneously, another 100 µL replicate was extracted for DNA and qPCR analysis. The sample was mixed with 200 mg of 0.1 mm zirconia/silica beads (Biospec products, Bartlesville, USA) and 900 µL of ASL lysis buffer (Qiagen, Germany), briefly vortexed, and incubated at 95°C for 5 min to lyse cells, followed by immediate placement on ice for 10 min. The sample was then bead-beaten on Precellys24 sample homogenizer (Bertin Technologies, Montigny-le-Bretonneux, France) at 8000 rpm for 2 × 60 s with 30 s pause to disrupt bacterial cell walls mechanically. Centrifugation of the sample at 2500 x *g* for 1 min followed, and 200 µL of the supernatant was withdrawn into the sample tube together with 20 µL of proteinase K for DNA extraction. Extraction was performed on an EZ1 Advanced XL instrument (Qiagen, Germany) according to the manufacturer's instructions. The extract was diluted in a 10-fold series of nuclease-free water and used as a template in the real-time PCR for generating a standard curve.

A real-time PCR targeting the d65_1178 gene, specific to *C. jejuni* Strain #65 and its ST type ST-104 (ST-21 CC) was conducted using a primer pair adapted from Atterby et al. (2018). The PCR was performed on a CFX96 Optics Module C1000 Touch Thermal Cycler (Bio-Rad Laboratories, USA). The reaction mixture contained: 1 x SsoAdvanced Universal SYBR Green Supermix, 0.3 µL of forward and reverse primer each, and 1 µL of the template. Reactions were run in triplicates. The amplification parameters were as follows; 98°C for 3 min, 40 cycles of 98°C for 15 s and 63°C for 60 s and followed by a melt curve ranging from 65 to 95°C as a check for assay specificity. Generated qPCR data was analyzed on Bio-Rad CFX Manager 3.1 software (Bio-Rad Laboratories, USA) and Microsoft Excel. Raw qPCR data are provided in Supplementary Figure 3 (Experiment 1) and Supplementary Figure 4 (Experiment 2). The amplification efficiency of the PCR reaction was 76% with $R^2$ of 0.9996.

All the cecal samples followed the same pre-treatment, DNA extraction procedure as the *C. jejuni #65* suspension, with minor pre-treatment modifications. Modifications included; 400 µL of ASL lysis buffer, added to the sample and vortexed briefly to homogenize. Then, 120 µL of the sample was used in downstream steps. Sample DNA extracts were analyzed by qPCR and sequencing. For quantification, DNA extracts were run on qPCR along with a standard (*C. jejuni #65*) DNA extract. The CT values obtained from sample runs were compared to that of the standard and transformed into CFU using the generated standard curve equation. The generated CFU was multiplied by five to compensate for a five times dilution of the sample performed during pre-treatment, a dilution not performed on the standard suspension. The ultimate quantification was expressed in CFU/ml by multiplication of 10.

## 2.7. 16S rRNA sequencing

One hundred forty cecal sample DNA extracts were sequenced using the Illumina Miseq PE 250 sequencing platform at Novogene Bioinformatics Technology Co., Ltd. (Beijing, China). The 16S rRNA gene V3–V4 regions were amplified using Illumina primer set 341F (CCTAYGGGRBGCASCAG) and 806R (GGACTACNNGGGTAT CTAAT) with a barcode. All template DNAs were normalized to the same concentration. PCR reactions were performed with Phusion® High-Fidelity PCR Master Mix (New England Biolabs, USA). PCR products were separated by electrophoresis on 2% agarose gel, purified with a Qiagen Gel Extraction Kit (Qiagen, Germany) and pooled at equal concentrations. Sequencing libraries were generated using NEBNext Ultra DNA Library Prep Kit (Illumina, USA) following the manufacturer's recommendations, and index codes were added. Library quality was assessed on the Qubit 2.0 Fluorometer (Thermo Fisher Scientific, USA) and the Bioanalyzer 2100 system (Agilent Technologies, USA).

## 2.8. Sequence analysis

The raw sequencing data were uploaded to the National Center for Biotechnology Information database (NCBI) with accession number PRJNA876811. The bioinformatics data processing was performed by Quantitative Insights into Microbial Ecology 2 – QIIME2 (version 2020.2.0) (Bolyen et al., 2019). The barcode and primer sequence of raw demultiplexed reads were trimmed off and further processed by DADA2 to denoise and dereplicate reads, merge pair-end reads and remove chimeras (Callahan et al., 2016). The truncation length of 221 bp was used for both forward and reverse reads. The phylogenetic tree was built using FastTree and MAFFT alignment (Katoh et al., 2002; Price et al., 2010). The SILVA SSU Ref NR 99132 dataset was first trimmed to the corresponding primer region and trained as a classify-sklearn taxonomy classifier (Pedregosa et al., 2012; Quast et al., 2013; Bokulich et al., 2018). Subsequently, the amplicon sequence variants (ASV) were assigned taxonomy using the resulting classifier. After trimming and quality filtering, the sequencing of 16S rRNA gene yielded a total of 4,539,867 sequences from 140 samples. The ASV table was rarefied according to the minimum reads per sample (i.e., 21,377 reads) (Weiss et al., 2017). The generalized UniFrac distance matrix (alpha = 0.5) and alpha rarefaction was generated using the QIIME2 diversity plugin (Chen et al., 2012; Bolyen et al., 2019).

## 2.9. Statistical analysis

The data generated from plate counts and qPCR from both experiments were organized in Microsoft Corporation (2018) and statistically analyzed in SAS version 9.4 (SAS Institute Inc, 2013). Plating data are graphically represented as scatter panel plots showing bacterial counts as log (CFU/ml) and qPCR data as a box plot; plots were generated with R and the package ggplot2 (Wickham, 2016; R

Core Team, 2021). Data from Experiments 1 and 2 were treated by the same pattern.

Statistical analyses of fecal plate count data were performed with a mixed effect linear model (Proc Mixed procedure in SAS) due to the repeated measure structure of the data. The model included treatment, days post-infection (dpi), and their interactions as fixed factors and pen as a random factor. To account for the repeated structure when several observations were made on the same birds (focals) at different dpi we included an error term with an unstructured covariance matrix. Post-hoc tests were conducted to compare *C. jejuni* load (log CFU/ml) at individual dpi among treatment groups as well as to compare all dpi within each treatment. In order to compare *C. jejuni* loads through the whole challenge period between four treatment groups, plate count data were expressed as the mean of all observed dpi samples within one treatment (colonization mean). qPCR data were analyzed with the same mixed-effect linear model and in the same pattern as the plating data. However, the pen as a random factor and repeated structure were removed from the model since only one cecal sample per pen was analyzed. Residual plots were inspected to ensure that residual were approximately normally distributed with equal variances for all models. Results are considered significant if $p < 0.05$.

For cecal microbiota, diversity analyses were performed with the q2-diversity plugin. The rarefied ASV table was used to calculate the number of observed ASV. Kruskal–Wallis rank test with Benjamini & Hochberg (B-H) correction was used to observe statistical differences in a number of observed ASV between groups (i.e., dpi and treatment, Kruskal and Wallis, 1952; Benjamini and Hochberg, 1995). Principal coordinate analysis was used to visualize the difference in the microbial composition based on the generalized UniFrac distances. Permutational multivariate analysis of variance (PERMANOVA) test of generalized UniFrac distance matrix with (B-H) correction was conducted to evaluate the difference among groups (Anderson, 2001). To identify bacterial taxa that differed in abundance between groups, we performed an analysis of composition of microbiomes (ANCOM) (Mandal et al., 2015).

# 3. Results

## 3.1. Higher LAB concentration and lower pH in silage than in haylage

Monthly enumeration of LAB during the experiment period revealed that silage contained 8.0, 7.4, and 7.2 log CFU/g of LAB, respectively, while haylage levels were 5.0, 3.8, and 3.0 log CFU/g. Consequently, silage contained ≥3 × 10-log (CFU/g) higher LAB concentrations than haylage and a gradual decrease in LAB concentrations was observed in both matters. The silage pH measurement just prior to the experiment showed pH 4.4 while haylage displayed pH 6.2.

## 3.2. *Campylobacter jejuni* colonization impacted by silage and haylage treatment in R-308 but not in RR as determined by culture, no significant treatment effects determined by qPCR

Culture results revealed *Campylobacter jejuni* negativity in all birds prior to the infection and successful *C. jejuni* colonization in both broiler types after the challenge. In both experiments, *C. jejuni* loads peaked within 3 days after the challenge and thereafter colonization intensity had decreasing tendency with time.

In R-308, there was an overall significant treatment effect ($p = 0.023$) observed. Specifically, a significantly lower *C. jejuni* colonization mean was observed in the silage ($p = 0.010$) and haylage ($p = 0.013$) groups in comparison to the control (Figure 2). At 1 dpi, colonization in the silage group was significantly lower (2.01 logs) in comparison to the control group ($p = 0.039$). However, at the end of the experiment (19 dpi), there was no significant difference in the colonization between any of the treatments. No significant effect of *LP*256 (directly provided via the drinking water) treatment on *C. jejuni* loads was observed. A comparison of *C. jejuni* colonization within each treatment at 1 and 19 dpi (start and end of colonization period) revealed no significant difference in bacterial load (CFU/ml). The same was true for colonization comparison between the 3 dpi (supposed peak of *C. jejuni* load) and 19 dpi.

As determined by qPCR (Figure 3), *C. jejuni* loads in ceca at 3 dpi (25 days of age) or 20 dpi (42 days of age) were not significantly affected by dietary treatments in R-308. A comparison of *C. jejuni* colonization within treatment revealed a decreasing pattern between 3 dpi and 20 dpi. However, the differences in *C. jejuni* CFU/ml were not statistically significant.

No significant effect of treatments on *C. jejuni* loads was observed in RR as determined by culture (Figure 4). However, colonization comparison between the start of the infection period (1 dpi) and end of the trial (32 dpi) within each treatment revealed significant changes with mean reductions in *C. jejuni* of 2.65 and 2.46 10-log (CFU/ml) for *LP*256 and haylage, respectively ($p = 0.006$ and $p = 0.017$, respectively). Colonization comparison between the supposed peak of bacterial load (3 dpi) and end of the trial (32 dpi) displayed significant *C. jejuni* reduction in all treatment groups; $p = 0.002$, $p = 0.001$, $p = 0.001$, and $p = 0.001$ for control, *LP*256, haylage and silage group, respectively.

At 3, 13, or 34 dpi, no significant treatment effects on the ceca *C. jejuni* loads were observed in RR as determined by qPRC (Figure 5). Comparing *C. jejuni* loads between the supposed peak of bacterial colonization (3 dpi; 34 days of age) and end of the trial (34 dpi; 63 days of age) revealed significant reductions in control, *LP*256, and haylage group ($p = 0.001$, $p = 0.001$, and $p = 0.024$, respectively). A comparison between cecal *C. jejuni* colonization at 13 dpi (42 days of age) and 34 dpi for each treatment displayed significant *C. jejuni* reductions in the control, *LP*256, and silage groups ($p = 0.001$, $p = 0.032$, and $p = 0.014$, respectively).

## 3.3. *Firmicutes* and *Bacteroidota* dominated both R-308 and RR cecal microbiota, with significant changes observed in their relative abundances after the *Campylobacter* challenge

Characterization of the cecal microbiota composition before and after the *C. jejuni* challenge in Experiments 1 and 2 was performed by 16S rRNA amplicon sequencing. A total of 140 samples were analyzed and altogether 675 amplicon sequence variants (ASVs) were identified, representing 122 taxonomic genera, 52 families, 33 orders, 13 classes, and 5 phyla. The rarefaction curves of observed ASVs revealed sufficient sequencing depth to capture species richness at all time points tested in Experiment 1 (Supplementary Figure 5) and Experiment 2 (Supplementary Figure 6).

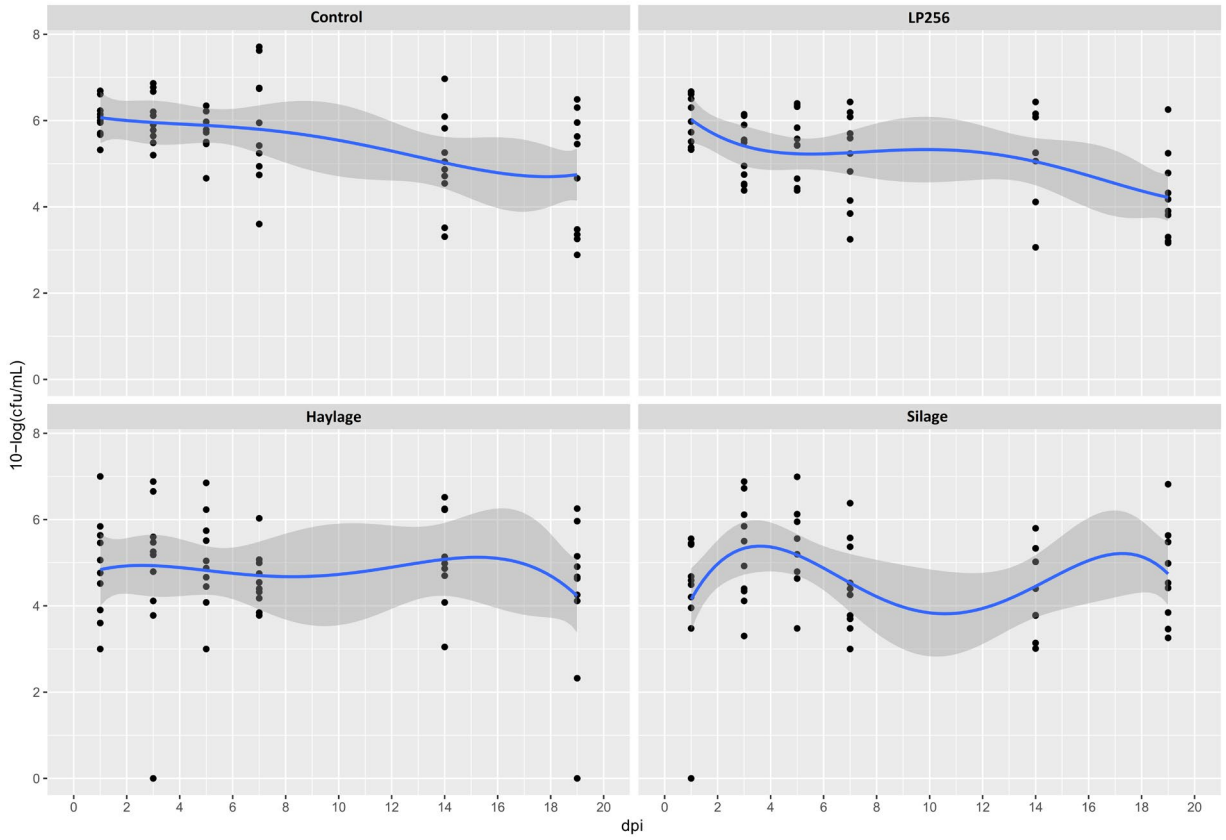


FIGURE 2
Culture-based colonization patterns of *C. jejuni* in four dietary treatment groups in Experiment 1. Black dots (data points) represent 10-log (CFU/ml) in individual fecal samples at a given day post-infection (dpi). The blue line is a smooth curve representing the trend of colonization based on the mean 10-log (CFU/ml) in each treatment with a 95% confidence band.

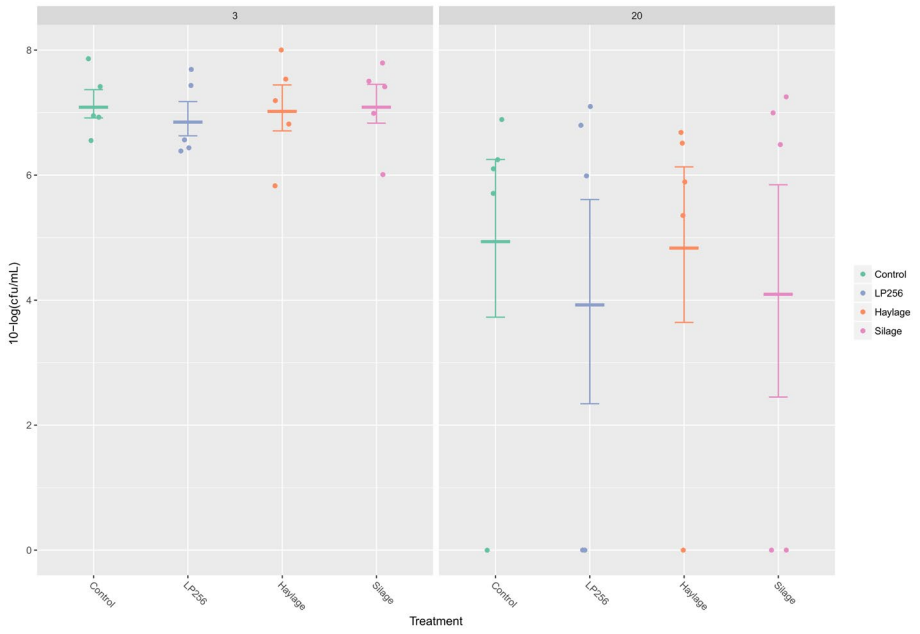


FIGURE 3
Quantitative PCR-based colonization dynamics of *C. jejuni* in the four dietary treatment groups at 3 and 20 days post-infection (dpi) in Experiment 1. The dots represent *C. jejuni* load (10-log CFU/ml) in individual caecal samples and line bars represent the mean 10-log CFU/ml with standard deviation.

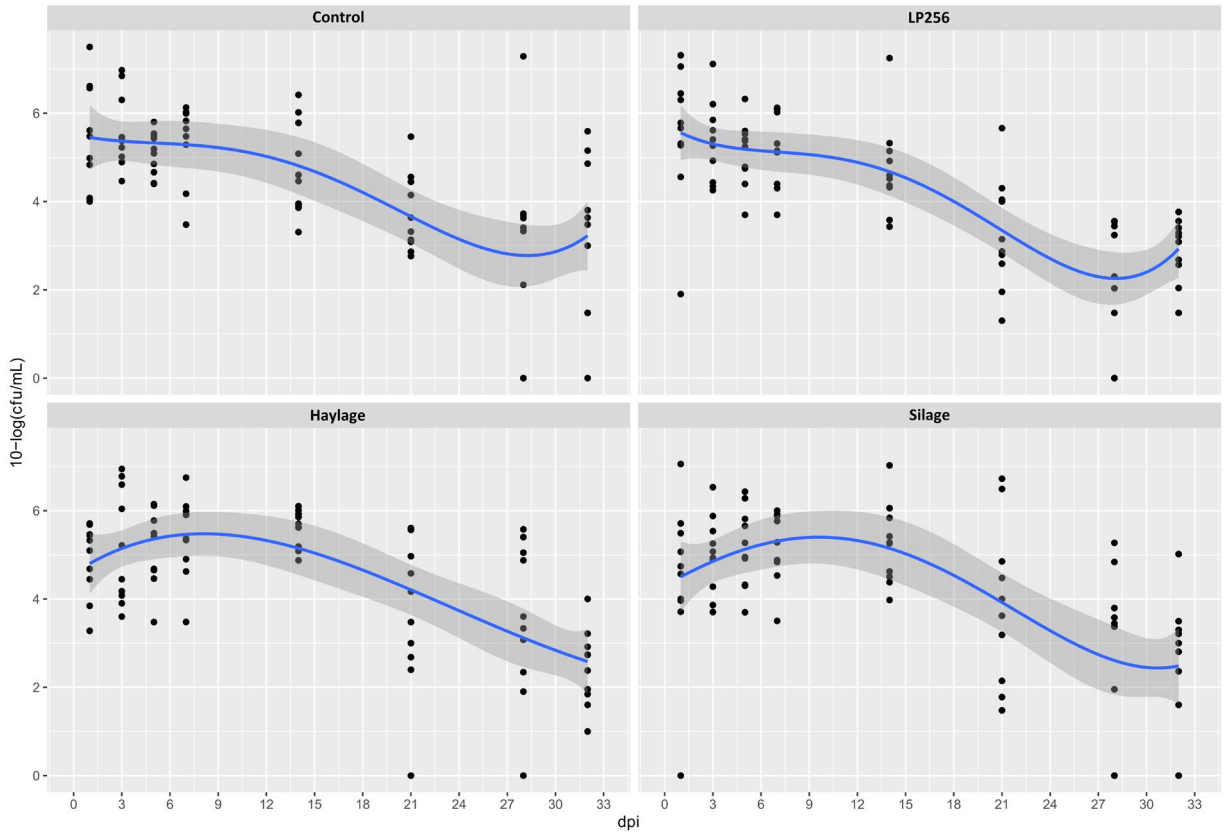


FIGURE 4
Culture-based colonization patterns of *C. jejuni* in four dietary treatment groups in Experiment 2. Black dots (data points) represent 10-log (CFU/ml) in individual fecal samples at a given day post-infection (dpi). The blue line is a smooth curve representing the trend of colonization based on the mean 10-log (CFU/ml) in each treatment with a 95% confidence band.

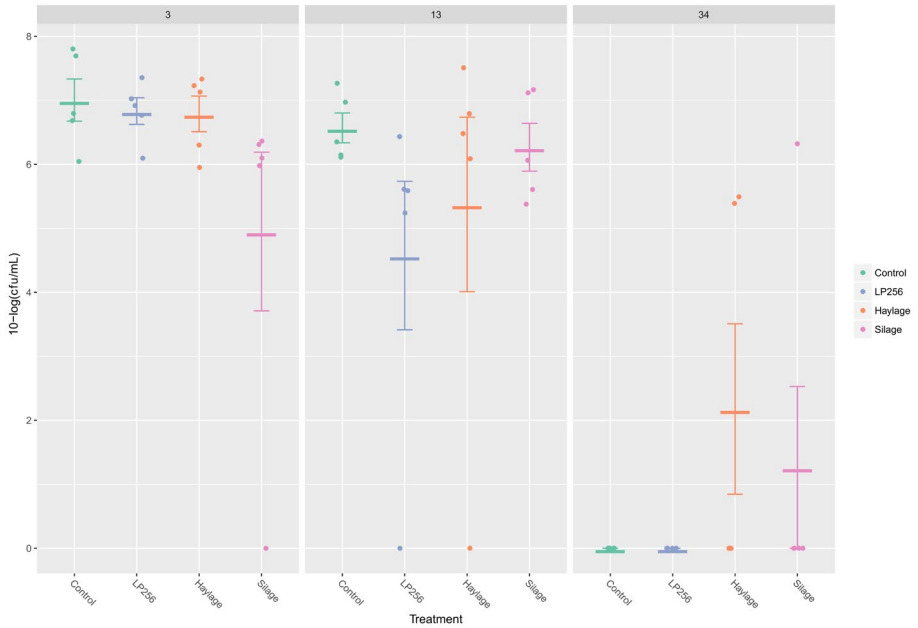


FIGURE 5
Quantitative PCR- based colonization dynamics of *C. jejuni* in the four dietary treatment groups at 3, 13, and 34 days post-infection (dpi) in Experiment 2. The dots represent *C. jejuni* load (10-log CFU/ml) in individual caecal samples and line bars represent the mean 10-log CFU/ml with standard deviation.

10.3389/fmicb.2023.1205797

In detail, 619 ASVs, representing 109 taxonomic genera and 5 phyla were observed in Experiment 1. Results of the principal coordinate analysis (PCoA) are shown in Figure 6 to visualize the variation of cecal microbiota between different days post-infection. Significant differences in the gut microbiota composition between different dpi were observed ($p = 0.001$), while no clear effect of the feed treatments on cecal microbiota composition was found; therefore, the treatments were pooled for further analysis.

At the phylum level, *Firmicutes* and *Bacteroidota* comprised more than 97.5% of the bacteria's relative abundance (RA) in all treatment groups at −1, 3, and 20 dpi, suggesting that they were the major components of the cecal microbiota (Figure 7). Since the different dietary treatments had no influence on the gut microbiota composition, treatments were pooled together and changes between different days post-infection were investigated. Changes in the RA at phylum level was observed after the *Campylobacter* challenge; a temporary decrease in the RA of phylum *Firmicutes* (mean RA at −1, 3, and 20 dpi was 84.2, 74.7, and 85.4% respectively) was substituted by a corresponding significant increase in *Bacteroidota* (mean RA at −1, 3, and 20 dpi was 14.5, 23.7, and 13.4%, respectively). The RA of phylum *Proteobacteria* decreased at 3 dpi and returned to a similar level as before the *C. jejuni* challenge at 20 dpi (mean RA at −1, 3, and 20 dpi was 1.3, 0.7, and 1.1% respectively). A significant increase in the RA of phyla *Campilobacterota* was observed at 3 dpi (mean RA of *Campilobacterota* at −1, 3, and 20 dpi was 0.01, 0.9, and 0.1% respectively). The RA of *Actinobacteriota* ranged from 0.02 to 0.04%.

At the genus level, the top 25 genera (Table 1) constituted 89% of the total sequencing read pool. Genus *Campylobacter* was added as the 26th genus due to the interest of this study. A description of major changes in the RA at the genus level between different dpi follows: genus *Bacteroides* was the most dominant in the cecal microbiota at −1 dpi and clearly most dominant after the *C. jejuni* challenge (3 dpi). Thereafter, a considerable decrease was observed to the advantage of other genera at 20 dpi (Table 1). *Clostridia* UCG-014 and uncultured *Ruminococcaceae* continuously increased in RA throughout the sampling points; where *Clostridia* UCG-014 became the most abundant genus at 20 dpi. A significant decrease in the RA of the twelfth most abundant genus *Lactobacillus* was observed after the *C. jejuni* challenge at 3 dpi. However, at 20 dpi the RA of this genus reached higher levels than before *C. jejuni* challenge. In the genera *Clostridia* vadinBB60 group and unclassified *Lachnospiraceae*, a decrease in RA appeared at 3 dpi and remained at a similar level at 20 dpi. The RA of the genera *Faecalibacterium* (the second most dominant bacterial genus in broilers' ceca), *Eisenbergiella*, *Subdoligranulum*, and *Escherichia-Shigella* decreased after *C. jejuni* challenge (3 dpi) but eventually, an increase was observed in all four genera at 20 dpi. As expected, the RA of genus *Campylobacter* significantly increased after the challenge (3 dpi) but had diminished at 20 dpi. Although clear general trends in the mean RA of different genera could be observed over the experiment as described above, there were high individual variations in the birds' cecal microbiota composition within the same treatment group at each infection time point (dpi).

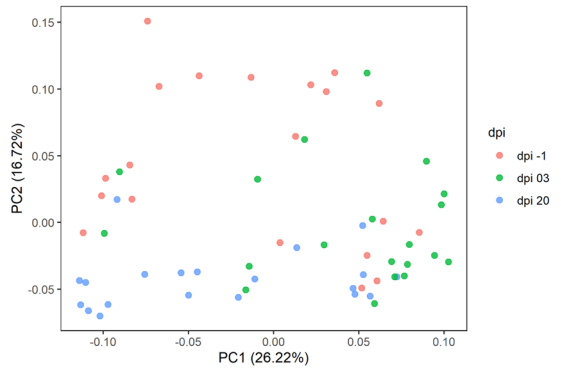


FIGURE 6
Principal coordinate analysis (PCoA) plot showing the differences in beta diversity based on generalized UniFrac distances between samples at −1, 3, and 20 days post-infection (dpi); represented by 20 caecal samples, respectively, for R-308. The dpi −1 is represented by samples before infection.

In Experiment 2, sequencing results comprised 671 ASVs, representing 121 taxonomic genera and 5 phyla. The results of the principal coordinate analysis are presented in the PCoA plot (Figure 8), where significant differences in the microbiota composition were observed ($p = 0.001$), while no clear effect of the feed treatments was found.

As seen in Experiment 1, cecal microbiota composition at the phylum level was dominated by *Firmicutes* and *Bacteroidota* also in Experiment 2; representing together at least 92.2% of the bacteria in all treatment groups (Figure 9) at −1, 3, 13, and 34 dpi. Proportional changes in RA were observed after the *C. jejuni* challenge (dpi 3) by an increase of phylum *Firmicutes* (mean RA at −1, 3, 13, and 34 dpi was 70.6, 84.5, 80.1, and 81.8% respectively) with a concomitant decrease of the taxonomic group *Bacteroidota* (mean RA at −1, 3, 13, and 34 dpi was 26.9, 13.6, 18.5, and 17.0% respectively). This was in contrast to the reverse pattern observed in Experiment 1. The RA of phylum *Proteobacteria* decreased after the infection (3 dpi), remained on a similar level at 13 dpi, and eventually increased again at 34 dpi; mean RA at −1, 3, 13, and 34 dpi was 2.4, 1.6, 1.3, and 2.1%, respectively. A significant increase in RA of the phylum *Campilobacterota* was observed at 3 dpi; mean RA at −1, 3, 13, and 34 dpi was 0.01, 0.3, 0.1, and 0.01%, respectively. The RA of phylum *Actinobacteriota* increased continuously throughout the experiment, ranging from 0.03–0.09%.

The top 25 genera (Table 2) constituted 91% of the total sequencing read pool. Genus *Campylobacter* was added as the 26th genus due to the interest of the study. A description of the trends in relative abundance at genus level during the experiment period follows: *Faecalibacterium* was the second most abundant genus at −1 dpi, the most abundant after the *C. jejuni* challenge (3 dpi), and clearly the most abundant at 13 and 34 dpi. *Bacteroides* dominated the cecal microbiota at −1 dpi. Despite a considerable decrease after *C. jejuni* challenge, the genus was the second most dominant at 3, 13, and 34 dpi. The RA of the genera *Clostridia* UCG-014, *Ruminococcus torques* group, and uncultured *Ruminococcaceae* peaked at 3 dpi, and thereafter gradually decreased at 13 and 34 dpi. Genus *Lactobacillus* was the ninth most abundant bacteria present in the ceca and its RA increased throughout all sampling points. Relative abundance of genera unclassified *Lachnospiraceae* and *Subdoligranulum* increased at 3 dpi, decreased at 13 dpi, and was maintained at a similar level at 34 dpi. In the genus *Clostridia* vadinBB60 group, a continuous decrease in RA was seen throughout the sampling points. *Escherichia-Shigella* decreased after the challenge and remained on the same level

10.3389/fmicb.2023.1205797

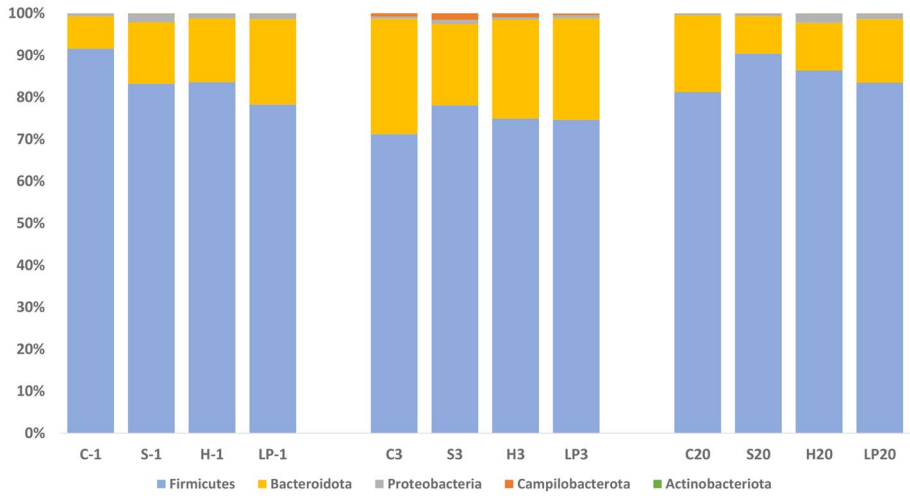


FIGURE 7
Phylum-level relative abundance (%) of broiler caecal microbiota in Experiment 1 (R-308) at each treatment and days post-infection (dpi): –1, 3, and 20. The treatment groups shown are the following: dietary treatment and dpi. C, control feed; S, diet based on 85% of pellets and 15% of silage; H, diet based on 85% of pellets and 15% of haylage; LP, control feed and water inoculated with $10^7$ CFU/mL of viable *L. plantarum* 256.

**TABLE 1** The mean and SD of relative abundance (%) of the top 25 genera of broiler cecal microbiota at each day post-infection (dpi) in Experiment 1.

| Family | Genus | –1 dpi (%) | 3 dpi (%) | 20 dpi (%) |
|---|---|---|---|---|
| Bacteroidaceae | *Bacteroides* | 14.5 ± 5.2 | 23.7 ± 3.3 | 13.4 ± 4.2 |
| Ruminococcaceae | *Faecalibacterium* | 9.4 ± 4.0 | 8.2 ± 3.9 | 13.7 ± 1.5 |
| Same as genus | *Clostridia* UCG-014 | 4.1 ± 0.7 | 9.9 ± 1.9 | 16.1 ± 3.4 |
| Same as genus | *Clostridia* vadinBB60 group | 12.7 ± 5.3 | 6.8 ± 2.7 | 6.4 ± 0.6 |
| Lachnospiraceae | unclassified *Lachnospiraceae* | 8.2 ± 1.6 | 6.9 ± 0.5 | 6.3 ± 0.9 |
| Lachnospiraceae | *Ruminococcus torques* group | 6.2 ± 0.9 | 6.7 ± 1.4 | 5.4 ± 0.9 |
| Lachnospiraceae | *Eisenbergiella* | 3.7 ± 0.9 | 2.6 ± 0.3 | 2.7 ± 0.6 |
| Ruminococcaceae | *Subdoligranulum* | 2.0 ± 1.3 | 1.8 ± 0.7 | 3.5 ± 1.1 |
| Ruminococcaceae | *Negativibacillus* | 2.4 ± 0.2 | 2.0 ± 1.2 | 2.1 ± 0.2 |
| Oscillospiraceae | *Colidextribacter* | 2.2 ± 0.3 | 2.5 ± 0.5 | 1.6 ± 0.2 |
| Ruminococcaceae | uncultured *Ruminococcaceae* | 1.6 ± 0.1 | 1.8 ± 0.2 | 2.2 ± 0.4 |
| Lactobacillaceae | *Lactobacillus* | 1.7 ± 0.7 | 0.9 ± 0.9 | 2.9 ± 1.2 |
| Oscillospiraceae | uncultured *Oscillospiraceae* | 1.3 ± 0.3 | 2.1 ± 0.4 | 1.8 ± 0.5 |
| Lachnospiraceae | *Lachnospiraceae* NK4A136 group | 2.6 ± 0.7 | 1.2 ± 0.2 | 1.4 ± 0.5 |
| Peptostreptococcaceae | unclassified *Peptostreptococcaceae* | 4.3 ± 7.6 | 0.1 ± 0.2 | 0.0 ± 0.0 |
| Same as genus | [*Eubacterium*]_coprostanoligenes_group | 1.4 ± 0.2 | 1.2 ± 0.1 | 1.6 ± 0.1 |
| Lachnospiraceae | *Lachnospiraceae* GCA-900066575 | 1.4 ± 0.3 | 1.2 ± 0.4 | 1.1 ± 0.4 |
| Oscillospiraceae | unclassified *Oscillospiraceae* | 1.1 ± 0.3 | 1.9 ± 0.7 | 0.5 ± 0.3 |
| Oscillospiraceae | *Oscillibacter* | 1.2 ± 0.3 | 1.2 ± 0.1 | 1.0 ± 0.2 |
| Lachnospiraceae | *Blautia* | 1.6 ± 0.5 | 1.0 ± 0.1 | 0.8 ± 0.2 |
| Lachnospiraceae | *Lachnoclostridium* | 1.5 ± 0.5 | 1.1 ± 0.2 | 0.8 ± 0.2 |
| Ruminococcaceae | *Ruminococcaceae* Incertae Sedis | 1.0 ± 0.3 | 1.1 ± 0.3 | 0.9 ± 0.1 |
| Enterobacteriaceae | *Escherichia-Shigella* | 1.2 ± 0.6 | 0.7 ± 0.2 | 1.1 ± 0.9 |
| Same as genus | *Bacilli*_RF39 | 0.6 ± 0.3 | 1.0 ± 0.2 | 1.4 ± 0.4 |
| Butyricicoccaceae | *Butyricicoccus* | 0.8 ± 0.1 | 1.0 ± 0.3 | 0.5 ± 0.2 |
| *Campylobacteraceae | **Campylobacter* | 0.01 ± 0.01 | 0.9 ± 0.5 | 0.1 ± 0.1 |

Genus *Campylobacter* (*) was added as the 26th genus due to the interest of the study.

at 13 dpi; thereafter an increase was observed at the end of the trial. The RA of *Campylobacter* significantly increased after the infection (3 dpi) and declined at 13 and 34 dpi. As observed in Experiment 1, a high individual variation in birds' cecal microbiota composition was observed also in Experiment 2.

## 4. Discussion

Previous studies have shown that probiotics can modulate broilers' gastrointestinal microbiota, provide beneficial health effects, and increase birds' resistance to pathogens (Pourabedin and Zhao, 2015). In particular, LAB have been shown to provide inhibitory effects on *C. jejuni* colonization, and feed additives containing such bacteria could therefore be a promising approach to reduce the occurrence of *Campylobacter* spp. in primary production (Guyard-Nicodème et al., 2016). Although some studies have reported promising effects, there are challenges related to the storage, distribution, and rationally feasible means of administration of such probiotics to the broilers (Krysiak et al., 2021). In this study, we assessed the possibility of providing LAB by the inclusion of grass silage inoculated with the strain *Lactiplantibacillus plantarum* 256 in the broiler's daily feed. According to Commission Regulation (EC) 889/2008 (2008), all birds kept in organic settings in the EU must have daily access to forage, with grass silage being one of the allowable options. With this requirement in mind, we sought to investigate whether the silage may serve as a diet component with the potential to reduce *C. jejuni* in broilers' guts. In addition, to evaluate whether the potential effect was caused by *L. plantarum 256* itself, we also tested the direct provision of this strain via drinking water.

Our results from colony counts after agar plate culturing for R-308 (Experiment 1) displayed lower *C. jejuni* mean colonization in the silage and haylage treatment groups and significantly lower *C. jejuni* colonization (2 logs) in the silage group compared to the control 1 day after the challenge. However, this effect did not last and no differences in colonization were observed between treatment groups at the end of the experiment period. This result suggests that silage and to some extent haylage could have an inhibitory effect against low loads of ingested *C. jejuni* in the R-308, but clearly could not protect the broilers from *C. jejuni* colonization. A similar initial inhibitory effect could not be observed in the RR where no differences in *C. jejuni* loads between the treatment groups were observed in Experiment 2. High LAB content and low pH in fermented feeds have been previously reported as promising feed attributes in order to reduce the Ross 308 broiler chickens' susceptibility to *Campylobacter* spp. colonization (Heres et al., 2004). In the current study, lactic acid bacteria counts in ensiled forage and pH evaluation revealed that silage contained notably higher LAB concentrations and lower pH in comparison to the haylage. This may partly explain why *C. jejuni* loads at the beginning of the challenge in Experiment 1 were significantly lower in the silage group compared to the control, while only a moderate (non-significant) reduction was observed in the haylage treatment.

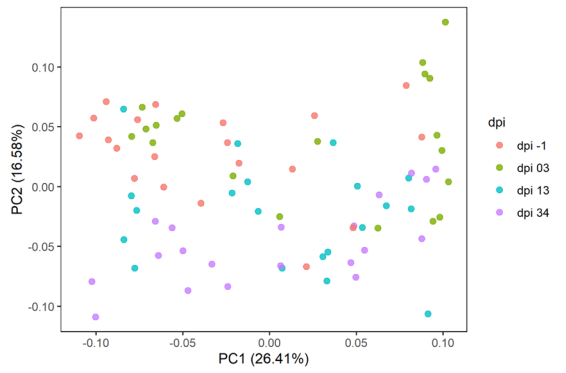


FIGURE 8
Principal coordinate analysis (PCoA) plot showing differences in beta diversity based on generalized UniFrac distances between samples at −1, 3, 13, and 34 days post-infection (dpi); represented by 20 samples, respectively, for RR. The dpi −1 is represented by samples before infection.

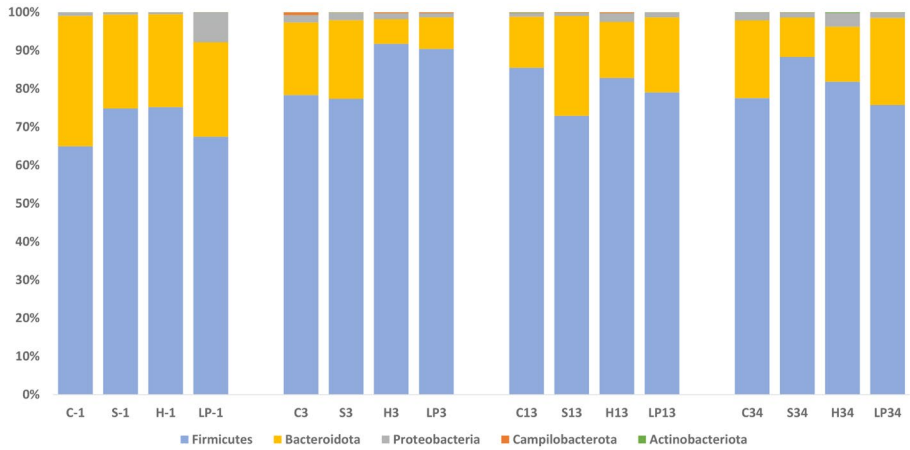


FIGURE 9
Phylum relative abundance (%) of broiler caecal microbiota in Experiment 2 (RR) at each treatment and days post-infection (dpi): −1, 3, 13, and 34. The treatment groups shown are the following: dietary treatment and dpi. C, control feed; S, diet based on 85% of pellets and 15% of silage; H, diet based on 85% of pellets and 15% of haylage; LP, control feed and water inoculated with $10^7$ CFU/mL of viable *L. plantarum* 256.

TABLE 2 The mean and SD of relative abundance (%) of the top 25 genera of broiler cecal microbiota at each day post-infection (dpi) in Experiment 2.

| Family | Genus | −1 dpi (%) | 3 dpi (%) | 13 dpi (%) | 34 dpi (%) |
|---|---|---|---|---|---|
| Ruminococcaceae | *Faecalibacterium* | 14.1 ± 4.8 | 14.7 ± 2.4 | 25.9 ± 4.2 | 27.9 ± 4.6 |
| Bacteroidaceae | *Bacteroides* | 25.9 ± 5.8 | 14.6 ± 8.7 | 18.5 ± 5.8 | 17.0 ± 5.7 |
| Same as genus | *Clostridia* UCG-014 | 6.9 ± 0.9 | 13.9 ± 3.2 | 9.5 ± 1.7 | 7.2 ± 2.6 |
| Lachnospiraceae | unclassified *Lachnospiraceae* | 5.9 ± 1.8 | 6.3 ± 0.4 | 5.0 ± 0.8 | 5.6 ± 0.7 |
| Ruminococcaceae | *Subdoligranulum* | 4.2 ± 1.4 | 6.1 ± 3.7 | 2.7 ± 0.7 | 3.0 ± 1.6 |
| Same as genus | *Clostridia* vadinBB60 group | 5.3 ± 1.8 | 5.0 ± 2.1 | 3.3 ± 0.6 | 2.1 ± 1.1 |
| Lachnospiraceae | *Ruminococcus torques* group | 4.1 ± 0.2 | 4.4 ± 0.6 | 3.6 ± 0.4 | 3.2 ± 0.7 |
| Lachnospiraceae | *Eisenbergiella* | 2.5 ± 0.6 | 2.1 ± 0.2 | 2.9 ± 0.9 | 2.8 ± 0.8 |
| Lactobacillaceae | *Lactobacillus* | 1.1 ± 0.5 | 2.0 ± 0.6 | 2.6 ± 0.4 | 3.1 ± 1.1 |
| Ruminococcaceae | *Negativibacillus* | 2.3 ± 0.1 | 1.8 ± 0.2 | 2.1 ± 0.4 | 2.4 ± 0.6 |
| Ruminococcaceae | uncultured *Ruminococcaceae* | 2.0 ± 0.3 | 2.2 ± 0.5 | 2.0 ± 0.3 | 1.9 ± 0.5 |
| Enterobacteriaceae | *Escherichia-Shigella* | 2.8 ± 3.4 | 1.3 ± 0.6 | 1.3 ± 0.7 | 1.7 ± 1.0 |
| Oscillospiraceae | *Colidextribacter* | 2.0 ± 0.3 | 1.8 ± 0.3 | 1.6 ± 0.4 | 1.3 ± 0.2 |
| Lachnospiraceae | *Lachnospiraceae* NK4A136 group | 1.1 ± 0.9 | 0.9 ± 0.1 | 1.7 ± 0.7 | 2.6 ± 3.3 |
| Same as genus | [*Eubacterium*] coprostanoligenes gr. | 1.6 ± 0.2 | 2.3 ± 0.6 | 1.5 ± 0.3 | 0.9 ± 0.3 |
| Oscillospiraceae | uncultured *Oscillospiraceae* | 1.6 ± 0.3 | 1.5 ± 0.2 | 1.2 ± 0.3 | 1.3 ± 0.3 |
| Oscillospiraceae | *Oscillibacter* | 1.3 ± 0.3 | 1.2 ± 0.1 | 1.1 ± 0.3 | 1.4 ± 0.3 |
| Same as genus | *Bacilli* RF39 | 1.0 ± 0.4 | 1.1 ± 0.5 | 1.2 ± 0.7 | 1.4 ± 0.6 |
| Lachnospiraceae | *Lachnoclostridium* | 1.1 ± 0.3 | 1.1 ± 0.2 | 0.8 ± 0.1 | 1.2 ± 0.4 |
| Lachnospiraceae | *Lachnospiraceae* GCA-900066575 | 0.9 ± 0.3 | 0.8 ± 0.2 | 0.8 ± 0.2 | 1.1 ± 1.1 |
| Oscillospiraceae | *Flavonifractor* | 0.7 ± 0.1 | 0.9 ± 0.2 | 0.7 ± 0.2 | 1.1 ± 0.3 |
| Erysipelatoclostridiaceae | *Erysipelatoclostridium* | 0.6 ± 0.3 | 1.2 ± 1.0 | 0.7 ± 0.5 | 0.4 ± 0.3 |
| Lachnospiraceae | *Blautia* | 0.7 ± 0.2 | 0.8 ± 0.2 | 0.6 ± 0.1 | 0.8 ± 0.1 |
| Ruminococcaceae | *Ruminococcus* | 0.4 ± 0.1 | 0.8 ± 0.4 | 1.2 ± 0.4 | 0.4 ± 0.2 |
| Ruminococcaceae | *Ruminococcaceae* Incertae Sedis | 0.8 ± 0.4 | 0.8 ± 0.2 | 0.6 ± 0.2 | 0.5 ± 0.2 |
| *Campylobacteraceae | **Campylobacter* | 0.01 ± 0.01 | 0.31 ± 0.29 | 0.13 ± 0.09 | 0.01 ± 0.01 |

Genus *Campylobacter* (*) was added as the 26th genus due to the interest of the study.

*In vivo* trials investigating the silage effect on *C. jejuni* colonization are currently rare. A study published by Ranjitkar et al. (2016) showed no significant differences in the load of *C. jejuni* between the treatment groups provided with different levels of crimped kernel maize silage in diets (replacement of 15 and 30% of pelleted feed with maize-silage) in comparison to the control. This discrepancy in results may be explained by differences in the type of silage, consumption levels, or by effects of broiler type and and age. The broiler type and age are also likely explanations as to why the reduction of *C. jejuni* loads were observed at the beginning of Experiment 1 in the R-308, while no effect was observed in the RR in Experiment 2. It is well known that fast-growing birds have a higher feed intake than slow-growing ones (Quentin et al., 2004; Sarica et al., 2020; Jong et al., 2021). For that reason, it was of interest to test the effects of silage in both fast- and slow-growing broilers. Hence, since a numerically higher intake of total mixed ratios, containing forage as silage and haylage, was observed in Ross 308 compared to Rowan Ranger birds (Valečková et al., 2020), it is possible that the inhibitory effect of silage on *C. jejuni* colonization seen at the beginning of Experiment 1 was related to the level of daily consumption of forage.

No significant treatment effect was seen on the reduction of *C. jejuni* in feces or ceca when *Lactiplantibacillus plantarum* 256 was directly provided in the drinking water to the R-308 or RR, neither by plate counts nor by qPCR. This suggests that although extracts from silage inoculated with this strain could inhibit *C. jejuni* growth *in vitro* (unpublished data), the presence of this strain in the broiler's intestinal tract at the level of administration ($10^7$ CFU/mL) used in this study could not effectively inhibit *C. jejuni* colonization. This could be related both to dosage and to the strain used. In a study by Arsi et al. (2015), 26 LAB isolates with the greatest inhibitory activity *in vitro* were further tested in a broiler trial where birds were challenged with $10^4$ CFU *C. jejuni* in a 100 µL suspension of tryptone salt broth. Only 3 out of these 26 isolates demonstrated a reduction in *Campylobacter* counts (approximate 1–2 log) in comparison to the control. *In vitro* assay results are known to not always translate into comparable results under *in vivo* settings, due to differences in the final probiotic supplement composition, its dose and application pattern, trial conditions, and thus different outcomes of the probiotic activity. In addition, *in vitro* studies do not take into account the variability and complexity of the birds' gastrointestinal environment

and their interaction with probiotics and *Campylobacter* strains (Smialek et al., 2021). Nevertheless, inhibitory effects on *C. jejuni in vivo* after direct administration of *Lactiplantibacillus* spp. have been demonstrated in several studies. For example, Saint-Cyr et al. (2017) showed that Ross broilers treated with oral gavage of *Lactobacillus salivarius* SMXD51 ($10^7$ CFU) at 24 h after hatch displayed a significant reduction in *C. jejuni* loads present in the gut at 14 days of age (0.82 logs) and 35 days of age (2.81 logs) in comparison to the control. Additionally, Neal-McKinney et al. (2012) reported that *Lactobacillus crispatus* JCM 5810 administered to broiler chickens by oral gavage ($10^8$ CFU) at the day of hatch and 4 days post-hatch was an effective competitive exclusion organism for *C. jejuni* resulting in a reduction in the total number of *C. jejuni* colonized broilers and lower microbial load at 21 days post-hatch.

In both experiments in this study, *C. jejuni* loads in feces peaked at the beginning of the challenge, after which a decrease over time was observed. This is in agreement with previous findings, e.g., Achen et al. (1998) found that 70% of the broilers were shedding *C. jejuni* within 48 h after artificial infection, and a steady decline in fecal shedding was observed after the third-week post-infection; at 6 weeks after infection, only 38% of the birds were shedding *C. jejuni* in their feces. In the current study, the decline of *C. jejuni* loads with time was more prominent in Experiment 2 (in the RR), where the comparison between the peak of *C. jejuni* bacterial load at 3 dpi to that at the end of the challenge at 34 dpi, displayed significant *C. jejuni* reduction in all treatment groups. However, this was likely due to the fact that in Experiment 2, *C. jejuni* colonization after the challenge was monitored for 2 weeks longer than in Experiment 1.

*Campylobacter jejuni* loads in cecal samples from both experiments were quantified using a qPCR assay. Comparison between cecal samples analyzed by qPCR and fecal samples analyzed by plate counting revealed higher numbers of *C. jejuni* in cecal samples in both experiments, consistent with previous studies (Berrang et al., 2000; Rudi et al., 2004). However, in some cases, *C. jejuni* loads in cecal samples were below the detection limit of the qPCR, despite fecal cultures being *C. jejuni* positive. This inconsistency can be attributed to the lower sensitivity of our qPCR, whose limit of detection was $3.3 \times 10^5$ CFU/g (Appendix 3) and is likely the reason for the significant *C. jejuni* reduction observed in Experiment 2 when different infection time points (3 dpi to 34 dpi and 13 dpi to 34 dpi) were compared. Consistent with the findings from the *C. jejuni* colony counts from fecal samples (except observation in the forage treatments in Experiment 1), there were no significant effects of the dietary treatments on the cecal *C. jejuni* loads in either of the two experiments. Similarly, there was no significant reduction in cecal *C. jejuni* loads between 3 dpi and the end of Experiment 1, but a significant reduction was seen at the end of Experiment 2 in *LP*256, haylage, and silage groups. This reduction seemed to be independent of the treatment, consistent with our culture-based results from fecal samples.

The broiler digestive tract is colonized by a wide variety of bacterial species, with the caecum being by far the most densely colonized and studied microbial site of the gut (Pourabedin and Zhao, 2015). Generally, the major phylum in the broiler cecal microbiota is *Firmicutes*, followed by two less abundant phyla, *Bacteroidota*, and *Proteobacteria* (Oakley et al., 2014; Kers et al., 2018). This is reflected in our current results from Illumina 16S amplicon sequencing of cecal samples at different infection time points throughout the two experiments, where *Firmicutes* was the most abundant phylum, followed by the phylum *Bacteroidota*. Lower relative abundances of *Proteobacteria*, *Campilobacterota* (as a result of the *C. jejuni* challenge), and *Actinobacteriota* were observed. Before the *C. jejuni* challenge (−1 dpi), a lower relative abundance of *Bacteroidota* was observed in all treatment groups in R-308, than its RA in RR. Based on results from previous studies by Connerton et al. (2018) and Richards et al. (2019), this difference could be due to the type of broiler used, but also due to the different ages of the birds at the *C. jejuni* exposure since the RR birds in Experiment 2 were challenged 7 days later that the R-308 in Experiment 1. *Actinobacteria* and *Proteobacteria* together represented less than 2 and 2.5% in R-308 and RR cecal samples, respectively, which aligns with their usual representation of around 2 to 3% in the total broiler cecal microbiota (Rychlik, 2020).

There were no significant effects of the different feed treatments on the broiler's cecal microbiota composition in either of the two different broiler types. However, several distinct changes in relative abundance related to the *C. jejuni* challenge were noted both on phylum and genus levels. In Experiment 1, a decrease in the RA of *Firmicutes* appeared in the R-308 after the *C. jejuni* challenge, which was accompanied by a parallel increase in the RA of *Bacteroidota*. In Experiment 2, the opposite was observed. Previous studies have reported changes in *Bacteroidota* abundance linked to interactions with *Campylobacter*, where, e.g., elevated RA of *Bacteroidetes* was found in *Campylobacter-positive* broilers (Sofka et al., 2015), in agreement with our observations at 3 dpi in R-308. Interestingly, the opposite correlation was observed in a study by Sakaridis et al. (2018) where the elevated abundance of *Firmicutes* and decreased *Bacteroidetes* levels were found in broilers with high *Campylobacter* counts, in line with our observations in RR after the *C. jejuni* challenge. This shows the complexity of gut microbiota interactions, where one stimulus (*C. jejuni* challenge in this case) may have opposing effects on the microbiota composition in two different broiler types.

In both experiments, the predominant phylum *Firmicutes* largely consisted of class Clostridia represented by the genera *Faecalibacterium*, *Clostridia* UCG-014, *Clostridia* vadinBB60 group, and unclassified *Lachnospiraceae*, with other bacteria belonging to families *Lachnosporaceae* and *Ruminococcaceae* at lower percentages. Phylum *Bacteroidota* on the other hand consisted of the sole genus *Bacteroides*. This genus is able to produce short-chain fatty acids, compounds contributing to maintaining mucosal integrity, immunity, and health of broilers (Ali et al., 2022). The most dominant genus in the phylum *Proteobacteria* was the facultatively anaerobic *Escherichia-Shigella*, whose abundance decreased after the *C. jejuni* challenge. This was in contrast to the genus *Clostridia* UCG-014, whose relative abundance increased after the *C. jejuni* challenge. Similar findings were reported by Awad et al. (2016), where 14-day-old Ross 308 broilers were challenged with $1 \times 10^8$ CFU of *C. jejuni* NCTC 12744. In that study, *C. jejuni* colonization was associated with an alteration of the gut microbiota with infected birds having a significantly lower abundance of *Escherichia coli*, while the level of *Clostridium* spp. was higher in infected birds compared to non-infected. However, it should be noted that the higher abundance of *Clostridium spp*. induced after the *C. jejuni* challenge was not straightforward in the present study, since a

concomitant decrease in the relative abundance of the genus *Clostridia* vadinBB60 group was observed. Notably, 23 out of the top 25 genera were commonly observed in both R-308 and RR. In spite of this fact, high individual variation in the birds' cecal microbiota composition within the same broiler type, treatment group, and at the same infection time point in relation to the *C. jejuni* challenge was observed. This is in agreement with a previous study where great individual microbiota variation between animals within a single uniformly derived and treated group, under highly controlled experimental conditions, was reported (Stanley et al., 2014). The authors of that study speculate that the likely reasons for this variation are the lack of exposure to maternally obtained bacteria and the sensitivity to colonization by environmental bacteria in hatcheries.

Our aim with this study was to compare different strategies to administer LAB in order to increase their content in the broilers' gut and create an unfavorable environment for *Campylobacter*. The relative abundance of genus *Lactobacillus* in both Experiments was relatively high, the twelfth most abundant bacteria in the gut in Experiment 1 and the ninth most abundant in Experiment 2. However, neither the addition of silage LAB (including *Lactiplantibacillus plantarum* 256) nor the *L. plantarum* 256 supplemented in water affected the relative abundance of *Lactobacillus* in broilers' ceca compared to the control birds that did not receive any LAB. Therefore, we speculate that the initial inhibition of *C. jejuni* growth in feces observed in the silage group in Experiment 1, may be pH dependent rather than due to the presence of LAB. In contrast, a possible effect of *C. jejuni* colonization on the *Lactobacillus* abundance was observed in sequencing data, where the relative abundance of the genus *Lactobacillus* decreased after the *C. jejuni* challenge in Experiment 1, independent of treatment. With the possible impact of lower *C. jejuni* abundance with time after the challenge, the highest presence of *Lactobacillus* was observed at 20 dpi. Interestingly, a linkage between the genera *Lactobacillus* and *Campylobacter* has been previously reported by Sofka et al. (2015), where LAB were found to be significantly higher, in total cultural colony counts, in *Campylobacter-negative* samples from broiler flocks in comparison to the *Campylobacter-positive* ones. Yet, the same correlation was not observed in Experiment 2, where the relative abundance of genus *Lactobacillus* increased after the *C. jejuni* challenge, and its abundance was increasing with time after the infection, independently of treatments. Moreover, even if the genus *Lactobacillus* had at −1 dpi relatively high abundance in RR ceca in the silage and LP256 group in comparison to the control (not significant), no effect of its presence on *Campylobacter* loads was observed after the infection.

Despite the fact that all tested birds were culture negative for *Campylobacter* the day before infection (−1 dpi), we unexpectedly observed a relative abundance of 0.01% of the genus *Campylobacter* in both experiments at −1 dpi. Because the same minor presence of this genus was observed in −1 dpi samples in both experiments, although birds were sampled 1 week apart, and no *C. jejuni* were detected by culture, it is highly unlikely that the 16S amplicon sequence variants reflect the actual presence of *C. jejuni*. If *C. jejuni* would have been present in the stable before the challenge, the level of abundance detected by 16S amplicon sequencing would likely differ between Experiments 1 and 2. Furthermore, the abundance of *C. jejuni* would have been higher since it is well established that after infection, broilers rapidly accumulate high numbers of *C. jejuni* in the cecal content within 3 days (Shanker et al., 1990). Therefore, we assume that contamination in DNA extraction has occurred.

In conclusion, the current study shows that grass silage inoculated with *L. plantarum* 256 (provided as TMR) or water supplemented with *LP*256 are not effective interventions against *C. jejuni* colonization in R-308 or RR broilers. Yet, the minor reductions in *C. jejuni* observed at 1 dpi in fecal samples from R-308 suggest that this approach could still be explored and optimized for better effects. However, it should be noted that due to the cfu/g expression, the reduction in *C. jejuni* load in one group may be artificially biased compared to the other groups.

Further optimization could involve a change from a grass-based silage to a wheat-based silage, as the latter is likely to be more palatable to the birds and hence result in a larger amount of LAB consumed. This could potentially induce greater gut colonization and a stronger inhibitory effect on *C. jejuni*. However, further research is needed to confirm this hypothesis, together with the evaluation of wheat-based silage inclusion levels on the broiler's performance. It is evident from this work that *C. jejuni* presence as well as broiler type and age had much greater effects on the cecal microbiota composition than the different feed additives.

## Data availability statement

The data presented in the study are deposited in the NCBI repository, accession number PRJNA876811, https://www.ncbi.nlm.nih.gov/bioproject/PRJNA876811.

## Ethics statement

The animal study was reviewed and approved by the Uppsala Ethics Committee for Animal Research, Uppsala, Sweden. Protocol number 5.8.18-16271/2017.

## Author contributions

HWall, EI, KK, and PE obtained the funding and designed the experiments, with HWall as the project leader. EV, HWall, EI, PE, HWang, and FD obtained samples during the study. EV analyzed, interpreted, and compiled the data. LS performed the bioinformatics analysis. FD and HWang performed the plating, DNA extraction, and qPCR analysis. EV wrote the major part of the manuscript, and PE and LS some parts. All authors contributed to the article and approved the submitted version.

## Funding

This work was supported by the SLU EkoForsk, Swedish University of Agricultural Sciences (2016.4.1-742-10).

## Conflict of interest

The authors declare that the research was conducted in the absence of any commercial or financial relationships that could be construed as a potential conflict of interest.

## Publisher's note

All claims expressed in this article are solely those of the authors and do not necessarily represent those of their affiliated organizations, or those of the publisher, the editors and the reviewers. Any product that may be evaluated in this article, or claim that may be made by its manufacturer, is not guaranteed or endorsed by the publisher.

## Supplementary material

The Supplementary material for this article can be found online at: https://www.frontiersin.org/articles/10.3389/fmicb.2023.1205797/full#supplementary-material

## References


Abd El-Hack, M. E., El-Saadony, M. T., Shafi, M. E., Qattan, S. Y. A., Batiha, G. E., Khafaga, A. F., et al. (2020). Probiotics in poultry feed: a comprehensive review. *J. Anim. Physiol. Anim. Nutr.* 104, 1835–1850. doi: 10.1111/jpn.13454

Achen, M., Morishita, T. Y., and Ley, E. C. (1998). Shedding and colonization of *Campylobacter jejuni* in broilers from day-of-hatch to slaughter age. *Avian Dis.* 42, 732–737. doi: 10.2307/1592708

Ali, Q., Ma, S., La, S., Guo, Z., Liu, B., Gao, Z., et al. (2022). Microbial short-chain fatty acids: a bridge between dietary fibers and poultry gut health—a review. *Anim. Biosci.* 35, 1461–1478. doi: 10.5713/ab.21.0562

Anderson, M. J. (2001). A new method for non-parametric multivariate analysis of variance. *Austral Ecol.* 26, 32–46. doi: 10.1111/j.1442-9993.2001.01070.pp.x

Arsi, K., Donoghue, A., Wooming, A., Blore, P., and Donoghue, D. (2015). The efficacy of selected probiotic and prebiotic combinations in reducing *Campylobacter* colonization in broiler chickens. *J. Appl. Poult. Res.* 24, 327–334. doi: 10.3382/japr/pfv032

Atterby, C., Mourkas, E., Méric, G., Pascoe, B., Wang, H., Waldenström, J., et al. (2018). The potential of isolation source to predict colonization in avian hosts: a case study in *Campylobacter jejuni* strains from three bird species. *Front. Microbiol.* 9:591. doi: 10.3389/fmicb.2018.00591

Awad, W. A., Mann, E., Dzieciol, M., Hess, C., Schmitz-Esser, S., Wagner, M., et al. (2016). Age-related differences in the luminal and mucosa-associated gut microbiome of broiler chickens and shifts associated with *Campylobacter jejuni* infection. *Front. Cell. Infect. Microbiol.* 6:154. doi: 10.3389/fcimb.2016.00154

Benjamini, Y., and Hochberg, Y. (1995). Controlling the false discovery rate: a practical and powerful approach to multiple testing. *J. R. Stat. Soc. Ser. B* 57, 289–300. doi: 10.1111/j.2517-6161.1995.tb02031.x

Berrang, M. E., Buhr, R. J., and Cason, J. A. (2000). *Campylobacter* recovery from external and internal organs of commercial broiler carcass prior to scalding. *Poult. Sci.* 79, 286–290. doi: 10.1093/ps/79.2.286

Bokulich, N. A., Kaehler, B. D., Rideout, J. R., Dillon, M., Bolyen, E., Knight, R., et al. (2018). Optimizing taxonomic classification of marker-gene amplicon sequences with QIIME 2's q2-feature-classifier plugin. *Microbiome* 6:90. doi: 10.1186/s40168-018-0470-z

Bolyen, E., Rideout, J. R., Dillon, M. R., Bokulich, N. A., Abnet, C. C., Al-Ghalith, G. A., et al. (2019). Reproducible, interactive, scalable and extensible microbiome data science using QIIME 2. *Nat. Biotechnol.* 37, 852–857. doi: 10.1038/s41587-019-0209-9

Callahan, B. J., McMurdie, P. J., Rosen, M. J., Han, A. W., Johnson, A. J., and Holmes, S. P. (2016). DADA2: high-resolution sample inference from Illumina amplicon data. *Nat. Methods* 13, 581–583. doi: 10.1038/nmeth.3869

Chen, J., Bittinger, K., Charlson, E. S., Hoffmann, C., Lewis, J., Wu, G. D., et al. (2012). Associating microbiome composition with environmental covariates using generalized UniFrac distances. *Bioinformatics* 28, 2106–2113. doi: 10.1093/bioinformatics/bts342

Commission Regulation (EC) 889/2008. (2008). No 889/2008 of 5 September 2008 laying down detailed rules for the implementation of Council Regulation (EC) No 834/2007 on organic production and labelling of organic products with regard to organic production, labelling and control. Available at: https://eur-lex.europa.eu/ (Accessed March 06, 2023).

Connerton, P., Flaujac Lafontaine, G., O'Kane, P., Ghaffar, N., Cummings, N., Smith, D., et al. (2018). The effect of the timing of exposure to *Campylobacter jejuni* on the gut microbiome and inflammatory responses of broiler chickens. *Microbiome* 6:88. doi: 10.1186/s40168-018-0477-5

Cosby, W. M., Axelsson, L. T., and Dobrogosz, W. J. (1989). Tn917 transposition in *Lactobacillus plantarum* using the highly temperature-sensitive plasmid pTV1Ts as a vector. *Plasmid* 22, 236–243. doi: 10.1016/0147-619x(89)90006-1

Crawley, K. (2015). Fulfilling 100% organic poultry diets: roughage and foraging from the range. Available at: https://orgprints.org/id/eprint/28090/7/28090.pdf (Accessed March 27, 2023).

Di Marcantonio, L., Marotta, F., Vulpiani, M. P., Sonntag, Q., Iannetti, L., Janowicz, A., et al. (2022). Investigating the cecal microbiota in broiler poultry farms and its potential relationships with animal welfare. *Res. Vet. Sci.* 144, 115–125. doi: 10.1016/j.rvsc.2022.01.020

EFSA (2020). Update and review of control options for *Campylobacter* in broilers at primary production. *EFSA J.* 18:e06090. doi: 10.2903/j.efsa.2020.6090

Guyard-Nicodème, M., Keita, A., Quesne, S., Amelot, M., Poezevara, T., Le Berre, B., et al. (2016). Efficacy of feed additives against Campylobacter in live broilers during the entire rearing period. *Poult. Sci.* 95, 298–305. doi: 10.3382/ps/pev303

Heres, L., Engel, B., Urlings, H. A., Wagenaar, J. A., and van Knapen, F. (2004). Effect of acidified feed on susceptibility of broiler chickens to intestinal infection by *Campylobacter* and *Salmonella*. *Vet. Microbiol.* 99, 259–267. doi: 10.1016/j.vetmic.2003.12.008

Heres, L., Engel, B., Van Knapen, F., Wagenaar, J. A., and Urlings, B. A. (2003). Effect of fermented feed on the susceptibility for *Campylobacter jejuni* colonisation in broiler chickens with and without concurrent inoculation of *Salmonella enteritidis*. *Int. J. Food Microbiol.* 87, 75–86. doi: 10.1016/s0168-1605(03)00055-2

Jong, I. C., Blaauw, X. E., van der Eijk, J. A. J., Souza da Silva, C., van Krimpen, M. M., Molenaar, R., et al. (2021). Providing environmental enrichments affects activity and performance, but not leg health in fast- and slower-growing broiler chickens. *Appl. Anim. Behav. Sci.* 241:105375. doi: 10.1016/j.applanim.2021.105375

Katoh, K., Misawa, K., Kuma, K., and Miyata, T. (2002). MAFFT: a novel method for rapid multiple sequence alignment based on fast Fourier transform. *Nucleic Acids Res.* 30, 3059–3066. doi: 10.1093/nar/gkf436

Kers, J. G., Velkers, F. C., Fischer, E. A. J., Hermes, G. D. A., Stegeman, J. A., and Smidt, H. (2018). Host and environmental factors affecting the intestinal microbiota in chickens. *Front. Microbiol.* 9:235. doi: 10.3389/fmicb.2018.00235

Kruskal, W. H., and Wallis, W. A. (1952). Use of ranks in one-criterion variance analysis. *J. Am. Stat. Assoc.* 47, 583–621. doi: 10.2307/2280779

Krysiak, K., Konkol, D., and Korczyński, M. (2021). Overview of the use of probiotics in poultry production. *Animals* 11:1620. doi: 10.3390/ani11061620

Mandal, S., Van Treuren, W., White, R. A., Eggesbø, M., Knight, R., and Peddada, S. D. (2015). Analysis of composition of microbiomes: a novel method for studying microbial composition. *Microb. Ecol. Health Dis.* 26:27663. doi: 10.3402/mehd.v26.27663

Microsoft Corporation. (2018). Microsoft Excel. Available at: https://office.microsoft.com/excel.

Neal-McKinney, J. M., Lu, X., Duong, T., Larson, C. L., Call, D. R., Shah, D. H., et al. (2012). Production of organic acids by probiotic lactobacilli can be used to reduce pathogen load in poultry. *PLoS One* 7:e43928. doi: 10.1371/journal.pone.0043928

Oakley, B. B., Lillehoj, H. S., Kogut, M. H., Kim, W. K., Maurer, J. J., Pedroso, A., et al. (2014). The chicken gastrointestinal microbiome. *FEMS Microbiol. Lett.* 360, 100–112. doi: 10.1111/1574-6968.12608

Pedregosa, F., Varoquaux, G., Gramfort, A., Michel, V., Thirion, B., Grisel, O., et al. (2012). Scikit-learn: machine learning in python. *J. Mach. Learn. Res.* 12, 2825–2830. doi: 10.48550/arXiv.1201.0490

Pourabedin, M., and Zhao, X. (2015). Prebiotics and gut microbiota in chickens. *FEMS Microbiol. Lett.* 362:fnv122. doi: 10.1093/femsle/fnv122

Prabhurajeshwar, C., and Chandrakanth, K. (2019). Evaluation of antimicrobial properties and their substances against pathogenic bacteria in-vitro by probiotic Lactobacilli strains isolated from commercial yoghurt. *Clin. Nutr. Exp.* 23, 97–115. doi: 10.1016/j.yclnex.2018.10.001

Price, M. N., Dehal, P. S., and Arkin, A. P. (2010). FastTree 2 – approximately maximum-likelihood trees for large alignments. *PLoS One* 5:e9490. doi: 10.1371/journal.pone.0009490

Quast, C., Pruesse, E., Yilmaz, P., Gerken, J., Schweer, T., Yarza, P., et al. (2013). The SILVA ribosomal RNA gene database project: improved data processing and web-based tools. *Nucleic Acids Res.* 41, D590–D596. doi: 10.1093/nar/gks1219

Quentin, M., Bouvarel, I., and Picard, M. (2004). Short- and long-term effects of feed form on fast- and slow-growing broilers. *J. Appl. Poult. Res.* 13, 540–548. doi: 10.1093/japr/13.4.540

R Core Team (2021). *R: A language and environment for statistical computing*. R Foundation for Statistical Computing: Vienna, Austria.

Ranjitkar, S., Lawley, B., Tannock, G., and Engberg, R. M. (2016). Bacterial succession in the broiler gastrointestinal tract. *Appl. Environ. Microbiol.* 82, 2399–2410. doi: 10.1128/AEM.02549-15

Richards, P., Fothergill, J., Bernardeau, M., and Wigley, P. (2019). Development of the Caecal microbiota in three broiler breeds. *Front. Vet. Sci.* 6:201. doi: 10.3389/fvets.2019.00201

Rinttilä, T., and Apajalahti, J. (2013). Intestinal microbiota and metabolites—implications for broiler chicken health and performance. *J. Appl. Poultry Res.* 22, 647–658. doi: 10.3382/japr.2013-00742

Rudi, K., Høidal, H. K., Katla, T., Johansen, B. K., Nordal, J., and Jakobsen, K. S. (2004). Direct real-time PCR quantification of *Campylobacter jejuni* in chicken fecal and cecal samples by integrated cell concentration and DNA purification. *Appl. Environ. Microbiol.* 70, 790–797. doi: 10.1128/aem.70.2.790-797.2004

Rychlik, I. (2020). Composition and function of chicken gut microbiota. *Animals* 10:103. doi: 10.3390/ani10010103

Saint-Cyr, M. J., Haddad, N., Taminiau, B., Poezevara, T., Quesne, S., Amelot, M., et al. (2017). Use of the potential probiotic strain *Lactobacillus salivarius* SMXD51 to control *Campylobacter jejuni* in broilers. *Int. J. Food Microbiol.* 247, 9–17. doi: 10.1016/j.ijfoodmicro.2016.07.003

Sakaridis, I., Ellis, R. J., Cawthraw, S. A., van Vliet, A. H. M., Stekel, D. J., Penell, J., et al. (2018). Investigating the association between the Caecal microbiomes of broilers and *Campylobacter* burden. *Front. Microbiol.* 9:927. doi: 10.3389/fmicb.2018.00927

Sarica, M., Yamak, U., Boz, M., Erensoy, K., Cilavdaroğlu, E., and Noubandiguim, M. (2020). Performance of fast, medium and slow growing broilers in indoor and free-range production systems. *South Afr. J. Anim. Sci.* 49, 1127–1138. doi: 10.4314/sajas.v49i6.16

SAS Institute Inc. (2013). *Base SAS® 9.4 procedures guide: statistical procedures*. Cary, NC: SAS Institute Inc.

Shanker, S., Lee, A., and Sorrell, T. C. (1990). Horizontal transmission of *Campylobacter jejuni* amongst broiler chicks: experimental studies. *Epidemiol. Infect.* 104, 101–110. doi: 10.1017/s0950268800054571

Smialek, M., Joanna, K., and Koncicki, A. (2021). The use of probiotics in the reduction of campylobacter spp. prevalence in poultry. *Animals* 11:1355. doi: 10.3390/ani11051355

Sofka, D., Pfeifer, A., Gleiss, B., Paulsen, P., and Hilbert, F. (2015). Changes within the intestinal flora of broilers by colonisation with *Campylobacter jejuni*. *Berl. Munch. Tierarztl. Wochenschr.* 128, 104–110. doi: 10.2376/0005-9366-128-104

Stanley, D., Geier, M. S., Hughes, R. J., Denman, S. E., and Moore, R. J. (2014). Highly variable microbiota development in the chicken gastrointestinal tract. *PLoS One* 8:e84290. doi: 10.1371/journal.pone.0084290

Sugiharto, S. (2016). Role of nutraceuticals in gut health and growth performance of poultry. *J. Saudi Soc. Agric. Sci.* 15, 99–111. doi: 10.1016/j.jssas.2014.06.001

Swedish Poultry Meat Association (2021). Årsrapport 2020. Available at: https://svenskfagel.se/wp-content/uploads/2022/03/arsrapport-2021-popular-slutgiltig-campylobacter.pdf (Accessed February 10, 2023).

Valečková, E., Ivarsson, E., Ellström, P., Wang, H., Mogodiniyai Kasmaei, K., and Wall, H. (2020). Silage and haylage as forage in slow and fast-growing broilers – effects on performance in *Campylobacter jejuni* infected birds. *Br. Poult. Sci.* 61, 433–441. doi: 10.1080/00071668.2020.1736515

Weiss, S., Xu, Z. Z., Peddada, S., Amir, A., Bittinger, K., Gonzalez, A., et al. (2017). Normalization and microbial differential abundance strategies depend upon data characteristics. *Microbiome* 5:27. doi: 10.1186/s40168-017-0237-y

Wickham, H (2016). *ggplot2: elegant graphics for data analysis*. Springer-Verlag: New York.

Yang, Y., Iji, P., and Choct, M. (2009). Dietary modulation of gut microflora in broiler chickens: a review of the role of six kinds of alternatives to in-feed antibiotics. *Worlds Poult. Sci. J.* 65, 97–114. doi: 10.1017/S0043933909000087

frontiers | Frontiers in Microbiology

TYPE Original Research
PUBLISHED 17 August 2023
DOI 10.3389/fmicb.2023.1238800



OPEN ACCESS

EDITED BY
Karolina Skonieczna-Żydecka,
Pomeranian Medical University, Poland

REVIEWED BY
Joseph Atia Ayariga,
Alabama State University, United States
Diego Fernández Lázaro,
University of Valladolid, Spain

*CORRESPONDENCE
Qing Zhou
✉ qingzhou112@sina.com
Zhiwei Li
✉ 039216235@njucm.edu.cn

†These authors have contributed equally to this work

RECEIVED 12 June 2023
ACCEPTED 03 August 2023
PUBLISHED 17 August 2023

CITATION
Chen S, Han H, Sun X, Zhou G, Zhou Q and Li Z (2023) Causal effects of specific gut microbiota on musculoskeletal diseases: a bidirectional two-sample Mendelian randomization study.
*Front. Microbiol.* 14:1238800.
doi: 10.3389/fmicb.2023.1238800



# Causal effects of specific gut microbiota on musculoskeletal diseases: a bidirectional two-sample Mendelian randomization study

Shuai Chen[1†], Huawei Han[1†], Xiaohe Sun[2], Guowei Zhou[3], Qing Zhou[4*] and Zhiwei Li[1*]

[1]Department of Orthopaedics, The Second Affiliated Hospital of Nanjing University of Chinese Medicine, Nanjing, China, [2]Department of Oncology, Jiangsu Province Hospital of Chinese Medicine, Affiliated Hospital of Nanjing University of Chinese Medicine, Nanjing, China, [3]Department of General Surgery, Jiangsu Province Hospital of Chinese Medicine, Affiliated Hospital of Nanjing University of Chinese Medicine, Nanjing, China, [4]Department of Ophthalmology, Children's Hospital of Nanjing Medical University, Nanjing, China

**Background:** Recent observational studies and clinical trials demonstrated an association between gut microbiota and musculoskeletal (MSK) diseases. Nonetheless, whether the gut microbiota composition has a causal effect on the risk of MSK diseases remains unclear.

**Methods:** Based on large-scale genome-wide association studies (GWAS), we performed a two-sample Mendelian randomization (MR) analysis to investigate the causal relationship between gut microbiota and six MSK diseases, namely osteoporosis (OP), fracture, sarcopenia, low back pain (LBP), rheumatoid arthritis (RA), and ankylosing spondylitis (AS). Instrumental variables for 211 gut microbiota taxa were obtained from the largest available GWAS meta-analysis ($n = 18{,}340$) conducted by the MiBioGen consortium. And the summary-level data for six MSK diseases were derived from published GWAS. The inverse-variance weighted (IVW) method was conducted as a primary analysis to estimate the causal effect, and the robustness of the results was tested via sensitivity analyses using multiple methods. The Bonferroni-corrected test was used to determine the strength of the causal relationship between gut microbiota and various MSK diseases. Finally, a reverse MR analysis was applied to evaluate reverse causality.

**Results:** According to the IVW method, we found 57 suggestive causal relationships and 3 significant causal relationships between gut microbiota and MSK diseases. Among them, *Genus Bifidobacterium* (β: 0.035, 95% CI: 0.013–0.058, $p = 0.0002$) was associated with increased left handgrip strength, *Genus Oxalobacter* (OR: 1.151, 95% CI: 1.065–1.245, $p = 0.0003$) was correlated with an increased risk of LBP, and *Family Oxalobacteraceae* (OR: 0.792, 95% CI: 0.698–0.899, $p = 0.0003$) was linked with a decreased risk of RA. Subsequently, sensitivity analyses revealed no heterogeneity, directional pleiotropy, or outliers for the causal effect of specific gut microbiota on MSK diseases ($p > 0.05$). Reverse MR analysis showed fracture may result in a higher abundance of *Family Bacteroidales* ($p = 0.030$) and sarcopenia may lead to a higher abundance of *Genus Sellimonas* ($p = 0.032$).

**Conclusion:** Genetic evidence suggested a causal relationship between specific bacteria taxa and six MSK diseases, which highlights the association of the "gut-bone/muscle" axis. Further exploration of the potential microbiota-related

mechanisms of bone and muscle metabolism might provide novel insights into the prevention and treatment of MSK diseases.

KEYWORDS

musculoskeletal diseases, gut microbiota, Mendelian randomization, sarcopenia, causality

# 1. Introduction

Musculoskeletal (MSK) diseases encompass a spectrum of pathologies that affect muscles, soft tissues, joints and the spine (Murray et al., 2012). Globally, all MSK diseases combined accounted for 21.3% of the total years lived with disability (YLDs), second only to mental and behavioral disorders (23.2%) (March et al., 2014; Smith et al., 2014). Disability due to MSK diseases has increased by 45% from 1990 to 2010, in particular sarcopenia, osteoporosis (OP) and osteoarthritis (OA), and is expected to continue to rise with an increasingly obese, sedentary, and ageing population (Vos et al., 2012). In addition, MSK diseases also impose a significant economic burden on both patients and the health care system (Sebbag et al., 2019). Recent epidemiological studies have revealed that MSK diseases-related lost productivity accounts for 2% of the gross domestic product (GDP) in the European Union (Bevan, 2015). According to data from the 2012 National Health Interview Survey (NHIS), the annual cost of direct treatment and lost wages for MSK diseases in the United States was estimated at $213 billion (Rosenfeld et al., 2018). Therefore, the prevention and management of MSK diseases has been globally recognized as a crucial public health issue that needs to be solved urgently.

The gut microbiota is a large and complex community of microbial species inhabiting the human gastrointestinal tract, which plays a critical role in human health and diseases (Li et al., 2022). Human gut microbiota can influence host physiology by regulating multiple processes, including inflammation, oxidative stress, immune function, and anabolic balance (Ticinesi et al., 2019). Growing evidence suggests that many MSK diseases, such as OP, OA, sarcopenia, and low back pain (LBP) are closely correlated with altered gut microbiota (Biver et al., 2019). According to a recent study by Xu et al., the gut microbiota compositions of patients with osteoporosis were significantly different from those of healthy controls, especially the enriched *Dialister* and *Faecalibacterium* genera (Xu et al., 2020). Another observational study indicated that the abundance of *Lactobacilli*, *Bacteroides*, and *Prevotella* is higher and the abundance of *Enterobacteriaceae* is lower in normal individuals than in those with sarcopenia (Castro-Mejia et al., 2020). In addition, the gut microbiota can also be involved in the development of rheumatoid arthritis (RA) and ankylosing spondylitis (AS) by altering intestinal barrier permeability, regulating expression levels of host hormones, and mediating immune responses (Asquith et al., 2019). Although the correlations between gut microbiota and Musculoskeletal (MSK) diseases have been reported by previous researches, these findings are mainly based on observational and cross-sectional analyses, and it is still unclear whether there is a causal link between the gut microbiome and MSK diseases.

Mendelian randomization (MR) is a groundbreaking analytical method that provides an unbiased estimation of the causal link between phenotypes (Smith and Ebrahim, 2003). Compared with traditional observational studies, the MR study uses genetic variation as instrumental variables (IVs) to avoid the influence of traditional confounding factors and reverse causality, which provides robust evidence on the mechanisms of disease pathogenesis and the efficacy of treatments (Davey and Hemani, 2014). Given the aforementioned findings and the MR method, our objective was to conduct a bidirectional two-sample MR analysis using extensive genome-wide association study (GWAS) data to explore the causality between specific gut microbiota and six MSK diseases, including OP, fracture, sarcopenia, LBP, RA, and AS.

# 2. Materials and methods

## 2.1. Study design

GWAS summary data focusing on the relationships between genetics and disease have been used to detect a causal relationship between the gut microbiome and six MSK diseases (OP, fracture, sarcopenia, LBP, RA, and AS) through bidirectional two-sample MR analysis (Visscher et al., 2012; Jia et al., 2019). Our first step was to determine whether the gut microbiome contributes to the prevention or promotion of six MSK diseases, by selecting the gut microbiome as the exposure and the six MSK diseases as the outcome. Furthermore, we examined changes in gut microbiota following the development of six MSK diseases. According to Bownden et al., the two-sample MR needs to satisfy the following three assumptions (Bowden et al., 2015): (Murray et al., 2012) The instruments of genetic variations should be robustly associated with gut microbiota; (b) The genetic variations should not be associated with any confounders of gut microbiota and six MSK diseases; (c) The genetic variations should affect six MSK diseases solely through gut microbiota, not via other pathways (Sanderson et al., 2019) (Figure 1A). All studies included in the cited GWASs were approved by relevant review committees and all participants provided informed consent. The flow chart of the MR analysis was presented in Figure 1B.

## 2.2. Genome-wide association studies sources

Our gut microbiota summary data came from a large multi-ethnic GWAS meta-analysis that included 18,340 European individuals and individuals from 24 cohorts (MiBioGen Consortium). Three different variable regions of the 16S rRNA gene were targeted in order to profile the microbial composition. And only the taxa found in >10% of the samples were included in the quantitative microbiome trait loci

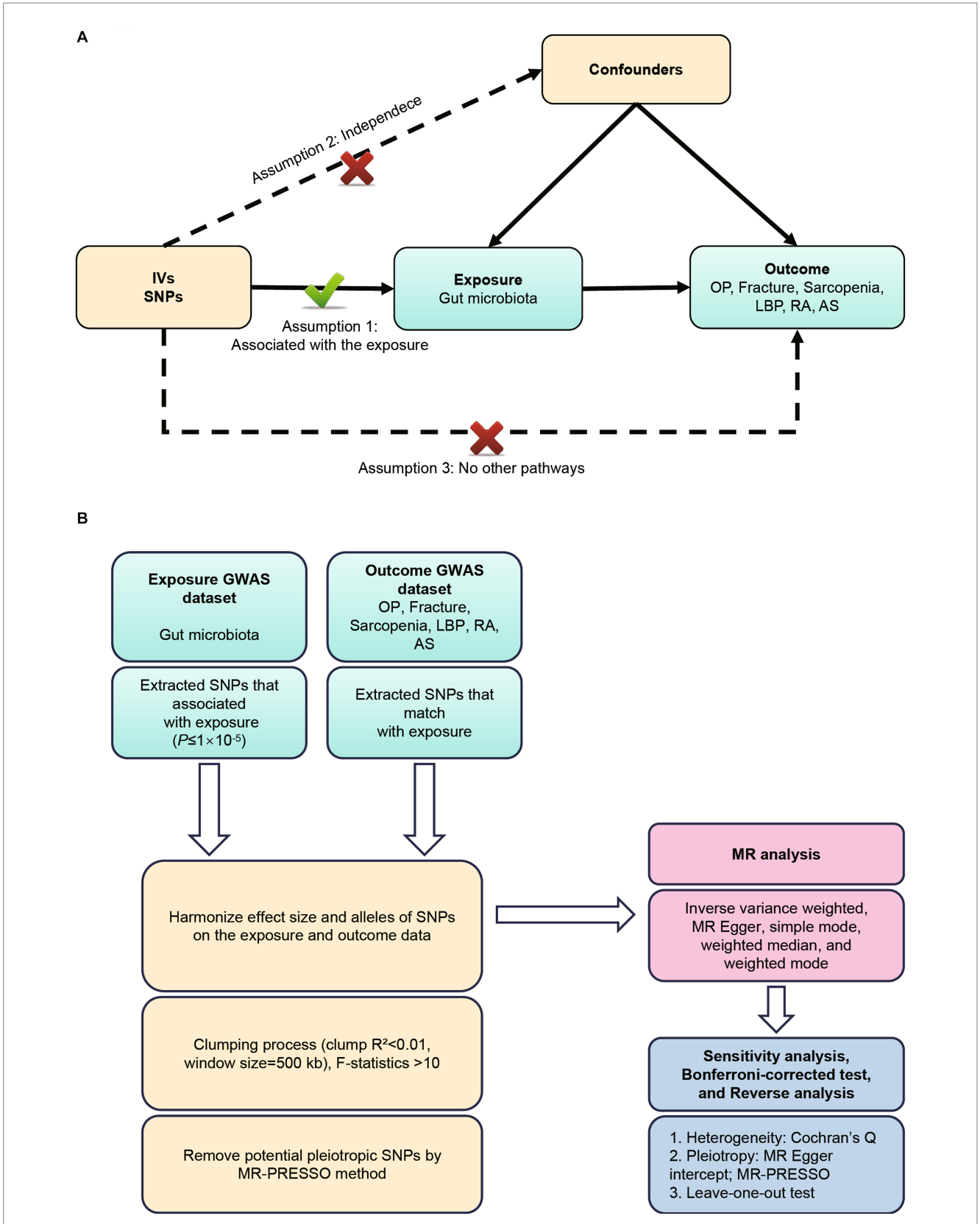


FIGURE 1
**(A)** Three assumptions of Mendelian randomization. **(B)** Flowchart of this Mendelian randomization study. MR, Mendelian randomization; MSK, musculoskeletal; OP, osteoporosis; LBP, low back pain; RA, rheumatoid arthritis; AS, ankylosing spondylitis.

(mbQTL) mapping study for each cohort. Furthermore, after adjustment for age, sex, technical covariates, and genetic principal components, Spearman's correlation analysis was conducted to identify genetic loci that affected the covariate-adjusted abundance of bacterial taxa (Kurilshikov et al., 2021).

In the study, we extracted GWAS summary statistics for six MSK diseases from publicly GWAS analyses. The GWAS summary data on OP were mainly extracted from UK Biobank, including 7,547 cases and 455,386 controls of European ancestry (Sudlow et al., 2015). Summary statistics for fracture were derived from a GWAS meta-analysis, including 44,502 cases and 415,887 controls of European ancestry (Morris et al., 2019). Summary data for ALM and handgrip strength were obtained from the UK Biobank study. An analysis of 450,243 UK Biobank cohort participants was conducted to quantify ALM-related values by summing fat-free mass (Pei et al., 2020). For handgrip strength, UK Biobank provided GWAS summary statistics on right and left handgrip strength based on 461,089 and 461,026 United Kingdom people, respectively (Sudlow et al., 2015). The data on LBP came from a meta-analysis including 13,178 cases and 164,682 controls of European ancestry (https://gwas.mrcieu.ac.uk/datasets/ukb-d-M13_LOWBACKPAIN). For RA, we collected summary statistics from a GWAS meta-analysis that includes 14,361 RA cases and 43,923 controls of European ancestry (Okada et al., 2014). The genetic data of AS risk were derived from a large GWAS involving 9,069 cases and 1,550 controls of European (Cortes et al., 2013). Detailed information on the demographic characteristics of selected summary-level GWASs applied in this study was shown in Supplementary Table S1.

## 2.3. Selection of genetic instrumental variables

During the selection of the optimal IVs, the following quality control steps were taken to ensure the validity and accuracy of the conclusions on the causal relationship between the gut microbiome and the six MSK diseases (Murray et al., 2012) The instrumental variables selected for analysis need to be highly related to the corresponding exposures (We choose significant SNPs based on a loose cutoff of $p < 1 \times 10^{-5}$ to ensure sufficient instrumental variables for screening). (March et al., 2014) The instrumental variables are mutually independent and avoid the offset caused by linkage disequilibrium (LD) between the SNPs ($r^2 < 0.01$, LD distance = 500 kb). (Smith et al., 2014) We eliminated instrumental variables with an F-statistic less than 10 to minimize potential weak instrument bias $F = R^2(n\text{-}k\text{-}1)/k(1\text{-}R^2)$ (n is the sample size, k is the number of included instrumental variables, and $R^2$ is the exposure variance explained by the selected SNPs).

## 2.4. Statistical analysis

The inverse variance weighted (IVW) method was employed as the main analysis, to obtain an unbiased estimate of the causal relationship between gut microbiota and MSK diseases. Furthermore, the weighted median, MR Egger, simple mode, and weighted mode methods were applied as additional methods to estimate causal effects under different conditions. The weighted median method could combine data on multiple genetic variants into a single causal estimate and provide a consistent estimate if at least half of the weight is derived from valid IVs (Bowden et al., 2016). The MR-Egger method could evaluate whether genetic variants have directional pleiotropy and provide a consistent estimate of the causal effect (Bowden et al., 2015). The intercept of MR-Egger regression was calculated to assess horizontal pleiotropy, and $p$ value >0.05 indicated that the possibility of pleiotropy effect in the causal analysis is weak (Verbanck et al., 2018). Cochran's Q test was derived from IVW estimation and used to detect heterogeneity among instrumental variables (Pierce and Burgess, 2013). In addition, we applied the Mendelian randomization pleiotropy residual sum and outlier (MR-PRESSO) method to determine horizontal pleiotropy and correct potential outliers. The leave-one-out method was used for sensitivity analysis, which sequentially removed one of the SNPs and used the remaining SNPs as instrumental variables for two-sample MR analysis to judge the degree of influence of causal association effect by a single SNP. In addition, we also performed a reverse-direction MR analysis to determine whether there was a reverse-direction causal relationship.

To obtain a more accurate assessment of the causal relationship, we applied Bonferroni correction to determine the significance of multiple-testing at each feature level ($p < 0.05/n$, where n is the number of bacterial taxa included in each feature level). Hence, the multiple-testing significance was $5.56 \times 10^{-3}$, $3.13 \times 10^{-3}$, $2.50 \times 10^{-3}$, $1.56 \times 10^{-3}$, and $4.20 \times 10^{-4}$, respectively, for phylum, class, order, family, and genus. The 'TwoSampleMR' package and the 'MRPRESSO' package in R software (version 4.1.3) were used for all MR analyses.

# 3. Results

## 3.1. Selection of instrumental variables

To begin with, 14,587 SNPs correlated with the gut microbiota were identified as IVs from the MiBioGen Consortium at a relatively loose significance level ($p < 1 \times 10^{-5}$). It contained 211 bacterial traits, including 131 genera, 35 families, 20 orders, 16 classes, and 9 phyla. After a series of quality control steps, 2,236 SNPs were finally included in the analysis. In addition, the F-statistics of all IVs were >10, indicating no evidence of weak instrument bias.

## 3.2. Causal effects of gut microbiota on musculoskeletal diseases

### 3.2.1. Causal effect of gut microbiota on osteoporosis risk

According to the results of the IVW method, the higher genetically predicted abundance of *Order NB1n* (OR: 0.998, 95% CI: 0.997–0.999, $p = 0.038$), *Genus Lachnospiraceae NK4A136 group* (OR: 0.996, 95% CI: 0.994–0.999, $p = 0.003$), *Genus Christensenellaceae R.7 group* (OR: 0.996, 95% CI: 0.991–1.000, $p = 0.028$) was associated with a reduced risk of OP (Table 1). In contrast, genetically predicted abundance of *Genus Howardella* (OR: 1.002, 95% CI: 1.000–1.003, $p = 0.033$), and *Genus Eubacterium oxidoreducens group* (OR: 1.003, 95% CI: 1.000–1.005, $p = 0.046$) was positively related to OP risk (Figure 2).

10.3389/fmicb.2023.1238800

TABLE 1 Mendelian randomisation (MR) results of causal effects between gut microbiome and the risk of osteoporosis.

| Group | Bacterial traits | Nsnp | Methods | SE | OR (95% CI) | *p*-value |
|---|---|---|---|---|---|---|
| *Order* | *NB1n* | 14 | MR Egger | 0.003 | 0.996 (0.990, 1.002) | 0.214 |
| | | | Weighted median | 0.001 | 0.998 (0.997, 1.000) | 0.103 |
| | | | Inverse variance weighted | 0.001 | 0.998 (0.997, 0.999) | 0.038 |
| | | | Simple mode | 0.002 | 0.999 (0.996, 1.002) | 0.412 |
| | | | Weighted mode | 0.002 | 0.999 (0.996, 1.002) | 0.393 |
| *Genus* | *Lachnospiraceae NK4A136 group* | 14 | MR Egger | 0.003 | 0.991 (0.985, 0.997) | 0.013 |
| | | | Weighted median | 0.002 | 0.997 (0.994, 1.001) | 0.177 |
| | | | Inverse variance weighted | 0.001 | 0.996 (0.994, 0.999) | 0.003 |
| | | | Simple mode | 0.003 | 0.998 (0.992, 1.004) | 0.576 |
| | | | Weighted mode | 0.004 | 0.998 (0.991, 1.005) | 0.604 |
| *Genus* | *Howardella* | 10 | MR Egger | 0.003 | 1.006 (0.999, 1.012) | 0.152 |
| | | | Weighted median | 0.001 | 1.001 (0.999, 1.003) | 0.506 |
| | | | Inverse variance weighted | 0.001 | 1.002 (1.000, 1.003) | 0.033 |
| | | | Simple mode | 0.002 | 1.000 (0.997, 1.003) | 0.812 |
| | | | Weighted mode | 0.002 | 1.000 (0.997, 1.004) | 0.809 |
| *Genus* | *Christensenellaceae R.7 group* | 10 | MR Egger | 0.005 | 0.993 (0.983, 1.004) | 0.233 |
| | | | Weighted median | 0.002 | 0.996 (0.991, 1.000) | 0.049 |
| | | | Inverse variance weighted | 0.002 | 0.996 (0.993, 1.000) | 0.028 |
| | | | Simple mode | 0.004 | 0.993 (0.985, 1.001) | 0.112 |
| | | | Weighted mode | 0.004 | 0.993 (0.985, 1.001) | 0.131 |
| *Genus* | *Eubacterium oxidoreducens group* | 5 | MR Egger | 0.005 | 1.000 (0.991, 1.010) | 0.924 |
| | | | Weighted median | 0.002 | 1.001 (0.998, 1.005) | 0.374 |
| | | | Inverse variance weighted | 0.001 | 1.003 (1.000, 1.005) | 0.046 |
| | | | Simple mode | 0.002 | 1.001 (0.997, 1.005) | 0.592 |
| | | | Weighted mode | 0.002 | 1.001 (0.998, 1.005) | 0.558 |

SNP, single nucleotide polymorphism; MR, mendelian randomization; SE, standard error; 95% CI, 95% confidence interval.

### 3.2.2. Causal effect of gut microbiota on fracture risk

The estimates of the IVW test showed that the genetically predicted four genera, namely, *Family Defluviitaleaceae* (OR: 1.005, 95% CI: 1.001–1.010, $p = 0.022$), *Family Bacteroidales S24.7 group* (OR: 1.007, 95% CI: 1.000–1.013, $p = 0.049$), *Genus Allisonella* (OR: 1.005, 95% CI: 1.001–1.009, $p = 0.015$), *Genus Defluviitaleaceae UCG011* (OR: 1.006, 95% CI: 1.001–1.011, $p = 0.019$) were positively associated with the risk of fracture (Table 2). And higher genetically predicted *Class Mollicutes* (OR: 0.994, 95% CI: 0.988–0.999, $p = 0.022$), *Genus Collinsella* (OR: 0.993, 95% CI: 0.986–1.000, $p = 0.047$), and *Phylum Tenericutes* (OR: 0.994, 95% CI: 0.988–0.999, $p = 0.022$) were linked with a decreased fracture risk (Figure 3).

### 3.2.3. Causal effect of gut microbiota on sarcopenia-related traits

The IVW results suggested that genetically predicted *Class Actinobacteria* (β: 0.026, 95% CI: 0.003–0.050, $p = 0.029$), *Family Bifidobacteriaceae* (β: 0.028, 95% CI: 0.004–0.052, $p = 0.024$), *Genus Alloprevotella* (β: 0.012, 95% CI: 0.002–0.022, $p = 0.021$), *Genus Bifidobacterium* (β: 0.028, 95% CI: 0.006–0.050, $p = 0.012$), *Genus Eisenbergiella* (β: 0.012, 95% CI: 0.000–0.025, $p = 0.049$), *Genus Parabacteroides* (β: 0.030, 95% CI: 0.008–0.051, $p = 0.006$), *Genus Sellimonas* (β: 0.013, 95% CI: 0.004–0.022, $p = 0.003$), *Order Bifidobacteriales* (β: 0.028, 95% CI: 0.004–0.052, $p = 0.024$), *Phylum Actinobacteria* (β: 0.030, 95% CI: 0.003–0.056, $p = 0.027$) were linked to an increase in right handgrip strength, while *Genus Paraprevotella* (β: -0.014, 95% CI: −0.023–-0.004, $p = 0.007$) and *Genus Prevotella9* (β: -0.014, 95% CI: −0.027–0.000, $p = 0.042$) were associated with an decrease in right handgrip strength (Table 3). Similarly, we found that genetically predicted *Family Bifidobacteriaceae* (β: 0.035, 95% CI: 0.011–0.060, $p = 0.005$), *Genus Eubacterium nodatum group* (β: 0.010, 95% CI: 0.002–0.017, $p = 0.013$), *Genus Bifidobacterium* (β: 0.035, 95% CI: 0.013–0.058, $P < 0.001$), *Genus Parabacteroides* (β: 0.029, 95% CI: 0.007–0.051, $p = 0.011$), *Genus Sellimonas* (β: 0.013, 95% CI: 0.005–0.021, $p = 0.002$), *Order Bifidobacteriales* (β: 0.035, 95% CI:

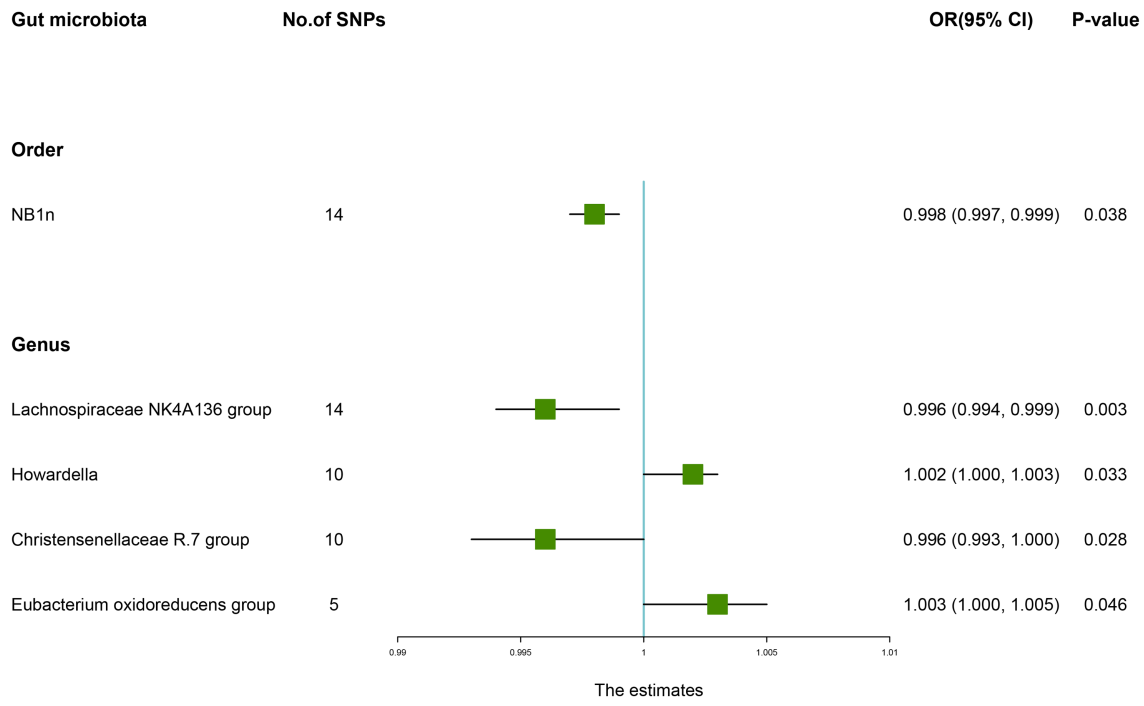


FIGURE 2
Forest plot of the causality between gut microbiota with the risk of osteoporosis. The estimates: Inverse variance weighted (IVW) results of gut microbiota and osteoporosis risk; *p*-value: *p*-value of the estimate. OR, odds ratio; SNP, single-nucleotide polymorphism.

0.011–0.060, $p = 0.005$) were also positively associated with left grip (Figures 4A,B). And the MR estimates of MR Egger and weighted median indicated that genetically predicted *Family Bifidobacteriaceae*, *Order Bifidobacteriales* were positively related to right and left handgrip strength ($P < 0.05$), suggesting *Family Bifidobacteriaceae*, *Order Bifidobacteriales* were protective factors for sarcopenia (Table 4).

In addition, the estimates of IVW indicated that genetically predicted *Family Bacteroidaceae* (β: 0.041, 95% CI: 0.010–0.071, $p = 0.008$), *Genus Bacteroides* (β: 0.041, 95% CI: 0.010–0.071, $p = 0.008$), *Genus Lachnospira* (β: 0.037, 95% CI: 0.000–0.073, $p = 0.049$), *Genus Phascolarctobacterium* (β: 0.024, 95% CI: 0.002–0.046, $p = 0.031$) were positively correlated with ALM (Table 5). And genetically predicted *Genus Eubacterium fissicatena group* (β: -0.017, 95% CI: −0.034–-0.000, $p = 0.044$), which suggested that a 1-SD increase in genetically determined *Genus Eubacterium fissicatena group* was correlated with an increase in ALM by 0.017 g (Figure 4C).

### 3.2.4. Causal effect of gut microbiota on low back pain risk

As presented in Table 6, there was a causal correlation between four microbiotas and LBP. According to the results of the IVW method, higher genetically predicted *Family Prevotellaceae* (OR: 1.182, 95% CI: 1.038–1.346, $p = 0.012$), *Genus Oxalobacter* (OR: 1.151, 95% CI: 1.065–1.245, $P < 0.001$), *Genus Tyzzerella3* (OR: 1.121, 95% CI: 1.032–1.217, $p = 0.007$) were correlated with a higher risk of LBP. However, *Class Melainabacteria* (OR: 0.891, 95% CI: 0.808–0.984, $p = 0.022$) was linked with a lower risk of LBP, which indicated that a 1-SD increase in *Class Melainabacteria* was correlated with a 10.9% decrease in LBP risk (Figure 5).

### 3.2.5. Causal effect of gut microbiota on rheumatoid arthritis risk

As shown in Table 7, the IVW results suggested that genetically predicted *Class Clostridia* (OR: 1.368, 95% CI: 1.033–1.812, $p = 0.029$), *Family Clostridialesvadin BB60 group* (OR: 1.200, 95% CI: 1.018–1.416, $p = 0.032$), *Family Desulfovibrionaceae* (OR: 1.253, 95% CI: 1.008–1.558, $p = 0.042$), *Family Streptococcaceae* (OR: 1.296, 95% CI: 1.038–1.620, $p = 0.022$), *Genus Desulfovibrio* (OR: 1.255, 95% CI: 1.020–1.544, $p = 0.032$), *Genus Ruminococcaceae UCG013* (OR: 1.365, 95% CI: 1.057–1.763, $p = 0.017$), *Genus Turicibacter* (OR: 1.218, 95% CI: 1.005–1.476, $p = 0.044$), and *Order Clostridiales* (OR: 1.349, 95% CI: 1.042–1.748, $p = 0.023$) were positively associated with the risk of RA. By contrast, there was evidence that increasing abundance of *Family Christensenellaceae* (OR: 0.750, 95% CI: 0.578–0.973, $p = 0.031$), *Family Oxalobacteraceae* (OR: 0.792, 95% CI: 0.698–0.899, $P < 0.001$), *Genus Oxalobacter* (OR: 0.825, 95% CI: 0.722–0.943, $p = 0.005$), *Genus Ruminococcaceae UCG002* (OR: 0.805, 95% CI: 0.667–0.971, $p = 0.023$), *Order Bacillales* (OR: 0.850, 95% CI: 0.743–0.972, $p = 0.018$), and *Phylum Cyanobacteria* (OR: 0.783, 95% CI: 0.635–0.965, $p = 0.022$) have a protective effect on RA risk (Figure 6).

### 3.2.6. Causal effect of gut microbiota on ankylosing spondylitis risk

According to the IVW method, genetically predicted *Family Lactobacillaceae* (OR: 0.696, 95% CI: 0.527–0.919, $p = 0.011$), *Family Rikenellaceae* (OR: 0.680, 95% CI: 0.491–0.942, $p = 0.020$), *Genus Howardella* (OR: 0.802, 95% CI: 0.650–0.991, $p = 0.041$), *Genus Anaerotruncus* (OR: 0.671, 95% CI: 0.454–0.991, $p = 0.045$) were

10.3389/fmicb.2023.1238800

TABLE 2 Mendelian randomisation (MR) results of causal effects between gut microbiome and the risk of fracture.

| Group | Bacterial traits | Nsnp | Methods | SE | OR (95% CI) | *p*-value |
|---|---|---|---|---|---|---|
| *Class* | *Mollicutes* | 12 | MR Egger | 0.009 | 0.992 (0.974, 1.010) | 0.400 |
| | | | Weighted median | 0.004 | 0.994 (0.986, 1.002) | 0.140 |
| | | | Inverse variance weighted | 0.003 | 0.994 (0.988, 0.999) | 0.022 |
| | | | Simple mode | 0.006 | 0.993 (0.981, 1.005) | 0.301 |
| | | | Weighted mode | 0.006 | 0.995 (0.983, 1.006) | 0.374 |
| *Family* | *Defluviitaleaceae* | 12 | MR Egger | 0.008 | 1.006 (0.990, 1.021) | 0.494 |
| | | | Weighted median | 0.003 | 1.005 (0.998, 1.011) | 0.149 |
| | | | Inverse variance weighted | 0.002 | 1.005 (1.001, 1.010) | 0.022 |
| | | | Simple mode | 0.005 | 1.006 (0.995, 1.016) | 0.324 |
| | | | Weighted mode | 0.005 | 1.005 (0.995, 1.015) | 0.359 |
| *Family* | *Bacteroidales S24.7 group* | 9 | MR Egger | 0.016 | 1.019 (0.988, 1.051) | 0.277 |
| | | | Weighted median | 0.004 | 1.004 (0.997, 1.011) | 0.245 |
| | | | Inverse variance weighted | 0.003 | 1.007 (1.000, 1.013) | 0.049 |
| | | | Simple mode | 0.006 | 1.003 (0.992, 1.015) | 0.554 |
| | | | Weighted mode | 0.005 | 1.002 (0.991, 1.012) | 0.776 |
| *Genus* | *Allisonella* | 8 | MR Egger | 0.014 | 1.007 (0.980, 1.036) | 0.613 |
| | | | Weighted median | 0.002 | 1.003 (0.998, 1.008) | 0.272 |
| | | | Inverse variance weighted | 0.002 | 1.005 (1.001, 1.009) | 0.015 |
| | | | Simple mode | 0.004 | 1.002 (0.995, 1.009) | 0.597 |
| | | | Weighted mode | 0.004 | 1.002 (0.995, 1.009) | 0.562 |
| *Genus* | *Collinsella* | 10 | MR Egger | 0.014 | 0.994 (0.967, 1.021) | 0.656 |
| | | | Weighted median | 0.005 | 0.994 (0.985, 1.003) | 0.169 |
| | | | Inverse variance weighted | 0.004 | 0.993 (0.986, 1.000) | 0.047 |
| | | | Simple mode | 0.007 | 0.994 (0.980, 1.008) | 0.421 |
| | | | Weighted mode | 0.007 | 0.995 (0.981, 1.008) | 0.477 |
| *Genus* | *Defluviitaleaceae UCG011* | 10 | MR Egger | 0.009 | 1.002 (0.984, 1.020) | 0.838 |
| | | | Weighted median | 0.004 | 1.006 (0.999, 1.014) | 0.070 |
| | | | Inverse variance weighted | 0.003 | 1.006 (1.001, 1.011) | 0.019 |
| | | | Simple mode | 0.006 | 1.008 (0.995, 1.021) | 0.239 |
| | | | Weighted mode | 0.006 | 1.006 (0.994, 1.018) | 0.331 |
| *Phylum* | *Tenericutes* | 12 | MR Egger | 0.009 | 0.992 (0.974, 1.010) | 0.400 |
| | | | Weighted median | 0.004 | 0.994 (0.987, 1.001) | 0.114 |
| | | | Inverse variance weighted | 0.003 | 0.994 (0.988, 0.999) | 0.022 |
| | | | Simple mode | 0.007 | 0.993 (0.981, 1.066) | 0.331 |
| | | | Weighted mode | 0.006 | 0.995 (0.982, 1.007) | 0.416 |

SNP, single nucleotide polymorphism; MR, mendelian randomization; SE, standard error; 95% CI, 95% confidence interval.

negatively associated with the risk of AS (Table 8), while *Genus Ruminococcaceae NK4A214 group* (OR: 1.707, 95% CI: 1.190–2.449, $p = 0.045$) was positively linked with the AS risk (Figure 7).

### 3.2.7. Sensitivity analysis, Bonferroni-corrected test, and reverse analysis

We performed a series of sensitivity analyses to test the heterogeneity and horizontal pleiotropy of the selected IVs. Based on Cochran's Q test, we observed no significant heterogeneity ($p > 0.05$) (Table 9). All $p$ values of the MR-Egger intercept tests were > 0.05, which indicated no horizontal pleiotropy. Furthermore, we also did not discover any outliers through the MR-PRESSO global test (Table 9). Detailed scatter plots for each MR method analysis were shown in Supplementary Figures S2–S9. And results from a leave-one-out analysis demonstrated that no SNP was an influential outlier (Supplementary Figures S9–S16).

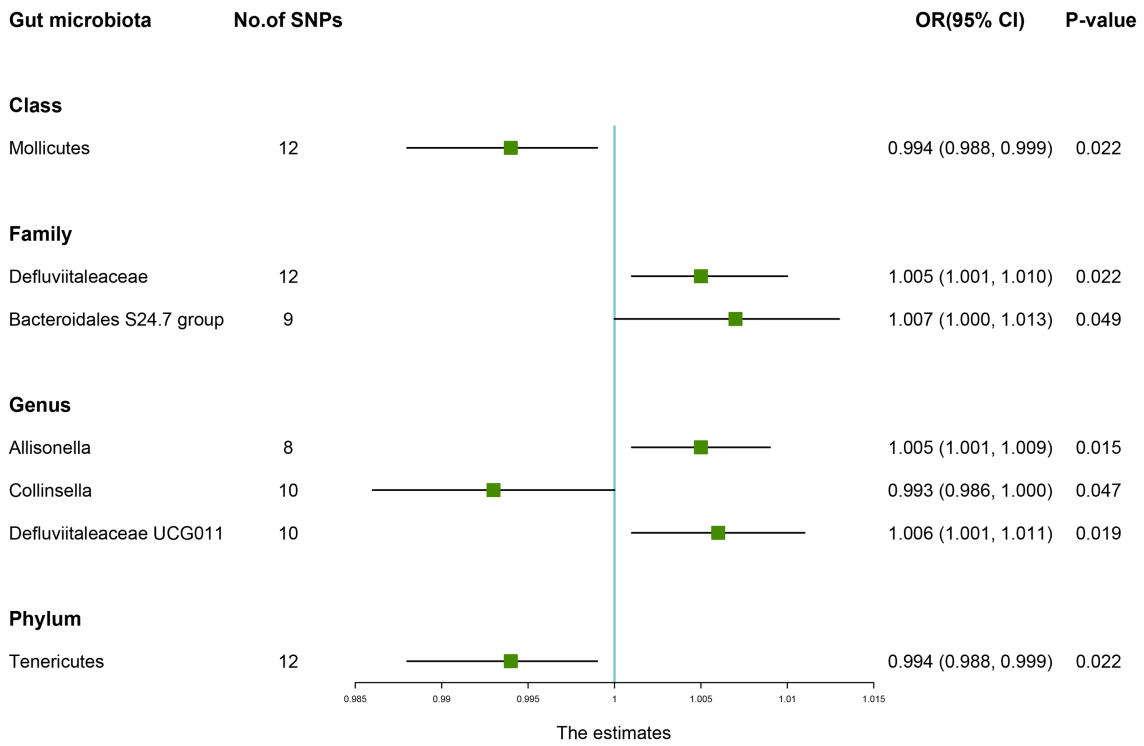


FIGURE 3
Forest plot of the causality between gut microbiota with the risk of fracture. The estimates: Inverse variance weighted (IVW) results of gut microbiota and fracture risk; *p*-value: *p*-value of the estimate. OR, odds ratio; SNP, single-nucleotide polymorphism.

According to the results of the Bonferroni-corrected test, *Genus Bifidobacterium* (β: 0.035, 95% CI: 0.013–0.058, $p = 0.0002$) was significantly correlated with left handgrip strength. In addition, higher level of *Genus Oxalobacter* retains a strong causal association with an increased risk of LBP (OR: 1.151, 95% CI: 1.065–1.245, $p = 0.0003$) and higher level of *Family Oxalobacteraceae* (OR: 0.792, 95% CI: 0.698–0.899, $p = 0.0003$) retains a strong causal association with a decreased risk of RA. In addition, reverse analysis demonstrates that fracture may result in a higher abundance of *Family Bacteroidales* ($p = 0.030$) and sarcopenia may lead to a higher abundance of *Genus Sellimonas* ($p = 0.032$) (Supplementary Table S10).

## 4. Discussion

To our knowledge, this was the first comprehensive and in-depth investigation of causal associations between gut microbiota and six common MSK diseases (OP, fracture, sarcopenia, LBP, RA, and AS) based on publicly available GWAS data. According to the findings of our study, a total of 57 gut microbiota were potentially causally associated with the progression of MSK diseases. After multiple testing corrections, we observed a significant causal relationship between *Genus Bifidobacterium*, *Genus Oxalobacter*, and *Family Oxalobacteraceae* with the risk of sarcopenia, LBP and RA, respectively. These findings might provide new ideas for the future treatment of MSK diseases by targeting the specific gut microbiota.

The gut microbiota consists of trillions of bacteria in the gastrointestinal tract, which have functions such as improving intestinal permeability, attenuating the inflammatory response, and participating in the immune regulation of the skeletal system (Rizzoli, 2019). In recent years, the "gut-bone/muscle" axis has received increasing attention in the field of bone health and orthopedic diseases and multiple studies indicated that gut microbiota composition is involved in the MSK disease pathogenesis through multiple pathways (Tu et al., 2021; Zhang et al., 2021). In our study, we discovered that genetically proxied higher abundance of *Genus Bifidobacterium* was significantly correlated with increased grip strength. And consistent directional effects for all analyses were observed in both MR Egger and weighted median methods, which suggests that *Bifidobacterium* might be a promising target for sarcopenia prevention. According to recent studies, *Bifidobacterium* has been identified as a critical taxon for frailty and sarcopenia in the elderly (Ticinesi et al., 2019). In a case–control study of elderly Chinese women, metagenomic sequencing of the gut microbiota revealed that the abundance of *Prevotella* and *Bifidobacterium* in the healthy control group was higher than those in the sarcopenia group (Wang et al., 2023). An animal experiment reported that *Bifidobacterium longum* could improve exercise-associated peripheral fatigue indicators (forelimb grip strength) and oxidative stress-related damage indicators in mice, which indicated *Bifidobacterium* may be involved in the occurrence and progression of age-related physical frailty and sarcopenia (Huang et al., 2020). In addition, a double-blind randomized clinical trial of older adults 65 aged 65 and over demonstrated that long-term intake of a prebiotic supplement containing *Bifidobacterium* significantly improved grip strength and reduced the level of fatigue (Buigues et al., 2016). *Bifidobacterium* might affect sarcopenia through its metabolites, such as short-chain fatty acids (acetate, propionate, and butyrate), which are important for immune regulation and metabolic

10.3389/fmicb.2023.1238800

TABLE 3 Mendelian randomisation (MR) results of causal effects between gut microbiome and hand grip strength (Right).

| Group | Bacterial traits | Nsnp | Methods | SE | β (95% CI) | *p*-value |
|---|---|---|---|---|---|---|
| *Class* | *Actinobacteria* | 22 | MR Egger | 0.030 | 0.046 (−0.013, 0.106) | 0.143 |
| | | | Weighted median | 0.010 | 0.013 (−0.006, 0.033) | 0.179 |
| | | | Inverse variance weighted | 0.012 | 0.026 (0.003, 0.050) | 0.029 |
| | | | Simple mode | 0.018 | 0.000 (−0.035, 0.034) | 0.994 |
| | | | Weighted mode | 0.017 | 0.007 (−0.026, 0.040) | 0.691 |
| *Family* | *Bifidobacteriaceae* | 21 | MR Egger | 0.034 | 0.146 (0.080, 0.213) | <0.001 |
| | | | Weighted median | 0.011 | 0.032 (0.010, 0.054) | 0.004 |
| | | | Inverse variance weighted | 0.012 | 0.028 (0.004, 0.052) | 0.024 |
| | | | Simple mode | 0.027 | 0.026 (−0.027, 0.080) | 0.345 |
| | | | Weighted mode | 0.014 | 0.066 (0.037, 0.094) | <0.001 |
| *Genus* | *Alloprevotella* | 6 | MR Egger | 0.048 | 0.020 (−0.074, 0.115) | 0.695 |
| | | | Weighted median | 0.007 | 0.015 (0.002, 0.028) | 0.020 |
| | | | Inverse variance weighted | 0.005 | 0.012 (0.002, 0.022) | 0.021 |
| | | | Simple mode | 0.009 | 0.015 (−0.003, 0.033) | 0.156 |
| | | | Weighted mode | 0.009 | 0.015 (−0.002, 0.032) | 0.141 |
| *Genus* | *Bifidobacterium* | 20 | MR Egger | 0.033 | 0.040 (−0.024, 0.104) | 0.233 |
| | | | Weighted median | 0.011 | 0.031 (0.010, 0.051) | 0.004 |
| | | | Inverse variance weighted | 0.011 | 0.028 (0.006, 0.050) | 0.012 |
| | | | Simple mode | 0.024 | 0.021 (−0.026, 0.068) | 0.393 |
| | | | Weighted mode | 0.021 | 0.069 (0.027, 0.111) | 0.004 |
| *Genus* | *Eisenbergiella* | 11 | MR Egger | 0.051 | 0.043 (−0.057, 0.144) | 0.423 |
| | | | Weighted median | 0.007 | 0.009 (−0.005, 0.023) | 0.224 |
| | | | Inverse variance weighted | 0.006 | 0.012 (0.000, 0.025) | 0.049 |
| | | | Simple mode | 0.011 | 0.009 (−0.012, 0.030) | 0.438 |
| | | | Weighted mode | 0.011 | 0.009 (−0.013, 0.030) | 0.452 |
| *Genus* | *Parabacteroides* | 6 | MR Egger | 0.033 | 0.012 (−0.053, 0.076) | 0.741 |
| | | | Weighted median | 0.014 | 0.028 (0.000, 0.056) | 0.047 |
| | | | Inverse variance weighted | 0.011 | 0.030 (0.008, 0.051) | 0.006 |
| | | | Simple mode | 0.019 | 0.034 (−0.003, 0.071) | 0.136 |
| | | | Weighted mode | 0.018 | 0.019 (−0.015, 0.054) | 0.326 |
| *Genus* | *Paraprevotella* | 13 | MR Egger | 0.016 | −0.015 (−0.048, 0.017) | 0.369 |
| | | | Weighted median | 0.007 | −0.017 (−0.031, −0.004) | 0.013 |
| | | | Inverse variance weighted | 0.005 | −0.014 (−0.023, −0.004) | 0.007 |
| | | | Simple mode | 0.011 | −0.017 (−0.040, 0.005) | 0.152 |
| | | | Weighted mode | 0.012 | −0.018 (−0.040, 0.005) | 0.157 |
| *Genus* | *Prevotella9* | 15 | MR Egger | 0.020 | −0.029 (−0.068, 0.011) | 0.177 |
| | | | Weighted median | 0.008 | −0.016 (−0.032, 0.001) | 0.062 |
| | | | Inverse variance weighted | 0.007 | −0.014 (−0.027, −0.000) | 0.042 |
| | | | Simple mode | 0.016 | −0.031 (−0.063, 0.001) | 0.077 |
| | | | Weighted mode | 0.017 | −0.031 (−0.065, 0.003) | 0.096 |
| *Genus* | *Sellimonas* | 11 | MR Egger | 0.020 | 0.036 (−0.003, 0.076) | 0.107 |
| | | | Weighted median | 0.006 | 0.012 (0.001, 0.023) | 0.029 |

*(Continued)*

TABLE 3 (Continued)

| Group | Bacterial traits | Nsnp | Methods | SE | β (95% CI) | *p*-value |
|---|---|---|---|---|---|---|
| | | | Inverse variance weighted | 0.004 | 0.013 (0.004, 0.022) | 0.003 |
| | | | Simple mode | 0.009 | 0.015 (−0.003, 0.032) | 0.127 |
| | | | Weighted mode | 0.009 | 0.014 (−0.004, 0.032) | 0.159 |
| *Order* | *Bifidobacteriales* | 21 | MR Egger | 0.034 | 0.146 (0.080, 0.213) | <0.001 |
| | | | Weighted median | 0.011 | 0.032 (0.010, 0.054) | 0.004 |
| | | | Inverse variance weighted | 0.012 | 0.028 (0.004, 0.052) | 0.024 |
| | | | Simple mode | 0.026 | 0.026 (−0.025, 0.078) | 0.330 |
| | | | Weighted mode | 0.015 | 0.066 (0.036, 0.096) | <0.001 |
| *Phylum* | *Actinobacteria* | 19 | MR Egger | 0.048 | 0.127 (0.033, 0.221) | 0.017 |
| | | | Weighted median | 0.011 | 0.011 (−0.011, 0.034) | 0.318 |
| | | | Inverse variance weighted | 0.014 | 0.030 (0.003, 0.056) | 0.027 |
| | | | Simple mode | 0.018 | 0.002 (−0.033, 0.038) | 0.904 |
| | | | Weighted mode | 0.017 | 0.002 (−0.031, 0.034) | 0.928 |

SNP, single nucleotide polymorphism; MR, mendelian randomization; SE, standard error; 95% CI, 95% confidence interval.

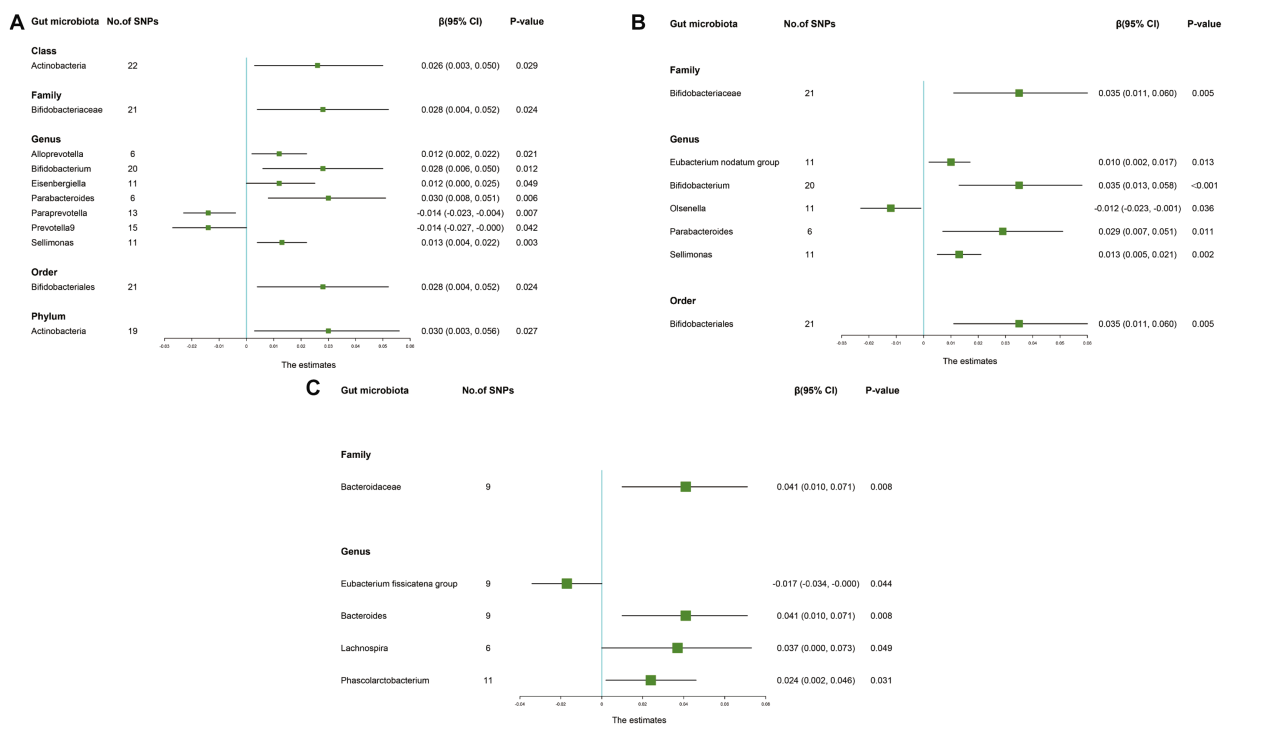


FIGURE 4
Forest plot of the causality between gut microbiota with sarcopenia-related traits. The estimates: Inverse variance weighted (IVW) results of gut microbiota and sarcopenia-related traits; *p*-value: *p*-value of the estimate. **(A)** Hand grip strength (Right); **(B)** Hand grip strength (Left); **(C)** Appendicular lean mass. SNP, single-nucleotide polymorphism.

homeostasis (Wang et al., 2015). *Bifidobacterium* also contributed to the absorption and utilization of vitamin D and minerals such as calcium, phosphorus, and iron, which are essential for muscle metabolism (Montazeri-Najafabady et al., 2019). Furthermore, *Bifidobacterium* was rich in genes encoding proteins related to the carbohydrate and amino acid transport and metabolism, influencing protein synthesis and nutrient utilization, which might also be one of the potential mechanisms by which *Bifidobacterium* prevents sarcopenia (Tu et al., 2023).

Our MR analysis also identified a causal relationship between *Genus Oxalobacter*, *Family Oxalobacteraceae* and the prevalence of LBP and RA, respectively. *Oxalobacter*, is a unique anaerobic bacterium that plays an important role in degrading dietary oxalate and stimulating oxalate secretion by the gut mucosa (Liu et al., 2017;

10.3389/fmicb.2023.1238800

TABLE 4 Mendelian randomisation (MR) results of causal effects between gut microbiome and hand grip strength (Left).

| Group | Bacterial traits | Nsnp | Methods | SE | β (95% CI) | *p*-value |
|---|---|---|---|---|---|---|
| *Family* | *Bifidobacteriaceae* | 21 | MR Egger | 0.034 | 0.159 (0.092, 0.226) | <0.001 |
| | | | Weighted median | 0.011 | 0.032 (0.009, 0.054) | 0.005 |
| | | | Inverse variance weighted | 0.013 | 0.035 (0.011, 0.060) | 0.005 |
| | | | Simple mode | 0.031 | 0.004 (−0.056, 0.065) | 0.888 |
| | | | Weighted mode | 0.026 | 0.081 (0.030, 0.131) | 0.005 |
| *Genus* | *Eubacterium nodatum group* | 11 | MR Egger | 0.017 | 0.012 (−0.022, 0.046) | 0.518 |
| | | | Weighted median | 0.005 | 0.006 (−0.005, 0.016) | 0.308 |
| | | | Inverse variance weighted | 0.004 | 0.010 (0.002, 0.017) | 0.013 |
| | | | Simple mode | 0.009 | 0.002 (−0.016, 0.021) | 0.803 |
| | | | Weighted mode | 0.010 | 0.002 (−0.017, 0.021) | 0.830 |
| *Genus* | *Bifidobacterium* | 20 | MR Egger | 0.033 | 0.046 (−0.020, 0.111) | 0.190 |
| | | | Weighted median | 0.011 | 0.031 (0.009, 0.053) | 0.006 |
| | | | Inverse variance weighted | 0.011 | 0.035 (0.013, 0.058) | <0.001 |
| | | | Simple mode | 0.029 | 0.014 (−0.043, 0.072) | 0.625 |
| | | | Weighted mode | 0.042 | 0.081 (−0.001, 0.162) | 0.067 |
| *Genus* | *Olsenella* | 11 | MR Egger | 0.021 | −0.034 (−0.076, 0.008) | 0.142 |
| | | | Weighted median | 0.006 | −0.014 (−0.025, −0.002) | 0.019 |
| | | | Inverse variance weighted | 0.006 | −0.012 (−0.023, −0.001) | 0.036 |
| | | | Simple mode | 0.009 | −0.013 (−0.031, 0.004) | 0.164 |
| | | | Weighted mode | 0.009 | −0.013 (−0.030, 0.004) | 0.157 |
| *Genus* | *Parabacteroides* | 6 | MR Egger | 0.038 | 0.042 (−0.032, 0.116) | 0.328 |
| | | | Weighted median | 0.015 | 0.027 (−0.001–0.056) | 0.06 |
| | | | Inverse variance weighted | 0.011 | 0.029 (0.007, 0.051) | 0.011 |
| | | | Simple mode | 0.022 | 0.030 (−0.014, 0.074) | 0.235 |
| | | | Weighted mode | 0.019 | 0.028 (−0.009, 0.065) | 0.204 |
| *Genus* | *Sellimonas* | 11 | MR Egger | 0.019 | 0.038 (0.001, 0.074) | 0.073 |
| | | | Weighted median | 0.006 | 0.012 (0.001, 0.023) | 0.035 |
| | | | Inverse variance weighted | 0.004 | 0.013 (0.005, 0.021) | 0.002 |
| | | | Simple mode | 0.009 | 0.012 (−0.007, 0.030) | 0.236 |
| | | | Weighted mode | 0.009 | 0.011 (−0.007, 0.029) | 0.261 |
| *Order* | *Bifidobacteriales* | 21 | MR Egger | 0.034 | 0.159 (0.092, 0.226) | <0.001 |
| | | | Weighted median | 0.012 | 0.032 (0.009, 0.054) | 0.006 |
| | | | Inverse variance weighted | 0.013 | 0.035 (0.011, 0.060) | 0.005 |
| | | | Simple mode | 0.034 | 0.004 (−0.062, 0.071) | 0.898 |
| | | | Weighted mode | 0.025 | 0.081 (0.031, 0.130) | 0.005 |

SNP, single nucleotide polymorphism; MR, mendelian randomization; SE, standard error; 95% CI, 95% confidence interval.

Daniel et al., 2021). Recently, intensive studies have reported that *Oxalobacter* is closely related to the pathogenesis of kidney stones, hyperoxaluria, and chronic kidney disease (CKD) (Sidhu et al., 1999; Turkmen and Erdur, 2015; Falony, 2018). In addition, Li et al. observed that the diversity and relative abundance of gut microbiota in individuals with RA were significantly different from those in healthy controls. Specifically, the relative abundance of *Pelagibacterium* was higher and *Oxalobacter* and *Blautia* were lower in patients with RA (Li et al., 2021), which was consistent with our findings. Numerous studies emphasized the key role of the gut microbiota in RA pathogenesis, through a variety of mechanisms, including the production of proinflammatory metabolites, impairment of the intestinal mucosal barrier, and regulation of hormones throughout the body (Zhao et al., 2022). However, studies on the role of *Oxalobacter* in LBP are currently limited. Thus, it is necessary to further study the possible role of *Oxalobacter* in LBP and RA development.

In addition, we also observed some promising gut microbiota were associated with the risk of OP and AS. Several mechanisms seem

TABLE 5 Mendelian randomisation (MR) results of causal effects between gut microbiome and appendicular lean mass.

| Group | Bacterial traits | Nsnp | Methods | SE | β (95% CI) | *p*-value |
|---|---|---|---|---|---|---|
| *Family* | *Bacteroidaceae* | 9 | MR Egger | 0.086 | 0.008 (−0.160, 0.176) | 0.927 |
| | | | Weighted median | 0.017 | 0.022 (−0.012, 0.056) | 0.197 |
| | | | Inverse variance weighted | 0.015 | 0.041 (0.010, 0.071) | 0.008 |
| | | | Simple mode | 0.025 | 0.019 (−0.031, 0.069) | 0.478 |
| | | | Weighted mode | 0.021 | 0.017 (−0.025, 0.058) | 0.456 |
| *Genus* | *Eubacterium fissicatena group* | 9 | MR Egger | 0.047 | −0.047 (−0.139, 0.046) | 0.353 |
| | | | Weighted median | 0.009 | −0.022 (−0.039, −0.006) | 0.009 |
| | | | Inverse variance weighted | 0.008 | −0.017 (−0.034, −0.000) | 0.044 |
| | | | Simple mode | 0.013 | −0.024 (−0.049, 0.002) | 0.103 |
| | | | Weighted mode | 0.012 | −0.023 (−0.047, 0.001) | 0.095 |
| *Genus* | *Bacteroides* | 9 | MR Egger | 0.086 | 0.008 (−0.160, 0.176) | 0.927 |
| | | | Weighted median | 0.018 | 0.022 (−0.013, 0.057) | 0.215 |
| | | | Inverse variance weighted | 0.015 | 0.041 (0.010, 0.071) | 0.008 |
| | | | Simple mode | 0.025 | 0.019 (−0.031, 0.068) | 0.477 |
| | | | Weighted mode | 0.023 | 0.017 (−0.029, 0.062) | 0.492 |
| *Genus* | *Lachnospira* | 6 | MR Egger | 0.098 | 0.186 (−0.007, 0.379) | 0.132 |
| | | | Weighted median | 0.020 | 0.036 (−0.003, 0.075) | 0.072 |
| | | | Inverse variance weighted | 0.019 | 0.037 (0.000, 0.073) | 0.049 |
| | | | Simple mode | 0.028 | 0.033 (−0.022, 0.087) | 0.290 |
| | | | Weighted mode | 0.027 | 0.032 (−0.020, 0.084) | 0.281 |
| *Genus* | *Phascolarctobacterium* | 11 | MR Egger | 0.053 | 0.022 (−0.082, 0.125) | 0.689 |
| | | | Weighted median | 0.013 | 0.014 (−0.011, 0.039) | 0.279 |
| | | | Inverse variance weighted | 0.011 | 0.024 (0.002, 0.046) | 0.031 |
| | | | Simple mode | 0.018 | 0.017 (−0.017, 0.052) | 0.347 |
| | | | Weighted mode | 0.018 | 0.017 (−0.018, 0.052) | 0.358 |

SNP, single nucleotide polymorphism; MR, mendelian randomization; SE, standard error; 95% CI, 95% confidence interval.

to offer preliminary explanation for the relationship between gut flora and OP. On the one hand, the gut microbiota could regulate the Treg/Th17 cells balance or relevant cytokines through the immune system, affecting the intestinal and systemic immune states, thereby establishing a dynamic balance between osteoblasts (OB) and osteoclasts (OC), which is important for normal bone mass maintenance (Locantore et al., 2020). On the other hand, microbial metabolites such as SFAs, secondary bile acid (SBA), and indole derivatives participate in the reconstruction of bone resorption, metabolism and fracture healing by providing energy to gut epithelium cells and promoting calcium and phosphorus absorption (Tu et al., 2021). In addition, intestinal flora imbalance could promote the systemic chronic inflammatory response, which is closely related to the occurrence of AS (Guggino et al., 2021). Stebbings et al. demonstrated that the abundance of *Lachnospiraceae*, *Prevotellaceae*, and *Bacteroidaceae* was higher and that of *Ruminococcaceae* and *Rikenellaceae* was lower in AS patients compared with the healthy controls (Stebbings et al., 2002). According to an animal study in mice, regulating the gut microbiota and improving gut barrier function could delay AS progression (Liu et al., 2019). On the basis of the above evidence, we can further investigate how specific gut microbiota affect OP and AS.

Reverse MR analysis showed that fracture may lead to a higher abundance of *Family Bacteroidales* and sarcopenia may result in a lower abundance of *Genus Sellimonas*. According to a case–control study of 50 elderly patients, in patients with fracture, the relative abundance of *Bacteroidales* was higher and *Lachnospirales* was lower compared to healthy controls, suggesting that altering the microbiome may be an effective way to reduce fracture risk (Rosello-Anon et al., 2023). Another study of postmenopausal Japanese women reported that *Bacteroidels* and *Rikenellaceae* may be involved in bone metabolism and fracture risk (Ozaki et al., 2021). Furthermore, an animal study has also revealed that the proportion of *Firmicutes* and *Bacteroidetes* increased significantly by 16S RNA sequencing in postmenopausal osteoporosis mice (Wen et al., 2020). In addition, *Sellimonas* has been shown to be involved in restoring the balance of the intestinal flora (Munoz et al., 2020). Despite this, there has been a very limited amount of literature about *Sellimonas*. Thus, the underlying mechanism warrants future investigation.

10.3389/fmicb.2023.1238800

TABLE 6 Mendelian randomisation (MR) results of causal effects between gut microbiome and the risk of low back pain.

| Group | Bacterial traits | Nsnp | Methods | SE | OR (95% CI) | *p*-value |
|---|---|---|---|---|---|---|
| *Class* | *Melainabacteria* | 10 | MR Egger | 0.161 | 0.848 (0.618, 1.162) | 0.334 |
| | | | Weighted median | 0.066 | 0.934 (0.820, 1.063) | 0.301 |
| | | | Inverse variance weighted | 0.050 | 0.891 (0.808, 0.984) | 0.022 |
| | | | Simple mode | 0.097 | 0.936 (0.774, 1.131) | 0.509 |
| | | | Weighted mode | 0.085 | 0.927 (0.784, 1.096) | 0.396 |
| *Family* | *Prevotellaceae* | 16 | MR Egger | 0.251 | 1.316 (0.804, 2.151) | 0.293 |
| | | | Weighted median | 0.086 | 1.149 (0.970, 1.362) | 0.107 |
| | | | Inverse variance weighted | 0.066 | 1.182 (1.038, 1.346) | 0.012 |
| | | | Simple mode | 0.157 | 1.139 (0.837, 1.551) | 0.421 |
| | | | Weighted mode | 0.154 | 1.125 (0.831, 1.522) | 0.459 |
| *Genus* | *Oxalobacter* | 11 | MR Egger | 0.187 | 1.037 (0.719, 1.496) | 0.848 |
| | | | Weighted median | 0.053 | 1.130 (1.018, 1.254) | 0.022 |
| | | | Inverse variance weighted | 0.040 | 1.151 (1.065, 1.245) | <0.001 |
| | | | Simple mode | 0.099 | 1.050 (0.864, 1.276) | 0.634 |
| | | | Weighted mode | 0.086 | 1.057 (0.893, 1.252) | 0.534 |
| *Genus* | *Tyzzerella3* | 13 | MR Egger | 0.241 | 1.053 (0.656, 1.690) | 0.834 |
| | | | Weighted median | 0.055 | 1.123 (1.009, 1.251) | 0.035 |
| | | | Inverse variance weighted | 0.042 | 1.121 (1.032, 1.217) | 0.007 |
| | | | Simple mode | 0.087 | 1.124 (0.948, 1.332) | 0.203 |
| | | | Weighted mode | 0.086 | 1.128 (0.953, 1.336) | 0.186 |

SNP, single nucleotide polymorphism; MR, mendelian randomization; SE, standard error; 95% CI, 95% confidence interval.

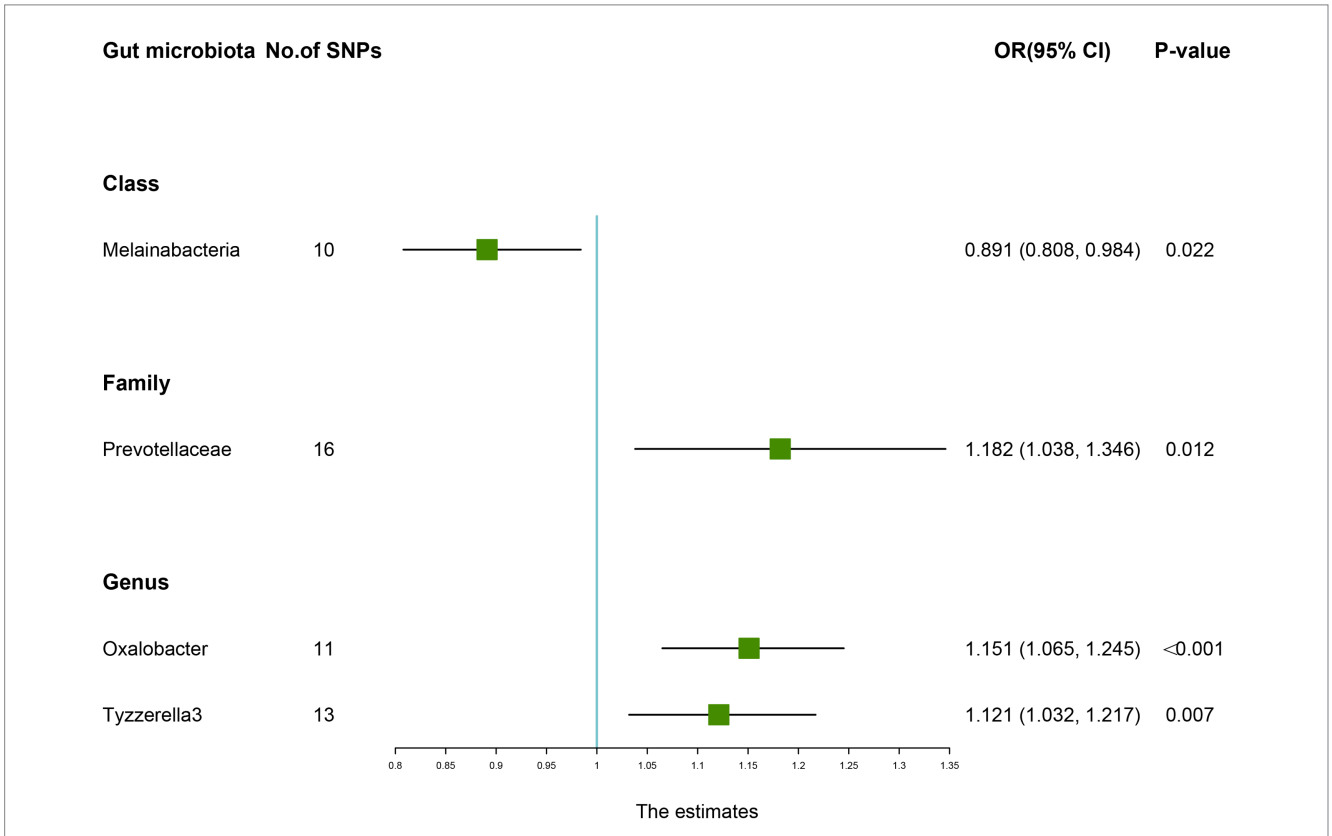


FIGURE 5
Forest plot of the causality between gut microbiota with the risk of low back pain. The estimates: Inverse variance weighted (IVW) results of gut microbiota and low back pain risk; *p*-value: *p*-value of the estimate. OR, odds ratio; SNP, single-nucleotide polymorphism.

TABLE 7 Mendelian randomisation (MR) results of causal effects between gut microbiome and the risk of rheumatoid arthritis.

| Group | Bacterial traits | Nsnp | Methods | SE | OR (95% CI) | *p*-value |
|---|---|---|---|---|---|---|
| *Class* | *Clostridia* | 9 | MR Egger | 0.648 | 1.589 (0.447, 5.655) | 0.497 |
| | | | Weighted median | 0.187 | 1.386 (0.960, 2.000) | 0.092 |
| | | | Inverse variance weighted | 0.143 | 1.368 (1.033, 1.812) | 0.029 |
| | | | Simple mode | 0.316 | 1.475 (0.793, 2.742) | 0.231 |
| | | | Weighted mode | 0.293 | 1.420 (0.800, 2.521) | 0.229 |
| *Family* | *Christensenellaceae* | 9 | MR Egger | 0.317 | 0.727 (0.390, 1.354) | 0.348 |
| | | | Weighted median | 0.164 | 0.765 (0.554, 1.055) | 0.104 |
| | | | Inverse variance weighted | 0.133 | 0.750 (0.578, 0.973) | 0.031 |
| | | | Simple mode | 0.230 | 0.790 (0.503, 1.240) | 0.293 |
| | | | Weighted mode | 0.213 | 0.772 (0.509, 1.171) | 0.252 |
| *Family* | *Clostridialesvadin BB60 group* | 12 | MR Egger | 0.231 | 1.101 (0.700, 1.732) | 0.715 |
| | | | Weighted median | 0.119 | 1.307 (1.036, 1.649) | 0.020 |
| | | | Inverse variance weighted | 0.084 | 1.200 (1.018, 1.416) | 0.032 |
| | | | Simple mode | 0.208 | 1.405 (0.934, 2.114) | 0.139 |
| | | | Weighted mode | 0.159 | 1.400 (1.025, 1.914) | 0.089 |
| *Family* | *Desulfovibrionaceae* | 9 | MR Egger | 0.280 | 1.202 (0.695, 2.080) | 0.531 |
| | | | Weighted median | 0.146 | 1.302 (0.978, 1.734) | 0.095 |
| | | | Inverse variance weighted | 0.111 | 1.253 (1.008, 1.558) | 0.042 |
| | | | Simple mode | 0.239 | 1.270 (0.795, 2.028) | 0.335 |
| | | | Weighted mode | 0.193 | 1.320 (0.905, 1.927) | 0.162 |
| *Family* | *Oxalobacteraceae* | 12 | MR Egger | 0.313 | 0.782 (0.424, 1.444) | 0.450 |
| | | | Weighted median | 0.086 | 0.774 (0.654, 0.915) | 0.002 |
| | | | Inverse variance weighted | 0.065 | 0.792 (0.698, 0.899) | <0.001 |
| | | | Simple mode | 0.127 | 0.778 (0.607, 0.997) | 0.059 |
| | | | Weighted mode | 0.125 | 0.776 (0.608, 0.991) | 0.047 |
| *Family* | *Streptococcaceae* | 13 | MR Egger | 0.498 | 1.535 (0.578, 4.078) | 0.408 |
| | | | Weighted median | 0.157 | 1.596 (1.173, 2.173) | 0.003 |
| | | | Inverse variance weighted | 0.114 | 1.296 (1.038, 1.620) | 0.022 |
| | | | Simple mode | 0.226 | 1.578 (1.012, 2.460) | 0.071 |
| | | | Weighted mode | 0.222 | 1.597 (1.033, 2.470) | 0.051 |
| *Genus* | *Desulfovibrio* | 9 | MR Egger | 0.304 | 1.066 (0.588, 1.935) | 0.839 |
| | | | Weighted median | 0.135 | 1.101 (0.845, 1.433) | 0.484 |
| | | | Inverse variance weighted | 0.106 | 1.255 (1.020, 1.544) | 0.032 |
| | | | Simple mode | 0.236 | 1.122 (0.706, 1.781) | 0.625 |
| | | | Weighted mode | 0.163 | 1.070 (0.777, 1.472) | 0.688 |
| *Genus* | *Oxalobacter* | 9 | MR Egger | 0.370 | 0.897 (0.435, 1.850) | 0.777 |
| | | | Weighted median | 0.093 | 0.800 (0.667, 0.959) | 0.014 |
| | | | Inverse variance weighted | 0.068 | 0.825 (0.722, 0.943) | 0.005 |
| | | | Simple mode | 0.137 | 0.874 (0.668, 1.143) | 0.335 |
| | | | Weighted mode | 0.137 | 0.795 (0.608, 1.040) | 0.111 |
| *Genus* | *Ruminococcaceae UCG002* | 18 | MR Egger | 0.366 | 0.326 (0.159, 0.667) | 0.007 |

*(Continued)*

TABLE 7 (Continued)

| Group | Bacterial traits | Nsnp | Methods | SE | OR (95% CI) | *p*-value |
|---|---|---|---|---|---|---|
| | | | Weighted median | 0.133 | 0.802 (0.618, 1.040) | 0.102 |
| | | | Inverse variance weighted | 0.096 | 0.805 (0.667, 0.971) | 0.023 |
| | | | Simple mode | 0.251 | 0.706 (0.432, 1.154) | 0.192 |
| | | | Weighted mode | 0.218 | 0.725 (0.473, 1.112) | 0.145 |
| *Genus* | *Ruminococcaceae UCG013* | 9 | MR Egger | 0.556 | 1.485 (0.499, 4.418) | 0.501 |
| | | | Weighted median | 0.174 | 1.529 (1.087, 2.150) | 0.019 |
| | | | Inverse variance weighted | 0.130 | 1.365 (1.057, 1.763) | 0.017 |
| | | | Simple mode | 0.243 | 1.557 (0.966, 2.510) | 0.118 |
| | | | Weighted mode | 0.223 | 1.531 (0.990, 2.369) | 0.097 |
| *Genus* | *Turicibacter* | 9 | MR Egger | 0.519 | 1.224 (0.442, 3.385) | 0.709 |
| | | | Weighted median | 0.133 | 1.144 (0.882, 1.483) | 0.322 |
| | | | Inverse variance weighted | 0.098 | 1.218 (1.005, 1.476) | 0.044 |
| | | | Simple mode | 0.220 | 1.093 (0.710, 1.681) | 0.677 |
| | | | Weighted mode | 0.197 | 1.103 (0.750, 1.623) | 0.614 |
| *Order* | *Bacillales* | 6 | MR Egger | 0.269 | 0.808 (0.476, 1.369) | 0.472 |
| | | | Weighted median | 0.087 | 0.875 (0.737, 1.038) | 0.139 |
| | | | Inverse variance weighted | 0.069 | 0.850 (0.743, 0.972) | 0.018 |
| | | | Simple mode | 0.120 | 0.892 (0.705, 1.128) | 0.383 |
| | | | Weighted mode | 0.103 | 0.900 (0.735, 1.101) | 0.367 |
| *Order* | *Clostridiales* | 10 | MR Egger | 0.594 | 1.289 (0.402, 4.132) | 0.680 |
| | | | Weighted median | 0.179 | 1.256 (0.885, 1.783) | 0.215 |
| | | | Inverse variance weighted | 0.132 | 1.349 (1.042, 1.748) | 0.023 |
| | | | Simple mode | 0.263 | 1.386 (0.829, 2.319) | 0.244 |
| | | | Weighted mode | 0.233 | 1.309 (0.828, 2.067) | 0.298 |
| *Phylum* | *Cyanobacteria* | 7 | MR Egger | 0.410 | 0.728 (0.326, 1.627) | 0.474 |
| | | | Weighted median | 0.136 | 0.752 (0.576, 0.981) | 0.028 |
| | | | Inverse variance weighted | 0.107 | 0.783 (0.635, 0.965) | 0.022 |
| | | | Simple mode | 0.197 | 0.740 (0.502, 1.089) | 0.164 |
| | | | Weighted mode | 0.182 | 0.746 (0.522, 1.064) | 0.153 |

SNP, single nucleotide polymorphism; MR, mendelian randomization; SE, standard error; 95% CI, 95% confidence interval.

Our study had several strengths. First of all, we used MR analysis to infer that the relationship between the gut microbiome and MSK diseases should be less susceptible to confounding and reverse causation than traditional observational analyses. Additionally, we analyzed the causal effect of each taxon on MSK diseases from the genus to the phylum level, which provides guidance for the prevention and treatment of MSK diseases by targeting specific gut microbiota in clinical practice. Third, the combination of stringent quality control procedures and multiple sensitivity analysis approaches enhances the credibility and robustness in the causal relationships inferred from the MR study. However, the present study also had some limitations that should be noted. Firstly, due to the lack of demographic data in the original study (e.g., gender, age, and race), we could not perform further subgroup analyses to obtain more specific effect relationships. Secondly, the GWAS data on gut microbiota used in this study are based on the population cohort from the largest macro-genome sequencing study to date. In the future, summary data of other gut microbiota needs to be obtained to provide a more comprehensive assessment of the causal relationship between gut microbes and the risk of MSK diseases. Last but not least, this study was confined to individuals of European origin and other populations require further MR studies since causal relationships may vary from race to race.

Overall, our study comprehensively evaluated the potential causal association between gut microbiota and six common MSK diseases. These findings provided new insights into the prevention, progression, and treatment of MSK diseases through targeting specific gut microbiota. In the future, more clinical trials and mechanism studies are needed to explore the exact mechanisms underlying the interactions between the gut microbiota and the prevalence of MSK diseases.

10.3389/fmicb.2023.1238800

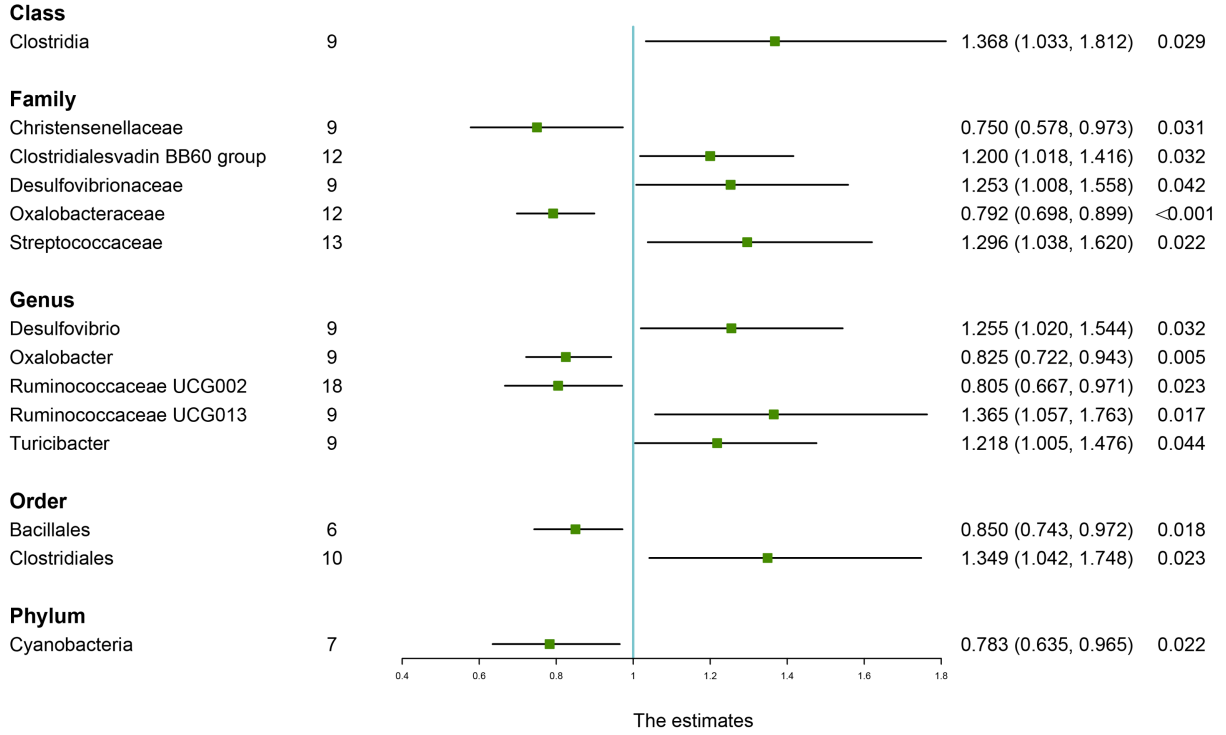


FIGURE 6
Forest plot of the causality between gut microbiota with the risk of rheumatoid arthritis. The estimates: Inverse variance weighted (IVW) results of gut microbiota and rheumatoid arthritis risk; *p*-value: *p*-value of the estimate. OR, odds ratio; SNP, single-nucleotide polymorphism.

TABLE 8 Mendelian randomisation (MR) results of causal effects between gut microbiome and the risk of ankylosing spondylitis.

| Group | Bacterial traits | Nsnp | Methods | SE | OR (95% CI) | *p*-value |
|---|---|---|---|---|---|---|
| *Family* | *Lactobacillaceae* | 9 | MR Egger | 0.350 | 0.615 (0.309, 1.221) | 0.207 |
| | | | Weighted median | 0.193 | 0.783 (0.537, 1.143) | 0.206 |
| | | | Inverse variance weighted | 0.142 | 0.696 (0.527, 0.919) | 0.011 |
| | | | Simple mode | 0.302 | 0.527 (0.292, 0.952) | 0.067 |
| | | | Weighted mode | 0.265 | 0.881 (0.523, 1.481) | 0.644 |
| *Family* | *Rikenellaceae* | 19 | MR Egger | 0.524 | 0.766 (0.274, 2.137) | 0.617 |
| | | | Weighted median | 0.224 | 0.600 (0.386, 0.931) | 0.023 |
| | | | Inverse variance weighted | 0.166 | 0.680 (0.491, 0.942) | 0.020 |
| | | | Simple mode | 0.409 | 0.546 (0.245, 1.216) | 0.156 |
| | | | Weighted mode | 0.418 | 0.542 (0.239, 1.230) | 0.160 |
| *Genus* | *Ruminococcaceae NK4A214 group* | 14 | MR Egger | 0.605 | 4.409 (1.347, 14.427) | 0.030 |
| | | | Weighted median | 0.261 | 1.950 (1.168, 3.255) | 0.011 |
| | | | Inverse variance weighted | 0.184 | 1.707 (1.190, 2.449) | 0.004 |
| | | | Simple mode | 0.493 | 2.448 (0.931, 6.440) | 0.093 |
| | | | Weighted mode | 0.411 | 2.448 (1.093, 5.484) | 0.049 |
| *Genus* | *Howardella* | 9 | MR Egger | 0.428 | 0.615 (0.266, 1.424) | 0.294 |
| | | | Weighted median | 0.157 | 0.882 (0.648, 1.200) | 0.423 |
| | | | Inverse variance weighted | 0.108 | 0.802 (0.650, 0.991) | 0.041 |
| | | | Simple mode | 0.257 | 0.964 (0.583, 1.595) | 0.890 |

*(Continued)*

TABLE 8 (Continued)

| Group | Bacterial traits | Nsnp | Methods | SE | OR (95% CI) | *p*-value |
|---|---|---|---|---|---|---|
| | | | Weighted mode | 0.259 | 0.980 (0.590, 1.626) | 0.939 |
| *Genus* | *Anaerotruncus* | 13 | MR Egger | 0.580 | 0.280 (0.090, 0.874) | 0.051 |
| | | | Weighted median | 0.289 | 0.801 (0.454, 1.411) | 0.442 |
| | | | Inverse variance weighted | 0.199 | 0.671 (0.454, 0.991) | 0.045 |
| | | | Simple mode | 0.436 | 0.946 (0.402, 2.223) | 0.900 |
| | | | Weighted mode | 0.426 | 0.900 (0.390, 2.074) | 0.808 |

SNP, single nucleotide polymorphism; MR, mendelian randomization; SE, standard error; 95% CI, 95% confidence interval.

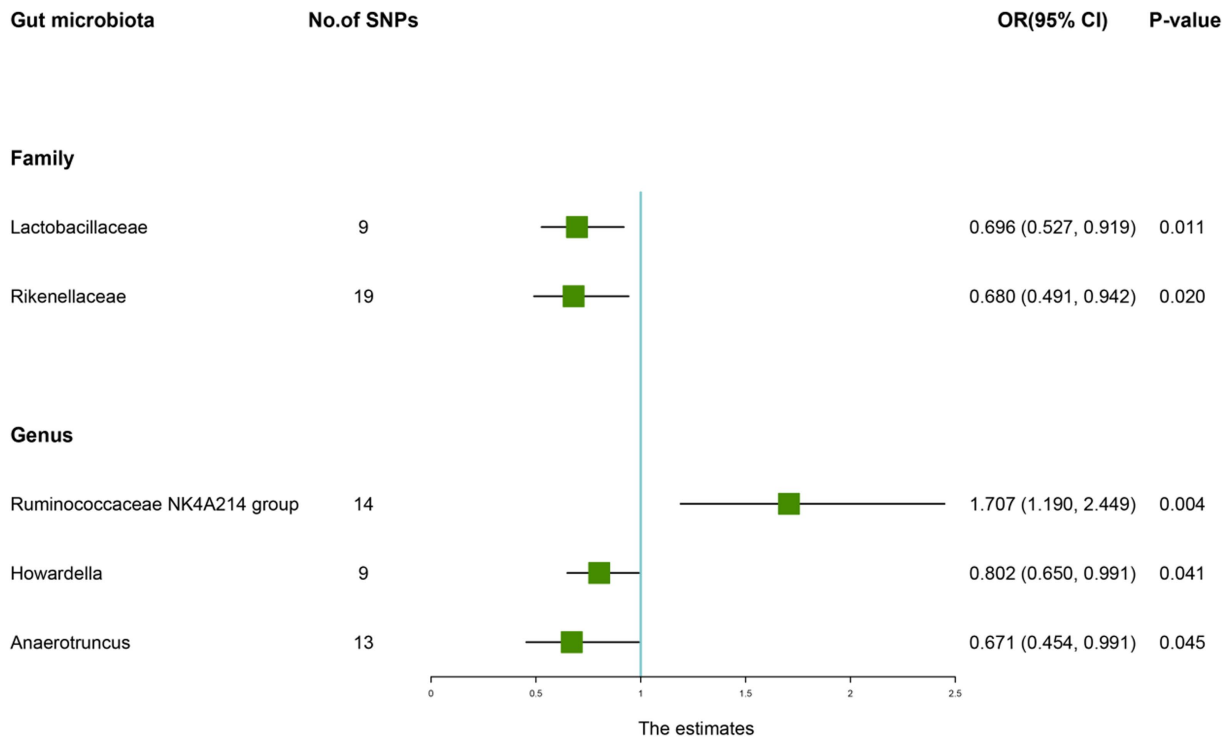


FIGURE 7
Forest plot of the causality between gut microbiota with the risk of ankylosing spondylitis. The estimates: Inverse variance weighted (IVW) results of gut microbiota and ankylosing spondylitis risk; *p*-value: *p*-value of the estimate. OR, odds ratio; SNP, single-nucleotide polymorphism.

## 5. Conclusion

In summary, our study provided evidence of a potential causal relationship between specific gut microbiota and MSK diseases through the bi-directional MR analysis. These findings opened up new avenues for exploring the underlying mechanisms by which gut microbiota influence MSK diseases and contributed to the development of targeted interventions and personalized treatments.

## Data availability statement

The original contributions presented in the study are included in the article/Supplementary material, further inquiries can be directed to the corresponding authors.

## Author contributions

SC collected data. HH, XS, and GZ organized the study and performed the statistical analysis. QZ and ZL drafted the manuscript. All authors contributed to the article and approved the submitted version.

## Funding

This work was supported by the Elderly Health Research Project of Jiangsu Commission of Health (LKZ2022008), the Natural Science Foundation of Nanjing University of Chinese Medicine (XZR2021060), and the Foundation of The Second Affiliated Hospital of Nanjing University of Chinese Medicine (SEZ202003).

10.3389/fmicb.2023.1238800

TABLE 9 Sensitivity analysis of the Mendelian randomization (MR) analysis results of gut microbiota and musculoskeletal diseases.

| Outcome | Bacterial traits | Cochran Q statistic | Heterogeneity *p*-value | MR-Egger Intercept | Intercept *p*-value | MR-PRESSO Global test *p*-value |
|---|---|---|---|---|---|---|
| Osteoporosis | *NB1n* | 4.318 | 0.987 | 0.000 | 0.413 | 0.987 |
| | *Lachnospiraceae NK4A136 group* | 11.362 | 0.581 | 0.000 | 0.086 | 0.514 |
| | *Howardella* | 5.752 | 0.765 | −0.001 | 0.28 | 0.77 |
| | *Christensenellaceae R.7 group* | 10.056 | 0.3 | 0.000 | 0.55 | 0.36 |
| | *Eubacterium oxidoreducens group* | 4.423 | 0.3 | 0.00 | 0.673 | 0.41 |
| Fracture | *Mollicutes* | 10.467 | 0.48 | 0.00 | 0.848 | 0.50 |
| | *Defluviitaleaceae* | 13.793 | 0.245 | 0.00 | 0.573 | 0.26 |
| | *Bacteroidales S24.7 group* | 12.199 | 0.14 | −0.0 | 0.4 | 0.18 |
| | *Allisonella* | 7.713 | 0.3 | 0.0 | 0.8 | 0.39 |
| | *Collinsella* | 3.987 | 0.91 | 0.00 | 0.9 | 0.92 |
| | *Defluviitaleaceae UCG011* | 8.947 | 0.44 | 0.00 | 0.6 | 0.46 |
| | *Tenericutes* | 10.467 | 0.489 | 0.000 | 0.848 | 0.521 |
| Hand grip strength (Right) | *Actinobacteria* | 43.759 | 0.119 | 0.002 | 0.360 | 0.209 |
| | *Bifidobacteriaceae* | 58.911 | 0.148 | −0.009 | 0.177 | 0.451 |
| | *Alloprevotella* | 3.621 | 0.605 | −0.001 | 0.871 | 0.645 |
| | *Bifidobacterium* | 48.382 | 0.268 | −0.001 | 0.969 | 0.327 |
| | *Eisenbergiella* | 12.407 | 0.259 | −0.004 | 0.372 | 0.280 |
| | *Parabacteroides* | 2.356 | 0.798 | 0.002 | 0.592 | 0.803 |
| | *Paraprevotella* | 7.685 | 0.809 | 0.001 | 0.721 | 0.809 |
| | *Prevotella9* | 21.374 | 0.092 | 0.002 | 0.441 | 0.098 |
| | *Sellimonas* | 8.671 | 0.371 | −0.000 | 0.865 | 0.394 |
| | *Actinobacteria* | 12.803 | 0.119 | 0.002 | 0.702 | 0.308 |
| Hand grip strength (Left) | *Bifidobacteriaceae* | 60.348 | 0.799 | −0.009 | 0.126 | 0.782 |
| | *Eubacterium nodatum group* | 9.233 | 0.510 | −0.000 | 0.908 | 0.530 |
| | *Bifidobacterium* | 50.120 | 0.133 | 0.001 | 0.847 | 0.100 |
| | *Olsenella* | 18.383 | 0.488 | 0.003 | 0.305 | 0.066 |
| | *Parabacteroides* | 5.492 | 0.359 | −0.001 | 0.728 | 0.446 |
| | *Sellimonas* | 6.242 | 0.620 | 0.000 | 0.990 | 0.651 |
| | *Bifidobacteriales* | 60.348 | 0.799 | −0.009 | 0.126 | 0.762 |
| Appendicular lean mass | *Bacteroidaceae* | 12.005 | 0.151 | 0.002 | 0.711 | 0.195 |
| | *Eubacterium fissicatena group* | 16.318 | 0.380 | 0.004 | 0.540 | 0.517 |
| | *Bacteroides* | 12.005 | 0.151 | 0.002 | 0.711 | 0.175 |
| | *Lachnospira* | 7.805 | 0.167 | −0.009 | 0.141 | 0.231 |
| | *Phascolarctobacterium* | 13.400 | 0.145 | −0.001 | 0.825 | 0.174 |
| Low back pain | *Melainabacteria* | 9.168 | 0.422 | −0.006 | 0.749 | 0.473 |

*(Continued)*

TABLE 9 (Continued)

| Outcome | Bacterial traits | Cochran Q statistic | Heterogeneity *p*-value | MR-Egger Intercept | Intercept *p*-value | MR-PRESSO Global test *p*-value |
|---|---|---|---|---|---|---|
| | *Prevotellaceae* | 19.450 | 0.194 | 0.014 | 0.448 | 0.200 |
| | *Oxalobacter* | 6.227 | 0.796 | −0.016 | 0.583 | 0.836 |
| | *Tyzzerella3* | 11.783 | 0.945 | 0.007 | 0.762 | 0.953 |
| Rheumatoid arthritis | *Clostridia* | 6.466 | 0.595 | −0.010 | 0.819 | 0.649 |
| | *Christensenellaceae* | 0.309 | 1.000 | 0.003 | 0.916 | 1.000 |
| | *Clostridialesvadin BB60 group* | 8.826 | 0.638 | 0.008 | 0.698 | 0.653 |
| | *Desulfovibrionaceae* | 4.510 | 0.808 | 0.004 | 0.876 | 0.824 |
| | *Oxalobacteraceae* | 5.470 | 0.906 | 0.002 | 0.968 | 0.937 |
| | *Streptococcaceae* | 10.513 | 0.571 | −0.013 | 0.734 | 0.600 |
| | *Desulfovibrio* | 10.225 | 0.250 | 0.017 | 0.583 | 0.287 |
| | *Oxalobacter* | 0.808 | 4.515 | −0.012 | 0.825 | 0.819 |
| | *Ruminococcaceae UCG002* | 18.311 | 0.369 | 0.066 | 0.021 | 0.388 |
| | *Ruminococcaceae UCG013* | 12.877 | 0.116 | −0.019 | 0.685 | 0.134 |
| | *Turicibacter* | 5.330 | 0.722 | 0.000 | 0.993 | 0.736 |
| | *Bacillales* | 2.280 | 0.809 | 0.007 | 0.855 | 0.840 |
| | *Clostridiales* | 6.184 | 0.721 | 0.003 | 0.939 | 0.760 |
| | *Cyanobacteria* | 6.867 | 0.333 | 0.009 | 0.862 | 0.422 |
| Ankylosing spondylitis | *Lactobacillaceae* | 4.146 | 0.844 | 0.016 | 0.710 | 0.843 |
| | *Rikenellaceae* | 10.762 | 0.904 | −0.009 | 0.814 | 0.903 |
| | *Ruminococcaceae NK4A214 group* | 13.561 | 0.405 | −0.073 | 0.126 | 0.443 |
| | *Howardella* | 6.444 | 0.598 | 0.042 | 0.542 | 0.543 |
| | *Anaerotruncus* | 10.645 | 0.560 | 0.063 | 0.138 | 0.582 |

MR-Egger, Mendelian randomization Egger.

## Acknowledgments

The authors are very grateful to Genetic Factors for Osteoporosis Consortium (GEFOS) and MiBioGen Consortium for their selfless public sharing of GWAS summary data, which provides us with great convenience to carry out this research.

## Conflict of interest

The authors declare that the research was conducted in the absence of any commercial or financial relationships that could be construed as a potential conflict of interest.

## Publisher's note



## Supplementary material

The Supplementary material for this article can be found online at: https://www.frontiersin.org/articles/10.3389/fmicb.2023.1238800/full#supplementary-material

# References


Asquith, M., Sternes, P. R., Costello, M. E., Karstens, L., Diamond, S., Martin, T. M., et al. (2019). HLA alleles associated with risk of ankylosing spondylitis and rheumatoid arthritis influence the Gut microbiome. *Arthritis Rheumatol.* 71, 1642–1650. doi: 10.1002/art.40917

Bevan, S. (2015). Economic impact of musculoskeletal disorders (MSDs) on work in Europe. *Best Pract. Res. Clin. Rheumatol.* 29, 356–373. doi: 10.1016/j.berh.2015.08.002

Biver, E., Berenbaum, F., Valdes, A. M., Araujo, D. C. I., Bindels, L. B., Brandi, M. L., et al. (2019). Gut microbiota and osteoarthritis management: an expert consensus of the European society for clinical and economic aspects of osteoporosis, osteoarthritis and musculoskeletal diseases (ESCEO). *Ageing Res. Rev.* 55:100946. doi: 10.1016/j.arr.2019.100946

Bowden, J., Davey, S. G., and Burgess, S. (2015). Mendelian randomization with invalid instruments: effect estimation and bias detection through egger regression. *Int. J. Epidemiol.* 44, 512–525. doi: 10.1093/ije/dyv080

Bowden, J., Davey, S. G., Haycock, P. C., and Burgess, S. (2016). Consistent estimation in Mendelian randomization with some invalid instruments using a weighted median estimator. *Genet. Epidemiol.* 40, 304–314. doi: 10.1002/gepi.21965

Buigues, C., Fernandez-Garrido, J., Pruimboom, L., Hoogland, A. J., Navarro-Martinez, R., Martinez-Martinez, M., et al. (2016). Effect of a prebiotic formulation on frailty syndrome: a randomized, double-blind clinical trial. *Int. J. Mol. Sci.* 17:17. doi: 10.3390/ijms17060932

Castro-Mejia, J. L., Khakimov, B., Krych, L., Bulow, J., Bechshoft, R. L., Hojfeldt, G., et al. (2020). Physical fitness in community-dwelling older adults is linked to dietary intake, gut microbiota, and metabolomic signatures. *Aging Cell* 19:e13105. doi: 10.1111/acel.13105

Cortes, A., Hadler, J., Pointon, J. P., Robinson, P. C., Karaderi, T., Leo, P., et al. (2013). Identification of multiple risk variants for ankylosing spondylitis through high-density genotyping of immune-related loci. *Nat. Genet.* 45, 730–738. doi: 10.1038/ng.2667

Daniel, S. L., Moradi, L., Paiste, H., Wood, K. D., Assimos, D. G., Holmes, R. P., et al. (2021). Forty years of *Oxalobacter formigenes*, a gutsy oxalate-degrading specialist. *Appl. Environ. Microbiol.* 87:e54421. doi: 10.1128/AEM.00544-21

Davey, S. G., and Hemani, G. (2014). Mendelian randomization: genetic anchors for causal inference in epidemiological studies. *Hum. Mol. Genet.* 23, R89–R98. doi: 10.1093/hmg/ddu328

Falony, G. (2018). Beyond Oxalobacter: the gut microbiota and kidney stone formation. *Gut* 67, 2078–2079. doi: 10.1136/gutjnl-2018-316639

Guggino, G., Mauro, D., Rizzo, A., Alessandro, R., Raimondo, S., Bergot, A. S., et al. (2021). Inflammasome activation in ankylosing spondylitis is associated with Gut Dysbiosis. *Arthritis Rheumatol.* 73, 1189–1199. doi: 10.1002/art.41644

Huang, W. C., Hsu, Y. J., Huang, C. C., Liu, H. C., and Lee, M. C. (2020). Exercise training combined with *Bifidobacterium longum* OLP-01 supplementation improves exercise physiological adaption and performance. *Nutrients* 12:12. doi: 10.3390/nu12041145

Jia, J., Dou, P., Gao, M., Kong, X., Li, C., Liu, Z., et al. (2019). Assessment of causal direction between Gut Microbiota-dependent metabolites and Cardiometabolic health: a bidirectional Mendelian randomization analysis. *Diabetes* 68, 1747–1755. doi: 10.2337/db19-0153

Kurilshikov, A., Medina-Gomez, C., Bacigalupe, R., Radjabzadeh, D., Wang, J., Demirkan, A., et al. (2021). Large-scale association analyses identify host factors influencing human gut microbiome composition. *Nat. Genet.* 53, 156–165. doi: 10.1038/s41588-020-00763-1

Li, C., Liu, C., and Li, N. (2022). Causal associations between gut microbiota and adverse pregnancy outcomes: a two-sample Mendelian randomization study. *Front. Microbiol.* 13:1059281. doi: 10.3389/fmicb.2022.1059281

Li, Y., Zhang, S. X., Yin, X. F., Zhang, M. X., Qiao, J., Xin, X. H., et al. (2021). The Gut Microbiota and its relevance to peripheral lymphocyte subpopulations and cytokines in patients with rheumatoid arthritis. *J Immunol Res* 2021, 6665563–6665569. doi: 10.1155/2021/6665563

Liu, M., Koh, H., Kurtz, Z. D., Battaglia, T., PeBenito, A., Li, H., et al. (2017). *Oxalobacter formigenes*-associated host features and microbial community structures examined using the American Gut project. *Microbiome* 5:108. doi: 10.1186/s40168-017-0316-0

Liu, B., Yang, L., Cui, Z., Zheng, J., Huang, J., Zhao, Q., et al. (2019). Anti-TNF-alpha therapy alters the gut microbiota in proteoglycan-induced ankylosing spondylitis in mice. *Microbiology* 8:e927. doi: 10.1002/mbo3.927

Locantore, P., Del, G. V., Gelli, S., Paragliola, R. M., and Pontecorvi, A. (2020). The interplay between immune system and Microbiota in osteoporosis. *Mediat. Inflamm.* 2020:3686748. doi: 10.1155/2020/3686749

March, L., Smith, E. U., Hoy, D. G., Cross, M. J., Sanchez-Riera, L., Blyth, F., et al. (2014). Burden of disability due to musculoskeletal (MSK) disorders. *Best Pract. Res. Clin. Rheumatol.* 28, 353–366. doi: 10.1016/j.berh.2014.08.002

Montazeri-Najafabady, N., Ghasemi, Y., Dabbaghmanesh, M. H., Talezadeh, P., Koohpeyma, F., and Gholami, A. (2019). Supportive role of probiotic strains in protecting rats from Ovariectomy-induced cortical bone loss. *Probiotics Antimicrob. Proteins* 11, 1145–1154. doi: 10.1007/s12602-018-9443-6

Morris, J. A., Kemp, J. P., Youlten, S. E., Laurent, L., Logan, J. G., Chai, R. C., et al. (2019). An atlas of genetic influences on osteoporosis in humans and mice. *Nat. Genet.* 51, 258–266. doi: 10.1038/s41588-018-0302-x

Munoz, M., Guerrero-Araya, E., Cortes-Tapia, C., Plaza-Garrido, A., Lawley, T. D., and Paredes-Sabja, D. (2020). Comprehensive genome analyses of Sellimonas intestinalis, a potential biomarker of homeostasis gut recovery. *Microb. Genom.* 6:6. doi: 10.1099/mgen.0.000476

Murray, C. J., Vos, T., Lozano, R., Naghavi, M., Flaxman, A. D., Michaud, C., et al. (2012). Disability-adjusted life years (DALYs) for 291 diseases and injuries in 21 regions, 1990-2010: a systematic analysis for the global burden of disease study 2010. *Lancet* 380, 2197–2223. doi: 10.1016/S0140-6736(12)61689-4

Okada, Y., Wu, D., Trynka, G., Raj, T., Terao, C., Ikari, K., et al. (2014). Genetics of rheumatoid arthritis contributes to biology and drug discovery. *Nature* 506, 376–381. doi: 10.1038/nature12873

Ozaki, D., Kubota, R., Maeno, T., Abdelhakim, M., and Hitosugi, N. (2021). Association between gut microbiota, bone metabolism, and fracture risk in postmenopausal Japanese women. *Osteoporos. Int.* 32, 145–156. doi: 10.1007/s00198-020-05728-y

Pei, Y. F., Liu, Y. Z., Yang, X. L., Zhang, H., Feng, G. J., Wei, X. T., et al. (2020). The genetic architecture of appendicular lean mass characterized by association analysis in the UK biobank study. *Commun. Biol.* 3:608. doi: 10.1038/s42003-020-01334-0

Pierce, B. L., and Burgess, S. (2013). Efficient design for Mendelian randomization studies: subsample and 2-sample instrumental variable estimators. *Am. J. Epidemiol.* 178, 1177–1184. doi: 10.1093/aje/kwt084

Rizzoli, R. (2019). Nutritional influence on bone: role of gut microbiota. *Aging Clin. Exp. Res.* 31, 743–751. doi: 10.1007/s40520-019-01131-8

Rosello-Anon, A., Chiappe, C., Valverde-Vazquez, M. R., Sanguesa-Nebot, M. J., Gomez-Cabrera, M. C., Perez-Martinez, G., et al. (2023). [translated article] pilot study to determine the association between gut microbiota and fragility hip fracture. *Rev. Esp. Cir. Ortop. Traumatol.* 67, T279–T289. doi: 10.1016/j.recot.2023.03.002

Rosenfeld, S. B., Schroeder, K., and Watkins-Castillo, S. I. (2018). The economic burden of musculoskeletal disease in children and adolescents in the United States. *J. Pediatr. Orthop.* 38, e230–e236. doi: 10.1097/BPO.0000000000001131

Sanderson, E., Davey, S. G., Windmeijer, F., and Bowden, J. (2019). An examination of multivariable Mendelian randomization in the single-sample and two-sample summary data settings. *Int. J. Epidemiol.* 48, 713–727. doi: 10.1093/ije/dyy262

Sebbag, E., Felten, R., Sagez, F., Sibilia, J., Devilliers, H., and Arnaud, L. (2019). The world-wide burden of musculoskeletal diseases: a systematic analysis of the World Health Organization burden of diseases database. *Ann. Rheum. Dis.* 78, 844–848. doi: 10.1136/annrheumdis-2019-215142

Sidhu, H., Schmidt, M. E., Cornelius, J. G., Thamilselvan, S., Khan, S. R., Hesse, A., et al. (1999). Direct correlation between hyperoxaluria/oxalate stone disease and the absence of the gastrointestinal tract-dwelling bacterium *Oxalobacter formigenes*: possible prevention by gut recolonization or enzyme replacement therapy. *J. Am. Soc. Nephrol.* 10, S334–S340.

Smith, G. D., and Ebrahim, S. (2003). 'Mendelian randomization': can genetic epidemiology contribute to understanding environmental determinants of disease? *Int. J. Epidemiol.* 32, 1–22. doi: 10.1093/ije/dyg070

Smith, E., Hoy, D. G., Cross, M., Vos, T., Naghavi, M., Buchbinder, R., et al. (2014). The global burden of other musculoskeletal disorders: estimates from the global burden of disease 2010 study. *Ann. Rheum. Dis.* 73, 1462–1469. doi: 10.1136/annrheumdis-2013-204680

Stebbings, S., Munro, K., Simon, M. A., Tannock, G., Highton, J., Harmsen, H., et al. (2002). Comparison of the faecal microflora of patients with ankylosing spondylitis and controls using molecular methods of analysis. *Rheumatology (Oxford)* 41, 1395–1401. doi: 10.1093/rheumatology/41.12.1395

Sudlow, C., Gallacher, J., Allen, N., Beral, V., Burton, P., Danesh, J., et al. (2015). UK biobank: an open access resource for identifying the causes of a wide range of complex diseases of middle and old age. *PLoS Med.* 12:e1001779. doi: 10.1371/journal.pmed.1001779

Ticinesi, A., Nouvenne, A., Cerundolo, N., Catania, P., Prati, B., Tana, C., et al. (2019). Muscle mass and function in aging: a focus on physical frailty and sarcopenia. *Nutrients* 11:11. doi: 10.3390/nu11071633

Tu, Y., Kuang, X., Zhang, L., and Xu, X. (2023). The associations of gut microbiota, endocrine system and bone metabolism. *Front. Microbiol.* 14:1124945. doi: 10.3389/fmicb.2023.1124945

Tu, Y., Yang, R., Xu, X., and Zhou, X. (2021). The microbiota-gut-bone axis and bone health. *J. Leukoc. Biol.* 110, 525–537. doi: 10.1002/JLB.3MR0321-755R

Turkmen, K., and Erdur, F. M. (2015). The relationship between colonization of *Oxalobacter formigenes* serum oxalic acid and endothelial dysfunction in hemodialysis

patients: from impaired colon to impaired endothelium. *Med. Hypotheses* 84, 273–275. doi: 10.1016/j.mehy.2015.01.010

Verbanck, M., Chen, C. Y., Neale, B., and Do, R. (2018). Detection of widespread horizontal pleiotropy in causal relationships inferred from Mendelian randomization between complex traits and diseases. *Nat. Genet.* 50, 693–698. doi: 10.1038/s41588-018-0099-7

Visscher, P. M., Brown, M. A., McCarthy, M. I., and Yang, J. (2012). Five years of GWAS discovery. *Am. J. Hum. Genet.* 90, 7–24. doi: 10.1016/j.ajhg.2011.11.029

Vos, T., Flaxman, A. D., Naghavi, M., Lozano, R., Michaud, C., Ezzati, M., et al. (2012). Years lived with disability (YLDs) for 1160 sequelae of 289 diseases and injuries 1990-2010: a systematic analysis for the global burden of disease study 2010. *Lancet* 380, 2163–2196. doi: 10.1016/S0140-6736(12)61729-2

Wang, I. K., Wu, Y. Y., Yang, Y. F., Ting, I. W., Lin, C. C., Yen, T. H., et al. (2015). The effect of probiotics on serum levels of cytokine and endotoxin in peritoneal dialysis patients: a randomised, double-blind, placebo-controlled trial. *Benef. Microbes* 6, 423–430. doi: 10.3920/BM2014.0088

Wang, Z., Xu, X., Deji, Y., Gao, S., Wu, C., Song, Q., et al. (2023). Bifidobacterium as a potential biomarker of sarcopenia in elderly women. *Nutrients* 15:15. doi: 10.3390/nu15051266

Wen, K., Tao, L., Tao, Z., Meng, Y., Zhou, S., Chen, J., et al. (2020). Fecal and serum Metabolomic signatures and microbial community profiling of postmenopausal osteoporosis mice model. *Front. Cell. Infect. Microbiol.* 10:535310. doi: 10.3389/fcimb.2020.535310

Xu, Z., Xie, Z., Sun, J., Huang, S., Chen, Y., Li, C., et al. (2020). Gut microbiome reveals specific Dysbiosis in primary osteoporosis. *Front. Cell. Infect. Microbiol.* 10:160. doi: 10.3389/fcimb.2020.00160

Zhang, Y. W., Li, Y. J., Lu, P. P., Dai, G. C., Chen, X. X., and Rui, Y. F. (2021). The modulatory effect and implication of gut microbiota on osteoporosis: from the perspective of "brain-gut-bone" axis. *Food Funct.* 12, 5703–5718. doi: 10.1039/d0fo03468a

Zhao, T., Wei, Y., Zhu, Y., Xie, Z., Hai, Q., Li, Z., et al. (2022). Gut microbiota and rheumatoid arthritis: from pathogenesis to novel therapeutic opportunities. *Front. Immunol.* 13:1007165. doi: 10.3389/fimmu.2022.1007165

frontiers | Frontiers in Microbiology

TYPE Original Research
PUBLISHED 23 August 2023
DOI 10.3389/fmicb.2023.1182460



OPEN ACCESS

EDITED BY
Rebeca Martín,
INRAE Centre Jouy-en-Josas, France

REVIEWED BY
Vinod Kumar Gupta,
Mayo Clinic, United States
Valeria D'Argenio,
University of Naples Federico II, Italy

*CORRESPONDENCE
Koen Venema
✉ k.venema@maastrichtuniversity.nl

RECEIVED 10 March 2023
ACCEPTED 01 August 2023
PUBLISHED 23 August 2023

CITATION
Ahmad MA, Karavetian M, Moubareck CA, Wazz G, Mahdy T and Venema K (2023) Association of the gut microbiota with clinical variables in obese and lean Emirati subjects. *Front. Microbiol.* 14:1182460. doi: 10.3389/fmicb.2023.1182460



# Association of the gut microbiota with clinical variables in obese and lean Emirati subjects

Manal Ali Ahmad[1], Mirey Karavetian[2], Carole Ayoub Moubareck[3], Gabi Wazz[4], Tarek Mahdy[5] and Koen Venema[6]*

[1]School of Nutrition and Translational Research in Metabolism (NUTRIM), Faculty of Health, Medicine and Life Sciences, Maastricht University, Maastricht, Netherlands, [2]Faculty of Kinesiology and Physical Education, University of Toronto, Toronto, ON, Canada, [3]College of Natural and Health Sciences, Zayed University, Dubai, United Arab Emirates, [4]Center of Excellence in Bariatric and Metabolic Surgery, Dr. Sulaiman Al Habib Hospital, Dubai, United Arab Emirates, [5]Department of Bariatric Surgery, Sharjah University, Sharjah, United Arab Emirates, [6]Centre for Healthy Eating and Food Innovation (HEFI), Maastricht University-Campus Venlo, Venlo, Netherlands

**Background:** Growing evidence supports the role of gut microbiota in obesity, yet exact associations remain largely unknown. Specifically, very little is known about this association in the Emirati population.

**Methods:** We explored differences in gut microbiota composition, particularly the Firmicutes/Bacteroidetes (F/B) ratio, between 43 obese and 31 lean adult Emirate counterparts, and its association with obesity markers, by using V3-V4 regions of 16 S ribosomal RNA gene sequencing data. Furthermore, we collected anthropometric and biochemical data.

**Results:** The two major phyla in obese and lean groups were Firmicutes and Bacteroidetes. We observed a significantly lower alpha diversity (Shannon index) in obese subjects and a significant difference in beta diversity and phylum and genus levels between the two groups. The obese group had higher abundances of Verrucomicrobia and Saccharibacteira and lower abundances of Lentisphaerae. *Acidaminococcus* and *Lachnospira* were more abundant in obese subjects and positively correlated with adiposity markers. No correlations were found between the gut microbiota and biochemical variables, such as fasting blood sugar, total cholesterol, HDL cholesterol, LDL cholesterol, and triglycerides.

**Conclusion:** We reveal significant differences in the gut microbiota between obese and lean adult Emiratis and an association between certain microbial genera of the gut microbiota and obesity. A better understanding of the interactions between gut microbes, diet, lifestyle, and health is warranted.

KEYWORDS

**gut microbiota, obesity, firmicutes, bacteroidetes, 16S rRNA, United Arab Emirates**

## 1. Introduction

Obesity is a multifactorial disease (Cannon and Kumar, 2009), declared by the World Health Organization (WHO) in 2016 as a pandemic (World Health Organization, 2016). Long-standing factors involved in obesity include excessive caloric intake and a sedentary lifestyle (Morgen and Sørensen, 2014). More recently, obesity was also found to present a complicated disequilibrium of the diversity, richness, and evenness of the bacterial component of the gut microbiota (Aguirre

and Venema, 2015), known as dysbiosis (Adlerberth and Wold, 2009; Round and Mazmanian, 2009). The latter has been proposed as part of the etiology of obesity (Davis, 2016) through its effect on digestion, regulation of metabolism, adipose tissue composition, short-chain fatty acid (SCFA) production, modulation of the production of gut peptides and hormones, among others (Corfe et al., 2015; Patrone et al., 2016). The human gut microbiota is primarily composed of Firmicutes and Bacteroidetes, which make up about 90% of all bacterial species, in addition to Actinobacteria, Fusobacteria, Proteobacteria, and Verrucomicrobia (Abenavoli et al., 2019; Rinninella et al., 2019). Nevertheless, substantial differences in composition and function in the microbiota between obese and healthy individuals have been established (Turnbaugh and Gordon, 2009; Tremaroli and Bäckhed, 2012; Pinart et al., 2021). In some studies, obesity in humans is typically characterized by high intestinal concentrations of Firmicutes and low concentrations of Bacteroidetes (Seganfredo et al., 2017; Crovesy et al., 2020); whereby the higher Firmicutes-to-Bacteroidetes ratio (F/B) among obese (Armougom et al., 2009; Furet et al., 2010; Kong et al., 2013) is potentially associated with a greater energy harvest from host diet (Turnbaugh et al., 2006). However, other studies show the opposite F/B ratio in obesity (Schwiertz et al., 2010), or no relation at all (Duncan et al., 2008) and thus, the cause-and-effect relationship between F/B and obesity is still to be elucidated.

Improvements in bacterial DNA sequencing allowed researchers to understand the gut microbiota and its composition and explore its complex relationship with health and disease (Gordon et al., 2007; Duncan et al., 2008). However, there are still gaps in our understanding of the role of the gut microbiota in the etiology of obesity and the effectiveness of interventions targeting gut microbiota for preventing and managing obesity (Tehrani et al., 2012), "e.g., it is still not entirely clear whether differences in the microbiota cause obesity, or whether obesity causes a difference in microbiota composition." Primarily, this is because most studies have used rodent models, which have different gut microbiota composition, fermentation process, and dietary practices than humans (Heinritz et al., 2013; Nguyen et al., 2015). Moreover, inconsistencies in human studies might be attributed to the different approaches to analyzing the composition of the gut microbiota, as well as the recruitment of subjects with ethnic differences and inter-individual dissimilarities in genetics, diets, and lifestyles which can shape the composition of the gut microbiota (Seganfredo et al., 2017; Crovesy et al., 2020; Pinart et al., 2021; Zeng et al., 2021). The characteristics of the gut microbiota in subjects with obesity are highlighted. Nevertheless, little is known about the association between gut microbiota and clinical variables (fasting blood sugar, total cholesterol, HDL cholesterol, LDL cholesterol, triglycerides, and anthropometrics) linked to obesity in humans. This warrants scientific investigations to explore microbial patterns associated with obesity markers.

In the Gulf countries, the prevalence of obesity is steadily increasing. Specifically, in the United Arab Emirates (UAE), the prevalence of overweight and obesity doubled between 1989 and 2017 (Radwan et al., 2018), and there are 27.8% of adults obese, according to the National Health Survey 2017–2018 (Sulaiman et al., 2017; Ministry of Health and Prevention, 2023). In this work, we aimed to profile the gut microbiota and its association with clinical variables and explore differences (through a comparative analysis) between obese and lean Emirate subjects. Exploring the gut microbiome of Emiratis adds a piece of the puzzle to our understanding of obesity, with the ultimate goal of uncovering preventive and interventional measures tailored to the Emirati population aiming to curb the obesity epidemic in the country.

## 2. Materials and methods

### 2.1. Study design

This is a cross-sectional study conducted among Emirati subjects living in the UAE. The present study is part of a pre-post study registered at clinicaltrials.gov (NCT04200521) and performed in the UAE.

### 2.2. Ethical considerations

Ethical approval was granted by the Research Ethics Committee of the Ministry of Health and Prevention of UAE (MOHP/DXB-REC-52/2018), the Dubai Health Care Regulatory Research Ethics Committee (DHCR-REC), and the Zayed University Ethical Committee Board (ZU19_51_F). The study followed the Declaration of Helsinki. Written informed consent was collected from all study subjects.

### 2.3. Participants and sample size

We determined the sample size by following standard calculations based on normal distributions. The sample size was calculated based on the change in F/B from pre- to post-bariatric surgery (Brant, 2015), based on the study by Damms-Machado et al. (2015). In that study, the mean(SD) fecal F/B increased significantly from 5.9 (2.1) to 10.4 (1.4) in 3 months post-bariatric surgery (Damms-Machado et al., 2015). To detect a similarly significant effect, two patients were needed to achieve 80% power at a two-sided alpha level of 5%. To allow for the high expected dropout rate, the minimum sample size was multiplied by 15. Hence, we targeted 30 Emirati obese adults residing in the UAE of both sex and planning to undergo the bariatric procedure. In addition, we recruited a sample of 30 age and sex-matched control subjects (lean adults living in the UAE).

### 2.4. Inclusion criteria

Emirati residents of UAE, aged between 18 and 60 years, of either sex, free of antibiotics for at least 3 months, falling into one of the two body mass index (BMI) categories were included: (1) obese with a BMI of $\geq$35 kg/m$^2$ and willing to undergo bariatric surgery; (2) lean counterparts with a BMI of 18.5–24.9 kg/m$^2$ and consenting to participate in the study.

Obese participants were recruited from one hospital in Dubai and another in Sharjah. In contrast, lean subjects were recruited from community settings in Dubai through word-of-mouth and flyer postings. Recruitment took place from October 2019 till March 2021.

## 2.5. Exclusion criteria

Individuals who consumed alcohol exceeding two drinks per day for men and one drink per day for women (Snetselaar et al., 2021), were pregnant at the time of the study, experienced significant weight loss (≥5%) in the past 3 months, or were not willing to consent for the study were excluded.

## 2.6. Outcome measures and data collection

General demographic characteristics collected from the patient included age and sex. Furthermore, health-related information was collected using a subjective screening questionnaire, including the presence of any chronic diseases such as dyslipidemia, diabetes, and hypertension, surgical history in the past 5 years, weight loss of at least 5% in the past 3 months, current intake of medication including antibiotics, and current consumption of prebiotic/probiotic/fiber supplement and probiotic foods, consumption of other nutrition supplements, and engagement in a physically active lifestyle and exercise.

Physical activity level was analyzed using two questions from our initial screening questionnaire. A "yes" or "no" answer was required for the following two questions: "Do you integrate physical activity in your daily routine" and "Do you incorporate any exercise program." Sedentary was denoted if "no" was answered to both questions; light physical activity if "yes" was only answered to the first question; moderate physical activity if "yes" was only responded to the second question; and high physical activity if "yes" was answered to both questions.

## 2.7. Anthropometric and clinical variables

For each participant, anthropometric measurements, lipid profile, fasting blood sugar (FBS), and microbiota analyses were done.

*Anthropometric data* were collected by trained research assistants and dietitians.

Body weight (kg): measured via portable Seca 762 scale (Vogel & Halke, Hamburg, Germany), following best practices, i.e., with light clothes and without shoes. Height (cm): measured using a portable stadiometer attached to the weighing scale following best practices, i.e., to the nearest 0.1 cm, without shoes, with the participant stretching to the maximum height while having the head positioned in the Frankfort plane. BMI (kg/m$^2$): calculated according to the standard formula by dividing weight in kilograms by squared height in meters. Waist circumference (WC) (cm): measured using a Seca 201 ergonomic circumference measuring tape, at the mid-point between the right iliac crest and the lower costal region, to the nearest 0.1 cm (Van der Kooy and Seidell, 1993). WC was categorized as appropriate (<94 cm in men and < 80 cm in women) or increased (≥94 cm for men and ≥80 cm for women; Ford, 2005).

Waist-to-height ratio (WHtR): calculated by dividing the WC (cm) by height (cm), whereby abdominal obesity was defined as a WHtR ≥0.5 (Ashwell and Gibson, 2016). Fat mass (FM) and Percent Body Fat (PBF): measured via bioelectrical impedance analyzer (BC-420 MA, Tanita Corporation, Tokyo, Japan) with the participants being well hydrated, without drinking caffeine for 12 h, not participating in excessive physical activity 24 h before the analysis, and wearing comfortable clothes. Elevated PBF was defined as PBF ≥ 25% and ≥ 35% in men and women, respectively (Romero-Corral et al., 2008).

## 2.8. Biochemical parameters

Total cholesterol (TC), low-density lipoprotein cholesterol (LDL-C), high-density lipoprotein cholesterol (HDL-C), triglycerides (TG), and FBS: measured after 12 h of fasting via portable Lux Meter Blood Test (Biochemical Systems International, S.p.A; Arezzo, Italy) following the manufacturer's instructions.

## 2.9. Stool sample collection

Stool samples were collected in Zymo DNA/RNA Shield fecal collection tubes and stored at room temperature. Two samples were collected from each participant, one of which was analyzed, and the second was held for accuracy verification. Sample collection followed standard protocols and regulations. Collection tubes (with a spoon attached to the cap for collecting 1 gram of feces) were pre-filled with DNA/RNA Shield™ (9 mL). The nucleic acids (DNA & RNA) in the samples are preserved at room temperature (DNA > 1 year, RNA up to 1 month).

## 2.10. DNA isolation and sequencing of the V3–V4 region of the 16S rRNA gene

DNA isolation and sequencing of the barcoded amplicons of the V3–V4 region of the 16S rRNA gene was done as per the protocols of Illumina (Illumina, Eindhoven, The Netherlands; Surono et al., 2022). The sequencing was performed using the Illumina MiSeq system (San Diego, CA, United States) using barcodes and the 2 × 300 bp protocol. We used Quantitative Insights Into Microbial Ecology: QIIME 2[1] software to analyze raw sequences; the latter were classified using the Silva database (version 132) as a reference 16S rRNA gene database. Reads were filtered, and only those present in at least 20% of the samples were taken.

### 2.10.1. Diversity analysis

*α Diversity indices*: observed-OTUs, Chao1 index, Phylogenetic diversity (Faith's PD), Pielou evenness, and Shannon diversity index, which were calculated with QIIME 2 and shown using the R software [R (4.1.x) (R Core Team)][2] in RStudio. The rarefaction curves were generated using the ggplot2 package for R. Rarefication depth was set at 3800.

*β Diversity* indices were visualized in a Principal Coordinate Analysis (PCoA) based on Bray–Curtis dissimilarity, Jaccard distance, and weighted and unweighted UniFrac using QIIME2 software.

1 https://qiime2.org/

2 http://www.R-project.org

TABLE 1 Demographic, anthropometric, and biochemical parameters between lean ($n$ = 31) and obese participants ($n$ = 43).

| | Lean [mean ± SD or $n$ (%)] | Obese [mean ± SD or n (%)] | Value of $p$ |
|---|---|---|---|
| Age (years) | 29.67 ± 10.73 | 29.95 ± 9.13 | 0.565 |
| Female | 19 (61.3) | 27 (62.8) | 0.896 |
| Weight (kg) | 62.39 ± 8.17 | 118.23 ± 25.6 | <0.001* |
| Height (cm) | 166.29 ± 8.38 | 165.16 ± 9.77 | 0.603 |
| BMI (kg/m$^2$) | 22.49 ± 1.93 | 43.12 ± 6.83 | <0.001* |
| WC (cm) | 76.70 ± 14.83 | 123.29 ± 17.76 | <0.001* |
| Appropriate | 23 (74.2) | 0 (0) | <0.001* |
| Increased risk | 8 (25.8) | 43 (100) | |
| WtHR | 0.48 ± 0.05 | 0.74 ± 0.08 | <0.001* |
| Normal | 16 (51.6) | 0 (0) | <0.001* |
| High | 15 (48.4) | 43 (100) | |
| PBF (%) | 26.62 ± 9.39 | 46.13 ± 30 | <0.001* |
| FM (kg) | 17.13 ± 7.12 | 53.8 ± 13.3 | <0.001* |
| MM (kg) | 43.14 ± 9.02 | 57.43 ± 11.76 | <0.001* |
| FFM in (kg) | 45.91 ± 9.27 | 62.08 ± 11.83 | <0.001* |
| FFMI (FFM kg/m$^2$) | 16.46 ± 2.22 | 22.77 ± 2.72 | <0.001* |
| FBS (mg/dL) Median (IQR) | 92 (87–98) | 97 (93.6–104) | 0.003* |
| HDL (mg/dL) | 43.63 ± 15.78 | 41.74 ± 11.05 | 0.547 |
| LDL (mg/dl) | 73.93 ± 20.99 | 98.65 ± 32.16 | <0.001* |
| TG (mg/dL) | 123.24 ± 35.49 | 128.53 ± 62.07 | 0.645 |
| TC (mg/dL) | 138 (120–159) | 161.6 (143–181.7) | 0.001* |
| TC/HDL ratio | 3.54 ± 1.10 | 4.18 ± 1.22 | 0.022* |

*Denotes statistical significance ($p$ < 0.05) between groups. Independent-sample $t$-test was used for normally distributed continuous variables with mean, and SD (Age, BMI, WC, WtHR, PBF, FM, MM, FFM, FFMI, LDL, HDL, TG, TC/HDL-c), Mann–Whitney U-test for skewed continuous variables (FBS, TC) with IQR and medians, and Chi-square test was used for categorical variables. BMI, body mass index; WC, waist circumference; PBF, percentage body fat; FM, fat mass; WtHR, waist-to-height ratio; MM, muscle mass; FFM, fat-free mass; FFMI, fat-free mass index; FBS, fasting blood sugar; HDL, high- density lipoprotein cholesterol; LDL, low-density lipoprotein cholesterol; TG, triglycerides; TC, total cholesterol; TC/HDL, total cholesterol to high-density lipoprotein cholesterol ratio.

The statistical significance of β diversity differences between the two groups was determined using Permutational Multivariate Analysis of Variance (PERMANOVA). The value of p was calculated through the Pairwise permanova method to compare β diversity between each category in all samples. Differences between obesity and lean samples (at phyla and genus levels) were analyzed via the non-parametric Kruskal–Wallis test corrected with the Benjamini–Hochberg false discovery rate (FDR) for multiple comparisons in Rstudio (the software package R (4.1.x), R Core Team, footnote 2).

The composition of the two groups was visualized using the Krona tool.[3]

Linear discriminant analysis (LDA) effect size (LEfSe) was used to explore microbial taxa with differential abundance between lean and obese (version 1.0).[4] Taxa showing LDA values above two at a value of $p$ <0.05 were considered enriched taxa in each group.

The non-parametric Spearman's rank-order correlations between the Amplicon Sequence Variant (ASVs) and continuous variables (BMI, WC, WHtR, PBF, FM, LDL, HDL, TC, TG, TC/HDL, and FBS) were calculated. $Q$-values, i.e., adjusted value of $p$s after the FDR, were considered significantly different at a cut-off of <0.05. The F/B ratio was calculated by dividing the relative abundances of Firmicutes and Bacteroidetes.

A heatmap of Spearman correlation analysis was generated in R software (ggplot2 package).

## 2.11. Statistical analyses

We analyzed 'participants' characteristics using the Statistical Package for the Social Sciences software version 21 (SPSS Inc. Chicago, IL, United States). We assessed the normality of the data using Skewness and Kurtosis. Normal data were summarized as mean (M) ± standard deviation (SD) and skewed data as median (Mdn) and interquartile range (IQR). Between-group differences were explored using independent samples t-test for normally distributed continuous variables, Mann–Whitney U-test for skewed continuous variables, and Chi-square for categorical values. A value of $p$ < 0.05 was used to denote statistical significance.

# 3. Results

The characteristics of participant groups are presented in Table 1. Forty-three obese subjects were included (37.2% men; mean ± SD age of 29.95 ± 9.13 years), whereas 31 lean subjects participated (38.7% men; mean ± SD age 29.67 ± 10.73 years). No significant differences in gender and age were observed between the groups. The obese group had higher anthropometric (BMI, WC, WHtR, and PBF) and biochemical parameters (FBS, LDL, TC, and TC/HDL-c ratio) than the lean group, as expected. There was no significant difference in lifestyle factors between the two groups (prebiotic, probiotic, fiber, alcohol consumption, and smoking). The level of physical activity in the obese group was mainly light and significantly lower than that of the lean group (Supplementary Table S1).

## 3.1. Differences in bacterial composition between the obese and lean groups

After filtering for taxa that were present in at least 20% of the samples, the microbiota was composed of eight phyla and 109 genera.

At the phylum level, Firmicutes (50% in lean vs. 47% in obese) and Bacteroidetes (44% in lean vs. 49% in obese) were the two most abundant bacterial phyla in the gut of obese and lean subjects. The obese group had significantly higher abundances of the phyla

3 https://github.com/marbl/Krona/wiki/KronaTools

4 http://huttenhower.sph.harvard.edu/galaxy/

Verrucomicrobia (0.5% in obese vs. 0.3% in lean, Benjamini-Hochberg correction, $q = 0.048$), and Saccharibacteira (0.003% in obese vs. 0.0009% in lean, $q = 0.0002$) than the lean group and significantly lower abundances of the phyla Lentisphaerae (0.03% in obese vs. 0.08% in lean, $q = 0.004$). However, there was no significant difference in the relative abundance of Bacteroidetes ($q = 0.12$), Firmicutes ($q = 0.32$), Fusobacteria ($q = 0.2$), Actinobacteria ($q = 0.54$), and Proteobacteria ($q = 0.85$) among the two groups. Furthermore, there was no significant difference in the F/B ratio between the obese (0.95) and lean group (1.1); $p = 0.315$ (Supplementary Figures S1A,B; Table 2).

## 3.2. Genus level

Taxonomic assignment was also performed at the genus level and revealed a total of 21 major genera with a significant difference between the obese and lean group, where 16 of these belonged to Firmicutes, as depicted in Table 3.

Of the 21 genera, *Acidaminococcus* and *Lachnospira* (belonging to the Firmicutes phylum) were higher in the obese group, while the remaining 19 were lower, including (a) from the Firmicutes phylum, an uncharacterized taxon in the Clostridiales.vadinBB60.group ($q = 0.001$), *Anaerotruncus* ($q = 0.001$), an uncharacterized Ruminococcaceae ($q = 0.003$), *Ruminococcaceae*.UCG.014 ($q = 0.004$), *Ruminococcaceae*.UCG.010 ($q = 0.008$), Family.XIII.UCG.001 (of the Clostridiales order, Family XIII; $q = 0.006$), an uncharacterized Erysipelotrichaceae ($q = 0.007$), *Christensenellaceae*.R.7.group ($q = 0.008$), *Lachnospiraceae*.UCG.010 ($q = 0.013$), *Ruminococcaceae*.UCG.005 ($q = 0.013$), *Ruminococcaceae*.UCG.002 ($q = 0.02$), *Ruminiclostridium*.6 ($q = 0.02$), an uncharacterized Lachnospiraceae ($q = 0.02$), *Lachnospiraceae*.NK4A136.group ($q = 0.04$), and (b) from the Bacteroidetes phylum, *Alistipes* ($q = 0.04$), *Odoribacter* ($q = 0.03$), *Barnesiella* ($q = 0.03$), (c) from the Proteobacteria phylum, an uncharacterized Rhodospirillaceae ($q = 0.001$), and (d) from the Verrucomicrobia phylum, *Victivallis* ($q = 0.002$; Table 3; Figures 1A,B; Supplementary Figures 2A,B).

We performed a Linear Discriminant Analysis Effect Size (LEfSe) on the taxa from the obese and lean groups. A total of 26 genera showed significantly different abundances between the two groups with LDA scores >2. In this case, 23 genera were higher in the lean group, and three genera were higher in the obese group, as shown in Figure 2.

TABLE 2 The gut microbial composition (relative abundance in %) of obese and lean participants (phylum level).

| Phylum | Lean (%) | Obese (%) | *q** |
|---|---|---|---|
| Firmicutes | 50 | 47 | 0.32 |
| Bacteroidetes | 44 | 49 | 0.12 |
| Proteobacteria | 4 | 3 | 0.85 |
| Actinobacteria | 0.6 | 0.5 | 0.54 |
| Verrucomicrobia | 0.3 | 0.5 | 0.04* |
| Lentisphaerae | 0.08 | 0.03 | 0.004* |
| Fusobacteria | 0.0003 | 0.0001 | 0.20 |
| Saccharibacteria | 0.0009 | 0.003 | 0.0002* |
| F/B ratio | 1.1 | 0.95 | 0.315 |

*$q \leq 0.05$ was considered statistically significant.

Of the three genera in the obese group, two belonged to Firmicutes (*Lachnospira* and *Acidaminococcus*) and one to Verrucomicrobia (*Akkermansia*). In the Kruskal-Wallis test, the latter was not statistically significant. In contrast, 17, 3, one, one, and one of the 23 genera for the lean group belonged to Firmicutes, Bacteroidetes, Actinobacteria, and Verrucumictobia phyla.

## 3.3. α- and β-Diversity (microbial diversity and richness, microbial dissimilarities)

According to the α -diversity metrics (Figure 3), obese adults showed significantly lower diversity (Shannon index, $p = 0.031$), coinciding with the lower observed OTUs ($p = 0.006$) and lower Chao1 richness estimator ($p = 0.008$). Furthermore, the obese group showed lower "Faith's phylogenetic diversity (PD; $p = 0.069$) and lower evenness ('Pielou's evenness, $p = 0.53$). However, the latter two were not statistically significant.

Principal coordinate Analysis (PCoA) based on unweighted UniFrac, weighted UniFrac, Bray–Curtis, and Jaccard showed a marked separation between the gut microbiota community of obese and lean groups, confirmed by the pairwise permanova analysis that indicated a significant difference in β-diversity between the two groups (Figure 4; $p = 0.009$; $p = 0.034$; $p = 0.029$; $p = 0.002$, respectively).

## 3.4. Correlation between gut microbiota (at genus level) and clinical variables

Certain microbes were positively or negatively correlated with BMI, WC, WHtR, PBF, and FM. Statistically significant correlations between microbes and anthropometric measurements are provided in (Supplementary Table S2) and the heat map (Figure 5).

Several taxa that were significantly lower in obese compared with lean using Kruskal–Wallis or LEfSe were negatively correlated with BMI, WC, WHtR, PBF, and FM (uncharacterized Rhodospirillaceae), (uncharacterized Clostridiales.vadinBB60.group), BMI, WHtR (*Victivallis*), BMI, WC and FM (uncharacterized Ruminococcaceae), BMI, WC, WHtR and FM (uncharacterized Erysipelotrichaceae), BMI & FM (*Lachnospiraceae*.UCG.010), BMI, WHtR and FM (*Christense nellaceae*.R.7.group, *Ruminococcaceae*.UCG.005, *Ruminococcaceae*.UCG.010, *Anaerotruncus*), BMI, WHtR, PBF and FM (Ruminococcaceae.UCG.014); BMI, PBF and FM (Family.XIII.UCG.001), WHtR (*Ruminococcaceae*.UCG.002). On the other hand, the taxa which were higher in the obese group presented positive correlations with BMI and FM (*Acidaminococcus*), and WHtR (*Lachnospira*); except for *Akkermansia,* which was prevalent in the obese group (LEfSe) was found to be negatively correlated with WHtR.

No correlations were found between the gut microbiota at the genus level and the following clinical variables: FBS, total cholesterol, HDL cholesterol, LDL cholesterol, and triglycerides. Furthermore, There were no correlations with age or gender.

# 4. Discussion

Recent research on the human gut microbiota has revealed its various roles in health and disease, with obesity being among the

TABLE 3 The difference in bacterial composition (relative abundance in %) between obese and lean subjects (genus level).

| Genus | Lean (%) | Obese (%) | q value |
|---|---|---|---|
| **Higher in lean subjects** | | | |
| *Clostridiales.vadinBB60. group.D_5-uncultured. Bacterium* | 0.1 | 0.01 | 0.001* |
| *Anaerotruncus* | 0.3 | 0.1 | 0.001* |
| *Ruminococcaceae.D_5__uncultured* | 0.7 | 0.2 | 0.003* |
| *Ruminococcaceae.UCG.014* | 1 | 0.4 | 0.004* |
| *Ruminococcaceae.UCG.010* | 0.4 | 0.05 | 0.008* |
| *Family.XIII.UCG.001* | 0.03 | 0.01 | 0.006* |
| *Erysipelotrichaceae.D_5__uncultured* | 0.2 | 0.02 | 0.007* |
| *Christensenellaceae.R.7.group* | 2 | 0.3 | 0.008* |
| *Rhodospirillaceae.D_5__uncultured* | 0.5 | 0.03 | 0.001* |
| *Victivallis* | 0.07 | 0.01 | 0.002* |
| *Alistipes* | 3 | 2 | 0.04* |
| *Lachnospiraceae.UCG.010* | 0.2 | 0.1 | 0.013* |
| *Ruminococcaceae.UCG.005* | 1 | 0.6 | 0.013* |
| *Ruminococcaceae.UCG.002* | 2 | 1 | 0.02* |
| *Ruminiclostridium.6* | 0.5 | 01 | 0.02* |
| *Lachnospiraceae.D_5__uncultured* | 0.2 | 0.1 | 0.02* |
| *Odoribacter* | 0.4 | 0.2 | 0.03* |
| *Barnesiella* | 0.6 | 0.2 | 0.03* |
| *Lachnospiraceae.NK4A136.group* | 1 | 0.9 | 0.04* |
| **Increased in obese peoples** | | | |
| *Acidaminococcus* | 0.1 | 0.7 | 0.01* |
| *Lachnospira* | 0.9 | 2 | 0.04* |

*$q \leq 0.05$ was considered statistically significant.

many conditions to which changes in the gut microbiota have been linked (Jinatham et al., 2018). Research on gut microbiota and obesity has mainly focused on Western populations, with limited studies on Arabs and almost none on Emiratis. This study pioneered in contrasting the fecal microbial composition of obese and lean Emirati people using 16S rRNA gene sequencing (V3-V4 region) and exploring its association with clinical parameters. It is difficult to compare this with previous studies in Western populations, because also diet, which differs between the Arabic and Western culture, also significantly affects microbiota composition.

To the best of our knowledge, the present cross-sectional study is first to provide insights into the relationships between clinical variables and the gut microbiota in obese and lean Emirati subjects. The α- diversity richness was significantly lower in the obese than the lean Emirate without significant difference in evenness. These data are in line with the majority of available studies (Pinart et al., 2021). Conversely, β-diversity, denoting dissimilarities in gut microbiota composition, showed significant differences between obese and lean; this also agrees with most available studies. Thus, the microbiota in the obese group presented fewer bacterial taxa, and lean samples showed a more diverse gut microbiota profile than obese samples based on Shannon index results. Controversy regarding relative abundance at genus and phylum level in individuals with obesity, compared with lean subjects, was observed.

Moreover, higher genera in the obese group correlated positively with BMI and FM (*Acidaminococcus*) and WHtR (*Lachnospira*). The exception was *Akkermansia* which was more prevalent in the obese group but was negatively associated with WHtR. This is in contrast to other studies (Gao X. et al., 2018; Jinatham et al., 2018), in different populations. On the other hand, genera higher in the lean group correlated negatively with adiposity (BMI, WC, WHtR, and FM).

The structure, function, and diversity of the gut microbiota in subjects with obesity differ from those of lean people (Cheng et al., 2019). In general, people with obesity show lower richness and biodiversity (Turnbaugh et al., 2009; Cotillard et al., 2013; Le Chatelier et al., 2013; Isolauri, 2017) similar to our findings, while Kocełak et al. (2013) and Kasai et al. (2015) found greater diversity richness in individuals with obesity. Le Chatelier et al. reported that subjects with obesity who have low bacterial richness present more overall adiposity, dyslipidemia, insulin resistance, and higher inflammation compared with obese individuals who have an elevated gut bacterial richness (Le Chatelier et al., 2013; Crovesy et al., 2020). In line with the literature, the present study revealed that Firmicutes and Bacteroidetes were the two most abundant bacterial phyla in the gut of obese and lean subjects without significant differences noted at the level of Firmicutes, Bacteroidetes (Pinart et al., 2021) nor F/B ratio (Castaner et al., 2018; Jinatham et al., 2018) between the two groups. It is well known that Firmicutes and Bacteroidetes predominate the gut microbiome

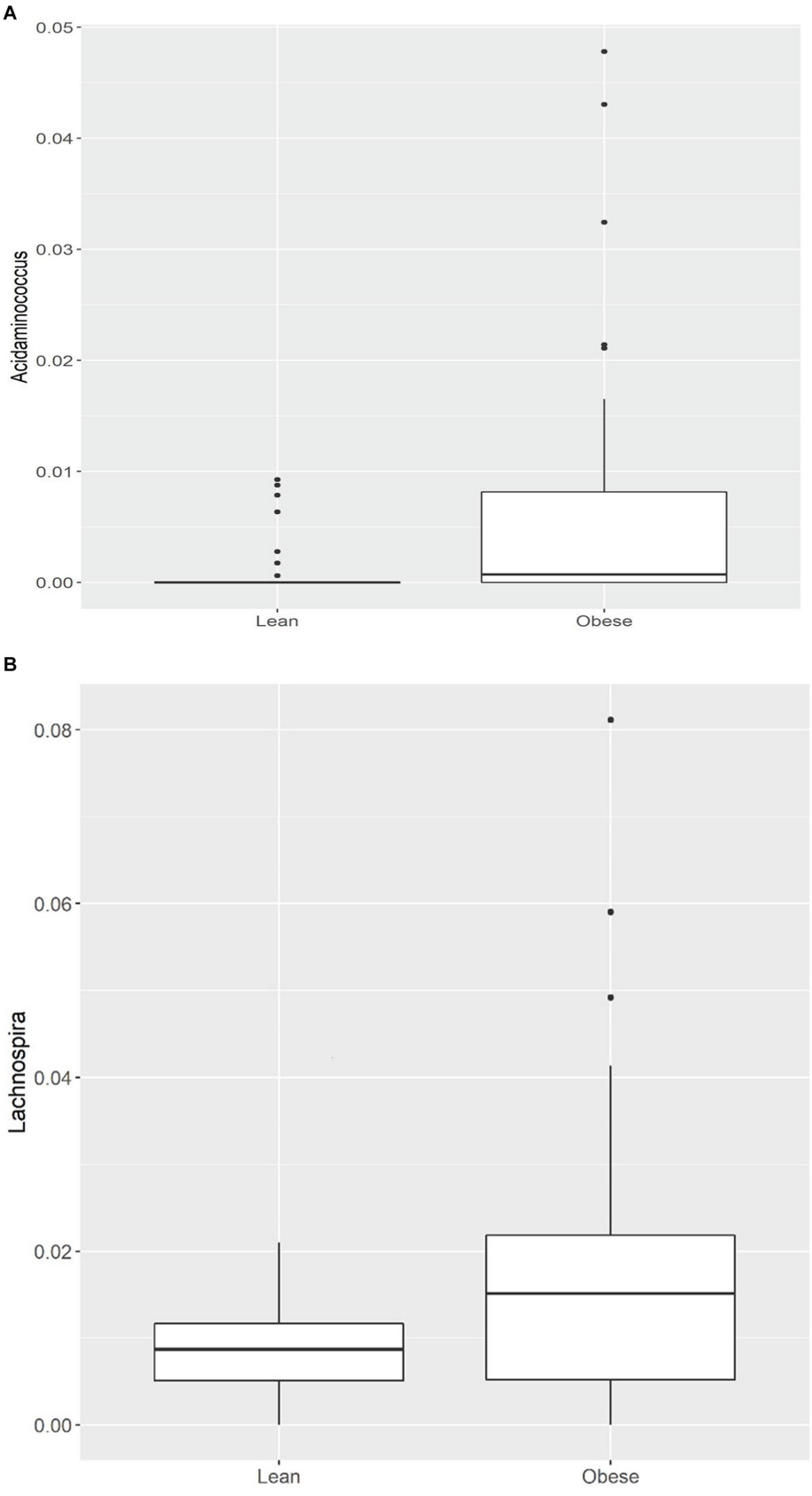


FIGURE 1
**(A)** Comparison of relative abundance of Acidaminococcus (genus level); **(B)** Comparison of relative abundance of Lachnospira (genus level) between lean and obese participants. *$q < 0.05$.

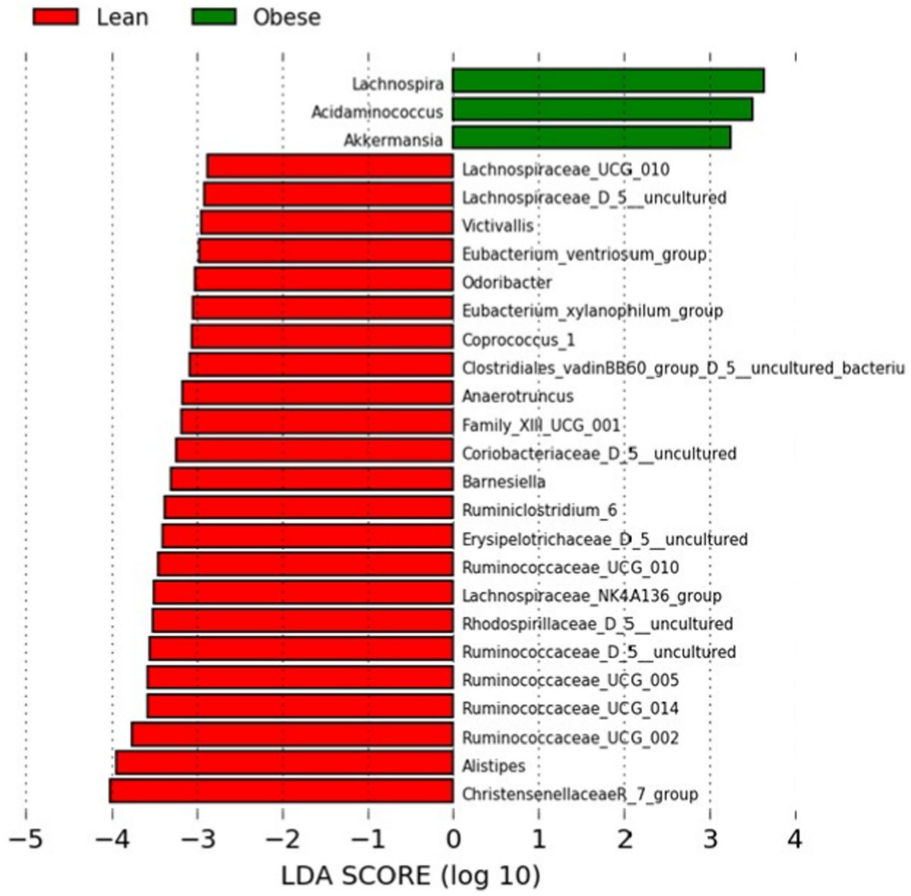


FIGURE 2
LEfSe analysis between the obese and lean groups (LDA score > 2). The LDA score (log10) for the more prevalent genera in the obese group is represented on a positive scale (green), and the LDA score for the more prevalent genera in the lean group is defined on a negative scale (red).

globally (Castaner et al., 2018). Scarce data on the gut microbiota of people in the Arabian Peninsula describe the dominance of Firmicutes and Actinobacteria as phyla in individuals from Saudi Arabia and the preponderance of either Firmicutes or Bacteroidetes in individuals from Kuwait (Plummer et al., 2020).

Of interest, it was believed in early reports that the ratio of Firmicutes and Bacteroidetes differs between lean and obese people, with a high ratio observed in the US (Plummer et al., 2020). However, this was later refuted, and the majority of evidence does not show significant differences in the relative abundance of Firmicutes (Pinart et al., 2021), whereas contradictory findings in the relative abundance of Bacteroidetes persist (Crovesy et al., 2020; Pinart et al., 2021).

The usefulness of a high F/B ratio as an indicator of obesity is still debatable and more complicated than a mere difference in the relative abundance between phyla (Turnbaugh and Gordon, 2009; Venema, 2010; Jinatham et al., 2018). The critical impact of some bacteria on human metabolism may be due to the number of less abundant bacteria or the higher abundance of other ones (Sonnenburg and Backhed, 2016). Gut microbiota geared towards the production of SCFA, rather than a simple increase in F/B ratio, may be associated with an increased energy harvest from 'one's diet leading to obesity. Investigating the association between energy harvest related to bacterial SCFA production and obesity is warranted (Venema, 2010; Jinatham et al., 2018). Furthermore, the F/B ratio may be strongly associated with metabolic markers of obesity, such as insulin resistance and metabolic syndrome, instead of obesity (Louis et al., 2016). Based on our results, a high F/B ratio may not be a valid global biomarker of obesity (Houtman et al., 2022). It is more likely that differences at the genus (and even species) level, compared with the phylum level, could be related to changes in metabolic function (Bauer et al., 2016). While significantly higher Lentisphaerae in lean individuals and Saccharibacteria and Verrucomicrobia in the obese group were reported, no differences in the relative abundance of Fusobacteria, Actinobacteria, and Proteobacteria are observed. The issue of differences between phyla in obese and lean individuals remains controversial in the literature (Pinart et al., 2021).

Similarly, differences between the obese and lean groups at the genus level remain controversial (Crovesy et al., 2020). Interestingly, in our study, the genus Lachnospiraceae NK4A136 was significantly higher in the lean group. Studies in mice suggest that this genus has a protective and anti-inflammatory effect being a potential butyrate producer (Companys et al., 2021). Furthermore, Companys et al. (2021) first identified the genus Lachnospiraceae NK4A136 as a biomarker of leanness in humans. Furthermore, in our study, as shown elsewhere (Gao R. et al., 2018), butyrate-producing Ruminococcus was higher in the lean group, denoting a more diverse microbiome profile.

Moreover, Christensenellaceae.group.7 (Firmicutes phylum) was significantly higher in the lean group. It is usually associated with a low BMI (Castaner et al., 2018), and when transplanted to mice, it

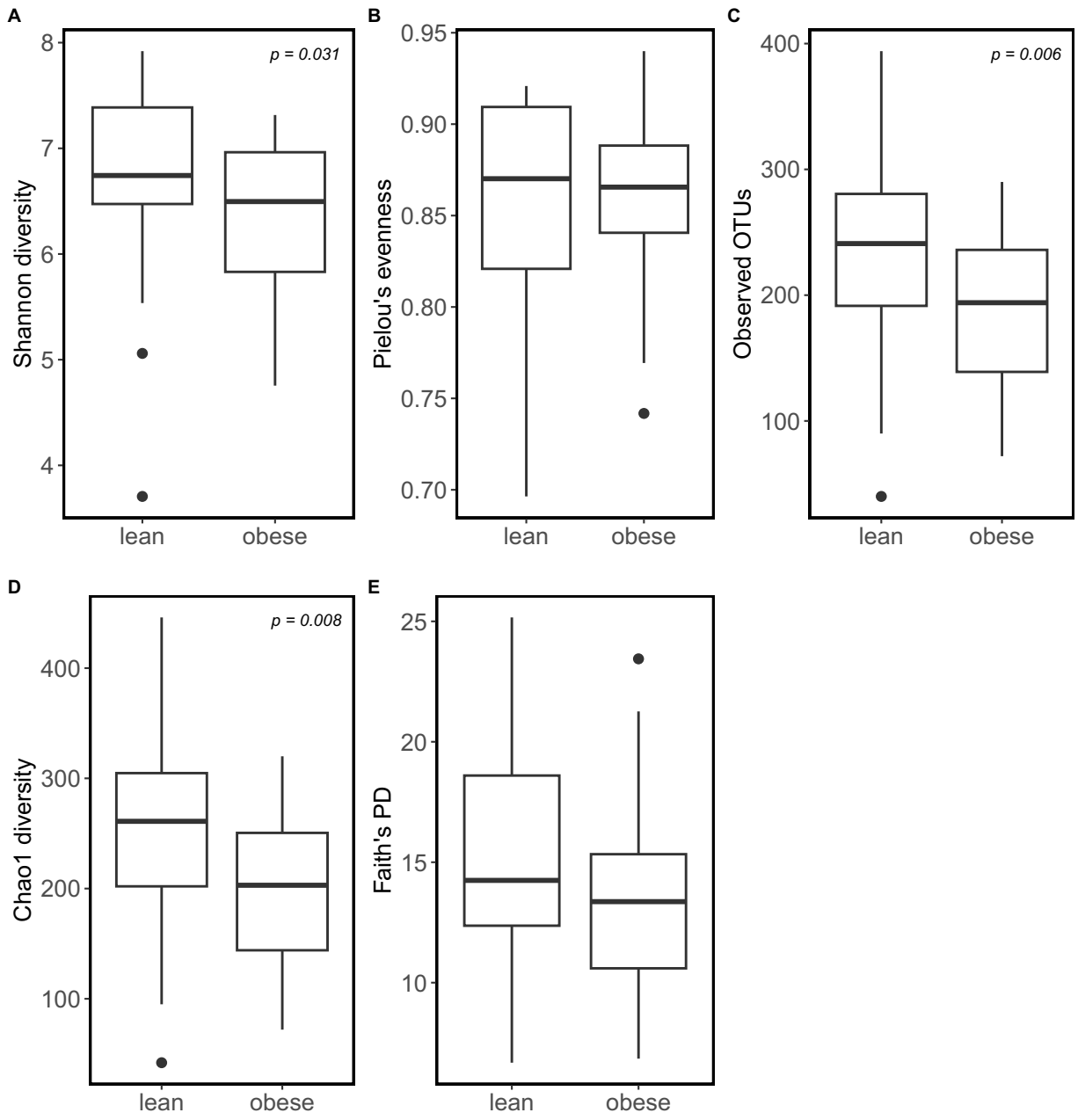


FIGURE 3
Obese individuals tend to have lower microbiome α-diversity. α-diversity was calculated using: **(A)** Shannon diversity; **(B)** Pielou's Evenness; **(C)** Observed_OTUs; **(D)** Choa1 diversity; **(E)** Faith's PD.

promotes a lean host phenotype and positively impacts the diversity of the community (Aguirre and Venema, 2015). The abundance of *Alistipes* was higher in the lean group; this new genus is significantly elevated in high-fat-diet-fed mice than in controls (Yang et al., 2022); individuals with obesity have a higher abundance of *Alistipes* (Crovesy et al., 2020). This aberrant finding may be related to the fact that Emirate adults could have a distinct gut microbiota composition given their varying dietary factors and lifestyle. In UAE, there is a transition towards energy-dense diets high in animal protein, total and saturated fatty acids, and simple sugars (Cheikh Ismail et al., 2020). High-fat diets are linked to considerable changes in the gut microbiota composition at the phylum and genus levels (Rosenbaum et al., 2015).

Our finding of a negative association between the genus *Lachnospiraceae* and PBF and BMI is also reported by Lippert et al. in older adults in Austria (Lippert et al., 2017), but not in a study with human stool from Ghanaian volunteers (Dugas et al., 2018). The negative correlation between bacterial taxa that were dominant in the lean group and the adiposity markers (BMI, WC, WHtR, FM, PBF) is unexpected, considering that most of these taxa belong to the Firmicutes phylum.

In contrast, genera that were higher in obese subjects positively correlated with BMI and FM (*Acidaminococcus*) as well as WHtR (*Lachnospira*), suggesting them as potential microbiota biomarkers of obesity (Companys et al., 2021). In addition, levels of *Acidamonicoccus*

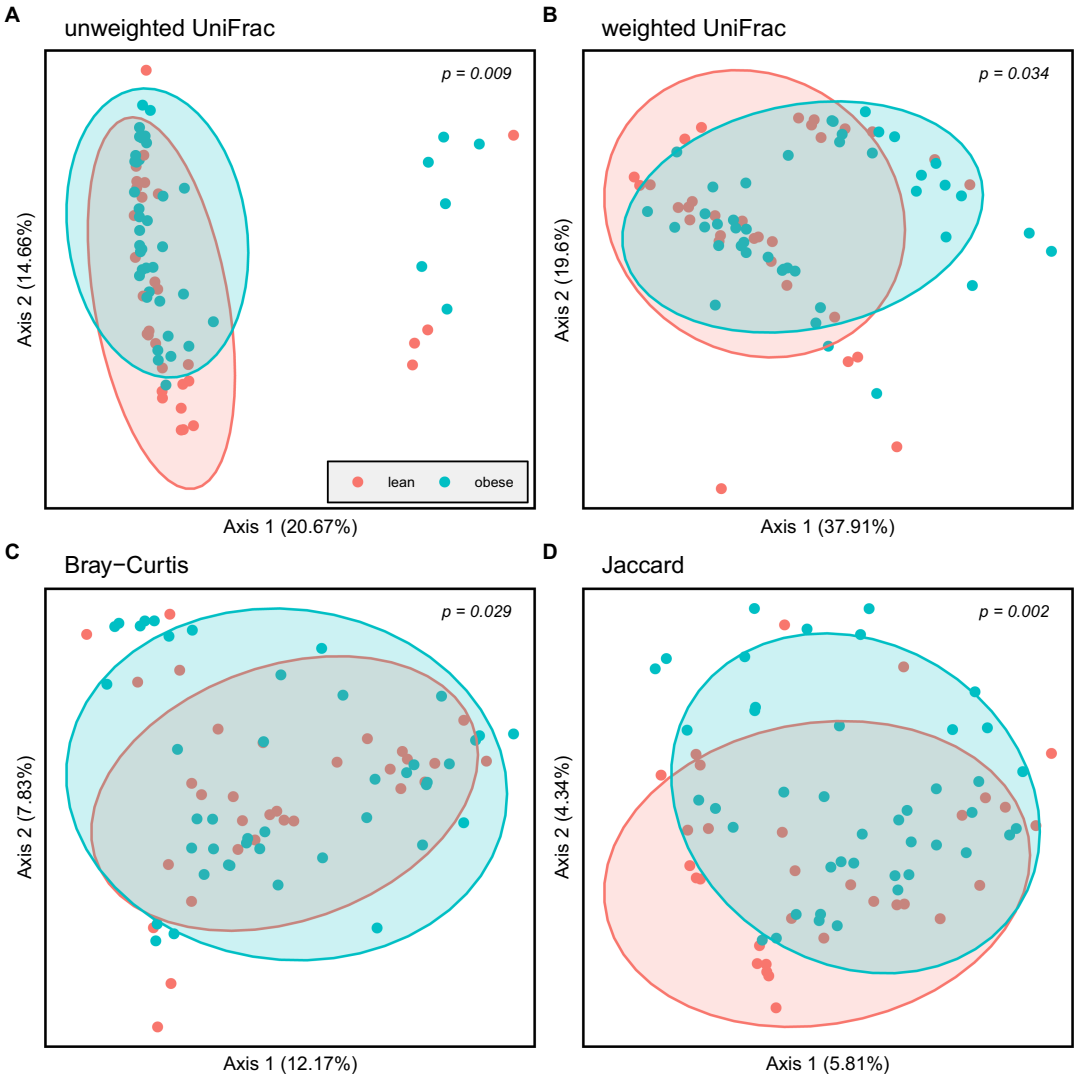


FIGURE 4
Principal coordinate Analysis (PCoA) based on: **(A)** Unweighted UniFrac; **(B)** Weighted UniFrac; **(C)** Bray–Curtis and **(D)** Jaccard; Obese (blue spheres) and lean participants (red spheres).

positively correlated with type 2 diabetes in the Saudi population (Al-Muhanna et al., 2022). Contrary to our results, a study in overweight adults showed that reduced *Lachnospira* abundance was associated with weight gain (Companys et al., 2021). These conflicting findings may have been attained because the two genera comprise various species whose role in obesity has not been thoroughly studied; such issues are still debatable (Aguirre and Venema, 2015).

Some of the identified microbial taxa correlated with adiposity but not other biochemical parameters, i.e., glucose and lipid homeostasis markers. It is tempting to assume that taxa showing negative correlations with adiposity are appropriate markers of metabolic health. Nevertheless, larger studies are required to ascertain such relationships (Palmas et al., 2021).

The presence of divergent results between this study and other studies in the literature might be attributed to the geographical location of the studies, given dietary and environmental variations known to affect gut microbiota (Al-Muhanna et al., 2022) or to many other factors, such as the population under study, gender, physical activity, drugs, ethnicity, and the season, as well as methods used to analyze the gut microbiota, such as different DNA extraction techniques, different areas of the 16S rRNA gene sequenced and primers used. The composition of the gut microbiota can be easily influenced, and all factors that affect it are difficult to control (Crovesy et al., 2020). The majority of available studies did not evaluate factors that can affect the gut microbiota, such as diet, physical activity, smoking, stress, and sleep, which might explain the possible differences found between studies (Rosenbaum et al., 2015; Aljazairy et al., 2022). Amongst these, the diet is likely to greatly impact the gut microbiota composition (Crovesy et al., 2020).

## 4.1. Strengths and limitations

This study provides meaningful insight into the relationship between gut microbiota and obesity, specifically in Emirati adults, and is a useful addition to the international microbiome reference dataset.

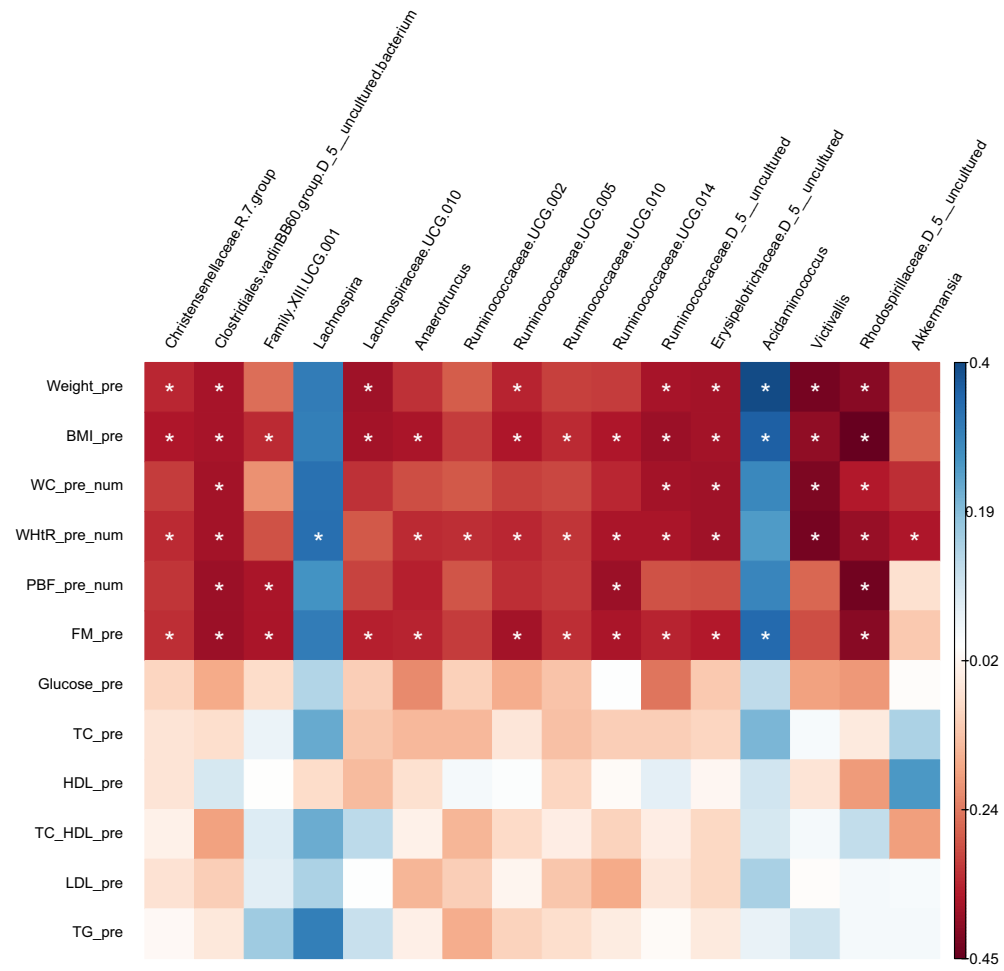


FIGURE 5
Heatmap of Spearman correlation analysis between gut microbiota (at genus level) and clinical variables.

Yet, this study is limited by its relatively small sample size. Furthermore, we did not adjust for a potential confounding factor such as dietary intake, hindering our ability to link unique gut microbiota profiles with specific diets. Finally, our results should be interpreted cautiously as they are based on observational data.

## 5. Conclusion

We revealed significant differences in microbiota between obese and lean subjects at phylum and genus levels. Remarkably, our study showed no significant differences in Firmicutes and Bacteroidetes or F/B ratio, suggesting that F/B cannot be used as a universal predictor biomarker for obesity in adults. Genera that were higher in obese subjects correlated positively with BMI and FM (Acidaminococcus) as well as WHtR (Lachnospira) and are genera that might serve as microbiota biomarkers of obesity in Emerati. In contrast, genera higher in the lean group correlated negatively with adiposity. Future studies are needed to confirm our results and to understand better the interplay between diet, lifestyle, gut microbiota, and health. Whether changes in the gut microbial composition are a cause or a consequence of obesity remains an open question.

## Data availability statement

The raw sequences and corresponding metadata have been archived in the Sequence Read Archive (SRA) repository at the NCBI under accession number PRJNA962831: http://www.ncbi.nlm.nih.gov/bioproject/962831.

## Ethics statement

The studies involving human participants were reviewed and approved by Ethical approval was granted by the Research Ethics Committee of the Ministry of Health and Prevention of UAE (MOHP/DXB-REC-52/2018), the Dubai Health Care Regulatory Research Ethics Committee (DHCR-REC), and the Zayed University Ethical Committee Board (ZU19_51_F). The study followed the Declaration of Helsinki. Written informed consent was collected from all study subjects. The patients/participants provided their written informed consent to participate in this study. The studies were conducted in accordance with the local legislation and institutional requirements. The participants provided their written informed consent to participate in this study.

## Author contributions

MA, MK, and KV: conceptualization, methodology, and data curation. MA and KV: software and supervision. MK, KV, and CM: validation. MA: formal analysis, investigation, and writing – original draft preparation. MK, KV, CM, GW, and TM: resources and writing – review and editing. MA, MK, KV, CM, GW, and TM: visualization. MK and KV: project administration. CA and KV: funding acquisition. All authors contributed to the article and approved the submitted version.

## Funding

This research was funded by Zayed University, Dubai, UAE (grant number R19054) and the Dutch Province of Limburg with a grant to the Centre for Healthy Eating and Food Innovation (HEFI) of Maastricht University – Campus Venlo (grant number HEFI-1).

## Acknowledgments

We thank the research assistants and students from the College of Natural and Health Sciences department at Zayed University in Dubai campus for their assistance in data collection, Dr. Sulaiman al Habib Hospital (Dubai, UAE), Al Qassimi Hospital (Sharjah, UAE), and the Research Institute for Medical and Health Sciences (Sharjah, UAE) for their collaboration and involvement in the study.

## Conflict of interest

The authors declare that the research was conducted without any commercial or financial relationships that could be construed as a potential conflict of interest.

## Publisher's note



## Supplementary material

The Supplementary material for this article can be found online at: https://www.frontiersin.org/articles/10.3389/fmicb.2023.1182460/full#supplementary-material

## References

Abenavoli, L., Scarpellini, E., Colica, C., Boccuto, L., Salehi, B., Sharifi-Rad, J., et al. (2019). Gut microbiota and obesity: a role for probiotics. *Nutrients* 11:2690. doi: 10.3390/nu11112690

Adlerberth, I., and Wold, A. (2009). Establishment of the gut microbiota in Western infants. *Acta Paediatr.* 98, 229–238. doi: 10.1111/j.1651-2227.2008.01060.x

Aguirre, M., and Venema, K. (2015). Does the gut microbiota contribute to obesity? Going beyond the gut feeling. *Microorganisms* 3, 213–235. doi: 10.3390/microorganisms3020213

Aljazairy, E. A. A., Al-Musharaf, S., Abudawood, M., Almaarik, B., Hussain, S. D., Alnaami, A. M., et al. (2022). Influence of adiposity on the gut microbiota composition of Arab women: a case-control study. *Biology* 11:1586. doi: 10.3390/biology11111586

Al-Muhanna, F. A., Dowdell, A. K., Al Eleq, A. H., Albaker, W. I., Brooks, A. W., Al-Sultan, A. I., et al. (2022). Gut microbiota analyses of Saudi populations for type 2 diabetes-related phenotypes reveals significant association. *BMC Microbiol.* 22, 1–9. doi: 10.1186/s12866-022-02714-8

Armougom, F., Henry, M., Vialettes, B., Raccah, D., and Raoult, D. (2009). Monitoring bacterial community of human gut microbiota reveals an increase in Lactobacillus in obese patients and methanogens in anorexic patients. *PLoS One* 4:e7125. doi: 10.1371/journal.pone.0007125

Ashwell, M., and Gibson, S. (2016). Waist-to-height ratio as an indicator of 'early health 'risk': simpler and more predictive than using a 'matrix' based on BMI and waist circumference. *BMJ Open* 6:e010159. doi: 10.1136/bmjopen-2015-010159

Bauer, P. V., Hamr, S. C., and Duca, F. A. (2016). Regulation of energy balance by a gut–brain axis and involvement of the gut microbiota. *Cell. Mol. Life Sci.* 73, 737–755. doi: 10.1007/s00018-015-2083-z.pdf

Brant, R. (2015). Inference for Means: Comparing Two Independent Samples. Web-Based Sample Size Calculators. Available at: http://newton.Stat.Ubc.Ca/~rollin/stats/ssize(2). (Accessed March 1, 2023).

Cannon, C. P., and Kumar, A. (2009). Treatment of overweight and obesity: lifestyle, pharmacologic, and surgical options. *Clin. Cornerstone* 9, 55–71. doi: 10.1016/S1098-3597(09)80005-7

Castaner, O., Goday, A., Park, Y. M., Lee, S. H., Magkos, F., Shiow, S. T. E., et al. (2018). The gut microbiome profile in obesity: a systematic review. *Int. J. Endocrinol.* 2018:4095789. doi: 10.1155/2018/4095789

Cheikh Ismail, L., Osaili, T. M., Mohamad, M. N., Al Marzouqi, A., Jarrar, A. H., Abu Jamous, D. O., et al. (2020). Eating habits and lifestyle during COVID-19 lockdown in the United Arab Emirates: a cross-sectional study. *Nutrients* 12:3314. doi: 10.3390/nu12113314

Cheng, L., Chen, Y., Zhang, X., Zheng, X., Cao, J., Wu, Z., et al. (2019). A metagenomic analysis of the modulatory effect of *Cyclocarya paliurus* flavonoids on the intestinal microbiome in a high-fat diet-induced obesity mouse model. *J. Sci. Food Agric.* 99, 3967–3975. doi: 10.1002/jsfa.9622

Companys, J., Gosalbes, M. J., Pla-Pagà, L., Calderón-Pérez, L., Llauradó, E., Pedret, A., et al. (2021). Gut microbiota profile and its association with clinical variables and dietary intake in overweight/obese and lean subjects: a cross-sectional study. *Nutrients* 13:2032. doi: 10.3390/nu13062032

Corfe, B. M., Harden, C. J., Bull, M., and Garaiova, I. (2015). The multifactorial interplay of diet, the microbiome and appetite control: current knowledge and future challenges. *Proc. Nutr. Soc.* 74, 235–244. doi: 10.1017/S0029665114001670

Cotillard, A., Kennedy, S. P., Kong, L. C., Prifti, E., Pons, N., Le Chatelier, E., et al. (2013). Dietary intervention impact on gut microbial gene richness. *Nature* 500, 585–588. doi: 10.1038/nature12480

Crovesy, L., Masterson, D., and Rosado, E. L. (2020). Profile of the gut microbiota of adults with obesity: a systematic review. *Eur. J. Clin. Nutr.* 74, 1251–1262. doi: 10.1038/s41430-020-0607-6

Damms-Machado, A., Mitra, S., Schollenberger, A. E., Kramer, K. M., Meile, T., Konigsrainer, A., et al. (2015). Effects of surgical and dietary weight loss therapy for obesity on gut microbiota composition and nutrient absorption. *Biomed. Res. Int.* 2015:806248. doi: 10.1155/2015/806248

Davis, C. D. (2016). The gut microbiome and its role in obesity. *Nutr. Today* 51, 167–174. doi: 10.1097/nt.0000000000000167

Dugas, L. R., Bernabé, B. P., Priyadarshini, M., Fei, N., Park, S. J., Brown, L., et al. (2018). Decreased microbial co-occurrence network stability and SCFA receptor level correlates with obesity in African-origin women. *Sci. Rep.* 8:17135. doi: 10.1038/s41598-018-35230-9

Duncan, S. H., Lobley, G., Holtrop, G., Ince, J., Johnstone, A., Louis, P., et al. (2008). Human colonic microbiota associated with diet, obesity and weight loss. *Int. J. Obes.* 32, 1720–1724. doi: 10.1038/ijo.2008.155

Ford, E. S. (2005). Prevalence of the metabolic syndrome defined by the international diabetes federation among adults in the US. *Diabetes Care* 28, 2745–2749. doi: 10.2337/diacare.28.11.2745

Furet, J. P., Kong, L. C., Tap, J., Poitou, C., Basdevant, A., Bouillot, J. L., et al. (2010). Differential adaptation of human gut microbiota to bariatric surgery-induced weight loss: links with metabolic and low-grade inflammation markers. *Diabetes* 59, 3049–3057. doi: 10.2337/db10-0253

Gao, X., Zhang, M., Xue, J., Huang, J., Zhuang, R., Zhou, X., et al. (2018). Body mass index differences in the gut microbiota are gender specific. *Front. Microbiol.* 9:1250. doi: 10.3389/fmicb.2018.01250

Gao, R., Zhu, C., Li, H., Yin, M., Pan, C., Huang, L., et al. (2018). Dysbiosis signatures of gut microbiota along the sequence from healthy, young patients to those with overweight and obesity. *Obesity (Silver Spring)* 26, 351–361. doi: 10.1002/oby.22088

Gordon, J. I., Turnbaugh, P., Ley, R., Hamady, M., Fraser-Liggett, C., and Knight, R. (2007). The human microbiome project. *Nature* 449, 804–810. doi: 10.1038/nature06244

Heinritz, S. N., Mosenthin, R., and Weiss, E. (2013). Use of pigs as a potential model for research into dietary modulation of the human gut microbiota. *Nutr. Res. Rev.* 26, 191–209. doi: 10.1017/S0954422413000152

Houtman, T. A., Eckermann, H. A., Smidt, H., and de Weerth, C. (2022). Gut microbiota and BMI throughout childhood: the role of firmicutes, bacteroidetes, and short-chain fatty acid producers. *Sci. Rep.* 12:3140. doi: 10.1038/s41598-022-07176-6

Isolauri, E. (2017). Microbiota and obesity. *Nestle Nutr Inst Workshop Ser* 88, 95–105. doi: 10.1159/000455217

Jinatham, V., Kullawong, N., Kespechara, K., Gentekaki, E., and Popluechai, S. (2018). Comparison of gut microbiota between lean and obese adult Thai individuals. *Microbiol Biotechnol Lett* 46, 277–287. doi: 10.4014/mbl.1711.11003

Kasai, C., Sugimoto, K., Moritani, I., Tanaka, J., Oya, Y., Inoue, H., et al. (2015). Comparison of the gut microbiota composition between obese and non-obese individuals in a Japanese population, as analyzed by terminal restriction fragment length polymorphism and next-generation sequencing. *BMC Gastroenterol.* 15:100. doi: 10.1186/s12876-015-0330-2

Kocełak, P., Zak-Gołąb, A., Zahorska-Markiewicz, B., Aptekorz, M., Zientara, M., Martirosian, G., et al. (2013). Resting energy expenditure and gut microbiota in obese and normal weight subjects. *Eur. Rev. Med. Pharmacol. Sci.* 17, 2816–2821.

Kong, L. C., Tap, J., Aron-Wisnewsky, J., Pelloux, V., Basdevant, A., Bouillot, J. L., et al. (2013). Gut microbiota after gastric bypass in human obesity: increased richness and associations of bacterial genera with adipose tissue genes. *Am. J. Clin. Nutr.* 98, 16–24. doi: 10.3945/ajcn.113.058743

Le Chatelier, E., Nielsen, T., Qin, J., Prifti, E., Hildebrand, F., Falony, G., et al. (2013). Richness of human gut microbiome correlates with metabolic markers. *Nature* 500, 541–546. doi: 10.1038/nature12506

Lippert, K., Kedenko, L., Antonielli, L., Kedenko, I., Gemeier, C., Leitner, M., et al. (2017). Gut microbiota dysbiosis associated with glucose metabolism disorders and the metabolic syndrome in older adults. *Benefic. Microbes* 8, 545–556. doi: 10.3920/BM2016.0184

Louis, S., Tappu, R.-M., Damms-Machado, A., Huson, D. H., and Bischoff, S. C. (2016). Characterization of the gut microbial community of obese patients following a weight-loss intervention using whole metagenome shotgun sequencing. *PLoS One* 11:e0149564. doi: 10.1371/journal.pone.0149564

Ministry of Health and Prevention. (2023). MoHAP Ramps Up Efforts to Improve Results of National Indicator on Prevalence of Obesity. Available at: https://mohap.gov.ae/en/media-center/news/4/3/2022/mohap-ramps-up-efforts-to-improve-results-of-national-indicator-on-prevalence-of-obesity (Accessed February 26, 2023).

Morgen, C. S., and Sørensen, T. I. (2014). Global trends in the prevalence of overweight and obesity. *Nat. Rev. Endocrinol.* 10, 513–514. doi: 10.1038/nrendo.2014.124

Nguyen, T. L. A., Vieira-Silva, S., Liston, A., and Raes, J. (2015). How informative is the mouse for human gut microbiota research? *Dis. Model. Mech.* 8, 1–16. doi: 10.1242/dmm.017400

Palmas, V., Pisanu, S., Madau, V., Casula, E., Deledda, A., Cusano, R., et al. (2021). Gut microbiota markers associated with obesity and overweight in Italian adults. *Sci. Rep.* 11, 1–14. doi: 10.1038/s41598-021-84928-w

Patrone, V., Vajana, E., Minuti, A., Callegari, M. L., Federico, A., Loguercio, C., et al. (2016). Postoperative changes in fecal bacterial communities and fermentation products in obese patients undergoing Bilio-intestinal bypass. *Front. Microbiol.* 7:200. doi: 10.3389/fmicb.2016.00200

Pinart, M., Dötsch, A., Schlicht, K., Laudes, M., Bouwman, J., Forslund, S. K., et al. (2021). Gut microbiome composition in obese and non-obese persons: a systematic review and meta-analysis. *Nutrients* 14:12. doi: 10.3390/nu14010012

Plummer, E., Bulach, D., Carter, G., and Albert, M. J. (2020). Gut microbiome of native Arab Kuwaitis. *Gut Pathogens* 12, 1–9. doi: 10.1186/s13099-020-00351-y

Radwan, H., Ballout, R. A., Hasan, H., Lessan, N., Karavetian, M., and Rizk, R. (2018). The epidemiology and economic burden of obesity and related cardiometabolic disorders in the United Arab Emirates: a systematic review and qualitative synthesis. *J. Obes.* 2018, 1–23. doi: 10.1155/2018/2185942

Rinninella, E., Raoul, P., Cintoni, M., Franceschi, F., Miggiano, G. A. D., Gasbarrini, A., et al. (2019). What is the healthy gut microbiota composition? A changing ecosystem across age, environment, diet, and diseases. *Microorganisms* 7:14. doi: 10.3390/microorganisms7010014

Romero-Corral, A., Somers, V. K., Sierra-Johnson, J., Thomas, R. J., Collazo-Clavell, M., Korinek, J., et al. (2008). Accuracy of body mass index in diagnosing obesity in the adult general population. *Int. J. Obes.* 32, 959–966. doi: 10.1038/ijo.2008.11

Rosenbaum, M., Knight, R., and Leibel, R. L. (2015). The gut microbiota in human energy homeostasis and obesity. *Trends Endocrinol. Metab.* 26, 493–501. doi: 10.1016/j.tem.2015.07.002

Round, J. L., and Mazmanian, S. K. (2009). The gut microbiota shapes intestinal immune responses during health and disease. *Nat. Rev. Immunol.* 9, 313–323. doi: 10.1038/nri2515

Schwiertz, A., Taras, D., Schäfer, K., Beijer, S., Bos, N. A., Donus, C., et al. (2010). Microbiota and SCFA in lean and overweight healthy subjects. *Obesity* 18, 190–195. doi: 10.1038/oby.2009.167

Seganfredo, F., Blume, C., Moehlecke, M., Giongo, A., Casagrande, D., Spolidoro, J., et al. (2017). Weight-loss interventions and gut microbiota changes in overweight and obese patients: a systematic review. *Obes. Rev.* 18, 832–851. doi: 10.1111/obr.12541

Snetselaar, L. G., de Jesus, J. M., DeSilva, D. M., and Stoody, E. E. (2021). Dietary guidelines for Americans, 2020–2025: understanding the scientific process, guidelines, and key recommendations. *Nutr. Today* 56, 287–295. doi: 10.1097/nt.0000000000000512

Sonnenburg, J. L., and Backhed, F. (2016). Diet-microbiota interactions as moderators of human metabolism. *Nature* 535, 56–64. doi: 10.1038/nature18846

Sulaiman, N., Elbadawi, S., Hussein, A., Abusnana, S., Madani, A., Mairghani, M., et al. (2017). Prevalence of overweight and obesity in United Arab Emirates expatriates: the UAE national diabetes and lifestyle study. *Diabetol. Metab. Syndr.* 9, 1–9. doi: 10.1186/s13098-017-0287-0

Surono, I. S., Simatupang, A., Kusumo, P. D., Waspodo, P., Verbruggen, S., Verhoeven, J., et al. (2022). Effect of different functional food supplements on the gut microbiota of Prediabetic Indonesian individuals during weight loss. *Nutrients* 14:781. doi: 10.3390/nu14040781

Tehrani, A. B., Nezami, B. G., Gewirtz, A., and Srinivasan, S. (2012). Obesity and its associated disease: a role for microbiota? *Neurogastroenterol Motility* 24, 305–311. doi: 10.1111/j.1365-2982.2012.01895.x

Tremaroli, V., and Bäckhed, F. (2012). Functional interactions between the gut microbiota and host metabolism. *Nature* 489, 242–249. doi: 10.1038/nature11552

Turnbaugh, P. J., and Gordon, J. I. (2009). The core gut microbiome, energy balance and obesity. *J. Physiol.* 587, 4153–4158. doi: 10.1113/jphysiol.2009.174136

Turnbaugh, P. J., Hamady, M., Yatsunenko, T., Cantarel, B. L., Duncan, A., Ley, R. E., et al. (2009). A core gut microbiome in obese and lean twins. *Nature* 457, 480–484. doi: 10.1038/nature07540

Turnbaugh, P. J., Ley, R. E., Mahowald, M. A., Magrini, V., Mardis, E. R., and Gordon, J. I. (2006). An obesity-associated gut microbiome with increased capacity for energy harvest. *Nature* 444, 1027–1031. doi: 10.1038/nature05414

Van der Kooy, K., and Seidell, J. C. (1993). Techniques for the measurement of visceral fat: a practical guide. *Int. J. Obes.* 17, 187–196.

Venema, K. (2010). Role of gut microbiota in the control of energy and carbohydrate metabolism. *Curr Opin Clin Nutr Metab Care* 13, 432–438. doi: 10.1097/MCO.0b013e32833a8b60

World Health Organization. (2016). Obesity and Overweight. Available at: https://www.who.int/news-room/fact-sheets/detail/obesity-and-overweight (Accessed March 5, 2023).

Yang, J., Wei, H., Zhou, Y., Szeto, C.-H., Li, C., Lin, Y., et al. (2022). High-fat diet promotes colorectal tumorigenesis through modulating gut microbiota and metabolites. *Gastroenterology* 162, 135–149.e2. doi: 10.1053/j.gastro.2021.08.041

Zeng, Q., Yang, Z., Wang, F., Li, D., Liu, Y., Wang, D., et al. (2021). Association between metabolic status and gut microbiome in obese populations. *Microb Genom* 7:000639. doi: 10.1099/mgen.0.000639

frontiers | Frontiers in Microbiology

TYPE Original Research
PUBLISHED 07 September 2023
DOI 10.3389/fmicb.2023.1210517



OPEN ACCESS

EDITED BY
Ekaterina Avershina,
Oslo University Hospital, Norway

REVIEWED BY
Naga Betrapally,
National Cancer Institute (NIH), United States
Ruiyue Yang,
Peking University, China

*CORRESPONDENCE
Yogendra Padwad
✉ yogendra@ihbt.res.in
Rajesh Pandey
✉ rajeshp@igib.in

RECEIVED 26 April 2023
ACCEPTED 21 August 2023
PUBLISHED 07 September 2023

CITATION
Chhimwal J, Anand P, Mehta P, Swarnkar MK, Patial V, Pandey R and Padwad Y (2023) Metagenomic signatures reveal the key role of phloretin in amelioration of gut dysbiosis attributed to metabolic dysfunction-associated fatty liver disease by time-dependent modulation of gut microbiome.
*Front. Microbiol.* 14:1210517.
doi: 10.3389/fmicb.2023.1210517



# Metagenomic signatures reveal the key role of phloretin in amelioration of gut dysbiosis attributed to metabolic dysfunction-associated fatty liver disease by time-dependent modulation of gut microbiome

Jyoti Chhimwal [1,2], Prince Anand [1,2], Priyanka Mehta [2,3], Mohit Kumar Swarnkar [4], Vikram Patial [1,2], Rajesh Pandey [2,3]* and Yogendra Padwad [1,2]*

[1]Pharmacology and Toxicology Laboratory, Dietetics and Nutrition Technology Division, CSIR-Institute of Himalayan Bioresource Technology (CSIR-IHBT), Palampur, India, [2]Academy of Scientific and Innovative Research (AcSIR), Ghaziabad, India, [3]INtegrative GENomics of HOst-PathogEn (INGEN-HOPE) Laboratory, CSIR-Institute of Genomics and Integrative Biology (CSIR-IGIB), New Delhi, India, [4]Biotechnology Division, CSIR-Institute of Himalayan Bioresource Technology (CSIR-IHBT), Palampur, India

The importance of gut-liver axis in the pathophysiology of metabolic dysfunction-associated fatty liver disease (MAFLD) is being investigated more closely in recent times. However, the inevitable changes in gut microbiota during progression of the disease merits closer look. The present work intends to assess the time-dependent gut dysbiosis in MAFLD, its implications in disease progression and role of plant-derived prebiotics in its attenuation. Male C57BL/6J mice were given western diet (WD) for up to 16 weeks and phloretin was administered orally. The fecal samples of mice were collected every fourth week for 16 weeks. The animals were sacrificed at the end of the study and biochemical and histological analyses were performed. Further, 16S rRNA amplicon sequencing analysis was performed to investigate longitudinal modification of gut microbiome at different time points. Findings of our study corroborate that phloretin alleviated the metabolic changes and mitigated circulating inflammatory cytokines levels. Phloretin treatment resists WD induced changes in microbial diversity of mice and decreased endotoxin content. Prolonged exposure of WD changed dynamics of gut microbiota abundance and distribution. Increased abundance of pathogenic taxa like *Desulfovibrionaceae, Peptostreptococcus, Clostridium,* and *Terrisporobacter* was noted. Phloretin treatment not only reversed this dysbiosis but also modulated taxonomic signatures of beneficial microbes like *Ruminococcus*, *Lactobacillus,* and *Alloprevotella*. Therefore, the potential of phloretin to restore gut eubiosis could be utilized as an intervention strategy for the prevention of MAFLD and related metabolic disorders.

KEYWORDS

**gut microbiome, MAFLD, phloretin, 16S rRNA, metagenome**

# 1. Introduction

The global burden of metabolic dysfunction-associated fatty liver disease (MAFLD) or previously called non-alcoholic fatty liver disease (NAFLD) is a pharmacological challenge with a prevalence of 21–30% among adults worldwide (Mitra et al., 2020). NAFLD could eventually lead to non-alcoholic steatohepatitis (NASH), associated with fibrosis, cirrhosis, and finally to hepatocellular carcinoma (HCC), which is a foremost cause of liver-related morbidity and mortality (Chhimwal et al., 2021). Both, NAFLD and NASH are emerging as a modern public health concern. The association of NAFLD or MAFLD with other life style disorders viz. obesity, type 2 diabetes and cardiovascular diseases contribute toward morbidity and mortality related to liver disease (Ismaiel and Dumitraşcu, 2019). The opportunities for the right treatment regimen are still evolving and development of safe and targeted pharmacotherapy is possibly the utmost need for the treatment of MAFLD. The molecular basis of MAFLD development is not well understood but the "multiple hit" concept emphasizes the role of gut microbiota, insulin resistance, and adipokines produced by adipose tissues which generally attributed to the occurrence of dysfunctional lipid metabolism, oxidative stress and hepatic inflammation (Ji et al., 2019).

The number of bacteria in the stomach is estimated to be 10 times that of human cells (over $10^{14}$) (Ji et al., 2019). The complex relationship of gut microbes and human host is reciprocally beneficial but at the same time, gut dysbiosis is linked with different chronic metabolic diseases, including MAFLD (Fan and Pedersen, 2021). Gut microbiome has attracted considerable attention due to its crucial role in the pathogenesis and development of MAFLD via the gut-liver axis. The liver health is highly reliant on the gut health, as any disruptions in the intestinal barrier expose liver to the pathogenic microorganisms and their toxic byproducts (De Muynck et al., 2021). Disturbance in gut microbiota leads to increased abundance of harmful microbes like endotoxin and ethanol producing bacteria and production of substances like choline and trimethylamine from its precursor phosphatidylcholine (Lee et al., 2020a). The patients with MAFLD also been reported having altered microbial populations in the gut (Tsai et al., 2020). Nevertheless, the impact of liver and gut microbiome and its dysbiosis on MAFLD biology and its potential interactions with the host phenome are largely unexplored, which confines our mechanistic understanding of metagenomic association with the disease (Sookoian et al., 2020). Additionally, majority of the studies of gut microbiota in MAFLD solely pertain on the endpoints and discuss the culminating changes occurred after the progression of the disease. Efforts toward comprehending the sequential changes in gut dysbiosis during progression of MAFLD would be useful to elucidate and essentially a focus of this manuscript.

Diet appears to be a crucial determinant in regulating gut microbiota composition, which is implicated in several metabolic processes including MAFLD (Quesada-Vázquez et al., 2020). The gut microbiota plays a role in the extraction of calories from diet and regulates fat storage. An unbalanced microbiome can result in excessive calorie extraction and fat accumulation (Davis, 2016). Previous studies have established a correlation between alterations in the gut microbiota caused by the western diet (WD) and the development of MAFLD (Romualdo et al., 2022; Yang et al., 2023). However, the paucity of long-term dietary studies or interventions with repeated fecal sample timepoints and post-intervention follow-ups limits current knowledge of how dietary habits alter the gut microflora and its impact on MAFLD progression. Therefore, the present study was conducted to better understand the correlation between WD induced gut dysbiosis and MAFLD progression utilizing a time-dependent approach, as well as implications of this finding for possible therapeutic approaches. Many dietary, phytomolecules and prebiotic-based strategies have been reported in promoting healthy gut microbiota, growth and associated benefits (Carrera-Quintanar et al., 2018; Beane et al., 2021). Phloretin, a dihydrochalcone flavonoid derived from apples or pears, is one such nutraceutical that has been shown to alter the gut microbiota associated with colitis (Wu et al., 2019). Phloretin is also effective in ameliorating MAFLD by regulating AMP-activated protein kinase (AMPK) pathways (Liou et al., 2020). In our previous study, we discussed how phloretin restored hepatic autophagy to slow the course of MAFLD (Chhimwal et al., 2022). However, it would be interesting to see if the modulation of gut microbiota could be attributed to the efficacy of orally administered phloretin in ameliorating MAFLD. In this study, taking advantage of the susceptibility of gut microbiota to over-nutrition, we looked at how the gut microflora changes over the course of 16 weeks of WD feeding. Further, we explored the potential of phloretin to maintain metabolic homeostasis while altering the gut microflora associated with MAFLD over time.

# 2. Materials and methods

## 2.1. Animals used in the study

Six-weeks-old, adult male C57BL/6J mice, weighing 25 ± 3 g were procured from CSIR-Indian Institute of Integrative Medicine, Jammu, India. The animals were caged into individually ventilated cages (IVC) under standard laboratory temperature and humidity conditions and allowed free access to standard mouse chow pellet feed and water *ad libitum*. Both animal handling procedures and protocols were approved by the Institutional Animal Ethical Committee (IAEC) and carried out as per the guidelines of Committee for the Purpose of Control and Supervision of Experiments on Animals (CPCSEA).

## 2.2. Experimental design

C57BL/6J mice were randomly separated into three groups ($n = 6$).

1. *Group 1 (Control):* The animals of this group were provided standard pellet feed and served as control group.
2. *Group 2 (WD):* The animals were fed on WD (44.4% kcal from carbohydrates, 40.1% kcal from fat, supplemented with 0.15% cholesterol) along-with HFCS (high fructose corn syrup, 42%) in drinking water for 16 weeks.
3. *Group 3 (WD + P):* The animals received phloretin [dissolved in 0.5% sodium carboxymethyl cellulose (CMC-Na) solution] by oral gavage at 200 mg/kg body weight dose along with WD and HFSC water. The dose of phloretin was optimized using previous research (Chhimwal et al., 2022).

Figure 1A illustrates the overall treatment regimen. Mice in control and WD group receive equal volume of CMC-Na solution orally to normalize the handling stress. The fecal samples of mice were collected every fourth week. The body weight and food intake of mice were measured weekly. At the end of the study, the animals were euthanized by $CO_2$ asphyxiation and the liver tissues were excised after the dissection of animals and stored for further analysis.

## 2.3. Serum biochemistry

Serum triglyceride (TG), total cholesterol (TC), low-density lipoprotein cholesterol (LDL-C), and high-density lipoprotein cholesterol (HDL-C) levels were determined by colorimetry based automated bioanalyzer using designated colorimetric kits (ERBA, Transasia, India), as per manufacturer's protocol.

## 2.4. ELISA for serum insulin and inflammatory cytokines

The serum concentrations of insulin and inflammatory cytokines (IL-6 and TNF-α) were assessed using designated ELISA kits (RayBiotech, GA, USA), as per manufacturer's instructions.

## 2.5. Estimation of fecal endotoxin level

To determine the fecal bacterial endotoxin concentration, 200 mg of fecal samples were homogenized and further sonicated in 1 ml of PBS. The supernatants were collected and subjected to endotoxin estimation using commercially available chromogenic endotoxin ELISA kit (MyBioSource, CA, USA) following manufacturer's instructions.

## 2.6. Histopathology and ORO staining in liver tissue

Formalin-fixed liver tissues were processed for histopathology as described by Chhimwal et al. (2020) and then sliced into 4 μM thick section to perform hematoxylin and eosin (H&E) and Picrosirius red staining following procedure reported previously (Chhimwal et al., 2020). Further, snap frozen liver specimens were embedded in OCT medium and sliced at 10 μm thickness with the help of cryotome (Lieca, Wetzlar, Germany). Followed by fixation in 10% buffered formalin for 10 min, and rinsed in water for 5 min. Fixed sections were then stained with freshly prepared 0.4% ORO staining solution for 10 min at RT followed by counter stain with Mayer's hematoxylin and again washed with running water for 5 min. Stained liver sections were then envisioned under bright field in EVOS FL Auto 2 microscope (Thermo Fisher Scientific, MA, USA). MAFLD scoring was done according to previously described method (Chhimwal et al., 2021).

## 2.7. RNA isolation and RT-qPCR

Total RNA was isolated from liver tissue using TRIzol TRI Reagent (Sigma, MO, USA). Briefly, 50 mg of liver tissue was homogenized in one ml of TRI reagent and the supernatant was collected by centrifugation at 12,000 *g* for 5 min at 4°C. To separate the aqueous layer containing nucleic acids, 0.2 ml chloroform was added per ml of collected supernatant and centrifuged (12,000 *g*; 15 min; 4°C). The upper aqueous layer was collected and an equal volume of 70% ethanol was added to it. The mixture was then passed through the column provided in RNeasy Mini Kit (Qiagen, Hilden, Germany) and further RNA was isolated using the manufacturer's protocol. The quality and quantity of RNA samples were checked by NanoDrop (Thermo Fisher Scientific, MA, USA). RT-qPCR reactions were executed using RT-qPCR ROX Mix Kit supplied by Thermo Fisher Scientific. GAPDH was used as reference gene. Primers sequences (forward and reverse) are listed in Supplementary Table 1. All the data (analyzed by $2^{-\Delta\Delta Ct}$ method) were adjusted to reference gene and displayed as fold change versus the control group.

## 2.8. DNA isolation, library preparation, and 16S rRNA sequencing

Total bacterial DNA was isolated from all 72 samples using QIAamp PowerFecal Pro DNA Kit (Qiagen, Hilden, Germany) according to manufacturer's instructions. The quality and quantity of DNA samples were checked by Qubit 2.0 fluorometer (Thermo Fisher Scientific, MA, USA). The amplicon PCR was carried out using the primers 341F (5′-CCTACGGGNGGCWGCAG-3′) and 805R (5′-GACTACHVGGGTATCTAATCC-3′) to amplify the V3–V4 region of the bacterial 16S rRNA gene. Following the PCR purification, the Nextera XT indexed adapters (Illumina, CA, USA) were added to the ends of the primers. KAPA HiFi HotStart ReadyMix (2X) (Roche, Basel, Switzerland) was used for all PCR reactions. The purified libraries were then subjected to quality check on Qubit 2.0 fluorometer (Thermo Fisher Scientific, MA, USA) and Agilent 2100 Bioanalyzer system (Agilent, Singapore). The libraries were then sequenced and 250 bp paired-end reads were generated on the Illumina platform using MiSeq Reagent Kit v3 (600 cycle) (Illumina, CA, USA). By sequencing all the samples in a single MiSeq run, any potential batch effects were eliminated.

## 2.9. Processing of raw sequencing data

Computing and data processing was performed using the computing resource on Google cloud platform. Trimming of raw reads was done by remove primers using cutadapt (Martin, 2011) and low-quality bases (<Q30). These high-quality reads were considered for denoising, merging of paired-end reads, removal of chimeric sequences, and to pick unique amplicon sequence variants (ASVs) using the DADA2 plugin within qiime2 (Caporaso et al., 2010; Callahan et al., 2016). For taxonomic assignments of these ASVs, Silva database (sequences along with taxonomy, version silva-138-99) were downloaded (Quast et al., 2013). Further, unclassified ASVs from the same family, genus or

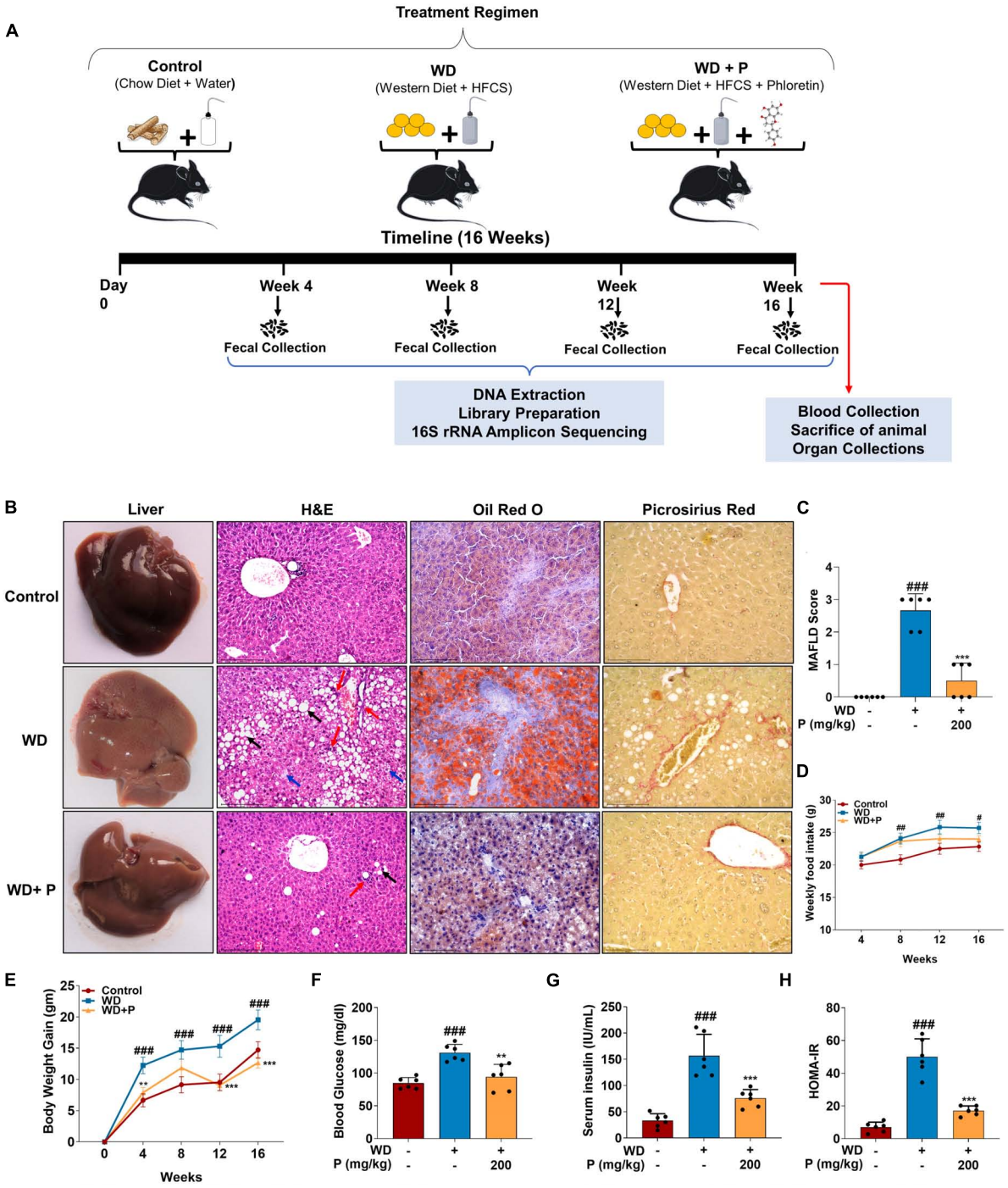


FIGURE 1
Phloretin improved pathological injury, hepatic lipid deposition and insulin resistance in western diet (WD) fed mice ($n$ = 6). **(A)** Schematic diagram illustrating treatment regimen. **(B)** Representative images of liver along with H&E (scale bars, 200 μm; black arrows represent macrosteatosis, blue arrows represent microsteatosis, and red arrows represent inflammatory focci), Oil Red O staining (scale bars, 100 μm) from each group and Picrosirius red staining (scale bars, 100 μm; red color represent fibrous tissues). **(C)** Graphical representation of semi-quantitative scoring of MAFLD in different groups. **(D)** Graphical representation of weekly food intake in different groups. **(E)** Graphical representation of body weight gain in different groups. **(F)** Blood glucose level in different groups. **(G)** Serum insulin level in different groups. **(H)** Graphical representation of HOMA-IR in all groups. The symbols "#," "##," "###" represent $p < 0.05$, $p < 0.01$, and $p < 0.001$, respectively vs. control group; the symbols "**," "***" represent $p < 0.01$, $p < 0.001$, respectively vs. WD group.

species were differentiated using consecutive numbering (1, 2, 3, and so on). Selected sequences, extracted using V3–V4 primers, were used to train the naïve Bayes classifier and this trained classifier was used to predict the complete taxonomy of each ASV. This training and testing were done using feature-classifier fit-classifier-naive-bayes, and feature-classifier classify-sklearn plugins within qiime2. Furthermore, functional potential of these microbial communities was evaluated using Phylogenetic Investigation of

Communities by Reconstruction of Unobserved States (PICRUSt, version 2; maximum nearest sequenced taxon index = 2) (Langille et al., 2013). Abundance of each ASV and predicted KEGG (kyoto encyclopedia of genes and genomes) metabolic pathways were used for downstream statistical analysis (Kanehisa and Goto, 2000).

## 2.10. Statistical analysis

One-way or two-way (wherever applicable) ANOVA was performed to analyze data using GraphPad Prism statistical analysis software (version 8.0.2), in order to determine the statistical significance of the differences among groups. Data are represented as mean ± SD ($n$ = 6) and $p$-value < 0.05 was considered as significant. R statistical interface was used to perform all microbial community ecology analyses. Because of low sequencing depth in 2 out of total of 72 samples, 70 samples were considered for downstream analysis. ASV counts were used to access the microbial richness, diversity and ASVs relative abundances were used to calculate distances between each sample using vegan and ape packages in R (Paradis and Schliep, 2019). Bray–Curtis distances were used for the ordination analysis. Adonis function in R was used to calculate permutational multivariate analysis of variance (PERMANOVA) for each variable. To identify significantly discriminating taxa and pathways, "indicator species analysis" was performed using labdsv package and variance partition analysis performed using Variance Partition package in R (Hoffman and Schadt, 2016; Roberts et al., 2019). Indicator species analysis (ISA) is one of the most used statistical methods in microbial ecology. The benefit of using ISA is that it provides the features (taxa/pathways) which are significantly discriminating across groups ($p$-value) and at the same time their prevalence within the group (IndVal score). Cumulative abundances of selected taxa and functions were shown in different plots. Kruskal–Wallis test was applied to check the statistical significance of discriminating features (taxa/pathways). To understand the co-occurrence of microbial taxa among all three experimental groups, compositional corrected correlations were performed using Compositionality Corrected by REnormalization and PErmutation (CCREPE) function in R (Schwager et al., 2019). All strong ($r$ > 0.5) significant correlations ($p$ < 0.05) were used to construct the co-occurrence network plots in Cytoscape (Shannon et al., 2003). Neighborhood Connectivity was used to access the overall network topology.

# 3. Results

## 3.1. Western diet contributed to MAFLD onset by triggering lipid accumulation, pathological, and fibrotic changes in liver and altering metabolic homeostasis

Effects of WD on pathophysiology of animal and induction of MAFLD has been evaluated through different parameters. ORO staining in **Figure 1B** shows that WD-fed mice had significant micro and macro-vesicular fat deposition in the hepatocytes. The H&E staining of liver sections revealed ballooning degeneration along with multifocal necrotic regions and invasive mononuclear cells indicating hepatic inflammation ($p$ < 0.001; **Figure 1C**). In comparison to the control group, WD feeding resulted in mild to moderate fibrous tissue deposition surrounding steatotic cells and vessels. We also observed a significant increase in feed intake in WD-fed mice over the course of 16 weeks. This resulted in an average 20 g of weight gain in WD mice, which is more than 30% of the weight of control mice ($p$ < 0.001) (**Figures 1D, E**). Further, we observed that the blood glucose and serum insulin levels were significantly elevated ($p$ < 0.001) in WD fed mice (**Figures 1F, G**).

## 3.2. Phloretin reduced pathological injury, hepatic fat deposition, fibrosis, blood glucose, and insulin resistance in WD fed mice

Treatment with phloretin substantially reduced the fat deposition in the liver while preserving normal hepatic architecture (**Figure 1B**). In comparison to the WD group, phloretin administration was observed to significantly ($p$ < 0.001) decrease the extent of degenerative alterations in the liver (**Figures 1B, C**). Administration of phloretin also lowered the fibrotic changes in the liver as compared to the WD group. Furthermore, as compared to the WD group, we observed a 40% reduction ($p$ < 0.001) in body weight gain of phloretin treated mice, however, no significant change was observed in weekly food intake (**Figures 1D, E**). Phloretin treatment also resulted in a significant ($p$ < 0.01, $p$ < 0.001, respectively) reduction in blood glucose and serum insulin levels thereby maintaining homeostasis model assessment-estimated insulin resistance (HOMA-IR) (**Figures 1F–H**).

## 3.3. Continuous exposure to WD resulted in dyslipidemia, overexpression of lipogenic marker genes, inflammation, and increased fecal endotoxin level as disease progresses

Western diet feeding resulted in dyslipidemia causing significant increase in serum triglycerides (TG) and cholesterol (TC) levels. Precisely, following 16 weeks of WD feeding, a ∼3-fold ($p$ < 0.001) increase in TG and ∼1.5-fold increase in both TC ($p$ < 0.01) and LDL-C ($p$ < 0.001) levels were observed (**Figures 2A–C**). Abnormal lipid metabolism is a defining feature of MAFLD, which is accompanied by alterations in the lipid metabolism pathway. Thus, we investigated the expression of genes encoding for fatty acid (FA) metabolism to govern the effect of phloretin on hepatic lipid metabolism. Our findings showed that the hepatic expression levels of lipogenic genes *SREBP-1c*, *ChREBP*, *CD36*, and *FASN* are elevated in response to WD, which contributes to *de novo* lipid synthesis (**Figure 2E**). In comparison to the control group, a 4.8-fold ($p$ < 0.001) and a 3.4-fold ($p$ < 0.001) elevation in the mRNA expression of *SREBP-1c* and *ChREBP* transcripts, respectively, as well as a 5.7-fold ($p$ < 0.001) increase in the FASN gene expression was detected in the liver of WD group mice. Apart from an increase in *SREBP-1c*, *ChREBP,* and

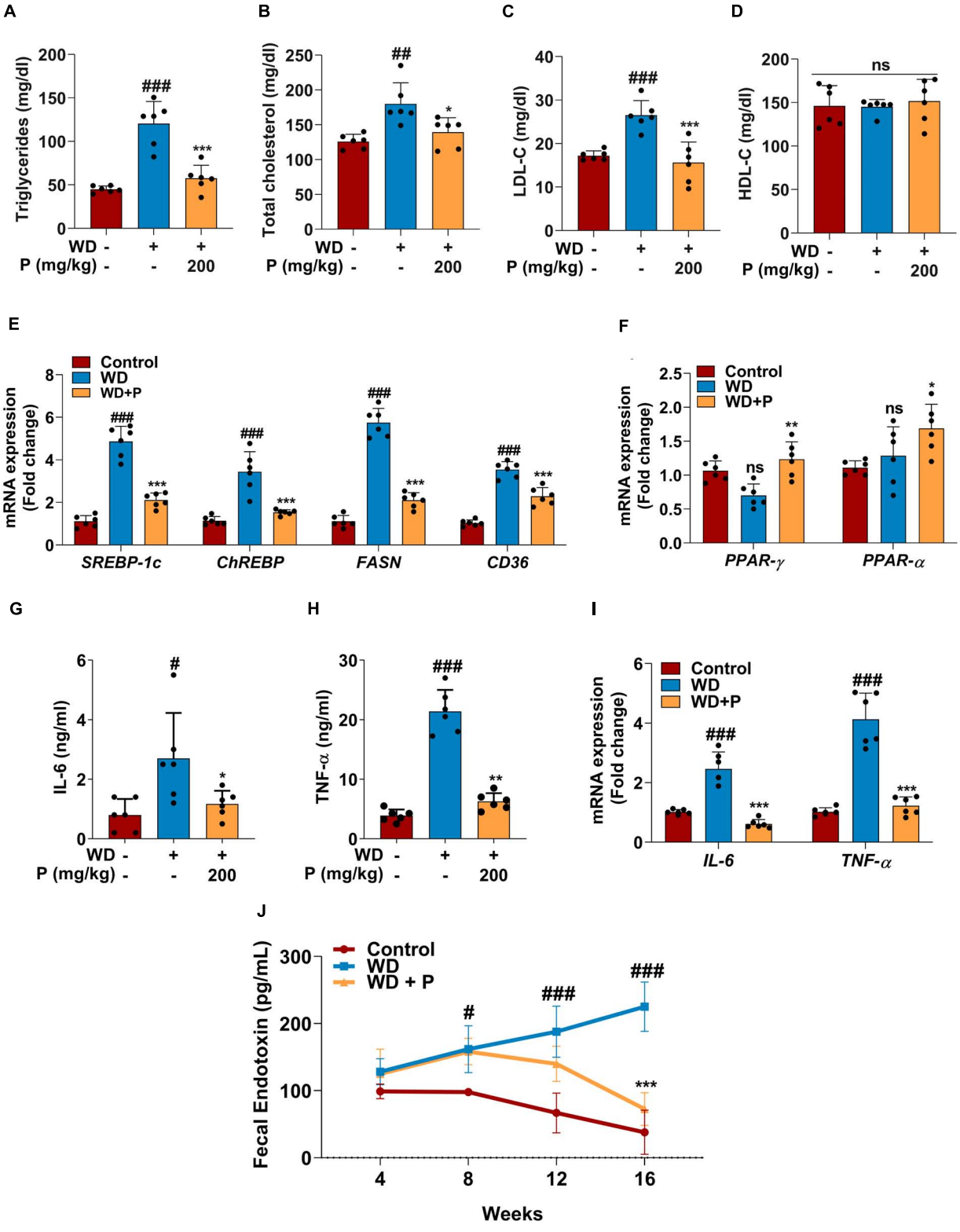


FIGURE 2
Phloretin maintained serum lipid profile, metabolic homeostasis and decreased the inflammatory markers in WD fed mice ($n$ = 6). Panels **(A–D)** denote the impact of phloretin on serum triglycerides, cholesterol, LDL-C, and HDL-C level, respectively. **(E)** Quantitative representation of the gene expression of *SREBP-1c*, *ChREBP*, *FASN*, and *CD36*, respectively in each group. **(F)** Quantitative representation of the gene expression of *PPAR-γ* and *PPAR-α*, respectively in each group. Panels **(G,H)** represent the serum concentrations of IL-6 and TNF-α level, respectively. **(I)** mRNA expression of *IL-6* and *TNF-α* in liver tissue from different groups. **(J)** Fecal endotoxin level in all group at different time points. The symbols "#," "##," "###" represent $p < 0.05$, $p < 0.01$, $p < 0.001$, respectively vs. control group; the symbols "*," "**," "***" represent $p < 0.05$, $p < 0.01$, $p < 0.001$, respectively vs. WD group; ns represents non-significant.

*FASN*, a 3.5-fold ($p < 0.001$) rise in the mRNA expression of *CD36* was also observed in WD fed mice. Further, in WD fed mice, the mRNA expression of *PPAR-γ* and *PPAR-α* showed a small but no significant alteration (Figure 2F).

Steatosis-induced inflammation plays a critical role in the progression of disease to more severe outcomes. Serum ELISA has been performed to evaluate the levels of inflammatory cytokine markers. Results revealed that exposure to WD augmented the circulating inflammatory cytokines viz. IL-6 (>3-fold; $p < 0.05$) and TNF-α (∼5-fold; $p < 0.001$) levels (Figures 2G, H). Further, the gene expression analysis revealed significant ($p < 0.001$; Figure 2I) elevation in *IL-6* and *TNF-α* expression after chronic exposure to WD. Additionally, Fecal endotoxin levels play critical role in assisting the inflammation and disease progression. The fecal endotoxin level was estimated in each group every fourth week. At week 4, a slightly elevated but not significant increase was observed in endotoxin level in feces of mice from WD and WD + P groups. However, continuous exposure to WD led to a substantial increase in the endotoxin release at 8th, 12th, and 16th week ($p < 0.05$, $p < 0.001$, $p < 0.001$, respectively) as compared to the control group (Figure 2J).

## 3.4. Phloretin improved abnormal lipid metabolism by modulating the expression of metabolism related genes

Phloretin treatment was found to improve lipid homeostasis and help in subverting the dyslipidemia in WD-fed mice. As illustrated in Figure 2, phloretin treatment of WD-fed mice prevented increase in TG ($p < 0.001$), TC ($p < 0.01$), and LDL-C ($p < 0.001$) levels (Figures 2A–C). However, no statistically significant difference was observed in the levels of HDL-C across all the groups (Figure 2D). Moreover, phloretin treatment reduced the expression of lipogenic marker genes. Importantly, we observed a 57 and 56% reduction ($p < 0.001$) in the expression of *SREBP-1c* and *ChREBP*, respectively on treatment with phloretin. Similarly, phloretin treatment resulted in a 2.7-fold ($p < 0.001$) and ∼1.6-fold ($p < 0.001$) downregulation of *FASN* and *CD36* genes, respectively (Figure 2E). Interestingly, phloretin supplement further upregulated the mRNA expression of *PPAR-γ* and *PPAR-α* by 1.7-fold ($p < 0.01$) and 1.3-fold ($p < 0.05$) respectively, facilitating hepatic FAs oxidation (Figure 2F).

## 3.5. Phloretin improved hepatic inflammation by mitigating inflammatory cytokines (IL-6 and TNF-α) levels and subverting the fecal endotoxin levels

On the contrary to the WD exposure, phloretin treatment significantly reduced the levels of inflammatory cytokine markets IL-6 and TNF-α their normal levels (Figures 2G, H). Phloretin, in instance, was found to cause a 2.3-fold ($p < 0.05$) and >3-fold ($p < 0.01$) decline in serum IL-6 and TNF-α levels, respectively. The gene expression of *IL-6* and *TNF-α* further demonstrated the ability of phloretin to diminish hepatic inflammation and consequently prevent the progression of NASH in mice ($p < 0.001$; Figure 2I). Furthermore, the endotoxin release initially increased in the feces of mice treated with phloretin, but prolonged exposure to phloretin decreased the endotoxin level to normal (Figure 2J). The result indicated the protective efficacy of phloretin against microbial toxic byproducts. These results suggested the potential of phloretin in mitigation of WD-induced imparities leading to MAFLD progression in mice.

## 3.6. Gut microbial diversity changes induced by prolonged exposure of WD and phloretin supplementation

To evaluate the role of gut-microbes in WD-induced disease progression and role of phloretin as counter strategies 16S rRNA sequencing and analysis of metagenome was performed. Post 16S rRNA sequencing, data was analyzed and microbial diversity was compared across the treatment groups at different time-points (Figure 3). Analysis of comparative microbial diversity and richness within groups at different time intervals revealed differences in diversity, as showed by the Shannon index and observed ASVs ($p < 0.05$). Significant differences were observed in diversity among WD groups versus control group, stratified across time points, prominent change was observed after 8 weeks (Figure 3A). Phloretin treatment reversed these changes at week 4, 8, and 12 but not at week 16. However, phloretin treatment maintained the overall diversity index similar to the control group (Figure 3B). Furthermore, there was a statistically significant difference ($p < 0.05$) in taxonomic richness between control and WD fed groups at week 8, 12, and 16. However, significant change in the richness ($p < 0.05$) between the WD and WD + P groups was observed only at week 12 (Figure 3C). Phloretin did not effectively alter the microbial richness at each time point; however, it managed to reverse the overall richness (Figure 3D). Overall, these results indicated that phloretin treatment resists WD induced changes in microbial diversity and richness in mice and indicates its prophylactic effects to maintain the diversity similar to healthy control group. Detailed Shannon and Simpson indices and observed ASVs of individual samples were given in Supplementary Table 2.

## 3.7. Long-term phloretin administration restored the microbial community structure that had been disrupted by WD feeding

Distance matrices suggest that WD fed mice exhibited distant diversity as compared to control and phloretin treatment group, which was comparatively less distant to the control group (Figure 3E). Additionally, separate comparative PCoA analysis at each time point exhibited a prominent difference in microbial diversity of WD as compared to control and WD + P (PERMANOVA $r^2$ ranging between 0.57 and 0.65) (Figure 3F). Results indicate that Bray–Curtis distance was higher between WD and control group across the timeline. On the other hand,

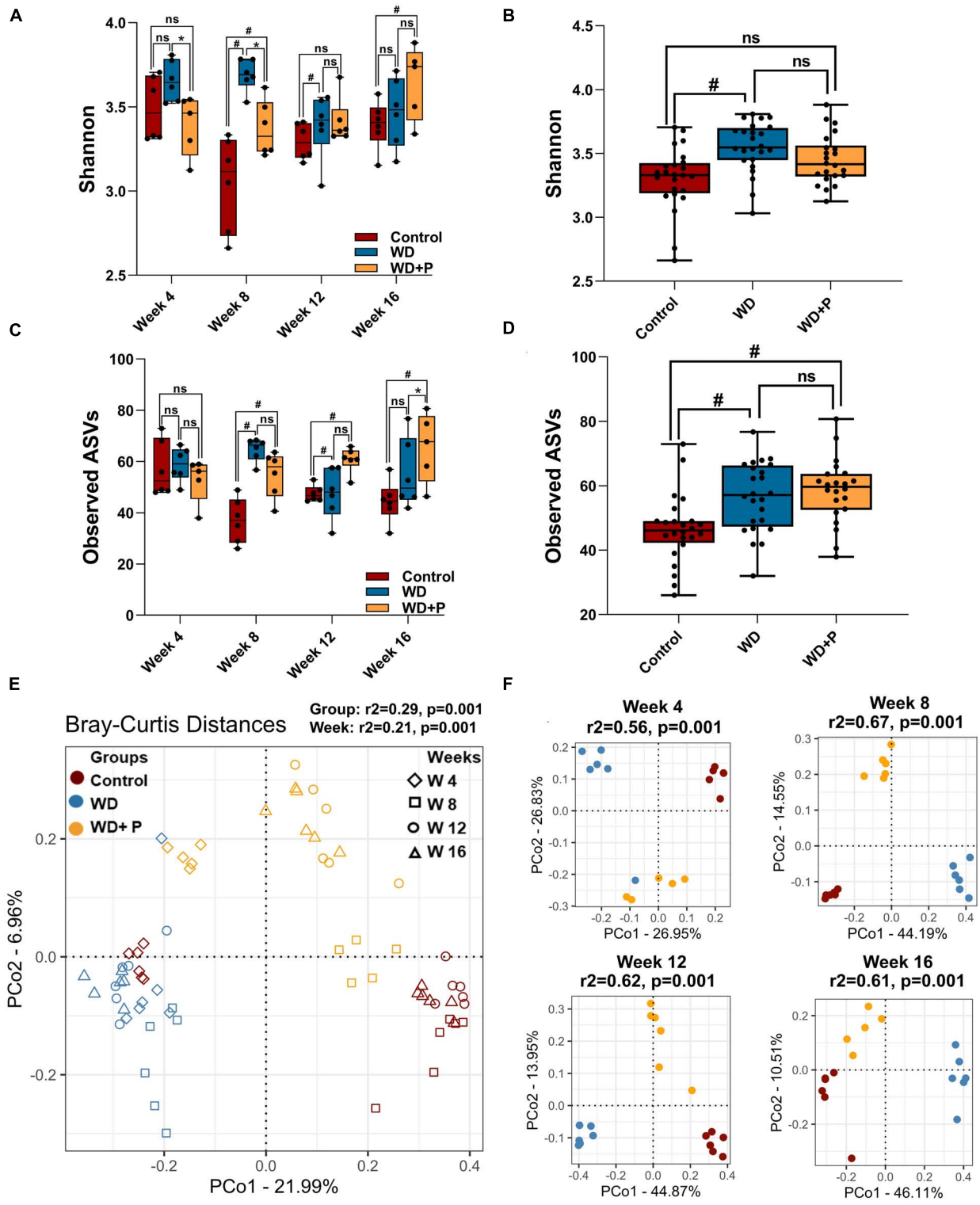


FIGURE 3
Microbial alpha and beta diversity was observed across different experimental groups ($n$ = 6). **(A)** Microbial diversity among different treatment groups across four time points, **(B)** overall diversity across different treatment independent of time **(C)** taxa richness among different treatment groups across four time points, **(D)** overall richness across different treatment independent of time. The symbol "#" represents $p < 0.05$ vs. control group and the symbol "*" represents $p < 0.05$ vs. western diet (WD) group according to Kruskal–Wallis test; ns represents non-significant. All the alpha diversity measures along with the metadata information are provided in the Supplementary Table 2. **(E,F)** PCoA analysis was performed on Bray–Curtis distances calculated on relative abundance of each species. **(E)** All experimental groups at different time points were considered. This shows the strong differences due to diet (PERMANOVA, $r^2$ = 0.29) as compared to the timepoints (PERMANOVA, $r^2$ = 0.21) and **(F)** differences between experimental groups at each time point such as week 4 (top left), week 8 (top right), week 12 (bottom left), and week 16 (bottom right) were observed. Strong differences (PERMANOVA, $r^2$ = 0.56–0.67) were observed among the treatment groups at each time point.

the diversity of the phloretin treatment group was comparatively less distant to control group. These outcomes substantiated that phloretin treatment restores the changes in microbial community composition.

## 3.8. Chronic WD exposure and phloretin supplementation both affected the dynamics of gut microbiota abundance and distribution

In order to evaluate the phylogenetic comparison of microbial communities, taxonomic signatures were identified in each experimental group at different timepoints. Relative abundance of different phylum and mean relative abundance of top 20 bacterial families were observed (**Figure 4**). After fourth week, relative abundance of *Firmicutes* was decreased and *Desulfobacterota* increased in the WD group as compared to control. In phloretin treatment group, no such observation was recorded for *Desulfobacterota*. In the eighth week, increase in *Campilobacterota* and decreased abundance of *Desulfobacterota* was observed in the phloretin treatment group similar to control but not in the WD group. After 12th week, *Campilobacterota* had largely decreased abundance in WD group as compared to the control and phloretin treatment groups. In 16th week, abundance of *Firmicutes* was decreased in the WD and phloretin treated groups as compared to the control. Large increase in abundance of *Desulfobacterota* was observed in the WD group, which was negligible in control and phloretin treated groups comparatively. Cumulatively, with increase in time abundance of *Campilobacterota* was increased and *Desulfobacterota* was decreased in the phloretin treatment group similar to control but dissimilar to the WD fed mice. Additionally, *Cyanobacteria* was found to be more abundant in control and phloretin treated mice as compared to control. Interestingly, abundance of *Proteobacteria* was found to be increased with time in the control group but decreased in the WD and phloretin treatment group (**Figure 4A**).

To delve deeper, mean relative abundance of top 20 bacterial families were analyzed. Abundance of *Muribaculaceae, Tannerellaceae, Desulfovibrionaceae,* and *Lachnospiraceae,* were increased in WD fed mice in comparison to control and phloretin treatment groups. Similarly, *Anaerovoraceae, Peptostreptococcaceae,* and *Erysipelotrichaceae* were least abundant or absent in the control group as compared to WD and phloretin treatment group. *Ruminococcaceae* was less abundant whereas *Selenomonadaceae* was completely absent in WD fed mice as compared to control group. Interestingly, abundance of *Helicobacteraceae* was more abundant in control as compared to the other groups. Although, it is highly unlikely that WDs with comparable nutrients would lead to decrease in *Helicobacteraceae* abundance observed in our study, but it is still a potential limitation of the present study. Finally, decreased abundance of *Lactobacillaceae* was observed after WD intake, which improves with the phloretin treatment (**Figure 4B** and **Supplementary Figure 1**). At the same time, pathogenic anaerobes like *Peptostreptococcaceae* were also found abundant in the WD fed group, which was least abundant or absent in the control group. The phloretin treatment group witnessed less abundance of these bacterial families and increased abundance of non-pathogenic *Lactobacillaceae* family (**Figure 4B** and **Supplementary Figure 1**). We also checked for the relative abundance of ASVs that had >1% occurrence and was plotted to observe the strain level difference amongst samples. The *Bacteroides-5* genus was observed to be more prevalent in WD group as compared to the control and phloretin treated groups, with an increase in dominance occurring over time. In comparison, ASVs belonging to the species *Bacteroides vulgatus* remained more dominant in the both control and phloretin treated group. **Supplementary Figure 2** illustrates the dynamic of the gut bacterial population among the groups over a period of 16 weeks and demonstrate the diet and treatment induced variations in taxa. Taxonomic signature analysis upholds the role of WD in alteration of microbial diversity dynamics and phloretin was found to restore these changes.

## 3.9. Heatmap signature revealed that phloretin reversed the ASVs-specific changes in gut microbiota occurred during progression of disease

Variance Partition analysis was performed to assess differentially abundant taxa in all experimental groups using diet pattern and time as independent variables. The diet pattern appeared to attribute more fraction of the variance as compared to time (weeks) (**Supplementary Table 3**). Heatmap signature of selected taxa (with a variable fraction value >0.25 of diet pattern) revealed the changes in abundance of observed ASVs at family, genus and species level across the treatment groups (**Figure 4C**). Hierarchical clustering heatmap revealed association of the selected taxa with the progression of MAFLD and phloretin treatment. On a larger extent, ASVs belonging to the genus *Blautia, Terrisporobacter, Alloprevotella, Muribaculaceae, Eubacterium, Clostridium, Parabacteroides, Allobaculum, Odoribacter*, and family *Desulfovibrionaceae, Paludibacteraceae*, was highly abundant in WD fed mice indicating a positive association with the progression of MAFLD. These taxa have been shown less abundant in control and WD + P groups, which suggests negative correlation with phloretin treatment. Interestingly, *Lactobacillus johnsonii* species were also abundant in the WD group. In contrast, several ASVs belonging to genus *Lactobacillus, Quinella, Prevotellaceae, Alloprevotella-1, Odoribacter-1, Bacteroides-1,* and species *B. vulgatus* and *Bacteroides caecimuris-1* showed negative association with WD intake and they started restoring to their normal abundance status in phloretin treatment group. Additionally, taxa from genus *Ruminococcus, Eubacterium coppostanoligenes 1, Hungatella, Bacteroides-5* and some species like *Bacteroides nordii*, and *Bacteroides uniformis* was highly abundant in WD + P group and was less abundant in both control and WD groups. Interestingly, *Bacteroides thetaiotaomicron* was also found abundant in WD + P group in the early phase but was least abundant in later phases of phloretin treatment. Findings indicates strong positive association of these taxa with phloretin treatment. These associations strongly suggests that WD intake changes the gut microbiota with progression of MAFLD and phloretin treatment not only reversed these changes but also modulated some other important taxa signatures.

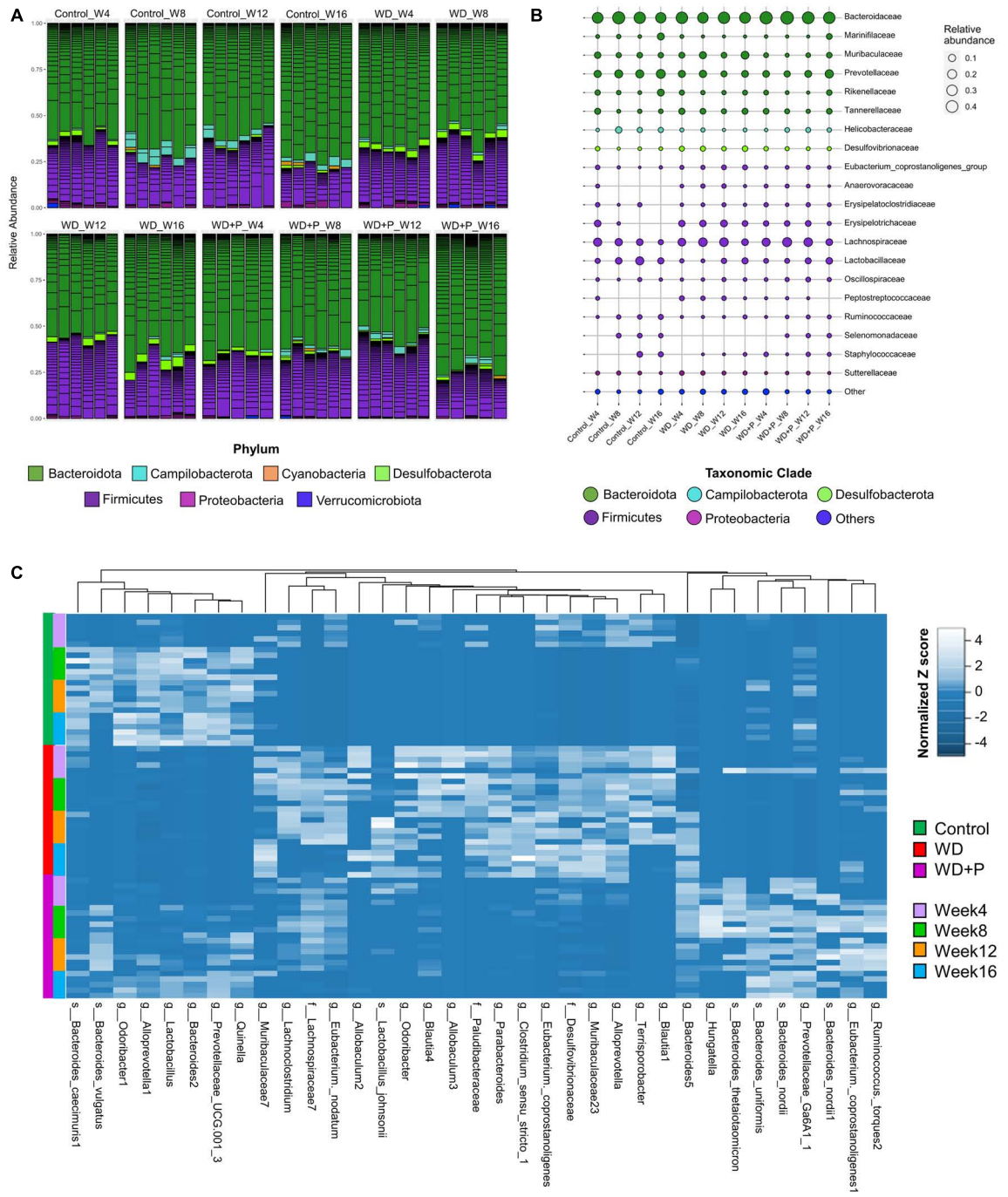


FIGURE 4
Taxonomic signatures of selected taxa identified in each experimental group ($n$ = 6). **(A)** Relative abundance of different bacterial phylum was observed, **(B)** mean relative abundance of top 20 bacterial families were observed, and **(C)** the abundance of selected ASVs using Variance Partition was shown using heatmap signatures, which demonstrated a disparity in their abundance in different group at each time point.

## 3.10. Differential bacterial abundance depicted the protective effect of phloretin against MAFLD associated gut dysbiosis

To delve deeper into the disease associated changes of microbial taxa signatures, cumulative relative abundance of taxonomic markers and distribution of selected taxonomic markers in ordination plot for each experimental group was evaluated. Taxonomic signatures were identified using ISA. Top 10 bacterial taxa (at families, genera and species level) were selected for each experimental group based on significant discrimination across groups ($p$-value) and their prevalence within the group (the maximum IndVal scores) (**Supplementary Table 4** and **Figure 5**). Clear demarcation between cumulative relative abundance (sum of relative abundances of all 10 representative

taxa) was observed across the experimental groups. Results indicate that highly abundant (>35 at week 16) signature marker taxa for control group (belonging to the genus *Lactobacillus, Alloprevotella-1, Bacteroides-2, Prevotellaceae, Odoribacter-1, Alistipes-8,* and *Quinella)* was relatively least abundant in the WD group (<8 at week 16) and was found to be restored after phloretin treatment (>15 at week 16), relative abundance at the start of the study was <10 in all the experimental groups (**Figure 5A**). Similarly, results suggested relatively high abundance of signature taxa of WD group (belonging to the family *Desulfovibrionaceae, Paludibacteraceae* and genus *Clostridium, Parabacteroides, Muribaculaceae, Odoribacter, Alloprevotella,* and species *L. johnsonii*) was present (>20 at week 16) as compared to the relative abundance of these taxa in control and WD + P group (<5 at week 16) (**Figure 5B**). Moreover, relative abundance of marker taxa of WD + P group (belonging to family *Lachnospiraceae-7,* genus *Prevotellaceae, Hungatella, Bacteroides,* and species *B. nordii, B. uniformis, Ruminococcus torques 1 and 2)* was decreased with time in WD + P and control groups (>25 at week 8 and <20 at week 16 for WD + P and >5 at week and <5 at week 16 in control) as compared to the WD group, where a time-dependent increment was observed (<10 at week 4 and >15 at week 16) (**Figure 5C**).

Distribution of selected taxonomic markers in ordination plot was done using PCoA analysis (**Figure 5D**). Colored ordination plots clearly indicate the higher abundance of ASVs from *Parabacteroides* and *Paludibacteraceae* in the WD group as compared to the control and WD + P groups (**Figures 5G, H**). Additionally, ASVs from *Lactobacillus, Alloprevotella* were highly abundant in control group and relatively more abundant in the WD + P group as compared to the WD group (**Figures 5E, F**). *B. nordii* was more abundant in the WD + P group as compared to the WD and control groups and *B. uniformis* was also found to be highly abundant in the WD + P group and week 12 and 16 of control groups as compared to the WD group (**Figures 5I, J**). It is important to note that all of these observations were largely time dependent, indicating a clear role of phloretin in reversing the effect of gut dysbiosis associated changes in microbial diversity in MAFLD. The samples from each group were then analyzed to create a Spearman's rank correlation matrix. The selected taxa from each group were used to calculate the distance matrix by Euclidean method. At the end of the fourth week, there was negligible distance between samples indicating all the group sharing similar microbial environment. Furthermore, in the 8th, 12th, and 16th weeks, the control and WD + P groups formed comparable clusters, whereas the WD group formed a distinct cluster (**Supplementary Figure 3**). The results indicated that the samples in WD group were more distant from the samples in the control and WD + P groups.

## 3.11. Prolonged exposure to WD caused loss of neighborhood connectivity among gut bacterial species

In order to examine the association between taxa in different groups, a co-occurrence network plot was created with all strong ($r > 0.5$) significant correlations ($p < 0.05$), and only those taxa were picked up that were positively associated to each other in each group. The neighborhood connectivity was found higher in the control group as compared to the WD and WD + P group. In particular, ASVs belonging to genus *Odoribacter-1* was found highly connected with other ASVs from genus *Lactobacillus, Alloprevotella-1, Bacteroides-2, Prevotellaceae, Alistipes-8, Quinella,* and species *Ruminococcus flavefaciens* with *r* value of 1 (**Figure 6A**). However, absence of *Odoribacter-1* and *R. flavefaciens* in the co-occurrence network of WD and WD + P groups lead to a decrease in neighborhood connectivity. Further, network density of taxa belonging to genus *Blautia-3, Bacteroides-5, Muribaculaceae-25,* and *Muribaculaceae-18* was also higher in the control group with network strength of <1. In contrast, in the WD group the neighborhood connectivity was dense only with taxa of genus *Bacteroides-5, Clostridium_sensu_stricto-1,* and species *Lactobacillus murinus, L. johnsonii* with *r* value of <1 (**Figure 6B**). However, the neighborhood connectivity was less frequent in the WD + P group as compared to control group but the correlation strength was higher in both control and WD + P group as compared to WD group indicating strong connectivity among bacterial species (**Figure 6C**). All of these observations indicated loss of neighborhood connectivity as well as network strength among species during the progression of MAFLD. However, phloretin treatment was ineffective in restoring connection, but it did maintain the strength of the network among species.

## 3.12. Functional prediction of gut bacteriome in response to WD and phloretin treatment

Western diet and phloretin supplementation both have been shown to affect the composition of the gut microbiota, and has potential to cause alterations in bacterial metabolic processes. KEGG pathway signatures were identified in whole microbiome and ISA was performed as a statistical test to determine significantly discriminating metabolic pathways in each group at different time points. A subset of level 3 metabolic pathways that are substantially linked with the course of MAFLD and have a statistically significant ($p < 0.05$) alteration was chosen for each experimental group. WD supplementation resulted in time-dependent enrichment in some of the lipid metabolism pathways, i.e., primary and secondary bile acid biosynthesis, FA elongation in mitochondria, biosynthesis of unsaturated FAs, and glycerophospholipid metabolism. Phloretin supplementation, on the other hand, has been shown to deplete these pathways (**Figure 7A**). Taking carbohydrate metabolism into account, fructose and mannose metabolism and tricarboxylic acid (TCA) cycle pathways were more abundant in the representative genomes of the taxa possessing a positive association with WD group. In contrast, their abundance appears to be decreased in the phloretin treatment group as compared to WD group. However, galactose metabolism, inositol phosphate metabolism and ascorbate and aldarate metabolism pathways were significantly upregulated by phloretin treatment as compared to WD group (**Figure 7B**). Vitamin metabolism pathways were also altered in the WD group with time dependent depletion of vitamin B6 and retinol metabolism pathways occurring simultaneously with enrichment of thiamin, biotin, and riboflavin metabolism and the induction of folate biosynthesis. However, it has been demonstrated that

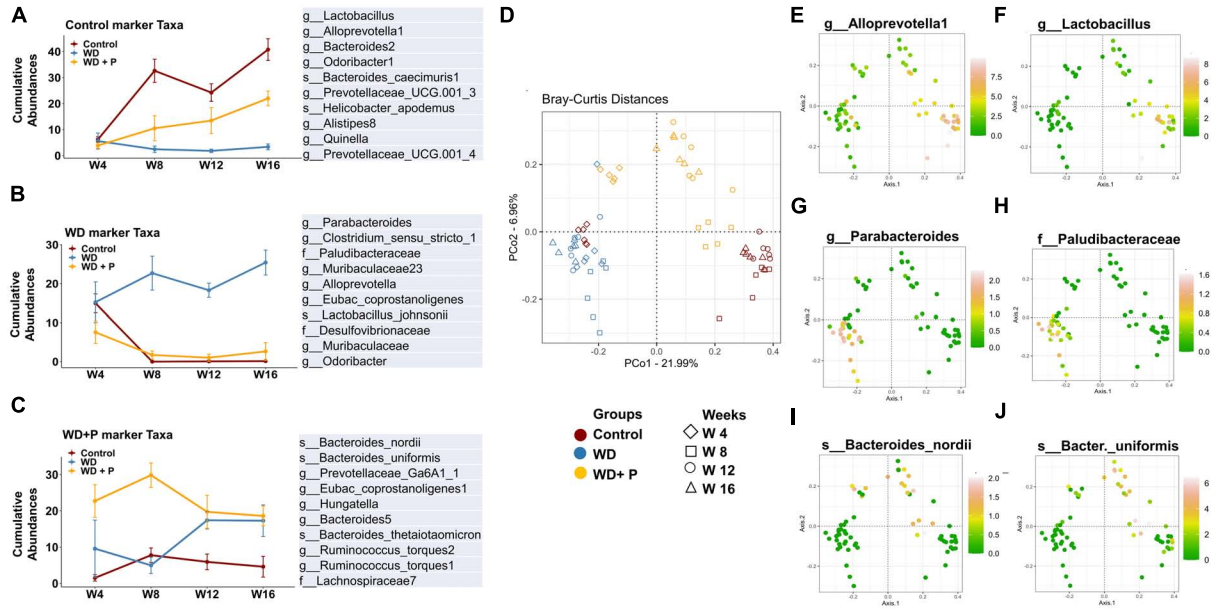


FIGURE 5
Cumulative relative abundance of taxonomic markers of each experimental group ($n$ = 6). Taxonomic signatures were identified using indicator species analysis. Top 10 bacterial species were selected for each experimental group based on the maximum IndVal scores. **(A)** Marker taxa of control group, **(B)** marker taxa of WD group, and **(C)** marker taxa of WD + P. **(D)** Distribution of samples from different experimental group in ordination plot. **(E–J)** Bray–Curtis distances PCoA ordination colored by the relative abundance of selected taxonomic markers of each experimental group. **(E,F)** Distribution of selected taxonomic markers from control group. **(G,F)** Distribution of selected taxonomic markers from WD group. **(I,J)** Distribution of selected taxonomic markers from WD + P group.

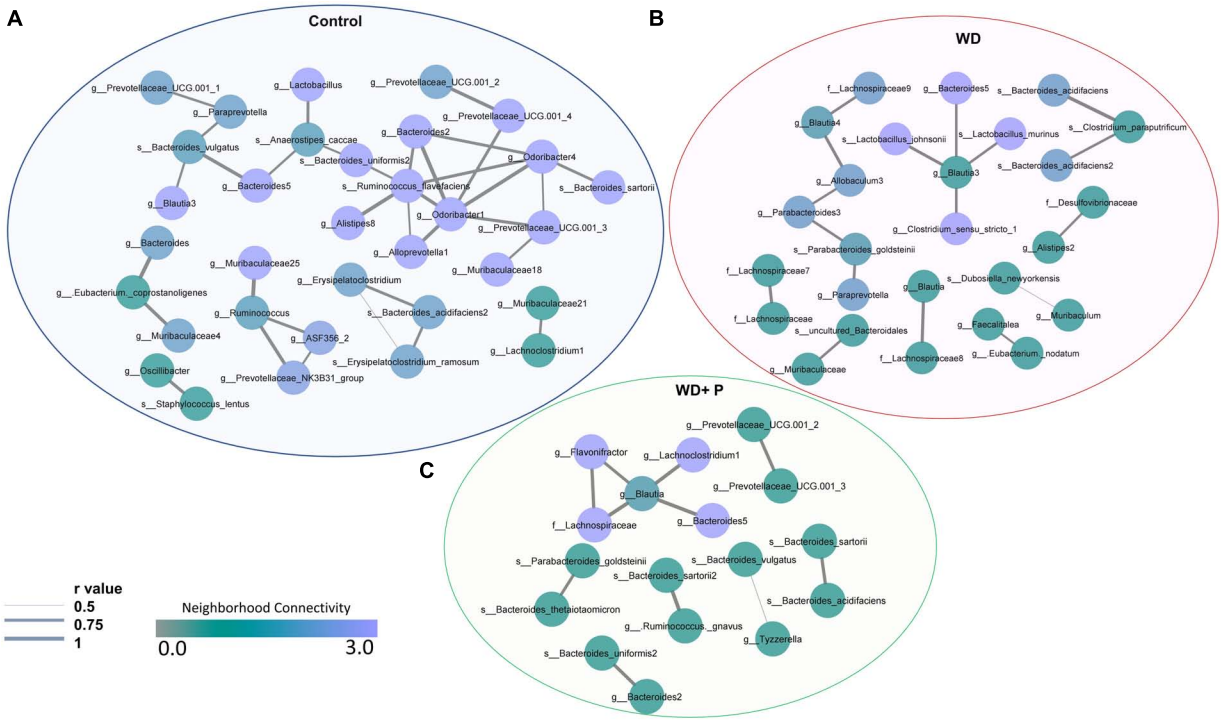


FIGURE 6
Co-occurrence network analysis using compositionally corrected correlations among different bacterial species ($n$ = 6). Network plot generated using the correlation of taxa **(A)** control diet samples, **(B)** WD samples, and **(C)** WD + P diet samples. Nodes represent each bacterial species whereas the thickness of edge represents the correlation strength ($r$ value from 0.5 to 1). Color of the node shows how dense the network is based on the neighborhood connectivity.

phloretin supplementation can help to reverse these alterations (**Figure 7C**). Amino acids metabolism pathways (excluding D arginine and D ornithine metabolism) were highly enriched in the representative genome from the WD group but less abundant in both control and WD + P groups (**Figure 7D**). WD group also showed enrichment with pathways involved in lipopolysaccharide biosynthesis at week fourth but depleted with time, as shown by related taxa in glycan biosynthesis and metabolism pathways. However, phloretin supplementation inhibited these pathways as the time progressed further (**Figure 7E**). Phloretin also facilitates drugs and xenobiotic metabolism by cytochrome P450 pathways in WD fed mice (**Figure 7F**). Moreover, the heatmap signature demonstrated the abundance of these marker pathways in each sample from each group during time intervals varying from 4th to 16th week (**Figure 7G**). Since these findings were merely correlations, we can only speculate that altered metabolic pathways were to account for the MAFLD phenotype; nevertheless, more research in this area is required.

## 4. Discussion

Metabolic dysfunction-associated fatty liver disease is becoming increasingly prevalent globally, representing challenge in terms of prevention and treatment. Recent investigation indicated that high fat/calorie rich diet contributed to the development of hepatic steatosis, which progressed to the even more severe NASH following continuous exposure to the diet (Kořínková et al., 2020). Moreover, the consumption of a high-fat/calorie-rich western-style diet causes remodeling of gut microbiota and metabolic dysfunction, which ultimately leads to the advancement of MAFLD or NAFLD (Bakhshimoghaddam and Alizadeh, 2021). However, it would be interesting to understand the dynamic of gut flora as the disease progresses. In light of this fact, the present study demonstrated the longitudinal changes in the gut microbial community as a result of WD feeding along the time course. Moreover, nutraceuticals of natural origin and traditional medicines have recently renewed interest as treatment alternatives in the pharmaceutical industries due to their therapeutic efficacy and fewer side effects. Phloretin is a phenolic dihydrochalcone, found in the apple and has been demonstrated to help prevent diabetes, oxidative injury, and obesity by preserving metabolic homeostasis (Alsanea et al., 2017; Nithiya and Udayakumar, 2017; Shen et al., 2020). Recent report highlighted that intraperitoneally injected phloretin can improve the symptoms of hepatic steatosis caused due to high-fat diet in mice (Liou et al., 2020) although, it would be intriguing to see if its effect on MAFLD is attributed to the remodeling of the gut flora when administered orally.

Findings of the study suggested that mice subjected to WD for an extended period exhibited a broad range of metabolic and histological alterations typical with NASH, including extensive lipid accumulation in the liver, ballooning of hepatocytes, and steatohepatitic foci (Godoy-Matos et al., 2020). However, the treatment of phloretin for 16 weeks was found to be effective in reversing pathological changes in the liver as well as decreasing hepatic lipid accumulation and fibrosis progression (**Figure 1B**). Insulin resistance is a critical factor in the pathogenesis of NAFLD (Armandi and Schattenberg, 2021). It has been shown previously that prolonged feeding of WD results in rise of fasting blood glucose, serum insulin, increased insulin resistance and other metabolic dysfunctions which ultimately leads to the development of NASH (Choi et al., 2017). Adding support to this, our findings revealed a substantial increase in levels of blood glucose and serum insulin after 16 weeks of WD exposure, indicating the development of insulin resistance. Importantly, phloretin restored the blood glucose and serum insulin levels and maintained the HOMA-IR in WD-fed mice (**Figures 1F–H**). Increase in circulating glucose and insulin levels associated with insulin resistance have been reported to stimulate *de novo* lipogenesis through the transcriptional regulation of *ChREBP* and *SREBP-1*, respectively (Lee et al., 2021a). The lipogenic marker *SREBP-1c* and its target gene *FASN* found to be upregulated in response to a western style diet, contributing to hepatic *de novo* lipogenesis (Li et al., 2016). Similarly, FA translocase, also known as CD36, is a protein that orchestrates a critical role in enhancing uptake of FAs in hepatocytes as well as some other cell types in the liver, and has been implicated in the advancement of hepatic steatosis (Fu et al., 2021). Phloretin downregulated the mRNA expression of *ChREBP*, *SREBP-1c*, *FAS,* and *CD36* indicating its ability to reduce hepatic *de novo* lipogenesis. Phloretin further contributed to the preservation of metabolic homeostasis by elevating the expression of *PPAR-α* and *PPAR-γ*. Phloretin also maintained the normal lipid profile indicating its protective effect against the dyslipidemia associated with MAFLD (**Figures 2A–D**). These findings were further corroborated by Liou et al. (2020) in which phloretin administration was reported to alleviate hepatic steatosis as well as dyslipidemia in mice fed with high-fat diet (Liou et al., 2020). Hepatic lipid buildup causes oxidative stress and the release of proinflammatory cytokines, which culminates in steatohepatitis (Hendrikx and Binder, 2020). Increased concentrations of circulatory pro-inflammatory cytokines viz. IL-6 and TNF-α were documented in the patient with NASH (Bocsan et al., 2017). According to the findings of the current investigation, WD feeding increased the levels of circulating inflammatory cytokines IL-6 and TNF-α as well as their hepatic gene expression, which was effectively reversed by the administration of phloretin (**Figures 2E–G**), indicating protective response of phloretin against hepatic inflammation. Furthermore, diet-induced gut dysbiosis changed nutritional absorption in the intestine as well as compromised intestinal permeability. This dysregulation increased the supply of nutrients, endotoxins, and microbial metabolites to the liver, resulting in increased hepatic fat deposition as well as increased inflammation (Jiang et al., 2020). It has recently been reported that the intake of WD for an extended period increases the level of endotoxin in the feces of mice (Lee et al., 2020b). Our findings revealed a time-dependent increase in the endotoxin levels in the feces of mice following prolonged exposure to a WD; however, phloretin supplementation could reversed these changes indicating its potential to influence the gut flora.

Recent investigations have established the link between gut dysbiosis and associated changes in microbial signatures and pathogenesis of NAFLD (Safari and Gérard, 2019; Astbury et al., 2020; Lee et al., 2020a; Li et al., 2021). However, very little emphasis was provided to study the time dependent changes in gut microbiota. Next generation sequencing and analysis of comparative microbial diversity and richness revealed significant

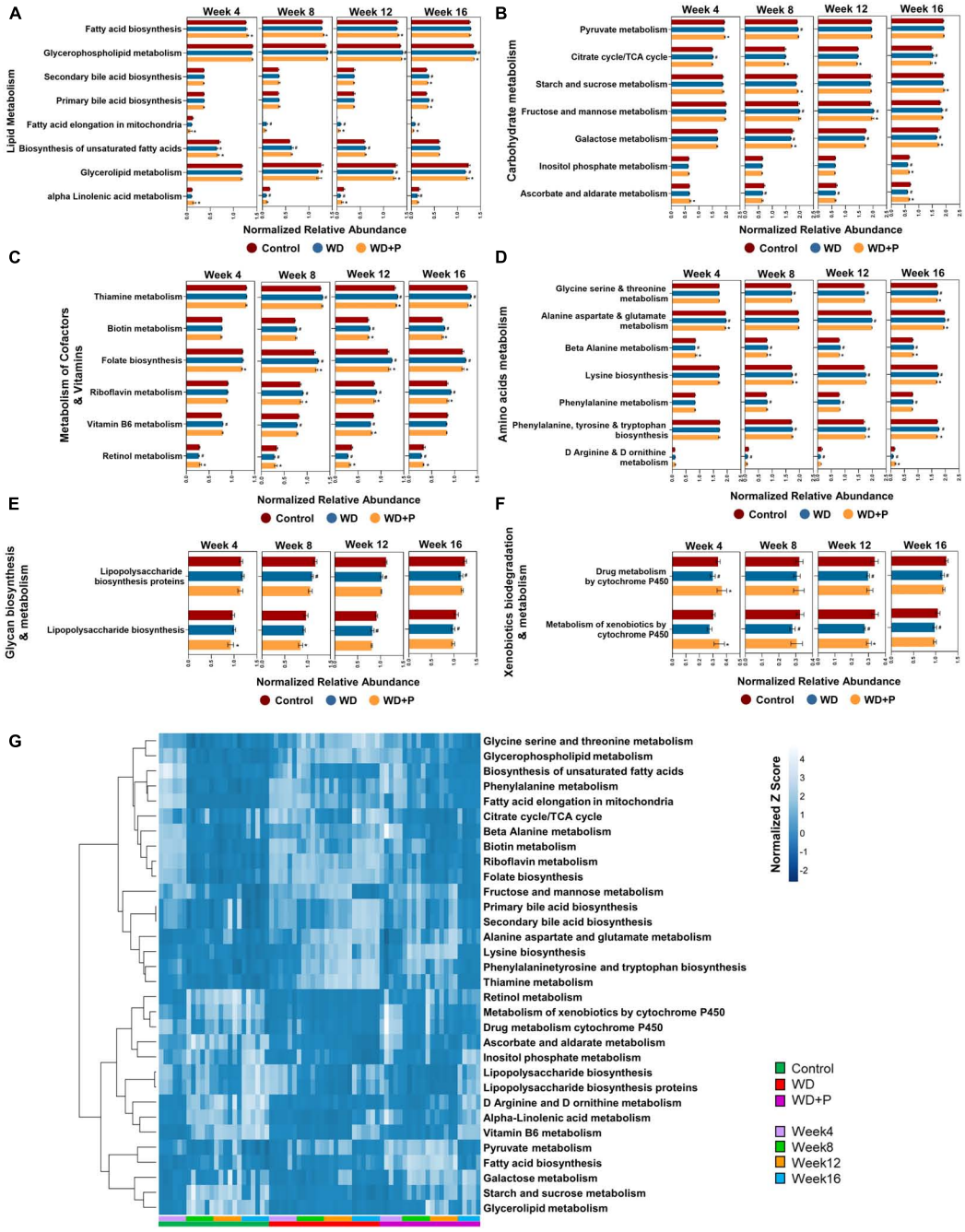


FIGURE 7
Functional prediction of gut bacteriome in response to WD and phloretin treatment ($n$ = 6). Normalized relative abundance of **(A)** lipid metabolism pathways, **(B)** carbohydrate metabolism pathways, **(C)** vitamin metabolism pathways, **(D)** amino acids metabolism pathways, **(E)** glycan biosynthesis and metabolism pathways, **(F)** xenobiotics biodegradation and metabolism pathways in each experimental group. **(G)** Heatmap signature of relative abundance of KEGG metabolism pathway in each group. The symbol "#" represents $p < 0.05$ vs. control group; the symbol "*" represents $p < 0.05$, vs. WD group.

changes in WD fed mice as compared to control. Despite minor differences in the phloretin treatment group over time, it has maintained the overall diversity index similar to the control group (Figure 3). The findings indicate that the WD has the potential to impact the diversity of gut microbes and might influence the progression of MAFLD by reducing the abundance of advantageous bacteria, while increasing the occurrence of detrimental bacteria linked to a higher risk of MAFLD. The results further surmises the role of phloretin treatment in resisting WD induced changes in microbial diversity and outlined its prophylactic effects.

To delve deeper into dynamics of gut microbiota abundance and distribution, taxonomic signatures were identified among groups. We observed that with increase in time, abundance of *Desulfobacterota* was decreased in the phloretin treatment group similar to control but dissimilar to the WD fed mice (Figure 4A). Prior investigations have revealed an increased abundance of

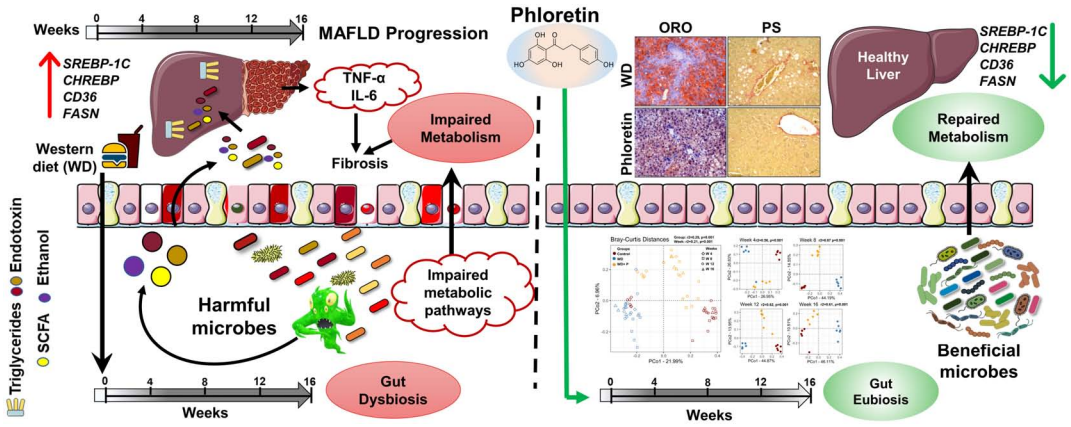


FIGURE 8
Graphical summary of the work.

*Desulfobacterota* in NAFLD (Bashiardes et al., 2016; Li et al., 2019) and also implicated in the activation of systemic inflammation (Shi et al., 2021). Increased abundance of *Desulfobacterota* in the WD group can be attributed to high fat diet mediated elevation in endotoxin levels and associated changes in inflammatory markers. Additionally, mean relative abundance of the top 20 families (**Figure 4B**) revealed an increased in *Muribaculaceae, Tannerellaceae, Desulfovibrionaceae,* and *Lachnospiraceae,* in the WD group similar to the earlier reports (Shen et al., 2017; Li et al., 2019; Hullar et al., 2021). Increased abundance of these obligate anaerobes responsible for production of toxic byproducts and ethanol indicate the ability of WD to induce gut dysbiosis. Moreover, similar to prior finding linking *Peptostreptococcus* to NASH in morbidly obese individuals (Sookoian et al., 2020), our findings revealed higher abundance of *Peptostreptococcus* in MAFLD mice. The family *Ruminococcaceae* and *Lactobacillaceae* was found to be substantially more abundant in the control and phloretin treated groups than in the WD group. The family *Ruminococcaceae* were shown to be more abundant in healthy individuals than in people with NAFLD, and their abundance decreased as the severity of fibrosis worsened (Jiang et al., 2015; Lee et al., 2020a). The importance of phloretin in reversing WD-induced alterations in microbial communities at the phylum and family levels was demonstrated by these findings.

Further, IndVal analysis of taxa (at family, genus and species level) across the treatment groups revealed an increase in the abundance of *Blautia, Terrisporobacter, Alloprevotella, Eubacterium, Clostridium_sensu_stricto, Parabacteroides, Allobaculum,* and *Paludibacetraceae* in WD fed mice indicating a positive association with the progression of MAFLD (**Figure 4C**). *Blautia* is associated with visceral fat accumulation and found highly abundant in NAFLD and/or NASH conditions including pediatric NAFLD (Safari and Gérard, 2019; Aron-Wisnewsky et al., 2020). Some of these taxa have previously been associated with hepatic damage, characterized by elevated transaminase levels, steatosis, lobular inflammation, and ballooning (Milton-laskibar et al., 2021). Increased abundance of these taxa in WD group is in correlation with the altered pathophysiology, disturbed homeostasis and aberrant lipid metabolism (**Figures 1**, **2**). Additionally, High abundance of anaerobic pathogenic taxa like *Terrisporobacter, Clostridium,* and *Peptostreptococcaceae* in WD groups clearly indicate the ability of WD induced gut dysbiosis to promote the growth of pathogenic microbes in MAFLD condition. Low abundance of these taxa in control and phloretin treated groups indicated that phloretin treatment might have a deleterious impact on their populations. Furthermore, in WD + P group, restored high abundance for *Lactobacillus, Prevotellaceae, Alloprevotella-1, Odoribacter-1, Ruminococcus,* and *Bacteroides-1* was observed, which was lost in WD group. Earlier studies have demonstrated a decrease in the abundance of family *Prevotellaceae* and genus *Lactobacillus*, *Odoribacter* in patients as well as in high fat diet-induced NAFLD (Boursier et al., 2016; Astbury et al., 2020; Pan et al., 2020; Milton-laskibar et al., 2021). Moreover, supplementation with *Lactobacillus* (*Lactobacillus acidophilus, Lactobacillus fermentum,* and *Lactobacillus plantarum*) lowers the progression of non-alcoholic steatosis in mice fed on WD (Lee et al., 2021b). However, genetic heterogeneity between strains at the genomic level can potentially have an impact on the disease state (Yan et al., 2020). According to our findings, different strains of the genus *Odoribacter, Alloprevotella,* and *Lactobacillus* have both favorable and detrimental effects on the pathophysiology of MAFLD (**Figure 5**). Along with it, *B. thetaiotaomicron*, a common component of gut microflora and an opportunistic pathogen was found in high abundance in WD + P group in fourth week, possibly due to the effect of WD challenge and attain low abundance with the progress of treatment in week 16. Further analysis of community co-occurrence and functional potential associated with these taxa support the microbial abundance observations. *R. flavefaciens* and *Odoribacter* both have been found to be beneficial against NAFLD (Iwao et al., 2020; Pan et al., 2021). These two taxa played a crucial role in maintaining community structure by increasing neighborhood connectivity; their absence in the co-occurrence network plot, on the other hand, resulted in a decrease in neighborhood connection (**Figure 6**). Previous studies have well reported that *Ruminococcaceae* is less abundant in the patients with progressive NAFLD than in healthy controls and serves as a major component of the microbiota in healthy individuals by preserving the homeostasis of the gut milieu (Qin et al., 2014; Lee et al., 2020a; Tsai et al., 2020). Furthermore, *Ruminococcaceae* family has been shown to effectively alter the microbial composition

of NAFLD toward a healthy gut microbiome through microbial interactions (Wu et al., 2020). These findings suggested that they could be used as strong probiotic supplement to help repair the structure of the gut microbial population in patients with NAFLD. Additionally, shift in gut bacterial diversity results in an alteration in the functional profile of bacterial communities as well. The WD group was highly enriched of taxa associated with FA biosynthesis and elongation, which could aggravate the MAFLD condition by promoting both hepatic lipid accumulation and inflammation (Kessler et al., 2014). In addition, long-term WD consumption led to an increase in bile acid biosynthesis pathways, which have been linked to MAFLD in the past (Mouzaki et al., 2016). TCA cycle pathways remained more dominant in WD group. Diet-induced hepatic insulin resistance and fatty liver have been attributed to an elevated TCA cycle (Satapati et al., 2012). Furthermore, WD caused disruption in retinol metabolism pathway which plays a critical role MAFLD progression (Saeed et al., 2021). Along with it, dysregulation of amino acid metabolism pathways has been linked to insulin resistance and altered liver metabolism in patients with liver fibrosis (Hasegawa et al., 2020). Our findings are consistent with previous study indicating that the majority of KEGG pathways associated with NASH and fibrosis patients were involved in the metabolism of carbohydrate, lipid, and amino acids (Boursier et al., 2016). Cytochrome P450 enzymes, found primarily in the liver, are responsible for the metabolism of potentially hazardous substances such as medications, xenobiotics, FAs, and bilirubin (Esteves et al., 2021). Pathways associated with Cytochrome P450 activity were also suppressed by long-term WD feeding. Nevertheless, WD-induced alterations in these metabolic pathways were prevented by phloretin supplementation (**Figure 7**). Observed high abundance of beneficial microbes and low abundance of pathogenic taxa is a characteristic of healthy gut, which is clearly visible in control and the phloretin treated group. These findings clearly indicate that WD intake alters the gut microbiota, leading to the accumulation of harmful pathogenic microbes with altered metabolic functions, which ultimately resulted in MAFLD progression. Phloretin treatment not only reversed this gut dysbiosis but also favored taxonomic signatures of beneficial microbes thereby slowing course of the disease in the long run. Furthermore, fecal microbiota transplantation (FMT), a method for altering the host microbiome and reversing gut microbiota dysbiosis toward eubiosis, is also widely used these days (Xue et al., 2022). The FMT from mice that had been given phloretin showed a positive effect on pre-clinical ulcerative colitis through modifying the gut microbial community (Wu et al., 2019). These findings strongly suggest that phloretin may have a therapeutic impact on MAFLD through altering the gut microbiota composition.

## 5. Conclusion

In summary (**Figure 8**), prolonged consumption of WD affects the alpha and beta diversity of gut microbiota as disease progresses. Further, WD feeding resulted in the accumulation of detrimental pathogenic microorganisms which exacerbate the disease pathology by increasing the toxic byproduct, e.g., endotoxin. The impact of genomic variation on pathogenicity, as well as their significance in the course of MAFLD, were also demonstrated by our findings. Phloretin administration, on the other hand, ameliorated WD induced liver steatosis, inflammation, fibrosis, and insulin resistance in mice by reshaping the microbial community composition and suppressing endotoxin release in a time-dependent manner. These findings substantiated the application of phloretin as a dietary intervention approach and as a functional food with favorable prebiotic and eubiotic effects against MAFLD. Additionally, findings of this study open doors for new interventional studies utilizing FMT to probe the uses and effects of phloretin and certain beneficial bacteria as symbiotic, either alone or in combination for the better management of the MAFLD.

## Data availability statement

The datasets presented in this study can be found in online repositories. The names of the repository/repositories and accession number(s) can be found below: https://www.ncbi.nlm.nih.gov/, PRJNA791189.

## Ethics statement

The animal study was approved by the Animal Ethical Committee (IAEC) of CSIR-IHBT, India. The study was conducted in accordance with the local legislation and institutional requirements.

## Author contributions

JC and YP conceptualized the study. JC and PA performed the major bench experiments, collection, analysis, and interpretation of the dataset, and writing of the manuscript. PM processed the NGS raw sequence data and performed *in silico* analysis. MS helped in the library preparation. VP performed the histopathology analysis. RP performed the MiSeq 16S rRNA sequencing and analysis, study-coordination, and writing of the manuscript. RP and YP edited the final version of the manuscript. All authors approved the final version of the manuscript.

## Funding

The Council of Scientific and Industrial Research (CSIR) of India funded this research through project ID MLP0204 and MLP0155.

## Acknowledgments

The authors gratefully acknowledges Director, CSIR-IHBT, Palampur, India for their encouragement and support. The authors

further express their gratitude to ChemBioIT Private Limited for facilitating the 16S rRNA analysis. JC is thankful to CSIR for providing fellowship. PA is thankful to Department of Science and Technology, India for providing DST-INSPIRE fellowship. JC and PA gratefully acknowledge AcSIR, India for Ph.D. registration. CSIR-IHBT communication number for this manuscript is 5009.

## Conflict of interest

The authors declare that the research was conducted in the absence of any commercial or financial relationships that could be construed as a potential conflict of interest.

## Publisher's note



## Supplementary material

The Supplementary Material for this article can be found online at: https://www.frontiersin.org/articles/10.3389/fmicb.2023.1210517/full#supplementary-material

## References

Alsanea, S., Gao, M., and Liu, D. (2017). Phloretin prevents high-fat diet-induced obesity and improves metabolic homeostasis. *AAPS J.* 19, 797–805. doi: 10.1208/S12248-017-0053-0

Armandi, A., and Schattenberg, J. M. (2021). Beyond the paradigm of weight loss in non-alcoholic fatty liver disease: From pathophysiology to novel dietary approaches. *Nutrients* 13:1977. doi: 10.3390/NU13061977

Aron-Wisnewsky, J., Vigliotti, C., Witjes, J., Le, P., Holleboom, A. G., Verheij, J., et al. (2020). Gut microbiota and human NAFLD: Disentangling microbial signatures from metabolic disorders. *Nat. Rev. Gastroenterol. Hepatol.* 17, 279–297. doi: 10.1038/S41575-020-0269-9

Astbury, S., Atallah, E., Vijay, A., Aithal, G. P., Grove, J. I., and Valdes, A. M. (2020). Lower gut microbiome diversity and higher abundance of proinflammatory genus Collinsella are associated with biopsy-proven nonalcoholic steatohepatitis. *Gut Microbes* 11, 569–580. doi: 10.1080/19490976.2019.1681861

Bakhshimoghaddam, F., and Alizadeh, M. (2021). Contribution of gut microbiota to nonalcoholic fatty liver disease: Pathways of mechanisms. *Clin. Nutr. ESPEN* 44, 61–68. doi: 10.1016/j.clnesp.2021.05.012

Bashiardes, S., Shapiro, H., Rozin, S., Shibolet, O., and Elinav, E. (2016). Non-alcoholic fatty liver and the gut microbiota. *Mol. Metab.* 5, 782–794. doi: 10.1016/j.molmet.2016.06.003

Beane, K. E., Redding, M. C., Wang, X., Pan, J. H., Le, B., Cicalo, C., et al. (2021). Effects of dietary fibers, micronutrients, and phytonutrients on gut microbiome: A review. *Appl. Biol. Chem.* 64, 1–18. doi: 10.1186/S13765-021-00605-6

Bocsan, I. C., Milaciu, M. V., Pop, R. M., Vesa, S. C., Ciumarnean, L., Matei, D. M., et al. (2017). Cytokines genotype-phenotype correlation in nonalcoholic steatohepatitis. *Oxid. Med. Cell. Longev.* 2017:4297206. doi: 10.1155/2017/4297206

Boursier, J., Mueller, O., Barret, M., Machado, M., Fizanne, L., Araujo-Perez, F., et al. (2016). The severity of NAFLD is associated with gut dysbiosis and shift in the metabolic function of the gut microbiota. *Hepatology* 63:764. doi: 10.1002/HEP.28356

Callahan, B. J., McMurdie, P. J., Rosen, M. J., Han, A. W., Johnson, A. J. A., and Holmes, S. P. (2016). DADA2: High-resolution sample inference from Illumina amplicon data. *Nat. Methods* 13, 581–583. doi: 10.1038/nmeth.3869

Caporaso, J. G., Kuczynski, J., Stombaugh, J., Bittinger, K., Bushman, F. D., Costello, E. K., et al. (2010). QIIME allows analysis of high-throughput community sequencing data. *Nat. Methods* 7, 335–336. doi: 10.1038/nmeth.f.303

Carrera-Quintanar, L., Roa, R. I. L., Quintero-Fabián, S., Sánchez-Sánchez, M. A., Vizmanos, B., and Ortuño-Sahagún, D. (2018). Phytochemicals that influence gut microbiota as prophylactics and for the treatment of obesity and inflammatory diseases. *Mediators Inflamm.* 2018:9734845. doi: 10.1155/2018/9734845

Chhimwal, J., Goel, A., Sukapaka, M., Patial, V., and Padwad, Y. (2022). Phloretin mitigates oxidative injury, inflammation, and fibrogenic responses via restoration of autophagic flux in in vitro and preclinical models of NAFLD. *J. Nutr. Biochem.* 107:109062. doi: 10.1016/j.jnutbio.2022.109062

Chhimwal, J., Patial, V., and Padwad, Y. (2021). Beverages and Non-alcoholic fatty liver disease (NAFLD): Think before you drink. *Clin. Nutr.* 40, 2508–2519. doi: 10.1016/j.clnu.2021.04.011

Chhimwal, J., Sharma, S., Kulurkar, P., and Patial, V. (2020). Crocin attenuates CCl 4-induced liver fibrosis via PPAR-γ mediated modulation of inflammation and fibrogenesis in rats. *Hum. Exp. Toxicol.* 39, 1639–1649. doi: 10.1177/0960327120937048

Choi, S. H., Leem, J., Park, S., Lee, C. K., Park, K. G., and Lee, I. K. (2017). Gemigliptin ameliorates western-diet-induced metabolic syndrome in mice. *Can. J. Physiol. Pharmacol.* 95, 129–139. doi: 10.1139/CJPP-2016-0026

Davis, C. D. (2016). The gut microbiome and its role in obesity. *Nutr. Today* 51:167. doi: 10.1097/NT.0000000000000167

De Muynck, K., Vanderborght, B., Van Vlierberghe, H., and Devisscher, L. (2021). The gut–liver axis in chronic liver disease: A macrophage perspective. *Cells* 10:2959. doi: 10.3390/cells10112959

Esteves, F., Rueff, J., and Kranendonk, M. (2021). The central role of cytochrome p450 in xenobiotic metabolism—a brief review on a fascinating enzyme family. *J. Xenobiotics* 11:94. doi: 10.3390/JOX11030007

Fan, Y., and Pedersen, O. (2021). Gut microbiota in human metabolic health and disease. *Nat. Rev. Microbiol.* 19, 55–71. doi: 10.1038/s41579-020-0433-9

Fu, Q., North, P. E., Ke, X., Huang, Y. W., Fritz, K. A., Majnik, A. V., et al. (2021). Adverse maternal environment and postweaning western diet alter hepatic CD36 expression and methylation concurrently with nonalcoholic fatty liver disease in mouse offspring. *J. Nutr.* 151:3102. doi: 10.1093/JN/NXAB249

Godoy-Matos, A. F., Silva Júnior, W. S., and Valerio, C. M. (2020). NAFLD as a continuum: From obesity to metabolic syndrome and diabetes. *Diabetol. Metab. Syndr.* 12, 1–20. doi: 10.1186/S13098-020-00570-Y/TABLES/5

Hasegawa, T., Iino, C., Endo, T., Mikami, K., Kimura, M., Sawada, N., et al. (2020). Changed amino acids in NAFLD and liver fibrosis: A large cross-sectional study without influence of insulin resistance. *Nutrients* 12:1450. doi: 10.3390/NU12051450

Hendrikx, T., and Binder, C. J. (2020). Oxidation-specific epitopes in non-alcoholic fatty liver disease. *Front. Endocrinol.* 11:941. doi: 10.3389/FENDO.2020.607011/BIBTEX

Hoffman, G. E., and Schadt, E. E. (2016). variancePartition: Interpreting drivers of variation in complex gene expression studies. *BMC Bioinformatics* 17:438. doi: 10.1186/S12859-016-1323-Z/FIGURES/5

Hullar, M. A. J., Jenkins, I. C., Randolph, T. W., Curtis, K. R., Monroe, K. R., Ernst, T., et al. (2021). Associations of the gut microbiome with hepatic adiposity in the multiethnic cohort adiposity phenotype study. *Gut Microbes* 13:1965463. doi: 10.1080/19490976.2021.1965463

Ismaiel, A., and Dumitraşcu, D. L. (2019). Cardiovascular risk in fatty liver disease: The liver-heart axis—literature review. *Front. Med.* 6:202. doi: 10.3389/fmed.2019.00202

Iwao, M., Gotoh, K., Arakawa, M., Endo, M., Honda, K., Seike, M., et al. (2020). Supplementation of branched-chain amino acids decreases fat accumulation in the liver through intestinal microbiota-mediated production of acetic acid. *Sci. Rep.* 10:18768. doi: 10.1038/S41598-020-75542-3

Ji, Y., Yin, Y., Li, Z., and Zhang, W. (2019). Gut microbiota-derived components and metabolites in the progression of non-alcoholic fatty liver disease (NAFLD). *Nutrients* 11:1712. doi: 10.3390/nu11081712

Jiang, W., Wu, N., Wang, X., Chi, Y., Zhang, Y., Qiu, X., et al. (2015). Dysbiosis gut microbiota associated with inflammation and impaired mucosal immune function

in intestine of humans with non-alcoholic fatty liver disease. *Sci. Rep.* 5:8096. doi: 10.1038/SREP08096

Jiang, X., Zheng, J., Zhang, S., Wang, B., Wu, C., and Guo, X. (2020). Advances in the involvement of gut microbiota in pathophysiology of NAFLD. *Front. Med.* 7:361. doi: 10.3389/FMED.2020.00361/BIBTEX

Kanehisa, M., and Goto, S. (2000). KEGG: Kyoto encyclopedia of genes and genomes. *Nucleic Acids Res.* 28, 27–30. doi: 10.1093/NAR/28.1.27

Kessler, S. M., Simon, Y., Gemperlein, K., Gianmoena, K., Cadenas, C., Zimmer, V., et al. (2014). Fatty acid elongation in non-alcoholic steatohepatitis and hepatocellular carcinoma. *Int. J. Mol. Sci.* 15:5762. doi: 10.3390/IJMS15045762

Kořínková, L., Pražienková, V., Černá, L., Karnošová, A., Železná, B., Kuneš, J., et al. (2020). Pathophysiology of NAFLD and NASH in experimental models: The role of food intake regulating peptides. *Front. Endocrinol.* 11:916. doi: 10.3389/FENDO.2020.597583/BIBTEX

Langille, M. G. I., Zaneveld, J., Caporaso, J. G., McDonald, D., Knights, D., Reyes, J. A., et al. (2013). Predictive functional profiling of microbial communities using 16S rRNA marker gene sequences. *Nat. Biotechnol.* 31, 814–821. doi: 10.1038/nbt.2676

Lee, G., You, H. J., Bajaj, J. S., Joo, S. K., Yu, J., Park, S., et al. (2020a). Distinct signatures of gut microbiome and metabolites associated with significant fibrosis in non-obese NAFLD. *Nat. Commun.* 11, 1–13. doi: 10.1038/s41467-020-18754-5

Lee, N. Y., Yoon, S. J., Han, D. H., Gupta, H., Youn, G. S., Shin, M. J., et al. (2020b). Lactobacillus and Pediococcus ameliorate progression of non-alcoholic fatty liver disease through modulation of the gut microbiome. *Gut Microbes* 11, 882–899. doi: 10.1080/19490976.2020.1712984

Lee, H., Bin, Do, M. H., Jhun, H., Ha, S. K., Song, H. S., et al. (2021a). Amelioration of hepatic steatosis in mice through *Bacteroides* uniformis CBA7346-mediated regulation of high-fat diet-induced insulin resistance and lipogenesis. *Nutrients* 13:2989. doi: 10.3390/NU13092989

Lee, N. Y., Shin, M. J., Youn, G. S., Yoon, S. J., Choi, Y. R., Kim, H. S., et al. (2021b). Lactobacillus attenuates progression of nonalcoholic fatty liver disease by lowering cholesterol and steatosis. *Clin. Mol. Hepatol.* 27:110. doi: 10.3350/CMH.2020.0125

Li, F., Ye, J., Shao, C., and Zhong, B. (2021). Compositional alterations of gut microbiota in nonalcoholic fatty liver disease patients: A systematic review and Meta-analysis. *Lipids Health Dis.* 20, 1–12. doi: 10.1186/S12944-021-01440-W/FIGURES/4

Li, J., Chanda, D., Van Gorp, P. J., Jeurissen, M. L. J., Houben, T., Walenbergh, S. M. A., et al. (2016). Macrophage stimulating protein enhances hepatic inflammation in a NASH model. *PLoS One* 11:e0163843. doi: 10.1371/JOURNAL.PONE.0163843

Li, Y., Li, J., Su, Q., and Liu, Y. (2019). Sinapine reduces non-alcoholic fatty liver disease in mice by modulating the composition of the gut microbiota. *Food Funct.* 10, 3637–3649. doi: 10.1039/C9FO00195F

Liou, C. J., Wu, S. J., Shen, S. C., Chen, L. C., Chen, Y. L., and Huang, W. C. (2020). Phloretin ameliorates hepatic steatosis through regulation of lipogenesis and Sirt1/AMPK signaling in obese mice. *Cell Biosci.* 10:114. doi: 10.1186/s13578-020-00477-1

Martin, M. (2011). Cutadapt removes adapter sequences from high-throughput sequencing reads. *EMBnet.journal* 17, 10–12. doi: 10.14806/EJ.17.1.200

Milton-laskibar, I., Marcos-Zambrano, L. J., Gómez-Zorita, S., Fernández-Quintela, A., de Santa Pau, E. C., Martínez, J. A., et al. (2021). Gut microbiota induced by pterostilbene and resveratrol in high-fat-high-fructose fed rats: Putative role in steatohepatitis onset. *Nutrients* 13:1738. doi: 10.3390/NU13051738

Mitra, S., De, A., and Chowdhury, A. (2020). Epidemiology of non-alcoholic and alcoholic fatty liver diseases. *Transl. Gastroenterol. Hepatol.* 5:16. doi: 10.21037/TGH.2019.09.08

Mouzaki, M., Wang, A. Y., Bandsma, R., Comelli, E. M., Arendt, B. M., Zhang, L., et al. (2016). Bile acids and dysbiosis in non-alcoholic fatty liver disease. *PLoS One* 11:e0151829. doi: 10.1371/JOURNAL.PONE.0151829

Nithiya, T., and Udayakumar, R. (2017). Protective effect of phloretin on hyperglycemia mediated oxidative stress in experimental diabetic rats. *Integr. Food Nutr. Metab.* 5:1000204. doi: 10.15761/ifnm.1000204

Pan, X., Kaminga, A. C., Liu, A., Wen, S. W., Luo, M., and Luo, J. (2021). Gut microbiota, glucose, lipid, and water-electrolyte metabolism in children with nonalcoholic fatty liver disease. *Front. Cell. Infect. Microbiol.* 11:1. doi: 10.3389/FCIMB.2021.683743/FULL

Pan, X., Wen, S. W., Kaminga, A. C., and Liu, A. (2020). Gut metabolites and inflammation factors in non-alcoholic fatty liver disease: A systematic review and meta-analysis. *Sci. Rep.* 10, 1–11. doi: 10.1038/s41598-020-65051-8

Paradis, E., and Schliep, K. (2019). ape 5.0: An environment for modern phylogenetics and evolutionary analyses in R. *Bioinformatics* 35, 526–528. doi: 10.1093/BIOINFORMATICS/BTY633

Qin, N., Yang, F., Li, A., Prifti, E., Chen, Y., Shao, L., et al. (2014). Alterations of the human gut microbiome in liver cirrhosis. *Nature* 513, 59–64. doi: 10.1038/nature13568

Quast, C., Pruesse, E., Yilmaz, P., Gerken, J., Schweer, T., Yarza, P., et al. (2013). The SILVA ribosomal RNA gene database project: Improved data processing and web-based tools. *Nucleic Acids Res.* 41, D590–D596. doi: 10.1093/NAR/GKS1219

Quesada-Vázquez, S., Aragonès, G., Del Bas, J. M., and Escoté, X. (2020). Diet, gut microbiota and non-alcoholic fatty liver disease: Three parts of the same axis. *Cells* 9:176. doi: 10.3390/CELLS9010176

Roberts, D. W., David, M., and Roberts, W. (2019). *Package "labdsv" Title Ordination and Multivariate Analysis for Ecology*. San Francisco, CA: Scribd, Inc.

Romualdo, G. R., Valente, L. C., Sprocatti, A. C., Bacil, G. P., de Souza, I. P., Rodrigues, J., et al. (2022). Western diet–induced mouse model of non-alcoholic fatty liver disease associated with metabolic outcomes: Features of gut microbiome-liver-adipose tissue axis. *Nutrition* 10:111836. doi: 10.1016/J.NUT.2022.111836

Saeed, A., Bartuzi, P., Heegsma, J., Dekker, D., Kloosterhuis, N., de Bruin, A., et al. (2021). Impaired hepatic vitamin A metabolism in NAFLD mice leading to vitamin A accumulation in hepatocytes. *Cell. Mol. Gastroenterol. Hepatol.* 11, 309–325.e3. doi: 10.1016/J.JCMGH.2020.07.006

Safari, Z., and Gérard, P. (2019). The links between the gut microbiome and non-alcoholic fatty liver disease (NAFLD). *Cell. Mol. Life Sci.* 76, 1541–1558. doi: 10.1007/S00018-019-03011-W

Satapati, S., Sunny, N. E., Kucejova, B., Fu, X., He, T. T., Méndez-Lucas, A., et al. (2012). Elevated TCA cycle function in the pathology of diet-induced hepatic insulin resistance and fatty liver. *J. Lipid Res.* 53, 1080–1092. doi: 10.1194/JLR.M023382

Schwager, E., Bielski, C., and George, W. (2019). *ccrepe: Ccrepe_and_nc.score, R package version 1.18.1*. Santo Domingo: Bioconductor.

Shannon, P., Markiel, A., Ozier, O., Baliga, N. S., Wang, J. T., Ramage, D., et al. (2003). Cytoscape: A software environment for integrated models of biomolecular interaction networks. *Genome Res.* 13, 2498–2504. doi: 10.1101/GR.1239303

Shen, F., Zheng, R. D., Sun, X. Q., Ding, W. J., Wang, X. Y., and Fan, J. G. (2017). Gut microbiota dysbiosis in patients with non-alcoholic fatty liver disease. *Hepatobiliary Pancreat. Dis. Int.* 16, 375–381. doi: 10.1016/S1499-3872(17)60019-5

Shen, X., Wang, L., Zhou, N., Gai, S., Liu, X., and Zhang, S. (2020). Beneficial effects of combination therapy of phloretin and metformin in streptozotocin-induced diabetic rats and improved insulin sensitivity: In vitro. *Food Funct.* 11, 392–403. doi: 10.1039/c9fo01326a

Shi, Y., Zou, Y., Xiong, Y., Zhang, S., Song, M., An, X., et al. (2021). Host gasdermin D restrains systemic endotoxemia by capturing *Proteobacteria* in the colon of high-fat diet-feeding mice. *Gut Microbes* 13:1946369. doi: 10.1080/19490976.2021.1946369

Sookoian, S., Salatino, A., Castaño, G. O., Landa, M. S., Fijalkowky, C., Garaycoechea, M., et al. (2020). Intrahepatic bacterial metataxonomic signature in non-alcoholic fatty liver disease. *Gut* 69, 1483–1491. doi: 10.1136/gutjnl-2019-318811

Tsai, M. C., Liu, Y. Y., Lin, C. C., Wang, C. C., Wu, Y. J., Yong, C. C., et al. (2020). Gut microbiota dysbiosis in patients with biopsy-proven nonalcoholic fatty liver disease: A cross-sectional study in Taiwan. *Nutrients* 12:820. doi: 10.3390/nu12030820

Wu, D., Jiao, N., Zhu, R., Zhang, Y., Gao, W., Fang, S., et al. (2020). Identification of the keystone species in non-alcoholic fatty liver disease by causal inference and dynamic intervention modeling. *bioRxiv* [Preprint]. doi: 10.1101/2020.08.06.240655

Wu, M., Li, P., An, Y., Ren, J., Yan, D., Cui, J., et al. (2019). Phloretin ameliorates dextran sulfate sodium-induced ulcerative colitis in mice by regulating the gut microbiota. *Pharmacol. Res.* 150:104489. doi: 10.1016/j.phrs.2019.104489

Xue, L., Deng, Z., Luo, W., He, X., and Chen, Y. (2022). Effect of fecal microbiota transplantation on non-alcoholic fatty liver disease: A randomized clinical trial. *Front. Cell Infect. Microbiol.* 12:759306. doi: 10.3389/fcimb.2022.759306

Yan, Y., Nguyen, L. H., Franzosa, E. A., and Huttenhower, C. (2020). Strain-level epidemiology of microbial communities and the human microbiome. *Genome Med.* 12:71. doi: 10.1186/S13073-020-00765-Y

Yang, M., Qi, X., Li, N., Kaifi, J. T., Chen, S., Wheeler, A. A., et al. (2023). Western diet contributes to the pathogenesis of non-alcoholic steatohepatitis in male mice via remodeling gut microbiota and increasing production of 2-oleoylglycerol. *Nat. Commun.* 14, 1–17. doi: 10.1038/s41467-023-35861-1

frontiers | Frontiers in Microbiology

TYPE Original Research
PUBLISHED 25 September 2023
DOI 10.3389/fmicb.2023.1269123



OPEN ACCESS

EDITED BY
Rebeca Martín,
INRAE Centre Jouy-en-Josas, France

REVIEWED BY
Leticia Abecia,
University of the Basque Country, Spain
Samara Paula Mattiello,
University of Tennessee Southern, United States

*CORRESPONDENCE
Yun Ma
✉ mayun@nxu.edu.cn
Yansheng Guo
✉ guoyansheng1978@163.com

RECEIVED 29 July 2023
ACCEPTED 31 August 2023
PUBLISHED 25 September 2023

CITATION
Mao Y, Wang F, Kong W, Wang R, Liu X, Ding H, Ma Y and Guo Y (2023) Dynamic changes of rumen bacteria and their fermentative ability in high-producing dairy cows during the late perinatal period. *Front. Microbiol.* 14:1269123. doi: 10.3389/fmicb.2023.1269123



# Dynamic changes of rumen bacteria and their fermentative ability in high-producing dairy cows during the late perinatal period

Yongxia Mao[1,2], Feifei Wang[1,2], Weiyi Kong[1,2], Ruiling Wang[1,2], Xin Liu[1,2], Hui Ding[1,2], Yun Ma[1,2]* and Yansheng Guo[1,2]*

[1]College of Animal Science and Technology, Ningxia University, Yinchuan, China, [2]Key Laboratory of Ruminant Molecular and Cellular Breeding of Ningxia Hui Autonomous Region, College of Animal Science and Technology, Ningxia University, Yinchuan, China

**Background:** High-producing dairy cows face varying degrees of metabolic stress and challenges during the late perinatal period, resulting in ruminal bacteria abundance and their fermentative ability occurring as a series of changes. However, the dynamic changes are still not clear.

**Aims/methods:** Ten healthy, high-producing Holstein dairy cows with similar body conditions and the same parity were selected, and ruminal fluid from the dairy cows at postpartum 0, 7, 14, and 21 d was collected before morning feeding. 16S rRNA high-throughput sequencing, GC-MS/MS targeted metabolomics, and UPLC-MS/MS untargeted metabolomics were applied in the study to investigate the dynamic changes within 21 d postpartum.

**Results:** The results displayed that the structures of ruminal bacteria were significantly altered from 0 to 7 d postpartum ($R = 0.486$, $P = 0.002$), reflecting the significantly declining abundances of Euryarchaeota and Chloroflexi phyla and *Christensenellaceae*, *Methanobrevibacter,* and *Flexilinea* genera ($P < 0.05$) and the obviously ascending abundances of *Ruminococcaceae*, *Moryella*, *Pseudobutyrivibrio,* and *Prevotellaceae* genera at 7 d postpartum ($P < 0.05$). The structures of ruminal bacteria also varied significantly from 7 to 14 d postpartum ($R = 0.125$, $P = 0.022$), reflecting the reducing abundances of *Christensenellaceae*, *Ruminococcaceae,* and *Moryella* genera ($P < 0.05$), and the elevating abundances of *Sharpea* and *Olsenella* genera at 14 d postpartum ($P < 0.05$). The metabolic profiles of ruminal SCFAs were obviously varied from 0 to 7 d postpartum, resulting in higher levels of propionic acid, butyric acid, and valeric acid at 7 d postpartum ($P < 0.05$); the metabolic profiles of other ruminal metabolites were significantly shifted from 0 to 7 d postpartum, with 27 significantly elevated metabolites and 35 apparently reduced metabolites ($P < 0.05$). The correlation analysis indicated that propionic acid was positively correlated with *Prevotellaceae* and *Ruminococcaceae* ($P < 0.05$), negatively correlated with *Methanobrevibacter* ($P < 0.01$); butyric acid was positively associated with *Prevotellaceae*, *Ruminococcaceae,* and *Pseudobutyrivibrio* ($P < 0.05$), negatively associated with *Christensenellaceae* ($P < 0.01$); valeric acid was positively linked with *Prevotellaceae* and *Ruminococcaceae* ($P < 0.05$); pyridoxal was positively correlated with *Flexilinea* and *Methanobrevibacter* ($P < 0.05$) and negatively correlated with *Ruminococcaceae* ($P < 0.01$); tyramine was negatively linked with *Ruminococcaceae* ($P < 0.01$).

**Conclusion:** The findings contribute to the decision of nutritional management and prevention of metabolic diseases in high-producing dairy cows during the late perinatal period.

KEYWORDS

high-producing dairy cow, metabolic challenges, rumen bacteria, ruminal fermentation capacity, late perinatal period

# 1. Introduction

In recent decades, improvements in breeding and nutritional technology have contributed to a sustained increase in milk production to meet the human demand for milk (Capper et al., 2009). Milk production has almost doubled in many countries around the world in the last 30 years (von Keyserlingk et al., 2013). However, the continued growth in milk production poses a serious challenge to the metabolism and health of dairy cows, especially in the late perinatal period (within 21 d after parturition) (Trevisi et al., 2012; Gross and Bruckmaier, 2019). When lactation initiates, dairy cows preferentially deliver nutrients to the mammary gland to supply energy requirements for lactation, which means the body requires higher energy and nutrient requirements than the dry period (Oftedal, 2011). Hence, dairy cows are prone to a physiological state of negative energy balance (NEB) after parturition due to lactation initiation and reduced dry matter intake (DMI) (Vossebeld et al., 2022). Although complex adaptation processes enable dairy cows to maintain the homeostasis of energy and nutrients, many individuals, especially high-producing individuals, fail to successfully cope with NEB (van Knegsel et al., 2013). High-producing cows experience varying degrees of metabolic stress at calving (LeBlanc, 2010). The metabolic challenges can affect the immune, metabolic, and endocrine systems, resulting in disorders in hormone, glucose, and lipid metabolisms of high-producing dairy cows during the late perinatal period (Esposito et al., 2014). The concentrations of many metabolic hormones and their receptors can change under the influence of parturition (Lucy et al., 2001). Leptin is a type of peptide hormone secreted by adipose tissue that can influence voluntary feeding in dairy cows (Ingvartsen and Boisclair, 2001). Low concentrations of leptin after parturition can lead to less DMI intake, proceeding to impact the fermentative ability of rumen bacteria in dairy cows (Wathes et al., 2007).

Ruminal bacteria participate in the digestion and nutrient absorption of ruminants (Pinnell et al., 2022), which ferment fiber in feed as short-chain fatty acids (SCFAs) to provide ~70% of energy for dairy cows (Indugu et al., 2017). The rumen bacteria tend to fluctuate due to the diet, environment, and physiological status (Bharanidharan et al., 2021). Lactation initiation and NEB result in obvious fluctuation in the abundance of rumen bacteria and concentrations of fermentation products in dairy cows (Pitta et al., 2014). Our previous study found that the abundance of rumen bacteria was significantly lower in dairy cows after parturition when compared with before parturition (Guo et al., 2023). The changes in ruminal bacterial composition after parturition can lead to some alterations in rumen metabolism (Plaizier et al., 2008; Auffret et al., 2017). A significant correlation is observed between SCFAs and bacteria abundances in the rumen (Liu et al., 2022). Some metabolites are associated with bacteria in the rumen (Fozia et al., 2013). Therefore, due to the parturition, lactation initiation, feed change, and adaptations, the changes in rumen bacteria abundance and their fermentative ability in high-producing dairy cows within 21 d after parturition are complicated and need to be further clarified.

Currently, 16S rRNA high-throughput sequencing has been successfully applied to study the structure and quantity of rumen and gut microbiota of dairy cows (Thoetkiattikul et al., 2013; Guo et al., 2015). GC-MS/MS-targeted metabolomics can be used to detect small molecules such as amino acids, lipids, and organic acids (Zhang et al., 2020) and has been widely used for the determination of metabolites in rumen fluid, blood, and urine of ruminants (Matthews et al., 2019). UPLC-MS/MS untargeted metabolomics has also been widely adopted to qualify and quantify rumen metabolites because of its high sensitivity and accuracy (Luo et al., 2019). Therefore, the combined application of the above technologies can provide a high feasibility to comprehensively reveal the dynamic changes in rumen bacteria and their fermentative ability in high-producing dairy cows within 21 d after parturition. In this study, the concentrations and correlations of ruminal bacteria, SCFAs, and other metabolites in high-producing dairy cows at 0, 7, 14, and 21 d postpartum were studied with 16S rRNA high-throughput sequencing, GC-MS/MS targeted metabolomics, and UPLC-MS/MS untargeted metabolomics, aiming to provide some references for nutritional regulation and prevention of metabolic diseases in high-producing cows during the late perinatal period.

# 2. Materials and methods

## 2.1. Collection and group of ruminal fluids

Ten healthy high-producing Holstein cows (body weight, 600 ± 20 kg; body condition score, 3.4–3.7; daily milk yield, above 35 kg; parity, 2–3) were selected from a dairy farm in Ningxia province, China. The temperature in the cowshed was between 10 and 20°C, with a relative humidity of 50–70%. The lighting time of the dairy cows was controlled for 16 h. All dairy cows were fed the same TMR diet after calving (Supplementary Table 1). Ruminal fluids were collected from the 10 dairy cows at postpartum 0, 7, 14, and 21 d before morning feeding and were grouped as A, B, C, and D, respectively. Ruminal fluids of each group were labeled as A1–A10, B1–B10, C1–C10, and D1–D10. The ruminal fluids were collected by the following method: One end of the pre-rinsed and

sterilized sampler with a metal filter was put into the rumen, and then, a 50 ml syringe fixed at the other end was used to extract the rumen fluid, discarding the first tube of rumen fluid to avoid saliva contamination and saving the second tube of rumen fluid. The supernatant from the rumen fluid after filtering and centrifugation was transferred to a 1.5 ml centrifuge tube and stored at −80°C for the succedent analyses.

## 2.2. 16s rRNA high-throughput sequencing of rumen bacteria communities

The total DNA of rumen bacteria was extracted from the four groups of rumen fluids using OMEGA Soil DNA Kit (M5635-02) (Omega Bio-Tek), and the purity and concentration of the genomic DNA were evaluated using 1% agarose gel electrophoresis. DNA was diluted to 1 ng-μl$^{-1}$ in sterile water as the template; 341F (CCTAYGGGRBGCASCAG) and 806R (GGACTACNNGGGTATCTAAT) were chosen as primers to amplify the V3–V4 highly variable region of the 16S rRNA gene of rumen bacteria in a thermocycling PCR system. Two percentage agarose gel electrophoresis and Qiagen Gel Extraction Kit (Qiagen, Hilden, Germany) were, respectively, used to verify and further purify the amplified products. DNA libraries were then constructed using TruSeq DNA PCR-Free Sample Preparation Kit (Illumina, San Diego, CA, USA) and quantified by the Qubit and Q-PCR methods before sequencing on the NovaSeq6000 platform (Illumina Inc., San Diego, CA, USA).

The valid sequences of all samples after filtering and removing chimeras of raw sequencing were clustered into operational taxonomic units (OTUs) with 97% consistency with UPARSE (v7.0.1001) software. The species annotation of OTUs was carried out with the Mothur and SILVA v132 of SSUrRNA databases. The bacterial community composition of each sample was counted at the phylum and genus levels. After homogenizing the data of each sample, alpha diversity indices including Shannon, Simpson, Chao1, and ACE were calculated using QIIME. The dilution curves of alpha diversity and principal coordinate analysis (PCoA) plots of beta diversity were plotted using R software (version 2.15.3). ANOSIM analysis based on Bray–Curtis distances was used to determine the differences in bacterial communities between the four groups, and the differential species among the four groups were visualized by the *t*-test.

## 2.3. Targeted GC-MS/MS metabolomic analysis of ruminal SCFAs

After thawing and mixing, 50 μl of the rumen fluid was taken into a 1.5 ml centrifuge tube, 100 μl of 36 % chromatographic grade phosphoric acid solution was added to fully mix and then 150 μl of chromatographic grade MTBE (methyl tert-butyl ether) solvent added to the internal standard. The mixed fluid was ultrasonically processed for approximately 5 min in an ice bath to extract SCFAs and then centrifuged at 12,000 r-min$^{-1}$ for 10 min at 4°C. In total, 90 μl of supernatant was transferred to the injection vial and stored at −20°C for subsequent targeted GC-MS/MS metabolomics analysis.

The acquisition conditions for GC-MS/MS analysis were as follows: chromatographic column was DB-FFAP column (30 m × 0.25 mm × 0.25 μm, Merck, USA), injection volume was 2 μl, injector temperature was 200°C, column flow rate was 1.2 ml-min$^{-1}$, and carrier gas was helium. Column temperature program was set as follows: 95°C was kept for 1 min; risen to 100°C at 25°C-min$^{-1}$ and then to 130°C at 17°C-min$^{-1}$ and held for 0.4 min; risen to 200°C at 25°C-min$^{-1}$, held for 0.5 min, and then run for 3 min. The temperatures of the electron ionization source, quadrupole, and transmission line were 230, 150, and 230°C, respectively; the ionization voltage was 70 eV, the scanning mode was multiple reaction monitoring (MRM), and the solvent delay time was 3.0 min.

Qualitative analysis of SCFAs was performed based on the retention time (RT), ion-pair formation, and secondary spectrum data. Quantitative analysis of SCFAs was carried out with MRM of triple quadrupole mass spectrometry. After the score and integral correction of peak areas, the standard curves and linear regression equations of SCFAs (acetic acid, propionic acid, isobutyric acid, butyric acid, isovaleric acid, valeric acid, and capric acid) were established. The concentrations of each SCFA in rumen fluid were calculated according to the linear regression equations. The obtained data of concentrations of each SCFA in rumen fluid were input into MetaboAnalyst 5.0 software, to perform targeted GC-MS/MS metabolomics analysis. Principal component analysis (PCA) of the software was applied to visualize the metabolic profiles (change trends) of ruminal SCFAs among groups, and orthogonal partial squares-discriminant analysis (OPLS-DA) of the software was used to calculate the variable importance in projection (VIP) values to classification. Univariate analysis of the software was used to calculate values of significance and fold change (FC) among the groups. The differential SCFAs among the groups were ascertained according to VIP $\geq$ 1, $P < 0.05$, FC $\geq$ 2, or FC $\leq$ 0.5.

## 2.4. Untargeted UPLC-MS/MS metabolomic analysis of other ruminal metabolites

The relative concentrations of other ruminal metabolites were determined by ultra-performance liquid chromatography-tandem mass spectrometry (UPLC-MS/MS). The chromatographic column was Waters ACQUITY UPLC HSS T3 C18 column (2.1 × 100 mm, 1.8 μm); mobile phase A was ultra-pure water with 0.04 % acetic acid; mobile phase B was acetonitrile with 0.04 % acetic acid; flow rate was 0.4 ml-min$^{-1}$; column temperature was 40°C; injection volume was 2 μl. The elution gradient was set as follows: A: B was 95:5 at 0 min, 5:95 at 11 min, 5:95 at 12 min, 95:5 at 12.1 min, and 95:5 at 14 min. The electrospray ion source temperature was 500°C, ion source gas I was 55 psi, gas II was 60 psi, and gas curtain gas was 25 psi, and the mass spectrometry voltage was 5,500 V (+),−4500 V (-).

Qualitative analysis of other ruminal metabolites was performed based on retention time, ion pair information, and secondary spectral data. Quantitative analysis of other ruminal metabolites was performed using MRM of triple quadrupole mass spectrometry. After obtaining UPLC-MS/MS data from different samples, the ion chromatographic peaks of metabolites were extracted, and the peak areas of each metabolite were corrected and

scored. The database containing sample numbers and peak areas was input into MetaboAnalyst 5.0 software to perform untargeted UPLC-MS/MS metabolomic analysis. The metabolic profiles of each group were analyzed by the PCA method; VIP values among the groups were calculated with the OPLS-DA method. The values of significance and FC among the groups were obtained with univariate analysis. The differential metabolites among the groups were confirmed according to VIP $\geq$ 1, $P < 0.05$, FC $\geq$ 2, or FC $\leq$ 0.5. Venn diagram was used to screen mutual differential metabolites among the groups.

## 2.5. Analysis of the correlation between rumen bacteria and metabolites

Spearman association analysis between the differential bacteria and metabolites was implemented with $M^2$IA software (https://m2ia.met-bioinformatics.cn/). The correlation coefficient, R, is between−1 and 1, |R| > 0.4 indicates a strong correlation. $P < 0.05$ indicates that the correlation is significant; $P < 0.01$ indicates that the correlation is highly significant. The strong correlations between metabolites and bacteria were presented as network plots.

# 3. Results

## 3.1. Diversity of ruminal bacteria in dairy cows within 21 d postpartum

After OTU clustering analysis, 10,594 OTUs were obtained for the valid sequences of rumen fluid samples from the four groups. The number of OTUs in groups A, B, C, and D was 2,778, 2,583, 2,554, and 2,679, respectively. A total of 2,078 OTUs were shared among the four groups, accounting for 19.61 % of the total OTUs. The rarefaction curves of the four groups tended to be flat, indicating the number of samples was reasonable and enough to reflect the structure and quantity of ruminal bacteria in postpartum dairy cows within 21 d (Supplementary Figure 1).

The results of alpha diversity are shown in Figure 1; the Shannon and Simpson indices between groups A and B, groups B and C, and groups C and D were not significant differences ($P > 0.05$), indicating the alteration in diversity of ruminal bacteria was steady in postpartum dairy cows within 21 d. The ACE and Chao1 indices in group B were significantly lower than those in group A ($P < 0.05$) and higher than those in group C ($P < 0.05$), while there was no distinct variation between the indices of groups C and D ($P > 0.05$), suggesting that the abundance of rumen bacteria occurred as a sharp fluctuation in high-producing dairy cows within 14 d postpartum. At the phylum and genus levels, the top ten species of the four groups of rumen fluid in the relative abundance are presented in Figure 2. Firmicutes and Bacteroidetes were the dominant phyla, and unidentified_*Ruminococcaceae*, unidentified_*Prevotellaceae*, *Methanobrevibacter*, unidentified_*Lachnospiraceae,* and unidentified_*Bacteroidales* were the dominant genera.

The principal coordinate analysis (PCoA) of beta diversity analysis showed the differences in rumen bacteria structure among the four groups (Figure 3). ANOSIM analysis further revealed that there were significant differences in rumen bacteria structure between groups A and B ($R = 0.486$, $P = 0.002$) and groups B and C ($R = 0.125$, $P = 0.022$), while there was no obvious difference between groups C and D ($R = 0.003$, $P = 0.391$) (Figure 3).

## 3.2. The differential bacteria in the rumen of dairy cows within 21 d postpartum

The differential bacteria at the phylum and genus levels among the four groups were obtained with the *t*-test (Figure 4). At the phylum level, the relative abundances of *Euryarchaeota* and *Chloroflexi* at 7 d postpartum were significantly lower than those at 0 d postpartum ($P < 0.05$). At the genus level, the relative abundances of unidentified_*Christensenellaceae*, *Methanobrevibacter* (belongs to Euryarchaeota phylum), and *Flexilinea* (belongs to Chloroflexi phylum) genera were significantly lower at 7 d postpartum than those at 0 d postpartum ($P < 0.05$). The relative abundances of unidentified_*Ruminococcaceae*, *Moryella*, *Pseudobutyrivibrio,* and unidentified_*Prevotellaceae* genera were significantly higher than those at 0 d postpartum ($P < 0.05$). Compared with 7 d postpartum, the relative abundances of *Moryella*, unidentified_*Christensenellaceae,* and unidentified_*Ruminococcaceae* genera significantly declined at 14 d postpartum ($P < 0.05$), while those of *Sharpea* and *Olsenella* clearly ascended ($P < 0.05$). No obviously changed bacterial phyla or genera were discovered between 14 and 21 d postpartum ($P > 0.05$).

## 3.3. Metabolic profiles of ruminal SCFAs in dairy cows within 21 d postpartum

Fluctuations in the metabolic profiles of ruminal SCFAs between the four groups were visualized with 2D scatter plots of PCA (Figure 5). The metabolic profiles between groups A and B were completely separated, but those between groups B and C and between groups C and D were largely merged. These fluctuations hinted that the rumen bacteria-producing SCFAs most likely occurred obvious alteration between 0 and 7 d postpartum and then gradually stabilized from 7 to 21 d postpartum.

According to the developed linear regression equations (Supplementary Table 2), the concentrations of SCFAs in rumen were calculated (Table 1). A clear difference in the concentrations of SCFAs between 0 and 7 d postpartum was also observed via the models of OPLS-DA (Figure 6). Combining VIP values from OPLS-DA, *P,* and FC values from univariate analysis, the differential ruminal SCFAs between the four groups were ascertained according to the standard of VIP $\geq$ 1, $P < 0.05$, FC $\geq$ 2, or FC $\leq$ 0.5. The concentrations of propionic acid, butyric acid, and valeric acid were significantly higher at 7 d postpartum than those at 0 d postpartum, while the concentrations of acetic acid, isobutyric acid, isovaleric acid, and caproic acid were not distinctly changed from 0 to 7 d postpartum. There were no significant differences in the concentrations of SCFAs between 7 and 14 d and between 14 and 21 d.

10.3389/fmicb.2023.1269123

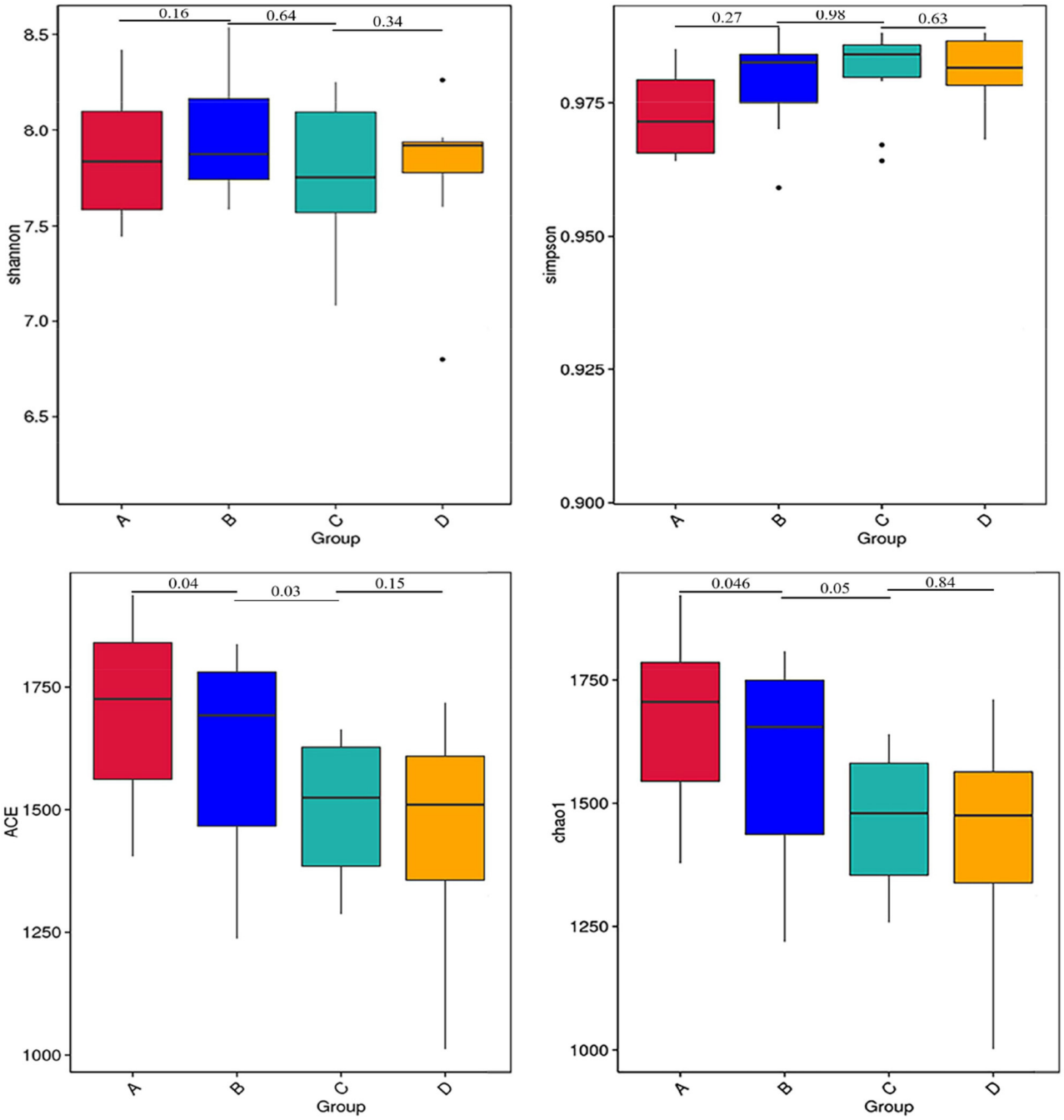


FIGURE 1
Alpha diversity indices of rumen bacteria in dairy cows within 21 d after calving. The differences observed for the alpha diversity (Shannon and Simpson indices) were not significant values ($P > 0.05$). The differences observed for the alpha diversity (ACE and Chao1 indices) between groups A and B and groups B and C were significant values ($P < 0.05$).

## 3.4. Metabolic profiles of other ruminal metabolites in dairy cows within 21 d postpartum

The changes in the metabolic profile of other ruminal metabolites among the four groups were also visualized by the 2D scatter plots of PCA (Figure 7). In accordance with the ruminal SCFAs, there was a clear separation in metabolic profiles between groups A and B, while there were large overlaps in metabolic profiles between groups B and C and between groups C and D. The results indicated that the digestive ability of ruminal bacteria to feed occurred a sharp alteration from 0 to 7 d postpartum and then stabilized after 7 d postpartum.

The OPLS-DA models were constructed to search the differential metabolites among the four groups (Figure 8). The OPLS-DA models presented the high discriminatory abilities to groups A and B ($R^2Y = 0.989$, $Q^2 = 0.87$), groups B and C ($R^2Y = 0.994$, $Q^2 = 0.515$), and groups C and D ($R^2Y = 0.989$, $Q^2 =$

10.3389/fmicb.2023.1269123

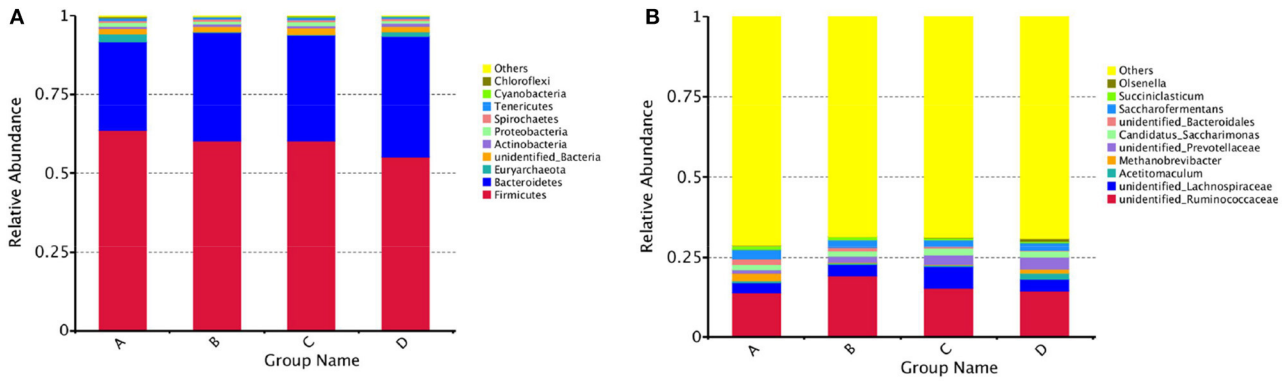


FIGURE 2
Histogram of the relative abundance of rumen species at the phylum and genus levels in dairy cows within 21 d after calving. **(A)** Bacteroidetes and Firmicutes were the dominant phyla in the rumen of dairy cows within 21 d postpartum, **(B)** unidentified_*Ruminococcaceae*, unidentified_*Prevotellaceae*, *Methanobrevibacter*, unidentified_*Lachnospiraceae*, and unidentified_*Bacteroidales* were the dominant genera.

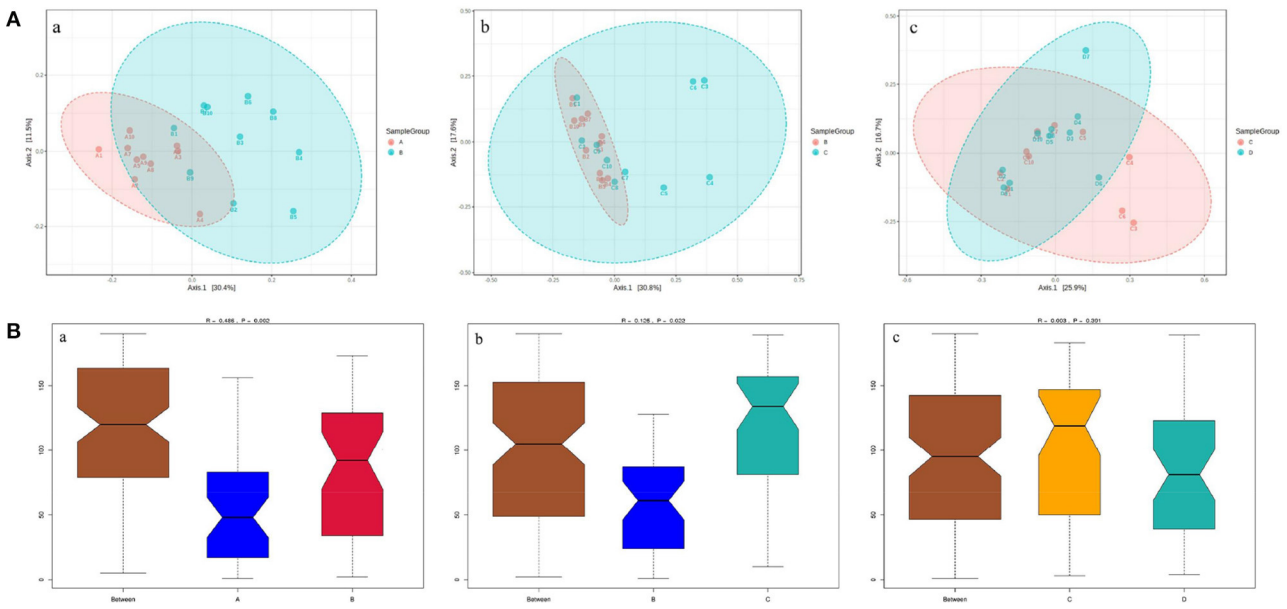


FIGURE 3
The PCoA diagrams **(A)** and boxplots **(B)** of rumen bacteria between groups A and B (a), B and C (b), and C and D (c) in dairy cows within 21 d after calving. **(A)** ANOSIM analysis of beta diversity indicated that the structure of ruminal bacteria sharply fluctuated within 14 d after parturition. **(B)** The Y-axis is the rank of the distance between the two groups, the X-axis represents intergroups; A, B, C, and D, respectively, represent their respective intragroups. R is between−1 and 1. $R > 0$ indicates significant differences between the two groups, $R < 0$, means no significant difference between the two groups.

0.442). $R^2Y$ close to 1 and $Q^2$ higher than 0.4 indicates a good model fitting. According to the standard of VIP $\geq$ 1, $P < 0.05$, FC $\geq$ 2, or FC $\leq$ 0.5, the intergroup differential metabolites were confirmed (Figure 9; Supplementary Table 3). A total of 27 metabolites were obviously elevated and 35 metabolites were reduced from 0 to 7 d postpartum. In total, 18 metabolites were clearly increased and 4 metabolites decreased from 7 to 14 d postpartum. Overall, 3 metabolites distinctly ascended and 8 metabolites descended from 14 to 21 d postpartum. In total, 5 differential metabolites were shared between the 4 groups (Figure 10). The levels of lactose, D-glucose, tyramine, and adenine in the rumen were significantly increased from 0 to 14 d and decreased from 14 to 21 d postpartum. The level of pyridoxal in the rumen was evidently significantly higher at 0 d postpartum than that at 7, 14, and 21 d postpartum (Figure 11).

## 3.5. Correlation between ruminal bacteria and metabolites in dairy cows within 21 d postpartum

The correlation network diagrams between rumen bacteria and metabolites were generated using $M^2IA$ software (Supplementary Figure 2). At the phylum level, *Chloroflexi*

10.3389/fmicb.2023.1269123

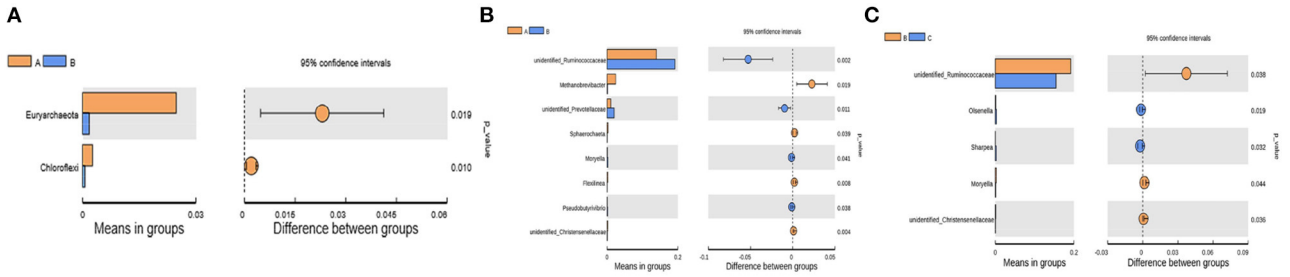


FIGURE 4
The differential rumen bacteria calculated from the *t*-test between groups A and B at the phylum and genus levels and between groups B and C at the genus level. **(A)** At the phylum level, the relative abundances of *Euryarchaeota* and *Chloroflexi* were significantly lower than those at 0 d postpartum ($p < 0.05$). **(B)** At the genus level, the relative abundances of unidentified_*Christensenellaceae*, *Methanobrevibacter,* and *Flexilinea* were significantly decreased within 7 d postpartum ($p < 0.05$), and unidentified_*Ruminococcaceae*, *Moryella*, *Pseudobutyrivibrio,* and unidentified_*Prevotellaceae* were significantly higher ($p < 0.05$). **(C)** The relative abundances of unidentified_*Christensenellaceae, Moryella* and unidentified_*Ruminococcaceae* significantly declined at 14 d postpartum compared with 7 d ($p < 0.05$), while those of *Sharpea* and *Olsenella* clearly increased ($p < 0.05$).

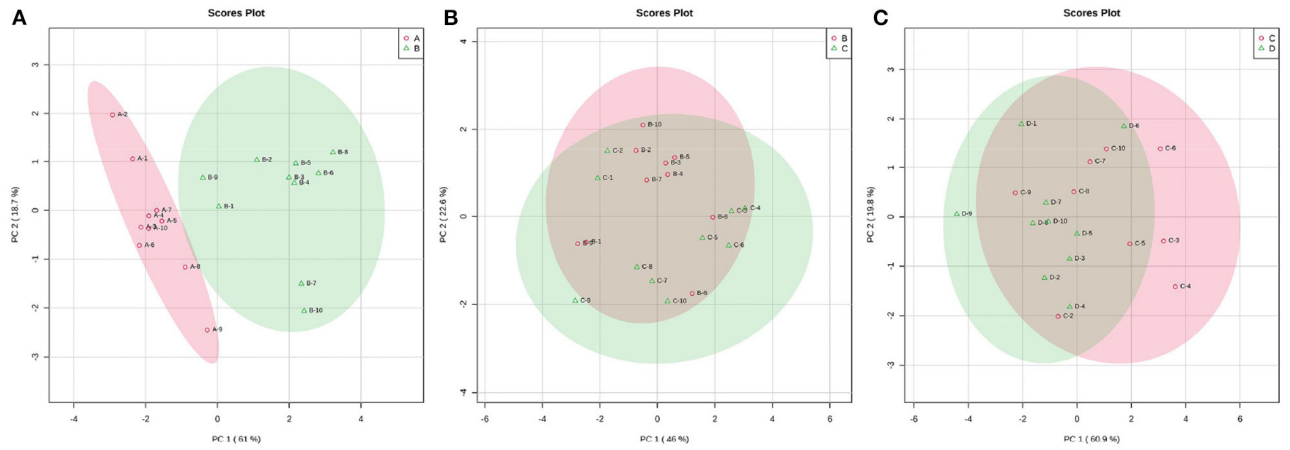


FIGURE 5
The 2D scatter plots of PCA of rumen SCFAs between groups A and B **(A)**, groups B and C **(B)**, and groups C and D **(C)**. The metabolic profiles of ruminal SCFAs were obviously waved within 7 d parturition and then gradually stabilized from 7 to 21 d postpartum.

was negatively correlated with propionic acid and valeric acid. *Euryarchaeota* was negatively associated with propionic acid. At the genus level, unidentified_*Prevotellaceae* showed a positive correlation with propionic acid, valeric acid, and butyric acid. *Flexilinea* was negatively correlated with propionic acid and valeric acid. *Methanobrevibacter* was negatively linked with propionic acid. Unidentified_*Ruminococcaceae* was positively associated with propionic acid, valeric acid, and butyric acid. Unidentified_*Christensenellaceae* was negatively associated with valeric acid, butyric acid, and propionic acid. *Pseudobutyrivibrio* showed a positive correlation with butyric acid. *Moryella* was positively associated with propionic acid and valeric acid. *Flexilinea* presented a positive association with pyridoxal. Unidentified_*Ruminococcaceae* was negatively correlated with pyridoxal and positively correlated with tyramine. *Methanobrevibacter* was positively linked with pyridoxal. The R- and *P*-values of bacteria with SCFAs and other metabolites are shown in Table 2.

# 4. Discussion

## 4.1. Changes in ruminal bacteria and metabolic profiles in high-producing dairy cows within 21 d postpartum

The present study certified that the change trends in rumen bacteria were basically consistent with the metabolic profiles of ruminal SCFAs and other metabolites. ANOSIM analysis of beta diversity indicated that the structure of ruminal bacteria was sharply fluctuated within 14 d after parturition. 2D scatter plots of PCA displayed that the metabolic profiles of ruminal SCFAs and other metabolic profiles were obviously waved within 7 d parturition. In addition, some studies found that Firmicutes and Bacteroidetes phyla were rumen-dominant bacteria in healthy dairy cows during the late perinatal period (Difford et al., 2018; Mingyuan et al., 2018; Wang et al., 2019), which is consistent with the results of the present study. Our study further testified that the abundances of *Firmicutes* and *Bacteroidetes* held at steady

TABLE 1 The concentrations (μg·mL-1) and the related parameters of SCFAs.

| Metabolites | Group A | Group B | A vs. B | | | Group C | B vs. C | | | Group D | C vs. D | | |
|---|---|---|---|---|---|---|---|---|---|---|---|---|---|
| | Mean ± SD | Mean ± SD | FC[a] | VIP[b] | *P*-Value | Mean ± SD | FC | VIP | *P*-value | Mean ± SD | FC | VIP | *P*-Value |
| Acetic acid | 634.00 ± 294.36 | 706.60 ± 261.78 | 1.12 | 1.30 | 0.59 | 1006.40 ± 256.23 | 1.42 | 1.73 | 0.02 | 1100.30 ± 272.47 | 1.09 | 1.35 | 0.46 |
| Propionic acid | 323.68 ± 165.61 | 660.50 ± 238.35 | 2.04 ↑ | 1.27 | 0.003** | 781.60 ± 323.67 | 1.46 | 1.15 | 0.12 | 706.60 ± 204.17 | 0.90 | 1.32 | 0.59 |
| Isobutyric acid | 36.64 ± 23.23 | 32.16 ± 13.77 | 0.88 | 1.10 | 0.63 | 23.86 ± 7.67 | 1.49 | 1.02 | 0.05 | 26.90 ± 10.12 | 0.85 | 1.26 | 0.33 |
| Butyric acid | 328.17 ± 149.00 | 693.90 ± 243.97 | 2.11↑[c] | 1.03 | 0.012* | 31.56 ± 7.85 | 0.98 | 0.85 | 0.91 | 46.36 ± 13.60 | 1.47 | 1.15 | 0.01 |
| Isovaleric acid | 34.96 ± 20.46 | 26.04 ± 11.06 | 0.75 | 0.87 | 0.27 | 30.36 ± 16.91 | 1.32 | 0.82 | 0.18 | 43.65 ± 17.91 | 0.90 | 0.52 | 0.57 |
| Valeric acid | 41.68 ± 21.69 | 86.28 ± 32.71 | 2.07↑ | 1.81 | 0.004** | 984.90 ± 392.93 | 1.05 | 0.46 | 0.83 | 832.40 ± 223.78 | 1.13 | 0.46 | 0.48 |
| Caproic acid | 14.17 ± 8.78 | 22.73 ± 13.63 | 1.60 | 0.08 | 0.13 | 126.00 ± 62.95 | 1.17 | 0.11 | 0.53 | 112.79 ± 32.97 | 1.44 | 0.26 | 0.12 |

[a]Fold change is the ratio of the relative peak intensity of the metabolites between the two groups (B/A, C/B, and D/C). [b]Variable importance projection value is calculated from the orthogonal partial squares discriminant analysis model. [c]↑ or ↓ shows the change trends of the differential metabolites in postpartum dairy cows (B/A, C/B, and D/C). The concentrations of propionic acid, butyric acid, and valeric acid were significantly higher within 7 d postpartum. * indicates $p < 0.05$, ** indicates $p < 0.01$.

level in the rumen of high-producing dairy cows within 21 d postpartum. However, the abundances of Euryarchaeota and Chloroflexi phyla were distinctly descended within 7 d postpartum. *Chloroflexi* plays a key role in methane production (Bovio et al., 2019). *Euryarchaeota*, also known as methanogenic bacteria, participates in the methanogenesis and degradation of other hydrocarbons (Baker et al., 2020). *Methanobrevibacter* belonging to *Euryarchaeota* is an important component of intestinal and rumen methanogenic archaea and is related to greater methane emission (Tapio et al., 2017). The abundance of the *Methanobrevibacter* genus was also obviously decreased within 7 d postpartum in this study. The production of methane in the rumen of dairy cows indicates loss of energy (Appuhamy et al., 2016; BetancurMurillo et al., 2022). High-producing dairy cows are prone to the metabolic status of NEB during the late perinatal period due to lactation initiation and lower DMI intake. Hence, the self-adaptive reduction in the abundance of rumen of *Euryarchaeota*, *Chloroflexi,* and *Methanobrevibacter* is beneficial to alleviate the metabolic stress of negative energy balance in postpartum high-producing dairy cows.

## 4.2. Correlation between ruminal bacteria and SCFAs in high-producing dairy cows within 21 d postpartum

SCFAs are the main products of feed fermented by ruminal bacteria; we found that the concentrations of ruminal propionic acid, butyric acid, and valeric acid were notably ascended within 7 d postpartum. As the important substrate for gluconeogenesis, propionic acid provides 40–70% of glucose (DeFrain et al., 2005), inhibits inflammation, and improves the immunity of the body (Walkenhorst et al., 2020). Butyric acid can regulate energy metabolism (Fukumori et al., 2022), inhibit the production of pro-inflammatory mediators stimulated by LPS and cytokines, and promote the release of anti-inflammatory cytokine IL-10 (Renato et al., 2011; Chang et al., 2014).

In this study, the relative abundances of unidentified_*Prevotellaceae* and *Pseudobutyrivibrio* were significantly increased and that of *Methanobrevibacter* decreased within 7 d postpartum. At the phylum level, *Bacteroidetes* and *Firmicutes* were the ruminal dominant bacteria in dairy cows within 21 d postpartum. Unidentified_*Prevotellaceae* of Bacteroidetes phylum is one of the most abundant bacterial genera in the rumen, accounting for 45–60% of the total bacterial population (Jiang et al., 2017). Unidentified_*Prevotellaceae* can decompose starch and protein (Xie et al., 2019) and synthesize propionate, butyrate, and valerate (Salonen et al., 2014; Baothman et al., 2016). *Pseudobutyrivibrio* genus of *Firmicutes* is an effective bacterium degrading hemicellulose, which can produce butyrate (Louis and Flint, 2017). *Methanobrevibacter* genus of *Euryarchaeota* phylum can utilize large amount of propionic acid during methane production (Shi et al., 2014; Poehlein et al., 2018).

Additionally, the study verified that the relative abundance of unidentified_*Ruminococcaceae* was significantly increased at 7 d postpartum and then evidently decreased at 14 d postpartum and that of unidentified_*Christensenellaceae* was distinctly reduced within 14 d postpartum. Unidentified_*Ruminococcaceae*, the main

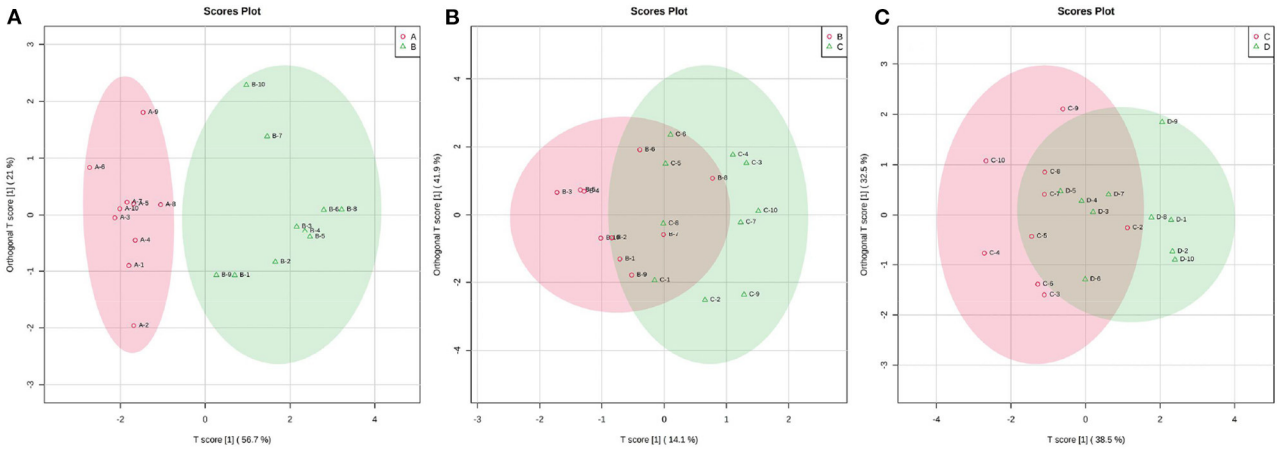


FIGURE 6
The 2D scatter plots of OPLS-DA of rumen SCFAs between groups A and B **(A)**, groups B and C **(B)**, and groups C and D **(C)**.

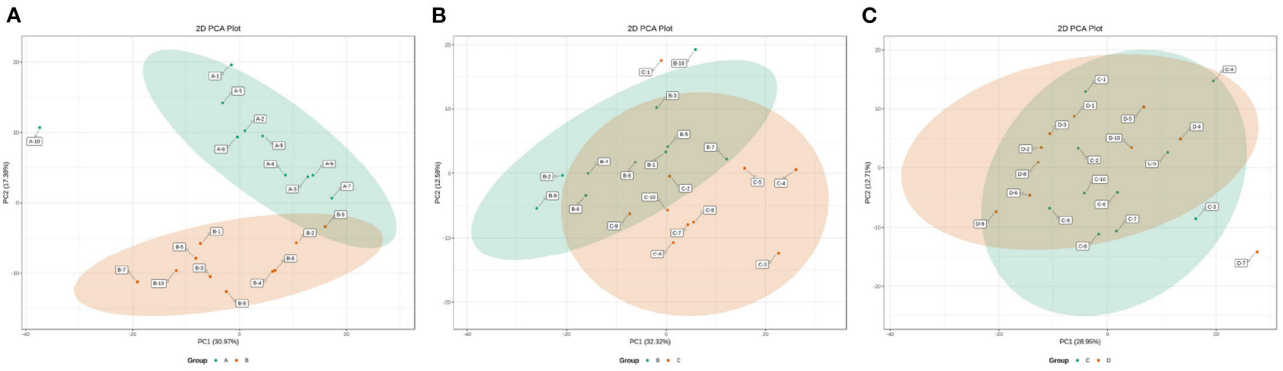


FIGURE 7
The 2D scatter plots of PCA of ruminal other metabolites between groups A and B **(A)**, groups B and C **(B)**, and groups C and D **(C)**.

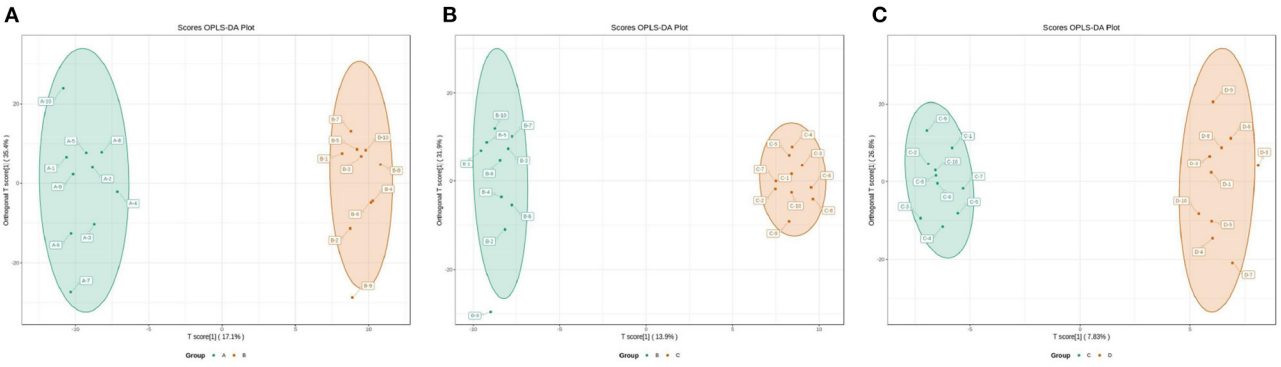


FIGURE 8
The 2D scatter plots of OPLS-DA of rumen other metabolites between groups A and B **(A)**, groups B and C **(B)**, and groups C and D **(C)**.

ruminal cellulose-degrading bacteria, can produce butyrate and valerate, participating in the release of inflammatory and cytotoxic factors, immune regulation, and intestinal homeostasis (Fanli et al., 2016; Daniela et al., 2019). *Christensenellaceae* have been reported to produce volatile fatty acids by utilizing a variety of sugars (Morotomi et al., 2012). Consequently, the levels of SCFAs in the rumen were closely linked to the abundance of SCFAs-producing and utilizing bacteria (Wang et al., 2021).

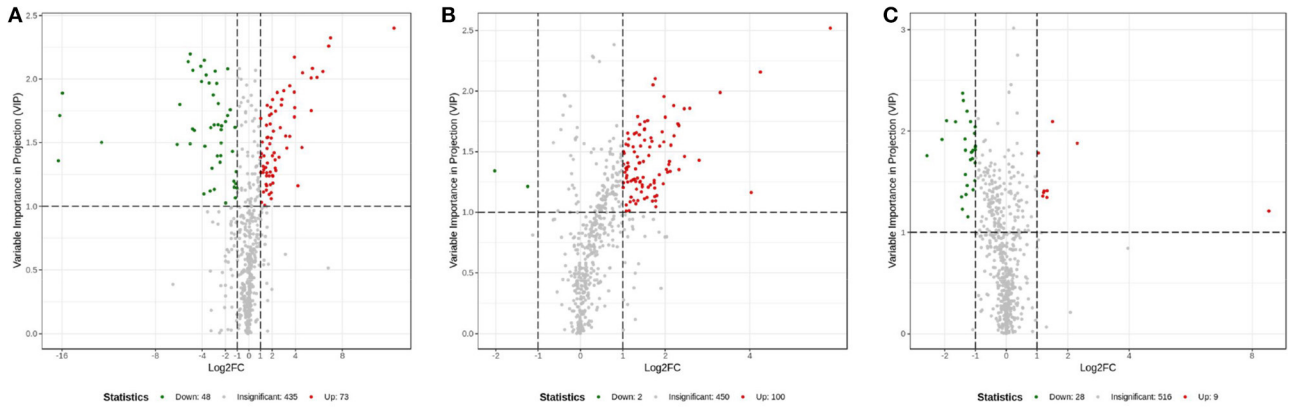


FIGURE 9
Volcanic plots of rumen other metabolites between groups A and B **(A)**, groups B and C **(B)**, and groups C and D **(C)**.


FIGURE 10
The Venn diagram of rumen differential metabolites between groups A and B, groups B and C, and groups C and D.

Hence, the correlation analysis was performed in this study to further validate the relationship between rumen bacteria and SCFAs. The results showed that unidentified_*Prevotellaceae* positively correlated with propionic acid, butyric acid, and valeric acid; *Methanobrevibacter* was negatively associated with propionic acid; unidentified_*Ruminococcaceae* was positively related to butyric acid, propionic acid, and valeric acid; unidentified_*Christensenellaceae* was negatively linked with butyric acid; and *Pseudobutyrivibrio* was positively correlated with butyric acid. In summary, these changes in the abundance of ruminal SCFAs-producing and utilizing bacteria may contribute to the high-producing dairy cows coping with the challenge of postpartum metabolic stress and inflammatory response.

## 4.3. Correlation between rumen bacteria and other metabolites in high-producing dairy cows within 21 d postpartum

In this study, the level of pyridoxal, the main component of vitamin B6, significantly declined 7 d postpartum and then clearly elevated within 14 d postpartum. The correlation analysis further certified that pyridoxal was negatively correlated with unidentified_*Ruminococcaceae* and positively associated with *Methanobrevibacter*. Rumen bacteria can synthesize B vitamins (Zinn et al., 1987). The synthesis of vitamin B6 in the rumen is negatively correlated with the abundance of fiber-degrading bacteria such as unidentified_*Ruminococcaceae* (Castagnino et al., 2016), which is consistent with the results of the present study. *Methanobrevibacter* facilitates the biosynthesis of most B vitamins in the small intestine (Jiang et al., 2022). However, it has not been reported whether *Methanobrevibacter* can promote the synthesis of B vitamins in rumen but its effect on the rumen has not been reported. Our study indicated that *Methanobrevibacter* in the rumen might aid the biosynthesis of B vitamin.

A highly significant positive correlation between tyramine content and unidentified_*Ruminococcaceae* was attested in the study. Biogenic amines are produced through the decarboxylation of some amino acids such as tyrosine and histidine under the action of bacterial amino acid decarboxylase (Aschenbach and Gäbel, 2000). The production of biogenic amines is closely related to the rumen bacteria (Phuntsok et al., 1998). *Ruminococcus gnavus* of Firmicutes phylum mediate the catabolism of phenylalanine, thus promoting the production of tyramine (Wu et al., 2023; Zhai et al., 2023). *Ruminococcus gnavus* is linked with tyramine generation (Yali et al., 2020).

Adenine is the precursor of ruminal microbial crude protein (MCP). MCP is generated *via* rumen microorganisms-fermenting feed in dairy cows (Lu et al., 2019). The efficiency of MCP synthesis in rumen ascends with the increase of DMI in dairy cows (Abdukarim, 2019). Protozoa synthesize their own nucleic acids utilizing free adenine and urine through the remedial pathway in the rumen (McAllan, 1982). We found that the level of adenine in the rumen was obviously elevated with 14 d postpartum and then

10.3389/fmicb.2023.1269123

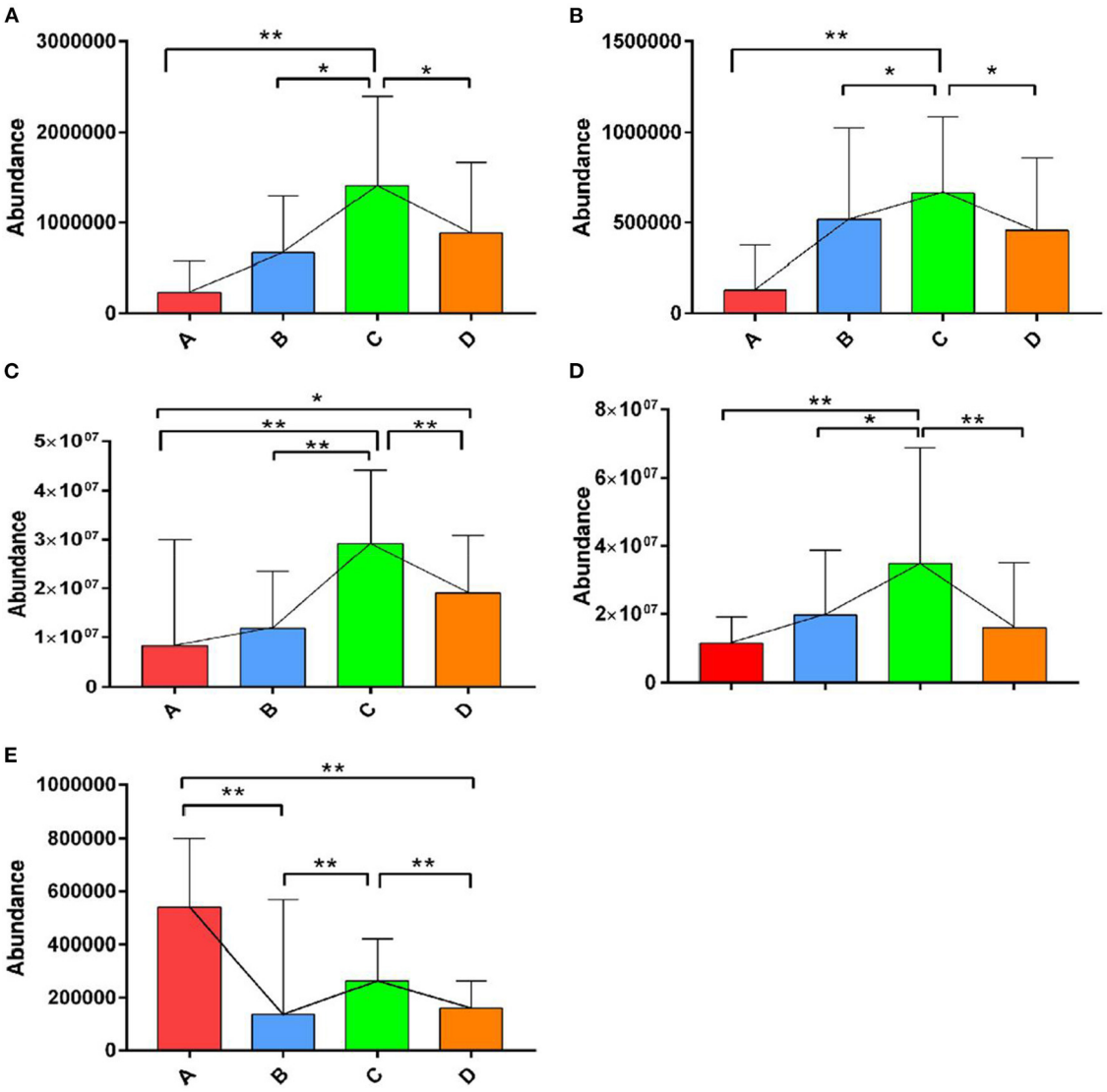


FIGURE 11
The relative abundances of the differential metabolites of D-glucose, lactose, tyramine, adenine, and pyridoxal in the four groups. ** indicates extremely significant difference ($p < 0.01$), and * indicates significant difference ($p > 0.05$). The levels of lactose **(A)**, D-glucose **(B)**, tyramine **(C)**, and adenine **(D)** in rumen were significantly increased from 0 to 14 d and decreased from 14 to 21 d postpartum. The level of pyridoxal **(E)** in rumen was evidently significantly higher at 0 d postpartum than that at 7, 14, and 21 d postpartum.

clearly dropped, and there was no correlation between adenine and bacteria. The results suggest that the level of adenine is most likely related to the relative abundance of protozoa in the rumen.

As the main starch-degrading bacteria in the rumen, unidentified_*Prevotellaceae* generates amylases that hydrolyze straight-chain or branched-chain starches into glucose and lactose through the pathway of sucrose, galactose, and starch metabolism (Richard et al., 2003). However, the soluble sugars are rapidly converted into volatile fatty acids (VFAs) in the rumen as the source of energy for organisms (Lucy et al., 2013). In this study, the change trends of lactose and D-glucose were found similar to those of adenine within 21 d postpartum, and there were no correlations between the two and unidentified_*Prevotellaceae* and other ruminal bacteria. The uncorrelation was highly possibly attributed to the rapid transformation of lactose into D-glucose.

## 5. Conclusion

To reveal the dynamic changes of rumen bacteria and metabolites in high-producing dairy cows after parturition, 16S rRNA high-throughput sequencing, GC-MS/MS targeted metabolomics, and UPLC-MS/MS untargeted metabolomics were used in this study, to comprehensively investigate the changes of ruminal bacterial abundance, SCFAs, and other metabolites in high-producing dairy cows at 0, 7, 14, and 21 d postpartum and the correlation between the three. The results suggested

10.3389/fmicb.2023.1269123

TABLE 2 The correlation table between rumen bacteria and SCFAs and other metabolites in postpartum dairy cows.

| Bacteria | SCFAs and other metabolites | *R* | *P* |
|---|---|---|---|
| At phylum level | | | |
| *Chloroflexi* | Propionic acid | −0.686 | 8.50E-04** |
| | Valeric acid | −0.614 | 4.00E-03** |
| *Euryarchaeota* | Propionic acid | −0.692 | 7.30E-04** |
| At genus level | | | |
| Unidentified_ *Prevotellaceae* | Propionic acid | 0.651 | 1.90E-03** |
| | Valeric acid | 0.52 | 0.019* |
| | Butyric acid | 0.513 | 0.04* |
| *Flexilinea* | Propionic acid | −0.759 | 1.00E-04** |
| | Valeric acid | −0.598 | 5.30E-03** |
| *Methanobrevibacter* | Propionic acid | −0.669 | 1.30E-03** |
| Unidentified_ *Ruminococcaceae* | Propionic acid | 0.657 | 1.60E-03** |
| | Valeric acid | 0.591 | 6.10E-03** |
| | Butyric acid | 0.556 | 0.011* |
| Unidentified_ *Christensenellaceae* | Propionic acid | −0.507 | 0.023* |
| | Valeric acid | −0.568 | 8.90E-03** |
| | Butyric acid | −0.695 | 6.80E-04** |
| *Pseudobutyrivibrio* | Butyric acid | 0.511 | 0.021* |
| *Moryella* | Propionic acid | 0.504 | 0.031* |
| | Valeric acid | 0.518 | 0.033* |
| *Flexilinea* | Pyridoxal | 0.481 | 0.032 |
| *Methanobrevibacter* | Pyridoxal | 0.459 | 0.042 |
| Unidentified_ *Ruminococcaceae* | Pyridoxal | −0.567 | 9.10E-03 |
| | Tyramine | 0.720 | 3.40E-04 |

* indicates $p < 0.05$, ** indicates $p < 0.01$. $|R| > 0.7$ means a very tight correlation is very close, |R| between 0.4 and 0.7 means a tight correlation.

that rumen bacteria and SCFAs and other metabolites took place various degrees of fluctuations during the late perinatal period affected by parturition stress and lactation initiation and that the levels of ruminal propionic acid, butyric acid, valeric acid, and pyridoxal presented obvious correlation with the Chloroflexi and Euryarchaeota phyla, as well as the *Prevotellacea, Flexilinea, Ruminococcaceae, Christensenellaceae, Moryella Pseudobutyrivibrio, and Methanobrevibacter* genera. The results would provide some references for the nutrition management and prevention of metabolic disease in postpartum high-producing dairy cows. The subsequent experiments should focus on the dynamic changes in rumen protozoa, archaea, and fungi and correlations with metabolites in postpartum high-producing dairy cows.

## Data availability statement

The datasets presented in this study can be found in online repositories. The names of the repository/repositories and accession number(s) can be found below: 16s rRNA NCBI-PRJNA1000975, UPLC-MS/MS EBI-MTBLS8333.

## Ethics statement

The animal study was approved by the Institutional Animal Care and Use Committee of Ningxia University (NXUC20200618). The study was conducted in accordance with the local legislation and institutional requirements.

## Author contributions

YoM: Data curation, Formal analysis, Methodology, Writing—original draft, Writing—review and editing. FW: Conceptualization, Formal analysis, Writing—review and editing. WK: Conceptualization, Methodology, Writing—review and editing. RW: Methodology, Resources, Writing—review and editing. XL: Methodology, Writing—review and editing. HD: Methodology, Writing—review and editing. YuM: Conceptualization, Formal analysis, Writing—review and editing. YG: Conceptualization, Supervision, Writing—review and editing.

## Funding

The author(s) declare financial support was received for the research, authorship, and/or publication of this article. This study was supported by the National Natural Science Foundation of China (32160848), the Ningxia Natural Science Foundation of Province (2023AAC03103), and the National Natural Science Foundation of China (31860719).

## Conflict of interest

The authors declare that the research was conducted in the absence of any commercial or financial relationships that could be construed as a potential conflict of interest.

## Publisher's note

All claims expressed in this article are solely those of the authors and do not necessarily represent those of

their affiliated organizations, or those of the publisher, the editors and the reviewers. Any product that may be evaluated in this article, or claim that may be made by its manufacturer, is not guaranteed or endorsed by the publisher.

## Supplementary material

The Supplementary Material for this article can be found online at: https://www.frontiersin.org/articles/10.3389/fmicb.2023.1269123/full#supplementary-material

## References


Abdukarim, Y. H. (2019). Factors affecting rumen microbial protein synthesis: a review. *Vet. Med. Open J.* 4, 27–35. doi: 10.17140/VMOJ-4-133

Appuhamy, J. A. D. R., France, J., and Kebreab, E. (2016). Models for predicting enteric methane emissions from dairy cows in north america, europe, and australia and new zealand. *Glob. Change Biol.* 22, 3039–3056. doi: 10.1111/gcb.13339

Aschenbach, J. R., and Gäbel, G. (2000). Effect and absorption of histamine in sheep rumen: significance of acidotic epithelial damage. *J. Anim. Sci.* 78, 464–470. doi: 10.2527/2000.782464x

Auffret, M. D., Dewhurst, R. J., Duthie, C., Rooke, J. A., John, W. R., and Freeman, T. C., et al. (2017). The rumen microbiome as a reservoir of antimicrobial resistance and pathogenicity genes is directly affected by diet in beef cattle. *Microbiome.* 5, 159. doi: 10.1186/s40168-017-0378-z

Baker, B. J., De Anda, V., Seitz, K. W., Dombrowski, N., Santoro, A. E., and Lloyd, K. G. (2020). Diversity, ecology and evolution of archaea. *Nat. Microbiol.* 5, 887–900. doi: 10.1038/s41564-020-0715-z

Baothman, O. A., Zamzami, M. A., Taher, I., Abubaker, J., and Abu-Farha, M. (2016). The role of gut microbiota in the development of obesity and diabetes. *Lipids Health Dis.* 15, 108. doi: 10.1186/s12944-016-0278-4

BetancurMurillo, C. L., AguilarMarín, S. B., and Jovel, J. (2022). Prevotella: a key player in ruminal metabolism. *Microorganisms.* 11, 1. doi: 10.3390/microorganisms11010001

Bharanidharan, R., Lee, C. H., Thirugnanasambantham, K., Ibidhi, R., Woo, Y. W., and Lee, H. G., et al. (2021). Feeding systems and host breeds influence ruminal fermentation, methane production, microbial diversity and metagenomic gene abundance. *Front. Microbiol.* 12:701081. doi: 10.3389/fmicb.2021.701081

Bovio, P., Cabezas, A., and Etchebehere, C. (2019). Preliminary analysis of chloroflexi populations in full-scale uasb methanogenic reactors. *J. Appl. Microbiol.* 126, 667–683. doi: 10.1111/jam.14115

Capper, J. L., Cady, R. A., and Bauman, D. E. (2009). The environmental impact of dairy production: 1944 compared with 2007. *J. Anim. Sci.* 87, 2160–2167. doi: 10.2527/jas.2009-1781

Castagnino, D. S., Seck, M., Beaudet, V., Kammes, K. L., Voelker Linton, J. A., and Allen, M. S., et al. (2016). Effects of forage family on apparent ruminal synthesis of b vitamins in lactating dairy cows. *J. Dairy Sci.* 99, 1884–1894. doi: 10.3168/jds.2015-10319

Chang, P. V., Hao, L., Offermanns, S., and Medzhitov, R. (2014). The microbial metabolite butyrate regulates intestinal macrophage function via histone deacetylase inhibition. *P. Natl. Acad. Sci. Usa.* 111, 2247–2252. doi: 10.1073/pnas.1322269111

Daniela, P. V., Daniela, P. V., Marjorie, K. D. L. F., Glauben, L., María, J. G., and Rodrigo, Q., et al. (2019). Short chain fatty acids (scfas)-mediated gut epithelial and immune regulation and its relevance for inflammatory bowel diseases. *Front. Immunol.* 10:1486. doi: 10.3389/fimmu.2019.01486

DeFrain, J. M., Hippen, A. R., Kalscheur, K. F., and Patton, R. S. (2005). Effects of feeding propionate and calcium salts of long-chain fatty acids on transition dairy cow performance *. *J. Dairy Sci.* 88, 983–993. doi: 10.3168/jds.S0022-0302(05)72766-1

Difford, G. F., Plichta, D. R., Løvendahl, P., Lassen, J., Noel, S. J., and Højberg, O., et al. (2018). Host genetics and the rumen microbiome jointly associate with methane emissions in dairy cows. *PLoS Genet.* 14:e1007580. doi: 10.1371/journal.pgen.1007580

Esposito, G., Irons, P. C., Webb, E. C., and Chapwanya, A. (2014). Interactions between negative energy balance, metabolic diseases, uterine health and immune response in transition dairy cows. *Anim. Reprod. Sci.* 144, 60–71. doi: 10.1016/j.anireprosci.2013.11.007

Fanli, K., Yutong, H., Bo, Z., Ruihong, N., Ying, L., and Jiangchao, Z. (2016). Gut microbiota signatures of longevity. *Curr. Biol.* 26, R832–R833. doi: 10.1016/j.cub.2016.08.015

Fozia, S., Souhaila, B., An, C. G., Nikolaos, P., Rupasri, M., and Suzanna, M. D., et al. (2013). The bovine ruminal fluid metabolome. *Metabolomics.* 9, 360–378. doi: 10.1007/s11306-012-0458-9

Fukumori, R., Doi, K., Mochizuki, T., Oikawa, S., Gondaira, S., and Iwasaki, T., et al. (2022). Sodium butyrate administration modulates the ruminal villus height, inflammation-related gene expression, and plasma hormones concentration in dry cows fed a high-fiber diet. *Anim. Sci. J.* 93:e13791. doi: 10.1111/asj.13791

Gross, J. J., and Bruckmaier, R. M. (2019). Invited review: metabolic challenges and adaptation during different functional stages of the mammary gland in dairy cows: perspectives for sustainable milk production. *J. Dairy Sci.* 102, 2828–2843. doi: 10.3168/jds.2018-15713

Guo, W., Li, Y., Wang, L., Wang, J., Xu, Q., and Yan, T., et al. (2015). Evaluation of composition and individual variability of rumen microbiota in yaks by 16s rrna high-throughput sequencing technology. *Anaerobe.* 34, 74–79. doi: 10.1016/j.anaerobe.2015.04.010

Guo, Y., Wang, F., Mao, Y., Kong, W., Wang, J., and Zhang, G. (2023). Influence of parturition on rumen bacteria and scfas in holstein cows based on 16s rrna sequencing and targeted metabolomics. *Animals*. 13:782. doi: 10.3390/ani13050782

Indugu, N., Vecchiarelli, B., Baker, L. D., Ferguson, J. D., Vanamala, J., and Pitta, D. W. (2017). Comparison of rumen bacterial communities in dairy herds of different production. *BMC Microbiol.* 17, 190. doi: 10.1186/s12866-017-1098-z

Ingvartsen, K. L., and Boisclair, Y. R. (2001). Leptin and the regulation of food intake, energy homeostasis and immunity with special focus on periparturient ruminants. *Domest. Anim. Endocrinol.* 21, 215–250. doi: 10.1016/S0739-7240(02)00119-4

Jiang, Q., Lin, L., Xie, F., Jin, W., Zhu, W., and Wang, M., et al. (2022). Metagenomic insights into the microbe-mediated b and k2 vitamin biosynthesis in the gastrointestinal microbiome of ruminants. *Microbiome.* 10, 109. doi: 10.1186/s40168-022-01298-9

Jiang, Y., Ogunade, I. M., Arriola, K. G., Qi, M., Vyas, D., Staples, C. R., et al. (2017). Effects of the dose and viability of saccharomyces cerevisiae. 2. Ruminal fermentation, performance of lactating dairy cows, and correlations between ruminal bacteria abundance and performance measures. *J. Dairy Sci.* 100, 8102–8118. doi: 10.3168/jds.2016-12371

LeBlanc, S. (2010). Monitoring metabolic health of dairy cattle in the transition period. *J. Reprod. Dev.* 56, S29–S35. doi: 10.1262/jrd.1056S29

Liu, J., Bai, Y., Liu, F., Kohn, R. A., Tadesse, D. A., and Sarria, S., et al. (2022). Rumen microbial predictors for short-chain fatty acid levels and the grass-fed regimen in angus cattle. *Animals.* 12:2995. doi: 10.3390/ani12212995

Louis, P., and Flint, H. J. (2017). Formation of propionate and butyrate by the human colonic microbiota. *Environ. Microbiol.* 19, 29–41. doi: 10.1111/1462-2920.13589

Lu, Z., Xu, Z., Shen, Z., Tian, Y., and Shen, H. (2019). Dietary energy level promotes rumen microbial protein synthesis by improving the energy productivity of the ruminal microbiome. *Front. Microbiol.* 10:847. doi: 10.3389/fmicb.2019.00847

Lucy, M., Jiang, H., and Kobayashi, Y. M. (2001). Changes in the somatotrophic axis associated with the initiation of lactation. *J. Dairy Sci.* 84, E113–E119. doi: 10.3168/jds.S0022-0302(01)70205-6

Lucy, M. C., Escalante, R. C., Keisler, D. H., Lamberson, W. R., and Mathew, D. J. (2013). Short communication: glucose infusion into early postpartum cows defines an upper physiological set point for blood glucose and causes rapid and reversible changes in blood hormones and metabolites. *J. Dairy Sci.* 96, 5762–5768. doi: 10.3168/jds.2013-6794

Luo, Z. Z., Shen, L. H., Jiang, J., Huang, Y. X., Bai, L. P., Yu, S. M., et al. (2019). Plasma metabolite changes in dairy cows during parturition identified using untargeted metabolomics. *J. Dairy Sci.* 102, 4639–4650. doi: 10.3168/jds.2018-15601

Matthews, C., Crispie, F., Lewis, E., Reid, M., O'Toole, P. W., and Cotter, P. D. (2019). The rumen microbiome: a crucial consideration when optimising milk and meat production and nitrogen utilisation efficiency. *Gut Microbes.* 10, 115–132. doi: 10.1080/19490976.2018.1505176

McAllan, A. B. (1982). The fate of nucleic acids in ruminants. *P. Nutr. Soc.* 41, 309–317. doi: 10.1079/PNS19820046

Mingyuan, X., Huizeng, S., Xuehui, W., Le Luo, G., and Jianxin, L. (2018). Assessment of rumen microbiota from a large dairy cattle cohort reveals the pan

and core bacteriomes contributing to varied phenotypes. *Appl. Environ. Microbiol.* 84:e0097018. doi: 10.1128/AEM.00970-18

Morotomi, M., Nagai, F., and Watanabe, Y. (2012). Description of christensenella minuta gen. nov., sp. nov., isolated from human faeces, which forms a distinct branch in the order clostridiales, and proposal of christensenellaceae fam. nov. *Int. J. Syst. Evol. Micr.* 62, 144–149. doi: 10.1099/ijs.0.026989-0

Oftedal, T. O. (2011). The evolution of milk secretion and its ancient origins. *Animal.* 6, 355–368. doi: 10.1017/S1751731111001935

Phuntsok, T., Froetschel, M. A., Amos, H. E., Zheng, M., and Huang, Y. W. (1998). Biogenic amines in silage, apparent postruminal passage, and the relationship between biogenic amines and digestive function and intake by steers. *J. Dairy Sci.* 81, 2193–2203. doi: 10.3168/jds.S0022-0302(98)75798-4

Pinnell, L. J., Reyes, A. A., Wolfe, C. A., Weinroth, M. D., Metcalf, J. L., and Delmore, R. J., et al. (2022). Bacteroidetes and firmicutes drive differing microbial diversity and community composition among micro-environments in the bovine rumen. *Front. Vet. Sci.* 9:897996. doi: 10.3389/fvets.2022.897996

Pitta, D. W., Kumar, S., Vecchiarelli, B., Shirley, D. J., Bittinger, K., and Baker, L. D., et al. (2014). Temporal dynamics in the ruminal microbiome of dairy cows during the transition period. *J. Anim. Sci.* 92, 4014–4022. doi: 10.2527/jas.2014-7621

Plaizier, J. C., Krause, D. O., Gozho, G. N., and McBride, B. W. (2008). Subacute ruminal acidosis in dairy cows: the physiological causes, incidence and consequences. *Vet. J.* 176, 21–31. doi: 10.1016/j.tvjl.2007.12.016

Poehlein, A., Schneider, D., Soh, M., Daniel, R., and Seedorf, H. (2018). Comparative genomic analysis of members of the genera methanosphaera and methanobrevibacter reveals distinct clades with specific potential metabolic functions. *Archaea.* 2018:7609847. doi: 10.1155/2018/7609847

Renato, T. N., Rui, C., Marco, A. R. V., and Hosana, G. R. (2011). Regulation of inflammation by short chain fatty acids. *Nutrients*. 3, 858–876. doi: 10.3390/nu3100858

Richard, F. T., John, K., and Xin, Q. (2003). Starch—composition, fine structure and architecture. *J. Cereal Sci.* 39, 151–165. doi: 10.1016/j.jcs.2003.12.001

Salonen, A., Lahti, L., Salojärvi, J., Holtrop, G., Korpela, K., and Duncan, S. H., et al. (2014). Impact of diet and individual variation on intestinal microbiota composition and fermentation products in obese men. *ISME J.* 8, 2218–2230. doi: 10.1038/ismej.2014.63

Shi, W., Moon, C. D., Leahy, S. C., Kang, D., Froula, J., and Kittelmann, S., et al. (2014). Methane yield phenotypes linked to differential gene expression in the sheep rumen microbiome. *Genome Res.* 24, 1517–1525. doi: 10.1101/gr.168245.113

Tapio, I., Snelling, T. J., Strozzi, F., and Wallace, R. J. (2017). The ruminal microbiome associated with methane emissions from ruminant livestock. *J. Anim. Sci. Biotechnol.* 8, 7. doi: 10.1186/s40104-017-0141-0

Thoetkiattikul, H., Mhuantong, W., Laothanachareon, T., Tangphatsornruang, S., Pattarajinda, V., and Eurwilaichitr, L., et al. (2013). Comparative analysis of microbial profiles in cow rumen fed with different dietary fiber by tagged 16s rrna gene pyrosequencing. *Curr. Microbiol.* 67, 130–137. doi: 10.1007/s00284-013-0336-3

Trevisi, E., Amadori, M., Cogrossi, S., Razzuoli, E., and Bertoni, G. (2012). Metabolic stress and inflammatory response in high-yielding, periparturient dairy cows. *Res. Vet. Sci.* 93, 695–704. doi: 10.1016/j.rvsc.2011.11.008

van Knegsel, A. T., van der Drift, S. G., Cermakova, J., and Kemp, B. (2013). Effects of shortening the dry period of dairy cows on milk production, energy balance, health, and fertility: a systematic review. *Vet. J.* 198, 707–713. doi: 10.1016/j.tvjl.2013.10.005

von Keyserlingk, M. A., Martin, N. P., Kebreab, E., Knowlton, K. F., Grant, R. J., and Stephenson, M., et al. (2013). Invited review: sustainability of the us dairy industry. *J. Dairy Sci.* 96, 5405–5425. doi: 10.3168/jds.2012-6354

Vossebeld, F., van Knegsel, A., and Saccenti, E. (2022). Phenotyping metabolic status of dairy cows using clustering of time profiles of energy balance peripartum. *J. Dairy Sci.* 105, 4565–4580. doi: 10.3168/jds.2021-21518

Walkenhorst, M., Leiber, F., Maeschli, A., Kapp, A. N., Spengler-Neff, A., and Faleschini, M. T., et al. (2020). A multicomponent herbal feed additive improves somatic cell counts in dairy cows - a two stage, multicentre, placebo-controlled long-term on-farm trial. *J. Anim. Physiol. Anim. Nutr.* 104, 439–452. doi: 10.1111/jpn.13297

Wang, H., He, Y., Li, H., Wu, F., Qiu, Q., and Niu, W., et al. (2019). Rumen fermentation, intramuscular fat fatty acid profiles and related rumen bacterial populations of holstein bulls fed diets with different energy levels. *Appl. Microbiol. Biot.* 103, 4931–4942. doi: 10.1007/s00253-019-09839-3

Wang, Y., Nan, X., Zhao, Y., Jiang, L., Wang, H., and Zhang, F., et al. (2021). Dietary supplementation of inulin ameliorates subclinical mastitis via regulation of rumen microbial community and metabolites in dairy cows. *Microbiol. Spectr.* 9:e0010521. doi: 10.1128/Spectrum.00105-21

Wathes, D. C., Cheng, Z., Bourne, N., Taylor, V. J., Coffey, M. P., and Brotherstone, S. (2007). Differences between primiparous and multiparous dairy cows in the inter-relationships between metabolic traits, milk yield and body condition score in the periparturient period. *Domest. Anim. Endocrinol.* 33, 203–225. doi: 10.1016/j.domaniend.2006.05.004

Wu, X., Chen, S., Yan, Q., Yu, F., Shao, H., and Zheng, X., et al. (2023). Gpr35 shapes gut microbial ecology to modulate hepatic steatosis. *Pharmacol. Res.* 189:106690. doi: 10.1016/j.phrs.2023.106690

Xie, F., Zhang, L., Jin, W., Meng, Z., Cheng, Y., and Wang, J., et al. (2019). Methane emission, rumen fermentation, and microbial community response to a nitrooxy compound in low-quality forage fed hu sheep. *Curr. Microbiol.* 76, 435–441. doi: 10.1007/s00284-019-01644-5

Yali, L., Yuanlong, H., Guangji, W., Xiao, Z., and Haiping, H. (2020). Gut microbial metabolites of aromatic amino acids as signals in host–microbe interplay. *Trends Endocrinol. Metab*. 31, 818–834. doi: 10.1016/j.tem.2020.02.012

Zhai, L., Huang, C., Ning, Z., Zhang, Y., Zhuang, M., and Yang, W., et al. (2023). Ruminococcus gnavus plays a pathogenic role in diarrhea-predominant irritable bowel syndrome by increasing serotonin biosynthesis. *Cell Host Microbe*. 31, 33–44. doi: 10.1016/j.chom.2022.11.006

Zhang, G., Zwierzchowski, G., Mandal, R., Wishart, D. S., and Ametaj, B. N. (2020). Serum metabolomics identifies metabolite panels that differentiate lame dairy cows from healthy ones. *Metabolomics*. 16, 73. doi: 10.1007/s11306-020-01693-z

Zinn, R. A., Owens, F. N., Stuart, R. L., Dunbar, J. R., and Norman, B. B. (1987). B-vitamin supplementation of diets for feedlot calves. *J. Anim. Sci.* 65, 9–15. doi: 10.2527/jas1987.651267x

frontiers | Frontiers in Microbiology

TYPE Original Research
PUBLISHED 27 September 2023
DOI 10.3389/fmicb.2023.1188458



OPEN ACCESS

EDITED BY
Karolina Skonieczna-Żydecka,
Pomeranian Medical University, Poland

REVIEWED BY
Kosuke Fujimoto,
Osaka Metropolitan University, Japan
Jocelyn M. Wessels,
McMaster University, Canada

*CORRESPONDENCE
Yun-Lang Cai
caiyl2021@163.com

RECEIVED 17 March 2023
ACCEPTED 08 September 2023
PUBLISHED 27 September 2023

CITATION
Ji X, Yang Q, Zhu X-L, Xu L, Guo J-Y, Rong Y and Cai Y-L (2023) Association between gut microbiota and endometriosis: a two-sample Mendelian randomization study. *Front. Microbiol.* 14:1188458. doi: 10.3389/fmicb.2023.1188458



# Association between gut microbiota and endometriosis: a two-sample Mendelian randomization study

Xuan Ji[1], Qi Yang[1], Xiu-Lin Zhu[2], Li Xu[1], Jie-Ying Guo[1], Yan Rong[1] and Yun-Lang Cai[3]*

[1]Medical School of Southeast University, Nanjing, Jiangsu Province, China, [2]Department of Obstetrics and Gynecology, Shanghai General Hospital, Shanghai, China, [3]Department of Obstetrics and Gynecology, Zhongda Hospital, Medical School of Southeast University, Nanjing, Jiangsu Province, China

**Background:** Recent studies have shown that an imbalance in gut microbiota (GM) may not always be associated with endometriosis (EMS). To investigate this further, we conducted a two-sample Mendelian randomization study.

**Methods:** MR analysis was performed on genome-wide association study (GWAS) summary statistics of GM and EMS. Specifically, the MiBioGen microbiota GWAS ($N$ = 18,340) was used as exposure. The FinnGen study GWAS (8,288 EMS cases and 68,969 controls) was used as outcome. We primarily used the inverse variance weighted (IVW) method to analyze the correlation and conducted a sensitivity analysis to verify its reliability.

**Results:** (1) MR analysis: The results of the IVW method confirmed that a total of 8 GM taxa were related to the risk of EMS. Class-*Melainabacteria* ($p$ = 0.036), family-*Ruminococcaceae* ($p$ = 0.037), and genus-*Eubacteriumruminantium* ($p$ = 0.015) had a protective effect on EMS, whereas order-*Bacillales* ($p$ = 0.046), family-*Prevotellaceae* ($p$ = 0.027), genus-*Anaerotruncus* ($p$ = 0.025), genus-*Olsenella* ($p$ = 0.036) and genus-*RuminococcaceaeUCG002* ($p$ = 0.035) could increase the risk of EMS. (2) Sensitivity analysis: Cochrane's Q test ($p$ > 0.05), MR-Egger intercept method ($p$ > 0.05), and leave-one-out method confirmed the robustness of MR results.

**Conclusion:** This study performed a MR analysis on two large national databases and identified the association between 8 GM taxa and EMS. These taxa could potentially be utilized for indirectly diagnosing EMS and could lead to novel perspectives in research regarding the pathogenesis, diagnosis, and treatment of EMS.

KEYWORDS

**endometriosis, gut microbiota, Mendelian randomization analysis, genome-wide association study, instrumental variables**

## 1. Introduction

Endometriosis (EMS) is a common benign gynecological disease, but it has similar manifestations to malignant tumors, such as hyperplasia, metastasis, and recurrence. It affects about 10% of reproductive-age women (Shafrir et al., 2018) and up to 50% of infertile women (Meuleman et al., 2009), which poses a significant global health burden.

EMS is defined as the implantation of endometrium-like tissue outside the uterus (usually including the ovary, fallopian tube, and pelvic tissue). Laparoscopy is the preferred diagnostic method, enabling a visual inspection of the affected area (Zondervan et al., 2020). Treatment includes surgical resection of the lesion and hormone drug therapy, but there are side effects and easy recurrence (Chen et al., 2018). There are many theories about the origins of endometriotic tissue. Sampson's theory of retrograde menstruation is the leading theory. However, it cannot explain why only about 10% of women with retrograde menstruation suffer from EMS (Talwar et al., 2022).

Numerous studies have indicated that an imbalance in the human gut microbiota (GM) could be a significant contributing factor to EMS. GM can affect the growth and diffusion of endometriotic tissue in various ways, as part of the endometriosis micro-environment (Salliss et al., 2021; Li et al., 2022). Leonardi et al. showed that the structure and composition of GM in patients with EMS would change significantly compared with healthy people, EMS is related to the increase of *Proteobacteria, Enterobacteriaceae*, *Streptococcus,* and *Escherichia coli (*Leonardi et al., 2020*)*. Huang et al. (2021) analyzed the composition of microbiota in the gut, cervical mucus, and peritoneal fluid of patients with EMS, and built a classifier model of EMS through a robust machine learning method. They found that GM was more conducive to the diagnosis of EMS than cervical microbiota. Hantschel et al. found that compared with healthy people, GM of patients with EMS was dominated by *Escherichia coli and Shigella* (Hantschel et al., 2019). However, these clinical observational studies cannot clarify the association between GM and EMS, because GM is affected by a variety of factors, including medicine, age, diet, etc.

Mendelian randomization (MR) analysis can reveal the causal relationship between exposure and outcome by using instrumental variables (IVs). Compared with randomized controlled studies, MR analysis can control confounding factors and reduce bias (Emdin et al., 2017). Recent studies have effectively employed MR analysis to examine the association between GM and different diseases (Chen et al., 2022; Liu et al., 2022; Shen et al., 2022). Nonetheless, the relationship between GM and EMS has not yet been investigated. In this study, we selected GM as the exposure and EMS as the outcome for MR analysis to investigate their correlation and provide a theoretical basis for further research on the pathogenesis of EMS. In addition, it can also provide new biological markers, which is helpful in formulating diagnosis and treatment strategies for EMS.

# 2. Methods

## 2.1. Study design and three assumptions of MR

We conducted a two-sample MR analysis to investigate the correlation between GM and EMS. The flowchart for the MR analysis is depicted in Figure 1. In addition, to reduce bias and obtain reliable results, we try to satisfy the following three assumptions when using MR analysis: (1) Correlation assumption: IVs are closely related to gut microbiota taxa, (2) Exclusive assumption: IVs do not affect endometriosis through other ways, and (3) Independence assumption: IVs are independent of confounding factors (Davies et al., 2018).

## 2.2. Data source and selection of IVs

### 2.2.1. Exposure data: GM

We obtained the summary-level data from a GWAS meta-analysis (data link: https://mibiogen.gcc.rug.nl). Kurilshikov et al. (2021) conducted a study on the impact of host genetics on GM composition. They collected genome-wide genotypes and 16S fecal microbiome data from 18,340 individuals across 24 cohorts based on the MiBioGen consortium. A total of 196 taxa have been included in the study, classified under five biological categories: phylum, class, order, family, and genus. It should be noted that participants of European origin were exclusively considered, and 15 GM taxa (unknown family or genus) without specific species names were excluded from the analysis.

To ensure the robustness of data and the accuracy of results, we conducted a quality inspection on the SNPs to obtain qualified IVs. Firstly, we selected IVs at $p < 1 \times 10^{-5}$ to acquire more comprehensive results (Lv et al., 2021; Liu et al., 2022). Secondly, to reduce the linkage disequilibrium (LD) between SNPs, we performed LD-clumping ($r^2 < 0.001$, distance = 10,000 kb) on all the IVs, and removed the SNPs that do not conform to the assumption. Thirdly, to prevent alleles from affecting the relationship between GM and EMS, we harmonized the exposure data and outcome data by removing palindrome SNPs.

### 2.2.2. Outcome data: EMS

We chose the most suitable GWAS from the IEU GWAS database, which we accessed on September 2022 (data link: https://gwas.mrcieu.ac.uk/). We gave priority to GWAS with a large number of samples and European descent queues. Specifically, We used the extract_outcome_Data function in R software to obtain the available complete GWAS summary statistics of EMS in the IEU GWAS database from the FinnGen cohort (GWAS ID: finn-b-N14_ENDOMETRIOSIS) (Garitazelaia et al., 2021). The FinnGen study utilized samples gathered by the National Network of the Finnish Biological Bank. They combined genomic data with EMS, consisting of 8,288 cases and 68,969 controls, and a total of 16,377,306 SNPs. In FinnGen, EMS is classified by using specific codes in the International Classification of Diseases (ICD). In ICD-10, it is defined as N80, in ICD-9 as 617, and in ICD-8 as 6,253 (Li et al., 2023).

## 2.3. Statistical analysis

We applied the "TwoSampleMR" package in the R software (Version 4.2.1) to perform all statistical analyses. We considered a correlation to be statistically significant if $p < 0.05$.

### 2.3.1. MR analysis

MR analysis was performed after selecting qualified SNPs to determine the correlation between GM and EMS. Since all GM taxa had multiple IVs, we mainly applied the inverse variance weighted (IVW) method to calculate the causal effect value between GM and EMS (Hemani et al., 2018). To determine the magnitude of the effect, the odds ratio (OR) value and 95% confidence interval (CI) are calculated. Additionally, the weighted median (WM) method (Bowden et al., 2016) and the MR-Egger test (Bowden et al., 2015) can be used as supplements to MR analysis. If the number of heterogeneous SNPs exceeds 50%, the WM result is used as a significant causal effect value.

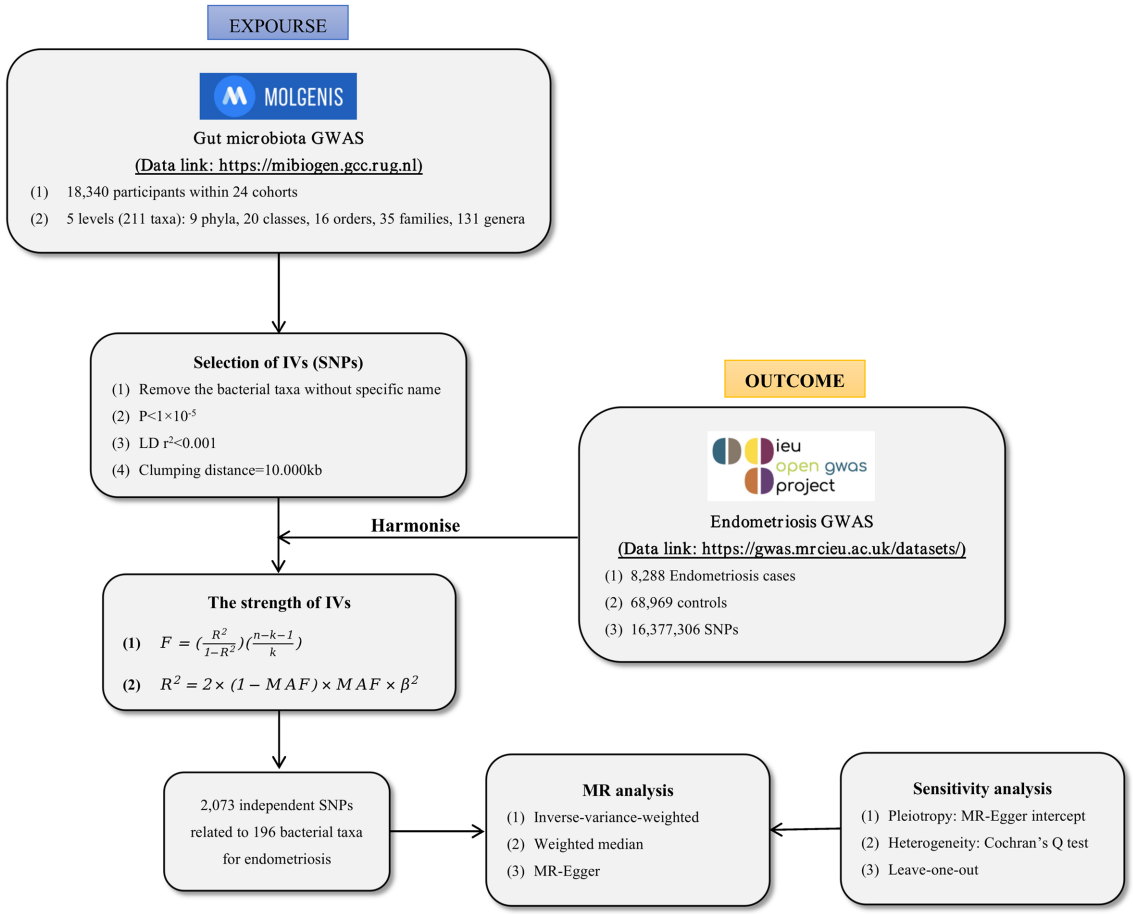


FIGURE 1
The flowchart of present MR analysis.

If the pleiotropic SNP is higher than 50%, the results of MR-Egger are still valid (Liu et al., 2022).

### 2.3.2. Sensitivity analysis

For the heterogeneity test, we utilized Cochrane's Q test. If $p > 0.05$, it is considered that there is no heterogeneity. We also employed the MR-Egger intercept method to test the pleiotropy, and the IVs with $p < 0.05$ were considered to have level pleiotropy. Furthermore, we used the leave-one-out method to detect if there was a significant association influenced by a single SNP. This method helped to further verify the robustness of our data (Xiang et al., 2021).

To test whether there were weak instrumental variables that affected the effect estimates of causality, we used F statistical to test the strength of IVs. F statistical and $R^2$ were calculated using the following equations (Palmer et al., 2012; Kamat et al., 2019).

$$F = \left(\frac{R^2}{1-R^2}\right)\left(\frac{n-k-1}{k}\right) \quad (1)$$

$$R^2 = 2\times(1-MAF)\times MAF\times\beta^2 \quad (2)$$

In the above equations, $R^2$ represents the variance explained by each IV, $n$ represents the sample size, k represents the number of IVs, and the full name of MAF is minor allele frequency.

If the results of the IVW method were statistically significant and there was an absence of heterogeneity and pleiotropy, it is reasonable to infer that GM is linked to EMS.

## 3. Results

### 3.1. Selection of IVs related to GM

After LD-clumping and palindrome removal, we identified 2,075 SNPs as IVs related to 196 taxa for EMS. The F-statistic of rs12938514 was 3.71. This SNP was included in 3 GM taxa (i.e., phylum-*Bacteroidetes*, class-*Bacteroidia*, and order-*Bacteroidales*). After removing it, The final MR analysis included 2,073 SNPs related to 196 GM taxa for EMS. All SNPs showed sufficient validity (F-statistic ranged from 12.18 to 88.43, all $F > 10$), indicating that the effect estimates of causality were unlikely to be affected by weak instrumental variables (Table 1). The key information of IVs is detailed in Supplementary Table S1.

## 3.2. Results of MR analysis

The results of the correlation between 196 GM taxa and EMS are detailed in Supplementary Table S2. After MR analysis, we determined 8 GM taxa that are relevant to the risk of EMS, composed of 1 class, 1 order, 2 families, and 4 genera (Figure 2). At the biological class classifications level, the results of the IVW method showed that *Melainabacteria* was associated with a lower risk of EMS (OR: 0.86, 95% CI: 0.75–0.99, $p = 0.036$). At the biological order classifications level, we observed that *Bacillales* was associated with a higher risk of EMS in the IVW method (OR: 1.11, 95% CI: 1.00–1.23, $p = 0.046$). At the biological family classifications level, the results of the IVW method indicated that *Prevotellaceae* could increase the risk of EMS (OR: 1.21, 95% CI: 1.02–1.42, $p = 0.027$), while *Ruminococcaceae* could reduce the risk of EMS (OR: 0.81, 95% CI: 0.66–0.99, $p = 0.037$). At the biological genus classifications level, the MR estimates of the IVW method demonstrated that *Eubacteriumruminantium* was negatively correlated with the risk of EMS (OR: 0.88, 95% CI: 0.79–0.98, $p = 0.015$), whereas *Anaerotruncus, Olsenella,* and *RuminococcaceaeUCG002* had positive associations with the risk of EMS (OR: 1.25, 95% CI: 1.03–1.53, $p = 0.025$ for *Anaerotruncus*; OR: 1.11, 95% CI: 1.01–1.22, $p = 0.036$ for *Olsenella*; OR: 1.20, 95% CI: 1.01–1.43, $p = 0.035$ for *RuminococcaceaeUCG002*).

In addition, the results of the WM method supported the relationship between *Melainabacteria, RuminococcaceaeUCG002,* and EMS (OR: 0.78, 95% CI: 0.65–0.94, $p = 0.008$ for *Melainabacteria*; OR: 1.23, 95% CI: 1.00–1.53, $p = 0.044$ for *RuminococcaceaeUCG002*). The relationship between *Ruminococcaceae* and EMS was supported by the MR-Egger test (OR: 0.54, 95% CI: 0.34–0.86, p = 0.037).

TABLE 1 The number and F-statistic range of SNPs.

| Level | Taxa | N.SNP | F- statistic range |
|---|---|---|---|
| Phylum | 9 | 101 | 16.97–58.16 |
| Class | 16 | 177 | 13.34–85.38 |
| Order | 20 | 214 | 16.53–85.37 |
| Family | 32 | 349 | 12.18–85.37 |
| Genus | 119 | 1,231 | 14.59–88.43 |
| Total | 196 | 2072 | 12.18–88.43 |

## 3.3. Results of sensitivity analysis

Supplementary Table S2 also details the results of pleiotropy and heterogeneity tests for all GM taxa. We tested the reliability of MR analysis results through sensitivity analysis (Table 2). The results of Cochran's Q test showed that there was no heterogeneity in Melainabacteria ($p = 0.301$), *Bacillales* ($p = 0.192$), *Prevotellaceae* ($p = 0.362$), *Ruminococcaceae* ($p = 0.431$), *Eubacteriumruminantium* ($p = 0.754$), *Anaerotruncus* ($p = 0.317$), *Olsenella* ($p = 0.598$), and *RuminococcaceaeUCG002* ($p = 0.071$) for EMS. Meanwhile, the MR-Egger regression method did not provide any evidence of

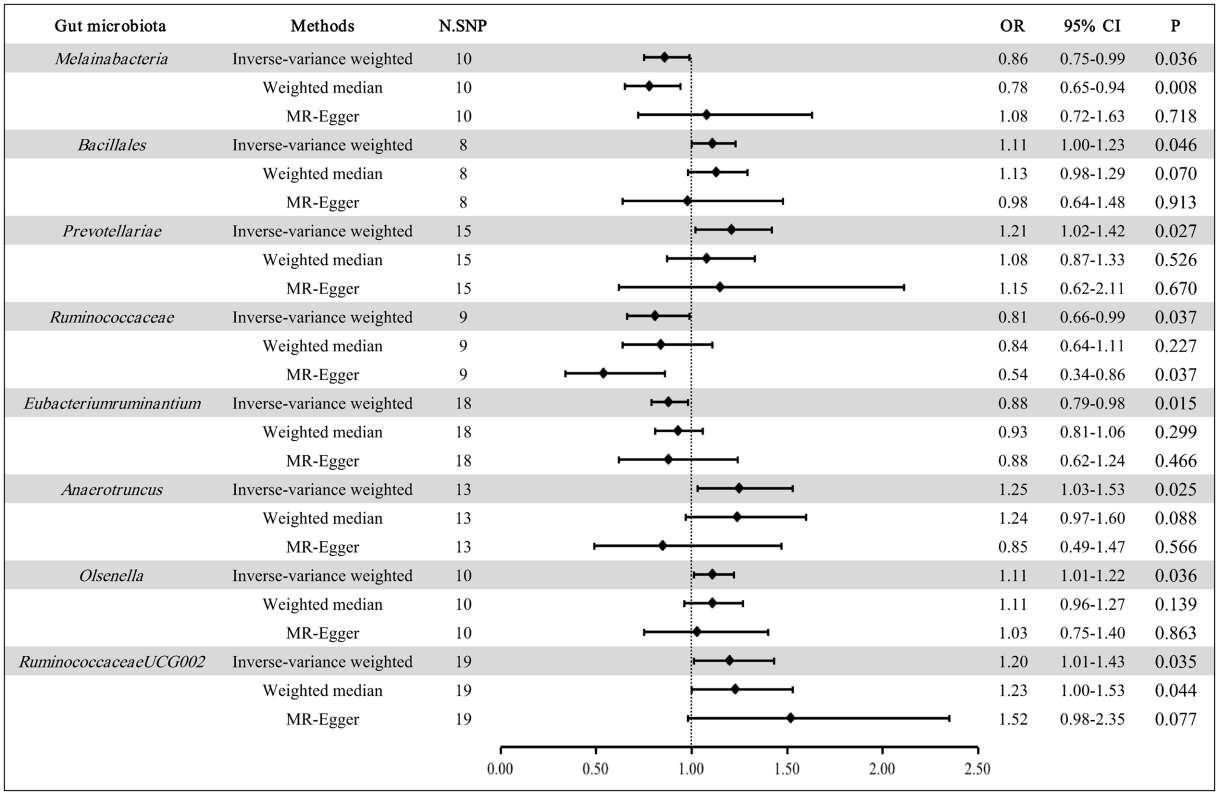


FIGURE 2
MR results of 8 GM taxa with a causal relationship to EMS.

TABLE 2 Sensitivity analysis between GM and EMS.

| Gut microbiota | MR-Egger-intercept_P | IVW_Q_P |
|---|---|---|
| *Melainabacteria* | 0.288 | 0.301 |
| *Bacillales* | 0.552 | 0.912 |
| *Prevotellariae* | 0.867 | 0.362 |
| *Ruminococcaceae* | 0.107 | 0.431 |
| *Eubacteriumruminantium* | 0.983 | 0.754 |
| *Anaerotruncus* | 0.166 | 0.317 |
| *Olsenella* | 0.629 | 0.598 |
| *RuminococcaceaeUCG002* | 0.269 | 0.071 |

pleiotropy in these GM taxa for EMS ($p = 0.288$ for *Melainabacteria*; $p = 0.552$ for *Bacillales*; $p = 0.867$ for *Prevotellaceae*; $p = 0.107$ for *Ruminococcaceae*; $p = 0.983$ for *Eubacteriumruminantium*; $p = 0.166$ for *Anaerotruncus*; $p = 0.629$ for *Olsenella*; $p = 0.269$ for *RuminococcaceaeUCG002*). In addition, the robustness of the results was further verified by the leave-one-out method (Supplementary Figures S1A–H).

Therefore, we could believe that *Melainabacteria, Bacillales, Prevotellaceae, Ruminococcaceae, Eubacteriumruminantium, Anaerotruncus, Olsenella,* and *RuminococcaceaeUCG002* were related to the risk of EMS.

## 4. Discussion

The study on the correlation between GM and EMS is affected by various confounding factors, so the conclusions of many studies are inconsistent. MR analysis can explore the causal relationship from exposure to results while controlling confounding factors (Emdin et al., 2017). Our study was the first to use a two-sample MR analysis to reveal the association between GM and EMS. By analyzing the summary statistics of GM and EMS GWAS, we identified 8 GM taxa that are associated with the risk of EMS. These findings provide important insights for the prevention and treatment of EMS.

The human gut contains a complex system of microorganisms known as microbiota that play a crucial role in maintaining human health. When there is an imbalance in the microbiota, it can lead to various diseases such as metabolic, immune, and neural-related disorders such as IBD, neurodegenerative diseases, PCOS, and EMS (Strandwitz, 2018; Zhang et al., 2021; Chadchan et al., 2022). More than 90% of GM maintaining the health and balance of the adult intestinal tract are composed of *Firmicutes, Bacteroides, Proteus,* and a small number of *Actinomycetes* (Quaranta et al., 2019). Svensson et al. (2021) used 16S rRNA sequencing to compare the GM between EMS patients and healthy people and found that the ratio of *Firmicutes* to *Bacteroides* in the case group was lower than that in the control group. On the contrary, Shan et al. (2021) found that patients with stage three or stage four EMS had a higher ratio of *Firmicutes* to *Bacteroides* than the healthy control group. In this study, *Bacillales, Ruminococcaceae, Eubacteriumruminantium,* and *RuminococcaceaeUCG002* belong to *Firmicutes*, while *Prevotellaceae* belongs to *Bacteroides*. However, the four GM taxa belonging to *Firmicutes* had opposite impacts on EMS, possibly because GM at the phylum level cover too many taxa, and the interaction between various taxa during the refinement process (e.g., the level of family and genus) may affect the observation of impacts.

In this study, *Ruminococcaceae* showed a negative correlation with the risk of EMS, which is consistent with the results of Huang et al. (2021). Huang et al. (2021) reported that the high abundance of *Ruminococcaceae* was positively correlated with the production of short-chain fatty acids (SCFA) and secondary bile acids (SBAs). In particular, butyric acid, as a SCFA, is believed to counteract gastrointestinal cancer and inflammation (Mao et al., 2021; Wozniak et al., 2022). Therefore, we hypothesize that the decrease of *Ruminococcaceae* may lead to a reduction in the concentration of protective metabolites. This reduction could lead to the development of EMS. However, the effect of butyric acid on female hormone synthesis is bidirectional. In an *in vitro* experiment conducted by Lu et al. (2017), it was discovered that at a lower concentration, butyric acid encouraged porcine granulosa cells (PGC) to secrete progesterone. However, at a higher concentration, butyric acid had a significant inhibitory effect on progesterone secretion. According to research conducted by Liu et al. (2022), it was found that premenopausal women who lack estrogen may develop nonalcoholic fatty liver disease due to the presence of butyric acid. The study also highlighted that butyric acid can regulate estrogen and progesterone levels in females. Interestingly, our study discovered a positive correlation between *RuminococcaceaeUCG002* and the risk of EMS, which contradicts the findings of *Ruminococcaceae*. We suspect that this result may be due to differences in their ability to produce butyric acid, but further investigation is needed to confirm this mechanism.

This study also found that *Eubacteriumruminantium* has the potential to lower the chances of developing endometriosis. This beneficial microbe can reduce intestinal inflammation, as well as improve conditions such as type 2 diabetes and obesity by producing SCFA. Additionally, *Eubacterium* can promote the health of both the intestines and liver by regulating bile acid metabolism (Mukherjee et al., 2020). These findings lead us to believe that *Eubacterium* may reduce the risk of EMS by producing protective metabolites and regulating the host's metabolism, immunity, and inflammation.

In recent, several studies have indicated that *Bacillus* may pose a risk for patients with encephalitis (Xu et al., 2020) and Graves disease (Yan et al., 2020) when compared to healthy individuals. Additionally, the abundance of *Bacillales* has been found to increase in those with SLE (Xiang et al., 2021), suggesting a potential role in inflammation promotion. These findings align with our research and lead us to believe that *Bacillales* may impact the progression of EMS by promoting pelvic inflammatory damage.

Research has shown that *Prevotellaceae*, a type of bacteria within the *Bacteroides* family, is linked to a higher risk of EMS. This finding aligns with the results of a study conducted by Huang et al. (2021). *Prevotellaceae* is capable of producing an enzyme called β-glucuronidase, which regulates estrogen levels and can convert bound estrogen to free estrogen. The free estrogen is then absorbed into the bloodstream through enterohepatic circulation, resulting in increased estrogen levels and the growth and shedding of ectopic endometrium (Khan et al., 2018). Additionally, *Prevotellaceae* has the potential to release lipopolysaccharide (LPS), which can activate macrophages and trigger the secretion of immune factors, ultimately promoting the proliferation of endometrial stromal cells (Sakamoto et al., 2003).

Recently, scientists have discovered non-photosynthetic *Melainabacteria* in the human gut. This research suggested that *Melainabacteria* could have a significant impact on human health. One advantage of *Melainabacteria* is that it competes for nutrients with cyanobacteria, which produce toxins that can harm the host. This competition can prevent cyanobacteria from occupying a place in the gut, thus protecting the host (Hu and Rzymski, 2022). Our study revealed that *Melainabacteria* is a protective factor against EMS and may be related to its resistance to cyanobacteria. We also found a causal relationship between *Anaerotruncus*, *Olsenella*, and EMS. *Anaerotruncus* belongs to *Verrucomicrobia*, and *Olsenella* belongs to *Actinobacteria*. Both of these bacteria increase the risk of EMS.

In our research, we made several important discoveries. Firstly, we were the first to uncover the link between GM and EMS through a two-sample MR analysis. Secondly, the GWAS database of GM that we used was the most comprehensive in recent years, covering five levels from genus to phylum. This made our study more reliable compared to smaller randomized controlled studies. Lastly, the GM taxa we found to be associated with EMS were completely different from those previously reported, which further emphasized the role of GM in EMS.

Of course, there were some limitations to our study: (1) GWAS in this study only included subjects of European descent, so the results could not be extended to other ethnic groups, (2) We were unable to determine the mutual causality between GM and EMS due to a lack of adequate IVs for reverse MR analysis, and (3) The study did not include analysis at the level of species or strains.

To sum up, we have used two large national databases (MiBioGen database $N = 18{,}340$ women; FinnGen database $N = 8{,}288$ women with EMS and 68,969 control women) and discovered a correlation between 8 GM taxa and EMS, which supports other, smaller studies demonstrating a link beween GM and EMS. The taxa we uncovered may become tools for the indirect diagnosis of EMS, while also providing new insights for further research into the pathogenesis, diagnosis, and treatment of the condition.

## Data availability statement

Publicly available datasets were analyzed in this study. This data can be found here: the summary-level data for gut microbiota can be downloaded from the MiBioGen database (data link: https://mibiogen.gcc.rug.nl) and the candidate datasets for endometriosis can be obtained from the IEU GWAS database (data link: https://gwas.mrcieu.ac.uk/).

## Author contributions

Y-LC and XJ designed this study. XJ wrote the manuscript, performed the statistical analysis, and literature search. QY, X-LZ, LX, J-YG, and YR assisted in statistical analysis, reviewed the article and provided critical feedback. Y-LC was responsible for manuscript revision. All authors contributed to the article and approved the submitted version.

## Acknowledgments

We are very grateful to FinnGen and MiBioGen Consortium for their selfless public sharing of GWAS summary data, which provides us with great convenience to carry out this research.

## Conflict of interest

The authors declare that the research was conducted in the absence of any commercial or financial relationships that could be construed as a potential conflict of interest.

## Publisher's note



## Supplementary material

The Supplementary material for this article can be found online at: https://www.frontiersin.org/articles/10.3389/fmicb.2023.1188458/full#supplementary-material

## References

Bowden, J., Davey, S. G., and Burgess, S. (2015). Mendelian randomization with invalid instruments: effect estimation and bias detection through egger regression. *Int. J. Epidemiol.* 44, 512–525. doi: 10.1093/ije/dyv080

Bowden, J., Davey, S. G., Haycock, P. C., and Burgess, S. (2016). Consistent estimation in Mendelian randomization with some invalid instruments using a weighted median estimator. *Genet. Epidemiol.* 40, 304–314. doi: 10.1002/gepi.21965

Chadchan, S. B., Singh, V., and Kommagani, R. (2022). Female reproductive dysfunctions and the gut microbiota. *J. Mol. Endocrinol.* 69, R81–R94. doi: 10.1530/JME-21-0238

Chen, I., Lalani, S., Xie, R. H., Shen, M., Singh, S. S., and Wen, S. W. (2018). Association between surgically diagnosed endometriosis and adverse pregnancy outcomes. *Fertil. Steril.* 109, 142–147. doi: 10.1016/j.fertnstert.2017.09.028

Chen, M., Xie, C. R., Shi, Y. Z., Tang, T. C., and Zheng, H. (2022). Gut microbiota and major depressive disorder: a bidirectional Mendelian randomization. *J. Affect. Disord.* 316, 187–193. doi: 10.1016/j.jad.2022.08.012

Davies, N. M., Holmes, M. V., and Davey, S. G. (2018). Reading Mendelian randomisation studies: a guide, glossary, and checklist for clinicians. *BMJ* 362:k601. doi: 10.1136/bmj.k601

Emdin, C. A., Khera, A. V., and Kathiresan, S. (2017). Mendelian Randomization. *JAMA* 318, 1925–1926. doi: 10.1001/jama.2017.17219

Garitazelaia, A., Rueda-Martínez, A., Arauzo, R., de Miguel, J., Cilleros-Portet, A., Marí, S., et al. (2021). A systematic two-sample Mendelian randomization analysis identifies shared genetic origin of endometriosis and associated phenotypes. *Life (Basel)* 11:11010024. doi: 10.3390/life11010024

Hantschel, J., Weis, S., Schäfer, K. H., Menger, M. D., Kohl, M., Egert, M., et al. (2019). Effect of endometriosis on the fecal bacteriota composition of mice during the acute phase of lesion formation. *PLoS One* 14:e0226835. doi: 10.1371/journal.pone.0226835

Hemani, G., Zheng, J., Elsworth, B., Wade, K. H., Haberland, V., Baird, D., et al. (2018). The MR-base platform supports systematic causal inference across the human phenome. *elife* 7:undefined. doi: 10.7554/eLife.34408

Hu, C., and Rzymski, P. (2022). Non-photosynthetic Melainabacteria (Cyanobacteria) in human gut: characteristics and association with health. *Life (Basel).* 12:undefined. doi: 10.3390/life12040476

Huang, L., Liu, B., Liu, Z., Feng, W., Liu, M., Wang, Y., et al. (2021). Gut microbiota exceeds cervical microbiota for early diagnosis of endometriosis. *Front. Cell. Infect. Microbiol.* 11:788836. doi: 10.3389/fcimb.2021.788836

Kamat, M. A., Blackshaw, J., Young, R., Surendran, P., Burgess, S., Danesh, J., et al. (2019). PhenoScanner V2: an expanded tool for searching human genotype-phenotype associations. *Bioinformatics* 35, 4851–4853. doi: 10.1093/bioinformatics/btz469

Khan, K. N., Fujishita, A., Hiraki, K., Kitajima, M., Nakashima, M., Fushiki, S., et al. (2018). Bacterial contamination hypothesis: a new concept in endometriosis. *Reprod. Med. Biol.* 17, 125–133. doi: 10.1002/rmb2.12083

Kurilshikov, A., Medina-Gomez, C., Bacigalupe, R., Radjabzadeh, D., Wang, J., Demirkan, A., et al. (2021). Large-scale association analyses identify host factors influencing human gut microbiome composition. *Nat. Genet.* 53, 156–165. doi: 10.1038/s41588-020-00763-1

Leonardi, M., Hicks, C., El-Assaad, F., El-Omar, E., and Condous, G. (2020). Endometriosis and the microbiome: a systematic review. *BJOG* 127, 239–249. doi: 10.1111/1471-0528.15916

Li, Y., Liu, H. Y., Ye, S. T., Zhang, B. M., Li, X. P., Yuan, J. P., et al. (2023). The effects of coagulation factors on the risk of endometriosis: a Mendelian randomization study. *BMC Med.* 21:195. doi: 10.1186/s12916-023-02881-z

Li, Y., Wang, K., Ding, J., Sun, S., Ni, Z., and Yu, C. (2022). Influence of the gut microbiota on endometriosis: potential role of chenodeoxycholic acid and its derivatives. *Front. Pharmacol.* 13:954684. doi: 10.3389/fphar.2022.954684

Liu, L., Fu, Q., Li, T., Shao, K., Zhu, X., Cong, Y., et al. (2022). Gut microbiota and butyrate contribute to nonalcoholic fatty liver disease in premenopause due to estrogen deficiency. *PLoS One* 17:e0262855. doi: 10.1371/journal.pone.0262855

Liu, B., Ye, D., Yang, H., Song, J., Sun, X., Mao, Y., et al. (2022). Two-sample Mendelian randomization analysis investigates causal associations between gut microbial genera and inflammatory bowel disease, and specificity causal associations in ulcerative colitis or Crohn's disease. *Front. Immunol.* 13:921546. doi: 10.3389/fimmu.2022.921546

Liu, K., Zou, J., Fan, H., Hu, H., and You, Z. (2022). Causal effects of gut microbiota on diabetic retinopathy: a Mendelian randomization study. *Front. Immunol.* 13:930318. doi: 10.3389/fimmu.2022.930318

Lu, N., Li, M., Lei, H., Jiang, X., Tu, W., Lu, Y., et al. (2017). Butyric acid regulates progesterone and estradiol secretion via cAMP signaling pathway in porcine granulosa cells. *J. Steroid Biochem. Mol. Biol.* 172, 89–97. doi: 10.1016/j.jsbmb.2017.06.004

Lv, W. Q., Lin, X., Shen, H., Liu, H. M., Qiu, X., Li, B. Y., et al. (2021). Human gut microbiome impacts skeletal muscle mass via gut microbial synthesis of the short-chain fatty acid butyrate among healthy menopausal women. *J. Cachexia. Sarcopenia Muscle* 12, 1860–1870. doi: 10.1002/jcsm.12788

Mao, J., Wang, D., Long, J., Yang, X., Lin, J., Song, Y., et al. (2021). Gut microbiome is associated with the clinical response to anti-PD-1 based immunotherapy in hepatobiliary cancers. *J. Immunother. Cancer* 9:e003334. doi: 10.1136/jitc-2021-003334

Meuleman, C., Vandenabeele, B., Fieuws, S., Spiessens, C., Timmerman, D., and D'Hooghe, T. (2009). High prevalence of endometriosis in infertile women with normal ovulation and normospermic partners. *Fertil. Steril.* 92, 68–74. doi: 10.1016/j.fertnstert.2008.04.056

Mukherjee, A., Lordan, C., Ross, R. P., and Cotter, P. D. (2020). Gut microbes from the phylogenetically diverse genus Eubacterium and their various contributions to gut health. *Gut Microbes* 12:1802866. doi: 10.1080/19490976.2020.1802866

Palmer, T. M., Lawlor, D. A., Harbord, R. M., Sheehan, N. A., Tobias, J. H., Timpson, N. J., et al. (2012). Using multiple genetic variants as instrumental variables for modifiable risk factors. *Stat. Methods Med. Res.* 21, 223–242. doi: 10.1177/0962280210394459

Quaranta, G., Sanguinetti, M., and Masucci, L. (2019). Fecal microbiota transplantation: a potential tool for treatment of human female reproductive tract diseases. *Front. Immunol.* 10:2653. doi: 10.3389/fimmu.2019.02653

Sakamoto, Y., Harada, T., Horie, S., Iba, Y., Taniguchi, F., Yoshida, S., et al. (2003). Tumor necrosis factor-alpha-induced interleukin-8 (IL-8) expression in endometriotic stromal cells, probably through nuclear factor-kappa B activation: gonadotropin-releasing hormone agonist treatment reduced IL-8 expression. *J. Clin. Endocrinol. Metab.* 88, 730–735. doi: 10.1210/jc.2002-020666

Salliss, M. E., Farland, L. V., Mahnert, N. D., and Herbst-Kralovetz, M. M. (2021). The role of gut and genital microbiota and the estrobolome in endometriosis, infertility and chronic pelvic pain. *Hum. Reprod. Update* 28, 92–131. doi: 10.1093/humupd/dmab035

Shafrir, A. L., Farland, L. V., Shah, D. K., Harris, H. R., Kvaskoff, M., Zondervan, K., et al. (2018). Risk for and consequences of endometriosis: a critical epidemiologic review. *Best Pract. Res. Clin. Obstet. Gynaecol.* 51, 1–15. doi: 10.1016/j.bpobgyn.2018.06.001

Shan, J., Ni, Z., Cheng, W., Zhou, L., Zhai, D., Sun, S., et al. (2021). Gut microbiota imbalance and its correlations with hormone and inflammatory factors in patients with stage 3/4 endometriosis. *Arch. Gynecol. Obstet.* 304, 1363–1373. doi: 10.1007/s00404-021-06057-z

Shen, W. D., Lin, X., Liu, H. M., Li, B. Y., Qiu, X., Lv, W. Q., et al. (2022). Gut microbiota accelerates obesity in peri−/post-menopausal women via Bacteroides fragilis and acetic acid. *Int. J. Obes.* 46, 1918–1924. doi: 10.1038/s41366-022-01137-9

Strandwitz, P. (2018). Neurotransmitter modulation by the gut microbiota. *Brain Res.* 1693, 128–133. doi: 10.1016/j.brainres.2018.03.015

Svensson, A., Brunkwall, L., Roth, B., Orho-Melander, M., and Ohlsson, B. (2021). Associations between endometriosis and gut microbiota. *Reprod. Sci.* 28, 2367–2377. doi: 10.1007/s43032-021-00506-5

Talwar, C., Singh, V., and Kommagani, R. (2022). The gut microbiota: a double-edged sword in endometriosis. *Biol. Reprod.* 107, 881–901. doi: 10.1093/biolre/ioac147

Wozniak, H., Beckmann, T. S., Fröhlich, L., Soccorsi, T., le Terrier, C., de Watteville, A., et al. (2022). The central and biodynamic role of gut microbiota in critically ill patients. *Crit. Care* 26:250. doi: 10.1186/s13054-022-04127-5

Xiang, K., Wang, P., Xu, Z., Hu, Y. Q., He, Y. S., Chen, Y., et al. (2021). Causal effects of gut microbiome on systemic lupus erythematosus: a two-sample Mendelian randomization study. *Front. Immunol.* 12:667097. doi: 10.3389/fimmu.2021.667097

Xu, R., Tan, C., He, Y., Wu, Q., Wang, H., and Yin, J. (2020). Dysbiosis of gut microbiota and short-chain fatty acids in encephalitis: a Chinese pilot study. *Front. Immunol.* 11:1994. doi: 10.3389/fimmu.2020.01994

Yan, H. X., An, W. C., Chen, F., An, B., Pan, Y., Jin, J., et al. (2020). Intestinal microbiota changes in Graves' disease: a prospective clinical study. *Biosci. Rep.* 40:undefined. doi: 10.1042/BSR20191242

Zhang, Z. J., Qu, H. L., Zhao, N., Wang, J., Wang, X. Y., Hai, R., et al. (2021). Assessment of causal direction between gut microbiota and inflammatory bowel disease: a Mendelian randomization analysis. *Front. Genet.* 12:631061. doi: 10.3389/fgene.2021.631061

Zondervan, K. T., Becke, C. M., and Missmer, S. A. (2020). Endometriosis. *N. Engl. J. Med.* 382, 1244–1256. doi: 10.1056/NEJMra1810764

frontiers | Frontiers in Microbiology

TYPE Original Research
PUBLISHED 06 October 2023
DOI 10.3389/fmicb.2023.1240891



OPEN ACCESS

EDITED BY
Rebeca Martín,
INRAE Centre Jouy-en-Josas, France

REVIEWED BY
Vijay Kumar Chava,
Bhagwan Mahavir Medical Research Centre, India
Jôice Dias Corrêa,
Pontifical Catholic University of Minas Gerais, Brazil

*CORRESPONDENCE
Aurea Simon-Soro
✉ asimon@us.es

RECEIVED 15 June 2023
ACCEPTED 18 September 2023
PUBLISHED 06 October 2023

CITATION
Saúco C, Rus MJ, Nieto MR, Barros C, Cantiga-Silva C, Lendines-Cordero D, Calderer-Ortiz M, Zurita-García M, Arias-Herrera S, Monsalve-Guil L, Segura-Egea JJ and Simon-Soro A (2023) Hyposalivation but not Sjögren's syndrome associated with microbial dysbiosis in women. *Front. Microbiol.* 14:1240891. doi: 10.3389/fmicb.2023.1240891



# Hyposalivation but not Sjögren's syndrome associated with microbial dysbiosis in women

Carlos Saúco[1], Maria J. Rus[1], María R. Nieto[1], Carolina Barros[2], Cristiane Cantiga-Silva[2], Débora Lendines-Cordero[3], Marta Calderer-Ortiz[1], Miriam Zurita-García[1], Santiago Arias-Herrera[4], Loreto Monsalve-Guil[1], Juan José Segura-Egea[1] and Aurea Simon-Soro[1]*

[1]Department of Stomatology, Faculty of Dentistry, University of Seville, Seville, Spain, [2]Department of Preventive and Restorative Dentistry, Dental School, São Paulo State University (UNESP), Araçatuba, Brazil, [3]Instituto Para el Estudio de la Biología de la Reproducción Humana (INEBIR), Seville, Spain, [4]Department of Dentistry, Faculty of Health Sciences, Universidad Europea de Valencia, Valencia, Spain

**Background:** Saliva modulates the environment of the oral biofilm through pH buffer, microbial attachment to host surfaces, and nutritional source. The ecology of stress occurs when a physical factor adversely impacts an ecosystem or its biotic components. Therefore, reduced salivary flow can affect oral-host balance. The leading causes of hyposalivation include disease-associated Sjögren's syndrome (SS) and menopausal women as aging-associated. However, little is known about the oral microbiome integrated with sex hormones in hyposalivation. This study aimed to characterize the hyposalivation microbiome caused by aging or disease affecting the salivary glands in women.

**Methods:** We included 50 women older than 40 years of age in any menopausal phase. We collected stimulated saliva from 25 women diagnosed with SS (SS) and 25 without SS (non-SS). The bacterial profile of the patients was obtained by 16S rRNA sequencing. Bioinformatics analysis used machine learning to analyze the cohort's signs, symptoms, and bacterial profile. Salivary estradiol as a sex hormone variation level was determined.

**Results:** We obtained that 79% of the SS group, and 52% of the non-SS group had hyposalivation. We found a negatively correlated *Prevotella*-age and *Rothia*-estradiol in the SS group. Highlight, we found that the cause of the hyposalivation in the study did not explain differences in microbial diversity comparing non-SS and SS groups. Therefore, microbial communities found in hyposalivation but not related to systemic conditions suggest that changes in the oral environment might underpin host-microbial balance.

**Conclusion:** The salivary microbiome was similar in women with and without SS. However, hyposalivation showed two distinctive clusters associated with the bacterial population profiles. Our study suggests that local ecological disturbances could drive the change in the microbiome.

KEYWORDS

**hyposalivation, Sjögren's syndrome, aging, saliva, estrogen, *Prevotella*, women's health**

# 1. Introduction

Hyposalivation is the condition characterized by a reduced production of saliva, which can be caused by several disorders (Smith et al., 2007; Einhorn et al., 2020). Hyposalivation has an overall prevalence of approximately 22%, with a higher incidence in women than in men and increases with age (Agostini et al., 2018; Pina et al., 2020; Pérez-Jardón et al., 2022). Reduced saliva production can be caused by various disorders, including pathological or age-related factors, as reported in previous studies (Ogle, 2020; Pina et al., 2020). Pathological hyposalivation can be triggered by autoimmune diseases such as Sjögren's syndrome or Mikulicz Syndrome, as well as by Parkinson's disease and the formation of neoplasms or bacterial infections of the salivary glands, leading to obstruction (sialadenitis) (Ogle, 2020). Age-related hyposalivation is linked to polymedication, with different drugs found to be associated with salivary gland dysfunction (Einhorn et al., 2020; Pina et al., 2020). Aging patients often report subjective symptoms of this condition, known as xerostomia (Smith et al., 2007; Pérez-Jardón et al., 2022). Saliva has many functions in the oral cavity that include moistening, lubrication, and protection of the oral cavity and esophagus, digestion, tasting, and smelling. It also plays a crucial role in maintaining oral health due to the presence of antimicrobial substances that maintain oral microbiome homeostasis (Holmberg and Hoffman, 2014; Dawes et al., 2015; Marsh et al., 2016). Therefore, salivary flow reduction can also affect microbial colonization, which ultimately contributes to biofilm formation (Marsh et al., 2016).

The oral cavity contains a diverse microbial community, consisting of more than 750 identified bacterial species (Human Oral Microbiome Database, n.d.). This community undergoes compositional changes over time, with the most distinct differences seen between childhood and late adulthood, and a stable period in between (Willis et al., 2022). A lower diversity of microbiota was found in elderly people and several taxa had been associated with age (Schwartz et al., 2021; Wells et al., 2022). A disruption in the balance of the oral microbial community can lead to dysbiosis, whether caused by an overgrowth of microorganisms or changes in the local host response. The dysbiotic state creates an environment that facilitates the development of disease (Roberts and Darveau, 2015). Notably, oral dysbiosis has been linked not only to oral diseases, such as caries and periodontal diseases but also to systemic health issues (Peng et al., 2022). For instance, the oral microbiome has been linked to rheumatoid arthritis and pulmonary diseases such as asthma, lung cancer, or pneumonia (Pathak et al., 2021; Sedghi et al., 2021).

Several factors can affect microbial populations in the oral cavity, including disease status, menstrual status, and salivary flow rate. For example, hyposalivation-affected individuals have been found to have an altered oral microbiome compared to those with normal salivary flow (Rusthen et al., 2019). Studies have also shown that SS can affect microbiome composition, with changes observed in the relative abundance of certain bacterial groups (Rusthen et al., 2019; Singh et al., 2021). However, the specific effects of SS on the oral microbiome are not yet fully understood, as conflicting results have been reported in the literature (Rusthen et al., 2019; Sharma et al., 2020; Singh et al., 2021). Menstrual status is a well-known factor that can cause significant changes in the vaginal microbiota (Farage et al., 2010). Studies have shown that it can also affect the oral microbiota by altering its richness and diversity during different menstrual phases (Krog et al., 2022). These changes are largely driven by estrogen, a hormone that is known to play a key role in the menstrual cycle. This hormone has been linked to the capacity of bacteria to coaggregate and participate in biofilm formation (Fteita et al., 2014).

In this study, we investigated the relationship between oral microbiota and hyposalivation in aging women considering different conditions such as menstrual state, hyposalivation, and SS. We collected clinical data and oral samples from these patients to analyze the bacteriome of their oral microbiota using 16S rRNA sequencing. The goal of this investigation was to identify potential microbial markers of these conditions and to elucidate the mechanisms linking oral microbiota dysbiosis with salivary gland hypofunction. This study could provide information on the role of the oral microbiota in systemic health and help identify new targets for the diagnosis and treatment of oral health related to women.

# 2. Materials and methods

## 2.1. Study design and sample selection

This is a case–control study conducted in the Dental Schools of the University of Seville and the European University of Valencia from January 2020 to June 2021. Saliva samples and clinical data were collected from a cohort of 25 women with Sjögren's syndrome and 25 controls of the same age and sex. The inclusion criteria were women between 40 and 70 years of age diagnosed with Sjögren syndrome according to the AEGG and ACR-EULAR 2016 guidelines. Exclusion criteria included incapacitating disease for independent collection of clinical data or biological samples, age less than 40 or over 70 years, antibiotics or antifungals in the last 3 months before sample collection, or mouthwashes with oral antiseptics in the month before sampling. Men and women who, according to the inclusion criteria, did not sign the informed consent for the study were also excluded. Subject recruitment was carried out between patients at the dental clinic of the Faculty of Dentistry of the University of Seville and the European University of Valencia.

## 2.2. Sample collection

Two saliva samples per patient were collected to determine pH, salivary flow rate, and estradiol levels, and to sequence the oral microbiome. First, saliva by drooling (SA), in a 50 mL sterile tube for 5 min. Subsequently, saliva was stimulated saliva (ST) by chewing paraffin pellets, in another 50 mL sterile tube for 5 min (Alvariño et al., 2021). The samples were kept at −80° C until processing.

## 2.3. Salivary measurement assays

The salivary flow was measured by decantation in a calibrated test tube for SA and ST. A normal salivary flow rate was established at

Abbreviations: SS, Sjögren's syndrome; SA, unstimulated saliva; ST, stimulated saliva; Normo, normosalivation; Hypo, hyposalivation; PRE, premenopause; POST, postmenopause; ER, estrogen receptor.

0.3 mL/min for SA and 1.5 mL/min for ST (Bartold et al., 2017). The salivary pH was determined in ST with a pH meter (Crison Basic 20). Estrogen levels were obtained using ST sample using an enzyme immunoassay kit for measuring salivary 17-β estradiol following the manufacturer's recommended protocol (Salimetrics. State College, PA). The assays were performed in duplicate with the average of the duplicate results used in the analyzes. Salivary estradiol values were measured in picograms per milliliter. Several samples were not measured for the estradiol assay due to the limited volume of saliva in subjects with extreme hyposalivation (7 samples). The other 3 samples were measured but obtained values below the detection limit. The normal levels of salivary estradiol ranged from 8–10 pg./mL based on the literature (Gavrilova and Lindau, 2009; Kozloski et al., 2014).

## 2.4. Collecting clinical data

To ensure consistency and standardization of sampling and oral clinical data collection, participating dentists underwent extensive calibration training sessions. These sessions were designed to align their sampling techniques, methodologies, and clinical criteria, thereby guaranteeing uniformity in the data collection process. Cohen's Kappa statistics were obtained for the degree of concordance between examiners (k = 0 0.83–0.71).

Oral and dental clinical data collection was based on oral mucosal examination and assessment of dental and periodontal status using a dental examination kit, dental mirror, caries probe, and millimeter periodontal probe. First, the alterations observed in oral structures covered by mucosa were recorded, specifying their location. Next, using the dental mirror and caries probe, the dental status was evaluated according to the DMFT index (Fejerskov and Kidd, 2008). This involved documenting the presence of caries lesions, fillings, tooth loss, fissures, fractures, hypoplasias, abutment teeth, dental crowns, and unerupted teeth. Periodontal status was determined through the Basic Periodontal Exam which provides a basis for a simple and fast examination and allows the evaluation of treatment needs (Dietrich et al., 2019). For data collection, the dentition is divided into canine-limited sextants, without recording the third molars. Sextants with only one tooth are excluded and the tooth is added to the adjacent sextant. The millimetered periodontal probe is introduced between the tooth and the gingiva to determine the depth of the gingivodental sulcus relative to the level of the gingival margin. Six probing points are performed on each tooth: mesial, midpoint, and distal of the vestibular and palatal/lingual side. The presence of dental calculus or other plaque retention factors is also assessed.

For coding purposes in the Basic Periodontal Exam, code 0 is assigned to sextants that do not have pockets of 4 mm or deeper, there is no calculus, overhanging fillings, and no bleeding after probing. Code 1 is for the sextants that, under these healthy conditions, show bleeding after probing. Code 2 is assigned to the sextants where dental calculus or other plaque retention factors such as overhanging fillings are observed. Code 3 is given to the sextant where the maximum probing depth in one or more teeth is between 4–6 mm. Code 4 is when one or more teeth have a probing depth greater than 6 mm. The * code is given to the sextant where there is an attachment loss of 7 mm or more, or if furcation involvement exists. Each sextant is assigned the highest value obtained.

Based on this scoring, the need for treatment is determined. The management of sextants with codes 0, 1, and 2 is as follows: Code 0, no treatment is required. Code 1 can be managed through oral hygiene instructions and supragingival prophylaxis. For Code 2, oral hygiene instructions, supragingival and selected subgingival prophylaxis, and removal of overhanging fillings are needed. In the presence of code 3, 4, or *, a thorough periodontal examination (periodontogram, plaque index, gingival index, tooth mobility, and panoramic radiography) is required for further information. Clinical management will consist of full-mouth prophylaxis and scaling and root planing for sextants with code 3. Patients with sextants scored as Code 4 or * will need comprehensive supragingival and subgingival prophylaxis, scaling and root planing, and periodontal surgery, with a continued emphasis on plaque control.

The basic health questionnaire was designed to collect the medical and pharmacological history of the participants and other aspects of their lifestyle, exercise, diet, toxic habits (tobacco and alcohol), and coffee. A menopause questionnaire was also included to determine the stage of menopause and the use of hormone therapy after the international classification of menopausal stages, premenopause (periodical menses), perimenopause (no periodical menses for the last 12 months), postmenopause (menses cessation >12 months) (The North American Menopause Society, 2023).

## 2.5. DNA extraction and 16S amplification

Microbial DNA was extracted from samples using the DNeasy Powersoil Pro Kit (Qiagen) following the manufacturer's instructions. The input gDNA 2 ng was amplified by PCR with 5x reaction buffer, 1 mM of dNTP mix, 500 nM each of the universal F/R PCR primer, and Herculase II fusion DNA polymerase (Agilent Technologies, Santa Clara, CA). The cycle condition for the 1st PCR was 3 min at 95 ° C for heat activation, and 25 cycles of 30 s at 95°C, 30 s at 55 ° C, and 30 s at 72°C, followed by a final extension of 5 min at 72 ° C. Sequencing libraries were prepared by amplifying the V3-V4 region of the 16S rRNA gene using the universal F/R PCR primer (Fw: 5'-TCGTCGGCAGCGTCAGATGTGTATAAGAGACAGCCTACGGGNGGCWGCAG; Rv: 5'-GTCTCGTGGGCTCGGAGATGTGTATAAGAGACAGGACTACHVGGGTATCTAATCC). The amplicons were purified with AMPure beads (Agencourt Bioscience, Beverly, MA). The purified product was quantified using qPCR according to the qPCR Quantification Protocol Guide (KAPA Library Quantification kits for Illumina Sequencing platforms) and qualified using TapeStation D1000 ScreenTape (Agilent Technologies, Waldbronn, Germany). Sequencing was performed using the MiSeqTM platform (Illumina, San Diego, United States). We included 3 samples as negative controls to test the contamination from DNA extraction reagents. Also, we sequenced a positive control using ZymoBIOMICS Microbial Community DNA Standard II (ZYMO) to test the amplification and microbial analysis procedure.

## 2.6. Bacteriome analysis

Microbiome analysis was performed with the bioinformatics platform QIIME2 v.2022.8.3 (Bolyen et al., 2019). Raw 16S rRNA gene sequences were quality filtered, denoised, and dereplicated with DADA2

using the denoise-paired plugin, designed for paired-end demultiplexed sequences (Callahan et al., 2016). Due to a decrease in quality, the forward and reverse read sequences were truncated at positions 278 and 205, respectively. The first 21 bases of the 5′ end of the sequences were also trimmed because of the low quality. Sequences with a Phred quality score below 20 were excluded from downstream analyzes. The amplified sequence variants (ASVs) obtained were aligned with the Greengenes 13_8 99% OTU reference sequence database using the classify sklearn Naive Bayes taxonomy classifier (McDonald et al., 2012; Bokulich et al., 2018). Alpha and Beta diversity was explored from a phylogenetic tree constructed with the Fasttree method based on the alignment of ASVs obtained with Mafft (Price et al., 2010; Katoh and Standley, 2013). Diversity metrics (Faith's phylogenetic diversity, UniFrac distance, Jaccard distance, and Bray–Curtis dissimilarity) were estimated using a diversity plugin at a sampling depth of 1,670 sequences per sample. Statistical analysis was carried out using R v4.2.2 (R Foundation for Statistical Computing, Austria, 2022). To assess the association between microbial and clinical variables, library rstatix v0.7.2 was used. Ggpubr v0.6.0 was used for the correlation coefficient using Pearson and the significance level. For alpha diversity, pairwise Wilcoxon rank sum between disease groups and salivary flow in Richness and Shannon indexes were considered. To analyze the differences between the disease and salivary flow groups in Beta diversity, a Permutational Multivariate Analysis of Variance (Anderson, 2017) was used. Library cluster v2.1.4 was installed to analyze the partition around medoids (Kaufman and Rousseuw, 1990).

# 3. Results

## 3.1. Hyposalivation in women over 40 years of age

To understand the relationship between hyposalivation and the oral microbiome in women, we collected saliva samples from 50 women over 40 years old. Of the total of 50 women, half were diagnosed with the known autoimmune disease Sjogren's syndrome affecting the salivary glands (Figure 1A). We also collected medical data, oral clinical exam, salivary estradiol, and pH that allowed us to correlate the microbial profile with the oral ecological aspects of the oral fluid (Table 1).

First, we analyzed the salivary flow of the women included in this study to measure SA and ST. When we associated saliva types with age, we obtained a negative correlation of ST flow and age but not in SA flow suggesting that saliva production could be affected after stimuli (Figure 1B, $R = -0.39$, $p = 0.005$). Focusing on disease groups, we found an uneven distribution of reduced saliva flow rate (Hypo) in both saliva collected types (Figure 1C). In the non-SS group, the study population was distributed 43% in SA and 53% in ST, while SS had 76% in SA and 92% in ST had reduced salivary flow rate (Hypo). Therefore, SS had accumulative factors of disease and aging that could affect salivary gland tissue and function, resulting in the reduction of SA and ST.

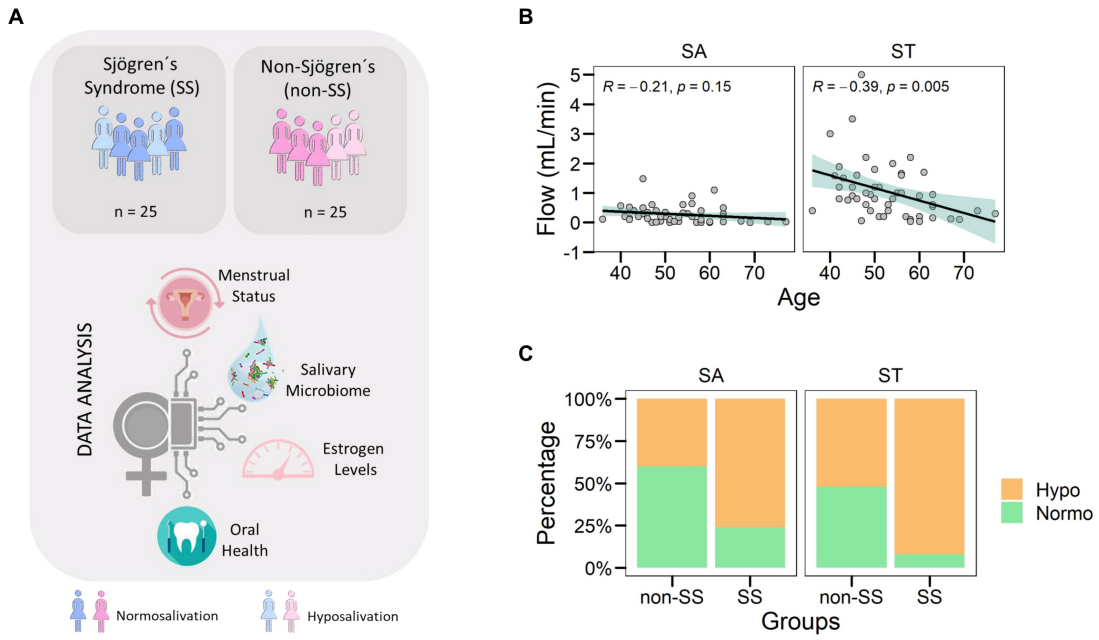


FIGURE 1
Hyposalivation in women over 40 years old. **(A)** Diagram showing the study workflow. Saliva samples were taken from a total of 50 women, 25 of them diagnosed with SS. After DNA extraction and sequencing, the microbiome population was obtained. Data were analyzed considering clinical data, disease condition, and age. **(B)** The correlation between age and salivary flow was assessed for both types of saliva collected. Each point corresponds to a sample. The green area corresponded to the 95% confidence interval of the linear model. **(C)** Distribution of samples by salivary types (SA and ST) and disease groups (non-SS and SS). The colors corresponded to salivary flow categories such as hyposalivation (Hypo) in yellow and normosalivation (Normo) in green.

## 3.2. Saliva microbiome in aging and disease

Hyposalivation not only reduces saliva volume but also might affect the biotic components of the oral cavity as its microbial community. To determine the microbiome in hyposalivation, we analyzed the stimulated saliva bacterial profile of the women included in the study. The microbial composition in hyposalivation (Hypo) and normosalivation (Normo) showed that the oral genera *Prevotella*, *Neisseria*, and *Rothia* highlighting *Streptococcus* are the most abundant taxa with 44% as the mean. When we characterized the bacteriome that separates women with SS, we found 16 and 10% for *Prevotella* for Hypos and Normo, respectively. However, the abundance of *Prevotella* decreased in the non-SS group by up to 8 and 7% for Hypo and Normo, respectively (Figure 2A). Then, our data showed a higher abundance of *Prevotella* related to SS condition.

TABLE 1 Characteristics of the study population.

| Variable | Women | Women SS | *p* |
|---|---|---|---|
| Age (mean (SD)) | 51.32 (6.21) | 54.44 (10.74) | 0.216 |
| Estradiol (mean (SD)) | 0.98 (0.90) | 0.77 (1.00) | 0.482 |
| SA (mean (SD)) | 0.40 (0.34) | 0.14 (0.18) | 0.002** |
| ST (mean (SD)) | 1.46 (1.14) | 0.63 (0.47) | 0.002** |
| *Menstrual status* | | | |
| Premenopause | 11 (44) | 11 (44) | |
| Postmenopause | 14 (56) | 14 (56) | |

Median, standard deviation and value of p of age, estrogen levels, SA, and ST. The distribution of patients with respect to their menstrual status is also included. (%) unless otherwise noted. SA, non-stimulated saliva; ST, stimulated saliva; SD, standard deviation.

Next, we analyze the alpha diversity of saliva flow and disease groups that showed no significant differences in richness or diversity for any of the groups (Figure 2B, $p > 0.05$). To assess whether the bacterial community was defined by saliva flow or disease in women, we analyzed beta diversity using weighted Unifrac distances (Figure 2C). We found a microbial community associated with saliva flow, while the diagnosis of Sjögren did not show a significant distribution ($p = 0.001$ and $p = 0.35$, respectively, PERMANOVA). Therefore, our results showed that the salivary bacterial community was independent of Sjögren's syndrome. However, *Prevotella* and *Streptococcus* might be associated with a disease.

## 3.3. *Streptococcus* and *Prevotella* defined microbial clusters

To assess the microbial profile of our cohorts independently of specific clinical features, we used an unsupervised classification method partition around medoids (Shi et al., 2022). The best number of k-medoids or clusters found in our data was k = 2 (Figure 3A). We obtained the main microorganisms separating the main 2 dimensions using Principal Component Analysis (Figure 3B). As a result, we obtained the main taxa separating the dimensions as *Streptococcus*, *Rothia*, *Granullicatella*, *Prevotella*, and *Fusobacteriaceae*. The bacterial genus Streptococcus (cursive) was associated with cluster 1 (Figure 3C left panel, $p < 0.001$) while *Prevotella* was associated with group 2 (Figure 3C right panel, $p < 0.01$). However, other taxa did not show significant differences in the cluster distribution. In particular, the non-SS group had a higher proportion of Streptococcus, while the SS group showed a higher proportion of *Prevotella*, as depicted in Figure 2A. Thus, intrinsic

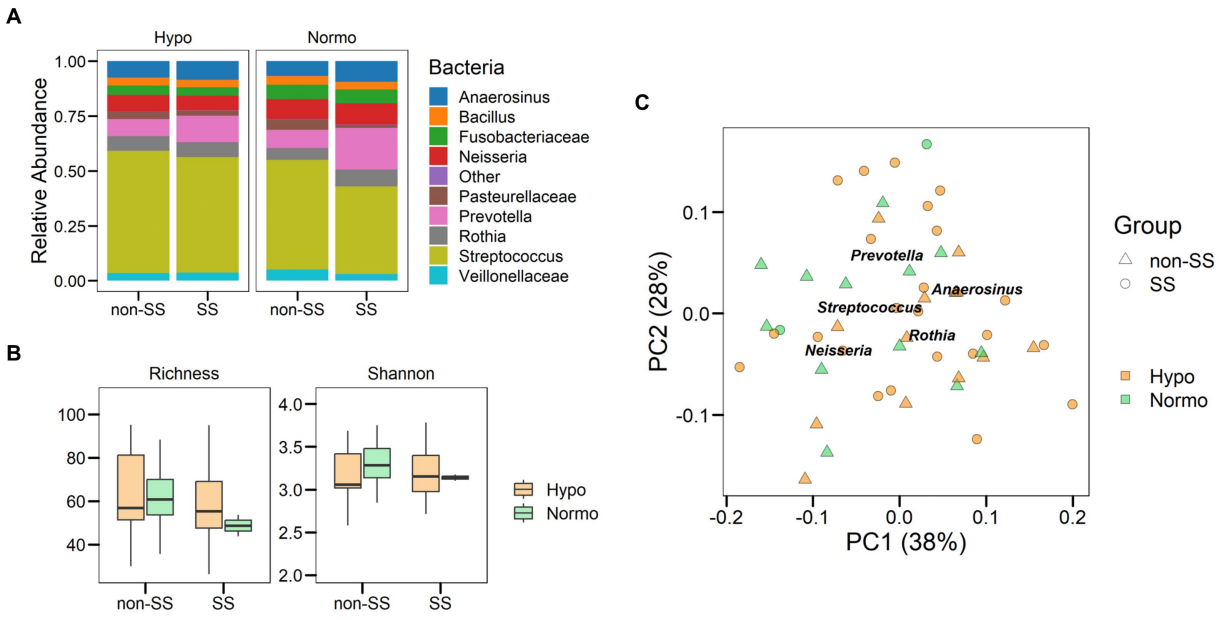


FIGURE 2
Saliva microbiome in aging and disease. **(A)** Relative abundance of bacterial taxa in Hypo and Normo as saliva flow categories considering SS and non-SS groups. Comparison of the abundances of the ten predominant bacteria detected after microbiome analysis with the relative abundance shown as a ratio. **(B)** Boxplot showing the alpha diversity richness and Shannon index. **(C)** Principal coordinate analysis showing the bacterial distribution according to health status and salivary condition. PC1 and PC2 explained 39 and 27% of the variance observed in the oral microbiome, respectively.

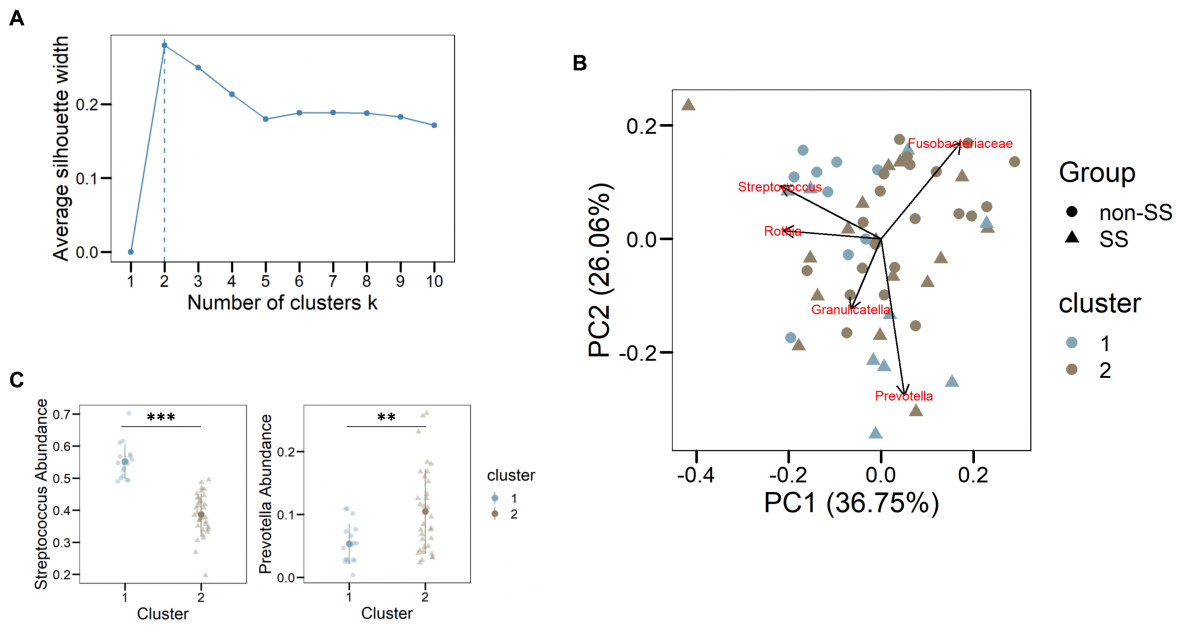


FIGURE 3
*Streptococcus* and *Prevotella* defined microbial clusters. **(A)** Number of clusters corresponding to the distribution of the oral microbiome according to PAM. The highest average silhouette width is found for two clusters, meaning that the best aggrupation is found for two clusters. **(B)** Principal component analysis with the distribution of the main bacterial taxa. The colors corresponded to the clusters assigned for each sample **(C)** Cluster distribution for the genera *Streptococcus* and *Prevotella* using the abundance of bacteria. ** <0.01, *** <0.001.

factors related to the host such as aging, disease, or salivary estradiol might condition the oral ecology and subsequently the salivary microbiome.

## 3.4. Oral ecological factors could explain *Prevotella* and *Rothia* modulation in women with Sjögren's syndrome

We investigate whether oral ecological factors explained the variation in microbial age or disease. First, we analyzed the correlation of salivary flow with bacterial abundance. It is important to emphasize that Sjögren's syndrome might affect the salivary glands. However, this finding strengthens the idea that *Prevotella* was associated with the SS environment even though 92% of the SS patients suffered hyposalivation. It should be noted that *Prevotella* is a known bacterial taxon associated with periodontal disease (Socransky et al., 1998). To investigate the association of *Prevotella* with periodontal disease, we analyzed the periodontal status of women and their relationship with the bacterial taxon (Figure 4A). We found that severe periodontal conditions (codes 3 and 4) were not significantly different from mild periodontal conditions (codes 1 and 2) in women. However, we found that individuals with healthy periodontium had a lower abundance of *Prevotella* compared to periodontal condition only in the SS group, but not significant. Highlight, *Prevotella* decreased with age in the SS group ($R = -0.48$, $p = 0.016$) but varied independently in the non-SS group (Figure 4B, $R = 0.12$, $p = 0.58$).

The oral microbial community can be modulated by intrinsic factors such as salivary estradiol. Therefore, variation in the concentration of the sex hormones might affect the microorganisms harbored in the oral cavity. Since our population was women over 40 years of age and hormones might decrease aging-related, we measured the concentration of salivary estradiol. We classified the menstrual status of women in premenopausal (PRE) and postmenopausal (POST) (Figure 4C). We found that salivary estradiol concentration in women was not significantly different for menstrual status ($p = 0.66$). The genus *Rothia* was negatively correlated with salivary estradiol only in women affected by Sjögren's syndrome, suggesting that autoimmune disease could affect oral bacteria (Figure 4D, $R = -0.64$, $p = 0.026$). However, *Streptococcus* was not correlated with salivary estradiol for both groups. Overall, we observed that *Prevotella* increased with saliva flow and periodontal status but decreased with age and estradiol levels in women with SS. Interestingly, any of the variables analyzed were not related to non-SS women.

# 4. Discussion

This case–control study aimed to investigate the composition of the oral microbiota in 50 women aged 40 to 70 years, including 25 women with Sjögren's syndrome and 25 women used as controls. Furthermore, the salivary flow was analyzed to investigate the relationship between hyposalivation and oral microbiota. The results showed a negative correlation between stimulated saliva flow and age, but not between unstimulated saliva flow and age. These findings suggest that saliva production may be affected during stimulation, while no significant changes in salivary flow are observed during rest. In SS, mononuclear cell infiltration and accumulation of adipose tissue cause salivary glands to block (Jonsson et al., 2018). Metabolic abnormalities associated with aging may contribute to this process and have also been linked to the development of SS (Hwang et al.,

10.3389/fmicb.2023.1240891

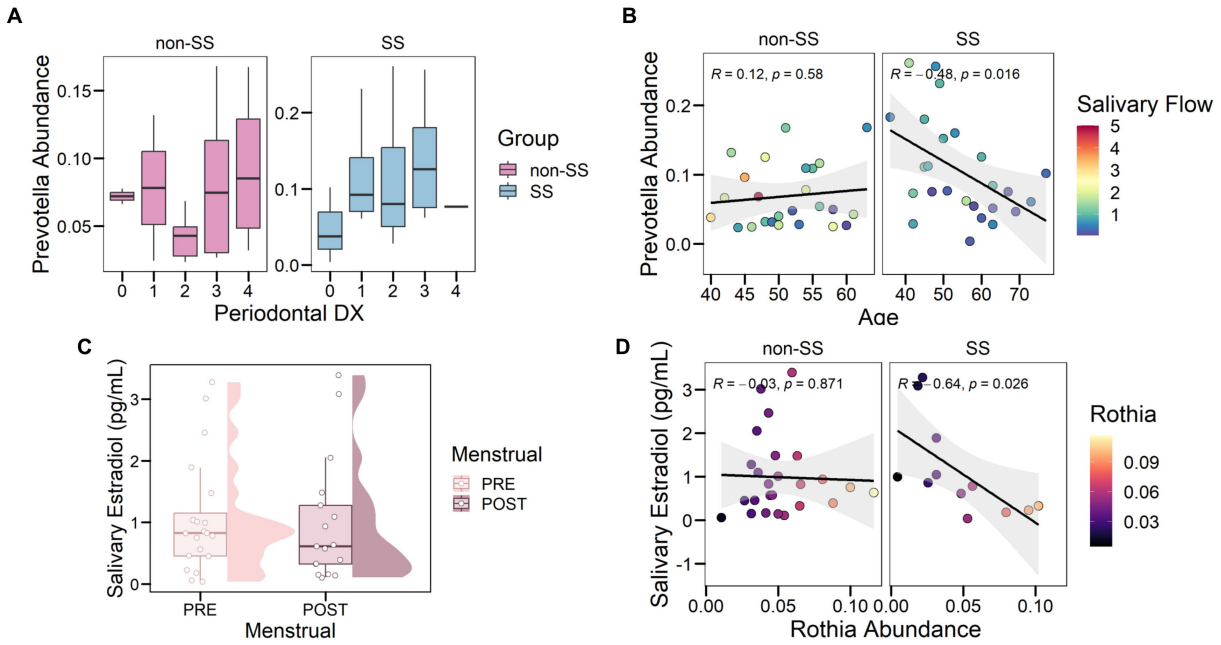


FIGURE 4
Oral Ecological Factors Modulated *Rothia* and *Prevotella* in Sjögren's Syndrome. **(A)** Relationship between *Prevotella* abundance and periodontal status. Periodontal categories go from 0 to 4 and read as follows. 0: No treatment required; 1: Instructions for oral hygiene and supragingival prophylaxis; 2: Instructions for oral hygiene, supragingival prophylaxis, localized subgingival prophylaxis and / or removal of overextended fillings; 3: Complete prophylaxis and scaling and root planning of sextants with code 3 (probing depth between 4–6 mm); 4: Supragingival and subgingival prophylaxis, scaling and root planning, and periodontal surgery. **(B)** Association between *Prevotella* abundance and age, dots are colored according to salivary flow (ml/min). **(C)** Boxplot of salivary estradiol levels with respect to menstrual status, including premenopausal women (PRE) and postmenopausal women (POST). **(D)** Correlation between salivary estradiol levels and the relative abundance of *Rothia*.

2021). The implications of the nervous system in SS, including cholinergic dysfunction, may explain the negative correlation between stimulated saliva flow and age in the SS group. Studies suggest independence of salivary gland damage and cholinergic dysfunction, highlighting the role of acetylcholine in salivary gland function in SS (Imrich et al., 2015; Naidu et al., 2022).

In all samples, the most abundant taxa were *Prevotella*, *Neisseria*, *Rothia*, and *Streptococcus*. Consistent with our findings, a similar pattern of abundant taxa was reported in a study by Rusthen et al. (2019) that compared SS and non-SS patients. The oral microbiota can be highly diverse, with several phyla associated with a healthy oral cavity. *Actinobacteria*, *Proteobacteria*, *Firmicutes*, *Bacteroidetes*, and *Fusobacteria* are predominant in the microbiome of healthy individuals (Verma et al., 2018; Li et al., 2022).

Several studies have investigated the association between Sjögren's syndrome and the oral microbiota. Our study did not find a significant salivary bacterial profile associated with SS disease, contrary to the groups related to salivary production. These results align with those described by Sembler-Møller et al. (2019), who found no significant differences in predominant genera or diversity between 24 SS patients and 36 non-SS controls. Similarly, Sharma et al. reported a comparable trend in their study, identifying three enriched genera such as *Bifidobacterium*, *Lactobacillus*, and *Dialister*, and decreased *Leptotrichia*. However, the study did not find significant differences between the bacterial microbiota of SS and non-SS groups (Sharma et al., 2020). Our results also did not show differences in terms of richness or diversity between the groups, which correlate with previous results (Sharma et al., 2020).

The microbial profile was assessed by separating microorganisms into two dimensions, with *Streptococcus* associated with cluster 1 and *Prevotella* with cluster 2. Interestingly, the non-SS group showed a higher proportion of Streptococcus, while the SS group exhibited a higher abundance of *Prevotella*. Tramice et al. analyzed the oral microbiome and observed a similar pattern, where Streptococcus and *Prevotella* were key factors in data distribution. However, the study did not explore the underlying reasons for this distribution (Tramice et al., 2022).

In our study, we examined the association between *Prevotella* and periodontal status but found no significant relationship. However, we did observe that healthy individuals with good periodontal health had lower levels of *Prevotella* compared to the SS group. A meta-analysis conducted by Yang et al. (2023) reported a positive correlation between *Prevotella* and periodontitis, suggesting also worse periodontal conditions in individuals with SS. However, it is important to note that the meta-analysis reported significant heterogeneity among the included studies.

Our study revealed a significant negative correlation between *Prevotella* spp. and age in the SS group, which was not associated with a reduction in salivary flow. This finding is consistent with previous reports that have suggested a predominance of *Prevotella* spp. in conditions such as poor oral health and advanced age (Yamashita and Takeshita, 2017). In a study by Deshpande et al. (2018), a negative

correlation was also observed between *P. melaninogenica* and age in the esophageal microbiota. However, considering this, a similar pattern should have been observed in the non-SS group as well. Other authors have reported negative correlations between age and other taxa at different oral sites, such as *Porphyromonas endodontalis*, *Alloprevotella tannerae*, *Filifactors* alocis, *Treponema* sp., *Lautropia mirabilis* and *Pseudopropionibacterium* sp._HMT_194 (Schwartz et al., 2021). This, along with our findings, suggests that aging may affect the oral microbiota and salivary flow.

We measured salivary estradiol levels in our study to investigate potential correlations with microbiota species. Seven samples were excluded from the analysis due to extreme hyposalivation. This limitation should be considered for future studies, which could involve the measurement of estradiol levels from alternative samples such as blood. This approach could establish correlations between salivary and blood estradiol levels, while also accounting for the hormonal status of the various individuals. Our results showed higher estradiol levels in the SS group compared to the non-SS group, without any significant differences in menstrual status. Previous research has suggested a negative association between estradiol levels and xerostomia (Agha-Hosseini et al., 2009; Soundarya et al., 2022). Soundarya et al. (2022) reported salivary estradiol levels in menstruating women, premenopausal women, and postmenopausal women. In contrast to our findings, their study observed higher mean estradiol levels in premenopausal women than in postmenopausal women. However, women with SS may have lower estrogen levels, as previously reported in the literature (McCoy et al., 2020), which may be related to the role of estradiol in the molecular pathways of salivary glands. These glands contain estrogen receptors (ER), specifically subtypes α and β which are predominantly found in the oral epithelium (Tsinti et al., 2009). ERα promotes proliferation, while ERβ triggers apoptosis through the activation of p38 upon stimulation (Galluzzo et al., 2007). Estradiol, which is detected in salivary glands by these receptors, has a specific role in the physiopathology of Sjogren's syndrome that has not yet been fully understood. However, previous research has shown a negative correlation between oral dryness and 17-β estradiol concentration, indicating that some aspect of the estrogen receptor pathway may be affected in SS (Agha-Hosseini et al., 2009).

In our study, we observed a negative correlation between salivary estradiol levels and the abundance of *Rothia* in the SS group. Previous research has reported a higher abundance of *Rothia* in breast tumor tissues, and estrogen is known to be a risk factor for this type of tumor (Kartti et al., 2023). However, we did not find any studies that specifically examined the relationship between sex hormones and *Rothia* species. In other species, such as *Streptococcus equi*. Subsp. Zooepidemicus, the presence of the β-glucuronidase gene has been reported (Krahulec and Krahulcová, 2007), suggesting a possible link between the metabolism of sexual hormones and microorganisms.

In conclusion, the oral microbiome is not solely determined by SS but rather by the hyposalivation condition. Stimulated saliva flow showed a negative correlation with age, indicating a decline in saliva production after stimulation, which can be further exacerbated in SS. Two main clusters of microorganisms were identified in the hyposalivation microbiome. *Rothia* and *Prevotella* showed a negative correlation with estradiol and age only in SS women, respectively. These findings contribute to our understanding of the salivary microbiome in the context of hyposalivation, aging, and disease.

## Data availability statement

The datasets presented in this study can be found in online repositories. The names of the repository/repositories and accession number(s) can be found at: https://www.ncbi.nlm.nih.gov/, PRJNA983278.

## Ethics statement

The present study was approved by the Ethics Committee of CEIC Hospital Universitario Ntra. Sra. De Valme 1,532-N$^{-21}$ and European University CIPI/22.201. The research was carried out following the guidelines of the Declaration of Helsinki on Medical Research in Human Subjects and Good Clinical Practice. Written informed consent was obtained from all participants. The studies were conducted in accordance with the local legislation and institutional requirements. The participants provided their written informed consent to participate in this study.

## Author contributions

MJR, MRN, CB, CC-S, MC-O, and DL-C: sample collection and dental examination. MRN, SA-H, LM-G, and JJS-E: recruitment of subjects and acquisition of clinical data. CS, MJR, and AS-S: conception and design of the study, data analysis. CS, MJR, AS-S, and MZ-G: data interpretation and drafting of the manuscript. All authors critically reviewed the manuscript and gave their final approval of the version to be published.

## Funding

This work was supported by the Spanish Ministry of Science and Innovation Grant ID PID2020-118557GA-I00 financiado por MCIN/AEI /10.13039/501100011033.

## Acknowledgments

The authors thank the Spanish Association of Sjögren Syndrome (AESS) and the Andalusian Association of Sjögren Syndrome (AASS) for their participation.

## Conflict of interest

The authors declare that the research was conducted in the absence of any commercial or financial relationships that could be construed as a potential conflict of interest.

## Publisher's note

# References


Agha-Hosseini, F., Mirzaii-Dizgah, I., Mansourian, A., and Khayamzadeh, M. (2009). Relationship of stimulated saliva 17β-estradiol and oral dryness feeling in menopause. *Maturitas* 62, 197–199. doi: 10.1016/j.maturitas.2008.10.016

Agostini, B. A., Cericato, G. O., Silveira, E. R. D., Nascimento, G. G., Costa, F. D. S., Thomson, W. M., et al. (2018). How common is dry mouth? Systematic review and Meta-regression analysis of prevalence estimates. *Braz. Dent. J.* 29, 606–618. doi: 10.1590/0103-6440201802302

Alvariño, C., Bagan, L., Murillo-Cortes, J., Calvo, J., and Bagan, J. (2021). Stimulated whole salivary flow rate: the most appropriate technique for assessing salivary flow in Sjögren syndrome. *Med. Oral Patol. Oral Cir. Bucal.* 26, e404–e407. doi: 10.4317/medoral.24736

Anderson, M. J. (2017). Permutational Multivariate Analysis of Variance (PERMANOVA). In *Wiley StatsRef: Statistics Reference Online* (eds N. Balakrishnan, T. Colton, B. Everitt, W. Piegorsch, F. Ruggeri and J. L. Teugels), 1–15.

Bartold, P., Compton, S., DePaola, L., Fida, Z., Fried, J., Gurenlian, J., et al. (2017). "Dry mouth" in *Prevention across the lifespan: a review of evidence- based interventions for common Oral conditions*. Eds. A. E. Spolarich and F. S. Panagakos (Charlotte, USA: Proffesional Audience Communications, Inc), 175–192.

Bokulich, N. A., Kaehler, B. D., Rideout, J. R., Dillon, M., Bolyen, E., Knight, R., et al. (2018). Optimizing taxonomic classification of marker-gene amplicon sequences with QIIME 2's q2-feature-classifier plugin. *Microbiome* 6:90. doi: 10.1186/s40168-018-0470-z

Bolyen, E., Rideout, J. R., Dillon, M. R., Bokulich, N. A., Abnet, C. C., Al-Ghalith, G. A., et al. (2019). Reproducible, interactive, scalable and extensible microbiome data science using QIIME 2. *Nat. Biotechnol.* 37, 852–857. doi: 10.1038/s41587-019-0209-9

Callahan, B. J., McMurdie, P. J., Rosen, M. J., Han, A. W., Johnson, A. J. A., and Holmes, S. P. (2016). DADA2: high-resolution sample inference from Illumina amplicon data. *Nat. Methods* 13, 581–583. doi: 10.1038/nmeth.3869

Dawes, C., Pedersen, A. M. L., Villa, A., Ekström, J., Proctor, G. B., Vissink, A., et al. (2015). The functions of human saliva: a review sponsored by the world workshop on Oral medicine VI. *Arch. Oral Biol.* 60, 863–874. doi: 10.1016/j.archoralbio.2015.03.004

Deshpande, N. P., Riordan, S. M., Castaño-Rodríguez, N., Wilkins, M. R., and Kaakoush, N. O. (2018). Signatures within the esophageal microbiome are associated with host genetics, age, and disease. *Microbiome* 6:227. doi: 10.1186/s40168-018-0611-4

Dietrich, T., Ower, P., Tank, M., West, N. X., Walter, C., Needleman, I., et al. (2019). Periodontal diagnosis in the context of the 2017 classification system of periodontal diseases and conditions – implementation in clinical practice. *Br. Dent. J.* 226, 16–22. doi: 10.1038/sj.bdj.2019.3

Einhorn, O. M., Georgiou, K., and Tompa, A. (2020). Salivary dysfunction caused by medication usage. *Physiol. Int.* 107, 195–208. doi: 10.1556/2060.2020.00019

Farage, M. A., Miller, K. W., and Sobel, J. D. (2010). Dynamics of the vaginal ecosystem—hormonal influences. *Infect. Dis. Res. Treat.* 3:IDRT.S3903. doi: 10.4137/IDRT.S3903

Fejerskov, O., and Kidd, E. (2008). *Dental caries: The disease and it's clinical management*. *2nd* Edn. Oxford: Blackwell Munksgaard.

Fteita, D., Könönen, E., Söderling, E., and Gürsoy, U. K. (2014). Effect of estradiol on planktonic growth, coaggregation, and biofilm formation of the *Prevotella intermedia* group bacteria. *Anaerobe* 27, 7–13. doi: 10.1016/j.anaerobe.2014.02.003

Galluzzo, P., Caiazza, F., Moreno, S., and Marino, M. (2007). Role of ERβ palmitoylation in the inhibition of human colon cancer cell proliferation. *Endocr. Relat. Cancer* 14, 153–167. doi: 10.1677/ERC-06-0020

Gavrilova, N., and Lindau, S. T. (2009). Salivary sex hormone measurement in a national, population-based study of older adults. *J. Gerontol. B Psychol. Sci. Soc. Sci.* 64B, i94–i105. doi: 10.1093/geronb/gbn028

Holmberg, K. V., and Hoffman, M. P. (2014). Anatomy, biogenesis and regeneration of salivary glands. *Monogr. Oral Sci.* 24, 1–13. doi: 10.1159/000358776

Human Oral Microbiome Database (n.d.). Version V3.1. Available at: https://www.homd.org (Accessed May 4, 2023).

Hwang, S.-H., Woo, J. S., Moon, J., Yang, S., Park, J.-S., Lee, J., et al. (2021). IL-17 and CCR9+α4β7− Th17 cells promote salivary gland inflammation, dysfunction, and cell death in Sjögren's syndrome. *Front. Immunol.* 12:721453. doi: 10.3389/fimmu.2021.721453

Imrich, R., Alevizos, I., Bebris, L., Goldstein, D. S., Holmes, C. S., Illei, G. G., et al. (2015). Predominant glandular cholinergic Dysautonomia in patients with primary Sjögren's syndrome. *Arthritis Rheumatol.* 67, 1345–1352. doi: 10.1002/art.39044

Jonsson, R., Brokstad, K. A., Jonsson, M. V., Delaleu, N., and Skarstein, K. (2018). Current concepts on Sjögren's syndrome – classification criteria and biomarkers. *Eur. J. Oral Sci.* 126, 37–48. doi: 10.1111/eos.12536

Kartti, S., Bendani, H., Boumajdi, N., Bouricha, E. M., Zarrik, O., Agouri H, E. L., et al. (2023). Metagenomics analysis of breast microbiome highlights the abundance of Rothia genus in tumor tissues. *J. Pers. Med.* 13:450. doi: 10.3390/jpm13030450

Katoh, K., and Standley, D. M. (2013). MAFFT multiple sequence alignment software version 7: improvements in performance and usability. *Mol. Biol. Evol.* 30, 772–780. doi: 10.1093/molbev/mst010

Kaufman, L., and Rousseuw, P. J. (1990) in *Finding groups in data*. eds. L. Kaufman and P. J. Rousseeuw (Hoboken, NJ, USA: John Wiley & Sons, Inc)

Kozloski, M. J., Schumm, L. P., and McClintock, M. K. (2014). The utility and dynamics of salivary sex hormone measurements in the National Social Life, health, and aging project, wave 2. *J. Gerontol. B Psychol. Sci. Soc. Sci.* 69, S215–S228. doi: 10.1093/geronb/gbu123

Krahulec, J., and Krahulcová, J. (2007). Characterization of the new β-glucuronidase from *Streptococcus equi* subsp. zooepidemicus. *Appl. Microbiol. Biotechnol.* 74, 1016–1022. doi: 10.1007/s00253-006-0745-3

Krog, M. C., Hugerth, L. W., Fransson, E., Bashir, Z., Nyboe Andersen, A., Edfeldt, G., et al. (2022). The healthy female microbiome across body sites: effect of hormonal contraceptives and the menstrual cycle. *Hum. Reprod.* 37, 1525–1543. doi: 10.1093/humrep/deac094

Li, X., Liu, Y., Yang, X., Li, C., and Song, Z. (2022). The Oral microbiota: community composition, influencing factors, pathogenesis, and interventions. *Front. Microbiol.* 13:895537. doi: 10.3389/fmicb.2022.895537

Marsh, P. D., Do, T., Beighton, D., and Devine, D. A. (2016). Influence of saliva on the oral microbiota. *Periodontol.* 70, 80–92. doi: 10.1111/prd.12098

McCoy, S. S., Sampene, E., and Baer, A. N. (2020). Association of Sjögren's syndrome with reduced lifetime sex hormone exposure: a case–control study. *Arthritis Care Res. (Hoboken)* 72, 1315–1322. doi: 10.1002/acr.24014

McDonald, D., Price, M. N., Goodrich, J., Nawrocki, E. P., DeSantis, T. Z., Probst, A., et al. (2012). An improved Greengenes taxonomy with explicit ranks for ecological and evolutionary analyses of bacteria and archaea. *ISME J.* 6, 610–618. doi: 10.1038/ismej.2011.139

Naidu, G. S. R. S. N. K., Sharma, A., Minz, R. W., Gupta, A., and Baishya, J. (2022). Peripheral nervous system involvement in Sjogren's syndrome and its impact on quality of life. *Clin. Exp. Med.* 23, 539–545. doi: 10.1007/s10238-022-00837-w

Ogle, O. E. (2020). Salivary gland diseases. *Dent. Clin. N. Am.* 64, 87–104. doi: 10.1016/j.cden.2019.08.007

Pathak, J. L., Yan, Y., Zhang, Q., Wang, L., and Ge, L. (2021). The role of oral microbiome in respiratory health and diseases. *Respir. Med.* 185:106475. doi: 10.1016/j.rmed.2021.106475

Peng, X., Cheng, L., You, Y., Tang, C., Ren, B., Li, Y., et al. (2022). Oral microbiota in human systematic diseases. *Int. J. Oral Sci.* 14:14. doi: 10.1038/s41368-022-00163-7

Pérez-Jardón, A., Pérez-Sayáns, M., Peñamaría-Mallón, M., Otero-Rey, E., Velasco-Ortega, E., López-López, J., et al. (2022). Xerostomia, the perception of general and oral health and health risk behaviours in people over 65 years of age. *BMC Geriatr.* 22:982. doi: 10.1186/s12877-022-03667-3

Pina, G. D. M. S., Mota Carvalho, R., Silva, B. S. D. F., and Almeida, F. T. (2020). Prevalence of hyposalivation in older people: a systematic review and meta-analysis. *Gerodontology* 37, 317–331. doi: 10.1111/ger.12497

Price, M. N., Dehal, P. S., and Arkin, A. P. (2010). FastTree 2 – approximately maximum-likelihood trees for large alignments. *PLoS One* 5:e9490. doi: 10.1371/journal.pone.0009490

R Foundation for Statistical Computing, Austria (2022). *R: A language and environment for statistical computing*. Available at: https://www.R.org/

Roberts, F. A., and Darveau, R. P. (2015). Microbial protection and virulence in periodontal tissue as a function of polymicrobial communities: symbiosis and dysbiosis. *Periodontol.* 69, 18–27. doi: 10.1111/prd.12087

Rusthen, S., Kristoffersen, A. K., Young, A., Galtung, H. K., Petrovski, B. É., Palm, Ø., et al. (2019). Dysbiotic salivary microbiota in dry mouth and primary Sjögren's syndrome patients. *PLoS One* 14:e0218319. doi: 10.1371/journal.pone.0218319

Schwartz, J. L., Peña, N., Kawar, N., Zhang, A., Callahan, N., Robles, S. J., et al. (2021). Old age and other factors associated with salivary microbiome variation. *BMC Oral Health* 21:490. doi: 10.1186/s12903-021-01828-1

Sedghi, L., DiMassa, V., Harrington, A., Lynch, S. V., and Kapila, Y. L. (2021). The oral microbiome: role of key organisms and complex networks in oral health and disease. *Periodontol.* 87, 107–131. doi: 10.1111/prd.12393

Sembler-Møller, M. L., Belstrøm, D., Locht, H., Enevold, C., and Pedersen, A. M. L. (2019). Next-generation sequencing of whole saliva from patients with primary Sjögren's syndrome and non-Sjögren's sicca reveals comparable salivary microbiota. *J. Oral Microbiol.* 11:1660566. doi: 10.1080/20002297.2019.1660566

Sharma, D., Sandhya, P., Vellarikkal, S. K., Surin, A. K., Jayarajan, R., Verma, A., et al. (2020). Saliva microbiome in primary Sjögren's syndrome reveals distinct set of disease-associated microbes. *Oral Dis.* 26, 295–301. doi: 10.1111/odi.13191

Shi, Y., Zhang, L., Peterson, C. B., Do, K.-A., and Jenq, R. R. (2022). Performance determinants of unsupervised clustering methods for microbiome data. *Microbiome* 10:25. doi: 10.1186/s40168-021-01199-3

Singh, M., Teles, F., Uzel, N. G., and Papas, A. (2021). Characterizing microbiota from Sjögren's syndrome patients. *JDR Clin. Trans. Res.* 6, 324–332. doi: 10.1177/2380084420940623

Smith, B. J., Valdez, I. H., and Berkey, D. B. (2007). "Oral Problems" in *Primary care geriatrics*. (Elsevier), 601–611.

Socransky, S. S., Haffajee, A. D., Cugini, M. A., Smith, C., and Kent, R. L. (1998). Microbial complexes in subgingival plaque. *J. Clin. Periodontol.* 25, 134–144. doi: 10.1111/j.1600-051X.1998.tb02419.x

Soundarya, B., Massillamani, F., Kailasam, S., Jayashree, G., Narmadha, N., and Sornaa, N. (2022). Salivary menopausal markers and Oral health status - a hidden hook up. *J. Midlife Health* 13, 157–162. doi: 10.4103/jmh.jmh_61_21

The North American Menopause Society (2023). *Menopause health questionnaire*.

Tramice, A., Paris, D., Manca, A., Guevara Agudelo, F. A., Petrosino, S., Siracusa, L., et al. (2022). Analysis of the oral microbiome during hormonal cycle and its alterations in menopausal women: the "AMICA" project. *Sci. Rep.* 12:22086. doi: 10.1038/s41598-022-26528-w

Tsinti, M., Kassi, E., Korkolopoulou, P., Kapsogeorgou, E., Moutsatsou, P., Patsouris, E., et al. (2009). Functional estrogen receptors alpha and beta are expressed in normal human salivary gland epithelium and apparently mediate immunomodulatory effects. *Eur. J. Oral Sci.* 117, 498–505. doi: 10.1111/j.1600-0722.2009.00659.x

Verma, D., Garg, P. K., and Dubey, A. K. (2018). Insights into the human oral microbiome. *Arch. Microbiol.* 200, 525–540. doi: 10.1007/s00203-018-1505-3

Wells, P. M., Sprockett, D. D., Bowyer, R. C. E., Kurushima, Y., Relman, D. A., Williams, F. M. K., et al. (2022). Influential factors of saliva microbiota composition. *Sci. Rep.* 12:18894. doi: 10.1038/s41598-022-23266-x

Willis, J. R., Saus, E., Iraola-Guzmán, S., Ksiezopolska, E., Cozzuto, L., Bejarano, L. A., et al. (2022). Citizen-science reveals changes in the oral microbiome in Spain through age and lifestyle factors. *NPJ Biofilms Microbiomes* 8:38. doi: 10.1038/s41522-022-00279-y

Yamashita, Y., and Takeshita, T. (2017). The oral microbiome and human health. *J. Oral Sci.* 59, 201–206. doi: 10.2334/josnusd.16-0856

Yang, B., Pang, X., Guan, J., Liu, X., Li, X., Wang, Y., et al. (2023). The association of periodontal diseases and Sjogren's syndrome: a systematic review and meta-analysis. *Front. Med. (Lausanne)* 9:904638. doi: 10.3389/fmed.2022.904638

frontiers | Frontiers in Microbiology

TYPE Original Research
PUBLISHED 23 November 2023
DOI 10.3389/fmicb.2023.1228845



OPEN ACCESS

EDITED BY
Rebeca Martín,
INRAE Center Jouy-en-Josas, France

REVIEWED BY
Sharanne Lee Raidal,
Charles Sturt University, Australia
Samara Paula Mattiello,
University of Tennessee Southern, United States

*CORRESPONDENCE
Birgit Walther
✉ birgit.walther@uba.de

†These authors share senior authorship

RECEIVED 25 May 2023
ACCEPTED 06 November 2023
PUBLISHED 23 November 2023

CITATION
Kauter A, Brombach J, Lübke-Becker A, Kannapin D, Bang C, Franzenburg S, Stoeckle SD, Mellmann A, Scherff N, Köck R, Guenther S, Wieler LH, Gehlen H, Semmler T, Wolf SA and Walther B (2023) Antibiotic prophylaxis and hospitalization of horses subjected to median laparotomy: gut microbiota trajectories and abundance increase of *Escherichia*. *Front. Microbiol.* 14:1228845. doi: 10.3389/fmicb.2023.1228845



# Antibiotic prophylaxis and hospitalization of horses subjected to median laparotomy: gut microbiota trajectories and abundance increase of *Escherichia*

Anne Kauter[1], Julian Brombach[2,3], Antina Lübke-Becker[2,3], Dania Kannapin[4], Corinna Bang[5], Sören Franzenburg[5], Sabita D. Stoeckle[4], Alexander Mellmann[6], Natalie Scherff[6], Robin Köck[6,7], Sebastian Guenther[8], Lothar H. Wieler[9], Heidrun Gehlen[4], Torsten Semmler[10], Silver A. Wolf[10†] and Birgit Walther[1,11*†]

[1]Advanced Light and Electron Microscopy (ZBS4), Robert Koch Institute, Berlin, Germany, [2]Center for Infection Medicine, Institute of Microbiology and Epizootics, Freie Universität Berlin, Berlin, Germany, [3]Veterinary Center for Resistance Research (TZR), Freie Universität Berlin, Berlin, Germany, [4]Equine Clinic, Surgery and Radiology, Freie Universität Berlin, Berlin, Germany, [5]Institute of Clinical Molecular Biology, Christian-Albrechts-University of Kiel, Kiel, Germany, [6]Institute of Hygiene, University of Münster, Münster, Germany, [7]Institute of Hygiene, DRK Kliniken Berlin, Berlin, Germany, [8]Pharmaceutical Biology, Institute of Pharmacy, Universität Greifswald, Greifswald, Germany, [9]Robert Koch Institute, Berlin, Germany, [10]Genome Sequencing and Genomic Epidemiology (MF2), Robert Koch Institute, Berlin, Germany, [11]Section Microbiological Risks (1.4), Department II Environmental Hygiene, German Environment Agency, Berlin, Germany

**Introduction:** Horse clinics are hotspots for the accumulation and spread of clinically relevant and zoonotic multidrug-resistant bacteria, including extended-spectrum β-lactamase producing (ESBL) Enterobacterales. Although median laparotomy in cases of acute equine colic is a frequently performed surgical intervention, knowledge about the effects of peri-operative antibiotic prophylaxis (PAP) based on a combination of penicillin and gentamicin on the gut microbiota is limited.

**Methods:** We collected fecal samples of horses from a non-hospitalized control group (CG) and from horses receiving either a pre-surgical single-shot (SSG) or a peri-operative 5-day (5DG) course of PAP. To assess differences between the two PAP regimens and the CG, all samples obtained at hospital admission ($t_0$), on days three ($t_1$) and 10 ($t_2$) after surgery, were screened for ESBL-producing Enterobacterales and subjected to 16S rRNA V1–V2 gene sequencing.

**Results:** We included 48 samples in the SSG ($n$ = 16 horses), 45 in the 5DG ($n$ = 15), and 20 in the CG (for $t_0$ and $t_1$, $n$ = 10). Two samples of equine patients receiving antibiotic prophylaxis (6.5%) were positive for ESBL-producing Enterobacterales at $t_0$, while this rate increased to 67% at $t_1$ and decreased only slightly at $t_2$ (61%). Shannon diversity index (SDI) was used to evaluate alpha-diversity changes, revealing there was no significant difference between horses suffering from acute colic (5DG, $SDI_{mean}$ of 5.90, SSG, $SDI_{mean}$ of 6.17) when compared to the CG ($SDI_{mean}$ of 6.53) at $t_0$. Alpha-diversity decreased significantly in both PAP groups at $t_1$, while at $t_2$ the onset of microbiome recovery was noticed. Although we did not identify a significant $SDI_{mean}$ difference with respect to PAP duration, the community structure (beta-diversity) was considerably restricted in samples of the 5DG at $t_1$, most likely due to the ongoing administration of antibiotics. An increased abundance of *Enterobacteriaceae,* especially *Escherichia*, was noted for both study groups at $t_1$.

**Conclusion:** Colic surgery and PAP drive the equine gut microbiome towards dysbiosis and reduced biodiversity that is accompanied by an increase of samples positive for ESBL-producing Enterobacterales. Further studies are needed to reveal important factors promoting the increase and residency of ESBL-producing Enterobacterales among hospitalized horses.

KEYWORDS

**horse, microbiome, gastrointestinal tract, microbiota, 16S rRNA gene sequencing, hospitalization, colic, *Escherichia***

## Introduction

Compared with other companion animals, horses more often acquire gastro-intestinal tract (GIT) disorders that may lead to long-term suffering or even death (Traub-Dargatz et al., 2001). The complex pain caused by disorders of the GIT in horses is commonly referred to as "colic" (Traub-Dargatz et al., 2001; Stockle et al., 2018) and often requires surgical intervention (Archer, 2019). The composition of the bacterial community residing within the GIT has been regarded as beneficial and a prerequisite for the health and well-being of hindgut fermenters such as Equidaes (reviewed in Kauter et al., 2019). Previous reports indicated that colonization with the physiological endogenous microbiota shields the equine GIT against either direct or indirect pathogen-induced damage and that these protective effects are disrupted in various enteric diseases (Costa et al., 2012; Weese et al., 2015). In addition, it has been reported as a consequence of the administration of antibiotics such as penicillin (Baverud et al., 2003), enrofloxacin or ceftiofur (Liepman et al., 2022), and doxycycline (Davis et al., 2006) that the enteric microbial community enters a dysbiotic state (Costa et al., 2015). However, among other factors, the state of the microbiota at the time of the (antibiotic) perturbation (diet, species, functional diversity, and redundancy) and the characteristics of the perturbation (e.g., route of administration, antimicrobial spectrum, and duration of the antibiotic course) determine the extent of any eventual dysbiosis (Schwartz et al., 2020).

Peri-operative antibiotic prophylaxis (PAP) is recommended to prevent adverse postoperative events, such as surgical site infections, in horses subjected to abdominal surgery due to acute colic (Dallap Schaer et al., 2012). The most commonly used PAP regimen for horses requiring median laparotomy consists of a combination of penicillin and gentamicin (P/G) for a period of 3–10 days (Dallap Schaer et al., 2012; Wormstrand et al., 2014; Teschner et al., 2015; Ceriotti et al., 2021). In contrast, the standard regimen for similar surgical interventions lacking complicating circumstances in human and small animal medicine is a short-term PAP, which is provided as a single-shot therapy 30–60 min prior to incision (as described in Stöckle et al., 2021). To investigate the effects of prolonged administration beyond this immediate peri-operative timeframe (> 24 h after surgery), we conducted a pilot study focusing on the clinical outcome (Stöckle et al., 2021), the extended-spectrum β-lactamase (ESBL)-producing *Escherichia coli* (EC) carriage rates (Kauter et al., 2021), and the microbiome composition (present study). Beyond others, our results indicated non-inferiority of a "single-shot" vs. a 5-day course of P/G PAP with respect to the patients' clinical outcomes (Stöckle et al., 2021). Regardless of the applied PAP-regimen, we noticed a worrisome increase of ESBL-EC carriage rates among horses during their hospital stay (Kauter et al., 2021).

Based on these previous observations, the current study aimed (i) to examine the extent of microbiome disturbance in hospitalized horses subjected to median laparotomy, (ii) to reveal alterations of the gut microbiota caused by a short and a long-term PAP regime, and (iii) to enable insights into changes of the microbiome that might play a role in the previously reported increased ESBL-EC carriage rates among equine patients.

## Materials and methods

### Study cohort and perioperative antibiotic prophylaxis

Horses diagnosed with acute abdominal pain (colic) that required median laparotomy were included in this study and were randomized 1: 1 to the PAP regimens in an open-label study as the different antibiotic regimens prevented blinding (for a detailed description of the controlled and randomized study, see in Stöckle et al., 2021). Briefly, horses assigned to the SSG received short term P/G PAP, while the 5DG group received P/G PAP for 5 consecutive days. In both groups, PAP consisted of parenteral administration of sodium penicillin G (22,000 IU/kg four times daily) and gentamicin (6.6 mg/kg), as previously recommended for colic surgery (Dallap Schaer et al., 2012; Durward-Akhurst et al., 2013; Southwood, 2014). Specimens of 10 non-hospitalized farm horses that were free of clinical symptoms for any apparent illnesses served as a control group (CG). All animals in the CG were sampled within at a 3-day interval ($t_0$ and $t_1$), similarly to the hospitalized animals (see description of sample collection), in order to ensure the representativeness of the samples of this group (for a detailed description of the study cohort and their respective clinical results, see Stöckle et al., 2021). A graphical abstract of the study outline is provided in Figure 1.

Inclusion criteria for study participation were: study participants had to be free of clinical signs of infectious diseases prior to surgery.

Abbreviations: 5DG, 5-day course of peri-operative antibiotic prophylaxis group; Bp, Base pair; CG, Control group; EC, *Escherichia coli*; ESBL, Extended-spectrum β-Lactamase; G, Gentamicin; GIT, Gastrointestinal tract; i.e., *id est*; Log2FC, $\log_2$ fold change; MDR, Multi-drug resistance; OTU, Operational taxonomic units; P, Penicillin; PAP, Perioperative antibiotic prophylaxis; PCA, Principal component analysis; SDI, Shannon diversity index; SSG, Single-shot of peri-operative antibiotic prophylaxis group.

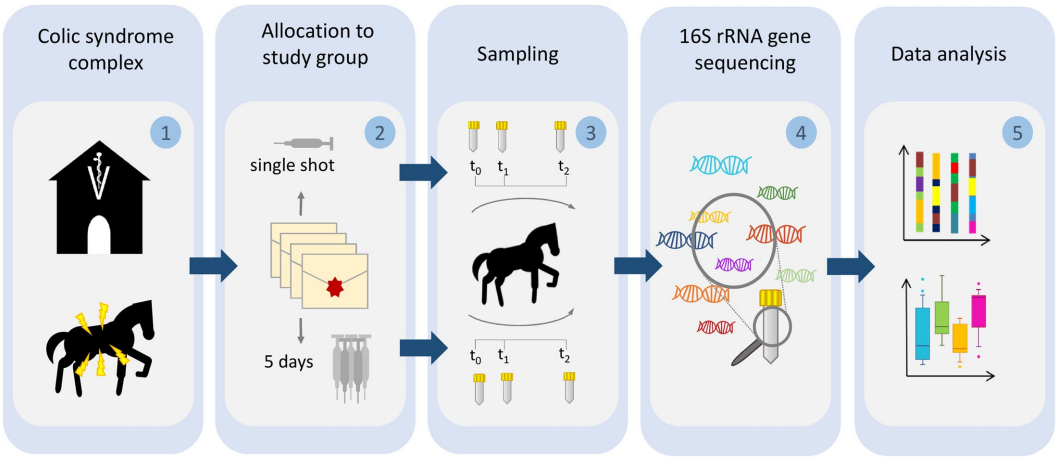


FIGURE 1
Illustration of the sampling procedure. Horses subjected to colic surgery were (1) sampled directly at hospital admission ($t_0$) and (2) allotted to either a single-shot perioperative antibiotic prophylaxis regimen or a 5-day-lasting protocol. Sampling was repeated for all horses on day 3 and 10 after surgery (3). All samples were subjected to DNA extraction and V1–V2 16S rRNA gene sequencing (4). Sequences were preprocessed and analyzed with respect to changes of microbiota composition, alpha and beta diversity (5).

Additionally, since the juvenile microbiome is known for continuing changes during the foals' gut maturation (Costa et al., 2016), all included horses were required to be 1 year or older. Equine patients were excluded from further consideration if their hospital stay had ended prematurely due to euthanasia and/or the antibiotic regimen they had originally been assigned to was not strictly followed, regardless of the particular reasons requiring these changes. Horses with incomplete sample sets ($t_0$, $t_1$, and $t_2$, see sample collection) or resection (enhanced rates of surgical site infections, SSIs) were excluded from this study. For additional details on the clinical characteristics of colic horses, see Stöckle et al. (2021).

## Sample collection

Fresh fecal samples were collected from each horse diagnosed with colic and undergoing midline celiotomy directly at hospital admission ($t_0$), as described previously (Walther et al., 2018; Kauter et al., 2021). A second sample was collected 3 days ($t_1$) after, and a third (final) sample, 10 days ($t_2$, hospital discharge) after surgery. In order to gain insights into the gut microbiome associated with non-hospitalized horses lacking clinical signs of gastro-intestinal disorders, control samples were obtained from 10 horses residing in a barn. All specimens were stored directly at −80°C and shipped on dry ice.

Identification of ESBL-producing Enterobacterales was previously described (Kauter et al., 2021). Briefly, samples were cultured on Brilliance™ ESBL Agar plates (Thermo Scientific, Germany) overnight. Colonies showing characteristic growth signatures of ESBL-producing Enterobacterales on chromogenic screening plates were further investigated. In case of distinct phenotypic appearances of presumptive ESBL-producing colonies on the plates, all isolates were subjected to an ESBL confirmation test according to the Clinical Laboratory Standards Institute's (CLSI) recommendations [Clinical and Laboratory Standards Institute (CLSI), 2020]. Species confirmation was achieved by matrix-assisted laser desorption/ionization-time of flight (MALDI-TOF) mass spectrometry (Bruker, Germany).

## DNA extraction and sequencing of the bacterial 16S rRNA V1-V2 region

The sequencing of bacterial DNA was performed by the Institute of Clinical Molecular Biology (IKMB) at the Christian-Albrechts University of Kiel. DNA was extracted using the QIAamp Fast DNA stool mini kit (QIAGEN, Hilden, Germany) automated on the QIAcube (QIAGEN, Hilden, Germany). For this, approximately 200 mg feces were transferred to 0.70 mm Garnet Bead tubes filled with 1 mL InhibitEx buffer. Subsequently, bead beating was performed using a SpeedMill PLUS (QIAGEN, Hilden, Germany) for 45 s at 60 Hz. Samples were then heated to 95°C for 5 min and afterwards centrifuged for 1 min at 10,000 rpm. 200 µL of the resulting supernatant were transferred to a 1.5 mL microcentrifuge tube, which was placed in the QIAcube for follow-up automated DNA isolation according to the manufacturer's protocol. DNA bound specifically to the QIAamp silica-gel membrane while contaminants passed through. PCR inhibitors were removed through means of InhibitEX (QIAGEN, Hilden, Germany), a unique adsorption resin, and an optimized buffer. DNA was diluted 1:10 prior to PCR, and 3 µL were used for further amplification. PCR-products were verified using agarose gel electrophoresis. PCR-products were then normalized using the SequalPrep Normalization Plate Kit (Thermo Fischer Scientific, Waltham, MA, United States), pooled equimolarily, and sequenced on an Illumina MiSeq v3 2 × 300 base pair (bp) platform (Illumina Inc., San Diego, CA, United States).

The V1–V2 region of the 16S rRNA gene was subsequently sequenced (Primerpair 27F-338R, dual MIDs inducing) on a MiSeq-platform (MiSeq Reagent Kit v2; Kozich et al., 2013). The resulting MiSeq raw fastq data were verified using an inhouse pipeline [Bcl2fastq Modul in CASAVA 1.8.2, Demultiplexing, FLASH software

(v1.2) (Magoč and Salzberg, 2011), and fastx toolkit und UCHIME (v6.0) (Edgar et al., 2011)]. Demultiplexing was performed based on zero mismatches within the barcode sequences.

## Analysis of 16S rRNA gene sequences

### Data preprocessing

Sequence reads were preprocessed as described (Mach et al., 2020). In brief, paired-end reads were merged into continuous sequences using the "join_paired_ends.py" script of QIIME (v1.9.1) (Caporaso et al., 2010) in "fastq-join" mode (Aronesty, 2013). Defined parameters allowed a minimum overlap of 6 bp and a maximum difference within the overlap region of 8%. Reads which did not meet these criteria were removed from further analysis. Next, seqkit (v0.16.1) (Shen et al., 2016) was utilized to filter out reads which were too short (≤300 bp) or too long (≥470 bp). The remaining sequences were then quality filtered using the "split_libraries_fastq.py" script of QIIME (v1.9.1) (Edgar, 2010) by applying a PHRED quality threshold of 20. Reads were hereby required to have 50% of their bases to be consecutively of high quality. A maximum of three consecutive low-quality bases were allowed before truncating a read. Reads containing any ambiguous bases ("N") were removed from further analysis.

### OTU clustering

Reads were clustered into operational taxonomic units (OTUs) using USEARCH (v11.0.667) (Edgar, 2010) and the Greengenes database (release 2013-08, gg_13_8_otus, 99_otus; DeSantis et al., 2006) with a 97% similarity cutoff. The "unnoise3" algorithm of USEARCH was utilized for additional filtering of chimeric OTUs. In order to improve taxonomic annotation, Greengenes OTUs as well as unmatched representative sequences were then mapped against the RDP database (v11.5) (Cole et al., 2014) using the SequenceMatch pipeline of rdptools (v2.0.3) (Cole et al., 2014), searching for the closest neighbor ($k = 1$) with a minimum sab score of 0.5. Counts were subsequently merged and the "filter_otus_from_otu_table.py" script of QIIME (v1.9.1) (Caporaso et al., 2010) was utilized to remove any singletons from the table (counts ≤3). Data were then exported using the biom (v 2.1.7) (McDonald et al., 2012) package and converted into the appropriate format for further data analysis. The resulting OTU table was then finalized by updating the available taxonomic labels with the recently released, new taxonomic names for bacterial phyla (Oren and Garrity, 2021).

### Sample size calculation

Sample-size calculation was performed as recommended for microbiome studies by utilizing a permutation-based extension of the multivariate analysis of variance (PERMANOVA) on a matrix of pairwise distances (Kelly et al., 2015). Subsequent study power estimation was performed through the R package micropower (v0.4) (Kelly et al., 2015). Unfiltered OTU tables were hereby subjected to random rarefaction in order to assess key population parameters, including mean and standard deviation per OTU based on both the presence/absence of individual taxa as well as their abundance (Weighted Jaccard Distance) for a comparison of two groups of fixed size ($n = 10$). These parameters were then further utilized to simulate a range of distance matrices and effect sizes in order to estimate the statistical power for identifying an effect size given a specified sample size and respective OTU table. Permutation-based sample-size estimation, according to Kelly et al. (2015), revealed that a subset of samples from 10 horses per study group were sufficient to identify differences in taxonomic composition of effect size 0.020 with $p = 0.05$ and a power of 80% (90% to identify an effect size of 0.035).

### Diversity estimation and OTUs assignation

The resulting OTU counts were randomly sub-sampled for each sample to a homogeneous level, defined by the counts of the lowest sample (12,178). OTU counts above 10,000 have been shown to provide adequate comparisons between differing sequencing depths for microbiome analyses (Mach et al., 2020). Rarefaction was performed by using the "rarefy_even_depth" function of phyloseq (v1.36.0) (McMurdie and Holmes, 2013) with rngseed = 1 in R (v4.1.1). Rarefied data were then utilized to assess the influence of antibiosis on the microbiome diversity among the equine patients and to visualize the distribution of taxa (OTUs) across the sample set. Within-sample diversity (alpha-diversity) was assessed through Shannon diversity indices (SDI) calculated using the R package microbiome (v1.14.0) (Lahti et al., 2017). Between-sample diversity (beta-diversity) was determined through the computation of Bray-Curtis distances by phyloseq (v1.36.0) (McMurdie and Holmes, 2013) on all OTUs of the rarefied table. The resulting diversity metrics were further visualized with ComplexHeatmap (v2.8.0) (Gu et al., 2016) and ggplot2 (v3.3.5) (Wickham et al., 2016) for subsequent comparisons between the study groups. Non-parametric Paired Wilcoxon Rank Sum tests were performed between groups of interest and results with a $p < 0.05$ were labeled as being significant. The Benjamini-Hochberg procedure was utilized for multiple-testing correction in order to limit the false discovery rate were applicable. OTUs were aggregated at selected taxonomic levels (including phlya) using the "aggregate_top_taxa" function of microbiome (v1.14.0) (Lahti et al., 2017). Differential taxa were identified between the PAP study groups (SSG/5DG) using the raw OTU table and the microbiomeExplorer R package (Reeder et al., 2021) with proportional normalization and the DESeq2 method (Love et al., 2014). Additional correlation analyses were also performed within the microbiome Explorer suite.

# Results

To explore the effects of both G/P PAP regimens and hospitalization on the gut microbiota of horses subjected to median laparotomy, microbiome sequencing and analysis were performed using sample sets obtained from a pilot study comparing the clinical outcomes of 67 patients that met the study's inclusion criteria (Stöckle et al., 2021). Overall, 48 samples from 16 horses representing the SSG and 45 samples of 15 horses belonging to the 5DG were comparatively evaluated. As a non-hospitalized CG, we included additional 20 samples of 10 horses that lacked any apparent signs of clinical illness, resulting in 113 samples (Supplementary Table 1). At hospital admission, two samples (6.5%) were positive for ESBL-producing Enterobacterales (Supplementary Table 1), while, regardless of the study group, the overall rate increased to 67% ($t_1$) and, only slightly decreased, at $t_2$ (61%). There was no difference in carriage of

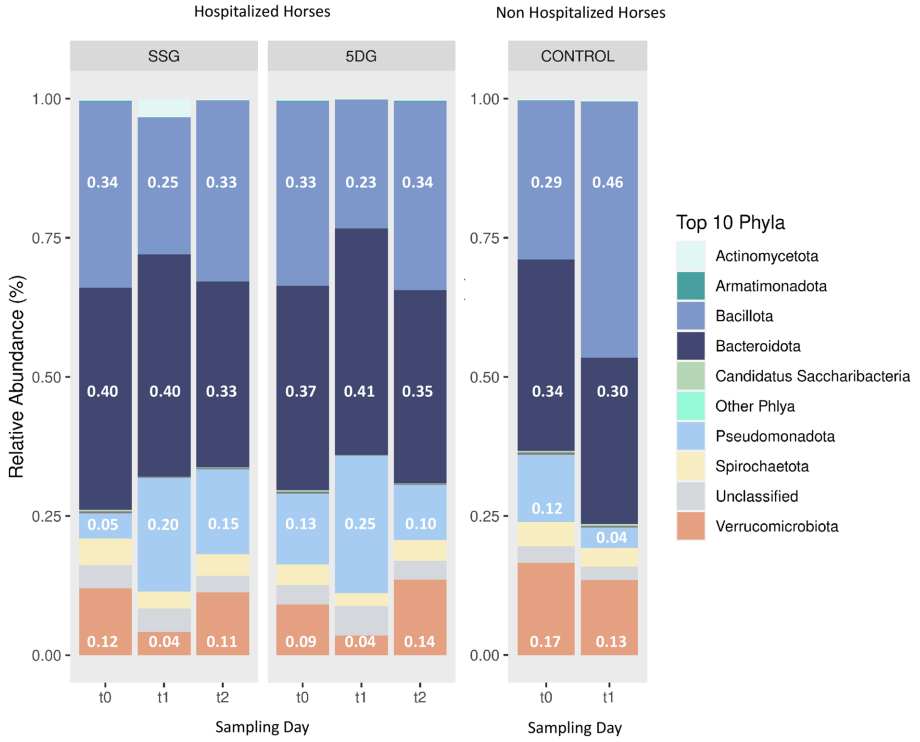


FIGURE 2
Taxonomic composition of microbiota in hospitalized horses. Stacked bar charts illustrating the relative abundances of the top 10 phyla for the single-shot group (SSG, $n = 16$) and the 5-day group (5DG, $n = 15$). $t_0$, Hospital admission (SSG/5DG)/first sampling round (CG); $t_1$ = 3 days after surgery (SSG/5DG)/3 days after first sampling (CG); $t_2$ = 10 days after surgery (SSG/5DG).

ESBL-producing Enterobacterales between the SSG and 5DG (Fisher's Exact Test, $p = 1$), while all CG samples were negative (Fisher's Exact Test, $p < 0.0001$).

In total, 4,896,645 high quality OTU counts (ranging between 12,178–220,454 counts per sample, median = 32,730) were obtained and assigned to 17,035 different OTUs across 330 different taxonomic entities at genus level. Further taxonomic assignment of these OTUs revealed the top 10 bacterial taxa (phylum level) based on their total counts across the sample set: The phyla *Bacteroidota* (38%; previously *Bacteroidetes*; Oren and Garrity, 2021) and *Bacillota* (33%; previously: *Firmicutes*; Oren and Garrity, 2021) were predominant in the equine fecal samples at hospital admission ($t_0$), followed by *Verrucomicrobiota* (11%), *Pseudomonadota* (9%; previously *Proteobacteria*; Oren and Garrity, 2021) and *Spirochaetota* (4%; Figure 2).

In addition, each horse harbored an individual composition of bacterial fecal communities, as presented in Supplementary Figure 1.

## Evaluation of gut microbiota profiles, microbiome disturbance, biodiversity, and microbiota trajectories

### Microbiota profiles at hospital admission

The SDI is a measure of a sample's diversity based on both, community richness and evenness. In the present study, SDI was selected to inspect the alpha-diversity within each sample and to compare these across study groups. Overall comparableness of the treatment groups was ensured by demonstrating the lack of significant difference in the mean SDI between both study groups at $t_0$ (Wilcoxon test, $p > 0.05$). As expected, visualization of beta-diversity ("between sample diversity") using ordination plots generated through principle component analysis (PCA) demonstrated an increased range of variance regarding the gut microbiota profiles of individual horses belonging to the SSG and the 5DG compared to the overall variance noticeable between the data points representing the CG samples (Figures 3A–C).

Of note, the mean SDI values of the CG samples were 6.42 and 6.44, respectively. At $t_0$, most of the enteral microbiota profiles associated with SSG horses (11 of 16) clustered within the framework set by the CG samples (Figure 3A). The $t_0$ microbiota profiles obtained for the 5DG, on the other hand, illustrated increased variance among the 5DG samples, and only four out of 15 samples clustered with the CG area, potentially indicating that more horses belonging to the 5DG had, in comparison to the SSG, gut microbiota perturbances at hospital admission (Figure 3B). This observation also seemed to correspond with the alpha-diversities, since the $t_0$ samples representing the SSG were associated with an $SDI_{mean}$ of 6.17, while the 5DG yielded an $SDI_{mean}$ of 5.90, however the difference lacked statistical significance (Figure 3D).

### Microbiota profiles at $t_1$

At $t_1$, most of the microbiota profiles obtained from fecal samples of the SSG (horses without antibiotics for at least 36 h) and the 5DG (horses at the third day of their 5-day course P/G PAP) visibly differed from those obtained at $t_0$ by shifting away

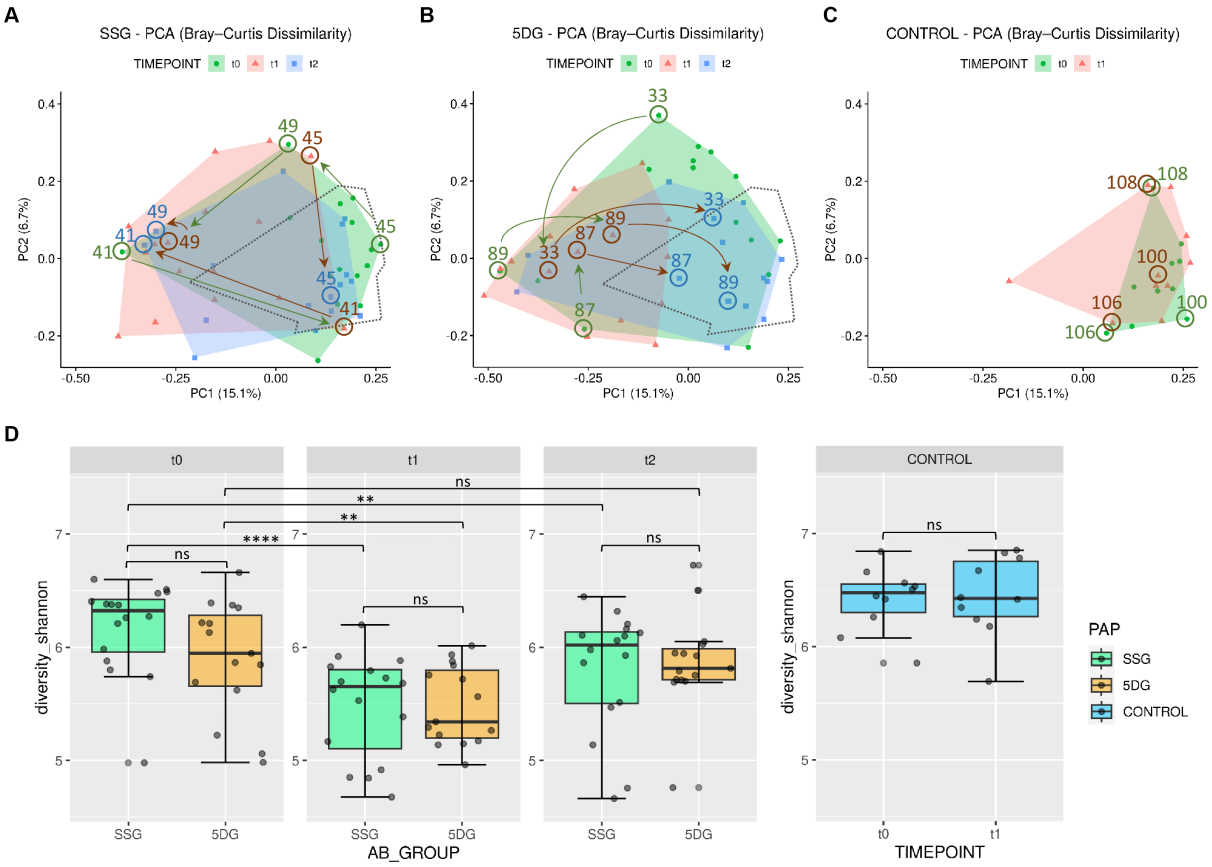


FIGURE 3
Diversity of the equine gut microbiome of hospitalized and non-hospitalized horses. **(A–C)** Principle component analysis (PCA) plots illustrating differences in gut microbiome composition (beta-diversity) based on unweighted Bray-Curtis dissimilarities across each group per sampling day. Axes represent the two dimensions that explain the largest proportion of variation across communities of each analysis. Distances between two data points reflect their similarity/dissimilarity with respect to sample composition. The colored areas represent the computed convex hull of data points from each sampling day, illustrating respective areas of minimal size. The area encompassing data points from the control group (CG) samples **(C)** is marked by a dotted line in **(A,B)** for direct comparison. Horses treated with peri-operative antibiotic prophylaxis (PAP) in the single-shot group (SSG) vs. the 5-day course group (5DG) show both large, intraindividual differences at $t_0$ **(A)** and a strong shift away from the area defined by the CG samples at $t_1$ **(B)**. Samples of both study groups converge back to the CG area at $t_2$. Numbered arrows indicate the trajectories of microbiota composition within selected horses. **(D)** Boxplots displaying the alpha-diversity indices (Shannon) for all three groups (SSG, $n = 16$; 5DG, $n = 15$; and control, $n = 10$; significance between groups: unpaired Wilcoxon Rank Sum tests, $^{**}p < 0.05$, $^{****}p < 0.0005$, ns, not significant).

from the center of the CG area, indicating perturbations (Figure 3B). This shift was accompanied by a significant reduction in mean alpha-diversity across both groups [SSG: SDI from $t_0 = 6.17$ to $t_1 = 5.48$ (paired Wilcoxon Test, $p = 0.000031$); 5DG: SDI from $t_0 = 5.90$ to $t_1 = 5.48$ (paired Wilcoxon Test, $p = 0.012$); Supplementary Table 1; Figure 3D]. In addition, the overall distances between 5DG samples seemed considerably restricted compared to the situation at $t_0$ (Figure 3B). Samples representing the SSG, on the other hand, were more widely scattered than samples representing the 5DG or even the CG, indicating an increased level of inter-individual differences among microbiome compositions for SSG horses at $t_1$.

## Microbiota profiles at $t_2$

At $t_2$, i.e., 10 (SSG) and 5 days (5DG) after the final PAP course was administered, the mean alpha-diversity of both study groups increased (SSG, $SDI_{mean} = 5.80$; 5DG, $SDI_{mean} = 5.87$), indicating the onset of microbiome recovery (Supplementary Table 1; Figure 3C).

## Common trajectories and inter-individual differences in microbiota profiles

To likewise illustrate common spatial shifts and individual deviation from common trajectories, data points representing samples of three individuals per group are highlighted in Figure 3.

### 5-day course of peri-operative antibiotic prophylaxis group

At $t_0$, the data points belonging to samples of equine patients 89, 33, and 87 clustered most distantly from the CG samples, indicating a considerable disturbance of the microbiome structure and composition at hospital admission. This finding is supported by the individual samples' low SDI values (5.05, 5.75, and 5.29; Supplementary Table 1). At $t_1$, samples 33 and 87 showed a different composition compared to the $t_0$ situation, but both points still clustered distantly from the CG area. Only the $t_1$ sample obtained from horse 89 showed some signs of movement toward the CG area (Figure 3B). At $t_2$, data points representing the samples of horses 33, 87, and 89 clustered within the CG area, indicating the onset of

microbiome recovery that was accompanied by a notable SDI increase (5.76, 6.02, and 5.76).

### Single-shot of peri-operative antibiotic prophylaxis group

The initial data point representing the $t_0$ sample of horse 45 (SDI 6.66) clustered near the area covered by the CG. While the corresponding data point at $t_1$ indicated an increase of gut microbiome disturbance accompanied by an SDI decrease to 5.97, the $t_2$ sample (SDI 6.15) clustered within the area framed by data points of the CG samples, once again indicating the onset of microbiome recovery.

However, some equine patients deviated from the aforementioned common temporal trajectory: The data points of horse 41 (SSG), for instance, indicated a considerable microbiome disturbance at $t_0$ (SDI 5.05) followed by a brief relative recovery at $t_1$ (SDI 5.99). Then, the data point of horse 41 shifted toward the opposite direction at $t_2$ (Figure 3A), a reversal that is accompanied by an SDI decrease to 5.59.

Taken together, samples of the CG seemed to represent an overall beneficial structure and composition of equine gut microbiota, since all patients' samples associated with an SDI > 5.8 clustered near or within the area covered by these samples, while samples associated with lower SDIs clustered elsewhere (Figure 3; Supplementary Table 1). Moreover, although a common temporal trajectory from hospital admission toward discharge was notable for the gut microbiota of most participants in both study groups, the temporal patterns of some horses deviated from these, emphasizing the individual nature of the GIT microbiome recovery process.

## Evaluation of gut microbiota alterations among horses receiving different PAP regimens after colic surgery

To gain insights into the putative effect of the different PAP regimens on the equine gut microbiota, log 2-fold changes (log2FC) were calculated based on OTU count changes on bacterial family level between sampling timepoints. Overall, the most prominent log2FC between $t_0$ and $t_1$ in the SSG were noticed for *Bacteroidaceae* (+5.16; $p < 0.05$), *Enterobacteriaceae* (+3.99; $p < 0.05$), and *Pseudomonadaceae* (+4.41; $p < 0.05$). Among the most prominent log2FC between $t_0$ and $t_1$ in samples of the 5DG were *Bacteroidaceae* (+2.96; $p < 0.05$) and *Pseudomonadaceae* (+3.33; $p < 0.05$).

### Divergence among microbiota composition on family level considering a baseline defined by the CG samples

In order to further investigate the relevance of the aforementioned observations and to better assess the influence of colic and midline laparotomy as well as antibiotic treatment on the abundances of specific bacterial families in the GIT of horses throughout this study, further log2FC values were determined based on the abundances calculated for the CG. Since the PCA confirmed the eligibility of the CG samples with respect to an overall favorable equine gut microbiota structure and composition, we determined the median relative abundance for bacteria (family level) among the CG samples. To enhance identification of relevant changes associated with microbiome disturbance among samples belonging to both study groups, the median for each bacterial family was calculated using the $t_0$ CG samples as a baseline. Then, log2FC for each sample/timepoint/study group/ were determined to pin-point variation that might have been overlooked by simply investigating mean abundances. In order to compensate for individual differences between the equine patients (i.e., age, diet, medical history, severity and duration of the acute colic episode, housing and social contacts), an interval comprising at least 85% of the SSG and 5DG samples was defined (Figure 4; log2FC ±2.5).

To identify the most deviations with high potential relevancy, further in-depth explorative analysis was restricted to bacterial families associated with at least five samples (SSG and 5DG) that clustered beyond the 85% interval (Figure 4, black arrows indicate bacterial families fulfilling the restriction criteria).

Directly at hospital admission and before any antibiotics were administered ($t_0$), six samples showed log2FC between 2.7 and 5.2 for *Streptococcaceae*, seven samples for *Bacteroidaceae* (log2FC between 2.9 and 8.6), seven samples for *Marinilabiliaceae* (log2FC between +2.8 and + 8.1), and six samples for *Enterobacteriaceae* (log2FC between +2.8 and + 5.9). Overall, lower values were noted for *Lachnospiraceae* (six samples, log2FC between −3.1 and − 5.4) and *Ruminicoccaceae* (five samples, log2FC between −2.7 and − 3.5; Figure 4, $t_0$; indicated by black arrows).

At $t_1$, increasing log2FC fulfilling the above mentioned criteria were noticed for *Clostridiaceae*, *Lactobacillaceae*, *Streptococcaceae*, *Veillonellaceae*, *Marinilabiliaceae*, and *Xanthomonadaceae*, but most prominently for *Bacteriodaceae* (22 samples, log2FC between +3.7 and + 9.5), *Comamonadaceae* (five samples, log2FC between +3.2 and + 11.6), *Enterobacteriaceae* (17 samples, log2FC between +2.7 and + 5.9), *Moraxellaceae* (six samples, log2FC between +3.5 and + 5.1), and *Pseudomonadaceae* (15 samples, log2FC between +2.8 and + 10.3; Figure 4). *Lachnospiraceae*, on the other hand, yielded log2FC between −2.7 and − 4.0 in five samples.

At $t_2$, deviation from the baseline interval (log2FC ≥ ±2.5) defined for bacterial families were recognized for *Bacteriodaceae* (11 samples, log2FC between +2.8 and + 9.3), *Enterobacteriaceae* (eight samples, log2FC between +2.6 and + 5.1), and *Lactobacillaceae* (nine samples, log2FC between +2.8 and + 5.9) followed by *Streptococcaceae*, *Veillonellaceae*, *Marinilabiliaceae*, *Comamonadaceae*, *Moraxellaceae*, and *Pseudomonadaceae* (Figure 4). Overall, a shift back to the baseline was directly recognizable for most of the displayed bacterial families.

Taken together, OTU abundances of many bacterial families deviated considerably from those associated with samples of the CG ($t_0$). In addition, overall deviation increased at $t_1$ and decreased at $t_2$, a result that is clearly in congruence with the SDI values and the trajectory pattern displayed by PCA (Figures 3A–D). Of note, clear differences between the study groups were not noticed in Figure 4. These results confirmed that although a common temporal trajectory pattern was recognizable, deviation of individuals contributed largely to the overall variances.

## Hospitalization, surgery, and administration of PAP is accompanied by a predominant converged trajectory pattern of *Escherichia* and *Bacteroides*

At $t_1$, deviations of *Bacteroidaceae* and *Enterobacteriaceae* stood out considering the baseline defined by the CG samples (Figure 4). Although relative abundances of OTUs within an individual sample depended on each other, we noticed stunning trajectories of OTUs


FIGURE 4
Changes of the fecal microbiome structure and composition during the study period. Illustration of log2FC abundance changes for bacterial families in each sample of both study groups with respect to a baseline calculated from the control group samples at $t_0$. To acknowledge individual variation and to enhance the chances of overall trend detection, an interval comprising the majority of samples (85% at $t_0$, $log_2$FC of 2.5) was calculated, illustrated as the blurred area per timepoint. Individual values that were zero (i.e., no abundance difference compared to the control) were not shown for better clarification. Data points belonging to samples from the SSG are marked by a triangle and those from the 5DG by a dot, while deviation from the baseline within at least five samples are indicated by a black arrow.

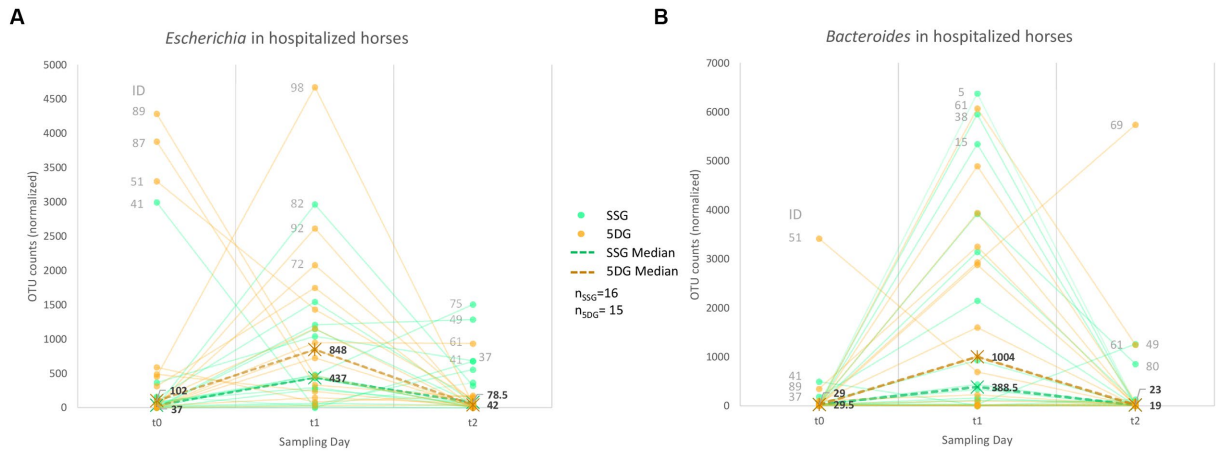


FIGURE 5
Abundance trajectories of OTUs assigned to the genera *Escherichia* **(A)** and *Bacteroides* **(B)**. Charts showing a trend line based on normalized OTU counts per sample/study group and timepoint. A dashed line indicates the median per group and sampling day.

assigned to *Bacteroides* and *Escherichia*, the predominating genera of the above-mentioned families within our sample set (Figure 5).

Apart from four horses (89, 87, 51, and 41), most study participants showed limited OTU counts ($median_{SSG}$ = 37; $median_{5DG}$ = 102) classified as *Escherichia* (genus level) at $t_0$, while the overall counts increased at $t_1$ (Figure 5A), with a median OTU counts of 437 (SSG) and 848 (5DG) in samples of both groups, respectively (SSG vs. 5DG, $t_0$: $p = 0.14$, $t_1$: $p = 0.086$, $t_2$: $p = 0.95$). This difference was significant between the SSG and 5DG from $t_1$ to $t_2$ (differences in counts, SSG vs. 5DG, $t_0$ to $t_1$: $p = 1$, $t_1$ to $t_2$: $p = 0.0019$). Of note, both study groups showed a decline to almost similar counts assigned to *Escherichia* at $t_2$ ($median_{SSG}$ = 79 OTU counts; $median_{5DG}$ = 42 OTU counts).

Interestingly, the hospitalized horses demonstrated a highly similar trajectory pattern for OTU counts assigned to the genus *Bacteroides*. Besides a single exception (horse 51, 5DG), both study groups had comparable counts for *Bacteroides* ($median_{SSG}$ = 29.5 OTU counts, $median_{5DG}$ = 29 OTU counts) at $t_0$ (SSG vs. 5DG, $t_0$: $p = 0.67$, $t_1$: $p = 0.45$, $t_2$: $p = 0.69$). Changes in differences were not significant across time points (differences in counts, SSG vs. 5DG, $t_0$ to $t_1$: $p = 0.89$, $t_1$ to $t_2$: $p = 0.92$).

At $t_1$, the OTU counts for *Bacteroides* doubled in abundance within the 5DG compared to the SSG ($median_{SSG}$ = 389, $median_{5DG}$ = 1,004 OTU, $p = 0.45$). However, the *Bacteroides* count level decreased once more at the last day of sampling ($t_2$) in both groups ($median_{SSG}$ = 19; $median_{5DG}$ = 23, $p = 0.69$).

In summary, the abundance counts of both *Escherichia* and *Bacteroides* seemed to be associated with a more pronounced increase among samples representing the 5DG, i.e., horses that received the long-term PAP, compared to horses belonging to the SSG at $t_1$. Correlation analysis revealed no obvious relationship between the two genera in the sample set investigated.

## Discussion

In the present study, we explored temporal alterations of the gut microbiota composition and the extent of its perturbation among hospitalized horses subjected to colic surgery that received either a short-term (SSG) or a 5-day course (5DG) of P/G PAP. Of note, comparison of fecal microbiota profiles of horses belonging to different cohorts or even between distinct individuals requires immense caution, since the intestinal microbiome is easily affected by external factors, including—but not limited to—exercise (Górniak et al., 2021), transport, fasting (Schoster et al., 2016) and diet (Al Jassim, 2006; Mshelia et al., 2018). In addition, Antwis et al. (2018) recently examined how spatial and social interactions affected the gut microbiome composition of semi-wild Welsh Ponies, revealing that up to 52.6% of the observed variation is attributable to individual variation.

At first, we determined the predominating microbial phyla in the sample set, revealing *Bacteroidota* (38%), *Bacillota* (33%) and *Verrucomicrobiota* (11%) as the top three main phyla at hospital admission ($t_0$) and in the CG (Figure 2). This result is in line with previous reports defining the *Bacteroidota* and *Bacillota* as the major phyla of the core bacterial community in equines (Morrison et al., 2018; Edwards et al., 2020).

### Gut microbiota diversity of hospitalized horses receiving colic surgery and P/G PAP elicits a predominant trajectory pattern from hospital admission to discharge

As summarized previously, most of the current clinical studies regarding the effects of antibiotics on the gut microbiome have been cross-sectional, while interventional or longitudinal approaches and comparisons to treatment-naive but diseased control groups are often missing (Zimmermann et al., 2021). As a result, it is difficult to differentiate between disease-mediated, drug-related hospitalization effects (Zimmermann et al., 2021), an aspect that clearly is a limitation with respect to the discussion of putative drug-related effects in the current study. Although the isolated and exact impact of the P/G regimen on the gut microbiota of horses participating in this study remains unknown due to the fact that our study was not an animal trial but a real-world scenario, recent research on the effect of parental administration of P/G on the developing infant gut microbiome clearly revealed an impact on Shannon diversity and overall gut microbiota composition (Reyman et al., 2022). However, at hospital admission and before antibiotic treatment and hospitalization ($t_0$), the mean alpha-diversity measured by SDIs revealed strong signals of an already compromised bacterial biodiversity in samples representing the SSG and the 5DG compared with those of the CG (Figure 3D), although only the latter difference was found to be significant. A loss of species diversity seems to be among the prominent characteristic of a disturbed gut microbiota (Ramirez et al., 2020). At hospital admission, a decrease in bacterial richness and diversity accompanied with a greater inter-individual variability was reported for horses admitted due to colic compared with horses presented for elective surgical procedures or even healthy horses (Stewart et al., 2018; Park et al., 2021). A similar trend was detected in the current study, demonstrating a considerable range of variation between microbiota profiles and microbiome perturbations among horses suffering from colic compared to horses free of abdominal pain or other enteral disorders.

A previous study by Costa et al. (2015) examined the effects of intramuscular administration of procaine penicillin and ceftiofur sodium, and oral trimethoprim sulfadiazine on the fecal microbiome of healthy horses. Although the administration route and duration, the cohort under investigation and the combination of antibiotics (P/G) differed in the present study, general similarities should be mentioned. The strongest perturbation of the microbiome was recognized directly after the final course of antibiotics, including a strong effect on the microbial community membership (Costa et al., 2015).

The most prominent peak of microbiome disturbance is characterized by significant SDI decreases at $t_1$ (i.e., 3 days after surgery/hospitalization; Figure 1). The considerable inter-individual distances between the microbiota profiles of 5DG horses at $t_0$ have diminished immensely at $t_1$, indicating a similar and consistent effect of the long-term PAP regimen on the gut microbiota composition that is specific for the long-term P/G PAP.

This observation is in line with the results of a recent study investigating the effects of commonly used antibiotics on the gut microbiome of healthy human volunteers before and after treatment, where the authors revealed drug-specific trajectories through the PCA space over time (Anthony et al., 2022). In strict contrast to the PCA of the 5DG in the present study, data points of the SSG showed increased inter-individual differences through the PCA space at $t_1$, indicating the lack of a common selective factor. Therefore, other more distinguishing factors associated with the distinct individual such as appetite, stress and/or pain, environmental bacteria or even the onset of GIT function and/or microbiome recovery (reviewed in Kauter et al., 2019) might be mirrored here.

At $t_2$, both study groups showed clear signs pointing toward the onset of microbiome recovery with respect to a rise of both $SDI_{mean}$, with most participants seeming to have already regained the baseline condition, since the difference between $t_0$ and $t_2$ lacked statistical differences (Figure 3). Interestingly, in a study of germ-free mice, the recovery of the gut microbiome after antibiotic treatment strongly depended on diet, community context and environmental reservoirs (Ng et al., 2019). The authors demonstrated that a reduction of environmental reservoirs impaired the process of microbiota recovery (Ng et al., 2019). This fact not only emphasizes the overall importance of the actual environmental bacteria in the immediate vicinity of hospitalized horses during microbiome recovery, but it also highlights the susceptibility of the equine gut microbiota to spatio-temporal local spreads of hospital-associated pathogens, explicitly including ESBL-EC, leading to worrisome carriage rates, as previously reported (Kauter et al., 2019).

Since studies on equine gut microbiomes are currently limited (Salem et al., 2019; Ang et al., 2022), it seems reasonable to assume

that some general effects occur across different mammalian species: Exposure of the gut microbiota to antibiotics or their active metabolites reduces its overall diversity, which is either temporarily or permanently conserved after end of antibiotic treatment (Costa et al., 2015; Ramirez et al., 2020; Arnold et al., 2021). Moreover, the effect might not be limited to a reduced microbial diversity, since a recent study on healthy human volunteers showed a worrisome increase of virulence- and resistance associated-factors immediately after antibiotic treatment (Palleja et al., 2018). Further studies on the equine gut metagenome (Ang et al., 2022) after exposure to different antibiotics are required to gain more insights with respect to spatial trends of virulence- and resistance gene occurrences and abundances.

## Alterations of the equine gut microbiota in the SSG and 5DG

At first, we analyzed the significant log2FC of the SSG and the 5DG. Samples of horses belonging to both study groups were associated with a significant abundance increase for *Bacteroidaceae*, *Enterobacteriaceae*, and *Pseudomonadaceae* from $t_0$ to $t_1$. A previous study that examined changes in the equine fecal microbiome during hospitalization because of colic reported a similar increase for *Bacteroides* (Stewart et al., 2021). The increased abundances noticed for *Enterobacteriaceae* at $t_1$ in both groups might enhance the risk of developing SSI for the equine patients, especially since multidrug-resistant Enterobacterales were often reported within horse clinics (Apostolakos et al., 2017; Walther et al., 2018; Shnaiderman-Torban et al., 2020), respectively in cases of SSI of horses subjected to laparotomy (Isgren et al., 2017; Dziubinski et al., 2020). Furthermore, significant changes were recognized regarding *Pseudomonadaceae*, a bacterial family that has been described as indicator of intestinal microbiome alterations in the human gut since an abundance increase seems to be associated with various gastrointestinal diseases (Alam et al., 2020; Chamorro et al., 2021).

Secondly, we explored the probable influence of the acute disease and other factors on the fecal microbiota. For this, we evaluated the abundance of different bacteria in fecal samples of both study groups compared to the control group at $t_0$, revealing considerable deviation of OTUs belonging to 15 different bacterial families (Figure 4). Overall, a common temporal trajectory pattern was recognizable regarding *Bacteroidaceae*, *Enterobacteriaceae*, and *Pseudomonadota*, with a strikingly increased proportion in almost all $t_1$ samples and decreasing, but still above-baseline level, OTU counts at $t_2$. In addition, we observed a reduced frequency of *Lachnospiraceae* for the horses diagnosed with colic, compared to the horses belonging to the CG, which is in line with recent findings (Stewart et al., 2019). Moreover, a reduction of *Lachnospiraceae* was previously described for horses suffering from enteral disorders (Costa et al., 2012; Weese et al., 2015).

Although differences between the study groups were limited, we observed interesting differences with respect to the effect of the distinct P/G PAPs on the microbiota. Horses that received the 5-day course of PAP showed the highest loss of inter-individual diversity (Figure 3B, $t_1$) which is clearly accompanied by the most prominent expansion of *Escherichia* (Figure 5). Further studies including metagenomic data are needed to reveal the particular dependences here.

## Gut microbiome perturbances are associated with increased *Escherichia* and *Bacteroides* abundances

Since penicillin and gentamicin were administered parenterally (Stöckle et al., 2021), the effect on the gut microbiome in general was expected to be lower than in cases when oral antibiotics where administered (Zhang et al., 2013). In the present study, however, the combined influences of (intestinal) illness, hospitalization, surgery and administration of P/G PAP showed a converged relative abundance trajectory of the genera *Escherichia* and *Bacteroides* over time, as demonstrated in the results (Figure 5). A recent review on the effects of distinct antibiotic classes on the GIT microbiome in humans highlighted an increase of *Enterobacteriaceae* and *Bacteroidaceae* after treatment with β-lactams in general (Patangia et al., 2022), which seems strikingly in line with the results presented here.

The obligatory anaerobic genus *Bacteroides* exclusively growing in the GIT of mammals is a major research focus of gut microbiology (reviewed in Wexler and Goodman, 2017). Since intrinsic resistance is reported for *Bacteroides* spp. [Pumbwe et al., 2006; Clinical and Laboratory Standards Institute (CLSI), 2020] at least an impact of a treatment-associated selective advantage can be assumed when considering the relative abundance increase among most of the fecal samples of both study group participants at $t_1$ (Figure 5), in particular for the 5DG.

Although many *Bacteroides* species play a crucial role in degrading polysaccharides of a plant-based diet (Pereira et al., 2021; Cheng et al., 2022), the specific importance and role of distinct *Bacteroides* species in hindgut fermentation has not been investigated yet. More research on the subject including metabolomic profiles gained from metagenome sequencing projects is clearly required to shed more light on this subject.

Apart from outliers (four horses, Figure 5), most of the horses participating in the present study revealed a low relative abundance of *Escherichia* at hospital admission. This observation is in line with the previously reported increase of ESBL-EC carriage rates among patients of both study groups over time, i.e., from hospital admission to discharge (Supplementary Table 1), that indicated local spread of, for instance, distinct ESBL-EC clonal lineages, as reported previously (Kauter et al., 2021). We further speculate that during P/G PAP, ESBL-EC had a selective advantage in the GIT of horses and therefore proliferate, resulting not only in increased carriage rates (Kauter et al., 2021), but also in unavoidable environmental contamination via feces-contaminated litter. Since the immediate environment is among the main sources of GIT-associated bacteria during microbiome recovery (Ng et al., 2019), environmental sources seem to play an overwhelming role with respect to ESBL-EC carriage rates. Since the specific needs and surroundings of hospitalized horses (bedding, boxes, and floor surfaces, reviewed in Gehlen et al., 2020) differ immensely from those of small animal or even human patients, the environment of equine clinics seems to play an important role in ESBL-EC accumulation and spread, including strains known for their pathogenic potential in humans and animals, i.e., isolates belonging to sequence type (ST)10 and ST410 (Kauter et al., 2021).

Taken together, the spread of *E. coli*, especially ESBL-EC in horse clinics, seems to be promoted by (i) the selective advantage of these bacteria toward β-lactam antibiotics and (ii) the fact that the fecal microbiota structure is re-modeled by other factors

occurring during the course of hospitalization, such as ingestion by food, contact to environmental sources or transmission via healthcare workers.

## Study limitations

The colic patients originated from different stables and unknown feeding situations prior to hospitalization. Once hospitalized, they were provided a stable diet, comparable to horses of the control group. Further differences existed between the control and treated hospitalized groups because horses were kept in different environments (barn vs. clinic).

## Conclusion

In the present study, we investigated the influence of two different PAP regimens (SSG vs. 5DG) in horses diagnosed with colic syndrome that were subjected to surgery with regard to changes of their gut microbiota composition. Colic surgery and PAP drive the equine gut microbiome toward dysbiosis and reduced biodiversity that is accompanied by a 10-fold increase of samples positive for ESBL-producing Enterobacterales (Kauter et al., 2021) and an abundance increase for Enterobacteriaceae. Further studies are needed to reveal the most important local sources of the resistant bacteria (i.e., environment, food, and contacts) and factors promoting the inclusion of ESBL-producing Enterobacterales in the equine gut microbiota.

# Data availability statement

The datasets presented in this study can be found in online repositories. The names of the repository/repositories and accession number(s) can be found at: https://www.ncbi.nlm.nih.gov/, BioProject: PRJNA906950.

# Ethics statement

Ethical approval was not required for the studies involving animals in accordance with the local legislation and institutional requirements, as the comparison of perioperative antibiotic regimens does not require approval. Written informed consent was obtained from the owners for the participation of their animals in this study.

# Author contributions

BW, AL-B, LW, and HG designed the project. AK, SS, HG, and BW conceived and designed the experiments. AK, DK, SS, JB, and AL-B performed laboratory analysis. CB and SF sequenced the samples. AK, SW, AL-B, BW, and TS analyzed the data. AK, SW, and BW wrote the first draft. AM, NS, RK, and SG helped to draft the manuscript and contributed to the discussion. All authors contributed to the article and approved the submitted version.

# Funding

This work was funded by the German Federal Ministry of Education and Research (BMBF) for #1Health-PREVENT (grants 01KI2009A, 01KI2009D, and 01KI2009F) within the German Research Network of Zoonotic Diseases. The funding bodies did not influence data interpretation or writing the manuscript. This work was also supported by the DFG Research Infrastructure NGS_CC (project 407495230) as part of the Next Generation Sequencing Competence Network (project 423957469). Sequencing was carried out at the Competence Center for Genomic Analysis (Kiel).

# Acknowledgments

We thank our colleagues from the Advanced Light and Electron Microscopy (ZBS 4) department of the Robert Koch Institute for their individual contribution and support. This manuscript was previously published as a preprint at: https://www.biorxiv.org/content/10.1101/2023.05.24.542119v1 (Kauter et al., 2023).

# Conflict of interest

The authors declare that the research was conducted in the absence of any commercial or financial relationships that could be construed as a potential conflict of interest.

# Publisher's note



# Supplementary material

The Supplementary material for this article can be found online at: https://www.frontiersin.org/articles/10.3389/fmicb.2023.1228845/full#supplementary-material

# References

Al Jassim, R. A. M. (2006). Supplementary feeding of horses with processed sorghum grains and oats. *Anim. Feed Sci. Technol.* 125, 33–44. doi: 10.1016/j.anifeedsci.2005.05.019

Alam, M. T., Amos, G. C. A., Murphy, A. R. J., Murch, S., Wellington, E. M. H., and Arasaradnam, R. P. (2020). Microbial imbalance in inflammatory bowel disease patients at different taxonomic levels. *Gut Pathog.* 12:1. doi: 10.1186/s13099-019-0341-6

Ang, L., Vinderola, G., Endo, A., Kantanen, J., Jingfeng, C., Binetti, A., et al. (2022). Gut microbiome characteristics in feral and domesticated horses from different geographic locations. *Commun. Biol.* 5:172. doi: 10.1038/s42003-022-03116-2

Anthony, W. E., Wang, B., Sukhum, K. V., D'souza, A. W., Hink, T., Cass, C., et al. (2022). Acute and persistent effects of commonly used antibiotics on the gut microbiome and resistome in healthy adults. *Cell Rep.* 39:110649. doi: 10.1016/j.celrep.2022.110649

Antwis, R. E., Lea, J. M. D., Unwin, B., and Shultz, S. (2018). Gut microbiome composition is associated with spatial structuring and social interactions in semi-feral Welsh Mountain ponies. *Microbiome* 6:207. doi: 10.1186/s40168-018-0593-2

Apostolakos, I., Franz, E., Van Hoek, A., Florijn, A., Veenman, C., Sloet-Van Oldruitenborgh-Oosterbaan, M. M., et al. (2017). Occurrence and molecular characteristics of ESBL/amp C-producing Escherichia coli in faecal samples from horses in an equine clinic. *J. Antimicrob. Chemother.* 72, 1915–1921. doi: 10.1093/jac/dkx072

Archer, D. C. (2019). Colic surgery: keeping it affordable for horse owners. *Vet. Rec.* 185, 505–507. doi: 10.1136/vr.l6062

Arnold, C. E., Pilla, R., Chaffin, M. K., Leatherwood, J. L., Wickersham, T. A., Callaway, T. R., et al. (2021). The effects of signalment, diet, geographic location, season, and colitis associated with antimicrobial use or Salmonella infection on the fecal microbiome of horses. *J. Vet. Intern. Med.* 35, 2437–2448. doi: 10.1111/jvim.16206

Aronesty, E. (2013). Comparison of sequencing utility programs. *Open Bioinform. J.* 7, 1–8. doi: 10.2174/1875036201307010001

Baverud, V., Gustafsson, A., Franklin, A., Aspan, A., and Gunnarsson, A. (2003). Clostridium difficile: prevalence in horses and environment, and antimicrobial susceptibility. *Equine Vet. J.* 35, 465–471. doi: 10.2746/042516403775600505

Caporaso, J. G., Kuczynski, J., Stombaugh, J., Bittinger, K., Bushman, F. D., Costello, E. K., et al. (2010). QIIME allows analysis of high-throughput community sequencing data. *Nat. Methods* 7, 335–336. doi: 10.1038/nmeth.f.303

Ceriotti, S., Westerfeld, R., Bonilla, A. G., and Pang, D. S. J. (2021). Use of clinical audits to evaluate timing of preoperative antimicrobials in equine surgery at a veterinary teaching hospital. *Front. Vet. Sci.* 8:630111. doi: 10.3389/fvets.2021.630111

Chamorro, N., Montero, D. A., Gallardo, P., Farfán, M., Contreras, M., De La Fuente, M., et al. (2021). Landscapes and bacterial signatures of mucosa-associated intestinal microbiota in Chilean and Spanish patients with inflammatory bowel disease. *Microb. Cell* 8, 223–238. doi: 10.15698/mic2021.09.760

Cheng, J., Hu, J., Geng, F., and Nie, S. (2022). Bacteroides utilization for dietary polysaccharides and their beneficial effects on gut health. *Food Sci. Human Wellness* 11, 1101–1110. doi: 10.1016/j.fshw.2022.04.002

Clinical and Laboratory Standards Institute (CLSI) (2020). *Performance Standards for Antimicrobial Susceptibility Testing CLSI Supplement M100*. Wayne, PA: Clinical and Laboratory Standards Institute

Cole, J. R., Wang, Q., Fish, J. A., Chai, B., Mcgarrell, D. M., Sun, Y., et al. (2014). Ribosomal database project: data and tools for high throughput rRNA analysis. *Nucleic Acids Res.* 42, D633–D642. doi: 10.1093/nar/gkt1244

Costa, M. C., Arroyo, L. G., Allen-Vercoe, E., Stämpfli, H. R., Kim, P. T., Sturgeon, A., et al. (2012). Comparison of the fecal microbiota of healthy horses and horses with colitis by high throughput sequencing of the V3-V5 region of the 16S rRNA gene. *PLoS One* 7:e41484. doi: 10.1371/journal.pone.0041484

Costa, M. C., Stampfli, H. R., Allen-Vercoe, E., and Weese, J. S. (2016). Development of the faecal microbiota in foals. *Equine Vet. J.* 48, 681–688. doi: 10.1111/evj.12532

Costa, M. C., Stampfli, H. R., Arroyo, L. G., Allen-Vercoe, E., Gomes, R. G., and Weese, J. S. (2015). Changes in the equine fecal microbiota associated with the use of systemic antimicrobial drugs. *BMC Vet. Res.* 11:19. doi: 10.1186/s12917-015-0335-7

Dallap Schaer, B. L., Linton, J. K., and Aceto, H. (2012). Antimicrobial use in horses undergoing colic surgery. *J. Vet. Intern. Med.* 26, 1449–1456. doi: 10.1111/j.1939-1676.2012.01024.x

Davis, J. L., Salmon, J. H., and Papich, M. G. (2006). Pharmacokinetics and tissue distribution of doxycycline after oral administration of single and multiple doses in horses. *Am. J. Vet. Res.* 67, 310–316. doi: 10.2460/ajvr.67.2.310

Desantis, T. Z., Hugenholtz, P., Larsen, N., Rojas, M., Brodie, E. L., Keller, K., et al. (2006). Greengenes, a chimera-checked 16S rRNA gene database and workbench compatible with ARB. *Appl. Environ. Microbiol.* 72, 5069–5072. doi: 10.1128/AEM.03006-05

Durward-Akhurst, S. A., Mair, T. S., Boston, R., and Dunkel, B. (2013). Comparison of two antimicrobial regimens on the prevalence of incisional infections after colic surgery. *Vet. Rec.* 172:287. doi: 10.1136/vr.101186

Dziubinski, N., Mählmann, K., Lübke-Becker, A., and Lischer, C. (2020). Retrospective identification of bacterial isolates from emergency laparotomy surgical site infections in horses. *J. Equine Vet.* 87:102927. doi: 10.1016/j.jevs.2020.102927

Edgar, R. C. (2010). Search and clustering orders of magnitude faster than BLAST. *Bioinformatics* 26, 2460–2461. doi: 10.1093/bioinformatics/btq461

Edgar, R. C., Haas, B. J., Clemente, J. C., Quince, C., and Knight, R. (2011). UCHIME improves sensitivity and speed of chimera detection. *Bioinformatics* 27, 2194–2200. doi: 10.1093/bioinformatics/btr381

Edwards, J. E., Shetty, S. A., Van Den Berg, P., Burden, F., Van Doorn, D. A., Pellikaan, W. F., et al. (2020). Multi-kingdom characterization of the core equine fecal microbiota based on multiple equine (sub)species. *Anim. Microb.* 2:6. doi: 10.1186/s42523-020-0023-1

Gehlen, H., Simon, C., Reinhold-Fritzen, B., Lübke-Becker, A., Kauter, A., Walther, B., et al. (2020). Basis-Hygienemaßnahmen für den Pferdetierarzt in Praxis und Klinik. *Berl. Munch. Tierarztl. Wochenschr.* 133 doi: 10.2376/1439-0299-2020-3

Górniak, W., Cholewińska, P., Szeligowska, N., Wołoszyńska, M., Soroko, M., and Czyż, K. (2021). Effect of intense exercise on the level of Bacteroidetes and Firmicutes Phyla in the digestive system of thoroughbred racehorses. *Animals* 11:290. doi: 10.3390/ani11020290

Gu, Z., Eils, R., and Schlesner, M. (2016). Complex heatmaps reveal patterns and correlations in multidimensional genomic data. *Bioinformatics* 32, 2847–2849. doi: 10.1093/bioinformatics/btw313

Isgren, C. M., Salem, S. E., Archer, D. C., Worsman, F. C., and Townsend, N. B. (2017). Risk factors for surgical site infection following laparotomy: effect of season and perioperative variables and reporting of bacterial isolates in 287 horses. *Equine Vet. J.* 49, 39–44. doi: 10.1111/evj.12564

Kauter, A., Brombach, J., Luebke-Becker, A., Kannapin, D., Bang, C., Franzenburg, S., et al. (2023). Antibiotic prophylaxis and hospitalization of horses subjected to median laparotomy: gut microbiota trajectories and abundance increase of Escherichia. bioRxiv [Preprint]. doi: 10.1101/2023.05.24.542119v1

Kauter, A., Epping, L., Ghazisaeedi, F., Lübke-Becker, A., Wolf, S. A., Kannapin, D., et al. (2021). Frequency, local dynamics, and genomic characteristics of ESBL-producing *Escherichia coli* isolated from specimens of hospitalized horses. *Front. Microbiol.* 12:671676. doi: 10.3389/fmicb.2021.671676

Kauter, A., Epping, L., Semmler, T., Antao, E.-M., Kannapin, D., Stoeckle, S. D., et al. (2019). The gut microbiome of horses: current research on equine enteral microbiota and future perspectives. *Anim. Microb.* 1:14. doi: 10.1186/s42523-019-0013-3

Kelly, B. J., Gross, R., Bittinger, K., Sherrill-Mix, S., Lewis, J. D., Collman, R. G., et al. (2015). Power and sample-size estimation for microbiome studies using pairwise distances and PERMANOVA. *Bioinformatics* 31, 2461–2468. doi: 10.1093/bioinformatics/btv183

Kozich, J. J., Westcott, S. L., Baxter, N. T., Highlander, S. K., and Schloss, P. D. (2013). Development of a dual-index sequencing strategy and curation pipeline for analyzing amplicon sequence data on the MiSeq Illumina sequencing platform. *Appl. Environ. Microbiol.* 79, 5112–5120. doi: 10.1128/AEM.01043-13

Lahti, L., Shetty, S., et al. (2017). Tools for microbiome analysis in R. Available at: https://microbiome.github.io/tutorials/ (Accessed September 20, 2022).

Liepman, R. S., Swink, J. M., Habing, G. G., Boyaka, P. N., Caddey, B., Costa, M., et al. (2022). Effects of intravenous antimicrobial drugs on the equine fecal microbiome. *Animals* 12:1013. doi: 10.3390/ani12081013

Love, M. I., Huber, W., and Anders, S. (2014). Moderated estimation of fold change and dispersion for RNA-seq data with DESeq2. *Genome Biol.* 15:550. doi: 10.1186/s13059-014-0550-8

Mach, N., Ruet, A., Clark, A., Bars-Cortina, D., Ramayo-Caldas, Y., Crisci, E., et al. (2020). Priming for welfare: gut microbiota is associated with equitation conditions and behavior in horse athletes. *Sci. Rep.* 10:8311. doi: 10.1038/s41598-020-65444-9

Magoč, T., and Salzberg, S. L. (2011). FLASH: fast length adjustment of short reads to improve genome assemblies. *Bioinformatics* 27, 2957–2963. doi: 10.1093/bioinformatics/btr507

Mcdonald, D., Clemente, J. C., Kuczynski, J., Rideout, J. R., Stombaugh, J., Wendel, D., et al. (2012). The biological observation matrix (BIOM) format or: how I learned to stop worrying and love the ome-ome. *GigaScience* 1:7. doi: 10.1186/2047-217X-1-7

Mcmurdie, P. J., and Holmes, S. (2013). Phyloseq: an R package for reproducible interactive analysis and graphics of microbiome census data. *PLoS One* 8:e61217. doi: 10.1371/journal.pone.0061217

Morrison, P. K., Newbold, C. J., Jones, E., Worgan, H. J., Grove-White, D. H., Dugdale, A. H., et al. (2018). The equine gastrointestinal microbiome: impacts of age and obesity. *Front. Microbiol.* 9:3017. doi: 10.3389/fmicb.2018.03017

Mshelia, E. S., Adamu, L., Wakil, Y., Turaki, U. A., Gulani, I. A., and Musa, J. (2018). The association between gut microbiome, sex, age and body condition scores of horses in Maiduguri and its environs. *Microb. Pathog.* 118, 81–86. doi: 10.1016/j.micpath.2018.03.018

Ng, K. M., Aranda-Díaz, A., Tropini, C., Frankel, M. R., van Treuren, W., O'Loughlin, C. T., et al. (2019). Recovery of the gut microbiota after antibiotics depends on host diet, community context, and environmental reservoirs. *Cell Host Microbe* 26, 650–665.e4. doi: 10.1016/j.chom.2019.10.011

Oren, A., and Garrity, G. M. (2021). Valid publication of the names of forty-two phyla of prokaryotes. *Int. J. Syst. Evol. Microbiol.* 71, 3491–3500. doi: 10.1099/ijsem.0.005056

Palleja, A., Mikkelsen, K. H., Forslund, S. K., Kashani, A., Allin, K. H., Nielsen, T., et al. (2018). Recovery of gut microbiota of healthy adults following antibiotic exposure. *Nat. Microbiol.* 3, 1255–1265. doi: 10.1038/s41564-018-0257-9

Park, T., Cheong, H., Yoon, J., Kim, A., Yun, Y., and Unno, T. (2021). Comparison of the fecal microbiota of horses with intestinal disease and their healthy counterparts. *Vet. Sci.* 8:113. doi: 10.3390/vetsci8060113

Patangia, D. V., Anthony Ryan, C., Dempsey, E., Paul Ross, R., and Stanton, C. (2022). Impact of antibiotics on the human microbiome and consequences for host health. *MicrobiologyOpen* 11:e1260. doi: 10.1002/mbo3.1260

Pereira, G. V., Abdel-Hamid, A. M., Dutta, S., D'alessandro-Gabazza, C. N., Wefers, D., Farris, J. A., et al. (2021). Degradation of complex arabinoxylans by human colonic Bacteroidetes. *Nat. Commun.* 12:459. doi: 10.1038/s41467-020-20737-5

Pumbwe, L., Ueda, O., Yoshimura, F., Chang, A., Smith, R. L., and Wexler, H. M. (2006). *Bacteroides fragilis* BmeABC efflux systems additively confer intrinsic antimicrobial resistance. *J. Antimicrob. Chemother.* 58, 37–46. doi: 10.1093/jac/dkl202

Ramirez, J., Guarner, F., Bustos Fernandez, L., Maruy, A., Sdepanian, V. L., and Cohen, H. (2020). Antibiotics as major disruptors of gut microbiota. *Front. Cell. Infect. Microbiol.* 10:572912. doi: 10.3389/fcimb.2020.572912

Reeder, J., Huang, M., Kaminker, J. S., and Paulson, J. N. (2021). MicrobiomeExplorer: an R package for the analysis and visualization of microbial communities. *Bioinformatics* 37, 1317–1318. doi: 10.1093/bioinformatics/btaa838

Reyman, M., Van Houten, M. A., Watson, R. L., Chu, M. L. J. N., Arp, K., De Waal, W. J., et al. (2022). Effects of early-life antibiotics on the developing infant gut microbiome and resistome: a randomized trial. *Nat. Commun.* 13:893. doi: 10.1038/s41467-022-28525-z

Salem, S. E., Maddox, T. W., Antczak, P., Ketley, J. M., Williams, N. J., and Archer, D. C. (2019). Acute changes in the colonic microbiota are associated with large intestinal forms of surgical colic. *BMC Vet. Res.* 15:468. doi: 10.1186/s12917-019-2205-1

Schoster, A., Mosing, M., Jalali, M., Staempfli, H. R., and Weese, J. S. (2016). Effects of transport, fasting and anaesthesia on the faecal microbiota of healthy adult horses. *Equine Vet. J.* 48, 595–602. doi: 10.1111/evj.12479

Schwartz, D. J., Langdon, A. E., and Dantas, G. (2020). Understanding the impact of antibiotic perturbation on the human microbiome. *Genome Med.* 12:82. doi: 10.1186/s13073-020-00782-x

Shen, W., Le, S., Li, Y., and Hu, F. (2016). Seq kit: a cross-platform and ultrafast toolkit for FASTA/Q file manipulation. *PLoS One* 11:e0163962. doi: 10.1371/journal.pone.0163962

Shnaiderman-Torban, A., Navon-Venezia, S., Dor, Z., Paitan, Y., Arielly, H., Ahmad, W. A., et al. (2020). Extended-Spectrum β-lactamase-producing Enterobacteriaceae shedding in farm horses versus hospitalized horses: prevalence and risk factors. *Animals* 10:282. doi: 10.3390/ani10020282

Southwood, L. L. (2014). Perioperative antimicrobials: should we be concerned about antimicrobial drug use in equine surgical patients? *Equine Vet. J.* 46, 267–269. doi: 10.1111/evj.12247

Stewart, H. L., Pitta, D., Indugu, N., Vecchiarelli, B., Engiles, J. B., and Southwood, L. L. (2018). Characterization of the fecal microbiota of healthy horses. *Am. J. Vet. Res.* 79, 811–819. doi: 10.2460/ajvr.79.8.811

Stewart, H. L., Pitta, D., Indugu, N., Vecchiarelli, B., Hennessy, M. L., Engiles, J. B., et al. (2021). Changes in the faecal bacterial microbiota during hospitalisation of horses with colic and the effect of different causes of colic. *Equine Vet. J.* 53, 1119–1131. doi: 10.1111/evj.13389

Stewart, H. L., Southwood, L. L., Indugu, N., Vecchiarelli, B., Engiles, J. B., and Pitta, D. (2019). Differences in the equine faecal microbiota between horses presenting to a tertiary referral hospital for colic compared with an elective surgical procedure. *Equine Vet. J.* 51, 336–342. doi: 10.1111/evj.13010

Stockle, S. D., Failing, K., Koene, M., and Fey, K. (2018). Postoperative complications in equine elective, clean orthopaedic surgery with/without antibiotic prophylaxis. *Tierarztl. Prax. Ausg. G Grosst. Nutz.* 46, 81–86. doi: 10.15653/TPG-170491

Stöckle, S. D., Kannapin, D. A., Kauter, A. M. L., Lübke-Becker, A., Walther, B., Merle, R., et al. (2021). A pilot randomised clinical trial comparing a short-term perioperative prophylaxis regimen to a long-term standard protocol in equine colic surgery. *Antibiotics* 10:10. doi: 10.3390/antibiotics10050587

Teschner, D., Barton, A. K., Klaus, C., and Gehlen, H. (2015). Antibiotikaeinsatz bei operierten Kolikpferden in Deutschland. *Pferdeheilkunde* 31, 235–240. doi: 10.21836/PEM20150305

Traub-Dargatz, J. L., Kopral, C. A., Seitzinger, A. H., Garber, L. P., Forde, K., and White, N. A. (2001). Estimate of the national incidence of and operation-level risk factors for colic among horses in the United States, spring 1998 to spring 1999. *J. Am. Vet. Med. Assoc.* 219, 67–71. doi: 10.2460/javma.2001.219.67

Walther, B., Klein, K.-S., Barton, A.-K., Semmler, T., Huber, C., Wolf, S. A., et al. (2018). Extended-spectrum beta-lactamase (ESBL)-producing Escherichia coli and *Acinetobacter baumannii* among horses entering a veterinary teaching hospital: the contemporary "Trojan horse". *PLoS One* 13:e0191873. doi: 10.1371/journal.pone.0191873

Weese, J. S., Holcombe, S. J., Embertson, R. M., Kurtz, K. A., Roessner, H. A., Jalali, M., et al. (2015). Changes in the faecal microbiota of mares precede the development of post partum colic. *Equine Vet. J.* 47, 641–649. doi: 10.1111/evj.12361

Wexler, A. G., and Goodman, A. L. (2017). An insider's perspective: Bacteroides as a window into the microbiome. *Nat. Microbiol.* 2:17026. doi: 10.1038/nmicrobiol.2017.26

Wickham, H., Chang, W., Henry, L., Pedersen, T.L., Takahashi, K., Wilke, C., et al. (2016). ggplot2: create elegant data visualisations using the grammar of graphics. R package version 2. Available at: https://ggplot2.tidyverse.org/reference/ggplot2-package.html (Accessed June 2022).

Wormstrand, B. H., Ihler, C. F., Diesen, R., and Krontveit, R. I. (2014). Surgical treatment of equine colic—a retrospective study of 297 surgeries in Norway 2005-2011. *Acta Vet. Scand.* 56:38. doi: 10.1186/1751-0147-56-38

Zhang, L., Huang, Y., Zhou, Y., Buckley, T., and Wang, H. H. (2013). Antibiotic administration routes significantly influence the levels of antibiotic resistance in gut microbiota. *Antimicrob. Agents Chemother.* 57, 3659–3666. doi: 10.1128/AAC.00670-13

Zimmermann, M., Patil, K. R., Typas, A., and Maier, L. (2021). Towards a mechanistic understanding of reciprocal drug-microbiome interactions. *Mol. Syst. Biol.* 17:e10116. doi: 10.15252/msb.202010116

frontiers | Frontiers in Microbiology

TYPE Original Research
PUBLISHED 29 November 2023
DOI 10.3389/fmicb.2023.1270974



OPEN ACCESS

EDITED BY
Edoardo Pasolli,
University of Naples Federico II, Italy

REVIEWED BY
Biswaranjan Pradhan,
Indian Institute of Technology Bhubaneswar, India
Jashbhai B. Prajapati,
Anand Agricultural University, India
Nitin Tyagi,
National Dairy Research Institute (ICAR), India

*CORRESPONDENCE
Rebeca Martin
✉ rebeca.martin-rosique@inrae.fr

RECEIVED 01 August 2023
ACCEPTED 23 October 2023
PUBLISHED 29 November 2023

CITATION
Carbonne C, Chadi S, Kropp C, Molimard L, Chain F, Langella P and Martin R (2023) *Ligilactobacillus salivarius* CNCM I-4866, a potential probiotic candidate, shows anti-inflammatory properties *in vitro* and *in vivo*. *Front. Microbiol.* 14:1270974. doi: 10.3389/fmicb.2023.1270974



# *Ligilactobacillus salivarius* CNCM I-4866, a potential probiotic candidate, shows anti-inflammatory properties *in vitro* and *in vivo*

Celia Carbonne, Sead Chadi, Camille Kropp, Lise Molimard, Florian Chain, Philippe Langella and Rebeca Martin*

Micalis Institute, AgroParisTech, INRAE, Université Paris-Saclay, Jouy-en-Josas, France

**Introduction:** The aim of this work was to characterize a new strain of *Ligilactobacillus salivarius* (CNCM I-4866) (CNCM I-4866) to address its potential as probiotic with a special focus on intestinal inflammation. Potential anti-inflammatory abilities of this strain were evaluated through *in vivo* and *in vitro* experiments.

**Methods:** Firstly, the strain was tested in a murine acute inflammation colitis model induced by DNBS. *In vitro* characterization was then performed with diverse tests: modulation capability of intestinal permeability; study of the impact on immunity profile through cytokines dosage; capacity to inhibit pathogens and adhere to intestinal cells lines. Production of metabolites, antibiotic resistance and survival to gastro-intestinal tract conditions were also tested.

**Results:** *In vitro* assay has shown a reduction of colonic damage and markers of inflammation after treatment with CNCM I-4866. Transcriptomic analysis performed on colons showed the capacity of the strain to down-regulate pro-inflammatory cytokines. *L. salivarius* CNCM I-4866 exerted anti-inflammatory profile by reducing IL-8 production by TNF-α stimulated cell and modulated cytokines profile on peripheral blood mononuclear cells (PBMC). It protected intestinal integrity by increasing trans-epithelial electrical resistance (TEER) on Caco-2 TNF-α inflamed cells. Additionally, *L. salivarius* CNCM I-4866 displayed inhibition capacity on several intestinal pathogens and adhered to eukaryotic cells. Regarding safety and technical concerns, CNCM I-4866 was highly resistant to 0.3% of bile salts and produced mainly L-lactate. Finally, strain genomic characterization allowed us to confirm safety aspect of our strain, with no antibiotic gene resistance found.

**Discussion:** Taken together, these results indicate that *L. salivarius* CNCM I-4866 could be a good probiotic candidate for intestinal inflammation, especially with its steady anti-inflammatory profile.

KEYWORDS

***Ligilactobacillus salivarius*, probiotic, DNBS inflammation, *in vitro*, anti-inflammatory**

## Introduction

Inflammatory bowel diseases (IBDs), including ulcerative colitis and Crohn's disease, are common chronic gastrointestinal diseases, mainly in Western countries (Aldars-Garcia et al., 2021). IBDs are characterized by inflammation bursting of the gastrointestinal tract driven by over-stimulation of the immune system. This deleterious inflammatory response includes the

overproduction of reactive oxygen species, damage to the intestinal epithelial barrier, and an imbalance in the immune response with the secretion of pro-inflammatory cytokines (Jakubczyk et al., 2020).

Even if IBD development is multifactorial, it has been shown that IBDs are linked with deregulation in the intestinal microbiota (Glassner et al., 2020). The intestinal microbiota is composed of more than trillions of different microorganisms, such as bacteria, fungi, or viruses. The majority of intestinal bacteria belong to four phyla: Bacillota, Bacteroidota, Pseudomonadota, and Actinomycetes (Thursby and Juge, 2017). The gut microbiota has many functions, such as host nutrient metabolism, immunomodulation, and protection against pathogens (Jandhyala et al., 2015). In the case of IBD, both the prevalence of pathobionts and/or the lack of key bacteria can promote IBD development and maintenance (Frank et al., 2007).

In the Bacillota phylum, the family Lactobacillaceae is a widely diverse group of Gram-positive bacteria, harboring 25 genera and almost 200 species. They exert an anaerobic metabolism, producing lactic acid through the fermentation of sugars, but are able to tolerate the presence of oxygen. Lactobacilli are widely studied for their potential beneficial properties. For example, some strains are shown to have a beneficial impact on restoring intestinal permeability (Chamignon et al., 2020), which is increased during inflammation. Another key role of some *Lactobacillus* strains is their ability to modulate the immune response in an inflammatory state by decreasing pro-inflammatory cytokine production or enhancing the levels of anti-inflammatory cytokines, such as IL-10 (Alard et al., 2018). Some *Lactobacillus* members are also known to be high producers of exopolysaccharides (EPSs), which have been recognized to directly infer the health-promoting properties of Lactobacilli (Juraskova et al., 2022; Martin et al., 2023).

*Ligilactobacillus salivarius,* formerly named *Lactobacillus salivarius,* is a homo-fermentative species. Many studies have been conducted on *L. salivarius* because of its useful properties for human health (Chaves et al., 2017). Indeed, beyond their capacity to alleviate inflammation-induced colitis in the murine model (Peran et al., 2005; Iyer et al., 2022), some *L. salivarius* strains are well known to exert antimicrobial activity (Tinrat et al., 2011; Messaoudi et al., 2013). Thereby, several strains of the Lactobacillaceae family were characterized these last years as potential probiotics for IBD, serving as complements to treatments in order to reduce disease-associated symptoms. Probiotics are defined as "live microorganisms, that, when administered in adequate amounts, confer a health benefit on the host" (Hill et al., 2014). Due to the wide range of applications of probiotics and their various mechanisms of action, the EFSA has proposed "Guidance on the characterization of microorganisms used as feed additives or as production organisms" (Rychen et al., 2018), suggesting safety and effectiveness criteria for their evaluation. These criteria include mostly physiological characterization and safety assessment by genomic analysis, particularly research for antibiotic resistance. Other key features to ensure the strain's ability to exert its beneficial activity are resistance to the gastrointestinal tract or adhesion to the intestinal mucosa.

In this study, we have assessed the probiotic capacities of *L. salivarius* CNCM I-4866 to target gut inflammation as the first step to characterize its potential beneficial effects on IBD management. Murine acute colitis assays and *in vitro* experiments were conducted to target some potentially beneficial effects observed *in vivo* (restoration of intestinal permeability and immunomodulatory response). Technological and safety parameters and genomic characterization were also explored to validate the safe status of this strain and its industrial interest.

# Materials and methods

## Growth of strains and eukaryotic cells

*Ligilactobacillus salivarius* CNCM I-4866 was isolated by SORBIAL company from the rumen of grazing lamb. *Ligilactobacillus salivarius* CNCM I-4866 and *Lacticaseibacillus rhamnosus* GG were grown in Man Rogosa and Sharpe (MRS) (Biokar, Solabia, France) at 37°C in aerobic conditions.

Bacterial cultures were centrifuged at 8000xg, washed twice in DPBS (Gibco, Thermo Fisher, USA), and resuspended in DPBS at an established concentration. These aliquots were used for *in vitro* and *in vivo* assays described below.

The human colon adenocarcinoma cell lines HT-29 and Caco-2 were obtained from the American Type Culture Collection (ATCC, United Kingdom). HT-29 cells were grown in Dulbecco's modified Eagle's medium supplemented with GlutaMAX (DMEM) (Gibco, Thermo Fisher) and 10% (v/v) of heat-inactivated fetal bovine serum (FBS, Eurobio, France). The Caco-2 cell line was cultured on DMEM GlutaMAX medium, 10% FBS, 1% non-essential amino acids (Gibco, Thermo Fisher), and 0.1% penicillin/streptomycin (Gibco, Thermo Fisher). The cultures were maintained at 37°C under 10% $CO_2$, and the medium was changed every 2 days.

## DNBS-induced colitis assays

For DNBS assays, 54 6-week-old male C57BL/6JrJ mice were obtained from Janvier Laboratory (Janvier, France) and maintained under specific pathogen-free (SPF) conditions in the animal facilities of the IERP Experimental Unit, INRAE. They were housed in four or five cages. Experiments were performed in accordance with European Union legislation on animal welfare and were approved by COMETHEA, a local committee on animal experimentation (no. 16744–201807061805486), and in compliance with the ARRIVE relevant guidelines. After a 7-day acclimation period, 54 mice were divided into 3 groups ($n = 8$ or $n = 10$ mice/group): the vehicle control group [no inflammation; Ethanol (EtOH)-Vehicle], the inflamed control group (inflammation-induced; DNBS-Vehicle), and the treated group (DNBS-CNCM I-4866). For 10 days, intra-gastric administration of DPBS (Vehicle) (Gibco, Thermo Fisher) (200 µL), 16% (v/v) glycerol, or the bacteria resuspended in DPBS ($10^9$ CFU/mL in 200 µL) was performed. Gavages were performed daily until the end of the experiment. After 7 days, the mice were anesthetized with an intraperitoneal injection of 0.1% ketamine and 0.06% xylazine. Subsequently, an intra-rectal injection of 2,4-dinitrobenzenesulfonic acid hydrate (Sigma, Switzerland) at a 2.75 mg/mice concentration dissolved in 30% ethanol in DPBS was injected. The vehicle control group received an intra-rectal injection of 30% ethanol in DPBS alone. After 3 days of the injection, blood was collected from the sub-mandibular vein, and mice were euthanized by cervical dislocation. The experiment procedure is presented in Figure 1.

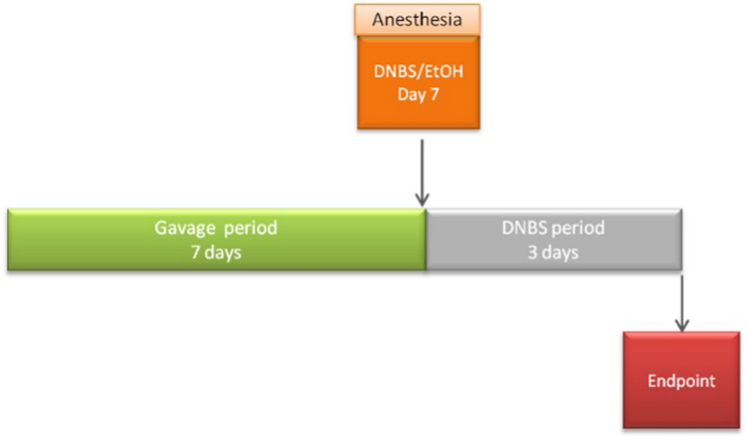


FIGURE 1
Procedure description of the acute DNBS model.

Macroscopic scores in terms of Wallace scores (Wallace et al., 1989), microscopic scores in terms of Ameho scores (Ameho et al., 1997), and myeloperoxidase (MPO) activity levels were determined on the colon samples as described before (Barone et al., 2018). The levels of lipocalin-2 (Mouse Lipocalin-2, R&D Systems, USA) and sCD14 (Mouse sCD14, R&D Systems, USA) were determined using ELISA, according to the manufacturer's instructions.

Transcriptomic analysis was performed on the colon samples of mice. In brief, samples were conserved in RNA at −80°C, and RNA was extracted afterward with the RNeasy kit (RNeasy kit, Qiagen, the Netherlands), following the manufacturer's instructions. Transcriptomic analysis was performed by the GENOM'IC platform at Cochin Institute using the 3'tag method. FASTQ files were then aligned using the STAR algorithm (version 2.7.6a) on the Ensembl release 101 reference. Reads were then counted using RSEM (v1.3.1), and the statistical analyses on the read counts were performed with R (version 3.6.3) and the DESeq2 package (DESeq2_1.26.0) to determine the proportion of differentially expressed genes between two conditions. The standard DESeq2 normalization method (DESeq2's median of ratios with the DESeq function) was used, with pre-filter of reads and genes (reads uniquely mapped on the genome, or up to 10 different loci with a count adjustment, and genes with at least 10 reads in at least 3 different samples). Following the package recommendations, the Wald test with the contrast function and the Benjamin–Hochberg FDR control procedure were used to identify the differentially expressed genes. Selected gene lists ($|\log2FoldChange| > 1.5$ and value of $p < 0.05$) were loaded into ingenuity pathway analysis (IPA) to analyze pathways and generate data.

## Anti-inflammatory *in vitro* assay on HT-29 cells

HT-29 cells were seeded into 24-well plates ($1 \times 10^5$ cells per well). After 6 days, when confluence was reached, the medium was replaced by a DMEM GlutaMAX medium with 5% FBS. After 24 h, on day 7, co-incubation with the bacterial cells was performed at a multiplicity of infection (MOI) of 40 in DMEM GlutaMAX, 0.1% penicillin/streptomycin, and 5% FBS and supplemented or not with TNF-α at a final concentration of 5 ng/mL (PeproTech, USA). DPBS was used as a negative control and butyrate at 10 mM as a positive control. After 6 h of co-incubation, supernatants were recovered and stored at −80°C. Interleukin (IL)-8 concentrations were quantified using the Human IL-8 ELISA MAX Standard Set (BioLegend, USA), according to the manufacturer's instructions. The absorbance was measured at 450 nm using the Infinite M200 Pro (TECAN, Switzerland).

## Transepithelial resistance measurements

Caco-2 cells were grown on Transwell inserts and kept at 37°C under 10% $CO_2$ until 80% confluence was reached. The medium was changed every 2 days. When optimal transepithelial resistance (TEER) values were reached (REMS AutoSampler, World Precision Instruments, USA), the fresh medium was added. Then, the strain *L. salivarius* CNCM I-4866 and *Lacticaseibacillus rhamnosus* GG (used as a positive control; Chamignon et al., 2020) at MOI 40 or the control (DPBS) were added to the apical compartment of the cells. After 3 h, 100 ng/mL of TNF-α was added to the basal compartment of Transwell plates. TEER was measured just before and 24 h after the treatments. The results were normalized to basal TEER as follows:

$$Ratio = \frac{TEERTreatmentT24 / TEERTreatmentT0}{TEERControlT24 / TEERControlT0}$$

## Immunomodulatory effects on PBMCs

Human peripheral blood mononuclear cells (PBMCs) isolated from the blood of healthy donors were obtained from StemCells (StemCells, Canada) and stored in liquid nitrogen. Five donors were selected according to the next selective criteria as follows: male individuals, BMI between 20 and 30, non-smokers, and with no allergies or diseases, such as asthma. After thawing, PBMCs were washed twice with Roswell Park Memorial Institute GlutaMAX medium (RPMI) (Gibco, Thermo Fisher) containing 10% FBS, and

DNase I was added to avoid aggregate formation. Then, cells were centrifuged at 200 *g* for 15 min at room temperature, and the supernatants were discarded. The washing step was performed twice, and then PBMCs were counted using the trypan blue method. Next, PBMCs were seeded at a rate of 1 million per 24-well plate. In total, 50 µL of fresh bacteria cultured in MRS (Difco, Thermo Fisher) was added at an MOI of 10, and co-cultures were maintained at 37°C in 5% $CO_2$ for 24 h. *Escherichia coli* TG1 was used as a control (Sokol et al., 2008). Finally, supernatants were collected, and interleukin-10 (IL-10), interleukin-12 (IL-12), and tumor necrosis factor (TNF-α) were quantified by ELISA using specific kits (Mabtech, Sweden), according to the manufacturer's guidelines.

## Ability to inhibit pathogen growth

Pathogen inhibition capacity against eight pathogens was determined. *Salmonella typhimurium, Salmonella enteritidis, Listeria monocytogenes* EDGE, *Escherichia coli* ATCC 700928, *Staphylococcus aureus* CNRZ 875, and *Clostridium perfringens* ATCC 13124 were obtained from the INRAE internal collection. *Helicobacter pylori* 26,695 was kindly provided by the Pasteur Institute (Dr. Hilde de Reuse team). *Campylobacter jejuni* BF was provided by the INRAE/ONIRIS Nantes collection. The first six strains were cultivated on Mueller Hinton (Thermo Fisher) at 37°C under aerobic conditions. *H. pylori* and *C. jejuni* were cultivated on Mueller Hinton agar supplemented with 5% sheep blood (Thermo Fisher) at 37°C in a micro-aerophilic atmosphere (bioMérieux, France). To perform inhibition tests, a lawn of each pathogen from a fresh suspension was made on Mueller Hinton. Holes were made in the agar with P100 sterile tips, to which 50 µL of filtered supernatants from a stationary-phase culture or control medium alone (MRS) was added. The results were read after 48 h of incubation as the diameter of inhibition (mm). To assess whether inhibition was due to acid production by the *L. salivarius* CNCM I-4866 strain, we performed the assay with supernatants neutralized at pH 7 with sodium hydroxide.

## Adhesion capacity tests

To assess bacterial adhesion capacity, Caco-2, HT-29, and its derivative, HT-29 MTX, were used. Cells were seeded into a 24-well tissue culture plate at a concentration of $1 \times 10^5$ cells/well, and adhesion was performed for 7 days for Caco-2 and HT-29 ATCC. For HT-29 MTX, after confluence (6 days), plates were incubated for an additional 14 days to allow cell differentiation (the medium was changed every day). In all cases, after 7 days or 21 days, wells were washed twice with DPBS, and fresh media without antibiotics were added. Each bacterial suspension was added at MOI 40 from a stationary-phase culture. After 3 h of incubation, monolayers were washed three times with DPBS to remove any bacteria that were not attached to the cells. Afterward, bacteria were disassociated by covering the monolayer with 150 µL of a 1% (v/v) Triton (Triton X-100, Sigma) solution in DPBS. Subsequently, 300 µL of DMEM was added in order to stop the reaction, and the number of viable adherent bacteria was determined by plating serial dilutions on MRS agar plates. Adhesion was expressed as the percentage of adhered bacteria with respect to the number of input bacteria, or DPBS as a negative control.

The adhesion test was also performed on mucin (Porcine gastric mucin, type III, Sigma). Mucin was prepared at 10 mg/mL in sterile DPBS and put on a 96-well plate overnight at 4°C. Adhesion assay was performed as described above, with an additional incubation at room temperature for 90 min after adding Triton solution.

## Determination of D-,L-lactate concentrations

D-lactate and L-lactate were measured in the supernatant of the bacterial culture at the stationary phase. The supernatant was precipitated with trichloroacetic acid (10%) and centrifuged at 20,000 *g* for 5 min at 4°C. Acid supernatants were neutralized with TEA 0.1 M at pH 9.15. Lactate was then measured with an enzymatic kit according to the manufacturer's instructions (Biosentec, France).

## Antibiotic resistance determinations

Phenotypic resistance to antibiotics was assessed according to the EFSA recommendations (European Food Safety Authority, 2018). Lactic acid bacteria susceptibility test medium (LSM agar) was prepared with 90% IST (Iso-Sensitest broth, Oxoid, United Kingdom), 10% MRS broth, and 1.5% granulated agar. Bacterial suspensions were streaked on plates to obtain a lawn, and antibiotic strips (bioMérieux) were used. The inhibition area with the corresponding concentration (minimum inhibitory concentration, MIC) was then determined and compared with the EFSA guidelines.

## Genomic characterization

Genomic DNA was extracted from 5 mL of culture with the first step of enzymatic lysis with the following cocktail: mutanolysin at 233.3 U/mL; lysostaphin at 13.3 U/mL, and lysozyme at 50 mg/mL, followed by incubation with RNAse A (Qiagen) at 10 mg/mL and proteinase K (Euromedex, France) at 50 mg/mL. Purification was performed with a DNA extraction kit (Genomic DNA Buffer Set and Genomic Tips, Qiagen), according to the manufacturer's instructions. DNA was resuspended in TE buffer, and the concentration was measured with NanoDrop (NanoDrop 1,000, Thermo Fisher). The genome was sequenced by Eurofins Genomics (France) using whole-genome sequencing with *de novo* assembly, with the PacBio method on single-molecule real-time (SMRT) cells, a 240-mn collection time, a mean length superior to 6,000 bp, and a genome coverage of 100 X. The analysis of the obtained reads began with a quality check and *de novo* assembly of contigs. Contigs were then circularized and mapped when possible.

The genome is available at NCBI (BioSample accession ID: SAMN37542358). The presence of antibiotic gene resistance was searched online on two databases, namely, CARD[1] and ResFinder.[2] According to the "EFSA statement on the requirements for whole genome sequence analysis of microorganisms intentionally used in the

1 https://card.mcmaster.ca/home

2 https://cge.food.dtu.dk/services/ResFinder/

food chain" (European Food Safety Authority, 2021), only hits with 80% identity and 70% length were reported. The presence of prophages in the genomes was determined *in silico* using Phaster.[3] Only intact prophages were considered. Potential bacteriocin activity was determined *in silico* using BAGEL4.[4]

## Bacteriophage induction essays

An induction assay was performed to establish if the intact prophage found with Phaster was active. In brief, induction with mitomycin C (Sigma) at 1 µg/mL was performed on culture at the beginning of the exponential phase. When the culture reached the stationary phase, 1 mL of culture was centrifuged (8,000 *g*, 10 mn, 4°C), and the supernatant was then filtered (0.22 µM) before being frozen at −20°C. *Listeria ivanovii* WSCL 3009 (Institute for Food and Health from the Technical University of Munich, Germany) was used as a receptor strain for B025 prophage. Two different protocols were performed with MRS agar (1.5%) and semi-solid MRS agar (0.75%), supplemented with 2 mM of $CaCl_2$ to increase phage absorption. On spot assay, 100 µL of receptor bacteria at the beginning of the exponential phase culture was poured with semi-solid agar on top of solid agar. In total, 10 µL of inducted supernatant or control was spotted on the surface of the Petri dish. On double lawn assay, 100 µL of receptor bacteria at the beginning of exponential phase culture was mixed with 100 µL of inducted supernatant or control. After 15 min of incubation at room temperature, 3 mL of semi-solid agar was added and then poured on solid agar. After 48 h of incubation, the presence of potential inhibition halos, indicating the presence of active phages, was observed.

## Active bacteriocin determination test

Potential bacteriocin activity was determined using a sensitive strain to enterolysin (which is the bacteriocin predicted for our strain): *Lactococcus lactis* IL403. The bacterial suspension was collected from the fresh colony of sensitive bacteria in sterile peptone water (McFarland 1) and streaked on LSM medium (medium prepared as described before). In total, 10 µL of supernatant was added to the agar. Three conditions were tested for each supernatant: filtered only; filtered and pH adjusted to 6; and filtered with pH 6 and 1 mg/mL of catalase, which inhibits potential $H_2O_2$ action. A bacterial growth medium was used as a negative control. Potential inhibition spots were observed after 48 h of incubation.

## Hemolytic activity

The hemolytic activity of our strain was determined by using blood agar, which was streaked with our strain and incubated at 37°C for 48 h. After incubation, the hemolytic activity was evaluated and classified based on the lysis of red blood cells in the medium around the colonies.

3 https://phaster.ca/

4 http://bagel4.molgenrug.nl/

## Bile salts and pH resistance

Tolerance to bile salts was studied to mimic the passage of the strains in the gastrointestinal tract. From stationary-phase culture, bacterial cells were exposed to 0% or 0.3% bile salts (Oxgall Powder, Sigma) for 1 h before viable cells were counted. Second, viable counts were performed after 24 h of growth of the *L. salivarius* CNCM I-4866 strain in media containing 0% or 0.3% bile salts.

Tolerance to acidic conditions was tested in the same conditions for bile salts by following the growth in media with a modified pH or after 1 h of exposition to a low pH and counting viable cells. We have performed assays at pH 2 and pH 4.

## Exopolysaccharide production: Ropy test and transmission electron microscopy

The production of potential exopolysaccharides (EPSs) by *L. salivarius* CNCM I-4866 was quantified with the Ropy phenotype test. In brief, a loop was used to observe EPS filament from a fresh colony on agar.

To determine bacterial structures, transmission electron microscopy (TEM) was performed by the microscopy and imaging platform (MIMA2, INRAE). The bacterial pellet obtained from an exponential phase was washed twice with phosphate buffer and recovered with 2% glutaraldehyde (EMS) in sodium cacodylate 0.1 M buffer. Suspensions were incubated for 1 h at room temperature. The pellet was then washed with sodium cacodylate in 0.1 M buffer (Fluka) and supplemented with 0.2 M sucrose. The sample was conserved at 4°C before being processed. The Hitachi HT7700 (Hitachi High-Tech, Japan) was used for microscopic observations.

# Results

## *Ligilactobacillus salivarius* CNCM I-4866 protects against DNBS-induced colitis inflammation

DNBS-induced colitis was performed to observe a potential protective effect of the strain on acute inflammation. A significant decrease was observed in the macroscopic scores of the treated group compared with the DNBS-Vehicle group, indicating lower inflammation in the treated group (Figure 2A). Microscopic scores and myeloperoxidase (MPO) activity determinations (Figures 2B,C) showed a tendency to recovery (with *p*-values of 0.0798 and 0.1038), reflecting an improvement in colonic epithelial structure and reduced immune cell infiltration.

Intestinal permeability is known to increase in cases of inflammation (Salvo-Romero et al., 2015). *Ligilactobacillus salivarius* I-4866 showed a tendency to decrease sCD14, an indicator of permeability, compared with the DNBS-Vehicle group (Figure 3A). Moreover, *L. salivarius* CNCM I-4866 treatment tended to decrease LCN-2 concentration in serum (Figure 3B), a biological marker of inflammation.

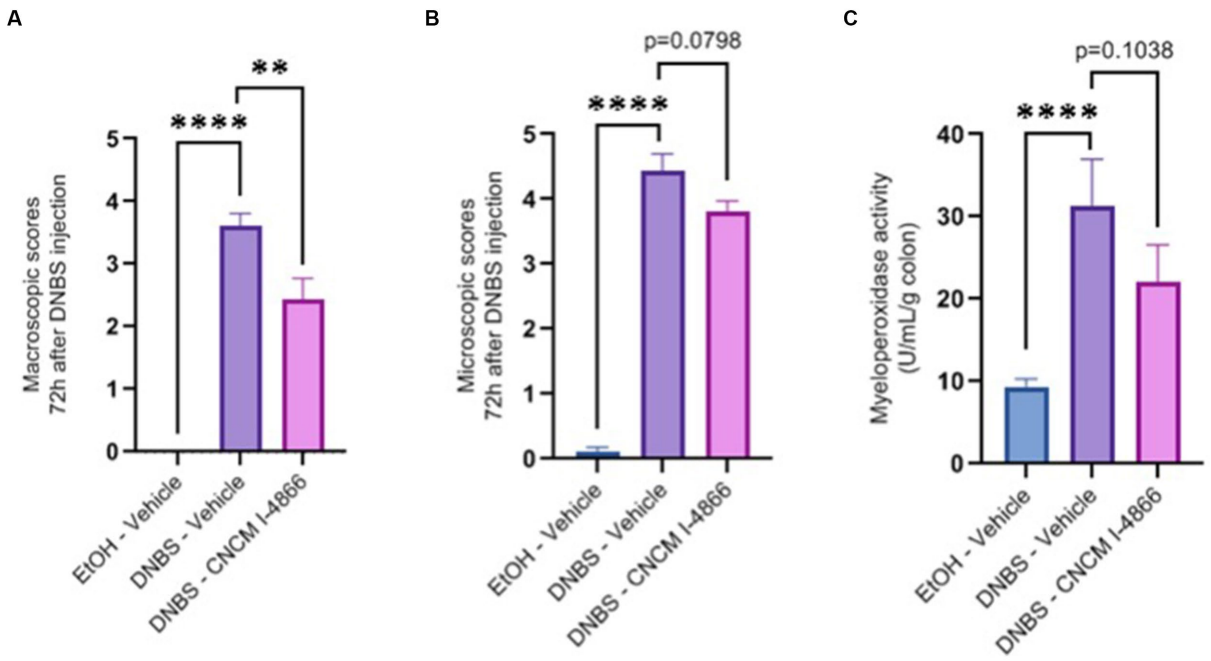


FIGURE 2
Effects of *L. salivarius* CNCM I-4866 on DNBS-induced colitis. **(A)** Colon macroscopic scores (Wallace scores); **(B)** colon microscopic scores (Ameho scores); and **(C)** levels of MPO activity in the colon. Results of Mann–Whitney *U*-tests compared with the DNBS-Vehicle group with the EtOH-Vehicle and treated groups: $*p < 0.05$, $**p < 0.01$, $***p < 0.001$, and $****p < 0.0001$.

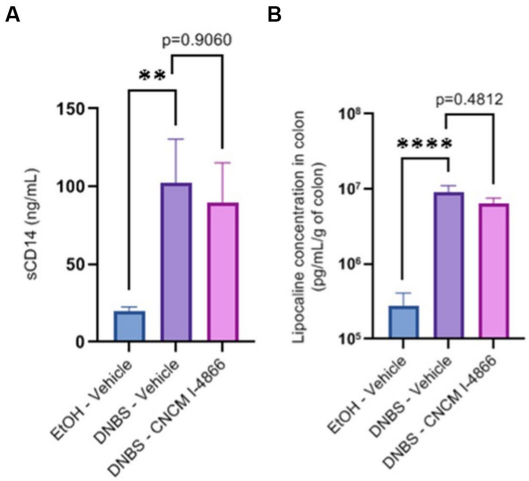


FIGURE 3
Effects of the *L. salivarius* 4,866 strain on inflammation markers in DNBS-induced colitis. **(A)** Levels of sCD14 in serum and **(B)** levels of lipocalin in the colon. Results of Mann–Whitney *U*-tests compared with the DNBS-Vehicle group with the EtOH-Vehicle and treated groups: $*p < 0.05$, $**p < 0.01$, $***p < 0.001$, and $****p < 0.0001$.

## Transcriptome analysis reveals that *Ligilactobacillus salivarius* 4,866 downregulates pro-inflammatory cytokine pathways

Comparative colonic transcriptomic analysis revealed that 22 genes were modulated between the DNBS-CNCM I-4866 and DNBS-Vehicle groups (Figure 4A). Among them, inflammatory cytokines were found. IL-1β was one of the genes linked to inflammation that was less expressed in the CNCM I-4866-treated group. Analysis of the specific signaling pathways modulated between these two groups (Figure 4B) also revealed that the tumor environment pathway is the top activated pathway in DNBS-Vehicle (Figure 4B). In addition, several pro-inflammatory cytokines (IL-1α, TNF, IL-1β, and IFNγ, among others) were also found as upstream regulators with significant *z*-scores (Figure 4C) when comparing the DNBS-Vehicle and DNBS-CNCM I-4866 groups. In other words, these results indicated that CNCM I-4866 treatment moderated the production of pro-inflammatory cytokines, as mentioned above. On the other hand, IL-10, an anti-inflammatory cytokine, had a negative *z*-score, indicating that it was downregulated in the DNBS-Vehicle group compared with the treated group. These results suggest that IL-10 could be more expressed in the colon of mice that have received CNCM I-4866.

## *Ligilactobacillus salivarius* 4866 displayed anti-inflammatory capabilities and restored intestinal permeability *in vitro*

The capacity of *L. salivarius* CNCM I-4866 to modulate TNF-α-induced secretion of IL-8, a major pro-inflammatory cytokine, and limit inflammation was conducted on HT-29 cells. In a similar way to the positive control butyrate (Lenoir et al., 2020), our strain has shown great ability to reduce IL-8 production on inflamed HT-29 cells (Figure 5A).

TEER results have shown that *L. salivarius* CNCM I-4866 treatment was able to maintain barrier integrity in Caco-2 cells

A

| log2FC | Gene | Description |
|---|---|---|
| -1,52 | Fam183b | Mus musculus Fam183b |
| 1,89 | Slc16a3 | Mus musculus solute carrier family 16 |
| 2,09 | Aldh1a3 | Mus musculus aldehyde dehydrogenase |
| 2,27 | Inhba | Mus musculus inhibin beta-A |
| 2,49 | Cd300lf | Mus musculus CD300 molecule |
| 2,53 | Apln | Mus musculus apelin |
| 2,87 | Il1b | Mus musculus interleukin 1 beta |
| 3,08 | Hdc | Mus musculus histidine decarboxylase |
| 3,13 | Mmp13 | Mus musculus matrix metallopeptidase 13 |
| 3,20 | Slc4a11 | Mus musculus solute carrier family 4 |
| 3,22 | Il11 | Mus musculus interleukin 11 |
| 3,26 | Mmp9 | Mus musculus matrix metallopeptidase 9 |
| 3,32 | Clps | Mus musculus colipase, pancreatic |
| 4,02 | Arg1 | Mus musculus arginase liver |
| 4,04 | S100a8 | Mus musculus S100 calcium binding protein A8 |
| 4,16 | S100a9 | Mus musculus S100 calcium binding protein A9 |
| 4,75 | Mmp8 | Mus musculus matrix metallopeptidase 8 |
| 5,44 | Mmp10 | Mus musculus matrix metallopeptidase 10 |
| 5,60 | Cstdc4 | Mus musculus cystatin domain |
| 7,65 | Ctrl | Mus musculus chymotrypsin-like |
| 34,43 | 1810028F09Rik | Mus musculus RIKEN cDNA |
| 35,02 | Gm10334 | Mus musculus Gm10334 |

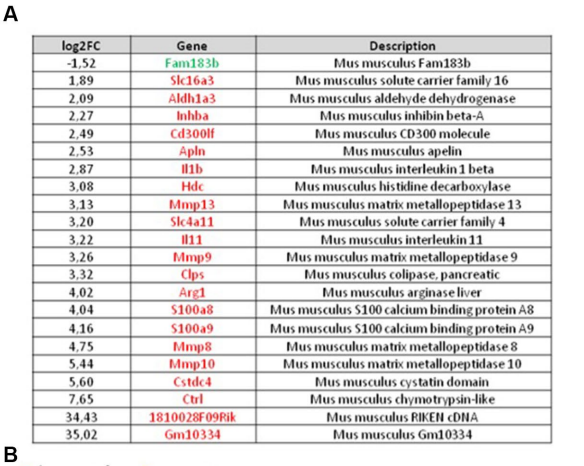


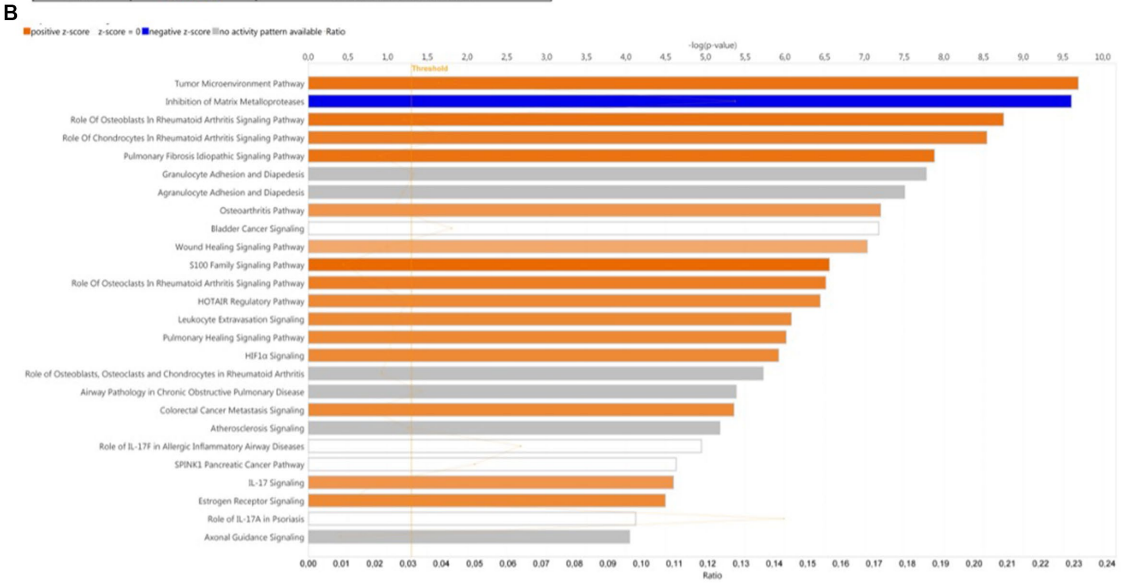


FIGURE 4
Transcriptomic analysis of mouse colons from the DNBS-Vehicle or DNBS-CNCM I-4866-treated group. **(A)** Modulation of genes between the DNBS-Vehicle group and DNBS-CNCM I-4866-treated group (adjusted value of $p < 0.05$ and $|\log2FoldChange| > 1.5$). Upregulated genes are in red and downregulated genes in green; **(B)** IPA canonical pathway display of the genes modulated in a comparison of DNBS-Vehicle versus DNBS-CNCM I-4866: the *y*-axis displays the -log of the value of *p*, which is calculated by a right-tailed Fisher's exact test. The orange- and blue-colored bars indicate predicted pathway activation or predicted inhibition, respectively. The orange points interconnected by a thin line represent the ratio; **(C)** Top 20 of affected upstream regulators (only cytokines are represented here) based on IPA. Red indicates activation, while blue indicates suppression.

challenged with TNF-α with a slight lower effect that the well-known probiotic candidate *L. rhamnosus* GG (Figure 5B).

Immunomodulatory effect analysis was also conducted on PBMC from five human donors with the same criteria. Pro-inflammatory cytokines (IL-12) and anti-inflammatory cytokines (IL-10) were dosed after co-incubation of PBMC cells with *L. salivarius* CNCM I-4866, *L. rhamnosus* GG, and the control *E. coli* TG1 (Figures 6A,B). *E. coli* TG1 is known to produce IL-10 and not IL-12, thus having an elevated IL-10/IL-12 ratio (Sokol et al., 2008). *Ligilactobacillus salivarius* CNCM I-4866 showed an anti-inflammatory profile based on its high production of IL-10 and high ratio of IL-10/IL-12 (Figure 6D). Moreover, TNF-α production was measured (Figure 6C) in order to determine the TNF-α /IL-10 ratio, which is also an indicator of the inflammatory profile. It appeared to be relatively low for *L. salivarius* CNCM I-4866 compared with *L. rhamnosus* GG and equivalent to the *E. coli* TG1 ratio (Figure 6E).

## *Ligilactobacillus salivarius* CNCM I-4866 had good adhesion capacities and was able to inhibit several pathogens due to its acid production

We have studied *L. salivarius* CNCM I-4866 ability to adhere to several cell lines: HT-29, HT-29 MTX, and Caco-2, as well as porcine mucin (Figure 7A). Comparatively to the reference strain *L. rhamnosus* GG, which is known to have a good adhesion capacity (Tuomola and Salminen, 1998; Ayeni et al., 2011), *L. salivarius* CNCM I-4866 has shown a good capacity to adhere to HT-29 and Caco-2 cells. Adhesion to HT-29 MTX cells and porcine mucin was more moderate but similar to *L. rhamnosus* GG control.

The ability of the strain supernatant to inhibit eight pathogens was also tested. *Ligilactobacillus salivarius* CNCM I-4866 supernatant inhibited four strains: *Escherichia coli, Staphylococcus aureus, Salmonella typhimurium,* and *S. enteritidis* (Figure 7B). This inhibition

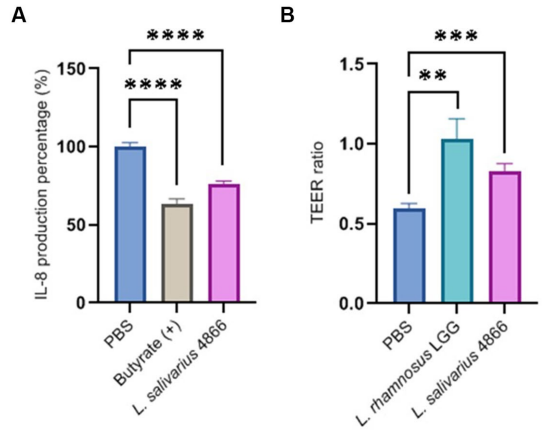


FIGURE 5
*In vitro* beneficial capacities of the *L. salivarius* CNCM I-4866 strain. **(A)** IL-8 production by HT-29 cells exposed to TNF-α in the presence of *L. salivarius* CNCM I-4866 and butyrate (positive control); **(B)** TEER ratio of Caco-2 cells monolayer exposed to TNF-α in the presence of *L. salivarius* CNCM I-4866 and *L. rhamnosus* GG. The results of Mann–Whitney *U*-tests comparing the DPBS control group with the other groups: $*p < 0.05$, $**p < 0.01$, $***p < 0.001$, and $****p < 0.0001$.

effect was lost when the pH of the supernatant was increased by adding sodium hydroxide, which indicates that the inhibition effect was probably due to lactic acid production.

## *Ligilactobacillus salivarius* CNCM I-4866 resisted bile salt exposition and showed no hemolytic activity

No significant difference was found after growth in media with 0.3% bile salts (Figure 8A) or after 1 h of exposition to 0.3% bile salts. Concerning tolerance to acidic conditions, *L. salivarius* CNCM I-4866 growth was found to be slightly impacted by pH 4 and inhibited at pH 2 (Figure 8B). Moreover, no hemolytic activity was found after the growth of *L. salivarius* CNCM I-4866 on blood agar.

## *Ligilactobacillus salivarius* CNCM I-4866 produced mainly L-lactate as a fermentation product

We have measured D-lactate and L-lactate production from the strain *L. salivarius* CNCM I-4866 which produced mostly L-lactate (Figure 8C).

## *Ligilactobacillus salivarius* CNCM I-4866 is a potential producer of exopolysaccharides

Finally, potential exopolysaccharide production was first assessed by the Ropy test. The Ropy test was positive (data not shown). This test was completed with a global analysis of the structure of *L. salivarius* CNCM I-4866 by transmission electron microscopy (Figures 9A,B). This result has shown a structure that is compatible with an EPS layer, suggesting EPS production by the strain.

## Antibiotic resistance analysis of *Ligilactobacillus salivarius* CNCM I-4866 strain *in vitro* and *in silico*

To ensure the health safety of *L. salivarius* CNCM I-4866, phenotypic resistance to several antibiotics was determined according to the EFSA recommendations (Table 1). The results showed that the strain is sensitive to ampicillin, gentamicin, streptomycin, erythromycin, clindamycin, tetracycline, and chloramphenicol and resistant to kanamycin.

Furthermore, the *L. salivarius* CNCM I-4866 genome was sequenced by whole-genome sequencing. Potential genes for antibiotic resistance were searched in online databases. No gene responsible for antibiotic resistance was found according to our thresholds.

## Analysis of the presence of bacteriophage and bacteriocin *in vitro* and *in silico*

Potential phage or bacteriocin production has been determined *in silico* and *in vitro*. *In silico* Phaster analysis highlighted the presence of an intact prophage, B025, a *Listeria* prophage (score of 120, length of 43.7 Kb, and region from 121,049 to 164,766 with a percentage of GC of 33.63%). Induction assay and research on lytic plaques with a sensitive strain for this phage have shown that this prophage was not active in our conditions (data not shown). Moreover, *in silico*, the bacteriocin enterolysin was found to be potentially active. After testing on a sensitive strain, no halo was observed, indicating that the bacteriocin was not active.

# Discussion

In Western countries, IBDs are widespread chronic diseases, with no curative treatment available for the moment (Aldars-Garcia et al., 2021). Therapies based on supplementation with beneficial microorganisms have been pointed out as a potential co-treatment in the management of the symptoms. This approach could be performed with traditional probiotics such as lactic acid bacteria (Doron et al., 2005; Cheng et al., 2020). In this study, we characterized a Lactobacillaceae strain, *L. salivarius* CNCM I-4866, as a potential probiotic strain to manage and moderate intestinal inflammation.

First, the anti-inflammatory properties of our strain were assessed in a DNBS-induced colitis model. This acute inflammation displays many related features of Crohn's disease, making it an approaching model for this pathology (Wallace et al., 1995). After treatment with CNCM I-4866, colon macroscopic scores improved significantly compared with DNBS control. These results were in accordance with microscopic scores, including damage to colonic epithelial structure and immune cell infiltration, which *L. salivarius* CNCM I-4866 tended to improve. To assess the immunomodulatory effects of the strain in our DNBS model, colonic MPO, an enzyme found in the intracellular granules of neutrophils, and serum LCN-2, a non-invasive marker of inflammation, were quantified. Administration of *L. salivarius* CNCM I-4866 tended to decrease both markers when compared with the DNBS control. Colonic inflammation has been proven to be linked with a dysfunction of intestinal barrier function and, therefore, an increase in permeability as it is observed in IBD patients (Michielan and D'Inca, 2015; Salvo-Romero et al., 2015). By determining sCD14

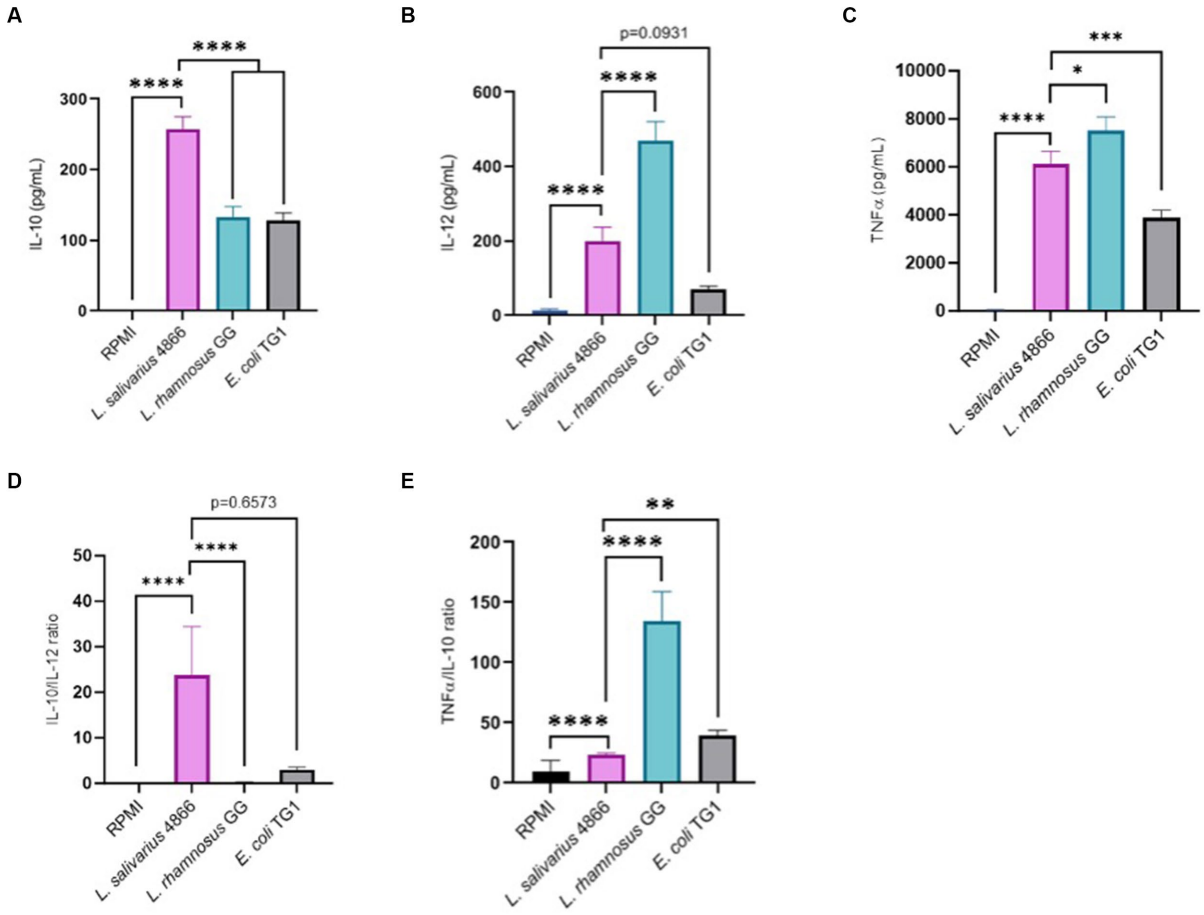


FIGURE 6
Anti-inflammatory profile based on co-incubation with human PBMCs. **(A)** IL-10 production by *L. salivarius* CNCM I-4866 strain after co-incubation with human PBMCs for five donors. *L. rhamnosus* GG and *E. coli* TG1 are used as controls with known effects; **(B)** IL-12 production by *L. salivarius* CNCM I-4866 strain after co-incubation with human PBMCs, for 5 donors. *L. rhamnosus* GG and *E. coli* TG1 are used as controls with known effects; **(C)** TNF-α production by *L. salivarius* CNCM I-4866 strain after co-incubation with human PBMCs, for 5 donors. *L. rhamnosus* GG and *E. coli* TG1 are used as controls with known effects; **(D)** IL-10/IL-12 ratio for *L. salivarius* CNCM I-4866 after co-incubation with human PBMCs. A low ratio is a marker of the pro-inflammatory profile, whereas a high ratio is a marker of the anti-inflammatory profile; **(E)** TNFα/IL-10 ratio for *L. salivarius* CNCM I-4866 after co-incubation with human PBMCs. A low ratio is a marker of an anti-inflammatory profile, whereas a high ratio is a marker of a pro-inflammatory profile. Results of Mann–Whitney U-tests comparing *L. salivarius* 4,866 with other groups: *$p < 0.05$, **$p < 0.01$, ***$p < 0.001$, and ****$p < 0.0001$.

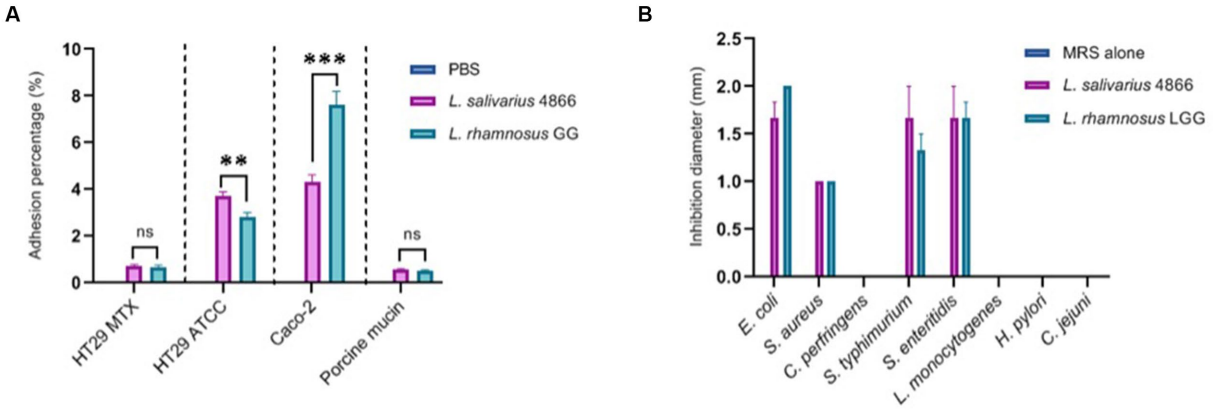


FIGURE 7
*Ligilactobacillus salivarius* CNCM I-4866 adhesion and pathogen inhibition *in vitro* **(A)** Adhesion percentage to HT-29 MTX, HT-29, Caco-2 cells, and to porcine mucin. Percentage is the ratio of viable count (CFU/ml) after co-incubation compared with the initial inoculum. *L. rhamnosus* GG was used as a positive control; **(B)** pathogen inhibition ability of eight pathogens in the *L. salivarius* CNCM I-4866 supernatant. *L. rhamnosus* GG was used as a positive control. Results of Mann–Whitney U-tests comparing *L. salivarius* 4866 and *L. rhamnosus* GG: **$p < 0.01$, ***$p < 0.001$.

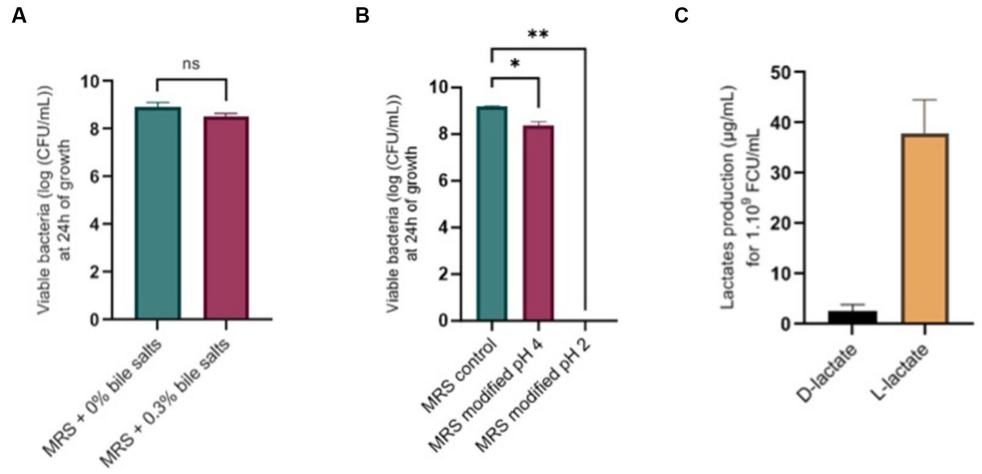


FIGURE 8
Physiological potentialities of *L. salivarius* CNCM I-4866. **(A)** Survival of *L. salivarius* CNCM I-4866 after 24-h growth in media with 0.3% or 0% bile salts, expressed in log of CFU/ml; **(B)** Survival of *L. salivarius* CNCM I-4866 after 24-h growth in media at pH 4 or pH 2, expressed in log of CFU/ml; **(C)** D-lactate and L-lactate production of *L. salivarius* CNCM I-4866. Results of Mann–Whitney *U*-tests: $*p < 0.05$, $**p < 0.01$, $***p < 0.001$, and $****p < 0.0001$.

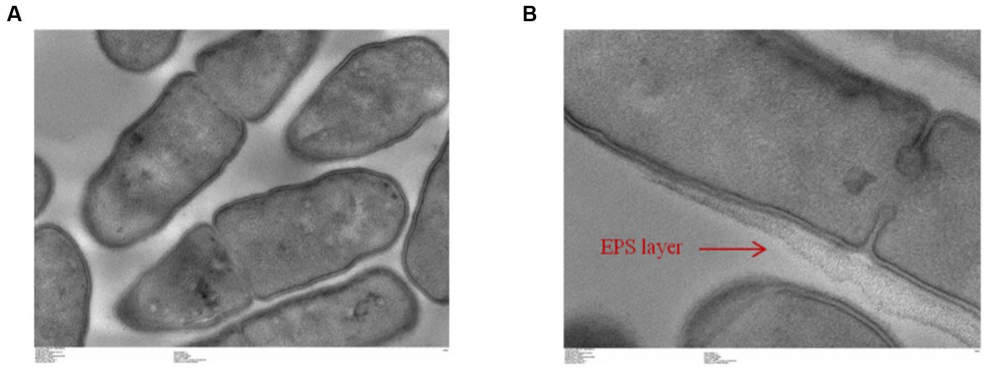


FIGURE 9
Transmission electronic microscopic visualization of *L. salivarius* CNCM I-4866 **(A,B)**.

levels in serum, we have observed that *L. salivarius* CNCM I-4866 tends to maintain intestinal barrier integrity in cases of inflammation. This model is a robust model for probiotic identification as it has employed other bacteria with well-known probiotic capacities, such as *Faecalibacterium prausnitzii* (Martin et al., 2014) or several *Lactobacillus* strains (Benitez-Cabello et al., 2020).

Additionally, colonic transcriptome analysis by comparing the DNBS-Vehicle group with the DNBS-*L. salivarius* CNCM I-4866-treated group has revealed that genes implied in inflammation and, more precisely, pro-inflammatory cytokine production were less expressed when mice were treated with CNCM I-4866. Conversely, based on the z-score, the expression of the anti-inflammatory cytokine IL-10 was higher in the treated group. The major pathway upregulated in DNBS-Vehicle is the tumor environment pathway, which includes not only cancer cells but also many immune cells that occur during inflammation development. Thereby, IL-1β is a major inflammatory cytokine that mediates other pro-inflammatory cytokines, such as TNF-α or IL-12 (Wang et al., 2017). As these cytokines were upregulated in the control DNBS group (DNBS-Vehicle) compared with the DNBS-CNCM I-4866 group, we can assume that our probiotic candidate has the ability to pacify gene expression linked to immune response. A previous study has shown an equivalent pattern of immunity modulation in a DSS-induced colitis model with a *Lactobacillus plantarum* strain (Wu et al., 2022). To summarize, *L. salivarius* CNCM I-4866 seems to alleviate inflammatory bursting caused by DNBS colitis.

Taken together, these *in vivo* findings indicate that the *L. salivarius* CNCM I-4866 strain could be a good probiotic candidate to manage and reduce intestinal inflammation found in IBD patients. To go further on the understanding of the beneficial properties of CNCM I-4866 and, more specifically, immunomodulatory effects, two cellular models were used: TNF-α-activated HT-29 cells and PBMCs. Consequently, the anti-inflammatory effect was evaluated by measuring pro-inflammatory cytokine (IL-8) concentration in a co-incubation model of HT-29 cells with *L. salivarius* CNCM I-4866 bacteria after the TNF-α challenge. IL-8 secretion was shown to

TABLE 1 Phenotypic antibiotic resistance according to the EFSA recommendations for *L. salivarius* CNCM I-4866.

| Antibiotic | MIC values (mg/L) | Cutoff values EFSA (mg/L) |
|---|---|---|
| Ampicillin | 0.25–0.38 | 4 |
| Gentamicin | 4 | 16 |
| Kanamycin | >256 | 64 |
| Streptomycin | 48 | 64 |
| Erythromycin | 0.5 | 1 |
| Clindamycin | 0.125 | 1 |
| Tetracycline | 0.75–1 | 8 |
| Chloramphenicol | 2 | 4 |

Minimal inhibitory concentration (MIC) values are compared with the cutoff values from the EFSA guidelines.

be increased in IBD patients and correlated with mucosal inflammation (Daig et al., 1996). De Oliveira et al. (2013) described that this interleukin is responsible for neutrophil activation in the case of inflammation. Previous studies have already evaluated probiotic aptitude with this parameter (Martin et al., 2019; Maillard et al., 2023). Our strain has shown a good ability to reduce IL-8 production as compared with inflamed cells alone, confirming the anti-inflammatory properties observed *in vivo*.

To have a better picture of the impact of *L. salivarius* CNCM I-4866 on immunity at the peripheral level, we have determined its capacity to regulate the production of IL-10, IL-12, and TNF-α on human PBMC cells. High secretion of IL-10 was measured with CNCM I-4866 by comparing it with controls. Rogler and Andus (1998) have described the importance of this cytokine in immune homeostasis in IBD patients as an anti-inflammatory response. On the other hand, the pro-inflammatory cytokine IL-12 leads to a Th1 immune-mediated response with the differentiation of T-helper cells. The IL-10/IL-12 ratio is described as a reliable indicator for establishing the inflammatory profile of a strain, with a high ratio associated with an anti-inflammatory profile (Foligne et al., 2007). By comparing it with the well-known probiotic *L. rhamnosus* GG, CNCM I-4866 produced significantly more IL-10 and less IL-12, revealing a high IL-10/IL-12 ratio. These results are in accordance with those of Foligne et al. (2007), who have shown that *L. salivarius* Ls33 has a pronounced anti-inflammatory profile based on the IL-10/IL-12 ratio. The low TNF-α/IL-10 ratio, compared with *L. rhamnosus* GG, allowed us to confirm this anti-inflammatory pattern. These outcomes, taken with *in vivo* and IL-8 results, point out a strong anti-inflammatory profile of *L. salivarius* CNCM I-4866.

As mentioned above, intestinal permeability is impacted in the case of inflammation and, therefore, in IBD pathologies. In the DNBS model, CNCM I-4866 tends to maintain barrier permeability by using the sCD14 marker. Furthermore, we have evaluated this capacity in an *in vitro* model. Caco-2 cells are exposed to TNF-α, which disrupts tight junctions and increases epithelial barrier permeability. *L. salivarius* CNCM I-4866 treatment was able to restore barrier integrity in Caco-2 cells challenged with TNF-α. A study has shown that *L. rhamnosus* GG could attenuate permeability dysfunction induced by TNF-α and IFNγ by inhibiting the NF-κB pathway (Donato et al., 2010). *Lactobacillus plantarum* MB452 was also found to enhance intestinal barrier function by modulating tight junction proteins (Anderson et al., 2010). For CNCM I-4866, the *in vivo* effect on permeability was not pronounced, but *in vitro* assay with TEER highlighted the beneficial property of maintaining the permeability of our strain. Additional experiments should be carried out for a better understanding of the partial transferability of these *in vitro* results to the *in vivo* preclinical context and to further analyze the underlying mechanisms.

Rossi et al. (2015) and Hidalgo-Cantabrana et al. (2016) have shown that EPS production by probiotics candidates was a key parameter for them to exert their anti-inflammatory properties. To continue with a deeper characterization of *L. salivarius* CNCM I-4866, we have thus determined EPS production. EPS secretion is known to be a criterion for an adequate probiotic candidate as it has health benefits (Juraskova et al., 2022). With electronic transmission microscopy, we have observed that our strain possesses a potential EPS. This observation is supported by the Ropy test, indicating that CNCM I-4866 produces Ropy-linked EPS. Several mechanisms are known to be implied in beneficial effects exerted by EPS, for example modulation of intestinal microbiota (Salazar et al., 2008).

Even if the underlying mechanisms are not well known, it is known that IBDs are linked to a microbiota imbalance between commensal and pathogenic bacteria. Indeed, some pathogen populations are increased in the case of IBD, such as *Salmonella, Escherichia coli,* or *Listeria monocytogenes* (Axelrad et al., 2021). As *L. salivarius* species are well known to exert antimicrobial activity (Tinrat et al., 2011; Messaoudi et al., 2013), we have evaluated this capacity for CNCM I-4866 against eight intestinal pathogens. *L. salivarius* CNCM I-4866 was able to inhibit two *Salmonella* strains: one *E. coli* strain and one *S. aureus* strain. This property, potentially due to lactic acid production, is an interesting feature that can be considered for further applications. In a previous study, Kang et al. (2017) highlighted the anti-microbial mechanisms of *L. salivarius* strains against *S. aureus*, such as the secretion of anti-staphylococcal proteins.

Beyond its health-beneficial properties, we wanted to ensure that *L. salivarius* CNCM I-4866 was a good probiotic candidate (European Food Safety Authority, 2018). As a potential human probiotic, tolerance to bile salts is essential, as it will allow the bacteria to reach the lower intestinal tract. Thereby, we have shown that *L. salivarius* CNCM I-4866 could resist 0.3% bile salts, corresponding to the physiological concentration in the human gastrointestinal tract (Chateau et al., 1994; Prete et al., 2020). This capacity constitutes an advantage for the *in vivo* survival of the strain. In previous studies, probiotic candidate strains were screened on this parameter, and *Lactobacillus* strains have also shown good survival at 0.3% bile salts (Khiralla et al., 2015). The ability to tolerate bile salts is commonly known due to bile salt hydrolase activities (Noriega et al., 2006). However, Pan et al. (2021) have described the fact that, for some *L. salivarius* strains, other mechanisms could be responsible for this property. The growth of our strain was impacted by the low pH (pH 4 and pH 2) that mimic the passage in the gastrointestinal tract and, more specifically, gastric conditions. However, probiotic strains are often administered orally in a protective vehicle that ensures the viability of strain during its passage through the gastrointestinal tract (Tee et al., 2014).

Adhesion to the intestinal mucosa constitutes a key parameter in selecting a probiotic, as it allows the strain to persist and exert its

health-beneficial effects for a longer period. *L. salivarius* CNCM I-4866 possessed good adhesion capacities on several cell lines and mucus at a similar or even better degree than the well-known probiotic, *L. rhamnosus* GG. Adhesion mechanisms are well described and can be either specific to adhesion proteins (fibronectin, collagen, mucin, and laminin) or unspecific to binding to hydrophobic surfaces (de Wouters et al., 2015). Additionally, CbpA protein was identified in *L. salivarius* REN as essential for its adhesion to the HT-29 line (Wang et al., 2017). For *L. rhamnosus* GG, functional analysis has revealed that SpaCBA pili act as an essential factor in adhesion and immunomodulation (Lebeer et al., 2012), as is the case of SpaFED pili for *L. rhamnosus* CNCM-I3690 (Martin et al., 2023).

Regarding safety concerns, antibiotic resistance constitutes a major issue nowadays, and the risk of resistance gene dissemination should be limited to its maximum (Li et al., 2020). Following the EFSA recommendations (European Food Safety Authority, 2021), no antibiotic-resistance gene was found in our strain. Nevertheless, phenotypic antibiotic resistance has highlighted the resistance to kanamycin. It is well described that *Lactobacillus* are frequently resistant to kanamycin due to intrinsic resistance (Anisimova and Yarullina, 2019; Campedelli et al., 2019). As no gene is detected, *L. salivarius* CNCM I-4866 is validated on safety aspects. Additionally, no hemolytic activity was found for our strain. Lactic acid bacteria, as their name suggests, are high producers of lactate. Iraporda et al. (2016) have established that L-lactate treatment could alleviate intestinal inflammation in a mouse TNBS model. However, it has been shown that D-lactate accumulation can lead to acidosis in people with short bowel syndrome (Mack, 2004). As *L. salivarius* CNCM I-4866 produces mostly L-lactate and very little D-lactate, this strain is suitable for these patients.

In conclusion, our study has shown that a new strain, *L. salivarius* CNCM I-4866, displays strong anti-inflammatory capacities *in vitro* and *in vivo*. Even if further research could be useful to better understand the mechanisms involved or to test this strain on moderate inflammation, CNCM I-4866 is confirmed to be a promising probiotic candidate to alleviate inflammation at the preclinical level on a DNBS model, mimicking IBD and, more specifically, Crohn's disease. Nevertheless, a human clinical trial should be performed to confirm its potential.

## Data availability statement

The data presented in the study are deposited in the biosamplehelp@ncbi.nlm.nih.gov repository, accession number SAMN37542358.

## Ethics statement

Ethical approval was not required for the studies on humans in accordance with the local legislation and institutional requirements because only commercially available established cell lines were used. The animal study was approved by Experiments were performed in accordance with European Union legislation on animal welfare and were approved by COMETHEA, our local committee on animal experimentation (n° 16744–201807061805486) and in compliance with the ARRIVE relevant guidelines. The study was conducted in accordance with the local legislation and institutional requirements.

## Author contributions

CC: Conceptualization, Formal analysis, Investigation, Methodology, Validation, Writing – original draft. SC: Investigation, Validation, Methodology, Writing – review & editing. CK: Investigation, Validation, Methodology, Writing – review & editing. LM: Investigation, Validation, Methodology, Writing – review & editing. FC: Investigation, Validation, Methodology, Writing – review & editing. PL: Conceptualization, Funding acquisition, Validation, Writing – review & editing. RM: Conceptualization, Funding acquisition, Investigation, Methodology, Project administration, Supervision, Validation, Writing – review & editing.

## Funding

The author(s) declare financial support was received for the research, authorship, and/or publication of this article. This project was funded by the SORBIAL company. The SORBIAL company played no role in data collection and interpretation.

## Acknowledgments

This study has benefited from the facilities and expertise of @BRIDGe (Université Paris-Saclay, INRAE, AgroParisTech, GABI, 78350 Jouy-en-Josas, France) and MIMA2-MET (Université Paris-Saclay, INRAE, AgroParisTech, GABI, 78350 Jouy-en-Josas, France). The authors wish to thank the staff of the INRAE Infectiology of Fishes and Rodents Facility (IERP-UE907, Jouy-en-Josas Research Center, France), where animal experiments have been performed. The IERP Facility belongs to the National Distributed Research Infrastructure for the Control of Animal and Zoonotic Emerging Infectious Diseases through *in vivo* investigation. The authors also want to thank Hilde de Reuse from the Pasteur Institute for kindly providing us with the *Helicobacter pylori* strain and ONIRIS Nantes for providing the *Campylobacter jejuni* strain.

## Conflict of interest

The authors declare that the research was conducted in the absence of any commercial or financial relationships that could be construed as a potential conflict of interest.

The author(s) declared that they were an editorial board member of Frontiers, at the time of submission. This had no impact on the peer review process and the final decision.

## Publisher's note

# References


Alard, J., Peucelle, V., Boutillier, D., Breton, J., Kuylle, S., Pot, B., et al. (2018). New probiotic strains for inflammatory bowel disease management identified by combining in vitro and in vivo approaches. *Benef Microbes* 9, 317–331. doi: 10.3920/BM2017.0097

Aldars-Garcia, L., Chaparro, M., and Gisbert, J. P. (2021). Systematic review: the gut microbiome and its potential clinical application in inflammatory bowel disease. *Microorganisms* 9:977. doi: 10.3390/microorganisms9050977

Ameho, C. K., Adjei, A., Harrison, E. K., Takeshita, K., Morioka, T., Arakaki, Y., et al. (1997). Prophylactic effect of dietary glutamine supplementation on interleukin 8 and tumour necrosis factor α production in trinitrobenzene sulphonic acid induced colitis. *Gut* 41, 487–493. doi: 10.1136/gut.41.4.487

Anderson, R. C., Cookson, A. L., McNabb, W. C., Park, Z., McCann, M. J., Kelly, W. J., et al. (2010). *Lactobacillus plantarum* MB452 enhances the function of the intestinal barrier by increasing the expression levels of genes involved in tight junction formation. *BMC Microbiol.* 10:316. doi: 10.1186/1471-2180-10-316

Anisimova, E. A., and Yarullina, D. R. (2019). Antibiotic resistance of LACTOBACILLUS strains. *Curr. Microbiol.* 76, 1407–1416. doi: 10.1007/s00284-019-01769-7

Axelrad, J. E., Cadwell, K. H., Colombel, J. F., and Shah, S. C. (2021). The role of gastrointestinal pathogens in inflammatory bowel disease: a systematic review. *Ther. Adv. Gastroenterol.* 14:17562848211004493. doi: 10.1177/17562848211004493

Ayeni, F. A., Sanchez, B., Adeniyi, B. A., de Los Reyes-Gavilan, C. G., Margolles, A., and Ruas-Madiedo, P. (2011). Evaluation of the functional potential of *Weissella* and *Lactobacillus* isolates obtained from Nigerian traditional fermented foods and cow's intestine. *Int. J. Food Microbiol.* 147, 97–104. doi: 10.1016/j.ijfoodmicro.2011.03.014

Barone, M., Chain, F., Sokol, H., Brigidi, P., Bermudez-Humaran, L. G., and Langella, P. (2018). A versatile new model of chemically induced chronic colitis using an outbred murine strain. *Front. Microbiol.* 9:565. doi: 10.3389/fmicb.2018.00565

Benitez-Cabello, A., Torres-Maravilla, E., Bermudez-Humaran, L., Langella, P., Martin, R., Jimenez-Diaz, R., et al. (2020). Probiotic properties of Lactobacillus strains isolated from Table olive biofilms. *Probiotics Antimicrob Proteins* 12, 1071–1082. doi: 10.1007/s12602-019-09604-y

Campedelli, I., Mathur, H., Salvetti, E., Clarke, S., Rea, M. C., and Torriani, S. (2019). Genus-wide assessment of antibiotic resistance in *Lactobacillus* spp. *Appl. Environ. Microbiol.* 85:e01738-18. doi: 10.1128/AEM.01738-18

Chamignon, C., Gueneau, V., Medina, S., Deschamps, J., Gil-Izquierdo, A., Briandet, R., et al. (2020). Evaluation of the probiotic properties and the capacity to form biofilms of various *Lactobacillus* strains. *Microorganisms* 8:1053. doi: 10.3390/microorganisms8071053

Chateau, N., Deschamps, A. M., and Sassi, H. (1994). Heterogeneity of bile salts resistance in the Lactobacillus isolates of a probiotic consortium. *Lett. Appl. Microbiol.* 18, 42–44. doi: 10.1111/j.1472-765X.1994.tb00796.x

Chaves, B. D., Brashears, M. M., and Nightingale, K. K. (2017). Applications and safety considerations of *Lactobacillus salivarius* as a probiotic in animal and human health. *J. Appl. Microbiol.* 123, 18–28. doi: 10.1111/jam.13438

Cheng, F. S., Pan, D., Chang, B., Jiang, M., and Sang, L. X. (2020). Probiotic mixture VSL#3: an overview of basic and clinical studies in chronic diseases. *World J. Clin. Cases* 8, 1361–1384. doi: 10.12998/wjcc.v8.i8.1361

Daig, R., Andus, T., Aschenbrenner, E., Falk, W., Schölmerich, J., and Gross, V. (1996). Increased interleukin 8 expression in the colon mucosa of patients with inflammatory bowel disease. *Gut* 38, 216–222. doi: 10.1136/gut.38.2.216

de Oliveira, S., Reyes-Aldasoro, C. C., Candel, S., Renshaw, S. A., Mulero, V., and Calado, A. (2013). Cxcl8 (IL-8) mediates neutrophil recruitment and behavior in the zebrafish inflammatory response. *J. Immunol.* 190, 4349–4359. doi: 10.4049/jimmunol.1203266

de Wouters, T., Jans, C., Niederberger, T., Fischer, P., and Ruhs, P. A. (2015). Adhesion potential of intestinal microbes predicted by Physico-chemical characterization methods. *PLoS One* 10:e0136437. doi: 10.1371/journal.pone.0136437

Donato, K. A., Gareau, M. G., Wang, Y. J. J., and Sherman, P. M. (2010). *Lactobacillus rhamnosus* GG attenuates interferon-gamma and tumour necrosis factor-alpha-induced barrier dysfunction and pro-inflammatory signalling. *Microbiology (Reading)* 156, 3288–3297. doi: 10.1099/mic.0.040139-0

Doron, S., Snydman, D. R., and Gorbach, S. L. (2005). Lactobacillus GG: bacteriology and clinical applications. *Gastroenterol. Clin. N. Am.* 34, 483–498. doi: 10.1016/j.gtc.2005.05.011

European Food Safety Authority (2018). Guidance on the characterisation of microorganisms used as feed additives or as production organisms. *EFSA J.* 16:e05206.

European Food Safety Authority (2021). EFSA statement on the requirements for whole genome sequence analysis of microorganisms intentionally used in the food chain. *EFSA J.* 19:e06506. doi: 10.2903/j.efsa.2021.6506

Foligne, B., Nutten, S., Grangette, C., Dennin, V., Goudercourt, D., Poiret, S., et al. (2007). Correlation between in vitro and in vivo immunomodulatory properties of lactic acid bacteria. *World J. Gastroenterol.* 13, 236–243. doi: 10.3748/wjg.v13.i2.236

Frank, D. N., St Amand, A. L., Feldman, R. A., Boedeker, E. C., Harpaz, N., and Pace, N. R. (2007). Molecular-phylogenetic characterization of microbial community imbalances in human inflammatory bowel diseases. *Proc. Natl. Acad. Sci. U. S. A.* 104, 13780–13785. doi: 10.1073/pnas.0706625104

Glassner, K. L., Abraham, B. P., and Quigley, E. M. M. (2020). The microbiome and inflammatory bowel disease. *J. Allergy Clin. Immunol.* 145, 16–27. doi: 10.1016/j.jaci.2019.11.003

Hidalgo-Cantabrana, C., Algieri, F., Rodriguez-Nogales, A., Vezza, T., Martinez-Camblor, P., Margolles, A., et al. (2016). Effect of a ropy exopolysaccharide-producing *Bifidobacterium animalis* subsp. lactis strain orally administered on DSS-induced colitis mice model. *Front. Microbiol.* 7:868. doi: 10.3389/fmicb.2016.00868

Hill, C., Guarner, F., Reid, G., Gibson, G. R., Merenstein, D. J., Pot, B., et al. (2014). Expert consensus document. The international scientific Association for Probiotics and Prebiotics consensus statement on the scope and appropriate use of the term probiotic. *Nat. Rev. Gastroenterol. Hepatol.* 11, 506–514. doi: 10.1038/nrgastro.2014.66

Iraporda, C., Romanin, D. E., Bengoa, A. A., Errea, A. J., Cayet, D., Foligne, B., et al. (2016). Local treatment with lactate prevents intestinal inflammation in the TNBS-induced colitis model. *Front. Immunol.* 7:651. doi: 10.3389/fimmu.2016.00651

Iyer, N., Williams, M. A., O'Callaghan, A. A., Dempsey, E., Cabrera-Rubio, R., Raverdeau, M., et al. (2022). *Lactobacillus salivarius* UCC118 dampens inflammation and promotes microbiota recovery to provide therapeutic benefit in a DSS-induced colitis model. *Microorganisms* 10:1383. doi: 10.3390/microorganisms10071383

Jakubczyk, D., Leszczynska, K., and Gorska, S. (2020). The effectiveness of probiotics in the treatment of inflammatory bowel disease (IBD)-a critical review. *Nutrients* 12:1973. doi: 10.3390/nu12071973

Jandhyala, S. M., Talukdar, R., Subramanyam, C., Vuyyuru, H., Sasikala, M., and Nageshwar Reddy, D. (2015). Role of the normal gut microbiota. *World J. Gastroenterol.* 21, 8787–8803. doi: 10.3748/wjg.v21.i29.8787

Juraskova, D., Ribeiro, S. C., and Silva, C. C. G. (2022). Exopolysaccharides produced by lactic acid Bacteria: from biosynthesis to health-promoting properties. *Foods* 11:156. doi: 10.3390/foods11020156

Kang, M. S., Lim, H. S., Oh, J. S., Lim, Y. J., Wuertz-Kozak, K., Harro, J. M., et al. (2017). Antimicrobial activity of *Lactobacillus salivarius* and *Lactobacillus fermentum* against *Staphylococcus aureus*. *Pathog. Dis.* 75. doi: 10.1093/femspd/ftx009

Khiralla, G. M., Mohamed, E. A. H., Farag, A. G., and Elhariry, H. (2015). Antibiofilm effect of *Lactobacillus pentosus* and *Lactobacillus plantarum* cell-free supernatants against some bacterial pathogens. *J. Biotech. Res.* 6, 86–95.

Lebeer, S., Claes, I., Tytgat, H. L., Verhoeven, T. L., Marien, E., von Ossowski, I., et al. (2012). Functional analysis of *Lactobacillus rhamnosus* GG pili in relation to adhesion and immunomodulatory interactions with intestinal epithelial cells. *Appl. Environ. Microbiol.* 78, 185–193. doi: 10.1128/AEM.06192-11

Lenoir, M., Martin, R., Torres-Maravilla, E., Chadi, S., Gonzalez-Davila, P., Sokol, H., et al. (2020). Butyrate mediates anti-inflammatory effects of *Faecalibacterium prausnitzii* in intestinal epithelial cells through Dact3. *Gut Microbes* 12, 1–16. doi: 10.1080/19490976.2020.1826748

Li, T., Teng, D., Mao, R., Hao, Y., Wang, X., and Wang, J. (2020). A critical review of antibiotic resistance in probiotic bacteria. *Food Res. Int.* 136:109571. doi: 10.1016/j.foodres.2020.109571

Mack, D.R. (2004). D(−)-lactic acid-producing probiotics, D(−)-lactic acidosis and infants. *Can. J. Gastroenterol.*. 2004;18, 671–675. doi: 10.1155/2004/342583

Maillard, F., Meynier, M., Mondot, S., Pepke, F., Galbert, C., Torres Maravilla, E., et al. (2023). From in vitro to in vivo: a rational flowchart for the selection and characterization of candidate probiotic strains in intestinal disorders. *Microorganisms* 11:906. doi: 10.3390/microorganisms11040906

Martin, R., Benitez-Cabello, A., Kulakauskas, S., Viana, M. V. C., Chamignon, C., Courtin, P., et al. (2023). Over-production of exopolysaccharide by *Lacticaseibacillus rhamnosus* CNCM I-3690 strain cutbacks its beneficial effect on the host. *Sci. Rep.* 13:6114. doi: 10.1038/s41598-023-32116-3

Martin, R., Chain, F., Miquel, S., Lu, J., Gratadoux, J. J., Sokol, H., et al. (2014). The commensal bacterium *Faecalibacterium prausnitzii* is protective in DNBS-induced chronic moderate and severe colitis models. *Inflamm. Bowel Dis.* 20, 417–430. doi: 10.1097/01.MIB.0000440815.76627.64

Martin, R., Chamignon, C., Mhedbi-Hajri, N., Chain, F., Derrien, M., Escribano-Vazquez, U., et al. (2019). The potential probiotic *Lactobacillus rhamnosus* CNCM I-3690 strain protects the intestinal barrier by stimulating both mucus production and cytoprotective response. *Sci. Rep.* 9:5398. doi: 10.1038/s41598-019-41738-5

Messaoudi, S., Manai, M., Kergourlay, G., Prevost, H., Connil, N., Chobert, J. M., et al. (2013). *Lactobacillus salivarius*: bacteriocin and probiotic activity. *Food Microbiol.* 36, 296–304. doi: 10.1016/j.fm.2013.05.010

Michielan, A., and D'Inca, R. (2015). Intestinal permeability in inflammatory bowel disease: pathogenesis, clinical evaluation, and therapy of leaky gut. *Mediat. Inflamm.* 2015:628157. doi: 10.1155/2015/628157

Noriega, L., Cuevas, I., Margolles, A., and De los Reyes-Gavilán, C. G. (2006). Deconjugation and bile salts hydrolase activity by Bifidobacterium strains with acquired resistance to bile. *Int. Dairy J.* 16, 850–855. doi: 10.1016/j.idairyj.2005.09.008

Pan, Q., Shen, X., Yu, L., Tian, F., Zhao, J., Zhang, H., et al. (2021). Comparative genomic analysis determines the functional genes related to bile salt resistance in *Lactobacillus salivarius*. *Microorganisms* 9:2038. doi: 10.3390/microorganisms9102038

Peran, L., Camuesco, D., Comalada, M., Nieto, A., Concha, A., Diaz-Ropero, M. P., et al. (2005). Preventative effects of a probiotic, *Lactobacillus salivarius* ssp. *salivarius*, in the TNBS model of rat colitis. *World J. Gastroenterol.* 11, 5185–5192. doi: 10.3748/wjg.v11.i33.5185

Prete, R., Long, S. L., Gallardo, A. L., Gahan, C. G., Corsetti, A., and Joyce, S. A. (2020). Beneficial bile acid metabolism from *Lactobacillus plantarum* of food origin. *Sci. Rep.* 10:1165. doi: 10.1038/s41598-020-58069-5

Rogler, G., and Andus, T. (1998). Cytokines in inflammatory bowel disease. *World J. Surg.* 22, 382–389. doi: 10.1007/s002689900401

Rossi, O., Khan, M. T., Schwarzer, M., Hudcovic, T., Srutkova, D., Duncan, S. H., et al. (2015). *Faecalibacterium prausnitzii* strain HTF-F and its extracellular polymeric matrix attenuate clinical parameters in DSS-induced colitis. *PLoS One* 10:e0123013. doi: 10.1371/journal.pone.0123013

Rychen, G., Aquilina, G., Azimonti, G., Bampidis, V., Bastos, M., Bories, G., et al. (2018). Guidance on the characterisation of microorganisms used as feed additives or as production organisms. *EFSA J.* 16:e05206. doi: 10.2903/j.efsa.2018.5206

Salazar, N., Gueimonde, M., Hernandez-Barranco, A. M., Ruas-Madiedo, P., and de los Reyes-Gavilan, C. (2008). Exopolysaccharides produced by intestinal Bifidobacterium strains act as fermentable substrates for human intestinal Bacteria. *Appl. Environ. Microbiol.* 74, 4737–4745. doi: 10.1128/AEM.00325-08

Salvo-Romero, E., Alonso-Cotoner, C., Pardo-Camacho, C., Casado-Bedmar, M., and Vicario, M. (2015). The intestinal barrier function and its involvement in digestive disease. *Rev. Esp. Enferm. Dig.* 107, 686–696. doi: 10.17235/reed.2015.3846/2015

Sokol, H., Pigneur, B., Watterlot, L., Lakhdari, O., Bermudez-Humaran, L. G., Gratadoux, J. J., et al. (2008). *Faecalibacterium prausnitzii* is an anti-inflammatory commensal bacterium identified by gut microbiota analysis of Crohn disease patients. *Proc. Natl. Acad. Sci. U. S. A.* 105, 16731–16736. doi: 10.1073/pnas.0804812105

Tee, W. F., Nazzarudin, R., Tan, Y. N., and Ayob, M. K. (2014). Effects of encapsulation on the viability of potential probiotic *Lactobacillus plantarum* exposed to high acidity condition and presence of bile salts. *Food Sci. Technol. Int.* 20, 399–404. doi: 10.1177/1082013213488775

Thursby, E., and Juge, N. (2017). Introduction to the human gut microbiota. *Biochem. J.* 474, 1823–1836. doi: 10.1042/BCJ20160510

Tinrat, S., Sumarn, S., and Mullika, T. C. (2011). Isolation and characterization of *Lactobacillus salivarius* MTC 1026 as a potential probiotics. *J. Gen. Appl. Microbiol.* 57, 365–378. doi: 10.2323/jgam.57.365

Tuomola, E. M., and Salminen, S. J. (1998). Adhesion of some probiotic and dairy Lactobacillus strains to Caco-2 cell cultures. *Int. J. Food Microbiol.* 41, 45–51. doi: 10.1016/S0168-1605(98)00033-6

Wallace, J. L., Le, T., Carter, L., Appleyard, C. B., and Beck, P. L. (1995). (1995). Hapten-induced chronic colitis in the rat: alternatives to Trinitrobenzene sulfonic acid. *J. Pharmacol. Toxicol. Methods* 33, 237–239. doi: 10.1016/1056-8719(95)00001-X

Wallace, JL.M.W., Morris, GP., and Beck, PL (1989). Inhibition of leukotriene synthesis markedly accelerates healing in a rat model of inflammatory bowel disease. *Gastroenterology* 96, 29–36. doi: 10.1016/0016-5085(89)90760-9

Wang, R., Jiang, L., Zhang, M., Zhao, L., Hao, Y., Guo, H., et al. (2017). The adhesion of *Lactobacillus salivarius* REN to a human intestinal epithelial cell line requires S-layer proteins. *Sci. Rep.* 7:44029. doi: 10.1038/srep44029

Wang, M., Zhao, J., Zhang, L., Wei, F., Lian, Y., Wu, Y., et al. (2017). Role of tumor microenvironment in tumorigenesis. *J. Cancer* 8, 761–773. doi: 10.7150/jca.17648

Wu, Y., Jha, R., Li, A., Liu, H., Zhang, Z., Zhang, C., et al. (2022). Probiotics (*Lactobacillus plantarum* HNU082) supplementation relieves ulcerative colitis by affecting intestinal barrier functions, immunity-related gene expression, gut microbiota, and metabolic pathways in mice. *Microbiol Spectr.* 10:e0165122. doi: 10.1128/spectrum.01651-22

frontiers | Frontiers in Microbiology

TYPE Original Research
PUBLISHED 15 December 2023
DOI 10.3389/fmicb.2023.1232173



OPEN ACCESS

EDITED BY
Rebeca Martín,
INRAE Centre Jouy-en-Josas, France

REVIEWED BY
Valerie Diane Valeriano,
Karolinska Institutet (KI), Sweden
Yuying Liu,
University of Texas Health Science Center at Houston, United States
Christelle Knudsen,
INRAE Occitanie Toulouse, France

*CORRESPONDENCE
Rita M. Hickey
✉ rita.hickey@teagasc.ie

RECEIVED 31 May 2023
ACCEPTED 06 November 2023
PUBLISHED 15 December 2023

CITATION
Walsh C, Owens RA, Bottacini F, Lane JA, van Sinderen D and Hickey RM (2023) HMO-primed bifidobacteria exhibit enhanced ability to adhere to intestinal epithelial cells. *Front. Microbiol.* 14:1232173. doi: 10.3389/fmicb.2023.1232173



# HMO-primed bifidobacteria exhibit enhanced ability to adhere to intestinal epithelial cells

Clodagh Walsh[1,2,3], Rebecca A. Owens[4], Francesca Bottacini[3,5], Jonathan A. Lane[2], Douwe van Sinderen[3] and Rita M. Hickey[1,3]*

[1]Teagasc Food Research Centre, Moorepark, Cork, Ireland, [2]Health and Happiness Group, H&H Research, Cork, Ireland, [3]APC Microbiome Ireland and School of Microbiology, University College Cork, Cork, Ireland, [4]Department of Biology, Maynooth University, Maynooth, Ireland, [5]Biological Sciences and ADAPT Research Centre, Munster Technological University, Cork, Ireland

The ability of gut commensals to adhere to the intestinal epithelium can play a key role in influencing the composition of the gut microbiota. Bifidobacteria are associated with a multitude of health benefits and are one of the most widely used probiotics for humans. Enhanced bifidobacterial adhesion may increase host-microbe, microbe-nutrient, and/or microbe-microbe interactions, thereby enabling consolidated health benefits to the host. The objective of this study was to determine the ability of human milk oligosaccharides (HMOs) to enhance bifidobacterial intestinal adhesion *in vitro*. This study assessed the colonisation-promoting effects of HMOs on four commercial infant-associated *Bifidobacterium* strains (two *B. longum* subsp. *infantis* strains, *B. breve* and *B. bifidum*). HT29-MTX cells were used as an *in vitro* intestinal model for bacterial adhesion. Short-term exposure of four commercial infant-associated *Bifidobacterium* strains to HMOs derived from breastmilk substantially increased the adherence (up to 47%) of these probiotic strains. Interestingly, when strains were incubated with HMOs as a four-strain combination, the number of viable bacteria adhering to intestinal cells increased by >90%. Proteomic analysis of this multi-strain bifidobacterial mixture revealed that the increased adherence resulting from exposure to HMOs was associated with notable increases in the abundance of sortase-dependent pili and glycosyl hydrolases matched to *Bifidobacterium bifidum*. This study suggests that HMOs may prime infant gut-associated *Bifidobacterium* for colonisation to intestinal epithelial cells by influencing the expression of various colonization factors.

KEYWORDS

HMO, *Bifidobacterium*, probiotics, prebiotics, colonization, breastmilk, hIECs

## 1 Introduction

Bifidobacterial strains are the most abundant colonizers in the gut of breast-fed infants, accounting for 50%–90% of the total bacterial population detected in their faeces (Milani et al., 2017). The successful adaptation of bifidobacteria to the infant gut has been largely attributed to their large arsenal of carbohydrate-active enzymes, which allows specific bifidobacterial strains to utilise breast-milk derived glycans such as human milk oligosaccharides (HMOs). HMOs act as prebiotics [defined as "a substrate that is selectively utilized by host microorganisms conferring a health benefit" (Gibson et al., 2017)] by promoting growth of beneficial intestinal bacteria and thereby generating short-chain fatty acids which are critical for gut health

(Pokusaeva et al., 2011). Due to their historical use and health-promoting properties, bifidobacterial strains are some of the most widely used and clinically documented probiotics. As probiotics, bifidobacteria contribute to host health through modulation of the intestinal microbiota, promotion of immune system development, maintenance of mucosal barrier integrity, and resistance to pathogenic colonization (Gareau et al., 2010). However, in order for bifidobacterial probiotics to impart their beneficial role, they not only need to compete with other gut commensals for nutrient acquisition, but also need to survive gastrointestinal transit and stably colonize the gastrointestinal tract (Morrin and Hickey, 2020). Adhesion to intestinal cells and/or mucus should therefore act as a key selection criterion when developing probiotic-containing products.

Recent studies have identified a plethora of bacterial features that have been shown to be involved in host–microbe interactions (Chang and Kao, 2019; Viljoen et al., 2020; Xiao et al., 2021). In this regard, cell surface components, termed adhesins, play an important role in allowing bifidobacteria to adhere to and interact with intestinal epithelial cells (Westermann et al., 2016). Many microbial adhesins display lectin-like properties and bind corresponding glycan receptors on the surface of the host cells via carbohydrate-recognition domains (CRDs). These interactions can be an important determinant of host and tissue tropism. Bacterial adhesion to human intestinal cells often involves the assembly of elongated, submicroscopic structures called pili (resembling "threads") or fimbriae (also known as short attachment pili or "hairs") (Nizet et al., 2017). Mounting evidence suggests that numerous bifidobacterial strains encode and express pilus-like structures (Foroni et al., 2011; O'Connell Motherway et al., 2011, 2019; Westermann et al., 2016). In recent years, several studies have indicated that certain milk components could enhance the adhesion ability of bifidobacterial strains by influencing the expression of these bacterial adhesins. For instance, González and colleagues found that the FimA fimbrial subunit and sortase-like fimbria-associated protein (involved in the assemblage of fimbriae) were highly upregulated during growth of *Bifidobacterium longum* in human milk and formula milk (González et al., 2008). Researchers have hypothesized that one such milk component contributing to this enhanced adhesion is the prebiotic fraction in human milk; HMO. An *in vitro* study by Chichlowski et al. demonstrated that exposure of *B. infantis* ATCC 15697 to breastmilk-derived HMO significantly increased adherence of the strain to HT-29 intestinal cells (Chichlowski et al., 2012). More recently, findings from Zhang et al. indicate that 2′-fucosyllactose (2′-FL), typically the most abundant HMO in breastmilk, promotes *B. bifidum* DNG6 adhesion to Caco-2 cells through increased expression of genes encoding adhesion proteins (Zhang et al., 2020). Likewise, incubation of *B. infantis* ATCC 15697 in the presence of 3′-siallylactose (3′-SL) and 6′-siallylactose (6′-SL), two predominant acidic oligosaccharides found in the milk of most mammals, substantially increased the adherence of the bacteria to HT-29 cells (Kavanaugh et al., 2013). Subsequent transcriptomic analysis revealed that this increased adherence was associated with heightened levels of tight-adherence protein TadE expression. This protein plays a pivotal role in orchestrating the assembly of type IVb pili surface appendages (Kavanaugh et al., 2013).

The objective of the current study was to assess the ability of HMOs to enhance adhesion of a community of bifidobacterial strains to mucus-secreting intestinal cells. As outlined by Xiao et al. the majority of current studies assessing colonization capabilities of probiotic strains have been performed using allochthonous strains (i.e., those isolated from fermented foods or plants and then studied in humans) and therefore do not perform well in their new ecosystem (Xiao et al., 2021). It is suggested that, if the goal is stable colonization, authochthonous strains (i.e., those of human origin) should instead be examined (Xiao et al., 2021). The present study focused on four autochthonous bifidobacterial strains of human origin that are of commercial interest due to their historical employment as ingredients in functional foods and their clinically documented health benefits (Giannetti et al., 2017; Wong et al., 2019; Xiao et al., 2019). Here, we investigated the adhesive properties of *Bifidobacterium bifidum* R0071, *Bifidobacterium infantis* R0033, *Bifidobacterium breve* M-16 V, and *Bifidobacterium longum* subsp. *infantis* (*B. infantis*) M-63, which are all shown to elicit potent immunomodulatory and protective effects *in vivo* (Giannetti et al., 2017; Wong et al., 2019; Xiao et al., 2019). Genomic mining and proteomic analyses were subsequently performed to understand the mechanisms underlying bifidobacterial adherence to intestinal cells. Previous work by our group has shown that positive co-operation between these bifidobacterial strains in utilising HMOs as a carbohydrate source resulted in higher cell numbers (Walsh et al., 2022). Given the evolution of these strains in a HMO-rich environment, we hypothesised that HMOs would not only influence the selective growth of these strains in a community setting, but also their specific adhesive ability. This study provides further insights into the role that HMOs play in selectively promoting bifidobacterial colonization in the infant gut and corroborates the notion that oligosaccharides acting as prebiotics also have the potential to enhance bifidobacterial adhesion.

## 2 Materials and methods

### 2.1 Generation of HMO-enriched fraction

Pooled human milk samples (of unknown secretor status) were kindly donated by Irvinestown Human Milk Bank (Co. Fermanagh, Ireland) and stored at −80°C on arrival. Briefly, lipids and proteins were removed from breastmilk as previously described (Quinn et al., 2018) before separation of lactose and HMO components using size-exclusion chromatography (BioGel P2, 92 × 5 cm; Bio-Rad Laboratories, Inc., Hercules, CA, United States). Peptide-free (quantified using Pierce colorimetric peptide assay) and low-trace lactose [quantified using high pH anion exchange chromatography (HPAEC) with pulsed amperometric detection (Dionex Corporation, Sunnyvale, CA, United States)] fractions were pooled and freeze-dried. The resultant HMO-enriched fraction was stored at 4°C prior to use in experiments. HPAEC analysis indicated that low levels of 2′-fucosyllactose (2′-FL) were found in the HMO-enriched fraction, likely due to the purification process where 2′-FL and lactose fractionated together. Therefore, the 2′-FL which had been eliminated during the size exclusion process was resubstituted using commercial 2′-FL (Friesland Campina), as previously described (Walsh et al., 2022), to give a powder representative of secretor HMO (designated S-HMO). S-HMO was used in adhesion studies at concentrations outlined in previous studies from our group (Walsh et al., 2022): final concentration of 5 g/L (3.8 g/L isolated HMO + 1.2 g/L 2′-FL). The composition of the S-HMO blend is shown in Supplementary Figure S1.

## 2.2 Epithelial cell line conditions

The human colonic adenocarcinoma cell line HT29-MTX [European Collection of Authenticated Cell Cultures (ECACC)] was used as a model of human intestinal epithelia. HT29-MTX cells were used for experiments at three different passages (passage numbers 38 to 41) to provide three biological replicates. Cells were routinely cultured in Dulbecco's Modified Eagle's Medium (DMEM) [10% Fetal Bovine Serum (FBS), 1% non-essential amino acids] (Merck, Darmstadt, Germany) in 75 $cm^2$ tissue culture flasks at 37°C with humidified atmosphere (5% $CO_2$). The cultures were passaged by detaching with trypsin when cells had reached approximately 90% confluence. Cells were seeded at a density of $1\times10^5$ cells/mL into 12-well plates (Cellbind; Corning, New York, United States). HT29-MTX cells were used once 100% confluency was reached (approximately $5\times10^6$ cells/well at day 12–14). Growth medium was changed every other day and supplemented with 2% FBS 24 h prior to use.

## 2.3 Bacterial strains and culture conditions

Commercial *Bifidobacterium* strains used in this study were obtained from Lallemand Health Solutions, France (*Bifidobacterium bifidum* R0071 and *Bifidobacterium infantis* R0033), and Morinaga Milk, Japan (*Bifidobacterium breve* M-16 V and *Bifidobacterium infantis* M-63). Strains were stored at −80°C in de Man-Rogosa-Sharpe (MRS) broth (Difco, BD, Ireland), supplemented with 50% (v/v) glycerol as a cryoprotectant. For routine experiments, strains were grown at 37°C under anaerobic conditions using MRS medium supplemented with 0.05% (wt/v) L-cysteine hydrochloride (Merck) and 0.01% (wt/v) mupirocin (Merck). Bacterial stocks were regularly checked for contamination by closely monitoring colony morphology during culturing. In addition, the bacterial stocks were routinely validated as being specific to their genera using bifidobacterial-specific PCR targeting the 16S region using primers g-Bifid-F (5′-CTCCTGGAAACGGGTGG-3′) and g-Bifid-R (5′-CTCCTGG AAACGGGTGG-3′) (Matsuki et al., 2004). Resultant amplicons were sequenced using Sanger sequencing.

## 2.4 Colonisation assays

### 2.4.1 Priming of bifidobacterial strains

For experiments, bifidobacterial strains derived from −80°C stock cultures were streaked on MRS agar supplemented with 0.05% (wt/v) L-cysteine HCl and incubated for 48 h at 37°C under anaerobic conditions. Single colonies of each strain were subsequently inoculated in supplemented MRS broth and sub-cultured twice before use in subsequent experiments. To obtain working cultures, supernatant of overnight culture was removed by centrifugation, after which the bacterial cell pellet was washed with phosphate buffer saline (PBS) (Merck) and resuspended in tissue culture media (2% FBS) such that the $OD_{600}$ of each bacterial culture was ~0.4 (corresponding to ~$5\times10^7$ CFU/mL, as determined by plate counts). The following bacterial combinations were assessed: single cultures of *B. bifidum* (R0071), *B. infantis* (R0033), *B. breve* (M-16 V), *B. infantis* (M-63) and a mixture of all four bifidobacterial strains (4Bif) containing equal volumes of each~$5\times10^7$ CFU/mL bacterial culture prepared as described above Bacterial suspension was added at a 1:1 ratio to DMEM tissue culture media (2% FBS) supplemented with 10 mg/mL of S-HMO or 2′-FL. Therefore, the final concentration of bacteria and carbohydrate at initiation of incubation was $2.5\times10^7$ CFU/mL and 5 mg/mL, respectively. Bacteria suspended in non-supplemented DMEM tissue culture media (without S-HMO or 2′-FL) was used as a control. Bacteria were exposed to oligosaccharides at 37°C under anaerobic conditions for 1 h before removal of residual oligosaccharides by centrifugation. The bacterial pellet was washed three times using PBS and centrifugation before resuspending in non-supplemented DMEM media prior to use in the assays.

### 2.4.2 Bacterial exposure to eukaryotic cells

Eukaryotic cells were washed twice with PBS, and 0.5 mL of bacterium:medium suspensions were added to the appropriate wells (corresponding to approximately 10–20 bacterial cells per eukaryotic cell). Bacteria were exposed to eukaryotic cells for 2 h at 37°C under anaerobic conditions, after which wells were washed three times with PBS to remove non-adherent bacteria, and then lysed with 0.1% Triton X100 (Merck) for 30 min. Bacteria within extracted lysates were quantified using two methods.

Firstly, viable bacteria adhering to cells were enumerated by serially diluting lysates and spread-plating (in triplicate) on MRS plates. Aliquots of the experimental inocula were retained, diluted, and plated to determine original CFU/mL. Results were expressed as adherent bacteria as a percentage of the original inoculum, thereby accounting for variations in the original inocula between treatment groups. Percentage adherent = [CFU/mL of recovered adherent bacteria/ CFU/mL of inoculum] × 100. Comparisons between strains and treatments groups were calculated as fold change. Fold change in adherence = Percentage adherent treatment group/ percentage adherent control group.

Secondly, bacterial numbers were determined using quantitative PCR (qPCR) as previously described (Walsh et al., 2022). Bacterial DNA was extracted using GenElute Bacterial Genomic DNA Kit (Merck) and quantified using a 480 Lightcycler platform (Roche Applied Science, Penzberg, Germany) using the following program: 95°C for 5 min followed by 40 cycles of 95°C for 10 s, 58°C for 20 s and 72°C for 30s. Species within the co-culture were enumerated using primers targeting the 16S rDNA gene region. For quantification of all *Bifidobacterium* strains present in samples, the primer pairs Bifid-F and g-Bifid-R were used. To determine *B. bifidum* cell numbers, primer pairs BiBIF-1 (5′-CCACATGATCGCATGTGATTG-3′) and BiBIF-2 (5′-CCGGATGCTCCATCACAC-3′) were employed. *B. breve* cells were quantified using primer pair BiBRE-1 (5′-CCACATGA TCGCATGTGATTG-3′) and BiBRE-2 (5′-ACAAAGTGCCTTGC TCCCT-3′), while *B. infantis* cell numbers were determined using primer pair BiINF-1 (5′-TTCCAGTTGATCGCATGGTC-3′) and BiINF-2 (5′-GGAAACCCCATCTCTGGGA-3′). The copy-number of a given species in co-culture was evaluated by comparing the cycle threshold (Ct) values with those from a standard curve of known copy number. Standard curves ($10^9$ to $10^2$ copy number/ µL) were established by performing 1 in 10 serial dilutions of 16S rDNA of the specified bifidobacterial species (in the case of *B. infantis* strains, M-63 was used as the reference rDNA). The cell numbers of species within co-culture (denoted by bifidobacteria/mL) were then deduced by comparing these copy number values with copy numbers of standards

with known cell numbers (as determined by viable count assessment). Cell numbers were calculated according to the formula (Quigley et al., 2013):

$$\frac{(C/\mu l)(TV)}{TCN} \times Tcfu/mL = bifidobacteria/mL\,(S)$$

Where; C/μL = Copy number/μL, TV = template volume (μL), TCN = total copy number of the standard used, T cfu/mL = total cell number of standard used, and bifidobacteria/mL(S) = cell number of test sample. Samples were run in triplicate, while standards and negative controls (where template DNA was replaced with PCR grade water) were run in duplicate.

## 2.5 Whole genome sequencing assembly and annotation

Following growth of R0071, R0033, M-16 V and M-63 as described in Section 2.3 above, bacterial cells were harvested, lysed, and total bacterial DNA was isolated. Genome sequences of the bifidobacterial strains were generated by Macrogen Inc. (Seoul, South Korea) using Pacific Biosciences SMRT RSII technology. The raw sequencing reads were *de novo* assembled using the Hierarchical Genome Assembly Process (HGAP) protocol RS_Assembly.2 implemented in the SMRT Analysis software v.2.3 with default parameters[1] as previously described (Bottacini et al., 2017).

Open Reading Frame (ORF) prediction and automatic annotation was performed using Prodigal v2.0[2] for gene predictions. BLASTP v2.2.26 (cut-off E-value of 0.0001) was used for sequence alignments against a combined bifidobacterial genome-based database, and MySQL relational database to assign annotations. Predicted functional assignments were manually revised and edited using similarity searches against the non-redundant protein database curated by the National Centre for Biotechnology Information[3] and PFAM database,[4] which allowed for *in silico* characterization of hypothetical proteins. GenBank editing and manual inspection was performed using Artemis v18.[5] Transfer RNA genes were identified employing tRNAscan-SE v1.4 and ribosomal RNA genes were detected based on the software package Rnammer v1.2 (38) supported by BLASTN v2.2.26.

## 2.6 Prediction of colonisation capabilities

Scientific literature databases including PubMed, Web of Science, UCC library, and Google Scholar were searched for studies providing mechanistic insight into probiotic colonization and survival in the gastrointestinal tract. A list of probiotic (*Lactobacillus* and *Bifidobacterium* genera) colonisation-related features (Supplementary Table S3) was then compiled from these studies which included gene-trait matching, transcriptomic, proteomic, and knock-out studies (Tanaka et al., 2000; Walter et al., 2005, 2007, 2008; Bron et al., 2007; Guglielmetti et al., 2008; Shkoporov et al., 2008; Gueimonde et al., 2009; Kankainen et al., 2009; Foroni et al., 2011; Frese et al., 2011, 2013; O'Connell Motherway et al., 2011; Sims et al., 2011; Fanning et al., 2012; González-Rodríguez et al., 2012; Turroni et al., 2013; Christiaen et al., 2014; Goh and Klaenhammer, 2014; Liu et al., 2014; Wilson et al., 2014; Call et al., 2015; Ganesh et al., 2018; Ishikawa et al., 2021). A Blast search was then performed (e-value cutoff of 1e-5, query cover cutoff of 50%) of the database against the bifidobacterial genomes of interest. Percent identity was recorded for each bifidobacterial strain of interest and classified as "low identity" = 30%–50%, "moderate identity" = 50%–70%, and "high identity" = 70%–100%.

The bifidobacterial sequences were also searched for sortase-dependent proteins since these proteins can play a pivotal role in adhesion and mucin-degradation. The bifidobacterial strains were surveyed for features containing the following sequence:

1. a signal peptide at the N-terminus
2. a pentaglycine recognition motif

- o LPXTG in the case of sortase A- and sortase C-dependent proteins
- o [L/I/V][S/A]XTG in the case of sortase E-dependent proteins

3. followed by a hydrophobic membrane-spanning region (verified using Protscale https://web.expasy.org/protscale/ and DeepTMHMM v1.0.13 https://dtu.biolib.com/DeepTMHMM)
4. positively charged residues at the C-terminus.

## 2.7 Proteomic analysis of colonisation-related factors

### 2.7.1 Sample preparation

Label-free quantitative proteomic analysis was carried out on the four-strain bifidobacterial mixture with/without S-HMO pre-treatment and after exposure to the HT29-MTX cell line. Sample groups included S-HMO-treated (S-HMO$^+$cells$^+$), and untreated bifidobacteria (S-HMO$^-$cells$^+$), following incubation with cells, and untreated bifidobacterial control (S-HMO$^-$ Cells$^-$) without incubation with HT29-MTX cells. Biological replicates of treated and control cells were prepared ($n = 3$ per condition).

HT29-MTX cells were seeded in 6-well plates and cultured until 100% confluence was reached. A bifidobacterial mixture containing equal amounts of *B. bifidum* R0071, *B. infantis* R0033, *B. breve* M-16 V, & *B. infantis* M-63 was prepared as outlined in section 2.4. This bacterial mixture was then incubated for 2 h in non-supplemented serum-free phenol-red free DMEM with and without HMO. For experiments, HT29-MTX cells were washed with PBS and treated with 3 mL bacterial solutions. The plates were then incubated at 37°C for 2 h in a humidified atmosphere (5% $CO_2$). As a control, bacteria were incubated under the same conditions in DMEM without HT29-MTX cells. After 2 h incubation, medium containing the treated bacteria was aspirated (Wei et al., 2014). Thereafter, bacteria were pelleted, washed three times in PBS and immediately frozen in liquid nitrogen. Adherent bacteria were also extracted from the system by detaching HT29-MTX cells with ice-cold PBS. Harvested cells were

1 https://github.com/PacificBiosciences/SMRT-Analysis
2 http://prodigal.ornl.gov
3 ftp://ftp.ncbi.nih.gov/blast/db/
4 http://pfam.sanger.ac.uk
5 http://www.sanger.ac.uk/resources/soft-ware/artemis/

immediately frozen in liquid nitrogen. All samples were stored at −70°C until protein extraction was performed.

### 2.7.2 Protein extraction and digestion

Cold lysis buffer (0.1 M TrisHCl, 10% glycerol, 20 mM EDTA, 50 mM NaCl, 1 mM PMSF, 1 μg/mL, pH 7.5) was added to each cell pellet and sonicated using a MS72 probe (3 × 10 s, cycle 6, 20% power), and placed on ice between each sonication round. An aliquot of each lysate was clarified by centrifugation and a Bradford protein assay (Bio-Rad) was used to determine the protein concentration. Total lysates (without clarification) were adjusted to 0.25 mg/mL protein concentration with 50 mM ammonium bicarbonate and heated at 95°C, for 5 min. Samples were reduced using dithiothreitol (DTT; 5 mM final, 15 min), alkylated using iodoacetamide (IAA; 15 mM final, 20 min, dark) and subjected to overnight trypsin digestion at 37°C (trypsin: 8 μg/mL final) in the presence of ProteaseMax (0.01% (w/v)). Digestion was stopped by addition of trifluoroacetic acid (1% (v/v)) and samples were dried under vacuum. Digests were resuspended in 0.5% (v/v) TFA prior to clean-up using C18 ZipTips (Millipore) according to manufacturer's instructions. Samples were dried under vacuum and stored at −70°C until LC–MS/MS analysis.

### 2.7.3 Label-free quantitative (LFQ) proteomic analysis

Peptide extracts (0.75 μg) were analysed by LC–MS/MS using the Thermo Q-Exactive mass spectrometer coupled to a Dionex Ultimate 3,000 RSLCnano, using a 2.25 h method for separation on an Easy-Spray PepMap™ column (50 cm × 75 μm, 2 μm particles). Samples were searched against a composite database containing the proteomes of R0071, M-16 V, and M-63, appended with the *Homo sapiens* proteome (downloaded from Uniprot 15/02/2019) using MaxQuant (v 1.6.2.10) with MaxLFQ algorithm included for protein ratio characterisation (Cox et al., 2014) and 1% FDR applied. Perseus (v 1.6.2.2) was used for data analysis (Tyanova et al., 2016). Proteins were filtered to exclude single peptide identifications and proteins matching a reverse or a contaminants database. Proteins were retained for analysis only if detected in at least two biological replicates from either comparator group. Qualitative results were based on unique protein detection in at least two biological replicates in a condition, with absence of detection in all replicates of the comparator set. Quantitative and qualitative results were combined prior to functional characterization.

### 2.7.4 Statistical analysis

Statistical analyses for adhesion assays were performed using technical triplicate data (three wells of each biological replicate) from biological triplicate experiments (across three successive passages of HT29-MTX cells). Graphs were created using PRISM v8 (GraphPad, La Jolla, CA) and were plotted as mean ± sd. Two-way univariate analysis of variance (ANOVA) and post-hoc Tukey tests were performed on bifidobacterial adhesion levels with the strain and carbohydrate source as factors. Statistical significance was accepted as $p \leq 0.05$. For proteomic data Perseus was used for statistical analysis, with quantitative results composed of proteins with a significant change in abundance [$p < 0.05$ (Student's t-test), fold change ≥2]. The distribution and intersection of proteins detected across strains and carbohydrate source was assessed using Venn Diagrams. The Venn Diagram was initially constructed using the Draw Venn Diagram tool at Bioinformatics & Evolutionary Genomics[6] and reformatted thereafter using Microsoft Powerpoint.

## 3 Results

### 3.1 Single strain and multi-strain adherence to HT29-MTX

Adherence of probiotic bacteria was evaluated using HT29-MTX human tumorigenic cell lines to mimic bifidobacterial adhesion to intestinal epithelial cells (IECs). Bifidobacterial strains were incubated with various carbohydrates (glucose, 2′-FL, or S-HMO) after which their ability to adhere to HT29-MTX cells was determined. The "secretor-HMO" (S-HMO) used in the experiments was obtained through the purification of pooled breast milk using gel-filtration chromatography. Initial screenings revealed that during the size exclusion process using Bio-Gel polyacrylamide beads, lactose and 2′-FL were found to co-fractionate. Consequently, all fractions containing high levels of lactose and 2′-FL were excluded from the final HMO-enriched mixture. While the most abundant α1,2-fucosylated HMO was removed from the resulting powder, the preparation still included other HMOs containing H-antigens such as difucosyllactose (DFL), lacto-N-fucopentaose I (LNFP I), and lacto-N-difucohexaose I (LNDFH I) (see Supplementary Figure S1). To create an ingredient representative secretor HMO, the previously eliminated 2′-FL was then reintroduced (usually a commercially produced 2′-FL) and designated as S-HMO.

As shown in Figure 1 and Supplementary Table S1, adhesion of bifidobacterial strains varied significantly depending on strain and carbon source. The lowest levels of adherence were observed with *B. breve* M-16 V in control group where glucose was the sole carbon source (7.2 ± 0.6% of original inoculum), while highest levels of adherence were observed with strain *B. bifidum* R0071 after exposure to S-HMO (13.8 ± 1.4% of original inoculum). Across all treatment groups, *B. bifidum* R0071 and *B. infantis* R0033 demonstrated significantly higher adherence when compared to *B. breve* M-16 V (Supplementary Table S1).

Addition of 2′-FL resulted in a marked increase in the adhesive ability of the *B. infantis* strains, as represented by a 1.26 fold increase in adhesion of M-63 ($p = 0.0007$) and a 1.15 fold increase in adhesion of R0033 ($p = 0.0456$) when compared to treatment of these strains in control media (Figure 1). Exposure of *B. bifidum* R0071 and *B. breve* M-16 V to 2′-FL had no significant impact on the adhesion of these strains to the cell line. However, exposure of each of the four *Bifidobacterium* strains to S-HMO significantly increased adherence to HT29-MTX cells by an average of 1.31 fold (*vs* control). The HMO-induced promotion of adhesion was observed, in particular, for *B. bifidum* R0071 which demonstrated significantly higher adhesion following S-HMO treatment when compared to the other strains (vs. R0033 $p = 0.0170$, vs. M-16 V and M-63 $p < 0.0001$, Supplementary Table S1). The adhesive ability of R0071 increased 1.37 fold after S-HMO treatment when compared to adhesion of the strain in control conditions ($p < 0.0001$). Interestingly, we also observed

6 http://bioinformatics.psb.ugent.be/webtools/Venn/

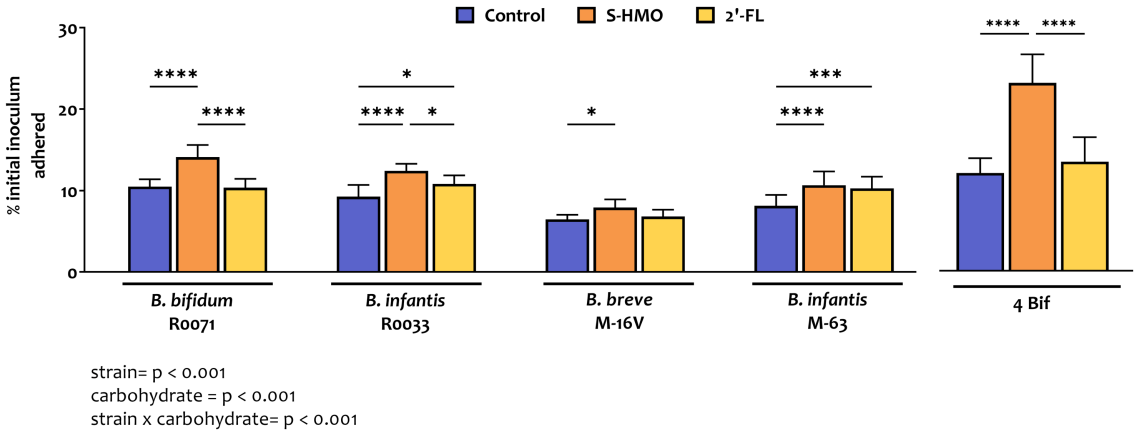


FIGURE 1
Levels of bifidobacterial adherence to HT29-MTX cells following pre-exposure to glucose control, breastmilk-derived human milk oligosaccharides (S-HMO), and 2′-fucosyllactose (2′-FL). Adherent bacteria are plotted as a percentage of the original inoculum. Percentage adherent=[CFU/mL of recovered adherent bacteria/ CFU/mL of inoculum]×100. R0071= *Bifidobacterium bifidum* R0071, R0033= *Bifidobacterium infantis* R0033, M-16V= *Bifidobacterium breve* M-16V, M-63= *Bifidobacterium infantis* M-63, 4Bif=four *Bifidobacterium* mixture. Analysis was calculated using technical triplicate data from biological triplicate experiments and data are means±SD. Univariate analysis of variance (ANOVA) and post-hoc Tukey tests were performed to determine the significant differences between the groups (**p* <0.05, ***p* <0.01, ****p* <0.001, *****p* <0.0001). Results of ANOVA are as outlined in figure where row factor=bifidobacterial strain(s), column factor=carbohydrate source, and interaction=bifidobacterial strain×carbohydrate source.

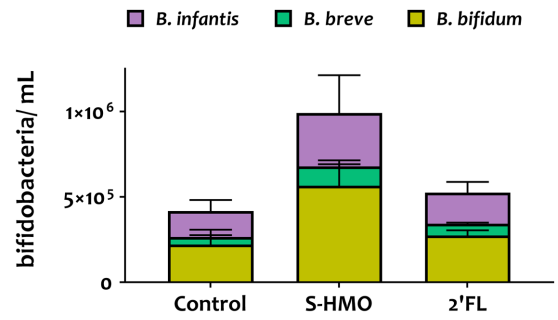


FIGURE 2
qPCR analysis of the adhered *Bifidobacterium* mixture (equal parts *Bifidobacterium bifidum* R0071, *Bifidobacterium infantis* R0033, *Bifidobacterium breve* M-16 V, *Bifidobacterium infantis* M-63) following pre-exposure to glucose control, breastmilk-derived human milk oligosaccharides (S-HMO), and 2′-fucosyllactose (2′-FL). Species within the bifidobacterial mixture were quantified using primers targeting the 16 s gene region of each species. Analysis was calculated using technical triplicate data from biological triplicate experiments and data are means ± SD.

higher adhesion levels of *B. infantis* R0033 when compared to its species counterpart *B. infantis* M-63 following exposure of the strains to S-HMO ($p = 0.0118$).

To assess whether a probiotic combination represents better colonists than single strains, the adhesive capacity of a bifidobacterial mixture containing equal amounts of all four strains was assessed using HT29-MTX cells. Substantial levels of bacterial adhesion occurred with this bifidobacterial consortium (Figures 1, 2). Notable increases in adhesion were observed in the control group when compared to colonization by single strains, although these increases were not significant in the case of *B. bifidum* R0071 (11.9 ± 1.8% in co-culture versus 10.5 ± 0.9% in *B. bifidum* R0071 alone, Supplementary Table S1). However, significant increases in adherence levels of the four-strain mixture were observed following S-HMO-exposure when compared to treatment with control media (Figure 1). A large proportion of the original inoculum (23.0 ± 3.5%) was found to have adhered to intestinal cells following treatment with HMOs, which corresponds to a 1.92 fold increase when compared to the non-supplemented control ($p < 0.0001$, Supplementary Table S1).

Quantitative PCR analysis targeting the 16S rRNA-encoding region allowed for quantification of cell numbers of each species within the four strain combination but did not distinguish between the two *B. infantis* strains. Nonetheless, qPCR analysis provided insights into the microbial composition of the adhered bacteria (Figure 2). Across all treatments, *B. bifidum* occupied the largest proportion of adhered bacteria accounting for 53.0, 57.8, and 52.3% in control, S-HMO, and 2′-FL treatment groups, respectively (Figure 2). As shown in Supplementary Table S2, significantly higher levels of adhered *B. bifidum* were detected following S-HMO exposure, when compared to the two other species present within the bifidobacterial combination (vs. *B. breve* $p < 0.0001$, vs. R0033 $p = 0.0157$).

## 3.2 Mining of bifidobacterial sequences for colonization-related features

To elucidate the key factors that are responsible for the observed differences in bifidobacterial adherence to intestinal cells, the bifidobacterial genomes were surveyed for colonisation-related factors. A literature search for studies assessing probiotic colonisation was performed and resulted in identification of 45 genes with a potential role in *Lactobacillus* and *Bifidobacterium* survival and persistence in the gut (Supplementary Table S3). Thereafter, the genomes of *B. bifidum* R0071, *B. breve* M-16 V, *B. infantis* R0033, and *B. infantis* M-63 were searched for homologs of these genes. All bifidobacterial strains studied here harboured genes associated with

microbe-host interactions (>50% coverage, e-value <1 e-5). Genes with high similarity (>70% identity) to bile salt hydrolase (*bsh*, shown to improve adhesion ability of *Lactobacillus plantarum*), transaldolase (*tal*, demonstrated to bind mucin in strains of *B. bifidum*), S-ribosylhomocysteine lyase (*luxS*, shown to be involved in biofilm production in *B. breve* UCC2003), early secretory antigen target 6-like protein (*esat-6* [*BBPR_0651*], found to be highly induced in *B. bifidum* PRL2010 following HT29 exposure), and hemolysin-like protein (*tlyC1*, shown to be involved in bile tolerance in *B. longum* BBMN68) were identified across all four genomes as well as genes involved in exopolysaccharide production such as undecaprenyl-phosphate galactosephosphotransferase *rfbP* (Figure 3; Supplementary Table S3).

The *tad* locus [as first described for the bifidobacterial genera in UCC2003 (O'Connell Motherway et al., 2011)], which encodes for site-determining protein TadZ, ATPase TadA, integral membrane proteins TadB and TadC, pre-pilin precursor Flp, and the pseudopilins TadE and TadF was found to be moderately conserved across the infant bifidobacterial strains studied here (as highlighted in Figure 3). Notably, we identified clear homologs (>70% identity) of all genes within the UCC2003 *tad* locus in *B. breve* M-16 V at *BBREV_0119* to *BBREV_0125* (Supplementary Table S3; Figure 3). Genes with homology (>50% coverage, e-value <1 e-5) to the UCC2003 *tad* locus were also identified in *B. bifidum* R0071 (at gene region *BBIF_1744-BBIF_1750*), although the level of genomic similarity was low (30%–50% identity) for *tadB*, *tadE*, and *tadF* (Supplementary Table S3; Figure 3). The *B. infantis* strains (R0033 and M-63) were found to harbour genes with moderate genomic similarity (50%–70% identity) to *tadA*, *tadB*, *tadC*, and *tadF* (Supplementary Table S3; Figure 3). However, no homologs to *tadE* were identified in either *B. infantis* strain.

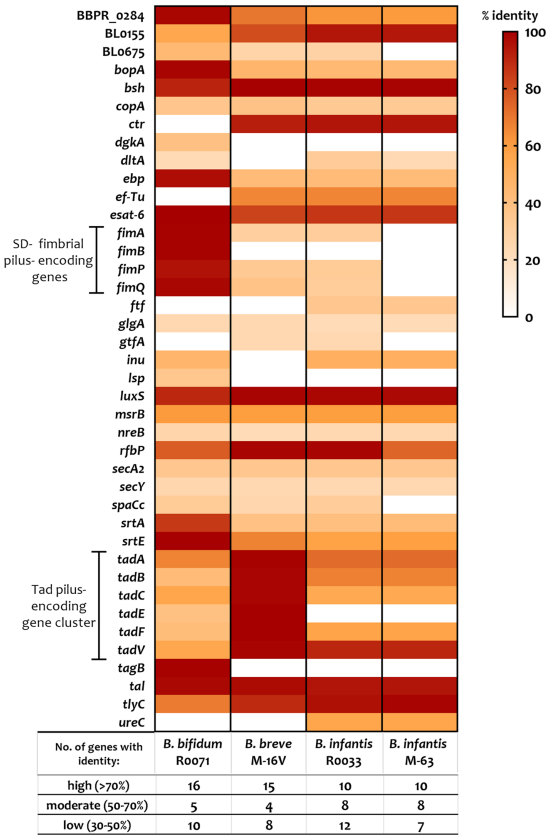


| No. of genes with identity: | *B. bifidum* R0071 | *B. breve* M-16V | *B. infantis* R0033 | *B. infantis* M-63 |
|---|---|---|---|---|
| high (>70%) | 16 | 15 | 10 | 10 |
| moderate (50-70%) | 5 | 4 | 8 | 8 |
| low (30-50%) | 10 | 8 | 12 | 7 |

FIGURE 3
Percentage identity of genes predicted to be involved in probiotic survival and persistence in the gut. Genes, including those associated with assemblage of sortase-dependent (SD-) fimbriae or Tad pili (as highlighted), were identified using a variety of sources including gene-trait matching, transcriptomic, proteomic, and knock-out studies (see Supplementary Table S3 for further information). Percent identity (classified as "low identity" = 30%–50%, "moderate identity" = 50%–70%, and "high identity" = 70%–100%) is based on BLAST searches using e-value cutoff of 1e-5 and query cover cutoff of 50%.

In contrast to the *tad* pili, genes encoding for fimbrial proteins such as FimA, FimB, FimP, and FimQ [as described in *B. bifidum* PRL2010 (Turroni et al., 2013)] were not found in all the bifidobacterial strains studied here (Supplementary Table S3; Figure 3). Genes with low homology (30–50%) to *fimA*, *fimP*, and *fimQ* were identified in *B. breve* M-16 V and *B. infantis* R0033, but not in *B. infantis* M-63 (Supplementary Table S3; Figure 3). On the other hand, clear homologs (>70% identity) of these fimbrial-associated genes were identified in *B. bifidum* R0071. The pilus shaft components encoded by *fimA* and *fimP* are polymerized and assembled with pilus tip components (encoded by *fimB* and *fimQ*) by an adjacent class C sortase (srtC). A further class of sortase enzymes [sortase E (srtE)] has also recently been found to be critical for bifidobacterial adhesion (Ishikawa et al., 2021). It is clear, therefore, that specific sortase enzymes may contribute to the adherence phenotypes observed in this study. These sortase-enzymes work by covalently attaching specific sortase-dependent proteins (SDPs) to the cell-wall of gram-positive organisms by recognizing a conserved C-terminal motif. Therefore, to understand if variances in SDPs could account for variances in adherence of the strains studied here, the bifidobacterial proteomes were searched for proteins with a signal peptide at the N-terminus, the srtC (LPXTG) or srtE ([L/I/V][S/A]XTG) recognition motif, followed by a stretch of hydrophobic amino acids and a positively charged C-terminus as previously described (Call and Klaenhammer, 2013; Ishikawa et al., 2021). We found nine such proteins in *B. breve* M-16 V (Supplementary Figure S2; Supplementary Table S4), 13 in *B. infantis* R0033 (Supplementary Figure S2; Supplementary Table S5), and 10 in *B. infantis* M-63 (Supplementary Figure S2; Supplementary Table S6). Analysis of the *B. infantis* strains revealed the presence of fimbrial proteins in R0033 (at BINF_1976 and BINF_1977, Supplementary Table S6), which contained the srtC-recognition motif LPXTG and, in the case of BINF_1977, a Von Willebrand Factor-type A (VWA) domain associated with binding of extracellular matrix components proteins and host cells (Supplementary Table S5). In contrast, no such srtC-dependent fimbrial proteins were identified in *B. infantis* M-63 (Supplementary Table S6).

In comparison to the lower numbers of SDPs identified in the other bifidobacterial strains, we identified 36 putative sortase-dependent proteins in *B. bifidum* R0071, including seven proteins containing the srtC-recognition motif and 29 proteins containing the srtE-recognition motif (Supplementary Figure S2; Supplementary Table S7). Of these putative srtE-dependent proteins identified in *B. bifidum* R0071, 15 were found to be glycosyl hydrolases (GHs) associated with degradation of HMOs and mucins such as those expressed on the epithelial cell surface, while the predicted srtC-dependent proteins (genetically) corresponded to the fimbrial proteins FimA/ FimP major pilin subunits or FimB/ FimQ minor pilin

subunits. In *B. bifidum* R0071 we identified six putative sortase-dependent pilus proteins arranged in three pilin clusters at *BBIF*_1805–1807 (*pil1*: *BBPR*_1820–1822 in PRL2010), *BBIF*_1693–1,695 (*pil2*: *BBPR*_1707–1709) and *BBIF*_0313–0315 (*pil3*: *BBPR*_0282–0284). A recent study has established that the presence of a stretch of polyG influences the on–off switch in the expression of these pili genes (Penno et al., 2022). Therefore, the identified pilin clusters in *B. bifidum* R0071 were searched for the presence of a G-tract up to 500 bp upstream and 200 bp downstream of the predicted gene start in the first gene of the operon. In comparison to PRL2010, which harbours only one G-tract containing pilus gene cluster (Penno et al., 2022), polyG sequences were found to be present in two pilus-specifying gene clusters in *B. bifidum* R0071. A G-tract was identified in the *pil3* gene cluster (*BBIF*_0313–0315) at the position 363939–36394911 (11 base pairs) and in the *pil1* gene cluster (*BBIF*_1805–1807) at the position 2216145 to 2216157 (13 base pairs).

## 3.3 Quantitative proteomic analysis of colonization-related factors

Label-free quantitative proteomic analysis was carried out on the four-strain bifidobacterial mixture after cell exposure and compared to control bacteria that had not been in contact with HT29-MTX cells. Furthermore, the impact of S-HMO pre-treatment on colonization-associated pathways was also assessed by comparing HMO-treated and untreated bifidobacteria following exposure to the human cell line. Preliminary screenings of the adhered cell lysate (which contained both lysed HT29-MTX cells and adhered bacteria) showed substantial masking of bacterial proteins. A total of 2,908 proteins were detected with only 12 proteins matched to bacterial proteins (2 × *B. infantis,* 2 × *B. breve,* and 8 × *B. bifidum*). The remaining 2,896 proteins were matched to human proteins. Since analysis of the adhered cell lysate did not allow for in-depth understanding of the impact of HMO and cell treatments on the bifidobacterial mixture, these samples were eliminated from subsequent analyses. Analysis of bifidobacteria aspirated from the cell apical compartment resulted in the identification of 2,191 bacterial proteins (which covered 37.4% of the proteome of the strains studied here) and 1,385 human proteins. Supplementary Figure S3 shows the distribution of shared or specific bacterial proteins by species (Supplementary Figure S3A) and by treatment (Supplementary Figure S3B). Of the 2,191 bacterial proteins identified, 170 proteins could not be distinguished based on species, with peptides matched to proteins in more than one species (Supplementary Figure S3A). Functional characterization confirmed that these shared proteins were not associated with bacterial adhesion. The remaining proteins detected during label-free quantitative proteomic analysis were matched exclusively to a single proteome in the database, with 393 from *B. bifidum*, 742 from *B. breve* and 886 from *B. infantis*.

To assess the influence of epithelial cell exposure on bifidobacterial proteome expression, a 2-fold increase or decrease in the level of protein abundance was used as a cut-off for statistically significant differentially abundant (SSDA) proteins ($p < 0.05$). Following treatment with cells (S-HMO$^-$cells$^+$), only two *B. infantis* proteins were found in higher abundance when compared to the control group; 30S ribosomal protein S17 (fold increase of 6.37) and sugar kinase (fold increase of 2.74) (Supplementary Table S9). A further two *B. infantis* proteins were uniquely detected after treatment with cells; DNA polymerase III delta subunit and uracil-xanthine transport protein (Supplementary Table S9). Similarly, treatment with cells resulted in increased abundances of only two *B. breve* proteins (30S ribosomal protein S17, and undecaprenyl-phosphate α-*N*-acetylglucosaminephosphotransferase) with a further two proteins uniquely detected after treatment with cells (prolipoprotein diacylglyceryl transferase and a transport protein) (Supplementary Table S10). In contrast, 42 *B. infantis* and 14 *B. breve* proteins decreased in abundance following incubation with HT29-MTX cells (S-HMO$^-$cells$^+$) (Figure 4A). Qualitative analysis revealed that a further 49 *B. infantis* and 60 *B. breve* proteins were no longer detected after cell-treatment (S-HMO$^-$cells$^+$). As shown in Figure 4B, pre-treatment with HMO shifted the proteome of these strains, with a number of *B. infantis* proteins, in particular, increasing in abundance. For *B. infantis* it was found that 31 proteins increased in abundance following HMO treatment. Functional characterization, however, revealed that the majority of these upregulated proteins (>90%) were associated with metabolism of HMO, including carbohydrate transporters, glycosyl hydrolases, and bifid shunt enzymes. For *B. breve* it was found that 4 proteins increased in abundance following pre-exposure to HMO (Figure 4B). Functional characterization again revealed that the majority of these proteins (75%) were associated with carbohydrate metabolism.

In contrast to *B. infantis* and *B. breve*, only nine *B. bifidum* proteins were detected at lower abundance after cell exposure (S-HMO$^-$cells$^+$) including 8 proteins detected exclusively in the control group (Figure 4A). On the other hand, incubation of the bifidobacterial mixture with HT29-MTX cells (S-HMO$^-$cells$^+$) resulted in an increased abundance of 225 *B. bifidum* proteins (including 71 uniquely detected proteins), many of which were further upregulated through pre-treatment with HMO (S-HMO$^+$cells$^+$) (Figure 4A; Supplementary Table S8). Within this group of upregulated *B. bifidum* proteins, we identified 27 with a potential function in probiotic colonization. The fold changes of these proteins (*vs* control) are summarized in Figure 5 and include cell surface pilus-associated proteins (Figure 5A), glycosyl hydrolases that have been shown to interact with the mucus layer (Figure 5B), and moonlighting proteins associated with bacterial adhesion (Figure 5C). Notably, we observed upregulation of numerous srtC-dependent proteins (as identified in section 3.3) following HT29-MTX exposure. These include Pil3 fimbrial subunits FimP (*BBIF*_0314) and FimQ (*BBIF*_0313) which increased 3.77 fold and 2.79 fold, respectively, following exposure to HT29-MTX cells (HMO$^-$cells$^+$) (Figure 5A; Supplementary Table S8). These proteins were further upregulated by pre-treatment with HMO (S-HMO$^+$cells$^+$); with FimP increasing 5.76 fold (vs control) and FimQ increasing 5.13 fold (vs control) (Figure 5A). The Pil1 major pilin (encoded by gene *BBIF*_1806) was also highly upregulated following S-HMO$^-$cells$^+$ and S-HMO$^+$cells$^+$ treatment (Figure 5A; Supplementary Table S8).

In addition to SrtC-dependent cell surface appendages, other *B. bifidum* R0071 colonization-related proteins were identified that were upregulated following cell +/− S-HMO treatment (Figure 5C). The majority of these upregulated proteins normally function as housekeeping genes or act as enzymes for glycolysis and are expressed intracellularly. However, these proteins have moonlighting properties and when expressed on the cell surface can facilitate cell adhesion. For example, cell treatment (S-HMO$^-$cells$^+$) resulted in significant upregulation of chaperone protein DnaK (2.39 fold increase vs.

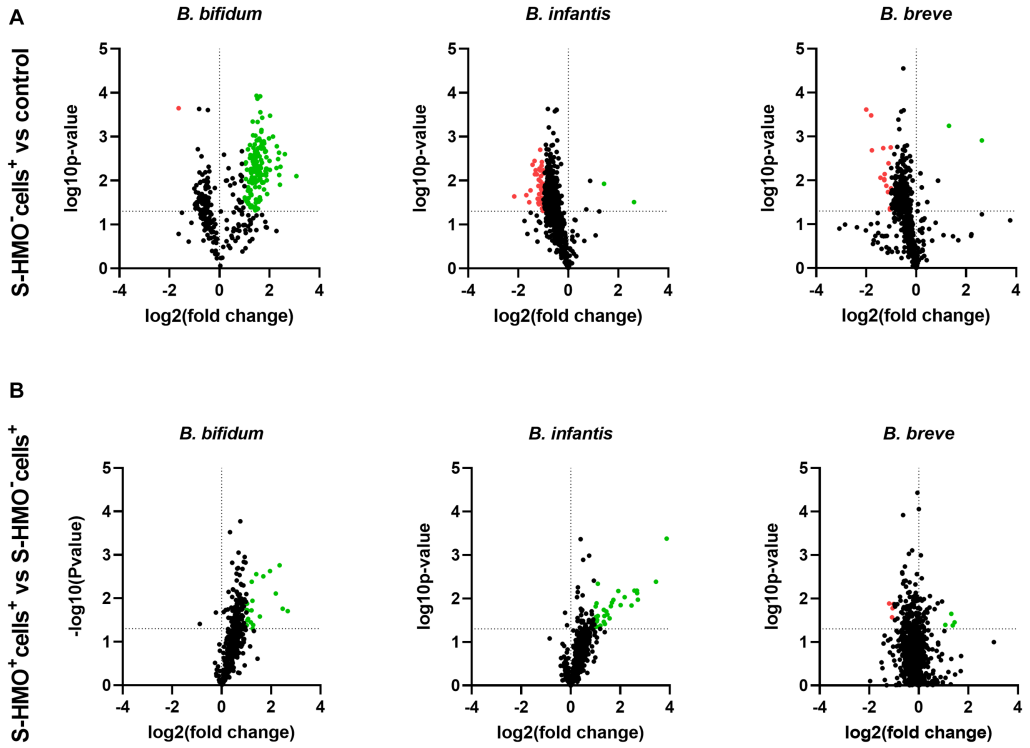


FIGURE 4
Volcano plots displaying quantitative changes in abundance of *Bifidobacterium bifidum, Bifidobacterium infantis,* and *Bifidobacterium breve* proteins following treatment **(A)** with and without mucus-secreting HT29-MTX cells (S-HMO⁻cells⁺ vs. S-HMO⁻cells⁻) **(B)** with mucus-secreting HT29-MTX cells with and without pre-exposure to S-HMO (S-HMO⁺cells⁺ vs. S-HMO⁻cells⁺) as detected using label-free quantitative proteomics. The horizontal line represents a value of p of 0.05. Proteins with a significant change in abundance [$p < 0.05$ (Student's *t*-test), fold change ≥2] are highlighted in red to indicate decreased abundance and green to indicate increased abundance.

control), chaperonin protein GroES (2.5 fold increase), chaperonin protein GroEL (3.11 fold increase), and S-ribosylhomocysteine lyase LuxS (2.12 fold increase) (Candela et al., 2007; Christiaen et al., 2014; Duranti et al., 2014; Wei et al., 2016; Zhu et al., 2016). Pre-treatment with HMO (S-HMO⁺cells⁺) resulted in significant increases in many moonlighting proteins (Figure 5C). These include elongation factor thermo unstable (EF-Tu), enolase (Eno), and glyceraldehyde phosphate dehydrogenase (Gap) which were upregulated 4.84 fold, 3.07 fold, and 3.84 fold, respectively, following incubation with both cells and HMO (S-HMO⁺cells⁺), which represents a significant increase when compared to treatment with cells alone (S-HMO⁻cells⁺) (Figure 5C; Supplementary Table S8).

Aside from upregulation of cell surface adhesins, we also observed significant upregulation of SrtE-dependent glycosyl hydrolase (GH) proteins in *B. bifidum* R0071 following exposure of the bifidobacterial mixture to mucus-secreting HT29-MTX cells. The cumulative effects of HMO and cell treatment (S-HMO⁺cells⁺) resulted in significant upregulation of numerous SrtE-dependent GH proteins (including β-galactosidases and fucosidases) when compared to treatment with cells alone (S-HMO⁻cells⁺) (Figure 5B).

## 4 Discussion

Our research specifically delved into the adhesive characteristics of four bifidobacterial strains: *Bifidobacterium bifidum* R0071, *Bifidobacterium longum* subsp. *infantis* R0033, *Bifidobacterium breve* M-16 V, and *Bifidobacterium longum* subsp. *infantis* M-63 in the presence of HMO. These strains have garnered considerable attention due to their well-documented health benefits, as substantiated by clinical investigations (Giannetti et al., 2017; Wong et al., 2019; Xiao et al., 2019). For instance, infants fed with a probiotic supplement comprising *B. bifidum* R0071, *B. infantis* R0033, and a *Lactobacillus* strain maintained elevated levels of fecal SIgA after a four-week treatment period (Xiao et al., 2019). *Bifidobacterium breve* M-16 V, another commonly used probiotic in infants, has exhibited promise in safeguarding against conditions such as necrotizing enterocolitis (NEC) and allergic diseases in infants, as extensively reviewed by Wong et al. in 2019 (Wong et al., 2019). Furthermore, a blend containing *B. infantis* M63, along with two other probiotic strains (including M-16 V), demonstrated superior management of functional abdominal pain and a notable enhancement in the quality of life among children with irritable bowel syndrome (IBS) (Giannetti et al., 2017). Notably, our previous research has highlighted the synergistic capabilities of these bifidobacterial strains when it comes to utilizing human milk oligosaccharides (HMOs) as a primary carbohydrate source, resulting in a marked increase in bacterial proliferation (Walsh et al., 2022).

Adherence of probiotic bacteria was evaluated using HT29-MTX human tumorigenic cell lines to mimic bifidobacterial adhesion to intestinal epithelial cells (IECs). The HT29-MTX cell line, which is able to constitutively produce mucin, has more physiologically

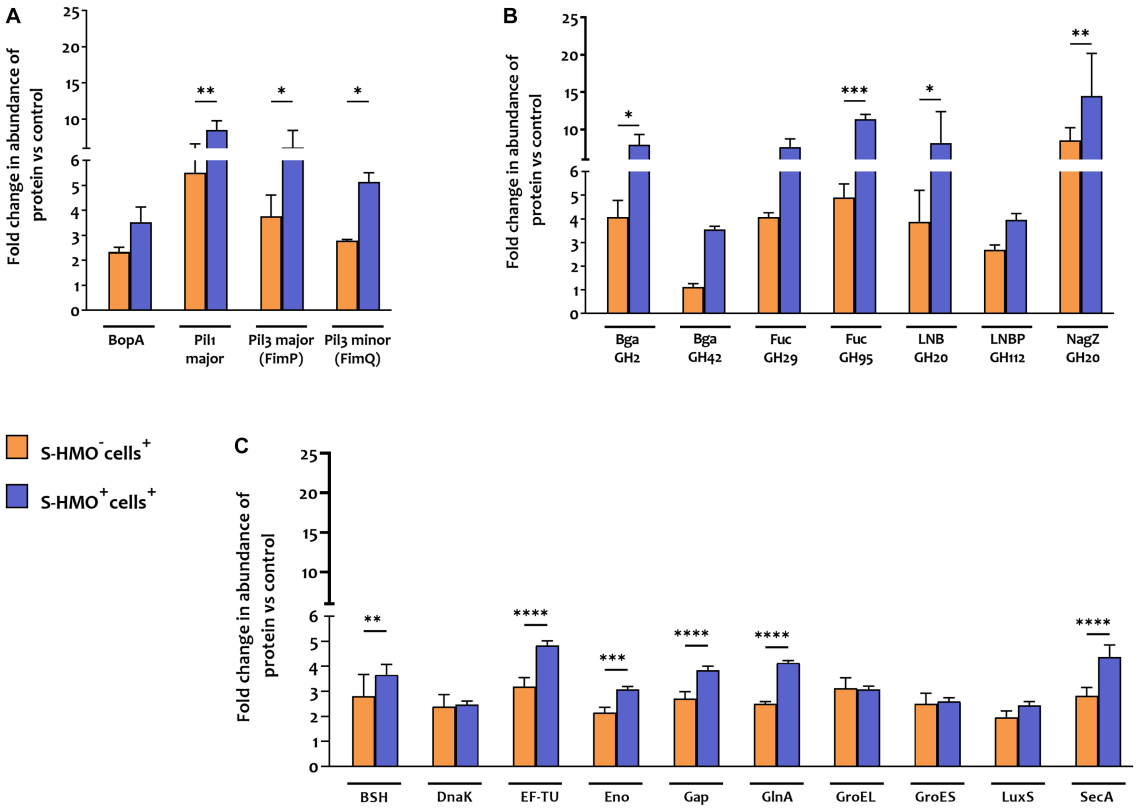


FIGURE 5
Proteins matched to *Bifidobacterium bifidum* R0071 with potential roles in bifidobacterial colonization that increased in abundance following treatment with cells (± S-HMO). **(A)** Cell surface adhesins **(B)** glycosyl hydrolases **(C)** secondary proteins involved in probiotic persistence. Protein abundance plotted as fold change versus negative control (S-HMO⁻cells⁻, without S-HMO or cell treatment). Analysis was calculated using technical triplicate data from biological triplicate experiments and data are means ± SD. Univariate analysis of variance (ANOVA) and post-hoc Tukey tests were performed to determine the significant differences between the groups (*$p < 0.05$, **$p < 0.01$, ***$p < 0.001$, ****$p < 0.0001$).

relevant characteristics when compared to HT29 cells alone due to the mucus layer formation, and has therefore been proposed as a more suitable cell line for studying host–microbe interactions. In agreement with other studies (Kavanaugh et al., 2013; Zhang et al., 2020) through the use of colonisation assays, we confirm that the adhesive potential of bifidobacterial strains can be substantially increased through treatment with milk oligosaccharides. These HMO-induced changes in bifidobacterial adhesion align with findings of Chicklowski et al., where increased adherence of *B. infantis* was observed resulting from exposure to breastmilk-derived HMOs (Chichlowski et al., 2012). However, in contrast to Chicklowski et al., the current study found that HMO-exposed *B. bifidum* had a higher rate of adhesion to intestinal cells compared to *B. infantis* or *B. breve* (Chichlowski et al., 2012). This agrees with previous studies which showed that *B. bifidum* PRL2010 displays higher levels of adhesion to extracellular matrix components (fibronectin, plasminogen, and laminin) when compared with *B. breve* and *B. infantis* (Turroni et al., 2013). Notably, proteomic analysis of the bifidobacterial combination revealed that many proteins within the *B. infantis* and *B. breve* proteome decreased in abundance following exposure to intestinal cells. This is likely a result of complex and dynamic interactions between the bacteria and host cells. These interactions can trigger various responses, including adaption to host immune responses, regulatory changes, and resource allocation, which collectively influence the protein expression profile of these bacteria during the assay.

Of note, we observed higher levels of adhesion in HMO-exposed *B. infantis* R0033 when compared to its species counterpart *B. infantis* M-63. Our findings verify that bacterial adhesion to intestinal epithelial cells is not only species-specific but also strain-specific. Interestingly, we have previously highlighted the strain-level differences between M-63 and R0033, with M-63 demonstrating superior growth on breastmilk-derived HMO (Walsh et al., 2022). It may be important, therefore, when assessing interactions of HMO and probiotics, to consider the growth phenotype but also the adherent phenotype resulting from a strain's exposure to HMO. Notably, findings from adhesion assays using a combination of all four strains have indicated that co-operation between strains may expand HMO acquisition capabilities to enhance gut colonization activity of strains. qPCR analysis of the bifidobacterial consortia revealed that, irrespective of the carbon source, *B. bifidum* R0071 occupied the largest proportion of bacteria adhering to HT29-MTX cells. Interestingly, recent studies have indicated that strains *of B. bifidum* adhere more strongly to infant mucus than adult mucus, while more adult-associated species such as *B. lactis* and *L. rhamnosus* adhere more strongly to adult mucus than to infant mucus. In general, the adhesion of *B. bifidum in vitro* is exceptionally strong among probiotics (Shibahara-Sone et al., 2016) and therefore the high levels

of adherence observed in this study may be expected. Such characteristics might arise from the vast array of sortase-dependent proteins specific to *B. bifidum* as described in a recent study (Ishikawa et al., 2021).

The survey of the bacterial genomes for colonisation-related factors revealed a number of components that bacteria can potentially interact with to adhere to mucus and epithelial surface glycans, e.g., outer-membrane proteins, adhesins, capsules and appendages such as pili, flagella, and fimbriae (Paone and Cani, 2020). Assembly of pilus-like appendages on the bacterial surface is thought to be pivotal for bifidobacterial gut colonization. In recent years, pilus encoding-gene clusters have been identified in many infant-derived bifidobacteria, most notably a type IVb tight adherence (Tad) pilus-encoding gene cluster in *B. breve* UCC2003 (O'Connell Motherway et al., 2011) and sortase-dependent pilus gene clusters in *B. bifidum* PRL2010 (Turroni et al., 2013). The fact that genes with homology to the UCC2003 *tad* locus were found in all our strains aligns with studies from O'Connell Motherway et al., where the authors found that the tad pilus-encoding locus was highly conserved across the bifidobacterial genera (O'Connell Motherway et al., 2011). That study suggested that such a phenomenon supports the notion of a ubiquitous pili-mediated host colonization and persistence mechanism for bifidobacteria (O'Connell Motherway et al., 2011, 2019).

In addition to tad pili, membrane-bound transpeptidase enzymes known as "sortases" have been found to play a critical role in facilitating bacterium-host cell crosstalk throughout the bifidobacterial genera. In fact, a recent study from Ishikawa et al. (2021) found that non-adhesive strains belonging to the *B. bifidum* species lacked a functional class E (housekeeping) sortase (Ishikawa et al., 2021). Class E sortases (srtE) work by anchoring proteins to the cell surface, while class C sortases (srtC) are responsible for constructing pilus polymers. Sortase-mediated surface structures are responsible, therefore, for cell attachment and nutrient uptake, amongst other functions. The small number of putative srtC-dependent clusters associated with pilus expression identified in *B. infantis* strains is in line with a previous study in which pilus-like structures were shown to be rare if at all present in *B. longum* subsp. *infantis* ATCC15697 (Foroni et al., 2011). Since pilus-like structures in *B. infantis* are rare, the srtC-dependent fimbrial units (containing VWA-domains) identified in R0033 may be notable. VWA-domains have been found in pilus proteins that bind to extracellular matrix components and host cells (Whittaker and Hynes, 2002). Follow-up studies are required to elucidate whether the expression of these fimbriae proteins in R0033 could account for its superior adherence over its *B. infantis* counterpart M-63. In contrast to the *B. infantis* and *B. breve* strains studied here, numerous srtC-dependent fimbrial proteins were identified in *B. bifidum* R0071. As described for *B. bifidum* PRL2010, the genome of *B. bifidum* R0071 encompasses three different loci (Pil1, Pil2, and Pil3) encoding the predicted biosynthetic machinery for the production of sortase-dependent pili (Turroni et al., 2013). Proteomic analysis of the bifidobacterial combination following exposure to intestinal cells revealed substantial upregulation of srtC-dependent pilin proteins within two pilus-specifying clusters (Pil1 and Pil3) but not Pil2. Recent studies have highlighted that the presence of a stretch of polyG influences the on–off switch in the expression of these pili genes. We confirm that polyG sequences were found downstream of the predicted gene start in Pil1 and Pil3, but not Pil2. The identification of polyG sequences is noteworthy, as productive replication slippage at G-tract sequences may be an important mediator of sortase-dependent pili expression and subsequent colonization of bifidobacterial strains within the gastrointestinal tract (Penno et al., 2022). Importantly, significant upregulation of the pilus proteins within the *B. bifidum* Pil1 and Pil3 clusters was observed following exposure of the bifidobacteria to HMO. The HMO-induced upregulation of srtC-dependent pilins aligns with findings from Foroni et al. where high production of pilus-like structure was observed following propagation of *B. bifidum* PRL2010 on fructooligosaccharides (Foroni et al., 2011). It is clear therefore, that expression of sortase-dependent pili by *B. bifidum* can be influenced by the presence of complex carbohydrates and may account for the increased adherence of this strain following exposure to S-HMO.

A somewhat less explored category of proteins known as "moonlighting proteins" (Huberts and van der Klei, 2010) may also play a critical role in bacterial adhesion. Most of these proteins typically serve as housekeeping genes or function as enzymes in glycolysis and are expressed intracellularly. Nevertheless, these proteins have been found to be multifunctional and, when expressed on the cell surface, have been reported to facilitate cell adhesion. In this current study, moonlighting proteins with primary functions as chaperone proteins such as DnaK and GroEL were more abundant in the *B. bifidum* R0071 proteome following co-cultivation with IECs. This aligns with previous research in *Lactobacillus johnsonii* (Bergonzelli et al., 2006) and *Bifidobacterium animalis* (Candela et al., 2010) which demonstrated a role for GroEL and DnaK in probiotic binding to mucins and plasminogen. However, in contrast to Kavanaugh et al., we found that exposure of bifidobacteria to HMO did not influence the expression of DnaK or GroEL (Kavanaugh et al., 2013), although these discrepancies could be accounted for differences in strains (multistrain vs. single strain of *B. infantis*), HMOs (breastmilk-derived HMO vs. combination of 3′-SL and 6′-SL), or analytical methods (transcriptomic vs. proteomic profiling). However, we identified numerous moonlighting proteins that serve as adhesins for bifidobacteria in higher abundance in the *B. bifidum* R0071 proteome following co-cultivation with HT29-MTX cells which were further upregulated following pre-exposure to HMO. These include enzymes typically associated with glycolysis and the bifid shunt pathway such as transaldolase (Tal), enolase (Eno), and glyceraldehyde-3-phosphate dehydrogenase (Gap) (Pokusaeva et al., 2011). This aligns with previous studies which have identified mucin-binding properties for transaldolase in *B. bifidum* (González-Rodríguez et al., 2012) and plasminogen-binding properties for enolase in *B. longum*, *B. bifidum*, *B. lactis*, and *B. breve* strains (Candela et al., 2007, 2009; Wei et al., 2014). Similar plasminogen binding capabilities have also been demonstrated for EF-Tu (Candela et al., 2007), which is another moonlighting protein which may facilitate cell adhesion and which was found at significantly higher abundances the *B. bifidum* R0071 proteome following IEC exposure and HMO pre-treatment. Overall, the proteomic profiling of moonlighting proteins outlined in this study indicates that bifidobacterial strains may be able to sense the conditions of their intestinal environment to detect receptors on IECs and respond by enhancing expression of adhesive molecules on the bacterial cell surface.

The mucus layer not only supplies attachment sites to commensal bacteria, it also serves as a nutrient source for organisms in the gut microbiota (Hansson, 2020; Paone and Cani, 2020). The turnover of the intestinal mucus layer involves mucus synthesis, secretion and

degradation, and represents a delicate process that needs to be regulated and balanced to ensure that mucus maintains an optimal protective function (Schneider et al., 2018). Recent studies have found that mucin adhesion is closely linked to mucin utilization (Ishikawa et al., 2021), with researchers highlighting that the class E housekeeping sortase is a critical component influencing adhesion of *B. bifidum* strains (Ishikawa et al., 2021). This aligns with the identification of SrtE-dependent glycosyl hydrolase proteins in R0071 following exposure the HT29-MTX cells and/ or HMO. Microbes most adept at mucin glycan degradation often encode sialidases and fucosidases to remove terminal structures which allows for greater accessibility to the extended core structures. The monosaccharides released by the action of these enzymes may be utilized by the bacteria themselves or released into the environment for scavenging bacteria (Luo et al., 2021). Proteomic analysis revealed significant upregulation of *B. bifidum* fucosidases belonging to GH29 and GH95 families, which hydrolyse Fucα1–2Gal and Fucα1–3/4Gal linkages, respectively. A SrtE-dependent GH33 exo-α-sialidase was detected that matched to *B. bifidum* R0071 which was found exclusively in bacteria exposed to mucus secreting intestinal cells. The fact that there was significant upregulation of fucosidases enzymes and an exo-α-sialidase in R0071 following incubation with IECs is notable. Studies have shown that the fucose released from mucin glycans by *B. bifidum* enables growth of *Eubacterium hallii*, a commensal species that produces butyrate and propionate from fermentation metabolites (Bunesova et al., 2018). Sialic acid residues are another highly sought-after nutrient source that are found terminating mucin glycan chains. To access this glycan residue intestinal bacteria express GH33 sialidases, which cleave terminal sialic acid residues. Previous studies have highlighted that cleavage of sialic acid residues from mucin oligosaccharides, catalyzed by *B. bifidum* GH33 sialidases, can support growth of *B. breve* UCC2003 (Egan et al., 2014). We hypothesize therefore that HMO-enhanced colonization of *B. bifidum* could also benefit other gut symbionts through mucin cross-feeding activities.

## 5 Conclusion

Overall, we confirm that adherence of bifidobacterial strains to intestinal epithelial cells is species- and strain-specific. Our results suggest that HMO, a prominent component of human breast milk, can promote interaction of infant-derived bifidobacteria and intestinal cells. In particular, we show that the presence of HMOs significantly improves the adhesion ability of a mixed community of commercial bifidobacterial strains. The adherence of bifidobacteria to intestinal epithelial cells is essential for their colonization, their ability to support a healthy gut environment, and their potential to confer various health benefits to the host. Recent studies have shown that certain bifidobacterial species, including *B. infantis*, are in danger of becoming extinct due to a multitude of factors including changes in breastfeeding habits in certain countries, C-sections deliveries, and antibiotic usage (Taft et al., 2022). Therefore, it has never been more important to explore a means to increase the colonization of beneficial bacteria such as bifidobacteria in the gut. Specifically, we show that carbohydrate sources are important environmental factors influencing adhesin expression levels particularly in *B. bifidum*, which may have knock-on effects positively influencing trophic interactions and social behavior among bifidobacterial species and between other intestinal microbes as has been shown previously for this species (Egan et al., 2014; Bunesova et al., 2018). We confirm that assembly and localization of surface proteins, including SrtC-dependent pili and moonlighting proteins, are key factors influencing *B. bifidum* adhesion. Our findings also verify that the class E housekeeping sortase may be a critical component influencing adhesion of *B. bifidum* strains by increasing bifidobacterial interaction with the mucin layer. Although *in vitro* experiments are key to understand the mechanisms of adhesion and select probiotic candidates with potential to adhere *in vivo*, it is difficult to extrapolate these results to the human intestinal tract where other factors such as peristaltic movements, host immune system, diet and genetics, or competition with resident microbiota could interfere with attachment. It is clear, therefore, that further clinical studies with probiotics, which incorporate specific combinations of probiotic consortia and HMOs, will be critical in understanding how the findings outlined here translate to the *in vivo* situation. Nevertheless, this study sheds light on the future use of oligosaccharides and bifidobacteria for nutritional intervention or clinical applications.

## Data availability statement

Genome data presented in this study for R0033 and R0071 is deposited in the Bacterial and Viral Bioinformatics Resource Center (BV-BRC) using the following links: R0033: https://www.bv-brc.org/view/Genome/1678.111, R0071: https://www.bv-brc.org/view/Genome/1678.107. Genome data for M-16V and M-63 is deposited in the NCBI repository, accession number OR940152-64.

## Author contributions

CW designed the experiments, performed the experiments and data analysis, prepared the original draft, and contributed to writing—reviewing and editing. RO contributed to proteomic analysis and writing—reviewing and editing. FB contributed to sequence assembly and annotation, writing—reviewing and editing. JL contributed to writing—reviewing and editing. DS and RH contributed to writing—reviewing and editing and supervision. All authors contributed to the article and approved the submitted version.

## Funding

The work was financially supported by H and H Group, Ireland. DS and RH are members of APC Microbiome Ireland funded by Science Foundation Ireland, through the Irish Government's National Development Plan (SFI/12/RC/2273-P1 and SFI/12/RC/2273-P2). FB is member of ADAPT Research Centre funded by Science Foundation Ireland (SFI/13/RC/2106_P2) at Munster Technological University. At the time of writing CW was in receipt of a Teagasc Walsh Scholarship. Mass spectrometry equipment for quantitative proteomics (Maynooth University) was funded by a competitive infrastructure award from Science Foundation Ireland (SFI) (12/RI/2346 (3)).

## Conflict of interest

CW and JL were employed by H & H Group, Ireland. RO has received costs for mass spectrometry services from H & H Group.

The remaining authors declare that the research was conducted in the absence of any commercial or financial relationships that could be construed as a potential conflict of interest.

## Publisher's note

All claims expressed in this article are solely those of the authors and do not necessarily represent those of their affiliated organizations, or those of the publisher, the editors and the reviewers. Any product that may be evaluated in this article, or claim that may be made by its manufacturer, is not guaranteed or endorsed by the publisher.

## Supplementary material

The Supplementary material for this article can be found online at: https://www.frontiersin.org/articles/10.3389/fmicb.2023.1232173/full#supplementary-material

## References


Bergonzelli, G. E., Granato, D., Pridmore, R. D., Marvin-Guy, L. F., Donnicola, D., and Corthésy-Theulaz, I. E. (2006). GroEL of *Lactobacillus johnsonii* La1 (NCC 533) is cell surface associated: potential role in interactions with the host and the gastric pathogen *Helicobacter pylori*. *Infection and immunity*, 74, 425–434.

Bottacini, F., Morrissey, R., Roberts, R. J., James, K., Van Breen, J., Egan, M., et al. (2017). Comparative genome and methylome analysis reveals restriction/modification system diversity in the gut commensal *Bifidobacterium breve*. *Nucleic Acids Res.* 46, 1860–1877. doi: 10.1093/nar/gkx1289

Bron, P., Meijer, M., Bongers, R., De Vos, W., and Kleerebezem, M. (2007). Dynamics of competitive population abundance of *Lactobacillus plantarum* ivi gene mutants in faecal samples after passage through the gastrointestinal tract of mice. *J. Appl. Microbiol.* 103, 1424–1434. doi: 10.1111/j.1365-2672.2007.03376.x

Bunesova, V., Lacroix, C., and Schwab, C. (2018). Mucin cross-feeding of infant bifidobacteria and *Eubacterium hallii*. *Microb. Ecol.* 75, 228–238. doi: 10.1007/s00248-017-1037-4

Call, E. K., Goh, Y. J., Selle, K., Klaenhammer, T. R., and O'Flaherty, S. (2015). Sortase-deficient lactobacilli: effect on immunomodulation and gut retention. *Microbiology* 161, 311–321. doi: 10.1099/mic.0.000007

Call, E., and Klaenhammer, T. (2013). Relevance and application of sortase and sortase-dependent proteins in lactic acid bacteria. *Front. Microbiol.* 4:73. doi: 10.3389/fmicb.2013.00073

Candela, M., Bergmann, S., Vici, M., Vitali, B., Turroni, S., Eikmanns, B. J., et al. (2007). Binding of human plasminogen to *Bifidobacterium*. *J. Bacteriol.* 189, 5929–5936. doi: 10.1128/JB.00159-07

Candela, M., Biagi, E., Centanni, M., Turroni, S., Vici, M., Musiani, F., et al. (2009). Bifidobacterial enolase, a cell surface receptor for human plasminogen involved in the interaction with the host. *Microbiology* 155, 3294–3303. doi: 10.1099/mic.0.028795-0

Candela, M., Centanni, M., Fiori, J., Biagi, E., Turroni, S., Orrico, C., et al. (2010). DnaK from *Bifidobacterium animalis* subsp. *lactis* is a surface-exposed human plasminogen receptor upregulated in response to bile salts. *Microbiology*, 156, 1609–1618.

Chang, C.-S., and Kao, C.-Y. (2019). Current understanding of the gut microbiota shaping mechanisms. *J. Biomed. Sci.* 26:59. doi: 10.1186/s12929-019-0554-5

Chichlowski, M., De Lartigue, G., German, J. B., Raybould, H. E., and Mills, D. A. (2012). Bifidobacteria isolated from infants and cultured on human milk oligosaccharides affect intestinal epithelial function. *J. Pediatr. Gastroenterol. Nutr.* 55, 321–327. doi: 10.1097/MPG.0b013e31824fb899

Christiaen, S. E. A., O'Connell Motherway, M., Bottacini, F., Lanigan, N., Casey, P. G., Huys, G., et al. (2014). Autoinducer-2 plays a crucial role in gut colonization and probiotic functionality of *Bifidobacterium breve* UCC2003. *PLoS One* 9:e98111. doi: 10.1371/journal.pone.0098111

Cox, J., Hein, M. Y., Luber, C. A., Paron, I., Nagaraj, N., and Mann, M. (2014). Accurate proteome-wide label-free quantification by delayed normalization and maximal peptide ratio extraction, termed Maxlfq. *Mol. Cell. Proteomics* 13, 2513–2526. doi: 10.1074/mcp.M113.031591

Duranti, S., Turroni, F., Lugli, G. A., Milani, C., Viappiani, A., Mangifesta, M., et al. (2014). Genomic characterization and transcriptional studies of the starch-utilizing strain *Bifidobacterium adolescentis* 22L. *Appl. Environ. Microbiol.* 80, 6080–6090. doi: 10.1128/AEM.01993-14

Egan, M., Motherway, M. O., Kilcoyne, M., Kane, M., Joshi, L., Ventura, M., et al. (2014). Cross-feeding by *Bifidobacterium breve* UCC2003 during co-cultivation with *Bifidobacterium bifidum* PRL2010 in a mucin-based medium. *BMC Microbiol.* 14:282. doi: 10.1186/s12866-014-0282-7

Fanning, S., Hall, L. J., Cronin, M., Zomer, A., MacSharry, J., Goulding, D., et al. (2012). Bifidobacterial surface-exopolysaccharide facilitates commensal-host interaction through immune modulation and pathogen protection. *Proc. Natl. Acad. Sci. U. S. A.* 109, 2108–2113. doi: 10.1073/pnas.1115621109

Foroni, E., Serafini, F., Amidani, D., Turroni, F., He, F., Bottacini, F., et al. (2011). Genetic analysis and morphological identification of pilus-like structures in members of the genus *Bifidobacterium*. *Microb. Cell Fact.* 10:S16. doi: 10.1186/1475-2859-10-S1-S16

Frese, S. A., Benson, A. K., Tannock, G. W., Loach, D. M., Kim, J., Zhang, M., et al. (2011). The evolution of host specialization in the vertebrate gut symbiont *Lactobacillus reuteri*. *PLoS Genet.* 7:e1001314. doi: 10.1371/journal.pgen.1001314

Frese, S. A., Mackenzie, D. A., Peterson, D. A., Schmaltz, R., Fangman, T., Zhou, Y., et al. (2013). Molecular characterization of host-specific biofilm formation in a vertebrate gut symbiont. *PLoS Genet.* 9:e1004057. doi: 10.1371/journal.pgen.1004057

Ganesh, B. P., Hall, A., Ayyaswamy, S., Nelson, J. W., Fultz, R., Major, A., et al. (2018). Diacylglycerol kinase synthesized by commensal *Lactobacillus reuteri* diminishes protein kinase C phosphorylation and histamine-mediated signaling in the mammalian intestinal epithelium. *Mucosal Immunol.* 11, 380–393. doi: 10.1038/mi.2017.58

Gareau, M. G., Sherman, P. M., and Walker, W. A. (2010). Probiotics and the gut microbiota in intestinal health and disease. *Nat. Rev. Gastroenterol. Hepatol.* 7, 503–514. doi: 10.1038/nrgastro.2010.117

Giannetti, E., Maglione, M., Alessandrella, A., Strisciuglio, C., De Giovanni, D., Campanozzi, A., et al. (2017). A mixture of 3 bifidobacteria decreases abdominal pain and improves the quality of life in children with irritable bowel syndrome: a multicenter, randomized, double-blind, placebo-controlled, crossover trial. *J. Clin. Gastroenterol.* 51, e5–e10. doi: 10.1097/MCG.0000000000000528

Gibson, G. R., Hutkins, R., Sanders, M. E., Prescott, S. L., Reimer, R. A., Salminen, S. J., et al. (2017). Expert consensus document: the International Scientific Association for Probiotics and Prebiotics (ISAPP) consensus statement on the definition and scope of prebiotics. *Nat. Rev. Gastroenterol. Hepatol.* 14, 491–502. doi: 10.1038/nrgastro.2017.75

Goh, Y. J., and Klaenhammer, T. R. (2014). Insights into glycogen metabolism in *Lactobacillus acidophilus*: impact on carbohydrate metabolism, stress tolerance and gut retention. *Microb. Cell Factories* 13, 1–12. doi: 10.1186/s12934-014-0094-3

González, R., Klaassens, E. S., Malinen, E., Vos, W. M. D., and Vaughan, E. E. (2008). Differential transcriptional response of *Bifidobacterium longum* to human milk, formula milk, and galactooligosaccharide. *Appl. Environ. Microbiol.* 74, 4686–4694. doi: 10.1128/AEM.00122-08

González-Rodríguez, I., Sánchez, B., Ruiz, L., Turroni, F., Ventura, M., Ruas-Madiedo, P., et al. (2012). Role of extracellular transaldolase from *Bifidobacterium bifidum* in mucin adhesion and aggregation. *Appl. Environ. Microbiol.* 78, 3992–3998. doi: 10.1128/AEM.08024-11

Gueimonde, M., Garrigues, C., Van Sinderen, D., De Los Reyes-Gavilán, C. G., and Margolles, A. (2009). Bile-inducible efflux transporter from *Bifidobacterium longum* NCC2705, conferring bile resistance. *Appl. Environ. Microbiol.* 75, 3153–3160. doi: 10.1128/AEM.00172-09

Guglielmetti, S., Tamagnini, I., Mora, D., Minuzzo, M., Scarafoni, A., Arioli, S., et al. (2008). Implication of an outer surface lipoprotein in adhesion of *Bifidobacterium bifidum* to Caco-2 cells. *Am. Soc. Microbiol.* 74, 4695–4702. doi: 10.1128/AEM.00124-08

Hansson, G. C. (2020). Mucins and the microbiome. *Annu. Rev. Biochem.* 89, 769–793. doi: 10.1146/annurev-biochem-011520-105053

Huberts, D. H., and van der Klei, I. J. (2010). Moonlighting proteins: an intriguing mode of multitasking. Biochimica et Biophysica Acta (BBA)-Molecular *Cell Research*, 1803, 520–525.

Ishikawa, E., Yamada, T., Yamaji, K., Serata, M., Fujii, D., Umesaki, Y., et al. (2021). Critical roles of a housekeeping sortase of probiotic *Bifidobacterium bifidum* in bacterium–host cell crosstalk. *iScience* 24:103363. doi: 10.1016/j.isci.2021.103363

Kankainen, M., Paulin, L., Tynkkynen, S., Von Ossowski, I., Reunanen, J., Partanen, P., et al. (2009). Comparative genomic analysis of *Lactobacillus rhamnosus* GG reveals pili containing a human-mucus binding protein. *Proc. Natl. Acad. Sci.* 106, 17193–17198. doi: 10.1073/pnas.0908876106

Kavanaugh, D. W., O'Callaghan, J., Buttó, L. F., Slattery, H., Lane, J., Clyne, M., et al. (2013). Exposure of *Bifidobacterium longum* subsp. *infantis* to milk oligosaccharides increases adhesion to epithelial cells and induces a substantial transcriptional response. *PLoS One* 8:e67224. doi: 10.1371/journal.pone.0067224

Liu, Y., An, H., Zhang, J., Zhou, H., Ren, F., and Hao, Y. (2014). Functional role of tlyC1 encoding a hemolysin-like protein from *Bifidobacterium longum* BBMN68 in bile tolerance. *FEMS Microbiol. Lett.* 360, 167–173. doi: 10.1111/1574-6968.12601

Luo, Y., Xiao, Y., Zhao, J., Zhang, H., Chen, W., and Zhai, Q. (2021). The role of mucin and oligosaccharides via cross-feeding activities by *Bifidobacterium*: a review. *Int. J. Biol. Macromol.* 167, 1329–1337. doi: 10.1016/j.ijbiomac.2020.11.087

Matsuki, T., Watanabe, K., Fujimoto, J., Kado, Y., Takada, T., Matsumoto, K., et al. (2004). Quantitative PCR with 16S RNA-gene-targeted species-specific primers for analysis of human intestinal bifidobacteria. *Appl. Environ. Microbiol.* 70, 167–173. doi: 10.1128/AEM.70.1.167-173.2004

Milani, C., Duranti, S., Bottacini, F., Casey, E., Turroni, F., Mahony, J., et al. (2017). The first microbial colonizers of the human gut: composition, activities, and health implications of the infant gut microbiota. *Microbiol. Mol. Biol. Rev.* 81:e00036-17. doi: 10.1128/MMBR.00036-17

Morrin, S. T., and Hickey, R. M. (2020). New insights on the colonization of the human gut by health-promoting bacteria. *Appl. Microbiol. Biotechnol.* 104, 1511–1515. doi: 10.1007/s00253-019-10336-w

Nizet, V., Varki, A., and Aebi, M. (2017). Microbial lectins: Hemagglutinins, adhesins, and toxins. *Essentials of Glycobiology*. 3:37.

O'Connell Motherway, M., Houston, A., O'Callaghan, G., Reunanen, J., O'Brien, F., O'Driscoll, T., et al. (2019). A Bifidobacterial pilus-associated protein promotes colonic epithelial proliferation. *Mol. Microbiol.* 111, 287–301. doi: 10.1111/mmi.14155

O'Connell Motherway, M., Zomer, A., Leahy, S. C., Reunanen, J., Bottacini, F., Claesson, M. J., et al. (2011). Functional genome analysis of *Bifidobacterium breve* UCC2003 reveals type IVb tight adherence (tad) pili as an essential and conserved host-colonization factor. *Proc. Natl. Acad. Sci.* 108, 11217–11222. doi: 10.1073/pnas.1105380108

Paone, P., and Cani, P. D. (2020). Mucus barrier, mucins and gut microbiota: the expected slimy partners? *Gut* 69, 2232–2243. doi: 10.1136/gutjnl-2020-322260

Penno, C., Motherway, M. O., Fu, Y., Sharma, V., Crispie, F., Cotter, P. D., et al. (2022). Maximum depth sequencing reveals an on/off replication slippage switch and apparent *in vivo* selection for bifidobacterial pilus expression. *Sci. Rep.* 12:9576. doi: 10.1038/s41598-022-13668-2

Pokusaeva, K., Fitzgerald, G. F., and Van Sinderen, D. (2011). Carbohydrate metabolism in Bifidobacteria. *Genes Nutr.* 6, 285–306. doi: 10.1007/s12263-010-0206-6

Quigley, L., McCarthy, R., O'Sullivan, O., Beresford, T. P., Fitzgerald, G. F., Ross, R. P., et al. (2013). The microbial content of raw and pasteurized cow milk as determined by molecular approaches. *J. Dairy Sci.* 96, 4928–4937. doi: 10.3168/jds.2013-6688

Quinn, E. M., Slattery, H., Thompson, A. P., Kilcoyne, M., Joshi, L., and Hickey, R. M. (2018). Mining Milk for factors which increase the adherence of *Bifidobacterium longum* subsp. *infantis* to intestinal cells. *Foods* 7:196. doi: 10.3390/foods7120196

Schneider, H., Pelaseyed, T., Svensson, F., and Johansson, M. E. (2018). Study of mucin turnover in the small intestine by in vivo labeling. *Sci. Rep.* 8:5760. doi: 10.1038/s41598-018-24148-x

Shibahara-Sone, H., Gomi, A., Iino, T., Kano, M., Nonaka, C., Watanabe, O., et al. (2016). Living cells of probiotic *Bifidobacterium bifidum* YIT 10347 detected on gastric mucosa in humans. *Benef. Microbes* 7, 319–326. doi: 10.3920/BM2015.0138

Shkoporov, A. N., Khokhlova, E. V., Kafarskaia, L. I., Pavlov, K. A., Smeianov, V. V., Steele, J. L., et al. (2008). Search for protein adhesin gene in *Bifidobacterium longum* genome using surface phage display technology. *Bull. Exp. Biol. Med.* 146, 782–785. doi: 10.1007/s10517-009-0423-4

Sims, I. M., Frese, S. A., Walter, J., Loach, D., Wilson, M., Appleyard, K., et al. (2011). Structure and functions of exopolysaccharide produced by gut commensal *Lactobacillus reuteri* 100-23. *ISME J.* 5, 1115–1124. doi: 10.1038/ismej.2010.201

Taft, D. H., Lewis, Z. T., Nguyen, N., Ho, S., Masarweh, C., Dunne-Castagna, V., et al. (2022). *Bifidobacterium* species colonization in infancy: a global cross-sectional comparison by population history of breastfeeding. *Nutrients* 14:1423. doi: 10.3390/nu14071423

Tanaka, H., Hashiba, H., Kok, J., and Mierau, I. (2000). Bile salt hydrolase of *Bifidobacterium longum*—biochemical and genetic characterization. *Appl. Environ. Microbiol.* 66, 2502–2512. doi: 10.1128/AEM.66.6.2502-2512.2000

Turroni, F., Serafini, F., Foroni, E., Duranti, S., O'Connell Motherway, M., Taverniti, V., et al. (2013). Role of sortase-dependent pili of *Bifidobacterium bifidum* PRL2010 in modulating bacterium–host interactions. *Proc. Natl. Acad. Sci.* 110, 11151–11156. doi: 10.1073/pnas.1303897110

Tyanova, S., Temu, T., Sinitcyn, P., Carlson, A., Hein, M. Y., Geiger, T., et al. (2016). The Perseus computational platform for comprehensive analysis of (prote)omics data. *Nat. Methods* 13, 731–740. doi: 10.1038/nmeth.3901

Viljoen, A., Mignolet, J., Viela, F., Mathelié-Guinlet, M., and Dufrêne Yves, F. (2020). How microbes use force to control adhesion. *J. Bacteriol.* 202:e00125-20. doi: 10.1128/jb.00125-20

Walsh, C., Lane, J. A., Van Sinderen, D., and Hickey, R. M. (2022). Human milk oligosaccharide-sharing by a consortium of infant derived *Bifidobacterium* species. *Sci. Rep.* 12:4143. doi: 10.1038/s41598-022-07904-y

Walter, J., Chagnaud, P., Tannock, G. W., Loach, D. M., Dal Bello, F., Jenkinson, H. F., et al. (2005). A high-molecular-mass surface protein (Lsp) and methionine sulfoxide reductase B (MsrB) contribute to the ecological performance of *Lactobacillus reuteri* in the murine gut. *Appl. Environ. Microbiol.* 71, 979–986. doi: 10.1128/AEM.71.2.979-986.2005

Walter, J., Loach, D. M., Alqumber, M., Rockel, C., Hermann, C., Pfitzenmaier, M., et al. (2007). D-alanyl ester depletion of teichoic acids in *Lactobacillus reuteri* 100-23 results in impaired colonization of the mouse gastrointestinal tract. *Environ. Microbiol.* 9, 1750–1760. doi: 10.1111/j.1462-2920.2007.01292.x

Walter, J., Schwab, C., Loach, D. M., Gänzle, M. G., and Tannock, G. W. (2008). Glucosyltransferase A (GtfA) and inulosucrase (Inu) of *Lactobacillus reuteri* TMW1.106 contribute to cell aggregation, in vitro biofilm formation, and colonization of the mouse gastrointestinal tract. *Microbiology* 154, 72–80. doi: 10.1099/mic.0.2007/010637-0

Wei, X., Wang, S., Zhao, X., Wang, X., Li, H., Lin, W., et al. (2016). Proteomic profiling of *Bifidobacterium bifidum* S17 cultivated under in vitro conditions. *Front. Microbiol.* 7:97. doi: 10.3389/fmicb.2016.00097

Wei, X., Yan, X., Chen, X., Yang, Z., Li, H., Zou, D., et al. (2014). Proteomic analysis of the interaction of *Bifidobacterium longum* NCC2705 with the intestine cells Caco-2 and identification of plasminogen receptors. *J. Proteome* 108, 89–98. doi: 10.1016/j.jprot.2014.04.038

Westermann, C., Gleinser, M., Corr, S. C., and Riedel, C. U. (2016). A critical evaluation of bifidobacterial adhesion to the host tissue. *Front. Microbiol.* 7:1220. doi: 10.3389/fmicb.2016.01220

Whittaker, C. A., and Hynes, R. O. (2002). Distribution and evolution of von Willebrand/integrin A domains: widely dispersed domains with roles in cell adhesion and elsewhere. *Mol. Biol. Cell* 13, 3369–3387. doi: 10.1091/mbc.e02-05-0259

Wilson, C. M., Loach, D., Lawley, B., Bell, T., Sims, I. M., O'Toole, P. W., et al. (2014). *Lactobacillus reuteri* 100-23 modulates urea hydrolysis in the murine stomach. *Appl. Environ. Microbiol.* 80, 6104–6113. doi: 10.1128/AEM.01876-14

Wong, C. B., Iwabuchi, N., and Xiao, J. Z. (2019). Exploring the science behind *Bifidobacterium breve* M-16V in infant health. *Nutrients* 11:1724. doi: 10.3390/nu11081724

Xiao, L., Gong, C., Ding, Y., Ding, G., Xu, X., Deng, C., et al. (2019). Probiotics maintain intestinal secretory immunoglobulin A levels in healthy formula-fed infants: a randomised, double-blind, placebo-controlled study. *Benef. Microbes* 10, 729–739. doi: 10.3920/BM2019.0025

Xiao, Y., Zhai, Q., Zhang, H., Chen, W., and Hill, C. (2021). Gut colonization mechanisms of *Lactobacillus* and *Bifidobacterium*: an argument for personalized designs. *Annu. Rev. Food Sci. Technol.* 12, 213–233. doi: 10.1146/annurev-food-061120-014739

Zhang, G., Zhao, J., Wen, R., Zhu, X., Liu, L., and Li, C. (2020). 2′-Fucosyllactose promotes *Bifidobacterium bifidum* DNG6 adhesion to Caco-2 cells. *J. Dairy Sci.* 103, 9825–9834. doi: 10.3168/jds.2020-18773

Zhu, D., Sun, Y., Liu, F., Li, A., Yang, L., and Meng, X.-C. (2016). Identification of surface-associated proteins of *Bifidobacterium animalis* ssp. *lactis* KLDS 2.0603 by enzymatic shaving. *J. Dairy Sci.* 99, 5155–5172. doi: 10.3168/jds.2015-10581

frontiers | Frontiers in Microbiology

TYPE Original Research
PUBLISHED 11 January 2024
DOI 10.3389/fmicb.2023.1301727



OPEN ACCESS

EDITED BY
Karolina Skonieczna-Żydecka,
Pomeranian Medical University, Poland

REVIEWED BY
Lorenzo Nissen,
University of Bologna, Italy
Paripok Phitsuwan,
King Mongkut's University of Technology Thonburi, Thailand

*CORRESPONDENCE
Claire Davies
✉ Claire.Davies@abvista.com

RECEIVED 25 September 2023
ACCEPTED 20 December 2023
PUBLISHED 11 January 2024

CITATION
Davies C, González-Ortiz G, Rinttilä T, Apajalahti J, Alyassin M and Bedford MR (2024) Stimbiotic supplementation and xylose-rich carbohydrates modulate broiler's capacity to ferment fibre.
*Front. Microbiol.* 14:1301727.
doi: 10.3389/fmicb.2023.1301727



# Stimbiotic supplementation and xylose-rich carbohydrates modulate broiler's capacity to ferment fibre

Claire Davies[1]*, Gemma González-Ortiz[1], Teemu Rinttilä[1,2], Juha Apajalahti[1,2], Mohammad Alyassin[3] and Michael R. Bedford[1]

[1]AB Vista, Wiltshire, United Kingdom, [2]Alimetrics Research Ltd., Espoo, Finland, [3]School of Applied Sciences, University of Huddersfield, Huddersfield, United Kingdom

Stimbiotics are a new category of feed additives that can increase fibre fermentability by stimulating fibre-degrading microbiota in the gut. The aim of this study was to test, *ex vivo*, if the microbiota of broilers fed a stimbiotic are better able to ferment different xylose-rich substrates in an ileal and a caecal environment. The ileal and caecal contents from broiler chickens fed a stimbiotic or from a control group were used as an inoculum in the *ex vivo* fermentation experiment. Different xylose-rich substrates including monomeric xylose (XYL), XOS with DP 2 to 6 (XOS), short DP XOS of 2 to 3 (sDP-XOS), long DP XOS of 4 to 6 (lDP-XOS) and de-starched wheat bran (WB), were added to each ileal and caecal inoculum in fermentation vessels. Total gas, short-chain fatty acids (SCFA) production, bacterial quantification, and carbohydrate utilisation were monitored for 9h post-inoculation. No significant interactions were observed in any of the parameters measured in either the ileal or caecal contents ($p>0.05$). Stimbiotic ileal inocula resulted in higher total gas ($p<0.001$) and volatile fatty acid (VFA) ($p<0.001$) production, increased numbers of *Lactobacillus* spp. ($p<0.001$), and decreased numbers of *Enterococcus* spp. ($p<0.01$) after 9h regardless of the xylose-rich substrate added. Stimbiotic caecal inocula resulted in a higher ratio of VFA to branched-chain fatty acids (BCFAs) by up to +9% ($p<0.05$). Ileal microbiota were found to preferentially metabolise WB, while caecal microbiota favoured XOS substrates, particularly lDP-XOS. These results indicate that stimbiotics can promote the abundance of lactic acid bacteria involved in the establishment of fibre-degrading bacteria and VFA content in the gut, which could have beneficial effects on broiler performance. Further, ileal and caecal microbiota differ in their utilisation of different substrates which may impact the effectiveness of different stimbiotic products.

KEYWORDS

**fibre fermentation, xylooligosaccharide, degree of polymerisation, ileal microbiota, caecal microbiota, SCFA, *ex vivo***

# 1 Introduction

The poultry gut microbiome is a complex and dynamic community of microorganisms that plays a major role in the health and productivity of poultry. The gut microbiome is responsible for a number of important functions including fibre fermentation, production of essential nutrients and energy, inhibition of pathogen colonisation, and development of the host's immune system (Carrasco et al., 2019). In broiler chickens, microbiota can ferment fibre in the distal ileum and the caecum. The microbial communities in these two intestinal compartments are distinct. The ileal microbial community is simple, with lactobacilli making up 80–90% of the bacteria. The primary metabolite of lactobacilli, lactic acid, plays a major role in lowering the pH of the ileum and preventing colonisation by pH-sensitive pathogenic bacteria (Rinttilä and Apajalahti, 2013). Dietary nutrients and microbial metabolites that are not absorbed in the small intestine can reach the lower intestine and caecum where they serve as a substrate for a much denser and more diverse microbial population. The primary end products of microbial fermentation are short chain fatty acids (SCFAs), including lactic acid and volatile fatty acids (VFAs) such as acetate, propionate and butyrate. In addition to serving as an energy source for the host, SCFAs are involved in maintaining intestinal function.

One way to promote a functional gut microbiome is through dietary supplementation with stimbiotics. Stimbiotics are a relatively new class of non-digestible feed additives that promote dietary fibre utilisation by the commensal microbiota through a smooth transition process (González-Ortiz et al., 2019). In contrast to prebiotics, stimbiotics are added at such low doses, effective as low as 50 g/t (Morgan et al., 2023), that they contribute little to the production of SCFAs through direct fermentation but instead are thought to signal fibre-digesting bacterial species to become more active and increase the fermentation of fibre already present in the diet (Ribeiro et al., 2018). Studies have shown that xylo-oligosaccharides (XOS) act as stimbiotics by selectively stimulating the growth and activity of beneficial bacteria commonly found in the gut such as *Lactobacillus* spp. and *Bifidobacterium* spp. (Okazaki et al., 1990; Courtin et al., 2008; Wang et al., 2010). XOS has been linked to improved fibre digestion, higher SCFA concentration, and better gut health in poultry (Morgan et al., 2019, 2022; Šimić et al., 2023) and swine (Liu et al., 2018; González-Solé et al., 2022). However, the typical assumption is that microbial adaptation to XOS occurs mainly in the caecum while the ileum remains largely understudied.

Much remains unknown about the mode of action of stimbiotics. *In vivo* studies are often complicated by individual variation between birds and the challenge of measuring transient intermediate metabolites, which are rapidly taken up by the host. *Ex vivo* studies offer a more controlled process where live microbial communities can be transplanted from the gut into a culture vessel. This approach allows conditions to be regulated and matched to the target intestinal segment, whilst fermentation dynamics can be monitored in real-time without interference from epithelial absorptive processes (Bedford and Apajalahti, 2018; Apajalahti and Rinttilä, 2019). In the present study, an *ex vivo* system was used to investigate whether feeding a stimbiotic to broiler chickens can modulate the microbiome and improve its fibre fermentation capabilities when exposed to different xylose-rich carbohydrate substrates. In addition, the extent to which different XOS and xylose-based products were fermented by gut bacteria from the ileum and caecum was investigated. The study aimed to test the following hypotheses: (1) microbiota from stimbiotic-supplemented birds have a higher preference for XOS fermentation over monomeric xylose or wheat bran; (2) microbiota from stimbiotic-supplemented birds have higher activity overall; (3) microbiota from the ileum are more specialised to metabolise simple carbohydrates (e.g., xylose, XOS, short degree polymerisation XOS) while microbiota from the caecum are more capable of metabolising more complex carbohydrates (long degree polymerisation XOS and wheat bran).

# 2 Materials and methods

## 2.1 Xylose-rich carbohydrate substrates

The xylose-rich carbohydrate substrates used in this study include: (1) monomeric D-xylose purchased from Sigma-Aldrich (St. Louis, MO, United States) with a purity of ≥99% (XYL); (2) xylo-oligosaccharides with degree of polymerisation (DP) between 2 and 6 (XOS); (3) xylo-oligosaccharides with a higher proportion of short DP (sDP-XOS); (4) xylo-oligosaccharides with a higher proportion of long DP (lDP-XOS); and (5) de-starched wheat bran (WB). The DP compositions of the different XOS substrates are shown in Figure 1. The sugar compositions of all substrates are shown in Table 1.

XOS, sDP-XOS, and lDP-XOS were provided by the School of Applied of Science, Huddersfield University (UK). Twenty grams of a corncob-derived XOS at 35% of purity and a degree of polymerisation (DP) between 2 and 6, was placed in a conventional Soxhlet extraction thimble using absolute ethanol (Fisher, Loughborough, UK) as a solvent. The extraction was carried out for 72 h with 32 extraction cycles per hour. The extraction solution was collected and dried, then redissolved in water and labelled as sDP-XOS. The remaining XOS in the substrate was then extracted with an 80% ethanol solution. The extraction solution was centrifuged at 4000 rpm for 30 min, filtered, evaporated to remove all the ethanol and excess water, concentrated, and labelled as lDP-XOS. The original corncob-derived XOS product was purified with 80% ethanol, recovered following the same steps of lDP-XOS, and labelled as XOS. All three extracts, sDP-XOS, lDP-XOS, and XOS, were analysed using the HPAEC-PAD method described in previous work (Alyassin et al., 2020). The analysis showed that sDP-XOS contained 80% xylobiose (X2), 16% xylotriose (X3) and 2.5% xylotetraose (X4), lDP-XOS contained 35% X2, 31% X3, 29% X4 and 6% xylopentaose (X5), and XOS contained 47% X2, 22% X3, 22% X4, 7.5% X5 and 1.5% xylohexaose (X6) (Figure 1).

De-starched WB was prepared enzymatically from commercial untreated WB (Korpelan Mylly Oy, Finland). Briefly, WB was suspended in 1:10 (w/v) sodium phosphate – bicarbonate buffer (pH 7.0) and the suspension was vigorously shaken for 15 min. Then 50 µL of heat-stable α-amylase (Sigma-Aldrich, St. Louis, MO, USA) was added and the suspension was incubated at 60°C for 60 min und er constant stirring, after which the sample was equilibrated at 37°C. The second step of de-starching was performed by adding 50 µL of amyloglucosidase (Sigma-Aldrich, St. Louis, MO, USA) to the suspension and incubated at 37°C for 30 min under constant stirring. After cooling to room temperature, the de-starched wheat sample was centrifuged (10,000 × g, 20 min, +4°C) and washed twice with deionised water prior to freeze-drying of the WB pellet.

10.3389/fmicb.2023.1301727

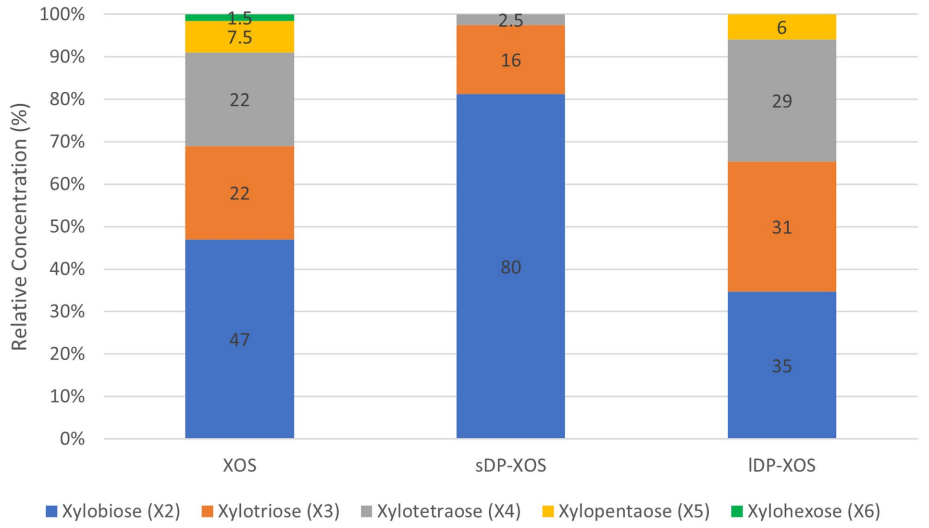


FIGURE 1
Relative concentration (%) of different length xylooligosaccharides in XOS substrates used in the study.

TABLE 1 Xylose-rich carbohydrate substrates used in the study.

| | Xylose | XOS | sDP-XOS | lDP-XOS | Wheat bran |
|---|---|---|---|---|---|
| Xylose | 5.00 | 2.55 | 3.56 | 5.05 | 0.20 |
| Arabinose | 0.00 | 0.29 | 0.54 | 0.31 | 0.11 |
| Mannose | 0.00 | 0.22 | 0.23 | 0.23 | 0.20 |
| Galactose | 0.00 | 0.29 | 0.28 | 0.40 | 0.19 |
| Glucose | 0.00 | 0.86 | 0.57 | 1.68 | 0.35 |

Sugar composition determined after acid hydrolysis (mg/mL).

## 2.2 *Ex vivo* incubation model

Ileum and caecum *ex vivo* fermentation experiments were conducted to mimic the luminal conditions of the ileum and caecum of broiler chickens. To prepare an authentic substrate medium for ileum fermentation, distal jejunal contents from 30 four-week-old Ross 308 broiler chickens fed a wheat-soya based diet without special additives (control birds) were collected, pooled, and homogenised. For the caecum fermentation, the substrate was prepared by combining distal ileal and caecal contents of the same birds. The jejunal and ileal/caecal digesta preparations were combined with an equal volume of pH 6.85 anaerobic buffer solution (0.02 M $K_2HPO_4$, 0.02 M $NH_4H_2PO_4$, 0.6 mmol $MgSO_4$) and centrifuged at 18,000 × g for 20 min to pellet the solids and bulk of bacteria. The pellet was discarded, and the clarified supernatants were used as the bacterial growth substrates in the *ex vivo* experiment.

The microbial inocula introduced for the respective ileum and caecum fermentation models comprised of fresh ileal or caecal digesta from four-week-old Ross 308 broilers fed either the wheat-soy-based control diet (Supplementary Table S1) or control diet amended with 100 g/t of stimbiotic product (Signis, AB Vista). No antibiotics, coccidiostats or other feed additives were included in these diets. Six control diet birds and six stimbiotic-fed birds were sacrificed. The intestinal contents were collected and maintained under anoxic conditions to retain viability of the bacteria until they were used for the inoculation of the simulation vessels (within 2 h of sacrificing the birds). The ileum simulation was initiated by adding 5.0 mL of the ileal substrate medium previously described, 50 mg of the xylose-rich carbohydrates, 0.1 g of ileal digesta inoculum of individual birds, and 5.0 mL of pH 6.85 buffer solution (20 mM $K_2HPO_4$, 20 mM $NH_4H_2PO_4$, 0.6 mM $MgSO_4$) to 20-ml serum bottles in an anaerobic chamber. The caecum simulation was initiated by adding 5.0 mL of the caecal substrate medium as previously described, 50 mg of the xylose-rich carbohydrates, 0.5 g of caecal digesta inoculum of individual birds and 5.0 mL of pH 6.85 buffer solution (20 mM $K_2HPO_4$, 20 mM $NH_4H_2PO_4$, 0.6 mM $MgSO_4$) to 20-ml serum bottles in an anaerobic chamber. To replicate genuine caecum conditions, the buffer was reduced to −340 mV with a mixture of NaS and cysteine.

Simulation vessels were sealed with thick butyl rubber stoppers, heated to 42°C, and continuously mixed in a gyratory shaker at 100 rpm. Each treatment was replicated in six vessels and the blank control was replicated in twelve vessels. These parallel vessels were considered biological replicates as the inocula were not pooled prior to introduction to simulation vessels. Instead, they were derived from individual birds fed either with the control or stimbiotic diet. The inoculation was done in a random order to avoid any potential systematic shifts or bias resulting from time of inoculation or freshness of the inoculum. The incubation of both the ileum and caecum simulations lasted for 9 h before the vessels were sampled for various analyses, as described below.

## 2.3 Sample analysis

### 2.3.1 Total gas production

Total gas production was measured in the simulation vessels at 3-h intervals by manually puncturing the rubber stopper with a needle that was connected to a high-precision glass syringe with a sensitive ground plunger and recording the volume of total gas released from the fermentation vessels.

TABLE 2 Real-time quantitative PCR assays used in the study.

| Target microorganism or group | Primer sequence (5′-3′) | Product size (bp) | Reference |
|---|---|---|---|
| Total eubacteria | F: TCCTACGGGAGGCAGCAGT | 466 | Nadkarni et al. (2002) |
| | R: GGACTACCAGGGTATCTAATCCTGTT | | |
| *Lactobacillus* spp. | F: AGCAGTAGGGAATCTTCCA | 341 | Rinttila et al. (2004) |
| | R: CACCGCTACACATGGAG | | |
| *Streptococcus* spp. | F: GGGGATAACTATTGGAAACGATA | 118 | Rinttilä et al. (2022) |
| | R: CCWACTAGCTAATACAACGCA | | |
| *Enterococcus* spp. | F: AYCAACCTGCCCTTCAGA | 147 | Unpublished |
| | R: GCRACTCGTTGTACTTCC | | |
| *Escherichia coli* | F: GGAGTAAAGTTAATACCTTTGCTC | 214 | Unpublished |
| | R: CCTCTACGAGACTCAAGCTT | | |
| *Lactobacillus salivarius* | F: TTTACTCTCTGTTAAAGAATGGCTTA | 146 | Unpublished |
| | R: GAGCTAAGGCCCCATAAGAA | | |
| *Lactobacillus crispatus* | F: CATGCAAGTCGAGCGAGC | 448 | Unpublished |
| | R: AATAAAGGCCAGTTACTACCTCTATC | | |
| *Lactobacillus reuteri* | F: TGGCCCAACTRATTGATGG | 188 | Unpublished |
| | R: CATCCCAGAGTGATAGCCA | | |

Amplification, standard, and melt curves for unpublished primers are provided in Supplementary Figure S1.

### 2.3.2 Fermentation end-products

Volatile fatty acids (VFA) and lactic acid were analysed as free acids in both the ileum and caecum simulation vessels after 9-h incubation using pivalic acid (Sigma-Aldrich, St. Louis, MO, United States) as an internal standard (Apajalahti et al., 2019). For this, 400 µL of sample and 2.4 mL of 1.0 mM pivalic acid solution were mixed, shaken vigorously for 5 min, and then centrifuged at 3000 × g for 10 min. Then, 800 µL of the supernatant was mixed with 400 µL of saturated oxalic acid solution, incubated at 4°C for 60 min, and then centrifuged at 18,000 × g for 10 min. The supernatant was analysed by gas chromatography (Agilent Technologies, Santa Clara, CA, USA) using a glass column packed with 80/120 Carbopack B-DA/4% Carbowax stationary phase, helium as the carrier gas, and a flame ionization detector. The quantified acids were acetic, propionic, butyric, valeric, isobutyric, 2-methylbutyric, isovaleric, and lactic acid.

### 2.3.3 Extraction of microbial DNA from ileum simulation samples

Subsamples from the ileum *ex vivo* experiment were collected for analysis of the abundance of different microbial species or genera using real-time quantitative PCR (qPCR). Microbial DNA was extracted from ileum simulation samples using the following protocol. First, 0.4 mL of each simulation sample was suspended in 1.6 mL of 50 mM phosphate-buffered saline with EDTA. Then, the suspension was shaken vigorously for 2 min. Next, the microcentrifuge tubes were centrifuged at 18,000 × g for 10 min to pellet the microbial cells. The pellet was resuspended in 600 µL of phosphate lysis buffer containing 100 mM Tris and 50 mM EDTA (pH 8.0). The suspension was transferred to a screw-cap microcentrifuge tube containing 20 µL of proteinase K (20 mg/mL; Roche Diagnostics GmbH, Mannheim, Germany) and 0.4 g of sterile glass beads (Scientific Industries Inc., Bohemia, NY, United States), and incubated at 65°C for 60 min with shaking for 30 s (1,400 rpm) at 10 min intervals. The microbial cells were disrupted by two 1 min rounds of bead beating (FastPrep-24™, MP Biomedicals, Irvine, CA, United States) at 6.5 m/s. Genomic DNA was then purified from the homogenates through phenol–chloroform–isoamyl alcohol (24:1) extraction with centrifugation at 10,000 × g for 10 min, followed by chloroform–isoamyl alcohol purification with centrifugation at 10,000 × g for 10 min. The DNA was precipitated by adding 0.6 volumes of 100% isopropanol and pelleted by centrifugation at 18,000 × g for 10 min. Finally, the DNA pellet was washed twice with 1 mL of ice-cold 70% ethanol, dried, and resuspended in 100 µL of Tris-EDTA buffer containing 10 mM Tris and 1.0 mM EDTA (pH 8.0) (AppliChem, Darmstadt, Germany).

### 2.3.4 qPCR analysis of ileal bacteria

The qPCR assays used in the study were selected based on prior knowledge of the consistently dominant bacteria found in the small intestines of broilers at Alimetrics Research experimental broiler facility. qPCR analyses were performed using an ABI Prism Sequence Detection System 7,500 instrument (Thermo Fisher Scientific Inc., Waltham, MA, United States). Amplifications were conducted in 15 µL volumes with SYBR Select Master Mix (Thermo Fisher Scientific Inc., Waltham, MA, USA), 0.25 µM of both primers, and 5 µL of 1:100 diluted template DNA or deionized sterile water as a no-template control. The rRNA gene-targeted primer sequences and PCR product sizes used for enumeration of the target microorganisms are listed in Table 2. Amplification, standard, and melt curves for unpublished primers are provided in Supplementary Figure S1. The qPCR assay development and optimization were conducted as described in Rinttilä et al. (2020). The thermal cycling conditions involved one cycle of preheating at 50°C for 2 min and an initial denaturation at 95°C for 10 min, followed by 40 cycles of denaturation at 95°C for 15 s and annealing and extension at the primer-specific annealing temperatures for 60s. To verify the specificity of amplifications based on the melting temperature of PCR products, a melt curve analysis was carried out alongside each qPCR

run. This involved slowly decreasing the temperature from 95 to 60°C, with fluorescence determination at 0.3°C intervals.

In each 96-well plate, synthetic small-subunit rRNA gene copies of the target microorganism (gBlocks® Gene Fragments, IDT, Coralville, IA, United States) were included in tenfold serial dilutions ranging from $1 \times 10^8$ to $1 \times 10^2$. The fractional cycle number at which the fluorescence passed the 0.3 fluorescence unit threshold was determined for the unknowns and compared with the standard curves. By accounting for the original volume of the starting material, elution volume, and PCR template dilution, the numbers of small subunit rRNA gene targets were determined per ml of ileum simulation sample. For data analysis, the rRNA gene copies/mL values were $\log_{10}$-transformed to achieve a normal distribution.

### 2.3.5 Carbohydrate analysis of ileal fermentation vessels and tested XOS products

For sugar analysis in the ileal simulation vessels after 9 h of incubation as well as xylose-rich test products, 0.5 g of sample was diluted in 4 mL of ice-cold water containing erythritol as an internal standard and vortexed for 5 min to extract soluble carbohydrates. Insoluble material was then spun down by centrifugation at 3,000 × g for 5 min. Two 200-ml aliquots were taken from the supernatant, one for the analysis of soluble monosaccharides (simple sugars) and the other for the analysis of total soluble carbohydrates.

For the determination of total soluble carbohydrates, the sample underwent acid hydrolysis by adding 200 mL of 2 moL/L $H_2SO_4$, sealing the vessel, and incubating at 100°C for 2 h. Subsequently, the hydrolysate was neutralised by adding 800 mL of 1 moL/L NaOH solution. The analysis of monosaccharides was performed on the original 200-ml sample without hydrolysis, but it was diluted with 1,000 mL of the $H_2SO_4$-NaOH solution to achieve the same ionic strength as the hydrolysed sample. 400 μL of the sample preparations were mixed with 800 mL of methanol to precipitate inorganic impurities, then 200 mL of the supernatant was evaporated to dryness. The monosaccharides in samples were converted to the corresponding oximes and derivatised with N,O-bis(trimethylsilyl)trifluoroacetamide as described by Zhang et al. (2018). Finally, the samples were analysed by gas chromatography mass spectroscopy (GC–MS) (Agilent 7,890-5975C GC-MSD equipped with a ZB-5 60 m × 250 mm × 0.25 mm column). Data was collected with a single ion mode and procedural calibration standards were used for quantification.

### 2.3.6 Statistical analysis

The statistical analyses were performed using JMP 16 Pro (SAS). A two-way analysis of variance evaluated the inoculum (Control vs. stimbiotic) and treatment (Control, XYL, XOS, sDP-XOS, lDP-XOS and WB) as main effects on gas production, SCFA, microbiota and disappearance of carbohydrates. The simulation vessel was considered a random effect. Means were separated by Student's t-test. Statements of significance were based on *p*-value of equal or less than 0.05.

# 3 Results

## 3.1 Total gas production

No interactions were observed for total gas production in either the ileum or the caecum and therefore, results of the main factors are shown in Figure 2. In general, in the ileal *ex vivo* simulation, gas was produced steadily over the 9 h fermentation period (Figure 2A). Ileal microbiota from stimbiotic birds produced more gas by the end of the 9 h incubation ($p < 0.001$) compared to the control, especially driven by the increased fermentation activity observed from 3 h to 6 h ($p < 0.05$) and 6 h to 9 h ($p < 0.05$). The different xylose-rich carbohydrate substrates did not influence gas production in the first 3 h of incubation (Figure 2C). Substrates, however, did influence the cumulative total gas production after the full 9 h incubation ($p < 0.001$). Ileal microbiota growing on WB were producing significantly ($p < 0.05$) more gas, followed by the unfractionated XOS and monomeric XYL, compared to the blank control treatment.

In the caecal *ex vivo* simulation, the greatest amount of gas was produced in the first 3 h of fermentation with longer periods of incubation resulting in a diminishing rate of gas production (Figure 2B). Caecal innocula from stimbiotic birds showed lower gas production in the first 3 h of incubation compared to innocula from control birds ($p < 0.001$). The different xylose-rich carbohydrate substrates significantly influenced gas production in all time ranges (Figure 2D) ($p < 0.001$). All vessels provided with a carbohydrate substrate, except for WB, produced significantly more gas than the blank control. The greatest amount of gas was produced by caecal microbiota exposed to XOS substrates, in particular the lDP-XOS, followed by sDP-XOS, XOS and monomeric XYL.

## 3.2 Fermentation end-products

No interactions were observed on the fermentation end-products after 9 h of incubation in the *ex vivo* experiment either with ileal or caecal innocula. The main effects are presented in Table 3. In the ileal simulation, supplementing diets with the stimbiotic resulted in higher VFA concentrations ($p < 0.0001$), but no differences were observed in the lactic acid concentration or the ratio between lactic acid and acetic acid ($p > 0.05$). All the xylose-rich substrates resulted in greater production of VFAs compared to the blank control ($p < 0.001$), but there was no significant difference between them. Lactic acid levels were highest when the ileal digesta was exposed to WB.

In the caecal simulation, the stimbiotic inoculum resulted in lower VFA concentrations ($p < 0.01$), higher lactic acid levels ($p < 0.05$), a higher lactic acid to acetic acid ratio ($p < 0.05$), and a higher VFA to BCFA ratio ($p < 0.05$). Substrates also influenced VFA ($p < 0.001$), lactic acid ($p < 0.001$) and the ratios of lactic acid to acetic acid ($p = 0.001$) and VFA to BCFA ($p < 0.001$). WB appeared to be a poor fermentation substrate for caecal microbes showing VFA concentrations similar to the control. In contrast, XYL > lDP-XOS > sDP-XOS > XOS presented higher VFA concentrations compared to WB and the control. lDP-XOS showed the highest caecal lactic acid concentration and lactic acid to acetic acid ratio compared to all the other substrates. Both XOS fractions, sDP-XOS and lDP-XOS, presented the highest VFA to BCFA ratio followed by the original XOS and monomeric XYL. WB did not influence the VFA to BCFA ratio compared to control ($p > 0.05$).

## 3.3 Ileal bacteria

No interactions or substrate effects were observed on microbiota after 9 h of incubation in the *ex vivo* assay with ileal digesta (Table 4).

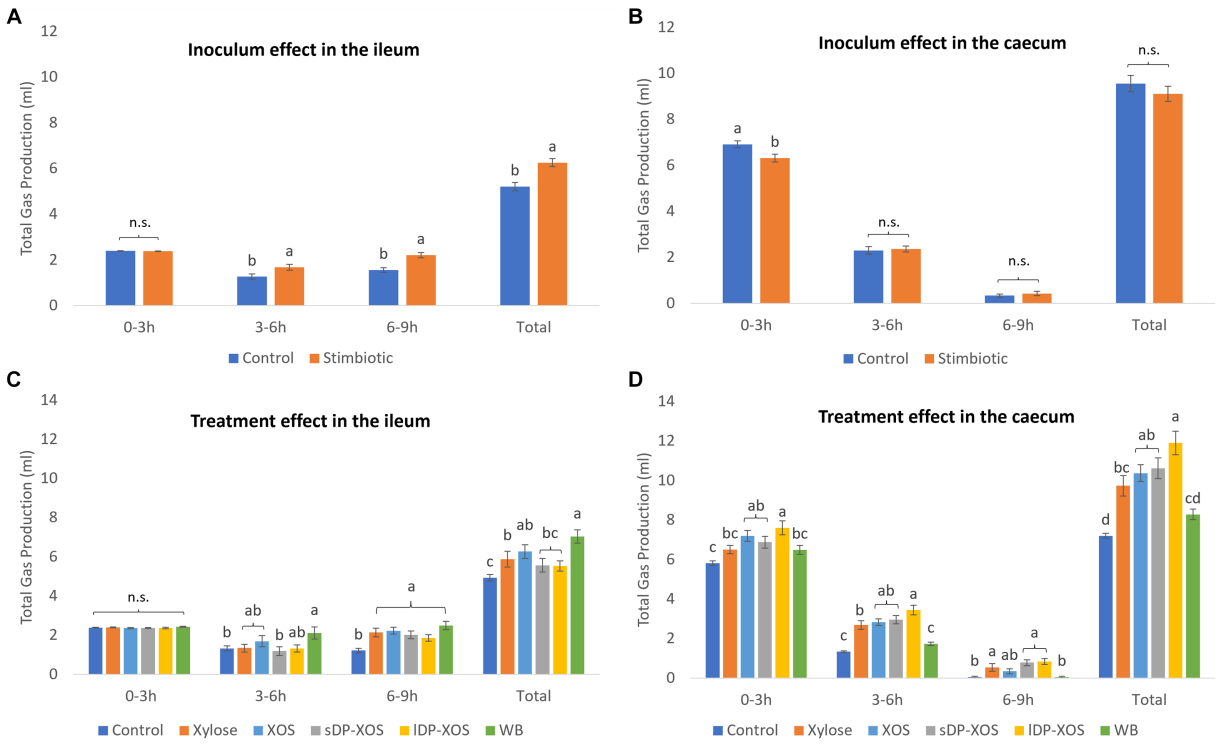


FIGURE 2
Gas produced (ml) during *ex vivo* fermentation ($n = 6$ for each treatment, n = 12 for the blank control). Inoculum effect on gas production in the ileum **(A)** and caecum **(B)**. Treatment effect on gas production in the ileum **(C)** and caecum **(D)**. Columns are grouped into different lengths of fermentation in hours. Significant differences ($p < 0.05$) within each time period are shown as different letters above each column. Bars indicate standard error of the mean.

Ileal inoculum from stimbiotic birds showed higher counts of total eubacteria ($p < 0.001$), *Escherichia coli* ($p < 0.001$), *Lactobacillus* spp. ($p < 0.001$), *L. salivarius* ($p < 0.001$) and *L. crispatus* ($p < 0.001$). Lower *Enterococcus* spp. counts were observed in stimbiotic inocula after 9 h of incubation ($p < 0.01$). *Streptococcus* spp. and *L. reuteri* were not influenced by inoculum ($p > 0.05$).

## 3.4 Carbohydrates

To evaluate the effect of the stimbiotic on the ability of the ileal microbial community to degrade the different xylose-rich carbohydrate substrates, the total carbohydrate content from the inoculum and substrates was measured before and after 9 h of incubation. The percentage loss of the different sugars are presented in Table 5. No interactions were observed. The inoculum from the stimbiotic-supplemented birds did not influence the loss of xylose, arabinose, mannose and glucose over the 9 h of the *ex vivo* experiment, however 2% more galactose disappeared compared to control inoculum ($p < 0.05$). The type of substrate had a more significant impact on the utilisation of sugars. Monomeric XYL and all XOS substrates decreased the utilisation of xylose compared to the control ($p < 0.05$), while no differences were observed between control and WB. Ileal arabinose disappearance was higher with all the substrates compared to the control, with sDP-XOS presenting the highest value, followed by XOS, lDP-XOS and WB, and XYL. XYL as a substrate did not influence mannose fermentation, in contrast all sources of XOS and WB increased its utilisation. Although substrate influenced the fermentation of galactose ($p = 0.002$), none of the products differed significantly from the control. No differences were observed in glucose disappearance with XYL, XOS, or sDP-XOS compared to the control, but lDP-XOS showed lower utilisation rate while WB clearly had higher utilisation.

# 4 Discussion

The aim of the current study was to investigate the reaction of the ileal and caecal microbiota from control or stimbiotic-supplemented birds when exposed to different xylose-rich carbohydrate substrates in an *ex vivo* experiment by measuring total gas production, fermentation end-products, bacterial counts, and loss of carbohydrates after 9 h of incubation. No interactions were observed in any of the parameters measured suggesting that the response of the bacterial communities to the different substrates provided was independent of the stimbiotic treatment for both intestinal compartments. Thus, the first hypothesis provided in this study was not confirmed. There may be several reasons for the lack of interactive effects. Firstly, bird age can have a significant effect on microbiota composition (Gong et al., 2008). In young birds, the gut microbiome is less well developed and more likely to be influenced by dietary changes, whereas older birds can efficiently utilise intransigent nutrients like dietary fibre (Lee et al., 2017; Craig et al., 2020). At 4 weeks old, the birds in this study should have had time to

10.3389/fmicb.2023.1301727

TABLE 3 Interactive effects of inoculum and substrate on fermentation end-products after 9 h of incubation in the *ex vivo* assay with ileal and caecal digesta.

| | | | VFA | Lactic acid | Lactic:Acetic | VFA:BCFA |
|---|---|---|---|---|---|---|
| Ileum | | | | | | |
| Inoculum | | | | | | |
| | | Control | 8.8 ± 1.14$^{b}$ | 22.4 ± 5.40 | 2.7 ± 0.93 | ND |
| | | Stimbiotic | 9.9 ± 1.14$^{a}$ | 22.9 ± 5.40 | 2.4 ± 0.93 | ND |
| Treatment | | | | | | |
| | | Control | 7.9 ± 1.11$^{b}$ | 20.2 ± 5.22$^{b}$ | 2.7 ± 0.90 | ND |
| | | Xylose | 10.0 ± 1.11$^{a}$ | 19.5 ± 5.22$^{b}$ | 2.0 ± 0.90 | ND |
| | | XOS | 9.4 ± 1.11$^{a}$ | 21.8 ± 5.22$^{b}$ | 2.4 ± 0.90 | ND |
| | | sDP XOS | 10.2 ± 1.11$^{a}$ | 24.3 ± 5.22$^{ab}$ | 2.5 ± 0.90 | ND |
| | | lDP XOS | 9.2 ± 1.11$^{a}$ | 21.8 ± 5.22$^{b}$ | 2.5 ± 0.90 | ND |
| | | Wheat bran | 9.6 ± 1.11$^{a}$ | 28.5 ± 5.22$^{a}$ | 3.1 ± 0.90 | ND |
| *p*-Value | | | | | | |
| | | Inoculum | <0.001 | 0.644 | 0.160 | – |
| | | Treatment | <0.001 | <0.001 | 0.089 | – |
| | | Interaction | 0.930 | 0.936 | 0.993 | – |
| Caecum | | | | | | |
| Inoculum | | | | | | |
| | | Control | 60.3 ± 5.30$^{a}$ | 2.0 ± 3.24$^{b}$ | 0.04 ± 0.08$^{b}$ | 143 ± 28$^{b}$ |
| | | Stimbiotic | 56.5 ± 5.30$^{b}$ | 3.6 ± 3.24$^{a}$ | 0.09 ± 0.08$^{a}$ | 156 ± 28$^{a}$ |
| Treatment | | | | | | |
| | | Control | 44.8 ± 5.12$^{d}$ | 1.2 ± 3.13$^{b}$ | 0.04 ± 0.08$^{b}$ | 70 ± 27$^{c}$ |
| | | Xylose | 68.3 ± 5.13$^{a}$ | 1.7 ± 3.13$^{b}$ | 0.03 ± 0.08$^{b}$ | 158 ± 27$^{b}$ |
| | | XOS | 60.5 ± 5.12$^{b}$ | 2.3 ± 3.13$^{b}$ | 0.06 ± 0.08$^{ab}$ | 183 ± 27$^{ab}$ |
| | | sDP XOS | 62.9 ± 5.12$^{ab}$ | 3.8 ± 3.13$^{ab}$ | 0.09 ± 0.08$^{ab}$ | 209 ± 27$^{a}$ |
| | | lDP XOS | 63.6 ± 5.12$^{ab}$ | 7.1 ± 3.13$^{a}$ | 0.15 ± 0.08$^{a}$ | 201 ± 27$^{a}$ |
| | | Wheat bran | 50.6 ± 5.12$^{c}$ | 0.8 ± 3.13$^{b}$ | 0.02 ± 0.08$^{b}$ | 74 ± 27$^{c}$ |
| *p*-value | | | | | | |
| | | Inoculum | 0.002 | 0.027 | 0.020 | 0.034 |
| | | Treatment | <0.001 | <0.001 | 0.001 | <0.001 |
| | | Interaction | 0.702 | 0.823 | 0.865 | 0.966 |

The values are reported in mmol/L as the mean ± standard deviation of 6 replicates for each substrate treatment and 12 replicates for the blank control. VFAs, volatile fatty acids; BCFA, branched-chain fatty acids. $^{a-c}$Means with a different superscript letter differ ($p < 0.05$). ND, non-detected.

develop a robust gut microbiome which may influence the response in the *ex vivo* experiment. Secondly, caecal emptying occurs several times a day in chickens. A recently emptied caecum can have a very different microbial composition to one that is full (Richards et al., 2019). Therefore, the timing of when inocula are taken adds another source of variation on top of the individual variation between birds. Thirdly, the concentration of the xylose-rich substrates used in the vessels was above the doses normally used *in vivo*. This may have led to saturation in the assay. Morgan et al. (2022) also observed that stimulating fibre-degrading bacteria with high levels of XOS in diets with little fermentable arabinoxylan can result in detrimental effects on the microbial balance and a proliferation of pathogenic bacteria species which outcompete the beneficial bacteria. Although no interactions were observed, the main effects are discussed in the next sections.

## 4.1 Effects of stimbiotic on the ileal and caecal microbial activity

This study found evidence that feeding broiler chickens a stimbiotic can modulate the microbiome and improve its fibre fermenting capabilities, however there were clear differences between the ileal and caecal microbial responses.

The stimbiotic effect stipulates that small doses of dietary additives can stimulate a fibre-degrading microbiome to increase fibre fermentability (González-Ortiz et al., 2019). In the literature, supplemental XOS doses range from as low as 2 g/t to 20,000 g/t, 50 g/t being the most tested dose across different studies showing positive effects (Morgan et al., 2023). The present study found evidence for this effect in the ileum where microbiota derived from birds fed a stimbiotic were significantly more active as demonstrated by higher

TABLE 4 Interactive effects of inoculum and substrate on microbiota after 9 h of incubation in the *ex vivo* assay with ileal digesta.

| | | Total eubacteria | *Streptococcus* spp | *Enterococcus* spp | *Escherichia coli* | *Lactobacillus* spp | *L. salivarius* | *L. reuteri* | *L. crispatus* |
|---|---|---|---|---|---|---|---|---|---|
| Inoculum | | | | | | | | | |
| | Control | 9.63 ± 0.21$^{b}$ | 8.39 ± 0.51 | 8.59 ± 0.25$^{a}$ | 9.10 ± 0.17$^{b}$ | 8.65 ± 0.47$^{b}$ | 6.43 ± 0.70$^{b}$ | 8.06 ± 0.63 | 8.61 ± 0.40$^{b}$ |
| | Stimbiotic | 9.90 ± 0.22$^{a}$ | 8.51 ± 0.51 | 8.43 ± 0.25$^{b}$ | 9.36 ± 0.18$^{a}$ | 9.23 ± 0.48$^{a}$ | 7.65 ± 0.71$^{a}$ | 8.06 ± 0.64 | 8.95 ± 0.40$^{a}$ |
| Treatment | | | | | | | | | |
| | Control | 9.73 ± 0.22 | 8.39 ± 0.51 | 8.48 ± 0.25 | 9.17 ± 0.17 | 8.91 ± 0.47 | 7.02 ± 0.71 | 7.97 ± 0.63 | 8.66 ± 0.40 |
| | Xylose | 9.84 ± 0.21 | 8.52 ± 0.49 | 8.53 ± 0.24 | 9.31 ± 0.17 | 8.85 ± 0.45 | 7.12 ± 0.68 | 7.96 ± 0.60 | 8.66 ± 0.38 |
| | XOS | 9.74 ± 0.21 | 8.30 ± 0.49 | 8.47 ± 0.24 | 9.16 ± 0.17 | 8.89 ± 0.45 | 6.88 ± 0.68 | 8.16 ± 0.60 | 8.81 ± 0.38 |
| | sDP XOS | 9.63 ± 0.21 | 8.42 ± 0.49 | 8.44 ± 0.24 | 9.15 ± 0.17 | 8.83 ± 0.45 | 6.78 ± 0.68 | 7.93 ± 0.61 | 8.77 ± 0.38 |
| | lDP XOS | 9.74 ± 0.21 | 8.42 ± 0.50 | 8.54 ± 0.24 | 9.26 ± 0.17 | 8.93 ± 0.46 | 7.07 ± 0.69 | 7.95 ± 0.62 | 8.74 ± 0.39 |
| | Wheat bran | 9.89 ± 0.21 | 8.65 ± 0.49 | 8.60 ± 0.24 | 9.30 ± 0.17 | 9.23 ± 0.45 | 7.39 ± 0.68 | 8.38 ± 0.61 | 9.03 ± 0.39 |
| *p*-value | | | | | | | | | |
| | Inoculum | <0.001 | 0.301 | 0.006 | <0.001 | <0.001 | <0.001 | 0.979 | <0.001 |
| | Treatment | 0.083 | 0.659 | 0.667 | 0.053 | 0.376 | 0.421 | 0.478 | 0.217 |
| | Interaction | 0.436 | 0.961 | 0.814 | 0.673 | 0.657 | 0.914 | 0.863 | 0.641 |

The values are reported as the mean ± standard deviation in log10 gene copies/ml produced as the mean of 6 replicates for each substrate treatment and 12 replicates for the blank control. $^{a\text{-}b}$Means with a different superscript letter differ ($p < 0.05$).

TABLE 5 Interactive effects of inoculum and substrate on disappeared total soluble sugars after 9 h of incubation in the *ex vivo* assay with ileal digesta.

| | | Xylose | Arabinose | Mannose | Galactose | Glucose |
|---|---|---|---|---|---|---|
| Inoculum | | | | | | |
| | Control | 34.3 ± 4.33 | 49.8 ± 2.37 | 47.0 ± 1.48 | 56.3 ± 2.74 $^{b}$ | 79.1 ± 1.11 |
| | Stimbiotic | 34.2 ± 4.33 | 48.8 ± 2.37 | 46.5 ± 1.48 | 58.2 ± 2.74 $^{a}$ | 80.5 ± 1.11 |
| Treatment | | | | | | |
| | Control | 45.1 ± 4.18$^{a}$ | 43.6 ± 2.29$^{d}$ | 35.5 ± 1.44$^{c}$ | 57.3 ± 2.65$^{ab}$ | 80.2 ± 1.07$^{b}$ |
| | Xylose | 21.3 ± 4.18$^{c}$ | 47.3 ± 2.29$^{c}$ | 36.4 ± 1.44$^{c}$ | 56.2 ± 2.65$^{b}$ | 79.7 ± 1.07$^{b}$ |
| | XOS | 32.5 ± 4.18$^{b}$ | 52.1 ± 2.29$^{b}$ | 52.7 ± 1.44$^{a}$ | 57.9 ± 2.65$^{ab}$ | 79.6 ± 1.07$^{b}$ |
| | sDP XOS | 32.5 ± 4.18$^{b}$ | 55.6 ± 2.29$^{a}$ | 53.3 ± 1.44$^{a}$ | 57.0 ± 2.65$^{ab}$ | 80.2 ± 1.07$^{b}$ |
| | lDP XOS | 25.4 ± 4.18$^{c}$ | 48.6 ± 2.29$^{c}$ | 50.6 ± 1.44$^{b}$ | 55.2 ± 2.65$^{b}$ | 74.2 ± 1.07$^{c}$ |
| | Wheat bran | 48.6 ± 4.18$^{a}$ | 48.6 ± 2.29$^{c}$ | 51.9 ± 1.44$^{ab}$ | 59.8 ± 2.65$^{a}$ | 82.0 ± 1.07$^{a}$ |
| *p*-value | | | | | | |
| | Inoculum | 0.903 | 0.074 | 0.111 | 0.002 | 0.126 |
| | Treatment | <0.001 | <0.001 | <0.001 | 0.002 | <0.001 |
| | Interaction | 0.645 | 0.980 | 0.681 | 0.984 | 0.782 |

The values reported are the mean % ± standard deviation of total soluble sugars loss of 6 replicates for each substrate treatment and 12 replicates for the blank control. $^{a\text{-}d}$Means with a different superscript letter differ ($p < 0.05$).

gas production, higher VFA concentrations, higher abundances of total eubacteria driven primarily by *Lactobacillus* spp., and greater utilisation of galactose. Thus, the second hypothesis in this study was supported. The stimbiotic in this study was a combination of xylanase and XOS. Both products have been demonstrated to positively influence cumulative bird performance through enhanced non-starch polysaccharide utilisation resulting in the proliferation of beneficial bacteria and SCFA production (González-Ortiz et al., 2021; Morgan et al., 2021; Singh et al., 2021). These effects are also supported by a recent holistic evaluation, which has identified that supplementing XOS into broiler diets reduces bird mortality and improves FCR (Morgan et al., 2023).

The ileal microbial community is mainly comprised of lactic acid producing bacteria (Rinttilä and Apajalahti, 2013). After 9 h of incubation in the *ex vivo* model, the lactic acid producing bacterial species *L. salivarius* and *L. crispatus* were both more abundant in the stimbiotic treatments. This is consistent with previous studies on swine where supplementation with XOS results in higher lactobacilli abundance in ileal, caecal, and faecal samples (Liu et al., 2018; Pan et al., 2019; Chen et al., 2021). In one *ex vivo* study, Moura et al. (2008) showed that when ileal inocula from piglets were provided with a XOS substrate, bifidobacteria and lactobacilli replication was enhanced. The primary metabolite of lactobacilli is lactic acid. Lactic acid plays

a major role in lowing the pH of the ileum and preventing colonization by pH-sensitive pathogenic bacteria (Pan et al., 2019). This was demonstrated in the current study by the lower abundance of *Enterococcus* spp. in stimbiotic treatments. Despite higher lactobacilli abundance in stimbiotic treatments, this study found no significant increase in lactic acid in the ileum fermentation model. This could be because lactic acid is an intermediary product that can be further metabolized into VFAs such as acetate, propionate and butyrate by other common intestinal microbes. This type of cross-feeding between bacteria has been observed *in vitro* by De Maesschalck et al. (2015) where lactic acid produced by *L. crispatus* during XOS fermentation was utilised by the butyrate-producing species *Anaerostipes butyraticus*. This explanation is consistent with the observation that although lactic acid concentration was unchanged, there were overall significantly higher concentrations of VFAs in stimbiotic treatments.

Xylanases are typically associated with the hydrolysis of arabinoxylans, however increased levels of fructose and galactose have also been observed *in vivo* after the addition of xylanase (Craig et al., 2020). Galactose likely originates from galactooligosaccharides or galactans which are found in soybean meal, a common protein source in poultry feed. The increased fermentation of galactose in stimbiotic treatments observed in this study could be due to the *in situ* release of galactose through xylanase action.

Caecal microbiota from stimbiotic-supplemented birds were less active in terms of gas and VFA production. Gas production was highest in the first 3 h of fermentation and then the rate of production declined, which may suggest a limiting resource that has been exhausted more rapidly by the stimbiotic effect. However, it is interesting to highlight the higher lactic acid concentrations, higher lactic acid:acetic acid ratio, and higher VFA:BCFA ratio promoted with the stimbiotic caecal inoculum. The increased lactic acid concentrations and higher lactic acid:acetic acid ratio may indicate the promotion of homofermentive lactic acid producing bacterial species over heterofermenters in the caecum by the stimbiotic treatment. The higher VFA:BCFA ratio (up to 9%) promoted with the stimbiotic demonstrates how the stimbiotic effect can reduce protein fermentation by providing caecal bacteria with carbohydrates, which are preferentially fermented over proteins (Xu et al., 2002; Sanchez et al., 2009). This can be beneficial for the host since increased caecal BCFA production may imply the concomitant production of toxic fermentation products such as ammonia and biogenic amines, which can inhibit growth and cause disease (Apajalahti and Vienola, 2016). Similar reduction of lower intestinal protein fermentation has been observed in piglets supplemented with the stimbiotic (Cho et al., 2020), and broiler chickens supplemented with a xylanase (Lee et al., 2017).

## 4.2 Effects of xylose-rich carbohydrate substrates on the ileal and caecal microbial activity

When comparing the different xylose-rich carbohydrate substrates, ileal microbiota showed a distinct preference for WB, which is observed by the greatest gas production and highest lactic acid concentrations. Previous *in vitro* studies using faecal inocula have similarly found that the amount of gas produced by microbiota varies depending on the substrate it is fermenting (Tao et al., 2019). Typically, longer chain oligosaccharides and more complex polysaccharides are less readily fermented and produce less gas (Moura et al., 2008; Hernot et al., 2009; Kaur et al., 2011). However, this study found no evidence in the gas production, fermentation end-products, or bacterial community, that shorter oligosaccharides are more readily fermented by ileal microbiota than longer ones. Thus, the third hypothesis in this study was not confirmed. It is possible that despite being the most complex substrate, wheat bran was preferred due to its sugar composition. Wheat bran had the lowest xylose content of the substrates used in this study and had proportionally higher glucose content. Across all treatments, glucose was the most fermented sugar (74–82% loss), while xylose was the least fermented (21–48% loss), suggesting a microbial preference for glucose. In addition, some studies have shown that the availability of glucose can delay the utilisation of lactic acid by lactic acid utilising bacteria resulting in lactic-acid accumulation (Duncan et al., 2004).

In contrast to the ileal results, wheat bran appeared to be a poor fermentation substrate for caecal microbiota. Wheat bran had the lowest gas production of all the substrates and was indistinguishable from the blank control in terms of statistical significance. However, all XOS-derived substrates promoted caecal microbial activity. In particular, lDP-XOS had the highest gas production, lactic acid concentration, and lactic to acetic acid ratio. Bacteria species vary significantly in their ability to use XOS of differing chain lengths depending on their ability to produce extra-and intracellular hydrolytic enzymes, as well as mono-and oligosaccharide transporters involved in carbohydrate metabolism (Rastall et al., 2022). This can make it difficult to predict how the diverse caecal microbiome will respond to XOS of different lengths. Wang et al. (2010) observed that *Bifidobacterium adolescentis* utilised DP3 and DP2 more rapidly than monosaccharides or DP4-7, while Dale et al. (2020) found evidence that caecal bacteria in broilers completely utilised DP4, but DP3 and DP2 were not fully utilised. The preference for higher DP XOS seen in this study suggests that longer chain oligosaccharides may be promising candidates for future products that can reach and be fermented in distal sections of the intestinal tract.

# 5. Conclusion

The *ex vivo* approach is a valuable tool for studying the impact of feed additives on microbial communities. The functional response of entire intestinal microbial communities can be studied in a more controlled way than in a live host environment. This study indicates that supplementing broiler diets with a stimbiotic promotes the abundance of lactic acid producing bacteria and SCFA content in the gut which could have beneficial effects on broiler performance. Ileal bacteria favoured glucose-rich wheat bran over XOS substrates, while caecal bacteria appeared to favour long-chain xylooligosaccharides. Against predictions, there was no indication that microbiota from stimbiotic birds were primed to favour XOS substrates when compared to microbiota from control birds. This study highlights some of the mechanisms by which stimbiotics can potentially impact broiler performance through microbiome modulation and demonstrates a methodology to identify promising future stimbiotic candidates.

## Data availability statement

The raw data supporting the conclusions of this article will be made available by the authors, without undue reservation.

## Author contributions

CD: Writing – original draft, Data curation, Formal analysis, Funding acquisition, Investigation, Methodology, Project administration, Resources, Supervision, Validation, Visualization. GG-O: Conceptualization, Data curation, Formal analysis, Funding acquisition, Investigation, Methodology, Project administration, Resources, Supervision, Validation, Visualization, Writing – original draft. TR: Conceptualization, Data curation, Formal analysis, Funding acquisition, Investigation, Methodology, Project administration, Resources, Supervision, Validation, Visualization, Writing – original draft. JA: Methodology, Conceptualization, Data curation, Funding acquisition, Investigation, Project administration, Supervision, Validation, Writing – review & editing. MA: Methodology, Resources, Writing – original draft. MB: Conceptualization, Data curation, Funding acquisition, Investigation, Methodology, Project administration, Resources, Supervision, Validation, Writing – review & editing.

## Ethics statement

The animal study was approved by The Regional Administrative Agency of Southern Finland (ESAVI). The study was conducted in accordance with the local legislation and institutional requirements.

## Funding

The author(s) declare that no financial support was received for the research, authorship, and/or publication of this article.

## Conflict of interest

CD, GG-O, TR, JA, and MB were employed by AB Vista. TR and JA were employed by Alimetrics Research Ltd.

The remaining author declares that the research was conducted in the absence of any commercial or financial relationships that could be construed as a potential conflict of interest.

## Publisher's note

All claims expressed in this article are solely those of the authors and do not necessarily represent those of their affiliated organizations, or those of the publisher, the editors and the reviewers. Any product that may be evaluated in this article, or claim that may be made by its manufacturer, is not guaranteed or endorsed by the publisher.

## Supplementary material

The Supplementary material for this article can be found online at: https://www.frontiersin.org/articles/10.3389/fmicb.2023.1301727/full#supplementary-material

## References

Alyassin, M., et al. (2020). 'Simultaneous determination of cereal monosaccharides, xylo- and arabinoxylo-oligosaccharides and uronic acids using HPAEC-PAD', *Food Chemistry*, 315, 126221. doi: 10.1016/j.foodchem.2020.126221

Apajalahti, J., and Rinttilä, T. (2019). 'Assessing the complex ecology of intestinal microbiome', in González-Ortiz, G., Bedford, M. R., Bach Knudsen, K. E., Courtin, C. M., and Classen, H. L. (eds) *The value of fibre – Engaging the second brain for animal nutrition*. The Netherlands: Wageningen Academic Publishers, pp. 279–296.

Apajalahti, J., and Vienola, K. (2016). Interaction between chicken intestinal microbiota and protein digestion. *Anim. Feed Sci. Technol.* 221, 323–330. doi: 10.1016/j.anifeedsci.2016.05.004

Apajalahti, J., Vienola, K., Raatikainen, K., Holder, V., and Moran, C. A. (2019). Conversion of branched-chain amino acids to corresponding isoacids-an in vitro tool for estimating ruminal protein degradability. *Front. Vet. Sci.* 6:311. doi: 10.3389/fvets.2019.00311

Bedford, M. R., and Apajalahti, J. (2018). "Exposure of a broiler to a xylanase for 35d increases the capacity of cecal microbiome to ferment soluble xylan" in *Poultry science association 107th annual meeting*. Oxford University Press, 98–99. Available at: www.poultryscience.org

Carrasco, J. M. D., Casanova, N. A., and Miyakawa, M. E. F. (2019). Microbiota, gut health and chicken productivity: what is the connection? *Microorganisms*. Wageningen Academic Publishers, 7, 1–15. doi: 10.3390/microorganisms7100374

Chen, Y., Xie, Y., Zhong, R., Liu, L., Lin, C., Xiao, L., et al. (2021). Effects of Xylo-oligosaccharides on growth and gut microbiota as potential replacements for antibiotic in weaning piglets. *Front. Microbiol.* 12, 1–12. doi: 10.3389/fmicb.2021.641172

Cho, H. M., González-Ortiz, G., Melo-Durán, D., Heo, J. M., Cordero, G., Bedford, M. R., et al. (2020). Stimbiotic supplementation improved performance and reduced inflammatory response via stimulating fiber fermenting microbiome in weaner pigs housed in a poor sanitary environment and fed an antibiotic-free low zinc oxide diet. *Plos One* 15, e0240264–e0240221. doi: 10.1371/journal.pone.0240264

Courtin, C. M., Swennen, K., Broekaert, W. F., Swennen, Q., Buyse, J., Decuypere, E., et al. (2008). Effects of dietary inclusion of xylooligo-saccharides, arabinoxylooligosaccha-rides and soluble arabinoxylan on the microbial composition of caecal contents of chickens. *J. Sci. Food Agric.* 88, 2517–2522. doi: 10.1002/jsfa.3373

Craig, A. D., Khattak, F., Hastie, P., Bedford, M. R., and Olukosi, O. A. (2020). Xylanase and xylo-oligosaccharide prebiotic improve the growth performance and concentration of potentially prebiotic oligosaccharides in the ileum of broiler chickens. *Br. Poult. Sci.* 61, 70–78. doi: 10.1080/00071668.2019.1673318

Dale, T., Hannay, I., Bedford, M. R., Tucker, G. A., Brameld, J. M., and Parr, T. (2020). The effects of exogenous xylanase supplementation on the in vivo generation of xylooligosaccharides and monosaccharides in broilers fed a wheat-based diet. *Br. Poult. Sci.* 61, 471–481. doi: 10.1080/00071668.2020.1751805

De Maesschalck, C., Eeckhaut, V., Maertens, L., De Lange, L., Marchal, L., Nezer, C., et al. (2015). Effects of Xylo-oligosaccharides on broiler chicken performance and microbiota. *Appl. Environ. Microbiol.* 81, 5880–5888. doi: 10.1128/AEM.01616-15

Duncan, S. H., Louis, P., and Flint, H. J. (2004). Lactate-utilizing bacteria, isolated from human feces, that produce butyrate as a major fermentation product. *Appl. Environ. Microbiol.* 70, 5810–5817. doi: 10.1128/AEM.70.10.5810-5817.2004

Gong, J., Yu, H., Liu, T., Gill, J. J., Chambers, J. R., Wheatcroft, R., et al. (2008). Effects of zinc bacitracin, bird age and access to range on bacterial microbiota in the ileum and caeca of broiler chickens. *J. Appl. Microbiol.* 104, 1372–1382. doi: 10.1111/j.1365-2672.2007.03699.x

González-Ortiz, G., dos Santos, T. T., and Bedford, M. R. (2021). Evaluation of xylanase and a fermentable xylo-oligosaccharide on performance and ileal digestibility of broiler chickens fed energy and amino acid deficient diets. *Anim. Nutr.* 7, 488–495. doi: 10.1016/j.aninu.2020.07.008

González-Ortiz, G., Gomes, G. A., Dos Santos, T. T., and Bedford, M. R. (2019). "Chapter 14 new strategies influencing gut functionality and animal performance" in *The value of fibre. Brill | Wageningen academic*, 233–254.

González-Solé, F., Solà-Oriol, D., Ramayo-Caldas, Y., Rodriguez-Prado, M., González Ortiz, G., Bedford, M. R., et al. (2022). Supplementation of xylo-oligosaccharides to suckling piglets promotes the growth of fiber-degrading gut bacterial populations during

the lactation and nursery periods. *Sci. Rep.* 12, 11594–11513. doi: 10.1038/s41598-022-15963-4

Hernot, D. C., Boileau, T. W., Bauer, L. L., Middelbos, I. S., Murphy, M. R., Swanson, K. S., et al. (2009). In vitro fermentation profiles, gas production rates, and microbiota modulation as affected by certain fructans, galactooligosaccharides, and polydextrose. *J. Agric. Food Chem.* 57, 1354–1361. doi: 10.1021/jf802484j

Kaur, A., Rose, D. J., Rumpagaporn, P., Patterson, J. A., and Hamaker, B. R. (2011). In vitro batch fecal fermentation comparison of gas and short-chain fatty acid production using "slowly fermentable" dietary fibers. *J. Food Sci.* 76, H137–H142. doi: 10.1111/j.1750-3841.2011.02172.x

Lee, S. A., Apajalahti, J., Vienola, K., González-Ortiz, G., Fontes, C. M. G. A., and Bedford, M. R. (2017). Age and dietary xylanase supplementation affects ileal sugar residues and short chain fatty acid concentration in the ileum and caecum of broiler chickens. *Anim. Feed Sci. Technol.* 234, 29–42. doi: 10.1016/j.anifeedsci.2017.07.017

Liu, J. B., Cao, S. C., Liu, J., Pu, J., Chen, L., and Zhang, H. F. (2018). Effects of dietary energy and lipase levels on nutrient digestibility, digestive physiology and noxious gas emission in weaning pigs. *Asian Australas. J. Anim. Sci.* 31, 1963–1973. doi: 10.5713/ajas.18.0087

Morgan, N. K., Gomes, G. A., and Kim, J. C. (2021). Comparing the efficacy of stimbiotic and a combination of xylanase and beta-glucanase, in broilers fed wheat-barley based diets with high or low AME. *Poult. Sci.* 100:101383. doi: 10.1016/j.psj.2021.101383

Morgan, N. K., Keerqin, C., Wallace, A., Wu, S. B., and Choct, M. (2019). Effect of arabinoxylo-oligosaccharides and arabinoxylans on net energy and nutrient utilization in broilers. *Anim. Nutr.* 5, 56–62. doi: 10.1016/j.aninu.2018.05.001

Morgan, N. K., Kim, E., and González-Ortiz, G. (2023). Holo-analysis of the effects of xylo-oligosaccharides on broiler chicken performance. *Br. Poult. Sci.* doi: 10.1080/00071668.2023.2280963

Morgan, N. K., Wallace, A., Bedford, M. R., and González-Ortiz, G. (2022). Impact of fermentable fiber, xylo-oligosaccharides and xylanase on laying hen productive performance and nutrient utilization. *Poult. Sci.* 101:102210. doi: 10.1016/j.psj.2022.102210

Moura, P., Cabanas, S., Lourenço, P., Gírio, F., Loureiro-Dias, M. C., and Esteves, M. P. (2008). In vitro fermentation of selected xylo-oligosaccharides by piglet intestinal microbiota. *Lwt* 41, 1952–1961. doi: 10.1016/j.lwt.2007.11.007

Nadkarni, M. A., Martin, F. E., Jacques, N. A., and Hunter, N. (2002). Determination of bacterial load by real-time PCR using a broad-range (universal) probe and primers set. *Microbiology* 148, 257–266. doi: 10.1099/00221287-148-1-257

Okazaki, M., Fujikawa, S., and Matsumoto, N. (1990). Effect of Xylooligosaccharide on the growth of Bifidobacteria. *Bifidobacteria Microflora* 9, 77–86. doi: 10.12938/bifidus1982.9.2_77

Pan, J., Yin, J., Zhang, K., Xie, P., Ding, H., Huang, X., et al. (2019). Dietary xylo-oligosaccharide supplementation alters gut microbial composition and activity in pigs according to age and dose. *AMB Express* 9:134. doi: 10.1186/s13568-019-0858-6

Rastall, R. A., Diez-Municio, M., Forssten, S. D., Hamaker, B., Meynier, A., Moreno, F. J., et al. (2022). Structure and function of non-digestible carbohydrates in the gut microbiome. *Benefic. Microbes* 13, 95–168. doi: 10.3920/BM2021.0090

Ribeiro, T., Cardoso, V., Ferreira, L. M. A., Lordelo, M. M. S., Coelho, E., Moreira, A. S. P., et al. (2018). Xylo-oligosaccharides display a prebiotic activity when used to supplement wheat or corn-based diets for broilers. *Poult. Sci.* 97, 4330–4341. doi: 10.3382/ps/pey336

Richards, P., Fothergill, J., Bernardeau, M., and Wigley, P. (2019). Development of the caecal microbiota in three broiler breeds. *Front. Vet. Sci.* 6, 1–19. doi: 10.3389/fvets.2019.00201

Rinttilä, T., and Apajalahti, J. (2013). Intestinal microbiota and metabolites-implications for broiler chicken health and performance. *J. Appl. Poult. Res.* 22, 647–658. doi: 10.3382/japr.2013-00742

Rinttila, T., Kassinen, A., Malinen, E., Krogius, L., and Palva, A. (2004). Development of an extensive set of 16S rDNA-targeted primers for quantification of pathogenic and indigenous bacteria in faecal samples by real-time PCR. *J. Appl. Microbiol.* 97, 1166–1177. doi: 10.1111/j.1365-2672.2004.02409.x

Rinttilä, T., Moran, C. A., and Apajalahti, J. (2022). DHA-rich Aurantiochytrium biomass, a novel dietary supplement, resists degradation by rumen microbiota without disrupting microbial activity. *Appl. Microbiol.* 2, 53–72. doi: 10.3390/applmicrobiol2010004

Rinttilä, T., Ülle, K., Apajalahti, J., Timmons, R., and Moran, C. A. (2020). Design and validation of a real-time PCR technique for assessing the level of inclusion of fungus-and yeast-based additives in feeds. *J. Microbiol. Methods* 171:105867. doi: 10.1016/j.mimet.2020.105867

Sanchez, J. I., Marzorati, M., Grootaert, C., Baran, M., van Craeyveld, V., Courtin, C. M., et al. (2009). Arabinoxylan-oligosaccharides (AXOS) affect the protein/carbohydrate fermentation balance and microbial population dynamics of the simulator of human intestinal microbial ecosystem. *Microb. Biotechnol.* 2, 101–113. doi: 10.1111/j.1751-7915.2008.00064.x

Šimić, A., González-Ortiz, G., Mansbridge, S. C., Rose, S. P., Bedford, M. R., Yovchev, D., et al. (2023). Broiler chicken response to xylanase and fermentable xylooligosaccharide supplementation. *Poult. Sci.* 102:103000. doi: 10.1016/j.psj.2023.103000

Singh, A. K., Mishra, B., Bedford, M. R., and Jha, R. (2021). Effects of supplemental xylanase and xylooligosaccharides on production performance and gut health variables of broiler chickens. *J. Anim. Sci. Biotechnol.* 12, 98–15. doi: 10.1186/s40104-021-00617-8

Tao, S., et al. (2019). 'In Vitro Fermentation Characteristics for Different Ratios of Soluble to Insoluble Dietary Fiber by Fresh Fecal Microbiota from Growing Pigs', *ACS Omega* 4, 15158–15167. doi: 10.1021/acsomega.9b01849

Wang, J., Sun, B., Cao, Y., and Wang, C. (2010). In vitro fermentation of xylooligosaccharides from wheat bran insoluble dietary fiber by Bifidobacteria. *Carbohydr. Polym.* 82, 419–423. doi: 10.1016/j.carbpol.2010.04.082

Xu, Z. R., Hu, C. H., and Wang, M. Q. (2002). Effects of fructooligosaccharide on conversion of L-tryptophan to skatole and indole by mixed populations of pig fecal bacteria. *J. Gen. Appl. Microbiol.* 48, 83–89. doi: 10.2323/jgam.48.83

Zhang, X., Junhui, Y., Jing, Y., Ting, C., Bei, X., Zhe, L., et al. (2018). Excellent low-temperature catalytic performance of nanosheet co-Mn oxides for total benzene oxidation. *Appl. Catal. A Gen.* 566, 104–112. doi: 10.1016/j.apcata.2018.05.039

frontiers | Frontiers in Microbiology

TYPE Original Research
PUBLISHED 26 February 2024
DOI 10.3389/fmicb.2024.1132151



OPEN ACCESS

EDITED BY
Rebeca Martín,
INRAE Centre Jouy-en-Josas, France

REVIEWED BY
Emily C. Hoedt,
The University of Newcastle, Australia
Md Abdullah Al Mamun,
Bangladesh Agricultural University, Bangladesh

*CORRESPONDENCE
Hilario Cuquetto Mantovani
✉ hcmantovani@wisc.edu
Polyana Pizzi Rotta
✉ polyana.rotta@ufv.br

RECEIVED 26 December 2022
ACCEPTED 13 February 2024
PUBLISHED 26 February 2024

CITATION
Quirino DF, Marcondes MI, Oliveira KR, Guimarães SEF, Silva JS, Suen G, Rossi LE, Cunha CS, Mantovani HC and Rotta PP (2024) Comparison of ruminal microbiota, *IL-1β* gene variation, and tick incidence between Holstein × Gyr and Holstein heifers in grazing system.
*Front. Microbiol.* 15:1132151.
doi: 10.3389/fmicb.2024.1132151



# Comparison of ruminal microbiota, *IL-1β* gene variation, and tick incidence between Holstein × Gyr and Holstein heifers in grazing system

Daiana Francisca Quirino[1], Marcos Inácio Marcondes[2], Kellen Ribeiro de Oliveira[1], Simone Elisa Facioni Guimarães[1], Juliana Soares da Silva[3], Garret Suen[4], Letícia Elisa Rossi[3], Camila Soares Cunha[5], Hilario Cuquetto Mantovani[6]* and Polyana Pizzi Rotta[1]*

[1]Department of Animal Science, Universidade Federal de Viçosa, Viçosa, Minas Gerais, Brazil, [2]Department of Animal Science, Washington State University, Pullman, WA, United States, [3]Department of Microbiology, Universidade Federal de Viçosa, Viçosa, Minas Gerais, Brazil, [4]Department of Bacteriology, University of Wisconsin, Madison, WI, United States, [5]School of Veterinary Medicine and Animal Science, Universidade Federal de Mato Grosso do Sul, Campo Grande, Mato Grosso do Sul, Brazil, [6]Department of Animal and Dairy Sciences, University of Wisconsin, Madison, WI, United States

**Introduction:** The variation in bacterial communities among breeds has been previously reported and may be one of the reasons why Holstein × Gyr dairy heifers have better development in grazing systems in tropical conditions. This study aimed to explore the ruminal microbiota composition, the *IL-1β* gene variation, tick incidence, and blood parameters of Holstein × Gyr (½ Holstein × ½ Gyr) and Holstein heifers grazing intensely managed Guinea grass (*Panicum maximum* Jacq. cv. Mombaça).

**Methods:** Sixteen heifers were divided into two groups consisting of 8 Holstein × Gyr and 8 Holstein heifers. The experimental period was comprised of 3 periods of 21 days. Ruminal samples were taken via the stomach tube technique. The sequencing of the V4 hypervariable region of the 16S rRNA gene was performed using the Illumina MiSeq platform. Counting and collection of ticks were conducted each 21 days. Blood and skeletal muscle tissue biopsies were performed at the end of the experiment.

**Results:** Firmicutes were the most abundant phyla present in both breed rumen samples and Bacteroidota showed differences in relative abundance between breed groups, with greater values for Holstein heifers ($p < 0.05$ with FDR correction). The 10 most abundant unique OTUs identified in each breed included several OTUs of the genus *Prevotella*. Holstein heifers had a greater tick count and weight (9.8 ticks/animal and 1.6 g/animal, respectively) than Holstein × Gyr (2.56 ticks/animal and 0.4 g/animal, respectively). We found nucleotide substitutions in the *IL-1β* gene that might be related to adaptation and resistance phenotypes to tick infestation in Holstein × Gyr heifers. Blood concentrations of urea, albumin, insulin-like growth factor 1, triiodothyronine, and thyroxine were greater in Holstein × Gyr than in Holstein heifers.

**Conclusion:** Adaptations in Holstein × Gyr heifers such as ruminal microbiota, tick resistance, nucleotide substitutions in *IL-1β* gene, and hormone concentration

suggest a better energy metabolism and thermoregulation resulting in better performance in tropical grazing systems.

KEYWORDS

crossbred heifer, Guinea grass, heat stress, pasture, rumen microbiology

# 1 Introduction

The Holstein × Gyr (½ Holstein × ½ Gyr), also known as the Girolando breed, is a popular crossbred among dairy producers in tropical regions (Mellado et al., 2011; Washburn and Mullen, 2014). The Girolando cattle allies milk production traits from Holstein and adaptability to tropical climate presented by Zebu breeds (Santos et al., 2011; Fraga et al., 2016). However, Holstein and crossbred genetics have been modified over the years (Washburn and Mullen, 2014), and the mechanisms behind different performance responses of purebred or crossbred young animals in tropical pasture-based systems are not fully understood. Abreu et al. (2022) suggested that Holstein heifers have less heat tolerance, demonstrated by the greater bite rate (20 vs. 17.3), and shorter grazing time spent in each meal compared to crossbred heifers. Therefore, the variation in performance of Holstein × Gyr and Holstein heifers might be explained by the ability to graze in high temperatures, which consequently impacts time spent in grazing and resting (Quirino et al., 2022), resistance to ectoparasites, and susceptibility to infectious diseases (Otto et al., 2018). Beyond the suggested differences above, we speculate that susceptibility to diseases and grazing behavior would also cause a significant change in the ruminal microbiota, which could impact the intake and performance of grazing animals (Uyeno et al., 2010).

The variation in bacterial communities among breeds has been previously reported (Uyeno et al., 2010; Paz et al., 2016). In addition, heat stress may impact the population of microorganisms essential for fiber digestion, and these changes are responsible for regulating nutrient cycling in the host (Church, 1993), consequently impacting animal performance and metabolism.

In addition to heat stress responses, Holstein animals are more susceptible to tick infestation because the physical barriers, including skin thickness, the density of fur coat, and odor, as well as the self-cleaning ability with larger space between tongue papillae are less effective in removing ticks in the larvae stage (Tabor et al., 2017). Infestations by ectoparasites such as the bovine tick *Rhipicephalus* (*Boophilus*) *microplus* may impact animal/herd performance due to secondary illnesses (Léger et al., 2013), and can even lead to animal death. Over 1 g in beef cattle weight might be lost daily for each engorging tick (Jonsson, 2006). The *IL-1β* gene is associated with the immune response and has been shown to be increased during tick infestation (Piper et al., 2008; Brannan et al., 2014; Thutwa et al., 2021). Greater polymorphism in the *IL-1β* gene may impact the animals' adaptive response to ticks, compromising the cascade of pro-inflammatory cytokines (Torina et al., 2020), activation of endothelium, and local upregulation of cell-surface adhesion (Rahman et al., 2016). Tick infestation is associated with lower productivity and decreased efficiency of feed utilization (Berman, 2011), and the Holstein animals are considered more susceptible to ticks (Glass and Coussens, 2005) in tropical grazing systems.

In addition, diet composition can induce significant changes in rumen microbiota, which in turn, is also influenced by host genetics (Liu et al., 2021). Menezes et al. (2011) observed a predominance of Prevotellaceae, Erysipelotrichaceae, and Veillonellaceae in grazing cows, while cows fed a total mixed ration had a predominance of Fibrobacteriaceae. However, a comparison between ruminal microbiota from crossbred (Holstein × Gyr) and purebred Holstein heifers in grazing systems has not yet been demonstrated, which might help explain the differences in digestibility, beyond feeding behavior, reported in previous studies (Oliveira Filho et al., 2018; Silvestre et al., 2021; Quirino et al., 2022). Thus, changes in ruminal microbiota and tick infestation potentially reduce the productivity of grazing animals, especially in Holstein animals. Therefore, for tropical systems, crossing taurine with zebu breeds can increase rusticity while maintaining production (Berman, 2011).

We hypothesized that Holstein × Gyr heifers perform better than Holstein heifers in grazing systems due to differences in the rumen microbiota, polymorphisms in the *IL-1β* gene, lower tick incidence, and greater concentrations of specific blood hormones that indicate better adaptability to tropical conditions. Therefore, this study aimed to evaluate the ruminal microbiota composition, polymorphisms in the *IL-1β* gene, tick incidence, and blood parameters from Holstein × Gyr and Holstein heifers managed in an intermittent grazing system of Guinea grass (*Panicum maximum* Jacq. cv. Mombaça) in tropical conditions.

# 2 Materials and methods

## 2.1 Experimental design and animal management

The study was conducted at the Universidade Federal de Viçosa (Viçosa, MG, Brazil), located in the Southwest region of Minas Gerais State (20,7604400S, 42,8,608,200 W), Brazil. The experiment was conducted during the summer season, from December 2016 to April 2017. The experiment was conducted following the standard procedures for Animal Care and Handling stated in the Universidade Federal de Viçosa guidelines process number 24/2018. Data on weather conditions were obtained from the Local Weather Station located 1.39 km from the experimental area. The experiment was composed of three periods of 21 days after an adaptation period to the diet and management of 45 days in a grazing system of Guinea grass. Before the trial, all animals received a preventive application of an anti-parasitic (Eprinex Pour-On, Boehringer

Ingelhein, São Paulo, São Paulo, Brazil) at 1 mL/10 kg body weight (BW). Sixteen heifers were used in this trial, and they were divided into four groups ($n = 4$) composed of four Holstein and four Holstein × Gyr (½ Holstein × ½ Gyr) heifers with two different BW assigned in a randomized block design with a repeated measure scheme. The groups averaged 258.6 ± 24.80 kg and 157.1 ± 24.99 kg BW and grazed two separate sets of 16 paddocks each. Blocks were considered a combination of a set of paddocks and animals' weights and treatments were randomized within each block (set of paddocks 1 had the heavier animals and set of paddocks 2 had the lighter animals).

Animals were managed in a rotational grazing system comprising 32 Guinea grass (*Panicum maximum* Jacq. cv. Mombaça) paddocks with an 800 $m^2$ area, fertilized with 200 kg of N/ha/yr. and 150 kg of $K_2O$/ha/yr., for 1 d grazing period. Each set of paddocks had a feeding area with a feed bunk, drinking fountains, and 4 $m^2$/animal of shade freely accessed by the animals. Each heifer group received a concentrate supplement (0.5% BW on DM basis) at 1200 h and mineral salt *ad libitum*. The concentrate composition is presented in Supplementary Table S1, and was manufactured in an animal feed factory at the Universidade Federal de Viçosa.

## 2.2 Ruminal sampling, DNA extraction, and sequencing

On the last day of each period, ruminal samples were taken without fasting at 0800 h using the stomach tube technique (Lodge-Ivey et al., 2009; Henderson et al., 2013; Kumar et al., 2015). The initial volume of rumen fluid (~200 mL) was discarded to avoid saliva contamination. A sample of approximately 50 mL was stored at −80°C for DNA extraction.

Genomic DNA was extracted from ruminal samples as described by Stevenson and Weimer (2009), using the phenol/chloroform method with bead beating for mechanical disruption of microbial cells. Samples were processed and sequenced separately for each experimental period. The V4 hypervariable region of the 16S rRNA gene was paired-end sequenced on the Illumina MiSeq platform following the manufacturer's guidelines (Illumina, Inc., San Diego, California, United States) at the University of Wisconsin-Madison (United States).

After sequencing, raw reads were demultiplexed and adapters were removed in Illumina Miseq software. Afterward, the sequences were filtered, and chimeras were removed, as well as reads shorter than 200 bp or longer than 500 bp. In addition, ambiguous sequences and homopolymers with more than 8 bp were removed. The paired-end sequences were joined, filtered, and cleaned using Mothur v.1.47.0 following MiSeq SOP (Schloss et al., 2009). V4 sequences were aligned using the SILVA v.138 16S rRNA gene reference database (Quast et al., 2012). Lastly, sequences were grouped into operational taxonomic units (OTUs) using uncorrected pairwise distances clustered with the furthest neighbor method based on a similarity cut-off of 97%. OTUs were normalized across samples, using the sample with the lowest number of sequences. For the bioinformatic analyses, sequences of the same treatment collected from three experimental periods were analyzed together and results are representative of the three sampling periods. The sequences obtained for all samples in the present study were submitted to Sequence Read Archive on the National Center for Biotechnology Information[1] under the accession number PRJNA 956552.

## 2.3 Tissue collection, DNA extraction, and sequencing

One muscle tissue sample was biopsied at d 80 by sampling 1 g of *Longissimus dorsi* from each animal using local subcutaneous lidocaine (10 mL at 5%). Samples were washed with a sterile saline solution (0.9%) and stored overnight (4°C) in RNA Later (Qiagen, Hilden, North Rhine, Westphalia, Germany) and subsequently at −80°C. DNA was extracted using the method described by Sambrook and Russell (2001).

Primers for 2 exons of gene *IL-1β* (GenBank AY851162.1; Supplementary Table S2) were designed using Primer-BLAST. PCR was performed with GoTaq® Master Mix (Promega Corporation, Madison, WI, United States) in a Veriti™ thermocycler (Applied Biosystems, Thermo Fisher Scientific, California, United States). The temperature cycles were as follows: initial denaturation at 95°C for 2 min, 40 denaturation cycles at 95°C for 1 min, annealing at 62°C and 63°C for 1 min for primers one and two, respectively, and extension at 73°C for 1.3 min followed by a final extension at 73°C for 5 min. PCR products were purified from agarose gel using the Wizard SV Gel and PCR clean-up System kit (Promega). Amplification products were sequenced using an AB3500 Genetic Analyzer (Applied Biosystems/Thermo Fisher Scientific, California, United States). Amplicons were forward and reverse sequenced in-house on a Sanger 3,500 Genetic Analyzer platform following the manufacturer's guidelines (Applied Biosystem Thermo Fisher Scientific, San Diego, California, United States).

Amplicon gene sequencing of the *IL-1β* gene data was processed using the BioEdit Sequence Alignment Editor version 7.0.5.3, and Muscle software version 3.8.31[2] was used to compare the sequences obtained with the reference gene *IL-1β* sequence (GenBank AY851162.1).

## 2.4 Weighing and tick counts and collection

Heifers were weighed on three consecutive days at the beginning and the end of the experiment. Before weighing, heifers were fasted for 12 h with free access to water. After weighing, animals were placed in paddocks until the next fasting period. At the end of each experimental period, tick counts were performed on the left side of the animal's body according to the methodology described by Wharton and Utech (1970). After tick collection, all animals received preventive treatment with a pour-on anti-parasitic (Eprinex® Pour-On, Boehringer Ingelhein, São Paulo, São Paulo, Brazil) at a dose of 1 mL/10 kg BW.

1 http://www.ncbi.nlm.nih.gov/sra

2 http://drive5.com/muscle/downloads.htm

## 2.5 Blood parameters

Blood samples were collected at d 80, by jugular vein puncture using vacuum tubes (BD Vacutainer® SST® II Advance®, São Paulo, Brazil). Blood serum was separated by centrifugation (2,700 × g for 20 min at 4°C) and frozen at −20°C. Urea (K056), glucose (K082), total protein (K031), albumin (K040), and triglycerides (K117) were quantified using an automatic biochemical analyzer (Mindray, BS200E, Shenzhen, China) and Bioclin kits. IGF-1 was analyzed by chemiluminescence using the UniCell Dxl Access Immunoassay System (Beckman Coulter Inc., Brea, United States). Total T3 and total T4 were analyzed using Beckman kits (ref. number 33,830 and 33,800, respectively, Beckman Coulter®, Brea, United States) in the Access 2 Immunoassay System (Beckman Coulter Inc., Brea, United States).

## 2.6 Statistical analysis

Statistical analysis was performed using the GLIMMIX procedure of SAS (SAS University Edition) using a randomized block design model with repeated measures:

$$Y_{ijklm} = \mu + T_i + P_k + (T \times P)_{ik} + B_l + \varepsilon_{ijklm}$$

where: μ = general mean, $T_i$ = fixed effect of treatment (breed) i, $P_k$ = fixed effect of period k, $T \times P_{ik}$ = fixed effect of the interaction between treatment *i* and period *k*, $B_l$ = random effect of block *l* (combined effect of weight and paddock), and $\varepsilon_{ijklm}$ = random errors with a mean 0 and variance $\sigma^2$, which is the variance between measurements within animals. Fifteen covariance structures were tested for each response variable and the one that provided the lower AIC was used. Data on tick counts and weight exhibited a non-normal distribution; all available distributions in the GLIMMIX procedure were tested using the same model described above and SHIFTED T (3) distribution was used (approached normality of residues).

Data with single observations per animal were analyzed using a randomized block design model:

$$Y_{ijk} = \mu + T_i + B_l + \varepsilon_{ijk}$$

where: μ = general mean, $T_i$ = fixed effect of treatment (breed) i, $B_l$ = random effect of block *l* (combined effect of weight and paddock), and $\varepsilon_{ijk}$ = random error with a mean 0 and variance $\sigma^2$.

For rumen microbiota statistical analysis, Past v.4.02 (Hammer et al., 2001) software was used to create Non-Metric Multidimensional Scaling (NMDS) plots based on the Bray–Curtis dissimilarity metric. Analysis of similarities (ANOSIM) was performed (number of permutations of 10.000) to evaluate significant differences between experimental groups using the same software. Beta diversity was also evaluated using two additional distance matrices (weighted and unweighted UniFrac) and Principal Coordinate Analysis (PCoA) as the ordination method. Permanova F-statistic and *p*-values were calculated according to Anderson (2001). Alpha diversity data were analyzed using SPSS v.22 (Norusis, 1993) for normality data using the Kolmogorov–Smirnov test. Subsequently, the Mann–Whitney non-parametric test was performed for independent samples to correlate Holstein × Gyr and Holstein data. Relative abundances of OTUs were analyzed using the Benjamini-Hochberg method to correct the false discovery rate at phylum, family, and genus levels. A two-sided White's non-parametric t-test was performed using STAMP v.1.2.3 (Parks et al., 2014).

To determine the OTUs most likely to explain the differences between breeds, LEfSe (Linear discriminant analysis Effect Size; Segata et al., 2011) was used to identify potential biomarkers associated with the phenotypes of interest. The statistical analyses were performed in the implementation of LEfSe on the server Galaxy (version 0.1). For this purpose, a standard table of the composition of bacterial OTUs for each breed was provided.

For all analyses, significant differences were declared when $p < 0.05$, and trends when $0.05 < p < 0.10$.

# 3 Results

## 3.1 Environmental conditions

Weather conditions varied along experimental periods, with a minimum temperature of 17.8°C and a maximum of 31.4°C. Relative humidity and Rainfall varied from 75.4% to 79.5% and 2.9 to 4.9 mm, respectively. The temperature-humidity index (THI) ranged from 68.8 to 72. Detailed information on weather data in each period was described by Quirino et al. (2022).

## 3.2 Forage allowance and chemical composition

The pre-grazing and post-grazing heights varied during the experiment, with average heights of 71.0 ± 2.91 and 43.8 ± 1.15 cm, respectively. The accumulated herbage per paddock (88.5 ± 5.13) and herbage allowance (11.0 ± 0.63) increased during periods and the major herbage accumulation occurred in periods 3 and 4 with DM of 27.4% and 25.8%, respectively, while grazing efficiency was superior (63.3%) when neutral detergent fiber was inferior (66.0%). Thus, the intake was not limited by forage allowance (Quirino et al., 2022).

## 3.3 Rumen microbiota composition

After cleaning and filtering the sequencing data, 2,062.650 high-quality sequence reads were obtained in total, with a minimum Good's coverage of 97% and a maximum value of 99% (Table 1). NMDS visualization did not show a clear separation between the microbial communities of Holstein × Gyr and Holstein heifers (Supplementary Figure 1). However, ANOSIM revealed a significant difference ($p < 0.01$) between the rumen microbiota composition of each breed (Supplementary Figure 1A). The NMDS analysis carried out separately between sampling days showed similar behavior, except for the first sampling, where no significant difference was observed between the breeds ($p = 0.11$; Supplementary Figure 1B). A significant difference between breeds was also observed (Permanova, $p < 0.05$) using weighted and unweighted UniFrac as phylogenetic distance metrics represented in a Principal Coordinate Analysis (PCoA; Figure 1). Alpha diversity metrics (Chao 1, Shannon, and Simpson

TABLE 1 Summary of sequencing data from ruminal samples from Holstein × Gyr and Holstein heifers (mean ± SD).

| Groups | | After filtering and clean-up | | After normalization | |
|---|---|---|---|---|---|
| | Good's coverage | Reads | OTUs | Reads | OTUs |
| Holstein | 0.98 ± 0.004 | 44,511 ± 12,765 | 2,398 ± 405 | 20,330 ± 256 | 1,958 ± 273 |
| Holstein × Gyr | 0.98 ± 0.005 | 41,299 ± 12,617 | 2,344 ± 382 | 20,371 ± 246 | 1,992 ± 217 |

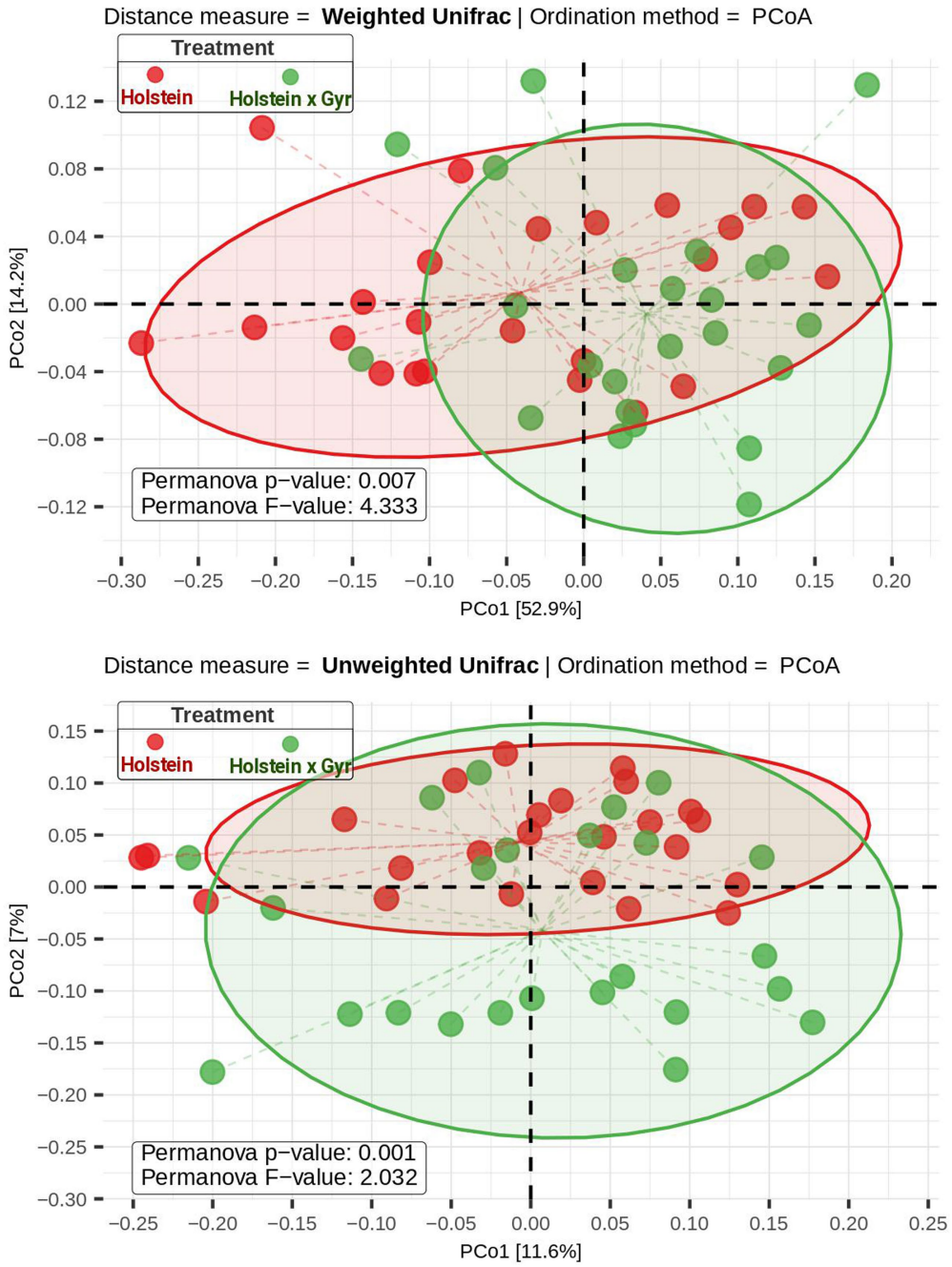


FIGURE 1
Beta diversity was evaluated using two distance matrices (weighted and unweighted UniFrac) and Principal Coordinate Analysis—PcoA as the ordination method. Permanova F-statistic and *p*-values were calculated and are shown in the PCoA plot. Holstein cattle is represented by red dots and Holstein × Gyr as green dots. Please note that some samples overlap in the plot.

indexes) were not different between breeds ($p = 0.77$, $p = 0.48$, $p = 0.32$, respectively; Supplementary Figure 2).

The taxonomic assignment of the bacterial sequences revealed a total of 23 phyla, 41 classes, 94 orders, 156 families, and 279 genera.

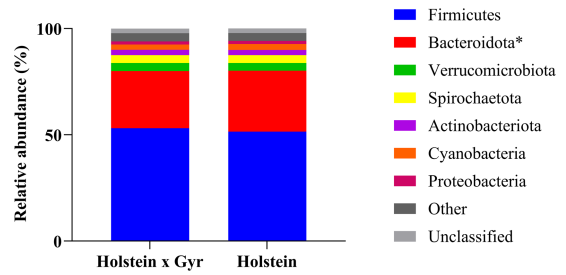


FIGURE 2
Bacterial community composition at the phylum level (relative abundances > 1.0%) in ruminal samples of Holstein × Gyr and Holstein heifers. *Different with $p < 0.05$ with FDR correction using two-sided White's non-parametric *t*-test.

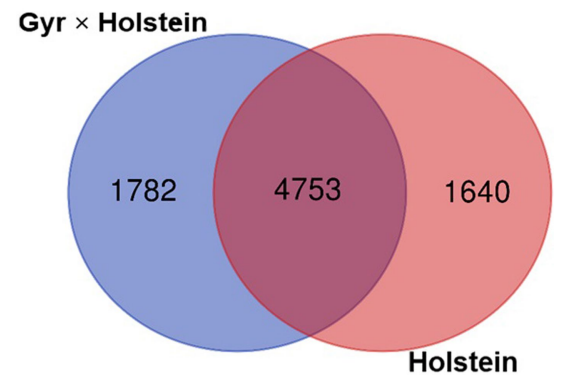


FIGURE 3
Venn diagram representing the number of OTUs that were shared between the Holstein × Gyr and Holstein breeds and those that appeared exclusively in each group.

The phylum Firmicutes was in higher abundance for both groups, with a greater relative abundance in Holstein × Gyr heifers (53.1% ± 2.08%) compared to Holstein heifers (51.5% ± 2.13%; Figure 2). The second most abundant phylum was Bacteroidota, which was different between breeds ($p = 0.03$ with FDR correction). Relative abundances were 26.9% ± 1.92% and 28.7% ± 2.23% for Holstein × Gyr and Holstein heifers, respectively. Unclassified phyla corresponded to 2.24% ± 0.43% for Holstein × Gyr heifers and 2.10% ± 0.52% for Holstein heifers.

At the family level, Prevotellaceae and Lachnospiraceae were the predominant groups in samples from both breeds, but no significant differences were observed ($p = 0.25$ with FDR correction; Supplementary Figure 3). As for the genus level, there were no significant differences in ruminal samples from both breeds. Genus *Prevotella* showed the greatest relative abundance in both heifer groups, being 10.6 ± 1.46 for Holstein × Gyr and 11.9 ± 1.95 for Holstein ($p = 0.33$ with FDR correction; Supplementary Figure 4).

The two breeds shared 4,753 OTUs, while 1,782 OTUs were observed only in the Holstein × Gyr breed and 1,640 OTUs were unique to the Holstein breed (Figure 3). Of the 4,753 OTUs shared between the two breeds, the most abundant (>0.5% relative abundance) are represented in Figure 4. OTU 0002 was found in highest abundance (3.7% relative abundance in the Holstein breed, and 2.3% in the Holstein × Gyr breed) and was classified as a member of the genus *Prevotella*. Members of the genus *Prevotella* also represented the most abundant OTUs shared by both breeds (14 OTUs out of 27 OTUs) and differences in relative abundances were detected for this genus between the two animal groups (Figure 4).

The 10 most abundant unique OTUs identified in each breed are listed in Supplementary Table S3, which includes several OTUs of the genus *Prevotella*. The OTUs classified as Prevotellaceae UCG-003 (0.08% ± 0.37%), *Prevotella* (0.07% ± 0.16%), and Bacteroidata unclassified (0.05% ± 0.24%) were found exclusively in Holstein × Gyr heifers (Supplementary Table S3). The unique OTUs identified in Holstein heifers were classified as Prevotellaceae unclassified (0.02% ± 0.06%), Lachnospiraceae unclassified (0.01% ± 0.03%), and *Prevotella* (0.01 ± 0.04%; Supplementary Table S3).

The OTUs that could explain the differences associated with Holstein × Gyr steers through LDA analysis, were OTU00004 (Christensenellaceae_R_7_group), OTU00005 (*Prevotella*), and OTU00020 (Lachnospiraceae_XPB1014-group). The OTUs that were considered indicators of the microbiota in Holsteins steers were OTU00036 (*Prevotella*), OTU00016 (NK4A214_group), and OTU00014 (*Methanobrevibacter*; Figure 5).

## 3.4 Tick incidence and polymorphisms in the *IL-1β* gene

Holstein heifers had a greater ($p = 0.06$; 9.8 ticks/animal) tick count than the Holstein × Gyr heifers (2.56 ticks/animal; Figure 6). Holstein heifers also had greater tick weight than Holstein × Gyr heifers (1.6 g/animal and 0.4 g/animal; $p < 0.05$). All heifers had more tick infestation in the third period ($p < 0.01$), resulting in greater tick weight ($p < 0.01$).

No mutations were identified at exon 1 of the gene *IL-1β* among 11 sequences analyzed in this study (five Holstein × Gyr and six Holstein heifers). However, mutations were found (Supplementary Figure 5) at Intron I in both breeds. At exon II, we confirmed the mutations described in the reference sequence from GenBank (AY851162.1) for eight of the analyzed sequences (four Holstein × Gyr and four Holstein; Table 2). For Holstein × Gyr heifers the higher presence of nucleotide variation was found in *IL-1β* at base position 2,126 of exon II. Holstein had the most variation at base position 2,184.

## 3.5 Blood parameters

The serum urea content ($p = 0.01$), IGF-1 ($p < 0.01$), T3 ($p = 0.02$), T4 ($p = 0.02$), and Albumin ($p < 0.01$) were greater in Holstein × Gyr than in Holstein heifers (Table 3). Breed did not influence serum concentrations of glucose ($p = 0.35$), total protein ($p = 0.25$), or triglycerides ($p = 0.16$).

# 4 Discussion

The present study was conducted to investigate factors contributing to the better performance of Holstein × Gyr heifers compared to Holstein heifers under tropical pastures. Previously,

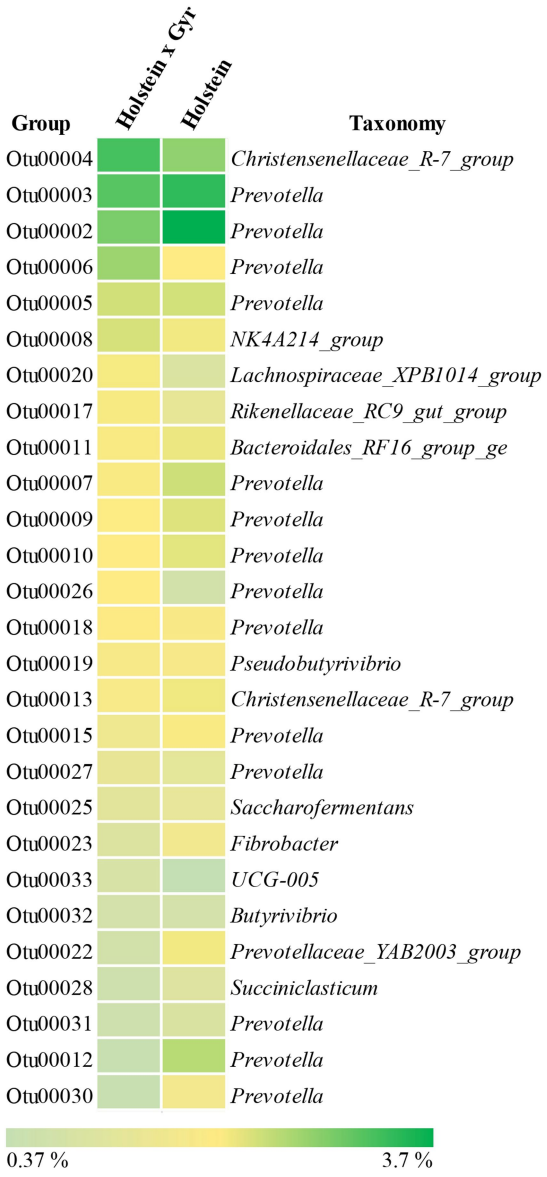


FIGURE 4
Heatmap of OTUs shared between Holstein × Gyr and Holstein with relative abundance above 0.5%.

Quirino et al. (2022) highlighted greater average daily gain and feed efficiency for Holstein × Gyr than Holstein heifers managed in an intermittent grazing system of Guinea grass (*Panicum maximum* Jacq. cv. Mombaça). Here, we evaluated differences in rumen microbiota composition, susceptibility to ticks, *IL-1β* nucleotide polymorphisms, and metabolic profile on blood samples aiming to identify factors explaining the better performance of Holstein × Gyr when grazing tropical pastures.

Significant differences in OTU abundance and membership were observed in the rumen microbial community of Holstein × Gyr and Holstein heifers. One OTU classified as *Prevotella* showed greater relative abundance in Holstein heifers. Although most of the OTUs were shared by both breeds, 27.3% of the OTUs detected in Holstein × Gyr heifers were found exclusively in this group. Similarly, 25.1% of the OTUs present in the rumen of Holstein heifers were not found in Holstein × Gyr. Notably, most observed differences were related to the phylum Bacteroidota and OTUs classified as members of the family Prevotellaceae and the genus *Prevotella*. In both Holstein x Gyr and Holstein animals, a large number of exclusive OTUs belonging to the genus *Prevotella* were observed and similar results were obtained in the analysis of indicator OTUs. Although amplicon sequencing has limited resolution to identify taxa at the species level, differences between breeds could be linked to *Prevotella* strains performing distinct functions in the rumen ecosystem of these animals.

*Prevotella* is a bacterial genus generally found in high abundance in the rumen of cattle (Thoetkiattikul et al., 2013; Pandit et al., 2018), probably due to its high genetic and functional diversity, which allows the colonization of various ecological niches in the rumen ecosystem (Jami and Mizrahi, 2012). *Prevotella* is metabolically versatile and capable of utilizing a range of substrates present in the rumen (Stevenson and Weimer, 2009; Jewell et al., 2015). *Prevotella* has been associated with greater concentrate intake due to its proteolytic and amylolytic activity in the rumen (McCann et al., 2014a,b), and some strains can also degrade hemicellulose and pectin (Dehority, 1991; Matsui et al., 1998).

Differences in microbial community composition may occur due to several factors, such as diet, heat stress, and management. For example, heat stress is known to affect animal eating habits, which could induce changes in the composition of the rumen microbiota (Uyeno et al., 2010). However, when animals are fed the same diet and subjected to the same management practices differences in rumen microbiota are less likely, as observed for Holstein × Gyr and Holstein heifers in the current study. It should be pointed out, however, that the animal gut microbiota can remain stable over a short period when animals are kept in a controlled environment, but the microbiome composition can vary in the longer term, which is a limitation of animal trials.

Firmicutes and Bacteroidota were the two most abundant phyla in the rumen of Holstein × Gyr heifers. However, the greater abundance of Firmicutes in Holstein × Gyr heifers may result from a compensation mechanism for decreasing *Prevotella* in the rumen (Jami et al., 2014). Prevotellaceae UCG-003, which was found only in Holstein × Gyr, has been associated with an increase in the production of organic acids in the rumen (Chen et al., 2021). An OTU classified as Bacteroidales unclassified was unique to the Holstein × Gyr heifers, and this taxon has been previously associated with ruminal biohydrogenation (Zhang et al., 2014). Also, the Bacteroidota phylum is related to the production of glycoside hydrolases that degrade substrates a range of substrates in the rumen, including cellulose, pectin, and starch (Hernández et al., 2022).

Tick infestation was low in the current study and may not have directly affected animal performance. This is probably because the animals were treated with anti-parasitic at the beginning of the experiment. Even with the same initial tick control, Holstein heifers had higher tick infestation. An even greater difference would probably be expected without preventive treatment of the animals in each group.

The *IL-1β* gene has been associated with inflammatory response and chronic inflammation (Brannan et al., 2014). The nucleotide sequence of this gene was analyzed since it has been associated with a response to tick infestation (Brannan et al., 2014), In addition, its polymorphism had been previously characterized and was confirmed by findings in the current study. According to the Genbank sequence (AY851162.1), we found nucleotide variations in the Bov-tA SINE

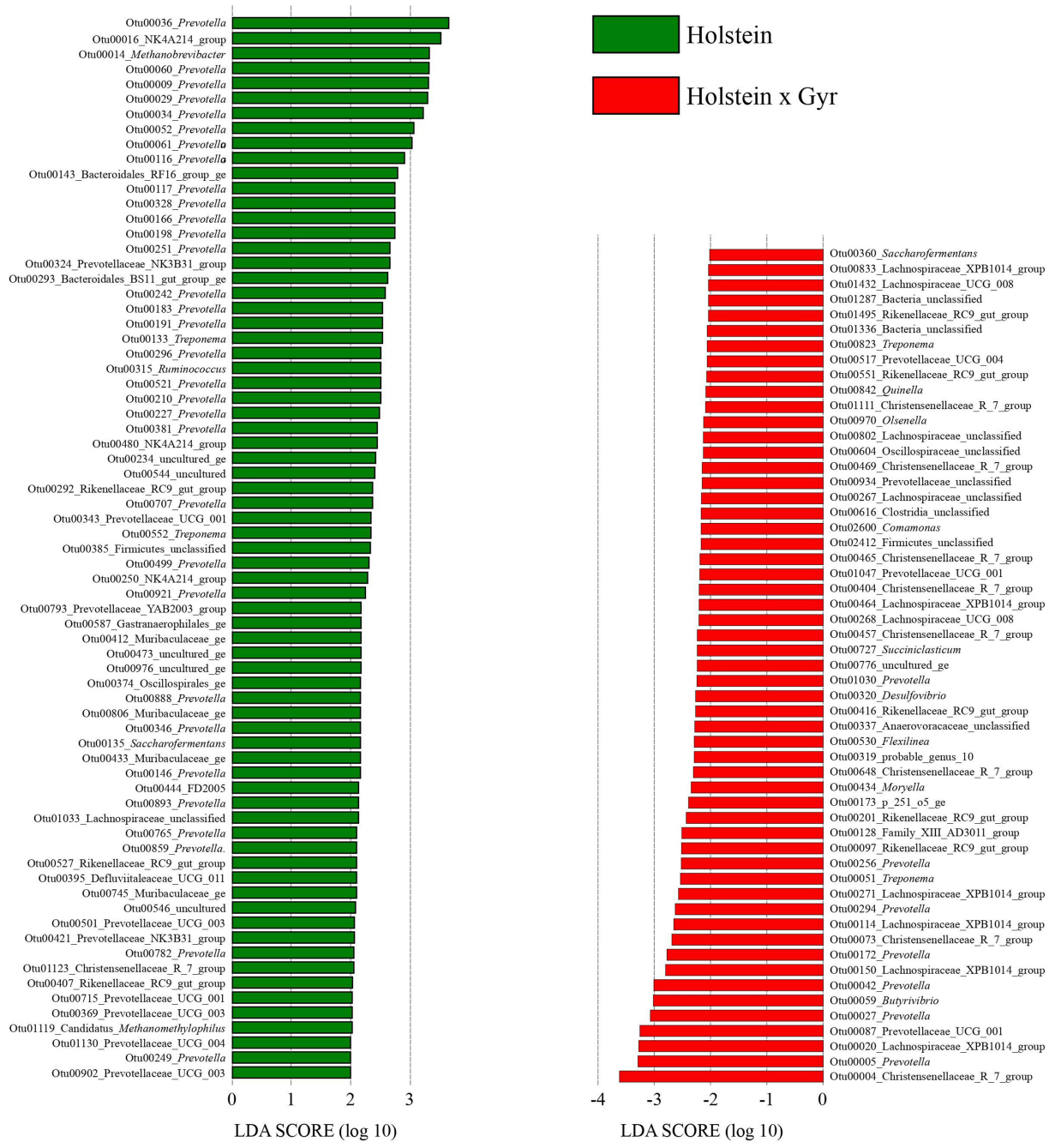


FIGURE 5
The plot was generated using the online LEfSe project. The length of the bar column represents the LDA score. The figure shows the microbial taxa with significant differences between the Holsteins × Gyr (green) and Holstein (red; LDA score > 2).

region, which is embedded in the intronic region. The Bov-tA SINE is a member of the retrotransposon family Bov-tA and is widely distributed in the ruminant genome (Lenstra et al., 1993). Bov-tA is composed of a tRNA-related region at the 5′ end and a Bov-A unit at the 3′ end (Okada and Hamada, 1997; Shimamura et al., 1999). According to Onami et al. (2007), the Bov-AX family is a candidate for use as a polymorphic DNA marker due to its polymorphic nature and abundance. Additionally, Bov-AX loci may be used for breed discrimination. The presence of mutations in the regulatory region of the gene *IL-1β*, confirms the highly polymorphic nature of the interleukin family (Wu and Wang, 2018) and highlights this region as a potential marker for tick infestation. Those mutations might explain the lower tick infestation in Holstein × Gyr heifers in tropical grazing systems, increasing the pro-inflammatory reaction when compared to Holstein. Moreover, the genomic characterization of immunological gene families may contribute to a better understanding of resistance phenotypes, particularly for mutations in conserved regions such as those described here, and may have relevant roles in general

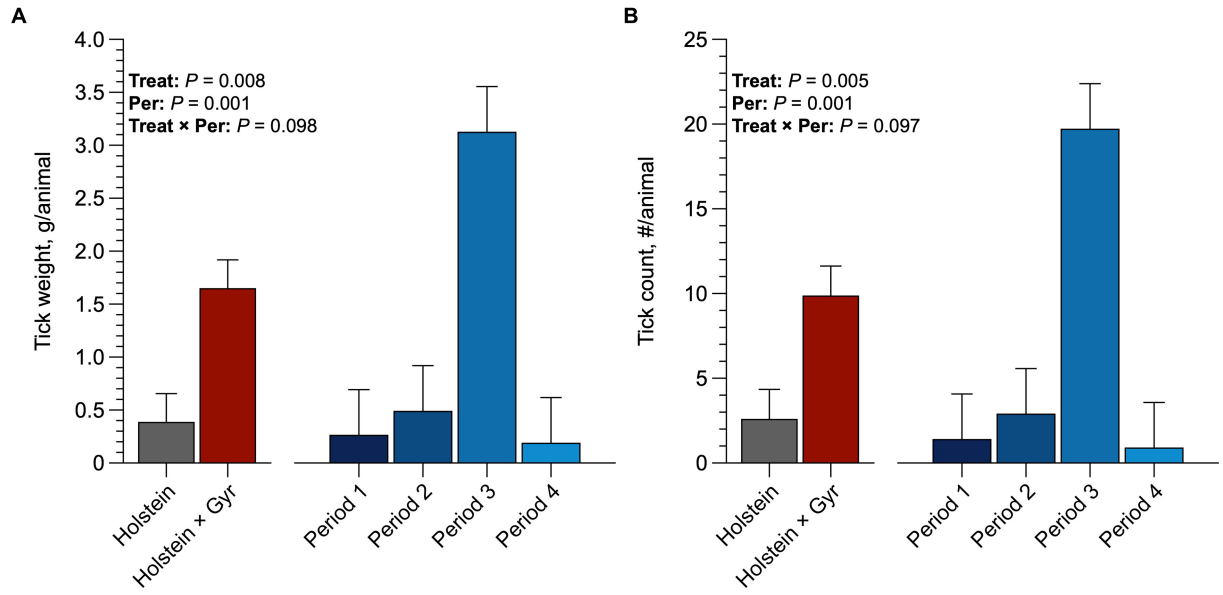


FIGURE 6
**(A)** Average tick count (number/animals) per breed and average per period of Holstein × Gyr and Holstein heifers in pasture of Guinea grass (*Panicum maximum* Jacq. cv. Mombaça). **(B)** Average tick weight (g/animals) per breed and average per period of Holstein × Gyr and Holstein heifers in pasture of Guinea grass (*Panicum maximum* Jacq. cv. Mombaça).

TABLE 2 **Mutations found in *IL-1β* gene in grazing heifers.**

| Base position | Holstein × Gyr | | Holstein | | Reference Sequence (*IL-1β* gene) |
|---|---|---|---|---|---|
| Intron 1 | Nucleotide | *N* | Nucleotide | *N*[a] | |
| 1,148 | A | 3 | A | 3 | G[b] |
| | G | 1 | R | 3 | |
| 1,235 | T | 3 | T | 3 | C[c] |
| | Y | 2 | Y | 3 | |
| 1,266 | G | 4 | G | 3 | A[d] |
| | R | 1 | R | 2 | |
| 1,378 | C | 3 | C | 3 | T[e] |
| | Y | 1 | Y[j] | 2 | |
| **Exon 2** | | | | | |
| 2,126 | A | 1 | - | - | R[f] |
| | G | 2 | G | 2 | |
| | R | 2 | - | - | |
| 2,184 | G | 4 | G | 4 | K[g] |
| | R | 1 | R | 2 | |
| 2,195 | G | 4 | G | 4 | K |
| 2,209 | C | 4 | C | 4 | M[h] |
| 2,253 | C | 4 | C | 4 | S[i] |

Despite such nucleotide variants, no differences in the aminoacidic composition were found. [a]N, number of animals. [b]A, adenine. [c]G, guanine. [d]C, cytosine. [e]T, tymine. [f]R, purine nucleotide. [g]K, nucleotide might be T or G. [h]M, nucleotide might be C or A. [i]S, nucleotide might be C or G. [j]Y, pyrimidine nucleotide.

adaptability that might be further investigated. The presence of most mutations in exon 2 of the IL-*1β* gene in Holstein × Gyr associated with less tick infestation and tick weight suggested the greater resistance of these animals.

Despite the presence of nucleotide variants in exon two, based on the reference sequence (GenBank AY851162.1), there were no predicted differences in the amino acid composition of the protein, and phenotypic changes are not expected. Such silent mutations

TABLE 3 Blood parameters of Holstein × Gyr and Holstein heifers under grazing conditions.

| Item | Breed | | | *P* |
|---|---|---|---|---|
| | Holstein × Gyr | Holstein | SEM[a] | |
| Urea, mg/dL | 29.82 | 22.70 | 1.780 | 0.014 |
| Glucose, mg/dL | 71.67 | 69.78 | 4.485 | 0.352 |
| Total protein, g/dL | 6.73 | 7.22 | 0.183 | 0.253 |
| Albumin, g/dL | 3.29 | 2.90 | 0.165 | 0.001 |
| Triglycerides, mg/dL | 30.07 | 24.25 | 2.783 | 0.162 |
| IGF 1, ng/mL | 270.67 | 165.94 | 39.933 | 0.001 |
| Total T3, ng/dL | 2.73 | 1.43 | 0.517 | 0.016 |
| Total T4, μ/dL | 9.98 | 5.51 | 1.677 | 0.016 |

[a]SEM, standard error of mean.

confirm the high variability in the *IL-1β* gene and together with the mutations identified in the Bov-tA family is necessary to understand the effect of these nucleotide substitutions on adaptability and parasite resistance in cattle. Also, an analysis of a larger number of animals might determine the haplotype structure of these breeds and pinpoint the role of each genetic group in the formation of crossbreeds and/or synthetic breeds.

Considering the greater forage dry matter intake and neutral detergent fiber intake for Holstein × Gyr heifers (Quirino et al., 2022), we had a greater concentration of serum urea, which may improve urea recycling. The fermentable carbohydrates are responsible for stimulating the transport of urea to the rumen (Nichols et al., 2022). However, the greater serum urea was not combined with glucose availability in the rumen. Therefore, urea cannot be recycled adequately and might not result in differences in total protein.

Spicer et al. (1990) suggested that serum IGF-1 may be affected by environmental conditions because cows in summer had lower milk IGF-1. Besides, Holstein × Gyr heifers presented greater concentrations of IGF-1, T3, and T4 which are associated with metabolic homeostasis and adaptation to the environment. This might indicate a better adaptation to tropical environments and better performance of Holstein × Gyr heifers. The IGF-1 participates in glucose homeostasis, reducing glucose blood levels and utilization by tissues (Kasprzak, 2021). Also, T4 and T3 were greater in Holstein × Gyr and these hormones are involved with body growth, skeletal development, energy metabolism, and temperature homeostasis (Silva et al., 2021). This could help explain why Holstein × Gyr heifers had a higher tolerance to heat stress (Cavalheira et al., 2021). Collectively, our results show that animals with better metabolism dynamics and adaptation to the environment can perform better, even without greater consumption (Quirino et al., 2022).

## 5 Conclusion

The rumen microbiota of Holstein × Gyr and Holstein heifers showed significant differences in community composition mainly associated with the phylum Bacteroidota and the abundance of members of the family Prevotellaceae and the genus *Prevotella*. The Holstein × Gyr heifers had less tick infestation compared to Holstein, which made these animals perform better. Additionally, the greater concentrations of IGF-1, T3, and T4 suggest that Holstein × Gyr heifers have better energy metabolism and thermoregulation and are more adapted to tropical grazing systems. *IL-1β* polymorphisms are still subject to further studies to disentangle the role of different nucleotide substitutions in tick resistance/susceptibility phenotype.

## Data availability statement

The datasets presented in this study can be found in online repositories. The names of the repository/repositories and accession number(s) can be found at: BioProject, PRJNA956552.

## Ethics statement

The animal study was approved by Animal Care and Handling stated in the Universidade Federal de Viçosa guidelines process number 24/2018. The study was conducted in accordance with the local legislation and institutional requirements.

## Author contributions

PR and MM designed the study. DQ, JS, HM, and LR conceived the study. DQ, KO, SG, CC, and PR wrote and edited the manuscript. GS and HM critically reviewed, edited, and finalized the manuscript for submission. All authors contributed to the article and approved the submitted version.

## Funding

This study was supported by Fundação de Amparo à Pesquisa do Estado de Minas Gerais—FAPEMIG (APQ-03278-18) and CAPES (PROEX 88887.844747/2023-00).

## Conflict of interest

The authors declare that the research was conducted in the absence of any commercial or financial relationships that could be construed as a potential conflict of interest.

## Publisher's note



## Supplementary material

The Supplementary material for this article can be found online at: https://www.frontiersin.org/articles/10.3389/fmicb.2024.1132151/full#supplementary-material

SUPPLEMENTARY FIGURE S1
Non-metric Multidimensional Scaling (NMDS) using Bray-Curtis dissimilarity as distance metric for OTUs in ruminal samples of Holstein × Gyr and Holstein heifers. The data in the upper panel **(A)** is representative of the three sampling periods combined while the lower panels **(B)** represent separate sampling periods.

SUPPLEMENTARY FIGURE S2
Alpha diversity indices of the ruminal samples of Holstein × Gyr and Holstein heifers (mean and standard deviation).

SUPPLEMENTARY FIGURE S3
Bacterial community composition at the family level (relative abundances > 1.0%) in ruminal samples of Holstein × Gyr and Holstein heifers.

SUPPLEMENTARY FIGURE S4
Bacterial community composition at the genus level (relative abundances > 1.0%) in ruminal samples of Holstein × Gyr and Holstein heifers.

SUPPLEMENTARY FIGURE S5
*IL1 β* intron 1 sequencing results. **(A)** The arrow indicates mutation in base number 1,148. **(B)** The arrow indicates mutation in base number 1,235. **(C)** The arrow indicates mutation in base number 1,266. **(D)** The arrow indicates mutation in base number 1,378.

## References

Abreu, M. B., Cunha, C. S., Costa, J. H. C., Miller-Cushon, E. K., Rotta, P. P., Machado, A. F., et al. (2022). Performance and feeding behavior of Holstein and Holstein × Gyr crossbred heifers grazing temperate forages. *Tropl. Anim. Health Prod.* 54:100. doi: 10.1007/s11250-022-03106-w

Anderson, M. J. (2001). A new method for non-parametric multivariate analysis of variance. *Austral Ecol.* 26, 32–46. doi: 10.1111/j.1442-9993.2001.01070.pp.x

Berman, A. (2011). Invited review: are adaptations present to support dairy cattle productivity in warm climates? *J. Dairy Sci.* 94, 2147–2158. doi: 10.3168/jds.2010-3962

Brannan, J. L., Riggs, P. K., Olafson, P. U., Ivanov, I., and Holman, P. J. (2014). Expression of bovine genes associated with local and systemic immune response to infestation with the lone star tick, *Amblyomma americanum*. *Ticks Tick Borne. Dis.* 5, 676–688. doi: 10.1016/j.ttbdis.2014.04.022

Cavalheira, L. R., Wenceslau, R. R., Ribeiro, L. S., Carvalho, B. C., Borges, A. M., and Camargo, L. S. A. (2021). Daily vaginal temperature in Girolando cows from three genetic composition under natural heat stress. *Transl. Anim.* 5, 1–9. doi: 10.1093/tas/txab138

Chen, H., Wang, C., Huasai, S., and Chen, A. (2021). Effects of dietary forage to concentrate ratio on nutrient digestibility, ruminal fermentation and rumen bacterial composition in Angus cows. *Sci. Rep.* 11:17023. doi: 10.1038/s41598-021-96580-5

Church, D. C. (1993). *The ruminant animal: Digestive physiology and nutrition*. Prospect Heights, IL: Waveland Press, Inc.

Dehority, B. A. (1991). Effects of microbial synergism on fibre digestion in the rumen. *Proc. Nutr. Soc.* 50, 149–159. doi: 10.1079/PNS19910026

Fraga, A. B., Silva, F. L., Hongyu, K., Santos, D. S., Murphy, T. W., and Lopes, F. B. (2016). Multivariate analysis to evaluate genetic groups and production traits of crossbred Holstein × zebu cows. *Tropl. Anim. Health Prod.* 48, 533–538. doi: 10.1007/s11250-015-0985-2

Glass, E., and Coussens, P. M. (2005). Functional genomics of host-pathogen interactions in species of veterinary importance. *Vet. Immunol. Immunopathol.* 105, 173–174. doi: 10.1016/j.vetimm.2005.02.005

Hammer, Ø., Harper, D. A. T., and Ryan, P. D. (2001). Past: Paleontological statistics software package for education and data analysis. *Palaeontol. Electron* 4, 1–9.

Henderson, G., Cox, F., Kittelmann, S., Miri, V. H., Zethof, M., Noel, S. J., et al. (2013). Effect of DNA extraction methods and sampling techniques on the apparent structure of cow and sheep rumen microbial communities. *PLoS One* 8:e74787. doi: 10.1371/journal.pone.0074787

Hernández, R., Mares, M. C., Jimenez, H., Reyes, A., and Caro-Quintero, A. (2022). Functional and phylogenic characterization of bacteria in bovine rumen using factionation of ruminal fluid. *Front. Microbiol.* 13:813002. doi: 10.3389/fmicb.2022.813002

Jami, E., and Mizrahi, I. (2012). Composition and similarity of bovine rumen microbiota across individual animals. *PLoS One* 7:e33306. doi: 10.1371/journal.pone.0033306

Jami, E., White, B. A., and Mizrahi, I. (2014). Potential role of the bovine rumen microbiome in modulating milk composition and feed efficiency. *PLoS One* 9:e85423. doi: 10.1371/journal.pone.0085423

Jewell, K. A., McCormick, C. A., Odt, C. L., Weimer, P. J., and Suen, G. (2015). Ruminal bacterial community composition in dairy cows is dynamic over the course of two lactations and correlates with feed efficiency. *Appl. Environ. Microbiol.* 81, 4697–4710. doi: 10.1128/AEM.00720-15

Jonsson, N. N. (2006). The productivity effects of cattle tick (*Boophilus microplus*) infestation on cattle, with particular reference to *Bos indicus* cattle and their crosses. *Vet. Parasitol.* 137, 1–10. doi: 10.1016/j.vetpar.2006.01.010

Kasprzak, A. (2021). Insulin-like growth factor 1 (IGF-1) signaling in glucose metabolism in colorectal cancer. *Int. Mol. Sci.* 22:6434. doi: 10.3390/ijms22126434

Kumar, S., Indugu, N., Vecchiarelli, B., and Pitta, D. W. (2015). Associative patterns among anaerobic fungi, methanogenic archaea, and bacterial communities in response to changes in diet and age in the rumen of dairy cows. *Front. Microbiol.* 6, 1–10. doi: 10.3389/fmicb.2015.00781

Léger, E., Vourc'h, G., Chevillon, C., and Mccoy, K. D. (2013). Changing distributions of ticks: causes and consequences. *Exp. Appl. Acarol.* 59, 219–244. doi: 10.1007/s10493-012-9615-0

Lenstra, J. A., Boxtel, J. A. F., Van Zwaagstra, K. A., and Schwerin, M. (1993). Short interspersed nuclear element (SINE) sequences of the Bovidae. *Anim. Genet.* 24, 33–39. doi: 10.1111/j.1365-2052.1993.tb00916.x

Liu, K., Zhang, Y., Yu, Z., Xu, Q., Zheng, N., Zhao, S., et al. (2021). Ruminal microbiota-host interaction and its effects on nutrient metabolism. *Anim. Nutr.* 7, 49–55. doi: 10.1016/j.aninu.2020.12.001

Lodge-Ivey, S. L., Browne-Silva, J., and Horvath, M. B. (2009). Technical note: bacterial diversity and fermentation end products in rumen fluid samples collected via oral lavage or rumen cannula. *J. Anim. Sci.* 87, 2333–2337. doi: 10.2527/jas.2008-1472

Matsui, H., Ushida, K., Miyazaki, K., and Kojima, Y. (1998). Use of ratio of digested xylan to digested cellulose (X/C) as an index of fiber digestion in plant cell-wall material by ruminal microorganisms. *Anim. Feed Sci. Technol.* 71, 207–215. doi: 10.1016/S0377-8401(97)00164-8

McCann, J. C., Wickersham, T. A., and Loor, J. J. (2014a). High-throughput methods redefine the rumen microbiome and its relationship with nutrition and metabolism. *Bioinform. Biol. Insights* 8, BBI.S15389–BBI.S15125. doi: 10.4137/BBI.S15389

McCann, J. C., Wiley, L. M., Forbes, T. D., Rouquette, F. M., and Tedeschi, L. O. (2014b). Relationship between the rumen microbiome and residual feed intake-efficiency of Brahman bulls stocked on bermudagrass pastures. *PLoS One* 9:e91864. doi: 10.1371/journal.pone.0091864

Mellado, M., Coronel, F., Estrada, A., and Ríos, F. G. (2011). Lactation performance of Holstein and Holstein x Gyr cattle under intensive condition in a subtropical environment. *Trop. Subtr. Agroec.* 14, 927–931.

Menezes, A. B., Lewis, E., O'Donovan, M., O'Neill, B. F., Clipson, N., and Doyle, E. M. (2011). Microbiome analysis of dairy cows fed pasture or total mixed ration diets. *FEMS Microbiol. Ecol.* 78, 256–265. doi: 10.1111/j.1574-6941.2011.01151.x

Nichols, K., Carvalho, I. P. C., Rauch, R., and Matín-Tereso, J. (2022). Review: unlocking the limitations of urea supply in ruminant diets by considering the natural mechanism of endogenous urea secretion. *Animal* 16:100537. doi: 10.1016/j.animal.2022.100537

Norusis, M. J. (1993). *SPSS for windows: base system user's guide*. SPSS:Chicago 5407–5412.

Okada, N., and Hamada, M. (1997). The 3′ ends of tRNA-derived SINEs originated from the 3′ ends of LINEs: a new example from the bovine genome. *J. Mol. Evol.* 44, S52–S56. doi: 10.1007/PL00000058

Oliveira Filho, C. A., Machado, F. S., Ferreira, A. L., Tomich, T. R., Maurício, R. M., Campos, M. M., et al. (2018). Nutritional plans on the intake, digestibility and performance of dairy heifers of different breed compositions. *Pesq. Agropec. Bras.* 53, 247–255. doi: 10.1590/S0100-204X2018000200014

Onami, J. I., Nikaido, M., Mannen, H., and Okada, N. (2007). Genomic expansion of the Bov-A2 retroposon relating to phylogeny and breed management. *Mamm. Genome* 18, 187–196. doi: 10.1007/s00335-007-9000-1

Otto, P. I., Guimarães, S. E., Verardo, L. L., Luísa Azevedo, A. S., Vandenplas, J., Soares, A. C., et al. (2018). Genome-wide association studies for tick resistance in *Bos taurus* x *Bos indicus* crossbred cattle: a deeper look into this intricate mechanism. *J. Dairy Sci.* 101, 11020–11032. doi: 10.3168/jds.2017-14223

Pandit, R. J., Hinsu, A. T., Patel, S. H., Jakhesara, S. J., Koringa, P. G., Bruno, F., et al. (2018). Microbiota composition, gene pool and its expression in Gir cattle (*Bos indicus*) rumen under different forage diets using metagenomic and metatranscriptomic approaches. *Syst. Appl. Microbiol.* 41, 374–385. doi: 10.1016/j.syapm.2018.02.002

Parks, D. H., Tyson, G. W., Hugenholtz, P., and Beiko, R. G. (2014). STAMP: statistical analysis of taxonomic and functional profiles. *Bioinformatics* 30, 3123–3124. doi: 10.1093/bioinformatics/btu494

Paz, H. A., Anderson, C. L., Muller, M. J., Kononoff, P. J., and Fernando, S. C. (2016). Rumen bacterial community composition in Holstein and Jersey cows is different under same dietary condition and is not affected by sampling method. *Front. Microbiol.* 7, 1–9. doi: 10.3389/fmicb.2016.01206

Piper, E. K., Jackson, L. A., Bagnall, N. H., Kongsuwan, K. K., Lew, A. E., and Jonsson, N. N. (2008). Gene expression in the skin of Bos taurus and *Bos indicus* cattle infested with the cattle tick, Rhipicephalus (Boophilus) microplus. *Vet. Immunol. Immunopathol.* 126, 110–119. doi: 10.1016/j.vetimm.2008.06.011

Quast, C., Pruesse, E., Yilmaz, P., Gerken, J., Schweer, T., Yarza, P., et al. (2012). The SILVA ribosomal RNA gene database project: improved data processing and web-based tools. *Nucleic Acids Res.* 41, D590–D596. doi: 10.1093/nar/gks1219

Quirino, D. F., Marcondes, M. I., Correa, P. V. F., Morais, V. C. L., Cunha, C. S., Silva, A. L., et al. (2022). Intake, performance, and feeding behavior of Holstein and Holstein × Gyr heifers grazing intensively managed tropical grasses during rainy season. *Animal* 16:100613. doi: 10.1016/j.animal.2022.100613

Rahman, S., Shering, M., Ogden, N. H., Lindsay, R., and Badawi, A. (2016). Toll-like receptor cascade and gene polymorphism in host-pathogen interaction in Lyme disease. *J. Inflamm. Res.* 9, 91–102. doi: 10.2147/JIR.S104790

Sambrook, J., and Russell, D. (2001). *Molecular cloning: A laboratory manual*, Cold Springs Harbour Press. Cold Spring Harbor, NY.

Santos, A. S., Valadares Filho, S. C., Detmann, E., Valadares, R. F. D., Ruas, J. R. M., and Amaral, P. M. (2011). Different forage sources for F1 Holstein × Gir dairy cows. *Livest. Sci.* 142, 48–58. doi: 10.1016/j.livsci.2011.06.017

Schloss, P. D., Westcott, S. L., Ryabin, T., Hall, J. R., Hartmann, M., Hollister, E. B., et al. (2009). Introducing mothur: open-source, platform-independent, community-supported software for describing and comparing microbial communities. *Appl. Environ. Microbiol.* 75, 7537–7541. doi: 10.1128/AEM.01541-09

Segata, N., Izard, J., Waldron, L., Gevers, D., Miropolsky, L., Garrett, W. S., et al. (2011). Metagenomic biomarker discovery and explanation. *Genome Biol.* 12, R60–R18. doi: 10.1186/gb-2011-12-6-r60

Shimamura, M., Abe, H., Nikaido, M., Ohshima, K., and Okada, N. (1999). Genealogy of families of SINEs in cetaceans and artiodactyls: the presence of a huge superfamily of tRNA derived families of SINEs. *Mol. Biol. Evol.* 16, 1046–1060. doi: 10.1093/oxfordjournals.molbev.a026194

Silva, T. A. C. C., Quigley, S. P., Kidd, L. J., Anderson, S. T., McLenna, S. R., and Poppi, D. P. (2021). Effect of high crude protein content diet during energy restriction and re-alimentation, on animal performance, skeletal growth and metabolism of bone tissue in two genotypes of cattle. *PLoS One* 16:0247718. doi: 10.1371/journal.pone.0247718

Silvestre, T., Lima, M. A., Santos, G. B., Pereira, L. G. R., Machado, F. S., and Tomich, T. R. (2021). Effects of feeding level and breed composition on intake, digestibility, and methane emissions of dairy heifers. *Animals* 11:586. doi: 10.3390/ani11030586

Spicer, L. J., Tucker, W. B., and Adams, G. D. (1990). Insulin-like growth factor-I in dairy cows: relationships among energy balance, body condition, ovarian activity, and estrous behavior. *J. Dairy Sci.* 73, 929–937. doi: 10.3168/jds.S0022-0302(90)78749-8

Stevenson, D. M., and Weimer, P. J. (2009). Erratum: dominance of Prevotella and low abundance of classical ruminal bacterial species in the bovine rumen revealed by relative quantification real-time PCR. *Appl. Microbiol. Biotechnol.* 83, 987–988. doi: 10.1007/s00253-009-2033-5

Tabor, A. E., Ali, A., Rehman, G., Rocha Garcia, G., Zangirolamo, A. F., Malardo, T., et al. (2017). Cattle tick *Rhipicephalus microplus*-host Interface: a review of resistant and susceptible host responses. *Front. Cell. Infect. Microbiol.* 7:506. doi: 10.3389/fcimb.2017.00506

Thoetkiattikul, H., Mhuantong, W., Laothanachareon, T., Tangphatsornruang, S., Pattarajinda, V., Eurwilaichitr, L., et al. (2013). Comparative analysis of microbial profiles in cow rumen fed with different dietary fiber by tagged 16S rRNA gene pyrosequencing. *Curr. Microbiol.* 67, 130–137. doi: 10.1007/s00284-013-0336-3

Thutwa, K., Wyk, J. B., Dzama, K., Scholtz, A. J., and Cloete, S. W. P. (2021). Expression of cytokine at tick attachement control sites of Namaqua Afrikaner, Dorper and south African mutton merino sheep. *Vet. Parasit.* 291:109384. doi: 10.1016/j.vetpar.2021.109384

Torina, A., Villari, S., Blanda, V., Vullo, S., La Manna, M. P., Azgomi, M. S., et al. (2020). Innate immune response to tick-borne pathogens: cellular and molecular mechanisms induced in the hosts. *Int. J. Mol. Sci.* 21:5437. doi: 10.3390/ijms21155437

Uyeno, Y., Sekiguchi, Y., Tajima, K., Takenaka, A., Kurihara, M., and Kamagata, Y. (2010). An rRNA-based analysis for evaluating the effect of heat stress on the rumen microbial composition of Holstein heifers. *Anaerobe* 16, 27–33. doi: 10.1016/j.anaerobe.2009.04.006

Washburn, S. P., and Mullen, K. A. E. (2014). Invited review: genetic considerations for various pasture-based dairy systems. *J. Dairy Sci.* 97, 5923–5938. doi: 10.3168/jds.2014-7925

Wharton, R. H., and Utech, K. B. W. (1970). The relation between engorgement and dropping of *Boophilus microplus* (Canestrini) (Ixodidae) to the assessment of tick numbers on cattle. *Aust. J. Entomol.* 9, 171–182. doi: 10.1111/j.1440-6055.1970.tb00788.x

Wu, J., and Wang, W. (2018). Association between interleukin family gene polymorphisms and recurrent aphthous stomatitis risk. *Nat. Genes Immun.* 20, 90–101. doi: 10.1038/s41435-018-0019-y

Zhang, R., Zhu, W., Zhu, W., Liu, J., and Mao, S. (2014). Effect of dietary forage sources on rumen microbiota, rumen fermentation and biogenic amines in dairy cows. *J. Sci. Food Agric.* 94, 1886–1895. doi: 10.1002/jsfa.6508

frontiers | Frontiers in Microbiology

TYPE Original Research
PUBLISHED 07 March 2024
DOI 10.3389/fmicb.2024.1321268



OPEN ACCESS

EDITED BY
Rebeca Martín,
INRAE Centre Jouy-en-Josas, France

REVIEWED BY
Xin Zhou,
First Teaching Hospital of Tianjin University of Traditional Chinese Medicine, China
George Grant,
University of Aberdeen, United Kingdom
Georgia Damoraki,
National and Kapodistrian University of Athens, Greece
Marcos Edgar Herkenhoff,
University of São Paulo, Brazil

*CORRESPONDENCE
Hong Zheng
✉ ysgzh@163.com

RECEIVED 16 October 2023
ACCEPTED 13 February 2024
PUBLISHED 07 March 2024

CITATION
Yao Y, Hu H, Chen L and Zheng H (2024) Association between gut microbiota and menstrual disorders: a two-sample Mendelian randomization study.
*Front. Microbiol.* 15:1321268.
doi: 10.3389/fmicb.2024.1321268



# Association between gut microbiota and menstrual disorders: a two-sample Mendelian randomization study

Yufan Yao[1], Haoran Hu[2], Longhao Chen[3] and Hong Zheng[1]*

[1]College of Basic Medical Science, Zhejiang Chinese Medical University, Hangzhou, China, [2]Hangzhou TCM Hospital of Zhejiang Chinese Medical University (Hangzhou Hospital of Traditional Chinese Medicine), Hangzhou, China, [3]The Third School of Clinical Medicine, Zhejiang Chinese Medical University, Hangzhou, China

**Background:** Evidence from observational studies and clinical trials suggests that the gut microbiota is associated with gynecological diseases. However, the causal relationship between gut microbiota and menstrual disorders remains to be determined.

**Methods:** We obtained summary data of gut microbiota from the global consortium MiBio-Gen's genome-wide association study (GWAS) dataset and data on menstrual disorders from the IEU Open GWAS project. MR-Egger, weighted median, inverse variance weighted, simple mode, and weighted mode were used to examine the causal association between gut microbiota and menstrual disorders. Thorough sensitivity studies were performed to confirm the data's horizontal pleiotropy, heterogeneity, and robustness.

**Results:** Through MR analysis of 119 kinds of gut microbiota and 4 kinds of clinical phenotypes, it was discovered that 23 different kinds of gut microbiota were loosely connected to menstrual disorders. After FDR correction, the results showed that only Escherichia/Shigella ($p = 0.00032$, $P_{FDR} = 0.0382$, OR = 1.004, 95%CI = 1.002–1.006) is related to menstrual disorders.

**Conclusion:** According to our MR Analysis, there are indications of a causal relationship between menstrual disorders and gut microbiota. This finding could lead to new discoveries into the mechanisms behind menstrual disorders and clinical research involving the microbiota.

KEYWORDS

**genetics, gut microbiota, menstrual disorder, Mendelian randomization, SNPs**

## 1 Introduction

Menstrual disorders are a common gynecological condition. Irregular menstrual cycles, long menstrual cycles, and increased or decreased menstrual blood volume are the main related manifestations (Chen W. et al., 2023). It causes considerable worry for women.

During the menstrual cycle, hormone and physiological changes can affect the richness and diversity of the urinary and reproductive microbiota (Holdcroft et al., 2023; Cao et al., 2024). Song et al. investigated vaginal microbiota changes at various periods of the menstrual cycle and discovered increased alpha diversity with decreased relative abundance of

*Lactobacillus* spp. and a greater percentage of other bacteria, including *Peptostreptococcus*, *Anaerococcus*, and *Streptococcus* species (Chen et al., 2017; Song et al., 2020). Research by Krog et al. demonstrated that during menstruation, women's vaginal microbiomes are more diverse. Furthermore, they discovered a rise in the non-resident bacteria that cause bacterial vaginosis; however, these bacteria decreased in the luteal and follicular phases (Krog et al., 2022; Grobeisen-Duque et al., 2023). According to a recent study, multiple gut microbiota functional pathways are significantly correlated with the severity score of dysmenorrhea symptoms (Chen C. et al., 2023). Women with more severe symptoms of dysmenorrhea had higher percentages of possibly pro-inflammatory bacteria in their vaginal microbiograms and lower percentages of *Lactobacillus* (Nabeh, 2023).

Some research has also been carried out on the effect of microbiota on menstruation. One study reported that deficiencies in the salivary and fecal microbiota led to significant changes in menstruation and that the diversity of the vaginal microbiota increased during menstruation due to the expansion of *Lactobacillus* during the follicular and luteal phases (Krog et al., 2022). Furthermore, microbial dysbiosis itself can result in elevated insulin levels and a condition known as insulin resistance because it triggers the immune system and stimulates the release of several pro-inflammatory cytokines. Menstrual issues result from this as it raises androgen production and throws off the natural balance between estrogen and progesterone (Tremellen and Pearce, 2012; Nabeh, 2023). Thus, menstruation and microorganisms are inextricably linked.

In the gastrointestinal system, the gut microbiota plays an important role in digestion regulation, but its importance goes much beyond that. The structure of the gut microbiota affects the onset and progression of metabolic and endocrine diseases (Mukherjee et al., 2023). Randomized controlled trials of the gut microbiota, as opposed to observational studies, may aid in proving causation. Unfortunately, due to objective elements such as technology, study methodology, and other confounding factors including age, environment, eating habits, and lifestyle, screening for strains still has substantial limits in early diagnosis and prognosis. It might be challenging to effectively control for these factors in observational studies (Sher et al., 2021). There is growing evidence that the human gut microbiota plays a role in gynecologic diseases (Flores et al., 2012; Lindheim et al., 2017; Parida and Sharma, 2019; Zhao et al., 2020; Zhou et al., 2020; Cao et al., 2024; Huang et al., 2024). If changes in the composition and/or function of the microbiota can be demonstrated to have clinically advantageous effects, then using the gut microbiota's functioning as an alternative to pharmaceutical intervention is possible.

Several studies have recently been conducted to study the association between the hormonal variations associated with the menstrual cycle and the gut microbiota. Reports claim that estrogen affects the gut microbiota in all parts of the body (Vieira et al., 2017). When women have sufficient estrogen in their bodies, their intestinal microbiota exhibits species diversity, with beneficial bacteria dominating and the growth of harmful bacteria being inhibited. Due to the presence of sex hormone receptors in the digestive tract, many healthy women suffer changes in gastrointestinal symptoms during the menstrual cycle (Bharadwaj et al., 2015; Mohib et al., 2018). For instance, early menstruation is characterized by lower stool consistency than mid-menstruation; visceral somatic impulses may be perceived more strongly, resulting in pain, bloating, and nausea, particularly on the first day of the menstrual cycle. In addition, hormonal changes during menstruation can lead to alterations in the function and activity of the body's microbiota. This is due to the microbiota's control over steroid hormone levels, including estrogen (Parida and Sharma, 2019), microbiota can metabolize sex hormones through numerous enzymes, such as hydroxysteroid dehydrogenase, which controls the balance of active and inactive steroids.

An analytical technique called Mendelian randomization (MR) is utilized to determine the causal connection between the observed relationships between modifiable exposures or risk factors and clinically relevant outcomes. To correlate with SNP outcome connections and merge them into a single causal estimate, two-sample MR analysis can utilize SNPs (exposure) from independent genome-wide association studies (GWASs). As the number of GWASs linking illnesses and the gut microbiota has risen rapidly (MiBioGen Consortium Initiative et al., 2018; Kurilshikov et al., 2021), large-scale pooled measurements have become more widespread, allowing two-sample MR analysis to have significantly enhanced statistical power (Kurilshikov et al., 2021). MR allows us to understand whether there is a causal relationship between intestinal flora and menstrual disorders, which can inform clinical and research studies.

GWASs have revolutionized the study of complex disease genetics by analyzing millions of genetic variants present in the genomes of several individuals to determine the connections between genotype and phenotype over the past decade (Visscher et al., 2017). A GWAS provides an agnostic method for studying the genetic basis of complex diseases. The GWAS directory has 427,870 associations and 6,041 articles as of October 2022.

# 2 Methods

## 2.1 Study design

This study is reported following the Strengthening the Reporting of Observational Studies in Epidemiology Using Mendelian Randomization guidelines (STROBE-MR, S1 Checklist) (Skrivankova et al., 2021a,b).

We assessed the causal relationship between 119 microbial communities and 4 clinical phenotypes based on a two-sample MR analysis. The research process is shown in Figure 1. MR uses genetic variation to represent risk factors, and therefore, valid instrumental variables (IVs) in causal inference must satisfy three key assumptions: (1) Exposure has a direct correlation with genetic variation; (2) There is no correlation between genetic variation and potential variables between exposure and result; (3) Other than exposure, genetic variation has no effect on outcome through other mechanisms (Bowden and Holmes, 2019) (Figure 2).

Abbreviations: MR, Mendelian randomization; EFMR (main), Diagnoses-main ICD10: N92.0 excessive and frequent menstruation with regular cycle; EFMR (secondary), Diagnoses-secondary ICD10: N92.0 excessive and frequent menstruation with regular cycle; IM (unspecified), Diagnoses-main ICD10: N92.6 irregular menstruation, unspecified; EFIM, Diagnoses-main ICD10: N92 excessive, frequent and irregular menstruation; GWAS, Genome-wide association study; IVs, Instrumental variables; IVW, Inverse variance weighted; FDR, False discovery rate; SCFA, Short-chain fatty acid.

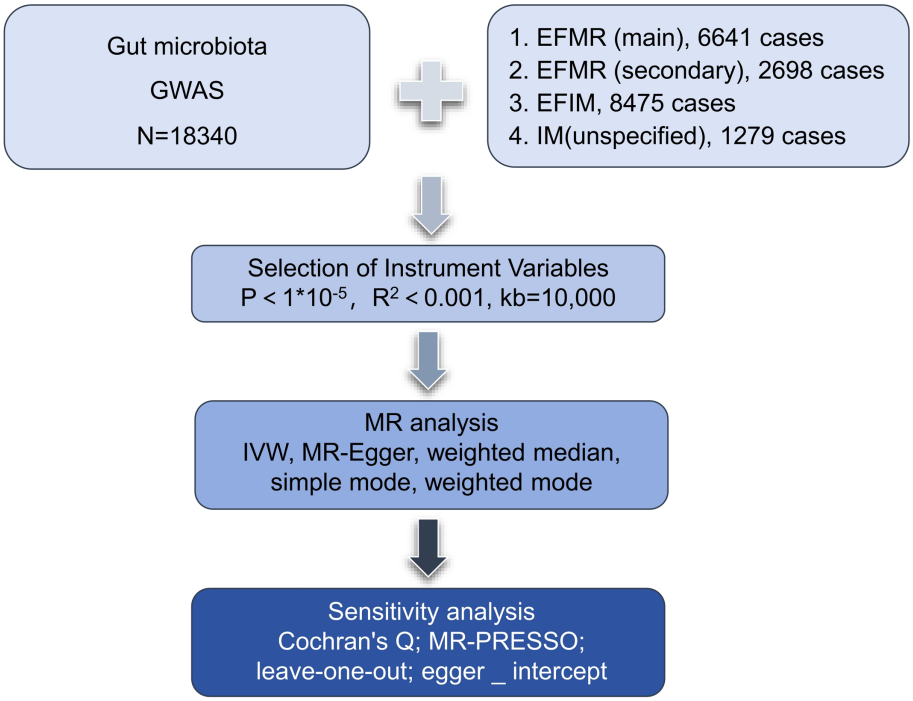


FIGURE 1
The flowchart of the study.

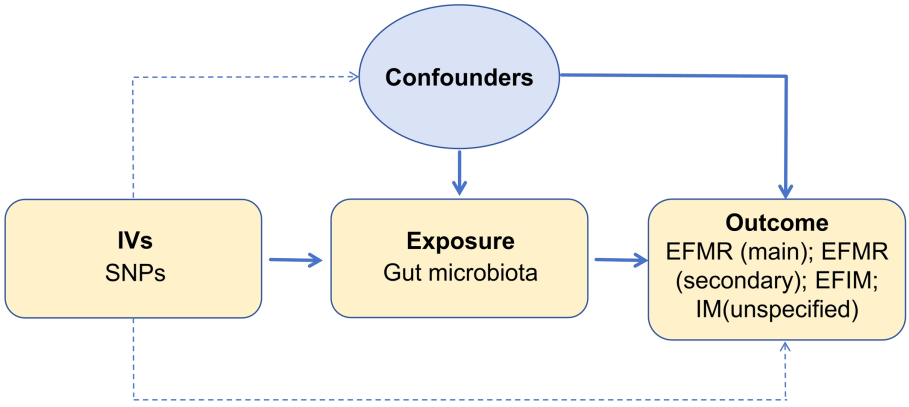


FIGURE 2
Three assumptions of MR analysis.

## 2.2 Exposure data

SNPs from the global consortium MiBio-Gen's GWAS dataset that are associated with the composition of the human gut microbiome were used as instrumental variables (IVs). In order to investigate the relationship between autosomal human genetic variants and the gut microbiome, this multi-ethnic large-scale GWAS brought together genotyping and 16 s ribosomal RNA gene sequencing data from 18,340 participants. A total of 211 taxa (131 genera, 35 families, 20 orders, 16 classes, and 9 phyla) were included (Long et al., 2023). In our study, we kept only data of genus.

## 2.3 Outcome data

Summary statistics for menstruation were obtained from a GWAS meta-analysis.[1] The genetic association data consisted: (1) The diagnostic criteria of diagnoses-main ICD10: N92.0 Excessive and frequent menstruation with regular cycle (EFMR (main)) containing 463,010 participants ($N = 6,641$ cases, 456,369 controls) with a total of 9,851,867 SNPs; (2) The diagnostic criteria of diagnoses-secondary

1 https://gwas.mrcieu.ac.uk

ICD10: N92.0 Excessive and frequent menstruation with regular cycle (EFMR (secondary)) containing 463,010 participants ($N$ = 2,698 cases, 460,312 controls) with a total of 9,851,867 SNPs; (3) The diagnostic criteria of Diagnoses-main ICD10: N92.6 Irregular menstruation, unspecified (IM (unspecified)) containing 463,010 participants ($N$ = 1,279 cases, 461,731controls) with a total of 9,851,867 SNPs; (4) The diagnostic criteria of Diagnoses-main ICD10: N92 Excessive, frequent and irregular menstruation (EFIM) containing 361,194 participants ($N$ = 8,475 cases, 352,719 controls) with a total of 12,983,417 SNPs.

All cases and controls were Europeans. The diagnostic criteria for these four packets are based on ICD-10 criteria. Ethical endorsement was not sought for the study as it only used publicly available GWAS summary statistics and did not attempt to identify individual-level data. Because this is publicly published data by GWAS, other infections and disorders/issues have been ruled out.

## 2.4 Instrumental variable selection

The gut microbiota served as the exposure, while menstruation serves as a result. First, we set up the parameters for identifying IVs with a genome-wide significance of $p < 1 \times 10^{-5}$ and a chained unbalanced clustering algorithm with an R2 threshold of 0.001 over a 10,000 kb area to assure independence of IV exposure (R4.3.1 software; Package: TwoSampleMR; VariantAnnotation; gwasglue). Furthermore, we regarded IVs with F-statistics >10 as powerful tools and saved them for the analyses that followed in order to prevent the bias caused by weak instruments (R4.3.1 software; Package: ieugwasr).

## 2.5 MR analysis

In order to evaluate the causal link between exposure factors and outcome, we utilized MR-Egger, weighted median, inverse variance weighted (IVW), simple mode, and weighted mode (R4.3.1 software, package: TwoSampleMR; VariantAnnotation; gwasglue). The benefit of IVW is that it makes it possible to measure the situation objectively and without experiencing horizontal pleiotropy. Therefore, the results of multiple IVs are mainly based on the IVW method, supplemented by four other methods (Bowden et al., 2015). To ensure that each IV was associated with the same effector allele, we excluded palindromes and incompatible SNPs when harmonizing exposure and outcome statistics, and excluded SNPs linked to exposures that the GWAS outcome statistics were unable to match.

Several sensitivity studies were conducted to evaluate the results' robustness (R4.3.1 software, package: TwoSampleMR). MR-PRESSO was used to detect polybiotic effect bias and correct for polybiotic effects by rejecting outliers, and it has the ability to both detect and correct pleiotropy in MR analysis, and get a causal effect estimate (Bowden et al., 2016) and examine whether the results are driven by the directional horizontal pleiotropy (Burgess and Thompson, 2017). To ascertain whether a single SNP was responsible for the causal signal, leave-one-out analyses were carried out. The identified causal relationship can be regarded as directionally reasonable if the IVs account for more of the exposure difference than the outcome difference. We used Cochran's Q statistics and a two-sample MR package between instruments testing for heterogeneity. Evidence of heterogeneity and invalid instruments can be found when Q exceeds the number of instruments minus one, or a significant Q statistic at a $p$-value < 0.05 can mean the presence of heterogeneity (Greco et al., 2015; Bowden et al., 2019). To exclude false positive results, we corrected the MR results with the false discovery rate (FDR).

In addition, forest plots, scatter plots, leave-one-out, and funnel plots were used to demonstrate that the data are not heterogeneous and their stability.

# 3 Results

## 3.1 SNP selection

In total, 1,531 SNPs were employed for 119 different bacterial species as IVs in accordance with the selection criteria for Ivs. A total of 25 results were obtained (Figure 3). The F-statistics for the Ivs were all more than 10, respectively. Cochrane's Q test did not reveal any evidence of heterogeneity in the sensitivity analysis (Supplementary Table S1). The MR-PRESSO global test ($p > 0.05$) also did not find evidence of a multibiotic effect (Supplementary Table S1). Ultimately, after eliminating the polytomous SNPs identified by the MR-PRESSO outlier test ($p > 0.05$) and MR-Egger regression ($p > 0.05$), there was no evidence of horizontal pleiotropy of IVs (Supplementary Table S1). The forest plots, funnel plots, leave-one-out plots, and scatter plots are shown in Supplementary Figures S1–S4.

## 3.2 EFMR (main)

This study identified 11 gut microbiota were found to be associated with EFMR (main) in IVW (Figure 3). Specifically, IVW estimate suggests that *Eubacterium eligens group* (OR = 0.996, 95%CI = 0.993–1.000, $p = 0.037$), *Haemophilus* (OR = 0.996, 95%CI = 0.994–0.999, $p = 0.004$), *Phascolarcto bacterium* (OR = 0.998, 95%CI = 0.996–1.000, $p = 0.048$), *Cateni bacterium* (OR = 0.998, 95%CI = 0.996–1.000, $p = 0.045$), and *Blautia* (OR = 0.997, 95%CI = 0.994–1.000, $p = 0.038$) had a protective effect on this type of menstrual disorders (Table 1). *RuminococcaceaeUCG011* (OR = 1.002, 95%CI = 1.000–1.003, $p = 0.046$), *DefluviitaleaceaeUCG011* (OR = 1.002, 95%CI = 1.000–1.004, $p = 0.027$), *Escherichia/Shigella* (OR = 1.004, 95%CI = 1.002–1.006, $p = 0.0003$), *Lachnospira* (OR = 1.004, 95%CI = 1.001–1.008, $p = 0.023$), *Anaerotruncus* (OR = 1.004, 95%CI = 1.001–1.007, $p = 0.010$), and *Marvinbryantia* (OR = 1.003, 95%CI = 1.000–1.005, $p = 0.026$) had a negative effect on this type of menstrual disorders (Table 1).

After FDR correction, the results showed that only Escherichia/Shigella ($p = 0.00032$, $P_{FDR} = 0.0382$, OR = 1.004, 95%CI = 1.002–1.006) was related to EFMR (main). The forest plots, funnel plots, leave-one-out plots, and scatter plots of Escherichia/Shigella proved the stability of the results (Figure 4).

## 3.3 EFMR (secondary)

Our study identified six gut microbiota were found to be associated with EFMR (secondary) in IVW (Figure 3). IVW estimate suggests

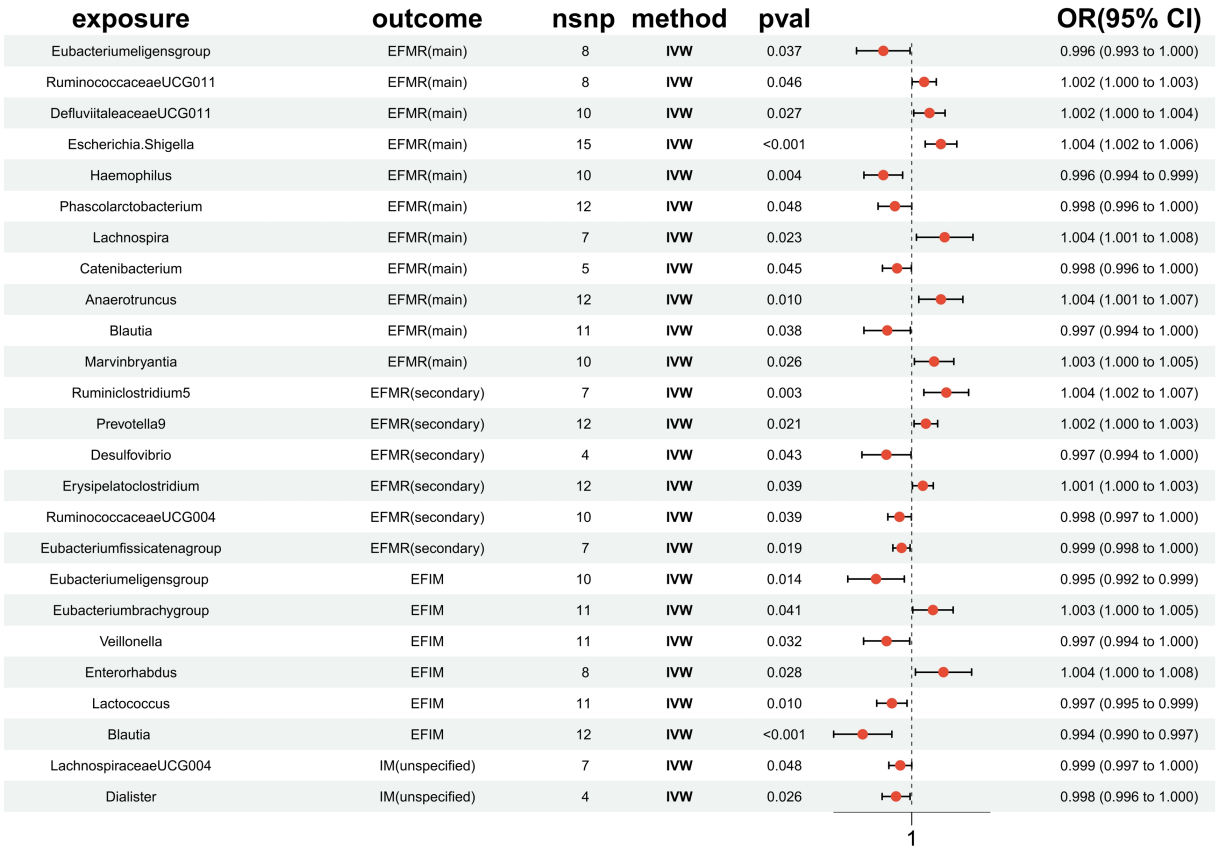


FIGURE 3
MR results of causal effects between gut microbiota and menstrual disorders. *p*-value, OR, odds ratio.

TABLE 1 MR results of causal effects between gut microbiota and EFMR (main).

| Disease type (outcome) | Gut microbiota (exposure) | Method | nSNPs | Beta | SE | *p*-value | OR | 95%CI |
|---|---|---|---|---|---|---|---|---|
| EFMR (main) | Eubacteriumeligens group | IVW | 8 | −0.004 | 0.002 | 0.037 | 0.996 | 0.993–1.000 |
| | RuminococcaceaeUCG011 | IVW | 8 | 0.002 | 0.001 | 0.046 | 1.002 | 1.000–1.003 |
| | DefluviitaleaceaeUCG011 | IVW | 10 | 0.002 | 0.001 | 0.027 | 1.002 | 1.000–1.004 |
| | Escherichia/Shigella | IVW | 15 | 0.004 | 0.001 | 0.0003 | 1.004 | 1.002–1.006 |
| | Haemophilus | IVW | 10 | −0.004 | 0.001 | 0.004 | 0.996 | 0.994–0.999 |
| | Phascolarctobacterium | IVW | 12 | −0.002 | 0.001 | 0.048 | 0.998 | 0.996–1.000 |
| | Lachnospira | IVW | 7 | 0.004 | 0.002 | 0.023 | 1.004 | 1.001–1.008 |
| | Catenibacterium | IVW | 5 | −0.002 | 0.001 | 0.045 | 0.998 | 0.996–1.000 |
| | Anaerotruncus | IVW | 12 | 0.004 | 0.001 | 0.010 | 1.004 | 1.001–1.007 |
| | Blautia | IVW | 11 | −0.003 | 0.002 | 0.038 | 0.997 | 0.994–1.000 |
| | Marvinbryantia | IVW | 10 | 0.003 | 0.001 | 0.026 | 1.003 | 1.000–1.005 |

that *Desulfovibrio* (OR = 0.997, 95%CI = 0.994–1.000, $p = 0.043$), *RuminococcaceaeUCG004* (OR = 0.998, 95%CI = 0.997–1.000, $p = 0.039$), and *Eubacterium fissicatena group* (OR = 0.999, 95%CI = 0.998–1.000, $p = 0.019$) had a protective effect (Table 2). *Ruminiclostridium5* (OR = 1.004, 95%CI = 1.002–1.007, $p = 0.003$), *Prevotella9* (OR = 1.002, 95%CI = 1.000–1.003, $p = 0.021$), and *Erysipelatoclostridium* (OR = 1.001, 95%CI = 1.000–1.003, $p = 0.039$) had a negative effect on this type of menstrual disorders (Table 2).

After FDR correction, we did not find a causal relationship between gut microbiota and EFMR (secondary).

## 3.4 EFIM

Six causal associations from gut microbiota to EFIM were identified by the IVW method (Figure 3). IVW estimate suggests that

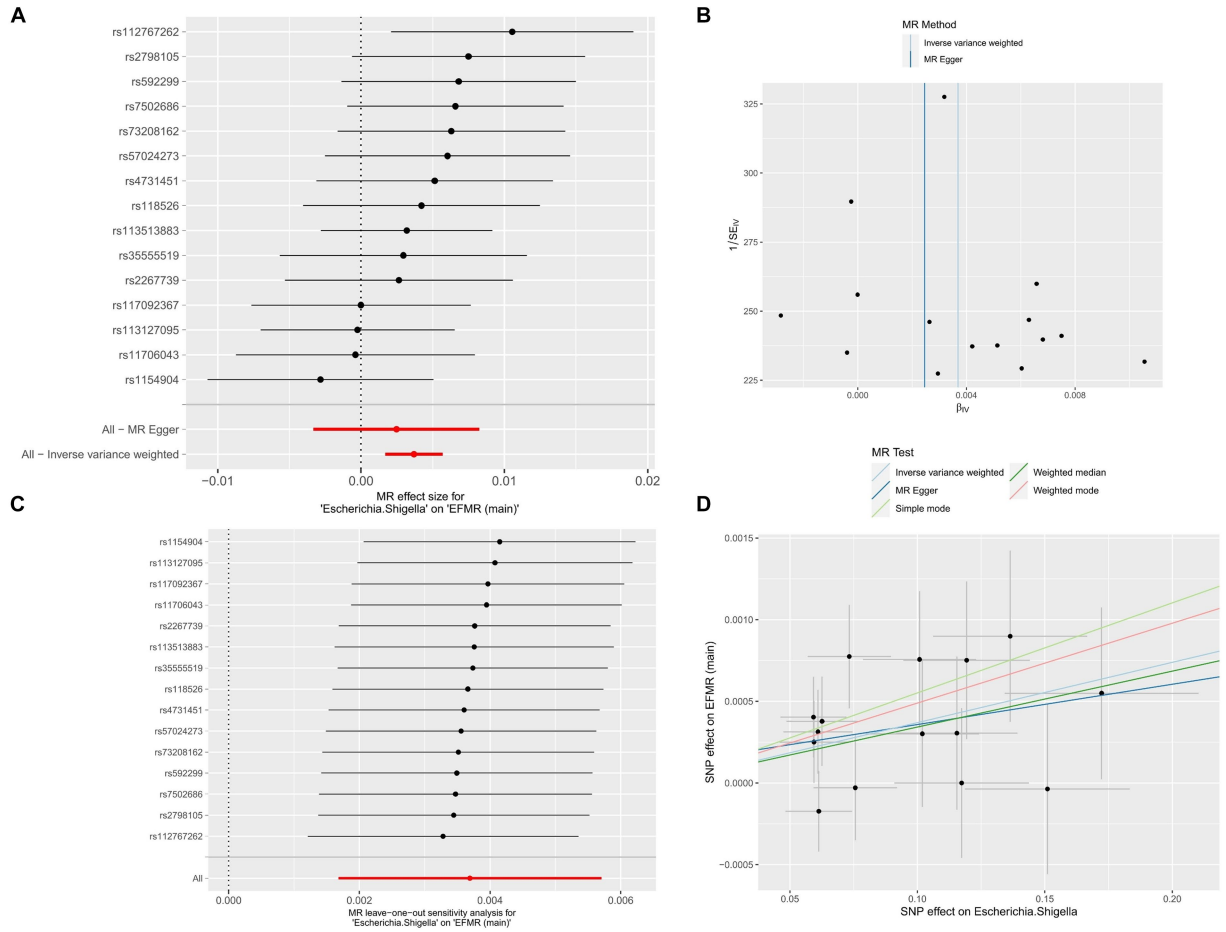


FIGURE 4
MR results of causal effects between Escherichia/Shigella and EFMR (main). **(A)** The forest plot of Escherichia/Shigella on EFMR (main). **(B)** The funnel plot of Escherichia/Shigella on EFMR (main). **(C)** The leave-one-out plot of Escherichia/Shigella on EFMR (main). **(D)** The scatter plot of Escherichia/Shigella on EFMR (main).

TABLE 2 MR results of causal effects between gut microbiota and EFMR (secondary).

| Disease type (outcome) | Gut microbiota (exposure) | Method | nSNPs | Beta | SE | *p*-value | OR | 95%CI |
|---|---|---|---|---|---|---|---|---|
| EFMR (secondary) | Ruminiclostridium5 | IVW | 7 | 0.004 | 0.001 | 0.003 | 1.004 | 1.002–1.007 |
| | Prevotella9 | IVW | 12 | 0.002 | 0.001 | 0.021 | 1.002 | 1.000–1.003 |
| | Desulfovibrio | IVW | 4 | −0.003 | 0.002 | 0.043 | 0.997 | 0.994–1.000 |
| | Erysipelatoclostridium | IVW | 12 | 0.001 | 0.001 | 0.039 | 1.001 | 1.000–1.003 |
| | RuminococcaceaeUCG004 | IVW | 10 | −0.002 | 0.001 | 0.039 | 0.998 | 0.997–1.000 |
| | Eubacteriumfissicatena group | IVW | 7 | −0.001 | 0.001 | 0.019 | 0.999 | 0.998–1.000 |

*Eubacterium eligens group* (OR = 0.995, 95%CI = 0.992–0.999, $p = 0.014$), *Veillonella* (OR = 0.997, 95%CI = 0.994–1.000, $p = 0.032$), *Lactococcus* (OR = 0.997, 95%CI = 0.995–0.999, $p = 0.010$), and *Blautia* (OR = 0.994, 95%CI = 0.990–0.997, $p = 0.001$) had a protective effect on this type of menstrual disorders (Table 3). *Eubacterium brachy group* (OR = 1.003, 95%CI = 1.000–1.005, $p = 0.041$) and *Enterorhabdus* (OR = 1.004, 95%CI = 1.000–1.008, $p = 0.028$) had a negative effect on this type of menstrual disorders (Table 3).

After FDR correction, we did not find a causal relationship between gut microbiota and EFIM.

## 3.5 IM (unspecified)

Two causal associations from gut microbiota to IM (unspecified) were identified (Figure 3). IVW estimate suggests that

TABLE 3 MR results of causal effects between gut microbiota and EFIM.

| Disease type (outcome) | Gut microbiota (exposure) | Method | nSNPs | Beta | SE | *p*-value | OR | 95%CI |
|---|---|---|---|---|---|---|---|---|
| EFIM | Eubacteriumeligens group | IVW | 10 | −0.005 | 0.002 | 0.014 | 0.995 | 0.992–0.999 |
| | Eubacteriumbrachy group | IVW | 11 | 0.003 | 0.001 | 0.041 | 1.003 | 1.000–1.005 |
| | Veillonella | IVW | 11 | −0.003 | 0.002 | 0.032 | 0.997 | 0.994–1.000 |
| | Enterorhabdus | IVW | 8 | 0.004 | 0.002 | 0.028 | 1.004 | 1.000–1.008 |
| | Lactococcus | IVW | 11 | −0.003 | 0.001 | 0.010 | 0.997 | 0.995–0.999 |
| | Blautia | IVW | 12 | −0.006 | 0.002 | 0.001 | 0.994 | 0.990–0.997 |

TABLE 4 MR results of causal effects between gut microbiota and IM.

| Disease type (outcome) | Gut microbiota (exposure) | Method | nSNPs | Beta | SE | *p*-value | OR | 95%CI |
|---|---|---|---|---|---|---|---|---|
| IM (unspecified) | LachnospiraceaeUCG004 | IVW | 7 | −0.001 | 0.001 | 0.048 | 0.999 | 0.997–1.000 |
| | Dialister | IVW | 4 | −0.002 | 0.001 | 0.026 | 0.998 | 0.996–1.000 |

*LachnospiraceaeUCG004* (OR = 0.999, 95%CI = 0.997–1.000, $p = 0.048$) and *Dialister* (OR = 0.998, 95%CI = 0.996–1.000, $p = 0.026$) had a protective effect on this type of menstrual disorders (Table 4).

After FDR correction, we did not find a causal relationship between gut microbiota and IM (unspecified).

## 4 Discussion

In order to determine the causal link between gut microbiota and menstrual disorders, we conducted a two-sample MR analysis in this study using gut microbiota summary statistics from the largest GWAS meta-analysis carried out by the MiBioGen consortium and "Menstrual disorders" summary statistics from the MRC-IEU, NA release data. As shown in our results, a total of 23 different kinds of gut microbiota have an effect on menstrual disorders [*Eubacteriumeligens group*, *Blautia* is repeated in EFMR (main) and EFIM], of which 12 intestinal flora are protective factors for menorrhagia, while the other 11 are risk factors for menorrhagia. While 23 groups of bacteria had a tentative association, only *Escherichia/Shigella* had a significant robust effect. After FDR correction, only *Escherichia/Shigella* was causally associated with menstrual disorders, as it increases, so does the risk of disease.

*Escherichia/Shigella* is an *Enterobacteriaceae* bacterium that has been shown to cause intestinal inflammation and increased intestinal permeability when overexpressed, making it a recognized pathogenic bacterium (Mukherjee et al., 2023). Its secreted lipopolysaccharide induces acute intestinal injury, increases blood–brain barrier permeability, and activates neuroinflammation (Dong et al., 2021). Some scholars have found that the proportion of *Escherichia/Shigella* and the number of *Streptococcus* in intestinal growth, whereas the number of *Akkermansia* and *Ruminococcaceae* decreases in patients with Polycystic ovary syndrome (Liu et al., 2022). An increase in the number of *Escherichia coli* and *Shigella* in the gut microbiome of patients with stage IIIIV endometriosis was found (Ata et al., 2019; Cao et al., 2024). *Escherichia coli* can also cause chronic endometritis (Cao et al., 2024). To our knowledge, this is the first time *Escherichia/Shigella* has been found to negatively affect menstruation. This could provide new ideas for future research and treatment of menstrual disorders.

Ravel and Brotman proposed the term "gut-vagina axis" in 2016 (Ravel and Brotman, 2016). In a previous study, 68% of the 63 bacterial species that were detected in the vagina or rectum had the same genotype, with 44% of the species present in both organs (El Aila et al., 2009), and species-level Spearman correlation coefficient analysis was used to identify individual BV-associated bacteria in the rectum and vagina of pregnant women (Fudaba et al., 2021). Oral probiotic strains were also found in the vagina (Reid et al., 2001; Morelli et al., 2004; Strus et al., 2012; Russo et al., 2018). These findings imply that vaginal germs may be able to be preserved in the rectum.

On the other hand, metabolites generated by the microbiota, such as short-chain fatty acids (SCFAs), may be viewed as collateral players in the gut-vaginal axis. There is no doubt that SCFAs have distinct functions in the gut and vagina (Amabebe and Anumba, 2020). While SCFAs in the vagina are linked to dysfunctional and pro-inflammatory states, SCFAs in the stomach serve advantageous purposes such maintaining barrier function (Aldunate et al., 2015). Due to the systemic circulation can carry SCFAs produced by gut bacteria to other organs (Dalile et al., 2019), it is possible that SCFAs have a role in the vaginal-gut axis. It is believed that vaginal bacteria's production of short-chain fatty acids adds to the dysbiotic environment (Aldunate et al., 2015). Excess short-chain fatty acids may be a possible cause of cervicovaginal inflammation, according to an *in vitro* investigation (Delgado-Diaz et al., 2020). Therefore, vaginal microecological dysregulation brought on by the flow of short-chain fatty acids from the gut to the vagina may cause menstruation abnormalities (Takada et al., 2023).

The estrobolome has the ability to deconjugate hepatically conjugated estrogens in the gastrointestinal system in addition to metabolites. Deconjugated estrogen is then reabsorbed to the systemic

circulation. When circulating estrogen reaches the distal epithelium of the vagina, it modifies the physiological traits of the cells that line the vagina, including the generation of mucus and glycogen. Since glycogen can be a vital source of energy for *Lactobacilli*, increased glycogen promotes *Lactobacillus* dominance in the vagina (Witkin, 2018; Linhares et al., 2019; Takada et al., 2023). Therefore, the number of *Lactobacillus* in the vaginal microbiota can be influenced by the number of bacteria in the gut microbiota that metabolize estrogen.

Evolutionary studies suggest that genes encoding the enzymes that catalyze the metabolism of dopamine, norepinephrine, and serotonin may have been passed from bacteria to host cells during the course of evolution (Iyer et al., 2004). Hormone receptors have even been detected on some microorganisms (Lyte, 1993; Nabeh, 2023). *Escherichia coli* growth depends on the transfer of iron from transferrin to bacteria, which is facilitated by catecholamines (Lyte et al., 2003). This suggests that microorganisms also interact with neurohormones, and we therefore speculate that *Escherichia/Shigella* may cause premenstrual dysphoric disorders by affecting neurohormone secretion, leading to menstrual disorders.

Fungus is also an integral part of the human body. A major member of the human fungal community has been identified as *Candida albicans* (Bradford and Ravel, 2017). *Candida albicans* can change from a commensal to a pathogenic condition when the human immune system is compromised, the intrinsic microbiota is dysregulated, or the mucosal gut barrier is compromised (Vergidis et al., 2016; Pappas et al., 2018). It has been proposed that, to differing degrees, at different phases of biofilm formation, Candida and *Escherichia coli* mutually govern the growth of biofilms (Bandara et al., 2009). *Escherichia coli* lipopolysaccharides directly regulate the production of *in vitro* biofilms, Candida species in particular, stimulating the growth of Pseudohyphae tropicalis and Nearly Naked Yeast, and inhibiting the growth of Pseudohyphae Duchenne. This stimulatory/inhibitory effect may be brought about by modifications in the number of cells inside the formed biofilm, modifications in cellular activity, or modifications in both (Bandara et al., 2009).

Cytoplasmic estrogen receptors found in certain species of *Candida* enable direct transcriptional responses to host hormones (Skowronski and Feldman, 1989). It has been demonstrated that estrogens interfere with neutrophil chemotaxis to the vaginal epithelium (Lasarte et al., 2016), and inhibit Th17 cell differentiation (Chen et al., 2015), resulting in increased host susceptibility to pathogens such as *Candida*. A hyperestrogenic state and raised vaginal pH are hallmarks of the premenstrual luteal phase, which is frequently linked to symptomatic *Candida* vaginitis (Galask, 1988). Researchers found that estrogen signaling increases *Candida albicans*' adherence to vaginal epithelial cells (Tarry et al., 2005). Therefore, *Escherichia coli* may have an effect on estrogen through *Candida albicans*, which needs to be verified by experimental and clinical trials.

In conclusion, we conducted a thorough analysis of the connections between various menstruation disorders and the gut flora. Our findings indicated that EFMR (main) had five positive and six negative causal directions; EFMR (secondary) had three positive and three negative causal directions; EFIM had four positive and two negative causal directions; and IR had two positive causal directions. After FDR correction, the results showed that only *Escherichia/Shigella* was related to menstrual disorders. The methods by which the gut microbiota mediates the development of menstruation problems may become clearer with the help of this study. Future scholars could target *Escherichia/Shigella* for research on menstrual disorders.

## 5 Weak point

The research has certain shortcomings. First, there were no data available at the species level and only a small number of instrumental variables included in the GWAS gut flora statistics. Secondly, we were not able to ascertain if the exposures and outcomes included in this study had overlapping participants in the GWAS data. Third, just the genus level of analysis was done on bacterial taxa. Fourth, a number of gut microbiota were not included in the IV selection phase due to our criterion, which may have caused some results to be overlooked.

## Data availability statement

The datasets presented in this study can be found in online repositories. The names of the repository/repositories and accession number(s) can be found in the article/Supplementary material.

## Ethics statement

This research has been conducted using published studies and consortia providing publicly available summary statistics. All original studies have been approved by the corresponding ethical review board, and the participants have provided informed consent. In addition, no individual-level data was used in this study. Therefore, no new ethical review board approval was required. Written informed consent to participate in this study was not required from the participants or the participants' legal guardians/next of kin in accordance with the national legislation and the institutional requirements.

## Author contributions

YY: Conceptualization, Data curation, Formal analysis, Investigation, Methodology, Software, Supervision, Validation, Visualization, Writing – original draft, Writing – review & editing. HH: Conceptualization, Data curation, Methodology, Software, Supervision, Writing – review & editing. LC: Data curation, Investigation, Methodology, Supervision, Writing – review & editing. HZ: Conceptualization, Data curation, Formal analysis, Funding acquisition, Investigation, Methodology, Project administration, Resources, Software, Supervision, Validation, Visualization, Writing – review & editing.

## Funding

The author(s) declare that no financial support was received for the research, authorship, and/or publication of this article.

## Acknowledgments

We acknowledged the MiBioGen consortium, UK Biobank investigators for making their datasets publicly available and we are

grateful for all the investigators and participants who contributed to those studies. In addition, thanks to Key Laboratory of Blood-stasis-toxin Syndrome of Zhejiang Province for your support.

## Conflict of interest

The authors declare that the research was conducted in the absence of any commercial or financial relationships that could be construed as a potential conflict of interest.

## Publisher's note

All claims expressed in this article are solely those of the authors and do not necessarily represent those of their affiliated organizations, or those of the publisher, the editors and the reviewers. Any product that may be evaluated in this article, or claim that may be made by its manufacturer, is not guaranteed or endorsed by the publisher.

## Supplementary material

The Supplementary material for this article can be found online at: https://www.frontiersin.org/articles/10.3389/fmicb.2024.1321268/full#supplementary-material

SUPPLEMENTARY FIGURE S1
Forest plots of EFMR (main), EFMR (secondary), EFIM, IM(unspecified).

SUPPLEMENTARY FIGURE S2
Funnel plots of EFMR (main), EFMR (secondary), EFIM, IM(unspecified)

SUPPLEMENTARY FIGURE S3
Leave-one-out plots of EFMR (main), EFMR (secondary), EFIM, IM(unspecified).

SUPPLEMENTARY FIGURE S4
Scatter plots of EFMR (main), EFMR (secondary), EFIM, IM(unspecified).

SUPPLEMENTARY TABLE S1
Results of Heterogeneity, Pleiotropy, MR-PRESSO.

SUPPLEMENTARY TABLE S2
MR results of EFMR (main), EFMR (secondary), EFIM, IM(unspecified).

## References


Aldunate, M., Srbinovski, D., Hearps, A. C., Latham, C. F., Ramsland, P. A., Gugasyan, R., et al. (2015). Antimicrobial and immune modulatory effects of lactic acid and short chain fatty acids produced by vaginal microbiota associated with eubiosis and bacterial vaginosis. *Front. Physiol.* 6:164. doi: 10.3389/fphys.2015.00164

Amabebe, E., and Anumba, D. O. C. (2020). Female gut and genital tract microbiota-induced crosstalk and differential effects of short-chain fatty acids on immune sequelae. *Front. Immunol.* 11:2184. doi: 10.3389/fimmu.2020.02184

Ata, B., Yildiz, S., Turkgeldi, E., Brocal, V. P., Dinleyici, E. C., Moya, A., et al. (2019). The Endobiota study: comparison of vaginal, cervical and gut microbiota between women with stage 3/4 endometriosis and healthy controls. *Sci. Rep.* 9:2204. doi: 10.1038/s41598-019-39700-6

Bandara, H. M. H. N., Yau, J. Y. Y., Watt, R. M., Jin, L. J., and Samaranayake, L. P. (2009). Escherichia coli and its lipopolysaccharide modulate *in vitro* Candida biofilm formation. *J. Med. Microbiol.* 58, 1623–1631. doi: 10.1099/jmm.0.012989-0

Bharadwaj, S., Barber, M. D., Graff, L. A., and Shen, B. (2015). Symptomatology of irritable bowel syndrome and inflammatory bowel disease during the menstrual cycle. *Gastroenterol. Rep.* 3, 185–193. doi: 10.1093/gastro/gov010

Bowden, J., Davey Smith, G., and Burgess, S. (2015). Mendelian randomization with invalid instruments: effect estimation and bias detection through Egger regression. *Int. J. Epidemiol.* 44, 512–525. doi: 10.1093/ije/dyv080

Bowden, J., Del Greco, M. F., Minelli, C., Davey Smith, G., Sheehan, N. A., and Thompson, J. R. (2016). Assessing the suitability of summary data for two-sample Mendelian randomization analyses using MR-Egger regression: the role of the I2 statistic. *Int. J. Epidemiol.* 45, 1961–1974. doi: 10.1093/ije/dyw220

Bowden, J., Del Greco, M. F., Minelli, C., Zhao, Q., Lawlor, D. A., Sheehan, N. A., et al. (2019). Improving the accuracy of two-sample summary-data Mendelian randomization: moving beyond the NOME assumption. *Int. J. Epidemiol.* 48, 728–742. doi: 10.1093/ije/dyy258

Bowden, J., and Holmes, M. V. (2019). Meta-analysis and Mendelian randomization: a review. *Res. Synth. Methods* 10, 486–496. doi: 10.1002/jrsm.1346

Bradford, L. L., and Ravel, J. (2017). The vaginal mycobiome: a contemporary perspective on fungi in women's health and diseases. *Virulence* 8, 342–351. doi: 10.1080/21505594.2016.1237332

Burgess, S., and Thompson, S. G. (2017). Interpreting findings from Mendelian randomization using the MR-Egger method. *Eur. J. Epidemiol.* 32, 377–389. doi: 10.1007/s10654-017-0255-x

Cao, W., Fu, X., Zhou, J., Qi, Q., Ye, F., Li, L., et al. (2024). The effect of the female genital tract and gut microbiome on reproductive dysfunction. *Biosci. Trends* 17, 458–474. doi: 10.5582/bst.2023.01133

Chen, C., Carpenter, J. S., Shin, A., Cross, T.-W. L., Ye, Y., Mitchell, C., et al. (2023). Dysmenorrhea symptoms and gut microbiome: a pilot study. *J. Pain* 24, 1–2. doi: 10.1016/j.jpain.2023.02.009

Chen, W., Chen, M., Tang, H., Wei, W., Shao, P., Dou, S., et al. (2023). Advances in diagnosis and treatment of perimenopausal syndrome. *Open Life Sci.* 18:20220754. doi: 10.1515/biol-2022-0754

Chen, R.-Y., Fan, Y.-M., Zhang, Q., Liu, S., Li, Q., Ke, G.-L., et al. (2015). Estradiol inhibits Th17 cell differentiation through inhibition of *RORγT* transcription by recruiting the ERα/REA complex to estrogen response elements of the *RORγT* promoter. *J. Immunol.* 194, 4019–4028. doi: 10.4049/jimmunol.1400806

Chen, C., Song, X., Wei, W., Zhong, H., Dai, J., Lan, Z., et al. (2017). The microbiota continuum along the female reproductive tract and its relation to uterine-related diseases. *Nat. Commun.* 8:875. doi: 10.1038/s41467-017-00901-0

Dalile, B., Van Oudenhove, L., Vervliet, B., and Verbeke, K. (2019). The role of short-chain fatty acids in microbiota–gut–brain communication. *Nat. Rev. Gastroenterol. Hepatol.* 16, 461–478. doi: 10.1038/s41575-019-0157-3

Delgado-Diaz, D. J., Tyssen, D., Hayward, J. A., Gugasyan, R., Hearps, A. C., and Tachedjian, G. (2020). Distinct immune responses elicited from Cervicovaginal epithelial cells by lactic acid and short chain fatty acids associated with optimal and non-optimal vaginal microbiota. *Front. Cell. Infect. Microbiol.* 9:446. doi: 10.3389/fcimb.2019.00446

Dong, S., Jiao, J., Jia, S., Li, G., Zhang, W., Yang, K., et al. (2021). 16S rDNA full-length assembly sequencing technology analysis of intestinal microbiome in polycystic ovary syndrome. *Front. Cell. Infect. Microbiol.* 11:634981. doi: 10.3389/fcimb.2021.634981

El Aila, N. A., Tency, I., Claeys, G., Verstraelen, H., Saerens, B., Dos Santos, L., et al. (2009). Identification and genotyping of bacteria from paired vaginal and rectal samples from pregnant women indicates similarity between vaginal and rectal microflora. *BMC Infect. Dis.* 9:167. doi: 10.1186/1471-2334-9-167

Flores, R., Shi, J., Fuhrman, B., Xu, X., Veenstra, T. D., Gail, M. H., et al. (2012). Fecal microbial determinants of fecal and systemic estrogens and estrogen metabolites: a cross-sectional study. *J. Transl. Med.* 10:253. doi: 10.1186/1479-5876-10-253

Fudaba, M., Kamiya, T., Tachibana, D., Koyama, M., and Ohtani, N. (2021). Bioinformatics analysis of Oral, vaginal, and rectal microbial profiles during pregnancy: a pilot study on the bacterial co-residence in pregnant women. *Microorganisms* 9:1027. doi: 10.3390/microorganisms9051027

Galask, R. P. (1988). Vaginal colonization by bacteria and yeast. *Am. J. Obstet. Gynecol.* 158, 993–995. doi: 10.1016/0002-9378(88)90111-1

Greco, M. F. D., Minelli, C., Sheehan, N. A., and Thompson, J. R. (2015). Detecting pleiotropy in Mendelian randomisation studies with summary data and a continuous outcome. *Stat. Med.* 34, 2926–2940. doi: 10.1002/sim.6522

Grobeisen-Duque, O., Mora-Vargas, C. D., Aguilera-Arreola, M. G., and Helguera-Repetto, A. C. (2023). Cycle biodynamics of Women's microbiome in the urinary and reproductive systems. *J. Clin. Med.* 12:4003. doi: 10.3390/jcm12124003

Holdcroft, A. M., Ireland, D. J., and Payne, M. S. (2023). The vaginal microbiome in health and disease-what role do common intimate hygiene practices play? *Microorganisms* 11:298. doi: 10.3390/microorganisms11020298

Huang, F., Cao, Y., Liang, J., Tang, R., Wu, S., Zhang, P., et al. (2024). The influence of the gut microbiome on ovarian aging. *Gut Microbes* 16:2295394. doi: 10.1080/19490976.2023.2295394

Iyer, L. M., Aravind, L., Coon, S. L., Klein, D. C., and Koonin, E. V. (2004). Evolution of cell–cell signaling in animals: did late horizontal gene transfer from bacteria have a role? *Trends Genet.* 20, 292–299. doi: 10.1016/j.tig.2004.05.007

Krog, M. C., Hugerth, L. W., Fransson, E., Bashir, Z., Nyboe Andersen, A., Edfeldt, G., et al. (2022). The healthy female microbiome across body sites: effect of hormonal contraceptives and the menstrual cycle. *Hum. Reprod.* 37, 1525–1543. doi: 10.1093/humrep/deac094

Kurilshikov, A., Medina-Gomez, C., Bacigalupe, R., Radjabzadeh, D., Wang, J., Demirkan, A., et al. (2021). Large-scale association analyses identify host factors influencing human gut microbiome composition. *Nat. Genet.* 53, 156–165. doi: 10.1038/s41588-020-00763-1

Lasarte, S., Samaniego, R., Salinas-Muñoz, L., Guia-Gonzalez, M. A., Weiss, L. A., Mercader, E., et al. (2016). Sex hormones coordinate neutrophil immunity in the vagina by controlling chemokine gradients. *J. Infect. Dis.* 213, 476–484. doi: 10.1093/infdis/jiv402

Lindheim, L., Bashir, M., Münzker, J., Trummer, C., Zachhuber, V., Leber, B., et al. (2017). Alterations in gut microbiome composition and barrier function are associated with reproductive and metabolic defects in women with polycystic ovary syndrome (PCOS): a pilot study. *PLoS One* 12:e0168390. doi: 10.1371/journal.pone.0168390

Linhares, I. M., Sisti, G., Minis, E., De Freitas, G. B., Moron, A. F., and Witkin, S. S. (2019). Contribution of epithelial cells to defense mechanisms in the human vagina. *Curr. Infect. Dis. Rep.* 21:30. doi: 10.1007/s11908-019-0686-5

Liu, L., Wang, H., Zhang, H., Chen, X., Zhang, Y., Wu, J., et al. (2022). Toward a deeper understanding of gut microbiome in depression: the promise of clinical applicability. *Adv. Sci.* 9:2203707. doi: 10.1002/advs.202203707

Long, Y., Tang, L., Zhou, Y., Zhao, S., and Zhu, H. (2023). Causal relationship between gut microbiota and cancers: a two-sample Mendelian randomisation study. *BMC Med.* 21:66. doi: 10.1186/s12916-023-02761-6

Lyte, M. (1993). The role of microbial endocrinology in infectious disease. *J. Endocrinol.* 137, 343–345. doi: 10.1677/joe.0.1370343

Lyte, M., Freestone, P. P., Neal, C. P., Olson, B. A., Haigh, R. D., Bayston, R., et al. (2003). Stimulation of *Staphylococcus epidermidis* growth and biofilm formation by catecholamine inotropes. *Lancet* 361, 130–135. doi: 10.1016/S0140-6736(03)12231-3

MiBioGen Consortium InitiativeWang, J., Kurilshikov, A., Radjabzadeh, D., Turpin, W., Croitoru, K., et al. (2018). Meta-analysis of human genome-microbiome association studies: the MiBioGen consortium initiative. *Microbiome* 6:101. doi: 10.1186/s40168-018-0479-3

Mohib, A., Zafar, A., Najam, A., Tanveer, H., and Rehman, R. (2018). Premenstrual syndrome: existence, knowledge, and attitude among female university students in Karachi. *Cureus* 10:e2290. doi: 10.7759/cureus.2290

Morelli, L., Zonenenschain, D., Del Piano, M., and Cognein, P. (2004). Utilization of the intestinal tract as a delivery system for urogenital probiotics. *J. Clin. Gastroenterol.* 38, S107–S110. doi: 10.1097/01.mcg.0000128938.32835.98

Mukherjee, A. G., Wanjari, U. R., Kannampuzha, S., Murali, R., Namachivayam, A., Ganesan, R., et al. (2023). The implication of mechanistic approaches and the role of the microbiome in polycystic ovary syndrome (PCOS): a review. *Meta* 13:129. doi: 10.3390/metabo13010129

Nabeh, O. A. (2023). New insights on the impact of gut microbiota on premenstrual disorders. Will probiotics solve this mystery? *Life Sci.* 321:121606. doi: 10.1016/j.lfs.2023.121606

Pappas, P. G., Lionakis, M. S., Arendrup, M. C., Ostrosky-Zeichner, L., and Kullberg, B. J. (2018). Invasive candidiasis. *Nat. Rev. Dis. Primers* 4:18026. doi: 10.1038/nrdp.2018.26

Parida, S., and Sharma, D. (2019). The microbiome–estrogen connection and breast Cancer risk. *Cell* 8:1642. doi: 10.3390/cells8121642

Ravel, J., and Brotman, R. M. (2016). Translating the vaginal microbiome: gaps and challenges. *Genome Med.* 8:35. doi: 10.1186/s13073-016-0291-2

Reid, G., Bruce, A. W., Fraser, N., Heinemann, C., Owen, J., and Henning, B. (2001). Oral probiotics can resolve urogenital infections. *FEMS Immunol. Med. Microbiol.* 30, 49–52. doi: 10.1111/j.1574-695X.2001.tb01549.x

Russo, R., Edu, A., and De Seta, F. (2018). Study on the effects of an oral lactobacilli and lactoferrin complex in women with intermediate vaginal microbiota. *Arch. Gynecol. Obstet.* 298, 139–145. doi: 10.1007/s00404-018-4771-z

Sher, N. M., Nazli, R., Zafar, H., and Fatima, S. (2021). Effects of lipid based multiple micronutrients supplement on the birth outcome of underweight pre-eclamptic women: a randomized clinical trial. *Pak. J. Med. Sci.* 38, 219–226. doi: 10.12669/pjms.38.1.4396

Skowronski, R., and Feldman, D. (1989). Characterization of an estrogen-binding protein in the yeast *Candida albicans* *. *Endocrinology* 124, 1965–1972. doi: 10.1210/endo-124-4-1965

Skrivankova, V. W., Richmond, R. C., Woolf, B. A. R., Davies, N. M., Swanson, S. A., VanderWeele, T. J., et al. (2021a). Strengthening the reporting of observational studies in epidemiology using mendelian randomization (STROBE-MR): explanation and elaboration. *BMJ* 375:n2233. doi: 10.1136/bmj.n2233

Skrivankova, V. W., Richmond, R. C., Woolf, B. A. R., Yarmolinsky, J., Davies, N. M., Swanson, S. A., et al. (2021b). Strengthening the reporting of observational studies in epidemiology using Mendelian randomization: the STROBE-MR statement. *JAMA* 326, 1614–1621. doi: 10.1001/jama.2021.18236

Song, S. D., Acharya, K. D., Zhu, J. E., Deveney, C. M., Walther-Antonio, M. R. S., Tetel, M. J., et al. (2020). Daily vaginal microbiota fluctuations associated with natural hormonal cycle, contraceptives, diet, and exercise. *mSphere* 5, e00593–e00520. doi: 10.1128/mSphere.00593-20

Strus, M., Chmielarczyk, A., Kochan, P., Adamski, P., Chełmicki, Z., Chełmicki, A., et al. (2012). Studies on the effects of probiotic Lactobacillus mixture given orally on vaginal and rectal colonization and on parameters of vaginal health in women with intermediate vaginal flora. *Eur. J. Obstet. Gynecol. Reprod. Biol.* 163, 210–215. doi: 10.1016/j.ejogrb.2012.05.001

Takada, K., Melnikov, V. G., Kobayashi, R., Komine-Aizawa, S., Tsuji, N. M., and Hayakawa, S. (2023). Female reproductive tract-organ axes. *Front. Immunol.* 14:1110001. doi: 10.3389/fimmu.2023.1110001

Tarry, W., Fisher, M., Shen, S., and Mawhinney, M. (2005). *Candida Albicans*: the estrogen target for vaginal colonization. *J. Surg. Res.* 129, 278–282. doi: 10.1016/j.jss.2005.05.019

Tremellen, K., and Pearce, K. (2012). Dysbiosis of gut microbiota (DOGMA) – a novel theory for the development of polycystic ovarian syndrome. *Med. Hypotheses* 79, 104–112. doi: 10.1016/j.mehy.2012.04.016

Vergidis, P., Clancy, C. J., Shields, R. K., Park, S. Y., Wildfeuer, B. N., Simmons, R. L., et al. (2016). Intra-abdominal candidiasis: the importance of early source control and antifungal treatment. *PLoS One* 11:e0153247. doi: 10.1371/journal.pone.0153247

Vieira, A. T., Castelo, P. M., Ribeiro, D. A., and Ferreira, C. M. (2017). Influence of Oral and gut microbiota in the health of menopausal women. *Front. Microbiol.* 8:1884. doi: 10.3389/fmicb.2017.01884

Visscher, P. M., Wray, N. R., Zhang, Q., Sklar, P., McCarthy, M. I., Brown, M. A., et al. (2017). 10 years of GWAS discovery: biology, function, and translation. *Am. J. Hum. Genet.* 101, 5–22. doi: 10.1016/j.ajhg.2017.06.005

Witkin, S. S. (2018). Lactic acid alleviates stress: good for female genital tract homeostasis, bad for protection against malignancy. *Cell Stress Chaperones* 23, 297–302. doi: 10.1007/s12192-017-0852-3

Zhao, X., Jiang, Y., Xi, H., Chen, L., and Feng, X. (2020). Exploration of the relationship between gut microbiota and polycystic ovary syndrome (PCOS): a review. *Geburtshilfe Frauenheilkd.* 80, 161–171. doi: 10.1055/a-1081-2036

Zhou, L., Ni, Z., Cheng, W., Yu, J., Sun, S., Zhai, D., et al. (2020). Characteristic gut microbiota and predicted metabolic functions in women with PCOS. *Endocr. Connect.* 9, 63–73. doi: 10.1530/EC-19-0522

frontiers | Frontiers in Microbiology

TYPE Original Research
PUBLISHED 12 March 2024
DOI 10.3389/fmicb.2024.1357415



OPEN ACCESS

EDITED BY
Karolina Skonieczna-Żydecka,
Pomeranian Medical University, Poland

REVIEWED BY
Chuanfa Liu,
The Chinese University of Hong Kong, China
Yaotong Hao,
Hebei Agricultural University, China

*CORRESPONDENCE
Tongzuo Zhang
✉ zhangtz@nwipb.cas.cn

RECEIVED 18 December 2023
ACCEPTED 26 February 2024
PUBLISHED 12 March 2024

CITATION
Gao H, Chi X, Song P, Gu H, Xu B, Cai Z, Jiang F, Li B and Zhang T (2024) Maintaining the native gut microbiota of bharal (*Pseudois nayaur*) is crucial in *ex situ* conservation.
*Front. Microbiol.* 15:1357415.
doi: 10.3389/fmicb.2024.1357415



# Maintaining the native gut microbiota of bharal (*Pseudois nayaur*) is crucial in *ex situ* conservation

Hongmei Gao[1,2], Xiangwen Chi[3], Pengfei Song[1,2,4], Haifeng Gu[1,2], Bo Xu[1,2,4], Zhenyuan Cai[1,2], Feng Jiang[1,2], Bin Li[1,2,4] and Tongzuo Zhang[1,2]*

[1]Key Laboratory of Adaptation and Evolution of Plateau Biota, Northwest Institute of Plateau Biology, Chinese Academy of Sciences, Xining, Qinghai, China, [2]Qinghai Provincial Key Laboratory of Animal Ecological Genomics, Xining, Qinghai, China, [3]Students' Affairs Division, Qinghai University, Xining, China, [4]College of Life Sciences, University of Chinese Academy of Sciences, Beijing, China

As wildlife protection continue to strengthen, research on the gut microbiota of wildlife is increasing. Carrying out conservation and research on endangered species in the Qinghai Tibet Plateau plays an important role in global biodiversity conservation. This study utilized 16S rRNA sequencing of fecal samples to investigate the composition, function, and changes of the gut microbiota of bharal in different environments, seasons, and genders. The results showed that Firmicutes and Bacteroidota were the dominant phyla and *UCG-005*, *Bacteroides*, *UCG-010* were the dominant genera of bharal. In the wild, the abundance of Firmicutes increased which was conducive to the decomposition and utilization of cellulose, hemicellulose, and carbohydrate. Due to the variety of food types and nutrition in different seasons, the composition and function of gut microbiota were obviously different between genders. Compared with zoo, higher alpha diversity, a more complex gut microbiota network structure, and stronger metabolic function were conducive bharal to adapting to the wild environment. In the zoo, captive bharals were fed foods rich in high fat and protein, which increased the abundance of Bacteroidota and reduced the alpha diversity of gut microbiota. A fixed diet unified the gut microbiota between genders of bharal. It is very important to pay attention to the impact of captive environments and maintain the native gut microbiota of wildlife.

KEYWORDS

**adaption, bharal (*Pseudois nayaur*), *ex situ* conservation, gut microbiota, Qinghai–Tibet Plateau**

## 1 Introduction

The Qinghai–Tibet Plateau holds a significant place in the terrestrial ecosystem of the planet due to its distinctive geography. This physical geography unit has fostered a wealth of wildlife resources, making it a crucial area for biodiversity conservation and research, not only in China but also the world (Wang et al., 2015). However, with the global climate change, the warming rate of this region has been twice as fast as the global average, leading to a severe biodiversity crisis in this area, even more severe than other regions (Luo et al., 2015). Therefore, it is crucial to carry out conservation and research on endangered species in the Qinghai–Tibet

Plateau to address the decreasing biodiversity issues in China and the world.

To better protect endangered wildlife, China government continuously strengthen the construction of both *in situ* conservation and *ex situ* conservation (Xu et al., 2019). Zoos as important places for *ex situ* conservation, it is a typical artificial enclosure environment. People provides nutritious food for wildlife, and frequent disinfection and sterilization, eliminating all pathogenic and harmful bacteria in environment. However, studies have shown that in an environment where "industrialization" environmental factors are increasing rapidly, they can seriously affect the composition and transmission of animal gut microbiota (Sonnenburg and Sonnenburg, 2019). We speculate that wildlife in zoos is often fed industrial foods such as refined feed, which may lead to imbalances in their gut microbiota and have negative impacts on their health. In a healthy state, the microbial community in the animal gastrointestinal tract remains relatively stable and plays a crucial role in regulating nutritional balance, energy conversion, immune response, adaptive evolution, and growth and development (Simpson et al., 2005; Ezenwa and Gerardo, 2012; Hicks et al., 2018). The gut microbiota has strong plasticity, and food (Ren et al., 2017), season (Gomez et al., 2016), genetic factors (Gomez et al., 2015), and habitat (Amato et al., 2013) can affect their diversity and function.

The bharal (*Pseudois nayaur*), belonging to the Cetartiodactyla, Bovidae, Caprinae, and Pseudois, is a Class II key protected wildlife in China. As a typical alpine animal, bharal is widely distributed and abundant species on the Qinghai–Tibet Plateau and its surrounding areas (Schaller, 1977). It also serves as the main prey for rare carnivores such as snow leopard, which is crucial for maintaining the stability of the ecosystem on the Qinghai–Tibet Plateau and protecting species diversity. In this study, we utilized 16S rRNA gene amplification technology to conduct high-throughput sequencing on fecal samples and discuss the composition, diversity, and function differences of gut microbiota in bharal under various factors. Conducting research on the gut microbiota and function of captive endangered wildlife is not only of great significance for the protection of wildlife, but also provides a new theoretical basis for the future health management of wildlife.

# 2 Materials and methods

## 2.1 Sample collection

In January 2018, 52 fresh fecal samples (WW) of wild bharal were collected from Huashixia Township, Maduo County, Qinghai Province, China. In August of the same year, we collected 45 bharal fecal samples (SW) from the same area. At the same time, we collected 22 fecal samples (WC and SC) of captive bharal at the Qinghai–Tibet Plateau Wildlife Park (longitude: 101.732657, latitude: 36.627469). The freshness of the samples was assessed based on the color and degree of air drying of the feces to ensure high-quality samples. We extracted DNA from the surface of bharal fecal samples using DNeasy Blood & Tissue Kit (QIAGEN), and used sex identification primers (SE47: CAGCCAACCTCCCTCTGC, SE48: CCCGCTTGGCTTGTCTG TTGC) (Weikard et al., 2006) for PCR amplification. The PCR amplification reaction conditions were pre denatured at 94°C for 5 min, Denaturation at 95°C for 30 s, annealing at 60°C for 1 min, and extension at 72°C for 10 min, 30 cycles. Two stripes for male and one stripe for female. We identified the gender of the samples and selected 66 of them for subsequent experiments, including WWM (WW group 17 males), WWF (WW group 13 females), SWM (SW group 4 males), SWF (SW group 10 females), WCM (WC group 8 males), WCF (WC group 3 females), SCM (SC group 8 males), and SCF (SC group 3 females).

## 2.2 Sequencing and annotation

Genomic DNA was extracted from 66 fecal samples using the CTAB method (Yan et al., 2008). The purity and concentration of DNA were tested, and the samples were diluted to 1 ng $\mu l^{-1}$ with sterile water. Complete PCR amplification (515F and 806R), product mixing and purification. The NEBNext® Ultra™ The IIDNA Library Prep Kit was used for library construction, and the constructed library was quantified using Qubit and Q-PCR. After library qualification, the Ion Torrent S5 XL was used for machine sequencing. Split each sample data from the offline data based on the barcode sequence and PCR amplification primer sequence. The barcode and primer sequence were removed, and used FLASH (V1.2.11) (Magoč and Salzberg, 2011) software concatenated the reads of the sample to obtain Raw Tags. Subsequently, Fastp software was used to perform quality control on the raw tags obtained, resulting in high-quality Clean Tags. Finally, we used Usearch software to compare clean tags with the database to detect and remove chimeras (Haas et al., 2011), and effective Tags were obtained. At same time, we used the DADA2 module in QIIME2 software to reduce the noise and filtered out sequences with an abundance less than 5 to obtain the Amplicon Sequence Variables (ASVs) information table. Next, we used the classify sklearn module to compare the obtained ASVs with the Silva138.1 database and obtain species information for each ASV. QIIME2's classify sklearn algorithm (Bokulich et al., 2018) was used to annotate each ASV with a pre trained Naive Bayes classifier, and obtained the corresponding species information and the distribution of species based on abundance.

At the same time, alpha diversity, and the abundance of ASVs were also calculated to determine species richness and evenness within each sample. Phylogenetic trees were constructed by aligning multiple sequences of ASVs, and community structure differences between groups were explored using PCoA (Principal Co-ordinates Analysis) and NMDS (Non-metric Multidimensional Scaling). Tax4Fun functional prediction was achieved using the nearest neighbor method based on minimum 16S rRNA sequence similarity. Specifically, the entire 16S rRNA gene sequence was extracted from prokaryotic organisms in the KEGG database and compared to the SILVA SSU Ref NR database using the BLASTN algorithm (BLAST bitscore >1,500) to establish a correlation matrix. The KEGG database was annotated using the UProC and PAUDA methods, and the entire genome functional information of prokaryotes was assigned to the SILVA database, enabling functional annotation of the SILVA database.

## 2.3 Data analysis

Alpha diversity can reflect the diversity of gut microbiota composition, and we choose Observed_Otus index (the number of observed specifications) to reflect the microbial community richness,

Shannon index to reflect the microbial community diversity, and Pielou_e index (Pielou's evenness index) to reflect the species evenness of microbial community. We used Qiime2 to calculate these alpha diversity indexes and plot rarefaction curves. Wilcoxon rank sum test was used to compare the alpha diversity indices among different groups to determine significant differences. To compare β diversity among groups, we used two similarity distance algorithms, Unweighted Unifrac, and Weighted Unifrac to calculate the distance between each sample at the ASVs level. An Anosim (analysis of similarities) and Adonis (permutational manova) were used to perform inter group (SCF-SCM, SWF-SWM, WCF-WCM, and WWF-WWM) difference tests (R Software, Version 3.5.3) (packages "vegan"). All species composition and functional abundance data were tested for normality using the Shapiro–Wilk test function in the *R*. Results with a *value of p* greater than 0.05 indicate that our data distribution follows normality. *T*-tests were used to analyze differences in the gut microbiota of bharal at the phylum and genus levels, based on factors such as environment, gender, and season. Due to unequal variances when comparing two groups, bilateral tests were chosen. We performed co-occurrence network analysis at the genus level and excluded genera with relative abundance less than 0.01 to reduce the impact of rare bacterial genera on the results. After calculating the network diagram in R (packages "igraph,"), we used Gephi (V0.10.1) software to adjust the image and calculated parameters such as average degree, average weighted degree, network diameter, average path length, density, and so on. Based on the results of modularity, we determined the size and color of each node in the network diagram. Other plots shown in this study were drawn using R (Version 3.5.3) and various software packages including "ggplot2," "reshape2" (Stacked histograms), "VennDiagram" (Petal diagram), "ggpubr" (box plot), and "vegan," "ggplot2" and "ade4" (PCoA and NMDS).

# 3 Results

## 3.1 Overview of gut microbiota in bharal

After sequencing 66 bharal fecal samples and filtering out low-quality base sequences, we obtained a total of 5,577,112 raw data for preliminary quality control. After filtering out chimeras, 5,236,180 high-quality sequences (clean reads) were used for subsequent analysis, with an average read length of 370 bp. The percentage of clean reads to raw reads was 93.92%. We randomly selected sequencing data from bharal fecal samples as the horizontal axis, and used microbial richness and community evenness index (at the ASVs level) as the vertical axis to draw rarefaction curve for bharal sequencing samples. As the sequencing depth continues to increase, the actual observed values of ASVs continue to rise (Figure 1A) and community evenness continue to decline (Figure 1B). When the sequencing quantity was 15,000, the curve gradually flattens out, and indicating that the quantity and quality of this sequencing were reliable, and the sequencing depth was sufficient to obtain most of the microbial information in the bharal fecal samples. The sequencing results can well reflect the diversity of gut microbiota in different environments, seasons, and genders of bharal.

In total 5,650 effective ASVs were identified in all samples, among them, the number of ASVs in the WWF (896.27 ± 112.91, mean ± SD) was the highest, followed by WWM (874.4 ± 98.26), WCM (775.88 ± 89.17), WCF (763 ± 49.07), SWM (536.5 ± 36.88), SWF (525.6 ± 55.64), SCM (427.5 ± 111.38), and SCF (320.67 ± 10.37), respectively. Among these groups, only 109 were shared, representing a mere 1.93% of the total ASVs. The highest proportion of ASVs were to be unique to WWM, with 1,582, accounting for 28% of the total ASVs. Subsequently, WWF (1,152, 20.39%), SWF (805, 14.25%), WCM (747, 13.22%), SCM (520, 9.2%), SWM (370, 6.55%), WCF (232, 4.11%), and SCF (133, 2.35%) were also identified (Figure 1C).

## 3.2 Composition and abundance analysis of gut microbiota in bharal

At the phylum level, the top 10 phyla of bacteria accounted for 98.17% of the gut microbiota. Firmicutes made up the highest proportion of the total bacterial content at 63.85% ± 10.87% (mean ± SD), followed by Bacteroidota (31.17% ± 9.62%), Verrucomicrobiota (0.90% ± 0.95%), Proteobacteria (0.78% ± 1.31%), Actinobacteriota (0.56% ± 0.75%), Spirochaeta (0.44% ± 0.61%), Cyanobacteria (0.21% ± 0.20%) Euryarchaeota (0.10% ± 0.17%), Campilobacterota (0.09% ± 0.19%), and Fibrobacterota (0.08% ± 0.20%). At the genus level, the top 10 genera were *UCG-005* (11.92% ± 3.72%), *Bacteroides* (7.82% ± 3.25%), *UCG-010* (7.23% ± 4.29%), *Alistipes* (5.72% ± 2.34%), *Rikenellaceae_RC9_gut_group* (5.45% ± 2.46%), *Christensenellaceae_R-7_group* (4.69% ± 2.32%), *RF39* (4.14% ± 2.10%), *Clostridia_UCG-014* (2.98% ± 1.91%), *F082* (2.47% ± 1.88%), and *Ruminococcus* (0.72% ± 0.63%). To visually represent the distribution of the top 10 bacterial in each sample, we created stacked histograms showing the relative abundance of gut microbiota at phylum level and genus level for each group (Figures 1D,E).

According to the functional predictions, Metabolism (ME) was the most important function at level 1 (Figure 2A), accounting for 45.30% ± 0.47% of the total functions, followed by Genetic Information Processing (GIP) (22.86% ± 0.15%), Environmental Information Processing (EIP) (12.85% ± 0.29%), Cellular Processes (CP) (8.47% ± 0.22%), Human Diseases (HD) (2.71% ± 0.04%), and Organismal Systems (OS) (1.97% ± 0.04%). At level 2 (Figure 2B), we conducted a comparative analysis of the main metabolic functions, including Carbohydrate Metabolism (CM) (11.41% ± 0.11%), Amino Acid Metabolism (ACM) (9.36% ± 0.12%), Energy Metabolism (EM) (4.43% ± 0.03%), Nucleotide Metabolism (NM) (4.13% ± 0.03%), Glycan Biosynthesis and Metabolism (GBM) (3.28% ± 0.27%), Metabolism of Cofactors and Vitamins (MCV) (3.14% ± 0.04%), Enzyme Families (EF) (2.41% ± 0.04%), Lipid Metabolism (LM) (2.34% ± 0.08%), Biosynthesis of Other Secondary Metabolites (BOSE) (1.46% ± 0.05%), Metabolism of Other Amino Acids (MOAA) (1.41% ± 0.03%), Xenobiotics Biodegradation and Metabolism (XBM) (0.99% ± 0.06%) and Metabolism of Terpenoids and Polyketides (MTP) (0.94% ± 0.04%).

## 3.3 Analysis of differences between different groups

In the PCoA analysis, for the captive environment, samples from each group clustered, summer and winter groups were clearly separated, but the separation of samples between different gender

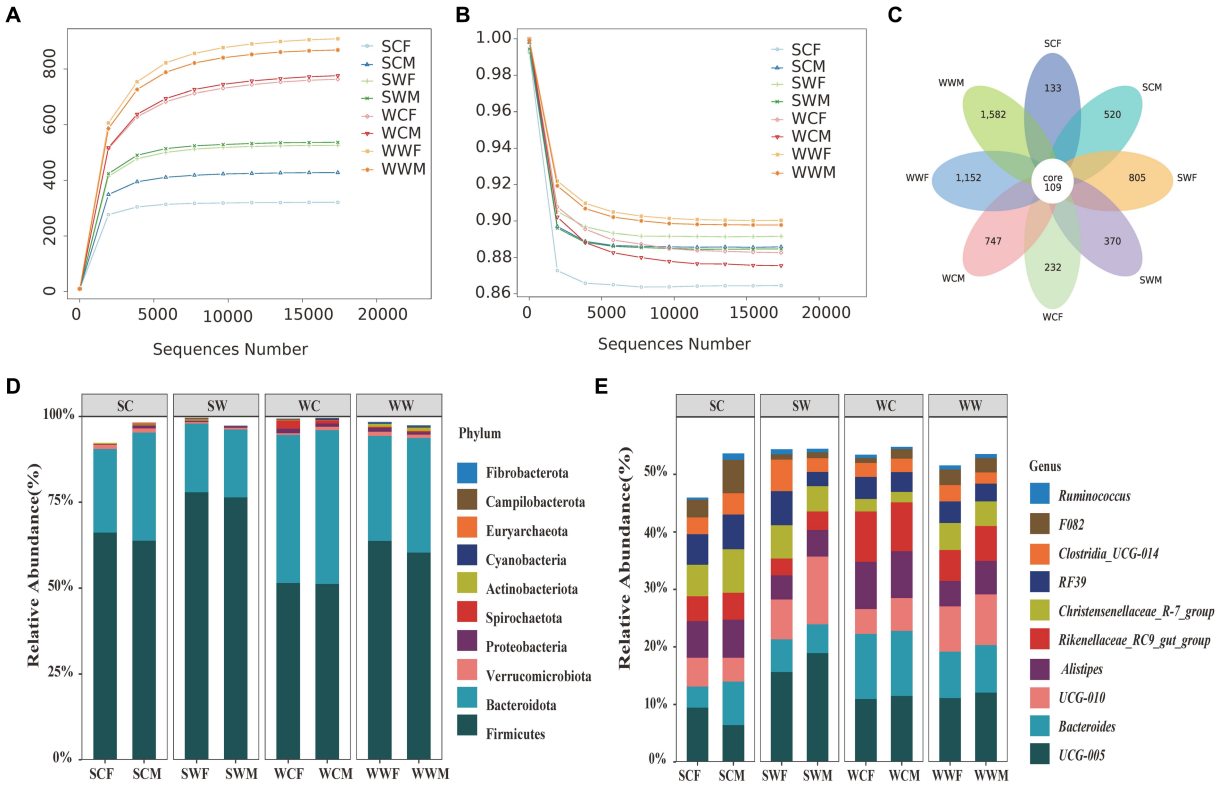


FIGURE 1
Rarefaction curves of community richness **(A)** and community evenness **(B)** of gut microbiome in bharal. Petal diagram of the number of ASVs among different groups **(C)**. Stacked histograms of the relative abundance of gut microbiota at phylum level **(D)** and genus level **(E)** of bharal.

groups were no significant difference during the same season (Figure 3A). In the wild environment, the summer and winter samples were clearly separated (Figure 3B), but within the same season, the samples of different gender groups were more distinctly separated in summer (Figure 3C), whereas they were mixed in winter (Figure 3D). In the NMDS analysis, the stress values are 0.052, 0.092, 0.079, and 0.071 (Figures 3E–H), respectively, which accurately reflected the degree of difference between samples. These prove that our grouping was reasonable and the difference results were reliable. The Anosim and Adonis analyses based on the Weighted Unifrac and Unweighted Unifrac distance algorithms jointly revealed that there were no significant differences observed among gender groups. However, it was observed that significant differences (adjust $p < 0.05$) exist among environmental groups. Among seasonal factors, except for SCF-WCF, all other groups showed significant differences (adjust $p < 0.05$) (Supplementary Appendix A). Based on the above analysis, we discovered significant differences in the gut microbiota of bharal across different seasons and environments. Therefore, in subsequent analyses, we will examine different factors.

## 3.4 The impact of gender on gut microbiota in bharal is small

In the alpha diversity analysis of bharal gut microbiota (Figure 4), there was no significant difference in the Pielou_e index and Shannon index, but the Observed_otus index was higher in SCM than in SCF. When analyzing inter-group differences between dominant phyla and genera, we found no significant difference in dominant phyla between groups. However, at the genus level, *UCG-005* and *UCG-002* in SCF were higher than those in SCM ($p < 0.05$), while *Bacteroides*, *F082*, and *Family_XIII_AD3011_group* in SCM were higher than in SCF ($p < 0.05$). In SWF, *RF39* and *Clostridia_UCG-014* were higher than in SWM ($p < 0.05$), while *UCG-014* was higher in SWM than in SWF ($p < 0.05$). In WWM, *Alistipes* was significantly higher than in WWF ($p < 0.05$), while *Clostridia_UCG-014*, *Monolobus*, and *UCG-002* were higher in WWF than in WWM ($p < 0.05$) (Figure 3). In functional analysis, at level 1, we found that only HD showed a higher WWM than WWF ($p < 0.05$), with no significant differences in other functions. At level 2, AAM shows that SWM was higher than SWF, and MCV, MTP and NM showed that SWF was higher than SWM ($p < 0.05$), and there was no significant difference in other functions (Supplementary Appendices B,C).

## 3.5 There are significant seasonal changes in gut microbiota of bharal

In the analysis of alpha diversity (Figure 4), whether in captivity or the wild, we observed a higher observed_otus index and Shannon index in winter compared to summer ($p < 0.05$). This suggests that the abundance and diversity of the gut microbiota of bharal was significantly higher in winter than in summer. In terms of inter-group

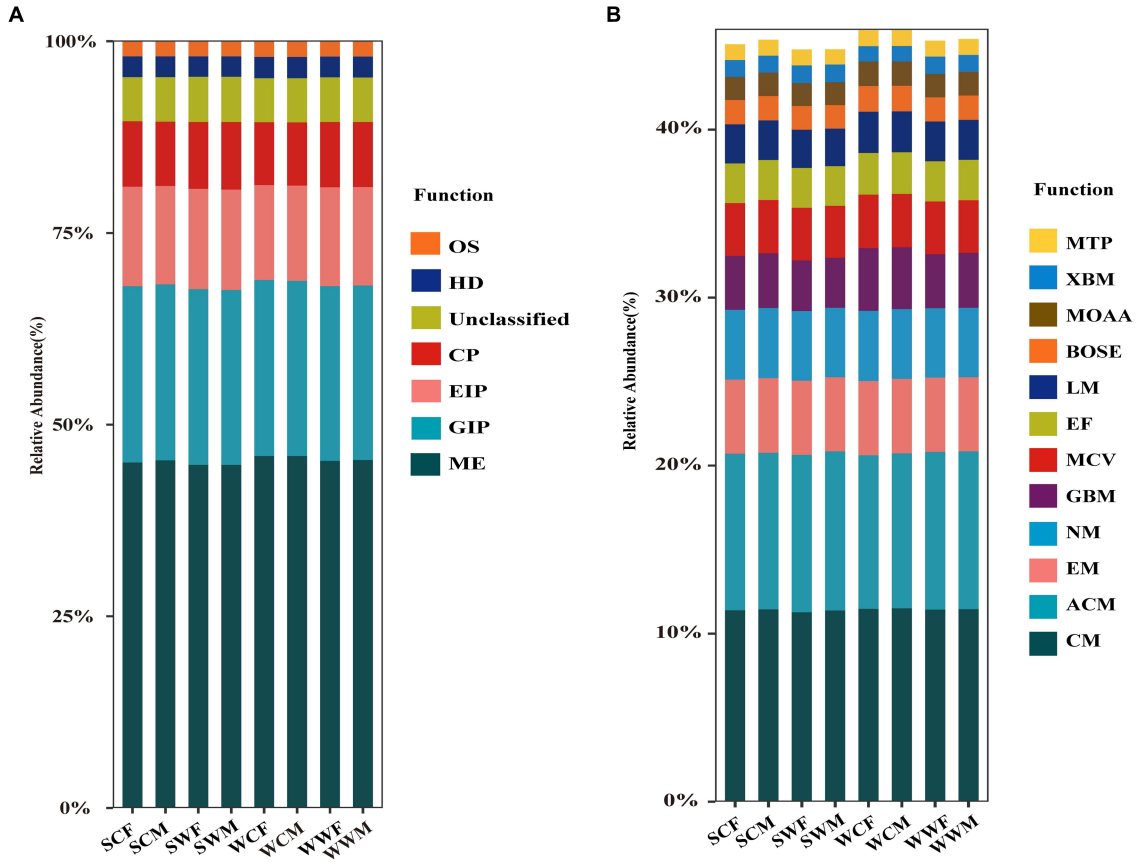


FIGURE 2
Relative abundance histogram of gut microbiota at level 1 **(A)** and level 2 **(B)** based on the KEGG database.

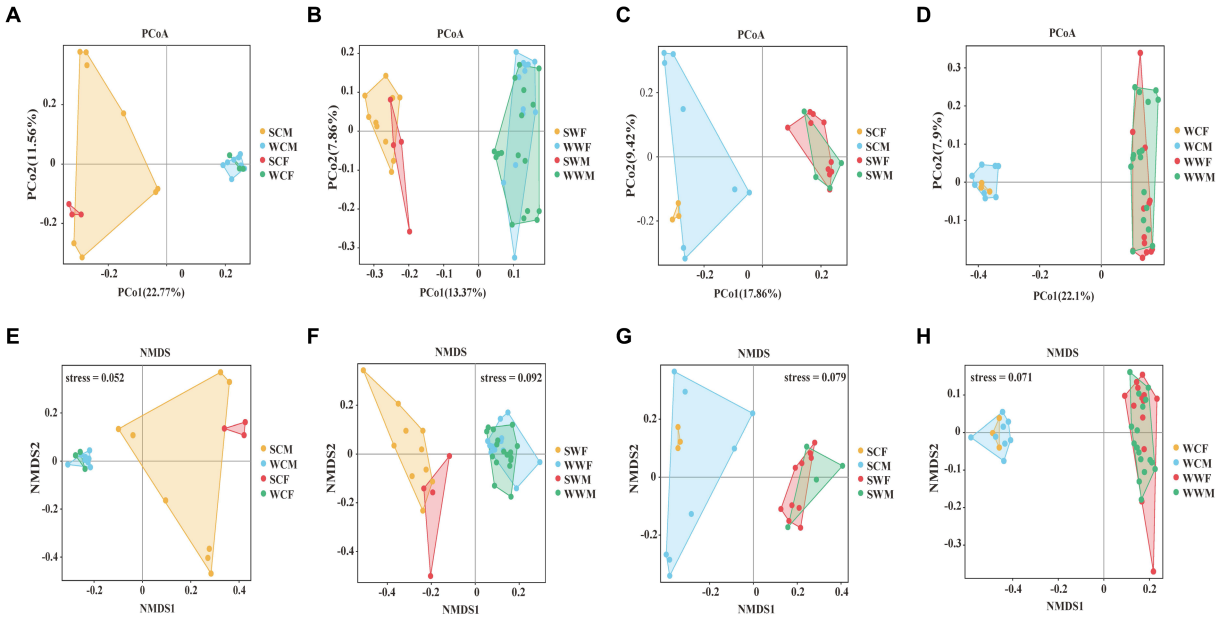


FIGURE 3
PCoA analysis **(A, B, C, D)** and NMDS analysis **(E, F, G, H)** of gut microbiome in different groups.

differences, at the phylum level, Bacteroidota was higher in winter ($p < 0.05$), while Firmicutes was higher in summer ($p < 0.05$). At the genus level, *F082* showed higher abundance in SC group ($p < 0.05$), but higher in WW group ($p < 0.05$). *Rikenellaceae_RC9_gut_group* was higher in WC group than in SC group ($p < 0.05$), *UCG-005* was higher in SW group than in WW group ($p < 0.05$), *Bacteroides* and

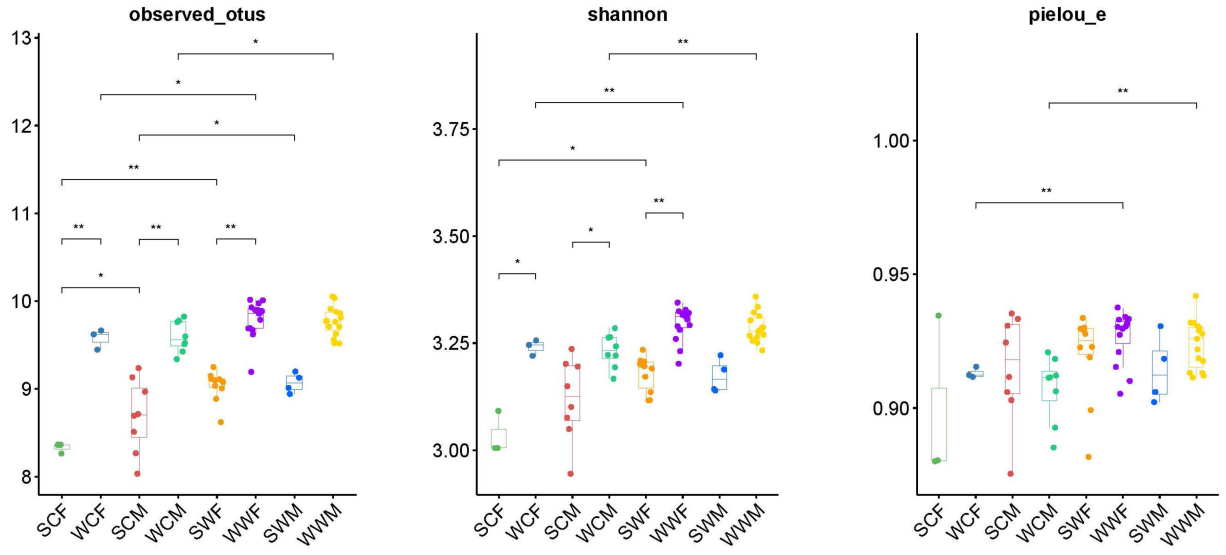


FIGURE 4
Differences analysis of alpha diversity (Observed_Otus index, Shannon index, and Pielou_e index). *$p < 0.05$, **$p < 0.01$.

*Rikenellaceae_RC9_gut_group* were higher in WW group than in SW group ($p < 0.05$).

Through functional prediction, it was observed that at level 1, ME, HD, and OS were higher in winter than in summer ($p < 0.05$), while CP was higher in summer than in winter ($p < 0.05$). GIP was only higher in SWF than WWF ($p < 0.05$), while EIP was higher in SWM than WWM ($p < 0.05$). At level 2, in the captive group, EM, EF and MOAA were higher in winter than in summer ($p < 0.05$). In the wild, BOSM, CM, EF, GBM, LM, and MOAA were higher in winter than in summer ($p < 0.05$). XBM was higher in summer than in winter ($p < 0.05$) in both in wild and captive groups (Supplementary Appendices B,C).

## 3.6 The environment has a significant impact on the gut microbiota of bharal

In the alpha diversity analysis (Figure 4), we observed that the observed_otus, Shannon index, and Pielou_e evenness index were significantly higher in the wild group compared to the captive group for both summer and winter ($p < 0.01$). When analyzing inter-group differences in dominant phyla and genera, all groups showed significantly higher levels of Bacteroidota in the captive compared to the wild, and significantly higher levels of Firmicutes in the wild compared to the captive, except for SCF and SWF groups. In terms of common bacterial genera, *F082* showed higher levels in the SC ($p < 0.05$), but higher levels in the WW ($p < 0.05$). *UCG-002* and *Rikenellaceae_RC9_gut_group* showed higher abundance in the captive environment compared to the wild in both seasons ($p < 0.05$). In winter, *Christenselelaceae_R-7_group*, *Monoglobus*, and *NK4A214_group* showed higher performance in the wild compared to the captive ($p < 0.05$).

Through functional prediction, we found that at level 1, ME, HD, and OS were higher in captivity than in the wild. CP was higher in wild than in captive. EIP is higher in WW than in WC, and OS was higher in WC than in WW. At level 2, BOSM, CM, EM, EF, GBM, LM, MCV, MOAA, and MTP were significantly higher in captive than in wild. However, when comparing the WCF-WWF group, BOSM, EF, GBM, MOAC, and MTP were higher in WWF than in WCF, and XBM was higher in the wild than in the captive in both seasons (Supplementary Appendices B,C).

## 3.7 Analysis of co-occurrence network of gut microbiota in bharal

The analysis revealed that the structure of gut microbial networks in bharal varied across seasons and environments, exhibiting varying levels of complexity. Specifically, the WW group had the most complex network structure, with 525 edges, followed by the SC group (337 edges), WC group (297 edges), and SW group (245 edges). Interestingly, the SC and WC groups had no negative edges, while SW had only 2 and WW had 190. The network diagram also showed that the modules of the network structure were distinct for each group. For instance, in the WC group, the purple module (20 nodes) was the most significant, followed by the green (19 nodes) and blue (18 nodes) modules. However, only *UCG-010* (15) and *UCG-009* (11) from the blue module had more than 10 edges, indicating they were part of the core area of the entire network. In the SC group, the purple (23 nodes), green (20 nodes), and blue (15 nodes) modules were the most important, followed by the black module (13 nodes). The genera with lines greater than or equal to 10 are *Christensenellaceae_R-6_group* (17 edges, blue module), *Family_XIII_AD3010_group* (15 edges, green module), *F081*(13 edges, green module), *UCG-001* (13 edges, green module), *NK4A213_group* (10 edges, purple module), *Methanobrevibacter* (10 edges, blue module), and *Candidatus_Soleaferrea* (10 edges, green module). In the SW group, the proportion of purple modules was relatively larger (68 nodes), followed by green modules (14 nodes). However, when looking at the statistics for the number of edges, only *Christensenellaceae_R-7_group* (10 nodes) in the purple module was found with 10 edges, while the remaining bacteria had less than 10 edges. In the WW group, compared to other groups, there were the most edges and the most complex structure.

The modules with the most nodes were green (30 nodes) and purple (30 nodes). In the edge count statistics, the genera with purple modules with more than 10 edges were *Christensenellaceae_R-7_group* (35 edges), *RF39* (30 edges), *NK4A214_group* (30 edges), *Clostridia_UCG-014* (28 edges), *UCG-002* (28 edges), *Monoglobus* (21 edges), *UCG-009* (14 edges), *Bacteroides* (13 edges), and *Lachnospiraceae_AC2044_group* (10 edges). For green module, the following genera had more than 10 edges were *Clostridia_vadinBB60_group* (19 edges), *UCG-010* (19 edges), *Victivallaceae* (18 edges), *Candidatus_Soleaferrea* (17 edges), *Izemoplasmatales* (17 edges), *Eubacterium_coprostanoligenes_group* (16 edges), *Phascolarctobacterium* (16 edges), *Ruminococcus* (13 edges), and *Alistipes* (10 edges) (Figure 5).

## 4 Discussion

Due to the small population and difficult-to-obtain the samples of endangered animals, collecting fresh feces through non-contact sampling has gradually become the best research method for conservation biology (Wei et al., 2019; Guo et al., 2020; Zhang et al., 2022). At the phylum level, the dominant phyla (abundance >1%) of bharal in different genders, seasons, and environments are Firmicutes and Bacteroidota, which is consistent with the results of most herbivorous gut microbiota (Chi et al., 2019; Li et al., 2022; Gao et al., 2023). As the dominant microbiome of bharal, these bacterial helps host to digest and decompose cellulose and hemicellulose in diet (Wu et al., 2016), which is great significance to the digestion, decomposition, and metabolism of bharal. In the alpha diversity analysis, we observed that there were significant differences based on environmental and seasonal factors. The diversity of gut microbiota in winter was higher than that in summer, while in the wild was higher than that in the captive, which is consistent with previous researches (Chi et al., 2019; Gao et al., 2020; Jiang et al., 2022). Alpha diversity is a quantitative indicator that indicates the diversity, stability, and community composition structure of the host's gut microbiota. It is also regarded as a crucial indicator of the host's overall health status (Shanahan, 2010; Lang et al., 2018). We believe that compared with captive bharal, the gut microbiota of wild bharal is more stable, which enhances wild populations' survival and adaptability.

In the analysis of gender impact, we found that even though the genera with differences between female and male individuals are different, they generally exhibit a pattern. The genera with higher relative abundance in the gut microbiota of female bharals (*UCG-005*, *UCG-002*, *RF39*, *and Clostridia_UCG-014*) belong to Firmicutes, while the genera with higher relative abundance in male bharals (*Bacteroides*, *F082*, *Alistipes*, and so on) belong to Bacteroidota. Previous studies have also shown similar results (Wang et al., 2020). We attribute these differences to variations in the physiological structure and sex steroid hormones such as estradiol and testosterone (Flores et al., 2012; Kaliannan et al., 2018). In captive environment, the gut microbiota function remained the same. However, in the wild, during winter when food is scarce, male, and female bharal exhibit a high degree of overlap in their dietary, resulting there was no difference in the structure and function of gut microbiota. However, during summer, there is a significant difference in food composition between male and female (Zhang, 2013). In the case, the composition and function of the gut microbiota of male and female bharal have changed. Male bharals prefer to consume high fiber foods, and Bacteroidota is beneficial to degrade cellulose (Li et al., 2021). Female bharals tend to consume high-quality food resources, Firmicutes increase the degradation of carbohydrates, fats, and proteins (Wu et al., 2020). These changes not only play an important role in the digestion and decomposition of different types of food, but also in adjusting functions that better adapt to the wild environment based on the host's characteristics.

In the analysis of seasonal impact, we found that Bacteroidota was higher in winter, while Firmicutes was higher in summer. This could be due to the higher levels of crude protein and fat in summer (Fan, 2002). The increase in Firmicutes abundance can benefit bharal to degrade carbohydrates (especially polysaccharides) and other substances such as protein, improve nutrient utilization, and maintain a balanced gut microbiota (Liu et al., 2020). At the genus level, *UCG-005* and *RF39* increase in abundance during summer, which were related to cellulose degradation and promotes the production of butyrate (Liang et al., 2021). The abundance of *Rikenellaceae_RC9_gut_group* and *Bacteroides* were higher in winter. Previous studies have shown that *Rikenellaceae_RC9_gut_group* was involved in the synthesis of dimethyl acetals during rumen fermentation, and was associated with the production of short chain fatty acids, especially propionate, which may enhance ruminant productivity in winter (Conte et al., 2022). The increased of *Bacteroides* was beneficial for improving host metabolism, regulating bile acids, short chain fatty acids, sugars, proteins, fat metabolism, and reducing fat deposition (Wahlström et al., 2016). Through these microbiota changes, the

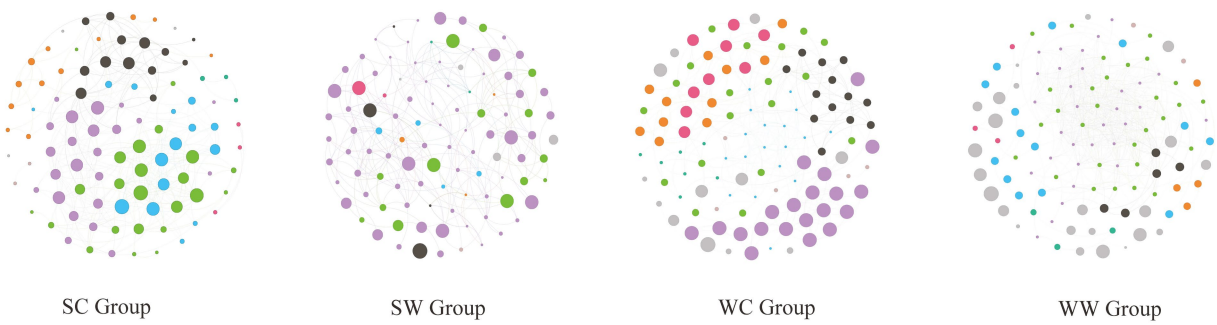


FIGURE 5
The structure of gut microbial networks in bharal among different groups.

utilization and adaptability of winter bharal to food resources were enhanced (Tremaroli and Backhed, 2012). In functional analysis, at level 1 and level 2, most metabolic functions were higher in winter. Compared to the captive group, the wild groups had more functions that increase in abundance during winter. The enhancement of metabolism and other functions is great significance for bharal to adapt the wild environment. It is worth noting that XBM was higher in summer than in winter. We speculate that there are abundant types of secondary compounds in summer food, and the enhancement of this function is conducive to the full utilization of food resources.

When analyzing differences in environmental factors, we found that captive bharals were fed artificial feed with high fat and protein content (Gao et al., 2020). Previous studies have shown that high crude fat content in the diet can lead to a decrease in the number of Bacteroidetes in the host and an increase in the number of Firmicutes (Ni, 2018), which is consistent with our findings. At the genus level, *F082* appeared to be more abundant in the captive group than wild group during summer, and may play a key role in the digestion of non-structural carbohydrates (Yi et al., 2022). *UCG-002* and *Rikenellaceae_RC9_gut_group* were increased which is conducive to the degradation and utilization of food and promotes the production of compounds such as acetate and propionate (Shabat et al., 2016; Liang et al., 2021). *Christensenellaceae_R-7_group*, *Monoglobus*, and *NK4A214_group* showed higher abundance in the wild group than in the captive group, which are mainly involved in the degradation of cellulose and hemicellulose and have a positive correlation with propionate, butyrate, and isobutyrate (Dai et al., 2022). These bacteria can promote acetate fermentation in the rumen, which usually has a slow energy supply but can sustain bharal in wild winter environments for a long time (Wu et al., 2022). In functional analysis, at level 1, the ME in the captive group was stronger than that in the wild group. At level 2, the enhanced metabolic functions in captive bharal were mainly related to material metabolism, likely due to the abundance of captive food. Enhancements in metabolic functions related to lipids, amino acids, and proteins can help captive bharal better utilize these foods. However, for wild bharal, during the winter when food is scarce, their enhanced metabolic functions tend to focus on the biosynthesis of metabolites, using limited food resources to synthesize useful compounds for themselves.

In co-occurrence network analysis, we removed rare bacteria (abundance <0.01%) to minimize their impact on the network structure (Galand et al., 2009). During winter, wild bharal had the most edges, the shortest average path length, and the most complex network structure. They also formed the most modules. We believe that the primary reason for these results is the lack of food resources in the wild during winter, which increases the interaction between microbial communities to optimize resource utilization and cope with harsh environments. In contrast, the captive bharal in summer should be the most comfortable compared to other groups, with a simpler relationship and structure between microbial communities. However, this simpler structure may also make it easier for some bacteria to be damaged, and their intestinal environment is more susceptible to damage than other groups. Through modular analysis and edge counting, we identified some key genera in the gut microbiota co-occurrence network of wild and captive bharal under different environments and seasons, which play a vital role in maintaining each functional module. Changes in the gut microbiota network structure of bharal are also a result of adaptation to environmental and seasonal changes.

Our findings indicate that the environment and season affect the gut microbiota of bharal. The captive environment has a significant impact on the gut microbiota composition and function of bharal. We need to attach the importance of maintaining the native gut microbiota of wild animals in captive environment. However, relying solely on 16S sequencing data to predict the gut microbiota function of bharal is inadequate. Therefore, we plan to use metagenomic sequencing to further analyze the gut microbiota function and metabolic pathways of bharal in different genders, seasons, and environments, providing a more comprehensive understanding of the impact of different factors on the gut microbiota of bharal.

## Data availability statement

The datasets presented in this study can be found in online repositories. The data presented in the study are deposited in the NCBI, accession number PRJNA1006445.

## Ethics statement

The animal studies were approved by the Northwest Institute of Plateau Biology, Chinese Academy of Sciences animal ethics committee. The studies were conducted in accordance with the local legislation and institutional requirements. Written informed consent was obtained from the owners for the participation of their animals in this study.

## Author contributions

HGa: Conceptualization, Data curation, Formal analysis, Funding acquisition, Investigation, Methodology, Project administration, Resources, Software, Supervision, Validation, Visualization, Writing – original draft, Writing – review & editing. XC: Conceptualization, Data curation, Formal analysis, Investigation, Methodology, Writing – review & editing. PS: Conceptualization, Data curation, Formal analysis, Investigation, Methodology, Writing – review & editing. HGu: Conceptualization, Data curation, Investigation, Project administration, Writing – review & editing. BX: Conceptualization, Data curation, Investigation, Methodology, Writing – review & editing. ZC: Data curation, Methodology, Project administration, Validation, Writing – review & editing. FJ: Conceptualization, Data curation, Project administration, Writing – review & editing. BL: Data curation, Investigation, Methodology, Writing – review & editing. TZ: Conceptualization, Data curation, Formal analysis, Funding acquisition, Methodology, Project administration, Resources, Writing – review & editing.

## Funding

The author(s) declare that financial support was received for the research, authorship, and/or publication of this article. This work was supported by the Second Tibetan Plateau Scientific Expedition and Research Program (STEP) (grant no. 2019QZKK0501) and the

Qinghai Province Science and Technology Plan (grant no. 2021-ZJ-951Q).

## Acknowledgments

We would like to express our heartfelt thanks to the keepers of the Qinghai–Tibet Plateau Wildlife Park for their help in collecting fecal samples from the bharal in zoo.

## Conflict of interest

The authors declare that the research was conducted in the absence of any commercial or financial relationships that could be construed as a potential conflict of interest.

## Publisher's note



## Supplementary material

The Supplementary material for this article can be found online at: https://www.frontiersin.org/articles/10.3389/fmicb.2024.1357415/full#supplementary-material

## References

Amato, K. R., Yeoman, C. J., Kent, A., Righini, N., Carbonero, F., Estrada, A., et al. (2013). Habitat degradation impacts black howler monkey (*Alouatta pigra*) gastrointestinal microbiomes. *ISME J.* 7, 1344–1353. doi: 10.1038/ismej.2013.16

Bokulich, N. A., Kaehler, B. D., Rideout, J. R., Dillon, M., Bolyen, E., Knight, R., et al. (2018). Optimizing taxonomic classification of marker-gene amplicon sequences with QIIME2's q2-feature-classifier plugin. *Microbiome* 6:90. doi: 10.1186/s40168-018-0470-z

Chi, X. W., Gao, H. M., Wu, G. S., Qin, W., Song, P. F., Wang, L., et al. (2019). Comparison of gut microbiota diversity between wild and captive bharals (*Pseudois nayaur*). *BMC Vet. Res.* 15:243. doi: 10.1186/s12917-019-1993-7

Conte, G., Dimauro, C., Daghio, M., Serra, A., Mannelli, F., McAmmond, B. M., et al. (2022). Exploring the relationship between bacterial genera and lipid metabolism in bovine rumen. *Animals* 16:100520. doi: 10.1016/j.animal.2022.100520

Dai, D., Pang, K., Liu, S., Wang, X., Yang, Y. K., Chai, S. T., et al. (2022). Effects of concentrate supplementation on growth performance, rumen fermentation, and bacterial community composition in grazing yaks during the warm season. *Animals* 12:1398. doi: 10.3390/ani12111398

Ezenwa, V. O., and Gerardo, N. M. (2012). Animal behavior and the microbiome. *Science* 338, 198–199. doi: 10.1126/science.1227412

Fan, Q. C. (2002). Quality analysis of several forage grasses in Cyperaceae in Qinghai. *J. Sichuan Grassl.*, 37–39. (In chinese)

Flores, R., Shi, J., Fuhrman, B., Xu, X., Veenstra, T. D., Gail, M. H., et al. (2012). Fecal microbial determinants of fecal and systemic estrogens and estrogen metabolites: a cross-sectional study. *J. Transl. Med.* 10:253. doi: 10.1186/1479-5876-10-253

Galand, P. E., Casamayor, E. O., Kirchman, D. L., and Lovejoy, C. (2009). Ecology of the rare microbial biosphere of the Arctic Ocean. *Proc. Natl. Acad. Sci. USA* 106, 22427–22432. doi: 10.1073/pnas.0908284106

Gao, H. M., Chi, X. W., Li, G. Y., Qin, W., Song, P. F., Jiang, F., et al. (2020). Gut microbial diversity and stabilizing functions enhance the plateau adaptability of Tibetan wild ass (*Equus kiang*). *Microbiology* 9, 1150–1161. doi: 10.1002/mbo3.1025

Gao, H. M., Jiang, F., Zhang, J. J., Chi, X. W., Song, P. F., Li, B., et al. (2023). Effects of ex situ conservation on diversity and function of the gut microbiota of the Tibetan wild ass (*Equus kiang*). *Integr. Zool.* 18, 1089–1104. doi: 10.1111/1749-4877.12726

Gomez, A., Petrzelkova, K., Yeoman, C. J., Vlckova, K., Mrázek, J., Koppova, I., et al. (2015). Gut microbiome composition and metabolomic profiles of wild western lowland gorillas (*Gorilla gorilla gorilla*) reflect host ecology. *Mol. Ecol.* 24, 2551–2565. doi: 10.1111/mec.13181

Gomez, A., Rothman, J. M., Petrzelkova, K., Yeoman, C. J., Vlckova, K., Umaña, J. D., et al. (2016). Temporal variation selects for diet–microbe co-metabolic traits in the gut of Gorilla spp. *ISME J.* 10, 514–526. doi: 10.1038/ismej.2015.146

Guo, W., Ren, K., Ning, R. H., Li, C. W., Zhang, H. M., Li, D. S., et al. (2020). Fecal microbiota transplantation provides new insight into wildlife conservation. *Glob. Ecol. Conserv.* 24:e01234. doi: 10.1016/j.gecco.2020.e01234

Haas, B. J., Gevers, D., Earl, A. M., Feldgarden, M., Ward, D. V., Giannoukos, G., et al. (2011). Chimeric 16S rRNA sequence formation and detection in sanger and 454-pyrosequenced PCR amplicons. *Genome Res.* 21, 494–504. doi: 10.1101/gr.112730.110

Hicks, A. L., Lee, K. J., Couto-Rodriguez, M., Patel, J., Sinha, R., Guo, C., et al. (2018). Gut microbiomes of wild great apes fluctuate seasonally in response to diet. *Nat. Commun.* 9:1786. doi: 10.1038/s41467-018-04204-w

Jiang, F., Song, P. F., Wang, H. J., Zhang, J. J., Liu, D. X., Cai, Z. Y., et al. (2022). Comparative analysis of gut microbial composition and potential functions in captive forest and alpine musk deer. *Appl. Microbiol. Biotechnol.* 106, 1325–1339. doi: 10.1007/s00253-022-11775-8

Kaliannan, K., Robertson, R. C., Murphy, K., Stanton, C., Kang, C., Wang, B., et al. (2018). Estrogen-mediated gut microbiome alterations influence sexual dimorphism in metabolic syndrome in mice. *Microbiome* 6:205. doi: 10.1186/s40168-018-0587-0

Lang, J. M., Pan, C., Cantor, R. M., Tang, W. H. W., Garcia-Garcia, J. C., Kurtz, I., et al. (2018). Impact of individual traits, saturated fat, and protein source on the gut microbiome. *MBio* 9, e01604–e01618. doi: 10.1128/mBio.01604-18

Li, B., Gao, H. M., Song, P. F., Liang, C. B., Jiang, F., Xu, B., et al. (2022). Captivity shifts gut microbiota communities in White-lipped deer (*Cervus albirostris*). *Animals* 12:431. doi: 10.3390/ani12040431

Li, Y., Lv, M., Wang, J., Tian, Z. H., Yu, B., Wang, B., et al. (2021). Dandelion (Taraxacum mongolicum hand.-Mazz.) supplementation-enhanced rumen fermentation through the interaction between ruminal microbiome and metabolome. *Microorganisms* 9:83. doi: 10.3390/microorganisms9010083

Liang, J., Kou, S., Chen, C., Raza, S. H. A., Wang, S. H., Ma, X., et al. (2021). Effects of *Clostridium butyricum* on growth performance, metabonomics and intestinal microbial differences of weaned piglets. *BMC Microbiol.* 21:85 (2021). doi: 10.1186/s12866-021-02143-z

Liu, W. S., Guo, X. Z., Chen, Y. L., Tang, Y. Q., Xiao, H. H., and Li, S. M. (2020). Analysis of microbial structure and function in the intestine of farmed black-spot frog. *J. Econ. Anim.*, 1–12. doi: 10.13326/j.jea.2019.1415

Luo, Z., Jiang, Z., and Tang, S. (2015). Impacts of climate change on distributions and diversity of ungulates on the Tibetan plateau. *Ecol. Appl.* 25, 24–38. doi: 10.1890/13-1499.1

Magoč, T., and Salzberg, S. L. (2011). FLASH: fast length adjustment of short reads to improve genome assemblies. *Bioinformatics* 27, 2957–2963. doi: 10.1093/bioinformatics/btr507

Ni, Y. T. (2018). *Effects of food change on intestinal microflora of plateau pika* Lanzhou, China: Lanzhou University.

Ren, T., Boutin, S., Humphries, M. M., Dantzer, B., Gorrell, J. C., Coltman, D. W., et al. (2017). Seasonal, spatial, and maternal effects on gut microbiome in wild red squirrels. *Microbiome* 5:163. doi: 10.1186/s40168-017-0382-3

Schaller, G. B. (1977). Mountain monarchs. Wild sheep and goats of the Himalaya *Q Rev Biol.* 43, 393–412.

Shabat, S. K., Sasson, G., Doron-Faigenboim, A., Durman, T., Yaacoby, S., Miller, M. E. B., et al. (2016). Specific microbiome-dependent mechanisms underlie the energy harvest efficiency of ruminants. *ISME J.* 10, 2958–2972. doi: 10.1038/ismej.2016.62

Shanahan, F. (2010). Probiotics in perspective. *Gastroenterology* 139, 1808–1812. doi: 10.1053/j.gastro.2010.10.025

Simpson, S., Ash, C., Pennisi, E., and Travis, J. (2005). The gut: inside out. *Science* 307:1895. doi: 10.1126/science.307.5717.1895

Sonnenburg, J. L., and Sonnenburg, E. D. (2019). Vulnerability of the industrialized microbiota. *Science* 366:eaaw9255. doi: 10.1126/science.aaw9255

Tremaroli, V., and Backhed, F. (2012). Functional interactions between the gut microbiota and host metabolism. *Nature* 489, 242–249. doi: 10.1038/nature11552

Wahlström, A., Sayin, S. I., Marschall, H. U., and Bäckhed, F. (2016). Intestinal crosstalk between bile acids and microbiota and its impact on host metabolism. *Cell Metab.* 24, 41–50. doi: 10.1016/j.cmet.2016.05.005

Wang, X. M., Wang, Y., Li, Q., Tseng, Z. J., Takeuchi, G. T., Deng, T., et al. (2015). Cenozoic vertebrate evolution and paleoenvironment in Tibetan plateau: Progress and prospects. *Gondwana Res.* 27, 1335–1354. doi: 10.1016/j.gr.2014.10.014

Wang, X., Zhang, Y., Wen, Q., Wang, Y., Wang, Z. X., Tan, Z., et al. (2020). Sex differences in intestinal microbial composition and function of Hainan special wild boar. *Animals* 10:1553. doi: 10.3390/ani10091553

Wei, F. W., Wu, Q., Hu, Y. B., Huang, G. P., Nie, Y. G., and Yan, L. (2019). Conservation metagenomics: a new branch of conservation biology. *Sci. China Life Sci.* 62, 168–178. doi: 10.1007/s11427-018-9423-3

Weikard, R., Pitra, C., and Kühn, C. (2006). Amelogenin cross-amplification in the family Bovidae and its application for sex determination. *Mol. Reprod. Dev.* 73, 1333–1337. doi: 10.1002/mrd.20554

Wu, Q., Chen, H., Zhang, F., Wang, W. K., Xiong, F. L., Liu, Y. Y., et al. (2022). Cysteamine supplementation in vitro remarkably promoted rumen fermentation efficiency towards propionate production via Prevotella enrichment and enhancing antioxidant capacity. *Antioxidants* 11:2233. doi: 10.3390/antiox11112233

Wu, H. L., Yuan, Y. H., and Pan, H. G. (2020). Comparison of fecal microbiota composition of blue sheep fed *Lolium perenne* versus *Sorghum sudanense*. *Can. J. Microbiol.* 67, 372–380. doi: 10.1139/cjm-2020-0333

Wu, X., Zhang, H., Chen, J., Shang, S., Wei, Q. G., Yan, J. K., et al. (2016). Comparison of fecal microbiota of dholes high-throughput Illumina sequencing of the V3-V4 region of the 16S RRNA gene. *Appl. Environ. Microbiol.* 100, 3577–3586. doi: 10.1007/s00253-015-7257-y

Xu, Z., Li, Z., Wu, Q. M., Pan, M., Zhang, X. G., Cui, D. Y., et al. (2019). Research status of wildlife environmental enrichment in ex-situ protected area, China. *Chin. J. Wildl.* 40, 1083–1089. doi: 10.19711/j.cnki.issn2310-1490.2019.04.037

Yan, M. M., Wei, G. C., Pan, X. H., Ma, H. L., and Li, W. Z. (2008). A method suitable for extracting genomic DNA from animal and plant-modified CTAB method. *Agric. Sci. Technol.* 18, 73–84. doi: 10.1007/s11442-008-0073-x

Yi, S., Dai, D., Wu, H., Chai, S. T., Liu, S. J., Meng, Q. X., et al. (2022). Dietary concentrate-to-forage ratio affects rumen bacterial community composition and metabolome of yaks. *Front. Nutr.* 9:927206. doi: 10.3389/fnut.2022.927206

Zhang, M. M. (2013). *Research on the Sexual Segregation of Blue sheep (Pseudois nayaur) in the Helan Mountains* Harbin, China: Northeast Forestry University.

Zhang, J. J., Gao, H. M., Jiang, F., Liu, D. X., Hou, Y. S., Chi, X. W., et al. (2022). Comparative analysis of gut microbial composition and functions in Przewalski's gazelle (*Procapra przewalskii*) from various habitats. *Front. Microbiol.* 13:913358. doi: 10.3389/fmicb.2022.913358

frontiers | Frontiers in Microbiology

TYPE Original Research
PUBLISHED 27 June 2024
DOI 10.3389/fmicb.2024.1396949



OPEN ACCESS

EDITED BY
Karolina Skonieczna-Żydecka,
Pomeranian Medical University, Poland

REVIEWED BY
Egil Andreas Joor Fischer,
Utrecht University, Netherlands
Cristiane Cantiga-Silva,
São Paulo State University (UNESP), Brazil

*CORRESPONDENCE
Eliška Eliasson
✉ eliska.valeckova@slu.se

†These authors have contributed equally to this work and share first authorship

RECEIVED 06 March 2024
ACCEPTED 06 June 2024
PUBLISHED 27 June 2024

CITATION
Eliasson E, Sun L, Cervin G, Pavia H, Tällberg G, Ellström P and Ivarsson E (2024) No colonization resistance to *Campylobacter jejuni* in broilers fed brown algal extract-supplemented diets. *Front. Microbiol.* 15:1396949. doi: 10.3389/fmicb.2024.1396949



# No colonization resistance to *Campylobacter jejuni* in broilers fed brown algal extract-supplemented diets

Eliška Eliasson[1*†], Li Sun[1†], Gunnar Cervin[2], Henrik Pavia[2], Gustav Tällberg[3], Patrik Ellström[4] and Emma Ivarsson[1]

[1]Department of Applied Animal Science and Welfare, Swedish University of Agricultural Sciences, Uppsala, Sweden, [2]Department of Marine Sciences, Tjärnö, University of Gothenburg, Strömstad, Sweden, [3]Zoonosis Science Center, Uppsala University, Uppsala, Sweden, [4]Zoonosis Science Center, Department of Medical Sciences, Uppsala University, Uppsala, Sweden

**Introduction:** *Campylobacter jejuni* gastroenteritis is the most commonly reported zoonosis within the EU, with poultry products regarded as the primary source of transmission to humans. Therefore, finding strategies to reduce *Campylobacter* colonization in broilers holds importance for public health. Recent studies suggest that supplementation of broiler feed with brown algal extracts, particularly laminarin, can provide beneficial effects on broiler gut health, growth performance, and gut microbiota. However, its effect on gut microbiota development and subsequent reduction of *Campylobacter* loads in broiler caeca during the later stages of the birds' lives remains unclear.

**Methods:** Experimental colonization of Ross 308 broilers with two different strains of *C. jejuni* was conducted, with groups fed either a basal diet or the same basal diet supplemented with 725 ppm algal extract from *Saccharina latissima* to provide 290 ppm laminarin. Fecal samples were collected for bacterial enumeration, and caecal samples were obtained before and after the *C. jejuni* challenge for the determination of microbiota development.

**Results and discussion:** No significant differences in fecal *C. jejuni* concentrations between the groups fed different diets or exposed to different *C. jejuni* strains were observed. This suggests that both strains colonized the birds equally well and that the laminarin rich algal extract did not have any inhibitory effect on *C. jejuni* colonization. Notably, 16S rRNA amplicon sequencing revealed detailed data on the caecal microbiota development, likely influenced by both bird age and *C. jejuni* colonization, which can be valuable for further development of broiler feed formulations aimed at promoting gut health.

KEYWORDS

**brown algae, *Saccharina latissima*, laminarin, *Campylobacter jejuni*, host specificity, microbiota, broiler**

## 1 Introduction

*Campylobacter jejuni* (*C. jejuni*) is a common gram-negative bacterial pathogen associated with foodborne illnesses in humans, and broiler chickens are known to be a significant reservoir for this bacterium (EFSA, 2020). Finding strategies to reduce *Campylobacter* colonization in broiler flocks is important for food safety and public health.

*Saccharina latissima* is a brown algae belonging to the family Laminariaceae and is rich in complex polysaccharides such as alginate, laminarin, and fucoidan

(Sharma et al., 2018). It has been proposed that laminarin could have prebiotic potential (Cherry et al., 2019). A study conducted on broiler chicks, where birds were fed a laminarin-rich extract from *Laminaria spp*. at 300 ppm, found that it exhibited promising effects on growth performance, protective immune responses, and beneficial effects on the gastrointestinal microbial profile (Venardou et al., 2021). Additionally, an increase in the expression of the cytokine interleukin 17A (IL17A) in the broiler's duodenum was observed. Interleukin 17A has been reported to be involved in the immune response against several infectious agents, including *Campylobacter* (Connerton et al., 2018). Sweeney and O'Doherty (2016) reported that supplementing the basal diet with laminarin at a concentration of 250 ppm during the initial stages of the chickens' life led to notable improvements in villus morphology and enhanced tight junction integrity in Ross 308 broilers. However, the same study reported no significant differences in *C. jejuni* colonization during experimental colonization (day three post-hatch to day 13) between broilers raised on an algal extract-supplemented diet and those raised on a conventional diet in the post-hatch period. Yet, the investigation of algal extracts' impact on the microbiota and *C. jejuni* bacterial load in broiler caeca during later stages of life remains unexplored in current scientific literature.

Although the epizootology of *C. jejuni* and its spread into broiler production is still not fully understood, it is well-known that wild birds constitute a natural reservoir for this pathogen (French et al., 2009; Waldenström et al., 2010; Griekspoor et al., 2013; Mourkas et al., 2022). Therefore, it is also likely that they play a role in the transmission of *C. jejuni* between wild animals, to domestic production, and further to humans. In wild birds, *C. jejuni* shows strong host specificity such that different bird taxa carry different genotypes of *C. jejuni* (Griekspoor et al., 2013). This specificity does not seem to correlate with the diet or habitat of the birds but rather with specific species associated microbiota. In a previous experiment, the relative colonization ability in mallard ducks (*Anas platyrhynchos*) was compared between *C. jejuni* strains of different host origins (Atterby et al., 2018). Not surprisingly, *C. jejuni* of mallard origin colonized the birds best. However, a strain from a song thrush (*Turdus philomelos*) was a very poor colonizer and could not establish long-term colonization in this species, whereas *C. jejuni* isolated from a broiler chicken could colonize the mallards. A similar experiment was previously performed on wild robins (*Erithacus rubecula*), where a song thrush strain of the same ST-type could colonize the birds for an average of 6.8 days whereas a strain isolated from a human could not establish colonization (Waldenström et al., 2010). These studies suggest that wild bird species might exhibit colonization resistance to *C. jejuni* genotypes that originate from distantly related hosts. On the other hand, there also exist generalist genotypes of *C. jejuni*, that can be found in many different host species (Gripp et al., 2011), and hence, colonization resistance does not seem to apply to such strains. Broiler chickens are known to harbor many different genotypes of *C. jejuni* and it is not known if this host species also shows colonization resistance to *C. jejuni* adapted to distantly related hosts.

The present study aimed to examine the impact of feed supplementation with a laminarin-rich algal extract from *Saccharina latissima* (*AE*) on the development of the caecal microbiota in broilers and assess its influence on resistance to intestinal colonization with *C. jejuni* upon experimental colonization. Groups of Ross 308 chickens were intraoesophagically inoculated at 17 days of age with two different *C. jejuni* strains, one of chicken origin and one isolated from a wild song thrush. Based on previous experiments, our hypothesis was that the *C. jejuni* strain isolated from chicken would exhibit superior colonization ability in broilers compared to the strain originating from song thrush and that any effect of the feed supplementation with *AE* would be more pronounced against the song thrush strain than the chicken strain.

## 2 Materials and methods

This study was conducted as part of a larger project where the effect of feeding brown algae (intact or as an *AE*) to broiler breeder hens was evaluated. Previously, the effect on hens' antibody response, egg quality, and the chick quality of their progeny was assessed (Ivarsson et al., 2023). In addition, the early development of hens' progenies with a main focus on early growth performance was examined (Supplementary Table 1). These progenies were subsequently utilized in the present study. The experiment was carried out at the Swedish Livestock Research Center of the Swedish University of Agricultural Sciences and was approved by the committee for animal ethics of the Uppsala region (approval number 5.8.18-10572/2019).

### 2.1 Housing

A total of 255 mixed-sex Ross 308 chicks were allocated into groups of 10-13 chickens in 24 experimental pens, the allocation of chicks to the rearing pens was determined prior to the hatching. The solid floor pens with dimensions 1.5 × 0.75 meters were bedded with wood shavings and equipped with feeders and nipple drinkers. The house temperature was initially set at 34°C during hatching (day 0) and then reduced to 33°C for the first 3 days. Thereafter, the temperature gradually decreased with age until reaching 23°C at day 24, remaining the same for the rest of the trial period. Lighting conditions consisted of a 24-h cycle during the first 2 days, after which the duration of light was reduced by 1 h daily until day eight, resulting in 18 h of light per day for the remaining period. All chickens were marked with color identification at hatch, which was replaced by a 1 cm × 1 cm laminated neck tag (Jolly Fine, Jolly, Italy) at 7 days of age. Two chickens from each replicate were used for the collection of fecal samples.

### 2.2 Experimental design and diets

The chicken facility with 24 experimental pens in total was divided into two parts, each consisting of 12 pens. Each part was split into two chick treatment groups: (1) basal diet formulated according to the nutrient requirement of Ross 308 (control - *C*), and (2) basal diet supplemented with 725 ppm algal extract (*AE*) sourced from *Saccharina latissima*. The supplemented diet was optimized to contain 290 ppm laminarin and was provided

from the first day of the animal's life until the end of the trial. Both chick diets were pelleted and formulated according to the nutrient requirement of Ross 308 (Aviagen., 2019). The algae used in the study were cultivated at sea on longlines in the Koster archipelago, located outside Tjärnö Marine Biological Laboratory on the Swedish West Coast (Thomas et al., 2022). In the experiment, dried algae were utilized as a substrate for the *AE*, with the detailed processing procedures described in Ivarsson et al. (2023). The resulting *AE* contained 41.6 % laminarin, analyzed enzymatically by measuring the β 1,3/1,6-glucan content using the K-YBGL 12/16 assay kit from Megazyme. Additionally, the ash content of the *AE* was determined to be 14.5% on a dry matter (DM) basis. The non-starch polysaccharide content was analyzed by the Uppsala method (Theander et al., 1995), and amounted to a total of 45.7% on a DM basis. The specific composition of the polysaccharides was as follows: 31% glucose, 2.2% fucose, 3.0% mannose, 1.8% galactose, 0.7% xylose, and 0.5% arabinose.

## 2.3 *Campylobacter jejuni* inoculation

At 17 days of age, the bird group size was reduced to four chickens per pen, and chicks were intraoesophagically inoculated with 1 ml of a PBS solution containing ~$10^2$ CFU of *C. jejuni* as determined by optical density at 405 nm. Two different *C. jejuni* strains were used and birds inoculated with each of the strains were kept apart in two different parts of the facility, separated by a flexible wall. *C. jejuni* strain #65 (ST-104, in ST-21 CC) was isolated from a broiler chicken in the UK and *C. jejuni* strain #3926 (ST-1315 in ST-1304 CCs) was isolated from a wild song thrush captured in Sweden. The bacterial concentration of the two inoculates was confirmed by CFU counts on blood agar plates after 24 h incubation at 42°C in a microaerobic atmosphere to be 2 x $10^2$ cfu/ml for *C. jejuni* strain #65 and 4 x $10^2$ cfu/ml for strain #3926.

## 2.4 Fecal and caecal samples collection

Fecal samples were taken from all birds 1 day before the inoculation, to ensure that the birds were culture-negative for *Campylobacter* before the challenge. Subsequently, samples were collected regularly throughout the experimental period at 1 day post-infection (dpi), 2 dpi, 3 dpi, 5 dpi, 7 dpi, 14 dpi, and 19 dpi for bacterial enumeration by culture on agar plates. Focal birds from each pen were placed individually in clean boxes and sterile cotton swabs were used to collect ~100 mg of fresh fecal matter per bird. Thereafter, samples were re-suspended in 1 ml Luria-Bertani (LB) medium complemented with 20% glycerol, followed by vortexing and centrifugation (100 × g for 15 s) for sedimentation of the fecal matter. Subsequently, six 20 µl aliquots were withdrawn from each sample and added to the first column of a 96-well plate containing 180 µl of PBS per well. The six replicates were serially diluted 10-fold and six dilution steps were plated in aliquots of 10 µl on modified charcoal cefoperazone deoxycholate agar (mCCDA) plates using an 8-channel pipette according to the 6 × 6 drop plate method described by Chen et al. (2003). Plates were left to dry for 10 min and incubated for 30 h at 42°C under microaerobic conditions (Campygen, Thermo Fisher, USA). After incubation, colonies were counted and a mean value was created from the six spots from the column that contained the highest number of well separated colonies. Results are presented for four treatments; chicken strain with control feed (Ch + *C*), chicken strain with algal extract (Ch + *AE*), song thrush strain with control feed (Th + *C*), and song thrush strain with algal extract (Th + *AE*).

Caecal samples were collected from two birds per pen at day 7, day 14, and day 37 of the experiment. Euthanasia was performed by administration of sodium pentobarbital intravenously through the wing vein. An aseptic procedure was followed to obtain caecal content, which was sampled into 2.0 ml screw cap microtubes (Sarstedt AG and Co, Germany) and immediately placed in liquid nitrogen. All samples were stored at−80°C until further analysis. The microbial composition of the caecal content was investigated by 16S rRNA amplicon sequencing.

## 2.5 DNA extraction, sequencing, and bioinformatics analysis

The DNA extraction of caecal digesta samples was conducted as previously described (Ivarsson et al., 2023). In brief, 400 microliters of ASL lysis buffer (Qiagen, Germany) were added to the thawed sample and homogenized. Thereafter, 120 µl suspension was used for bead beating on Precellys evolution homogenizer (Bertin Technologies SAS, France) at 8000 rpm for 2 × 60 sec with 30-s pauses. After centrifugation, 120 µl of the supernatant was used for DNA extraction using the EZ1 Advanced XL instrument (Qiagen, Germany) according to the manufacturer's instructions.

The caeca sample DNA extractions were sequenced at Novogene (Cambridge, UK), using the Illumina NovaSeq 6000 PE250 platform. The primer set targeting the V4 region of 16S rRNA gene 515F (GTGCCAGCMGCCGCGGTAA) and 806R (GGACTACHVGGGTWTCTAAT) were used for amplification. PCR reactions were performed with Phusion High-Fidelity PCR Master Mix (New England Biolabs, USA). PCR products (~400–450 bp) were separated by electrophoresis on 2% agarose gel, purified with a Qiagen Gel Extraction Kit (Qiagen, Germany), and pooled at equal concentrations. Sequencing libraries were generated using the NEBNext Ultra DNA Library Prep Kit (Illumina, USA), followed by quantification using Qubit (Thermo Fisher Scientific, USA) and sequencing.

The 16S rRNA gene sequencing data processing was performed as described in Sun et al. (2022), with the following modification: (1) using the truncation length of 221 bp for both forward and reverse reads; (2) the SILVA SSU Ref NR 99 138 dataset was used for taxonomic classification (Pedregosa et al., 2011); (3) the generalized UniFrac distance matrix (alpha = 0.5) was generated using the QIIME2 diversity plugin (Bolyen et al., 2019).

## 2.6 Statistical analysis

All statistical analysis was performed with R (R Core Team, 2019). To investigate the effect of dietary treatment and *Campylobacter* strain, Quasi-Poisson regression (Ver Hoef and

Boveng, 2007) was employed to analyse the plate counting data for C. jejuni, while Tukey's Honestly Significant Difference (HSD) test was utilized to conduct multiple pairwise comparisons. For sequencing data, the number of observed ASVs was calculated from rarefied ASV table. The Kruskal-Wallis rank test, followed by Dunn's test for pairwise comparisons with Benjamini and Hochberg (B–H) correction, was used to check for statistically significant differences in observed ASVs between treatment groups, using the QIIME2 q2-diversity plugin (Kruskal, 1952; Dunn, 1964; Benjamini and Hochberg, 1995). Permutational multivariate analysis of variance (PERMANOVA) of generalized UniFrac distance matrix with B-H correction was conducted to evaluate differences between the dietary and *Campylobacter* treatment groups, using the q2-diversity plugin (Anderson, 2001). Mixed effects linear models were fitted and analyzed using R packages lme4 (Bates et al., 2015), lmerTest (Kuznetsova et al., 2017), pbkrtest (Halekoh and Højsgaard, 2014), and emmeans (Searle et al., 1980). Age, feed treatment, and *Campylobacter* strain were used as fixed effects, and pen as a random effect. $P < 0.05$ was considered significant.

# 3 Results

## 3.1 *Campylobacter* colonization not influenced by *AE*

All birds were *Campylobacter jejuni* negative prior to the challenge and successful *C. jejuni* colonization in both strains was achieved after the challenge at 1 dpi (18 days of age). There was no significant effect of feed supplementation with *AE* on the colonization dynamics of either of the *C. jejuni* strains, as determined by CFU counts on agar plates (Figure 1). The levels of *C. jejuni* in birds that received *AE* in their diet (Ch + *AE* and Th + *AE*) were similar to *C. jejuni* levels in groups fed with the *C* diet (Ch + *C* and Th + *C*) at all sampling points. No significant differences were observed between the chicken and song thrush *C. jejuni* strains in their ability to colonize the broilers' gut, and similar colonization levels were observed from dpi 1 to dpi 19 in both *C* and *AE*-fed birds. *C. jejuni* colonization progressed rapidly from dpi 1 to dpi 2, and the peak was observed 3 days after the challenge (3 dpi) with $\sim 10^7$ CFU/g of feces. Thereafter, the colonization intensity for both strains remained at similar levels of $10^6$ CFU/g of feces on average until the end of the experiment.

## 3.2 Caecal microbiota composition shifts

Rarefaction curves of observed amplicon sequencing variants (ASVs) in caecal samples revealed sufficient sequencing depth to capture species richness at days 7, 14, and 37 after hatching (Supplementary Figure 1). The alpha diversity, as measured by the observed number of ASVs had the lowest count at day 7, followed by day 14, and the highest number of ASVs was present at day 37.

Principal coordinate analysis (PCoA) was used to display differences in the generalized UniFrac distance matrix at different sampling points after hatching (day 7, day 14, and day 37). The results demonstrate a distinct ASV clustering according to time after hatching (Kruskal-Wallis, $p < 0.001$) (Figure 2). The differences between sampling points day 7 and day 14 indicate an effect of age, whereas the microbiota composition at day 37 could be affected by age, cage effect or *C. jejuni* colonization (PERMANOVA, $p = 0.001$). No clear separation between groups fed with *AE* supplemented diet in comparison to the *C* groups was observed, indicating that the caecal microbiota composition was not significantly affected by supplementation with *AE*.

The relative abundance (RA) of the top 30 most prevalent ASVs in the caeca (Figure 3) accounted for ~80% of the total sequencing reads at day 7 and day 14. At day 37, this figure had dropped down to ~50%, concurrent with a substantial increase in the number of low abundant ASVs in the minor group; from 89 on day 14 to 285 and 297 on day 37 for the group infected with the thrush strain or the chicken strain, respectively. This minor group describes the group of ASVs, with each having an abundance lower than 0.55%. Since the caecal microbiota development was not significantly affected by supplementation with *AE*, the treatments were pooled for further analysis. In general, there was considerable individual variation in the caecal microbiota among the birds observed.

Examination of taxonomic composition revealed shifts in the caecal microbiota composition between the sampling points. Comparison of pre-*C. jejuni* challenge samples from day 7 and day 14 showed a considerable decrease in the RA of ASV *Escherichia-Shigella*_d46e at day 14, while *Eisenbergiella*_2799 showed a pronounced increase. At day 37 (post-challenge samples), the RA of both *Escherichia-Shigella*_d46e and *Eisenbergiella*_2799 had decreased to low percentages. In contrast, *Faecalibacterium*_4832 and *Faecalibacterium*_30c0 emerged as the dominant ASVs at day 37, with a minor representation at days 7 and 14. Unclassified *Enterobacteriaceae*_9451 showed the highest RA at day 7, with a decrease at day 14, and minimal presence at day 37. ASVs *Clostridium_sensu_stricto*_1_1d49 and *Clostridium_sensu_stricto*_1_9acb were present at day 7 and thereafter their RA was minimal. Conversely, ASVs *Clostridia*_UCG-014_a7ff and *Clostridia*_UCG-014_0bae were the most abundant at day 14 and diminished at day 37. The most abundant ASV classified as *Lactobacillus* was *Lactobacillus*_0df6, which had the highest RA at day 7, decreased by day 14, and was minimally present at day 37. Between day 14 and day 37, there was a distinct increase in the abundance of *Faecalibacterium*_54ef, *Bacilli*_RF39_2035, and *Anaeroplasma*_0af7. These ASVs were not present among the top 30 most abundant ASVs at day 7. The ASV *Subdoligranulum*_e0fc exhibited minor presence at days 7 and 14, with a considerable increase in its RA at day 37. A reduction in the RA of *Butyricicoccus*_6d52 was noted at day 37 in both groups (chicken and thrush strain), in contrast to its moderate abundance at days 7 and 14.

A PCoA plot of caecal samples obtained at day 37 after hatching revealed a significant clustering according to the *C. jejuni* strain used for the challenge (PERMANOVA, $p = 0.001$) (Figure 4). No effect of diet was observed at day 37.

At day 37, a significant difference ($p < 0.05$) in the RA of several ASVs was detected in caecal samples obtained from broilers challenged with the two different *C. jejuni* strains. The most abundant ASV within the group challenged with the song thrush strain was *Faecalibacterium*_30c0, exhibiting a significantly higher

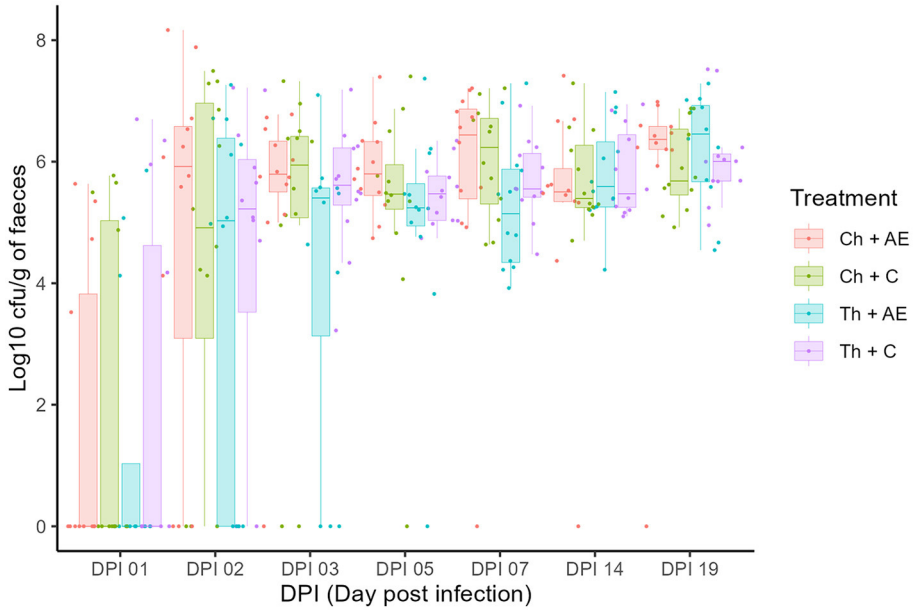


FIGURE 1
Colony forming unit counts of *Campylobacter jejuni* colonization in fecal samples at different dpi (days post-infection). Dots (data points) represent 10-log (CFU/ml) in individual fecal samples based on mean values of six replicate dots per plate at a given sampling point. Ch, chicken strain of *C. jejuni*; Th, song thrush strain of *C. jejuni*; C, control; AE, algal extract. Red = Ch + AE, Green = Ch + C, Blue = Th + AE, Purple = Th + C.

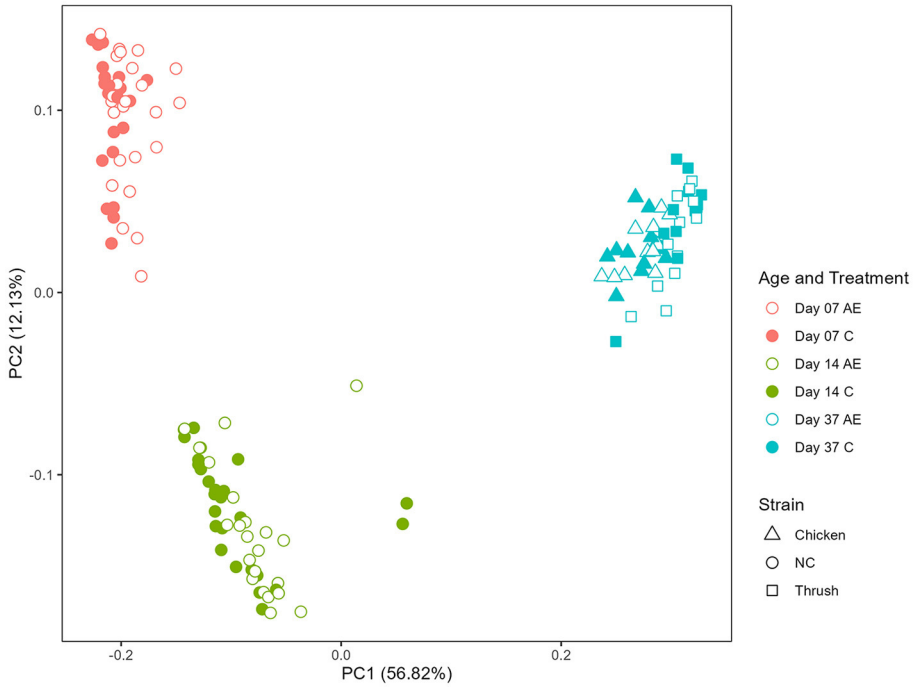


FIGURE 2
Principal coordinate analysis (PCoA) plot showing differences in generalized UniFrac distance matrix at different sampling points after hatching (day 7, day 14, and day 37). AE, algal extract; C, control; NC, non-challenged.

RA compared to the chicken strain samples (Figure 5). In contrast, the dominant ASV found in the samples from birds challenged with the chicken strain was *Faecalibacterium*_4832. Furthermore, a significantly higher abundance of ASVs *Anaeroplasma*_0af7 and *Faecalibacterium*_54ef was observed in the thrush strain samples than in the chicken strain samples (Figure 5). We cannot exclude that these differences were due to environmental factors as the birds challenged with the two different strains were caged in different parts of the stable, separated by a flexible wall.

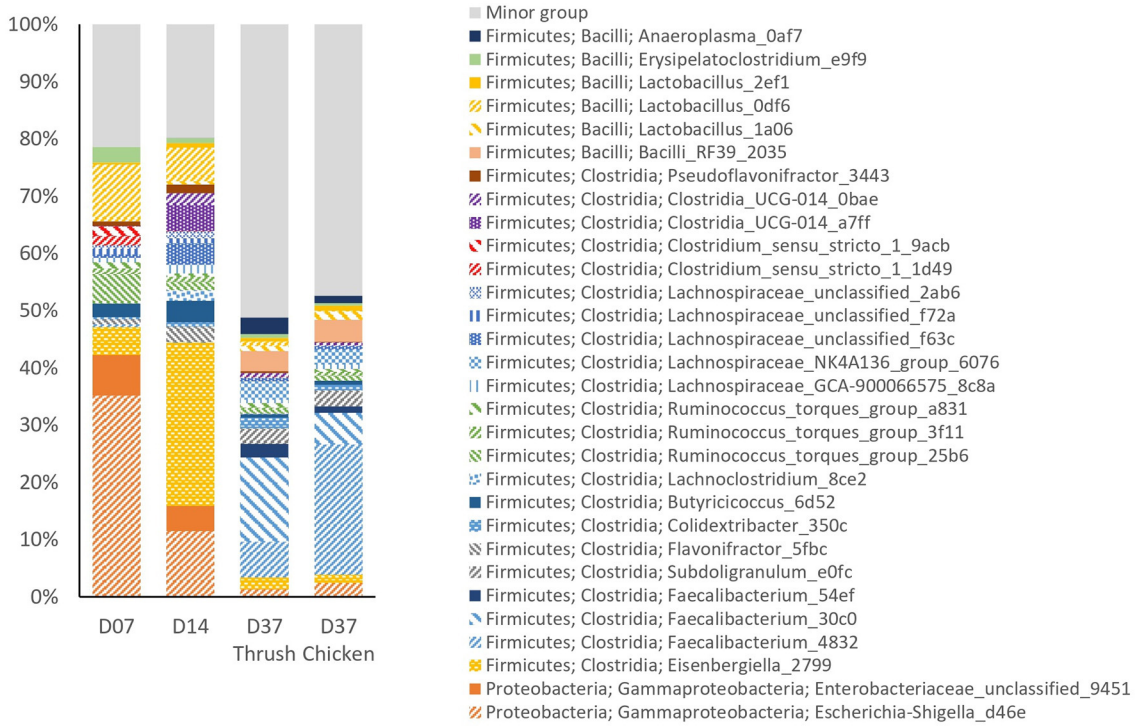


FIGURE 3
The relative abundance (%) of the top 30 most abundant ASVs in caecal samples at different ages (day 7, day 14, and day 37) and *Campylobacter* strains (song thrush and chicken).

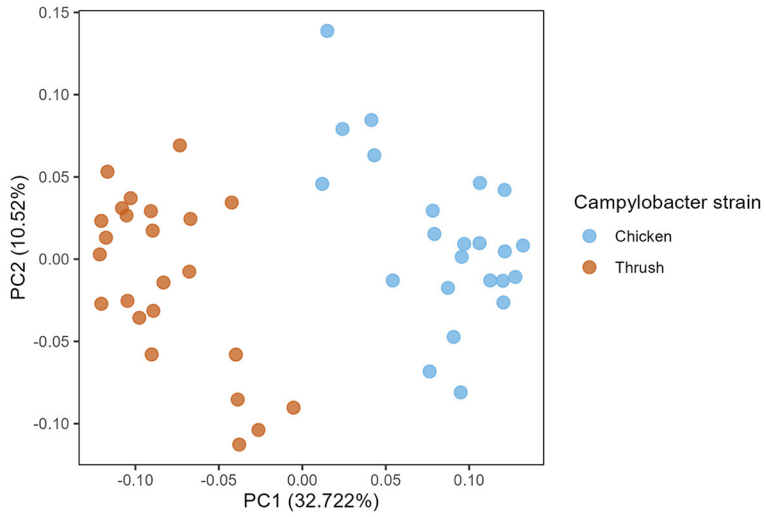


FIGURE 4
Principal coordinate analysis (PCoA) plot showing differences in generalized UniFrac distance matrix between different *Campylobacter* strains (chicken and song thrush origin) at age day 37.

## 4 Discussion

Identifying ways to reduce *Campylobacter jejuni* colonization in broilers' gut is desirable to minimize the risk of meat contamination during the slaughter process and thereby enhance the safety of poultry products for human consumption. Feed supplementation with prebiotics and probiotics may be an important component of the complex solution to this challenge.

Our study's results revealed that supplementation with 290 ppm laminarin had no significant effect on the colonization dynamics of two distinct strains of *C. jejuni*: the chicken origin strain #65 and the song thrush origin strain #3926. No significant differences in

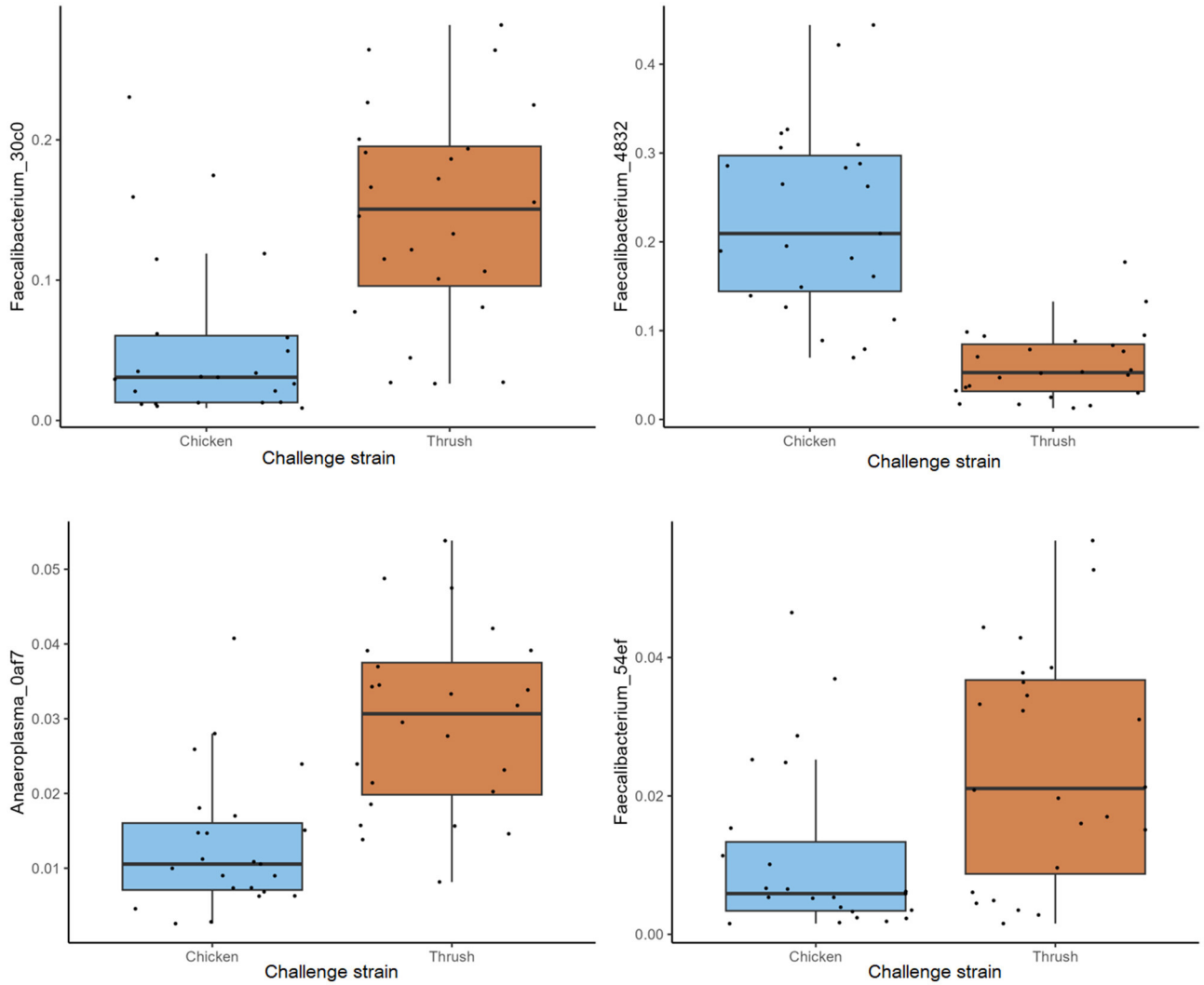


FIGURE 5
The relative abundance (%) of ASVs in caecal samples at day 37 with a significant difference ($p < 0.05$).

bacterial loads could be observed between the groups that received laminarin supplementation compared to the control groups at any time point during the study (Figure 1). These findings are in line with an earlier study by Sweeney and O'Doherty (2016), where the addition of purified laminarin extract (250 ppm) to the diet of broilers showed no significant impact on the suppression of *C. jejuni* during the initial post-hatch period. Taken together, this suggests that laminarin-rich algal extracts have a limited direct antimicrobial effect on reducing *C. jejuni* colonization in broiler caeca.

The chicken and song thrush origin *C. jejuni* strains exhibited comparable colonization dynamics during the whole experiment (Figure 1), indicating that the Ross 308 hybrid used in this study displayed similar susceptibility to colonization by both *C. jejuni* strains. This observation was in contrast to the study by Atterby et al. (2018) where dramatic differences in colonization patterns were observed in mallard ducks inoculated with either the chicken strain #65 or the song thrush strain #3926, both used in this study. In wild birds, *C. jejuni* shows strong host association that might be due to colonization resistance to specific *C. jejuni* genotypes (Griekspoor et al., 2013; Atterby et al., 2018). Our findings suggest that such colonization resistance against specific *C. jejuni* genotypes might be weaker in broiler chickens. However, further investigation utilizing a broader range of *C. jejuni* strains from diverse bird host origins is necessary to verify this. The fast establishment and continuous persistence of colonization observed in both strains highlight the efficiency with which *C. jejuni* establishes itself in the broilers' caeca. Colonization levels remained high from 3 dpi until the end of the experiment. These observations are in agreement with the results reported by Connerton et al. (2018), who documented the onset of *C. jejuni* colonization in broilers infected at 20 days of age within 2 days of exposure, with colonization persistence until the end of the study at day 35.

The caeca are known to be the most bacteria-dense part of the broiler's gastrointestinal tract and an important site for carbohydrate fermentation contributing to the birds' intestinal

health and nutrition (Waite and Taylor, 2014). To evaluate the impact of diet supplementation with *AE* on broiler microbiota development, caecal samples were analyzed by 16S rRNA amplicon sequencing and investigated at the ASV level. Principal Coordinate Analysis (Figure 2) used to visualize the dissimilarities within the generalized UniFrac distance matrix across different sampling points (day 7, day 14, and day 37) did not show any clear clustering of the groups that received feed supplemented with *AE* compared to the control groups. This suggests that the supplementation did not significantly influence the composition of the caecal microbiota in the current experiment. Yet, Venardou et al. (2021) found that supplementing the basal diet with 300 ppm of laminarin for 35 days led to an increase in both the relative and absolute abundance of *Bifidobacterium* in the caeca of Ross 308 broiler chickens, proposing this dosage to promote a beneficial gastrointestinal microbiota profile. However, it is worth mentioning that in that study broilers were not exposed to experimental *Campylobacter* challenge and that the influence of dietary supplements can vary based on diverse factors such as host physiological state, application pattern, housing effect, and dosage, which can yield different outcomes in their activity (Marco and Tachon, 2013; Salami et al., 2016). Additionally, pronounced individual variation observed in the caecal microbiota composition among the birds on all sampling points in the present study highlights the complexity of avian gut microbial communities (Stanley et al., 2013).

The age of the birds exerted a significant effect on the microbiota composition, as suggested by the distinct clustering of ASVs from each sampling point, correlating to the age of the birds (Figure 2). Furthermore, the rarefaction curves of observed ASVs revealed a consistent temporal increase in alpha diversity (Supplementary Figure 1). These observations find support in previous studies which have highlighted the age-dependent aspect of caecal microbiota development (Ivarsson et al., 2022; Boyner et al., 2023). Among changes in the gut microbiota solely connected to the age of the birds, a relatively high RA of ASVs *Clostridium_sensu_stricto*_1 as well as ASVs *Escherichia-Shigella*_d46e and unclassified *Enterobacteriaceae*_9451 (belonging to the phylum Proteobacteria), were observed at day 7, while their RA notably decreased at day 14 (Figure 3). Our observation aligns with a study conducted by Kers et al. (2020), suggesting that members of the genus *Clostridium sensu stricto* are among the first colonizers of the avian caeca, and that after a few days, members of the phylum Proteobacteria colonize the caeca, followed by an increase in Firmicutes later in the broiler's life.

Since the main aim of this study was to investigate if feeding broilers with *AE* had an effect on their resistance to *C. jejuni* colonization and if this could be explained by their caecal microbiota composition in contrast to birds fed control feed, we did not include a control group that was not challenged with *C. jejuni*. Regrettably, this fact renders us unable to draw direct conclusions on the relative effect of *C. jejuni* colonization vs. that of bird age on the caecal microbiota composition observed at day 37. However, this study provides valuable insights into caecal microbiota development during *C. jejuni* challenge, focusing on the ASV level rather than the higher taxonomic levels commonly discussed in broiler gut microbiota studies. Interestingly, the challenge with the two different *C. jejuni* strains at day 17 affected caecal microbiota composition differently by day 37 (Figure 5), suggesting an influence of *C. jejuni* colonization. ASVs classified as *Faecalibacterium* were pronounced at day 37, where ASV *Faecalibacterium*_4832 dominated in birds challenged with the chicken strain, while ASVs *Faecalibacterium*_30c0 and *Faecalibacterium*_54ef had significantly higher RA in the birds that received the song thrush strain. These findings are consistent with prior studies by Ocejo et al. (2019) and Thibodeau et al. (2015), who reported a positive association between *Faecalibacterium* and *Campylobacter* presence in broiler caeca. Moreover, similarities to our previous research (Valečková et al., 2023) were found, where *Faecalibacterium* emerged as the predominant genus in Ross 308 caeca 20 days after *C. jejuni* challenge. Furthermore, Liao et al. (2020) noted that *Faecalibacterium* dominated the caecal bacterial communities of *Campylobacter*-free broilers during the grower phase (7-14 days of age), while its prevalence decreased thereafter. In addition, in the current study, significantly higher RA of *Anaeroplasma*_0af7 was observed in birds that received the song thrush strain. Current reports about *Anaeroplasma* in broilers caeca in relation to *Campylobacter* presence are limited. However, Ocejo et al. (2019) identified *Anaeroplasma* as the main genus of the minor phyla Tenericutes, which was present at stable levels (0.002%−1.5%) throughout the productive period when analyzing the microbiome of chicken caeca in two different breeds (Ross-308 and Sasso-T451A), and management systems throughout their whole productive lifespan. It should be noted that the differences at ASV level seen at day 37 may also be due to environmental effects imposed by the fact that birds challenged with the two different *C. jejuni* strains were physically separated in the stable by a flexible wall (Kers et al., 2018).

Analyzing the RA of the top 30 most abundant ASVs revealed the pronounced reduction of ASV *Escherichia-Shigella*_d46e after the *C. jejuni* challenge. This observation aligns with results from Awad et al. (2016), where 14-day-old Ross 308 broilers were challenged with $1 \times 10^8$ CFU of *C. jejuni* NCTC 12744 and their microbial community composition was followed from day 1 to day 28 of age. The authors found that the presence of *C. jejuni* was associated with a significant reduction in *Escherichia coli* abundance compared to the non-challenged control birds. These findings may also be related to the observed decrease in RA of unclassified *Enterobacteriaceae*_9451 at day 37 in the present study. Furthermore, the RA of ASVs *Clostridia* UCG-014 decreased considerably post-challenge which aligns with the results from Pang et al. (2023), where a significant negative correlation between *Campylobacter* abundance and genera *Clostridia* was reported in caeca of 5 weeks old broilers. Additionally, a considerable increase in the RA of ASVs *Subdoligranulum*_e0fc and *Bacilli*_RF39_2035 at day 37, compared to their minimal presence prior to the challenge, along with a converse shift in the RA of *Eisenbergiella*_2799, *Butyricicoccus*_6d52, and *Lactobacillus*_0df6 in response to the challenge, aligns with our previous findings discussing the effect of *C. jejuni* presence on the broilers caeca microbial composition in Ross 308 (Valečková et al., 2023).

The observed increase in the species richness within the minor ASV group (Supplementary Figure 1) and the increased RA of ASVs within this group at day 37 (Figure 3) was likely attributed to the progressive divergence in the caecal microbiota

with age (Zhou et al., 2021). Ocejo et al. (2019) identified age as the strongest factor influencing the composition of caecal microbiota when the core microbiome was compared among Ross 308 broilers raised in a conventional system for 42 days with that of a 'slow-growing breed', Sasso T451A reared in an extensive farming system with outdoor access for 86-days. Interestingly, the same study reported different microbial taxa to be either positively or negatively correlated with *C. jejuni* RA, suggesting that both bird age and *C. jejuni* colonization can affect the caecal microbiota composition. Therefore, it can be speculated that the drastic increase in species richness observed on day 37 could have been an effect of the experimental *C. jejuni* challenge, where the host immune response triggered by *C. jejuni* colonization might selectively have promoted the profusion and growth of specific ASVs, resulting in an increase in microbial diversity as suggested in a study conducted by Pang et al. (2023). In their analysis of samples collected from five-week-old birds, the researchers observed that farms with *Campylobacter*-positive broilers had a higher species richness in the caecal microbiota and greater phylogenetic diversity in comparison to *Campylobacter*-negative farms. As stated above, it is important to note that the interpretation of pre- and post-challenge observations in the current study is obscured by the considerable age difference between the two sampling occasions, specifically 23 days. Further studies are therefore required to better understand changes in caecal microbiota composition related to *C. jejuni* colonization in general and the presence of different *C. jejuni* strains in particular.

In conclusion, the present study demonstrates that the supplementation of *AE* in broiler diets has no significant impact on either *C. jejuni* colonization after experimental challenge or the development of the caecal microbiota. The results suggest that the overall changes in the gut microbiota observed at different sampling points were mainly age-dependent. Furthermore, the results do not support the initial hypothesis that the chicken origin *C. jejuni* strain would exhibit better colonization ability in chickens compared to the strain originating from a song thrush. Yet, this study contributes to understanding the complex interactions influencing microbial communities in the broiler gut and provides insights for future interventions aimed at enhancing resistance to *Campylobacter* colonization in broilers.

## Data availability statement

The sequencing data are deposited in NCBI, accession number PRJNA1078836.

## Ethics statement

The animal study was approved by the Uppsala Ethics Committee for Animal Research, Uppsala, Sweden approval number (5.8.18-10572/2019). The study was conducted in accordance with the local legislation and institutional requirements.

## Author contributions

EE: Writing – review & editing, Writing – original draft, Visualization, Investigation. LS: Writing – review & editing, Writing – original draft, Visualization, Validation, Software, Methodology, Formal analysis, Data curation. GC: Writing – review & editing, Validation, Resources. HP: Writing – review & editing, Resources, Funding acquisition. GT: Writing – review & editing, Validation, Methodology, Investigation, Data curation. PE: Writing – review & editing, Writing – original draft, Validation, Supervision, Resources, Methodology, Investigation, Funding acquisition, Conceptualization. EI: Writing – review & editing, Supervision, Project administration, Investigation, Funding acquisition, Conceptualization.

## Funding

The author(s) declare that financial support was received for the research, authorship, and/or publication of this article. The work was supported by FORMAS, a Swedish Research Council for Sustainable Development (Grant number: 2016-00365).

## Acknowledgments

The authors wish to thank Dr. Annica Andersson and Professor Roger Andersson at the Department of Molecular Sciences, SLU, for great assistance with fiber analysis.

## Conflict of interest

The authors declare that the research was conducted in the absence of any commercial or financial relationships that could be construed as a potential conflict of interest.

## Publisher's note



## Supplementary material

The Supplementary Material for this article can be found online at: https://www.frontiersin.org/articles/10.3389/fmicb.2024.1396949/full#supplementary-material

# References


Anderson, M. J. (2001). A new method for non-parametric multivariate analysis of variance. *Austr. Ecol.* 26, 32–46. doi: 10.1111/j.1442-9993.2001.01070.pp.x

Atterby, C., Mourkas, E., Meric, G., Pascoe, B., Wang, H., Waldenström, J., et al. (2018). The potential of isolation source to predict colonization in avian hosts: a case study in *Campylobacter jejuni* strains from three bird species. *Front. Microbiol.* 9:591. doi: 10.3389/fmicb.2018.00591

Aviagen. (2019). *Ross Nutrition Specifications.* Available olnline aa: https://www.cipa.com.co/wp-content/uploads/2019/11/RossBroilerNutritionSpecs2019-EN.pdf (accessed November 24, 2023).

Awad, W. A., Mann, E., Dzieciol, M., Hess, C., Schmitz-Esser, S., Wagner, M., et al. (2016). Age-related differences in the luminal and mucosa-associated gut microbiome of broiler chickens and shifts associated with *Campylobacter jejuni* infection. *Front. Cell. Infect. Microbiol.* 6:154. doi: 10.3389/fcimb.2016.00154

Bates, D., Mächler, M., Bolker, B., and Walker, S. (2015). Fitting linear mixed-effects models using *lme*4. *J. Stat. Soft.* 67, 1–48. doi: 10.18637/jss.v067.i01

Benjamini, Y., and Hochberg, Y. (1995). Controlling the false discovery rate: a practical and powerful approach to multiple testing. *J. R. Stat. Soc. Ser. B Stat. Methodol.* 57, 289–300. doi: 10.1111/j.2517-6161.1995.tb02031.x

Bolyen, E., Rideout, J. R., Dillon, M. R., Bokulich, N. A., Abnet, C. C., Al-Ghalith, G. A., et al. (2019). Reproducible, interactive, scalable and extensible microbiome data science using QIIME 2. *Nat. Biotechnol.* 37, 852–857. doi: 10.1038/s41587-019-0209-9

Boyner, M., Ivarsson, E., Wattrang, E., Sun, L., Wistedt, A., Wall, H., et al. (2023). Effects of access to feed, water, and a competitive exclusion product in the hatcher on some immune traits and gut development in broiler chickens. *Br. Poult. Sci.* 12, 1–13. doi: 10.1080/00071668.2022.2163152

Chen, C.-Y., Nace, G. W., and Irwin, P. L. (2003). A 6× 6 drop plate method for simultaneous colony counting and MPN enumeration of *Campylobacter jejuni*, Listeria monocytogenes, and Escherichia coli. *J. Microbiol. Methods.* 55, 475–479. doi: 10.1016/S0167-7012(03)00194-5

Cherry, P., Yadav, S., Strain, C. R., Allsopp, P. J., McSorley, E. M., Ross, R. P., et al. (2019). Prebiotics from seaweeds: An ocean of opportunity? *Mar. Drugs* 17: 327. doi: 10.3390/md17060327

Connerton, P., Flaujac Lafontaine, G., O'Kane, P., Ghaffar, N., Cummings, N., Smith, D., et al. (2018). The effect of the timing of exposure to *Campylobacter jejuni* on the gut microbiome and inflammatory responses of broiler chickens. *Microbiome* 6:88. doi: 10.1186/s40168-018-0477-5

Core Team, R. (2019). *R: A Language and Environment for Statistical Computing.* Vienna: R Foundation for Statistical Computing.

Dunn, O. J. (1964). Multiple comparisons using rank sums. *Technometrics,* 6, 241–252. doi: 10.1080/00401706.1964.10490181

EFSA (2020). Update and review of control options for Campylobacter in broilers at primary production. *EFSA J.* 18:e06090. doi: 10.2903/j.efsa.2020.6090

French, N. P., Midwinter, A., Holland, B., Collins-Emerson, J., Pattison, R., Colles, F., et al. (2009). Molecular epidemiology of *Campylobacter jejuni* isolates from wild-bird fecal material in children's playgrounds. *Appl. Environ. Microbiol.* 75, 779–783. doi: 10.1128/AEM.01979-08

Griekspoor, P., Colles, F. M., McCarthy, N. D., Hansbro, P. M., Ashhurst-Smith, C., Olsen, B., et al. (2013). Marked host specificity and lack of phylogeographic population structure of *Campylobacter jejuni* in wild birds. *Mol. Ecol.* 22, 1463–1472. doi: 10.1111/mec.12144

Gripp, E., Hlahla, D., Didelot, X., Kops, F., Maurischat, S., Tedin, K., et al. (2011). Closely related *Campylobacter jejuni* strains from different sources reveal a generalist rather than a specialist lifestyle. *BMC Genom.* 12, 1–21. doi: 10.1186/1471-2164-12-584

Halekoh, U., and Højsgaard, S. (2014). A kenward-roger approximation and parametric bootstrap methods for tests in linear mixed models–the R package pbkrtest. *J. Stat. Softw.* 59, 1–32. doi: 10.18637/jss.v059.i09

Ivarsson, E., Wall, H., Boyner, M., Cervin, G., Pavia, H., Wattrang, E., et al. (2023). Effects of algal supplementation in feed to broiler breeders on transfer of nutrients and antibodies to chicks and quality of hatchlings. *Animal* 17:101020. doi: 10.1016/j.animal.2023.101020

Ivarsson, E., Wattrang, E., Sun, L., Cervin, G., Pavia, H., Wall, H., et al. (2022). Evaluation of early feed access and algal extract on growth performance, organ development, gut microbiota and vaccine-induced antibody responses in broiler chickens. *Animal* 16:100522. doi: 10.1016/j.animal.2022.100522

Kers, J. G., de Oliveira, J. E., Fischer, E. A., Tersteeg-Zijderveld, M. H., Konstanti, P., Stegeman, J. A., et al. (2020). Associations between phenotypic characteristics and clinical parameters of broilers and intestinal microbial development throughout a production cycle: a field study. *Microbiologyopen* 9:e1114. doi: 10.1002/mbo3.1114

Kers, J. G., Velkers, F. C., Fischer, E. A., Hermes, G. D., and Stegeman, J. A. (2018). Host and environmental factors affecting the intestinal microbiota in chickens. *Front. Microbiol.* 9:322066. doi: 10.3389/fmicb.2018.00235

Kruskal, W. H. (1952). Use of ranks in one-criterion variance analysis. *J. Am. Stat. Assoc.* 47, 583–621. doi: 10.1080/01621459.1952.10483441

Kuznetsova, A., Brockhoff, P. B., and Christensen, R. H. B. (2017). lmerTest package: tests in linear mixed effects models. *J. Stat. Softw.* 82:13. doi: 10.18637/jss.v082.i13

Liao, X., Shao, Y., Sun, G., Yang, Y., Zhang, L., Guo, Y., et al. (2020). The relationship among gut microbiota, short-chain fatty acids, and intestinal morphology of growing and healthy broilers. *Poult. Sci.* 99, 5883–5895. doi: 10.1016/j.psj.2020.08.033

Marco, M. L., and Tachon, S. (2013). Environmental factors influencing the efficacy of probiotic bacteria. *Curr. Opin. Biotechnol.* 24, 207–213. doi: 10.1016/j.copbio.2012.10.002

Mourkas, E., Yahara, K., Bayliss, S. C., Calland, J. K., Johansson, H., Mageiros, L., et al. (2022). Host ecology regulates interspecies recombination in bacteria of the genus Campylobacter. *Elife* 11:e73552. doi: 10.7554/eLife.73552.sa2

Ocejo, M., Oporto, B., and Hurtado, A. (2019). 16S rRNA amplicon sequencing characterization of caecal microbiome composition of broilers and free-range slow-growing chickens throughout their productive lifespan. *Sci. Rep.* 9:2506. doi: 10.1038/s41598-019-39323-x

Pang, J., Looft, T., Zhang, Q., and Sahin, O. (2023). Deciphering the association between Campylobacter colonization and microbiota composition in the intestine of commercial broilers. *Microorganisms* 11:1724. doi: 10.3390/microorganisms11071724

Pedregosa, F., Varoquaux, G., Gramfort, A., Michel, V., Thirion, B., Grisel, O., et al. (2011). Scikit-learn: machine learning in Python. *J. Mach. Learn. Res.* 12, 2825–2830.

Salami, S., Guinguina, A., Agboola, J., Omede, A., Agbonlahor, E., Tayyab, U., et al. (2016). In vivo and postmortem effects of feed antioxidants in livestock: a review of the implications on authorization of antioxidant feed additives. *Animal* 10, 1375–1390. doi: 10.1017/S1751731115002967

Searle, S. R., Speed, F. M., and Milliken, G. A. (1980). Population marginal means in the linear model: an alternative to least squares means. *Am. Stat.* 34, 216–221. doi: 10.1080/00031305.1980.10483031

Sharma, S., Neves, L., Funderud, J., Mydland, L. T., Øverland, M., Horn, S. J., et al. (2018). Seasonal and depth variations in the chemical composition of cultivated *Saccharina latissima*. *Algal Res.* 32, 107–112. doi: 10.1016/j.algal.2018.03.012

Stanley, D., Geier, M. S., Hughes, R. J., Denman, S. E., and Moore, R. J. (2013). Highly variable microbiota development in the chicken gastrointestinal tract. *PLoS ONE* 8:e84290. doi: 10.1371/journal.pone.0084290

Sun, L., Lundh, Å., Höjer, A., Bernes, G., Nilsson, D., Johansson, M., et al. (2022). Milking system and premilking routines have a strong effect on the microbial community in bulk tank milk. *J. Dairy Sci.* 105, 123–139. doi: 10.3168/jds.2021-20661

Sweeney, T., and O'Doherty, J. (2016). Marine macroalgal extracts to maintain gut homeostasis in the weaning piglet. *Domest. Anim. Endocrinol.* 56, S84–S89. doi: 10.1016/j.domaniend.2016.02.002

Theander, O., Åman, P., Westerlund, E., Andersson, R., and Pettersson, D. (1995). Total dietary fiber determined as neutral sugar residues, uronic acid residues, and Klason lignin (the Uppsala method): collaborative study. *J. AOAC Int.* 78, 1030–1044. doi: 10.1093/jaoac/78.4.1030

Thibodeau, A., Fravalo, P., Yergeau, É., Arsenault, J., Lahaye, L., Letellier, A., et al. (2015). Chicken caecal microbiome modifications induced by *Campylobacter jejuni* colonization and by a non-antibiotic feed additive. *PLoS ONE* 10:e0131978. doi: 10.1371/journal.pone.0131978

Thomas, J. B., Sterner, M., Nylund, G. M., Albers, E., Edlund, U., Undeland, I., et al. (2022). The effects of cultivation deployment-and harvest-timing, location and depth on growth and composition of *Saccharina latissima* at the Swedish west coast. *Aquaculture* 559:738443. doi: 10.1016/j.aquaculture.2022.738443

Valečková, E., Sun, L., Wang, H., Dube, F., Ivarsson, E., Kasmaei, K. M., et al. (2023). Intestinal colonization with *Campylobacter jejuni* affects broiler gut microbiota composition but is not inhibited by daily intake of Lactiplantibacillus plantarum. *Front. Microbiol.* 14:1205797. doi: 10.3389/fmicb.2023.1205797

Venardou, B., O'Doherty, J., Vigors, S., O'Shea, C., Burton, E., Ryan, M., et al. (2021). Effects of dietary supplementation with a laminarin-rich extract on the growth performance and gastrointestinal health in broilers. *Poult. Sci.* 100:101179. doi: 10.1016/j.psj.2021.101179

Ver Hoef, J. M., and Boveng, P. L. (2007). Quasi-Poisson vs. negative binomial regression: how should we model overdispersed count data? *Ecol.* 88, 2766–2772. doi: 10.1890/07-0043.1

Waite, D. W., and Taylor, M. W. (2014). Characterizing the avian gut microbiota: membership, driving influences, and potential function. *Front. Microbiol.* 5:223. doi: 10.3389/fmicb.2014.00223

Waldenström, J., Axelsson-Olsson, D., Olsen, B., Hasselquist, D., Griekspoor, P., Jansson, L., et al. (2010). *Campylobacter jejuni* colonization in wild birds: results from an infection experiment. *PLoS ONE* 5:e9082. doi: 10.1371/journal.pone.0009082

Zhou, Q., Lan, F., Li, X., Yan, W., Sun, C., Li, J., et al. (2021). The spatial and temporal characterization of gut microbiota in broilers. *Front. Vet. Sci.* 8:712226. doi: 10.3389/fvets.2021.712226

# Frontiers in Microbiology

**Explores the habitable world and the potential of microbial life**

The largest and most cited microbiology journal which advances our understanding of the role microbes play in addressing global challenges such as healthcare, food security, and climate change.

---

## Discover the latest Research Topics

See more →


**Frontiers**

Avenue du Tribunal-Fédéral 34
1005 Lausanne, Switzerland
frontiersin.org

**Contact us**

+41 (0)21 510 17 00
frontiersin.org/about/contact